Green Energy and Technology

Om Prakash
Anil Kumar

Solar Drying Technology

Concept, Design, Testing, Modeling, Economics, and Environment

Springer

Green Energy and Technology

More information about this series at http://www.springer.com/series/8059

Om Prakash • Anil Kumar
Editors

Solar Drying Technology

Concept, Design, Testing, Modeling, Economics, and Environment

Springer

Editors
Om Prakash
Department of Mechanical Engineering
Birla Institute of Technology, Mesra
Ranchi, Jharkhand, India

Anil Kumar
Department of Energy (Energy Centre)
Maulana Azad National Institute of Technology
Bhopal, Madhya Pradesh, India

ISSN 1865-3529 ISSN 1865-3537 (electronic)
Green Energy and Technology
ISBN 978-981-10-3832-7 ISBN 978-981-10-3833-4 (eBook)
DOI 10.1007/978-981-10-3833-4

Library of Congress Control Number: 2017949696

© Springer Nature Singapore Pte Ltd. 2017
This work is subject to copyright. All rights are reserved by the Publisher, whether the whole or part of the material is concerned, specifically the rights of translation, reprinting, reuse of illustrations, recitation, broadcasting, reproduction on microfilms or in any other physical way, and transmission or information storage and retrieval, electronic adaptation, computer software, or by similar or dissimilar methodology now known or hereafter developed.
The use of general descriptive names, registered names, trademarks, service marks, etc. in this publication does not imply, even in the absence of a specific statement, that such names are exempt from the relevant protective laws and regulations and therefore free for general use.
The publisher, the authors and the editors are safe to assume that the advice and information in this book are believed to be true and accurate at the date of publication. Neither the publisher nor the authors or the editors give a warranty, express or implied, with respect to the material contained herein or for any errors or omissions that may have been made. The publisher remains neutral with regard to jurisdictional claims in published maps and institutional affiliations.

Printed on acid-free paper

This Springer imprint is published by Springer Nature
The registered company is Springer Nature Singapore Pte Ltd.
The registered company address is: 152 Beach Road, #21-01/04 Gateway East, Singapore 189721, Singapore

Foreword by Akhtar Kalam

At the present situation, for the major chunk of global population, satisfying their basic needs like energy, food, clean water and housing cannot be achieved because of the demand for energy is far much higher than the supply.

In this age of energy crisis, there is a strong urge to look for renewable energy sources for the fulfillment of our basic energy need. It is not only provide the energy security but save our precious environment from greenhouse gasses. Solar energy has emerged as one of the prominent renewable energy. Solar radiation is another term used for electromagnetic radiation. By the proper utilization of the radiation, various important activities can be done like drying, water purification, electricity generation, space heating, crop cultivation etc. For developing nations like India, solar food processing is the newest and efficient advanced technology introduced for addressing different problems faced by our citizens. The technology which includes food processing and storage using solar energy can indirectly aid in removing poverty. We do not produce less; the fact is that much of our produce goes as waste as we do not have proper food processing and preservation mechanism in our country. By introducing solar drying technology to our farmers, a revolution can be started and absolute poverty and hunger can be wiped from our country.

In majority of Asian countries, agriculture mostly dominates economy. More than half the population is employed in agriculture but still the demand outdoes the supply. One of the major reasons for this being lack of efficient preservation and storage techniques. One of the most popular techniques for preserving food in most of the Asian countries is drying of crops by employing solar energy. Application of solar energy in drying for preserving agricultural and marine produce is in practice since ages. This was done using direct solar radiations.

Solar dryers have huge applications in agriculture and industrial sector; especially from an energy point of view, dryers are the most useful devices. These can save energy, save plenty of time, occupy minimal surface area, enhance life and quality of products and most importantly are ecofriendly. Drying rice using solar dryers has been well known for many years especially in the countries producing rice, such as

Thailand and the other Asian countries. Solar dryers can be used effectively for low temperature drying and hence can be used effectively to dry agricultural produce, flowers, herbs etc. Thus, solar dryers overcome various disadvantages of artificial mechanical dryers, reducing the total amount of fuel energy required.

This book has 5 sections and covers 23 chapters. These 5 sections are:

(i) Concept of Solar Drying
(ii) Design and Testing of Solar Drying Systems
(iii) Modelling of Solar Drying Systems
(iv) Environomical Impact of Solar Drying Systems
(v) Innovation in Solar Drying

This book edited by Dr. Anil Kumar, who was a respected researcher at the Energy Technology Research Centre, Department of Mechanical Engineering, Faculty of Engineering, Prince of Songkla University, Hat Yai, Thailand, and at present, Assistant Professor, Dept. of Energy (Energy Centre), Maulana Azad National Institute of Technology, Bhopal (India), and Dr. Om Prakash, Assistant Professor, Department of Mechanical Engineering, from Birla Institute of Technology Mesra, Ranchi-India, is extremely well written and the authors of various chapters have substantial analytical and theoretical knowledge in the subject. A comprehensive review of the various designs, details of construction and operational principles of the wide variety of practically-realised designs of solar-energy drying systems has been presented. I commend this book to all undergraduates, postgraduates, researchers and academics interested in acquiring knowledge in this important area. The appropriateness of each design type for application by rural farmers and others in developing countries has been discussed. Some very recent developments in solar drying technology have also been highlighted.

Akhtar Kalam

Smart Energy Research Unit, College
of Engineering and Science
(D524 or D332)
Victoria University
Ballarat Road, Footscray, 3011, VIC,
Australia

Foreword by D. P. Kothari

Solar energy is an ancient subject. In India, the Sun is considered to be God. Women worship the Sun. In fact, all forms of energy emanates from the Sun only. In the future, solar energy will form the major chunk of the energy supplied. India is lucky to have Sun for 220 days in most parts out of 365 days.

There are several aspects of solar science and engineering which the students, teachers, researchers and industry personnel have to study, such as solar power generation by PV and solar thermal, solar refrigeration, solar cooker, solar cooling and heating, solar drying, and solar architecture. Out of these, solar drying finds a special place.

The book *Solar Drying Technology: Concept Design Testing Modeling Economics and the Environment* edited by my friends Dr. Om Prakash and Dr. Anil Kumar will fulfil the long felt need of a book in this vital area. It will prove to be a good text/reference book.

The main strength of this book is its beauty of combining theory and practice in various chapters written by well-known international experts in the area.

Both the editors are well known to me and they have done a fabulous job. As a co-author/co-editor of more than 50 books and as one who has also worked in solar energy and was in the illustrious company of great solar energy experts like Prof. M.S. Sodha, Prof. S.S. Mathur, Prof. H.P. Garg, Prof. G.N. Tiwari, Prof. T.C. Kandpal and other erstwhile colleagues in the Center for Energy studies, IIT Delhi for 30 years, I can safely vouch for the quality of the book. I am sure the readers will immensely benefit by this book.

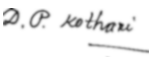

Indian Institute of Technology, Delhi
New Delhi, 110016, Delhi, India

D. P. Kothari

Foreword by Trilochan Mohapatra

Food preservation is very important for food safety and security. Food and Agriculture Organization (FAO) estimated that 852 million people worldwide are undernourished. The global challenge to ensuring food and nutritional security for the fast-growing human population can be addressed through technological development and innovation in agricultural sector. Technology intervention is essential to safeguard against post-harvest losses of agri-produce that continue to happen owing to primitive methods of harvests, handling and storage.

Drying of agricultural products is one of the important methods to preserve and enhance shelf-life. Although open sun drying is a very common and cost- effective method, its advantage is partly upset due to quantitative and qualitative losses caused by rodents, birds, insects, dust, rain, over drying and/or under drying. It is extremely important, therefore, to develop energy-efficient drying operations to conserve conventional energy without affecting the quality of the end product. In this regard, solar dryers not only meet the drying requirements of crops, fish and animal products, but also save time, energy and money.

I am happy to record that this book is a joint venture of national and international experts whose ideas have been meticulously compiled by the editors highlighting the concept, design, testing, modelling, economics and environmental perspectives of solar dryers for plausible reading and functional adoption. The editors and the authors deserve appreciation for this timely effort.

Trilochan Mohapatra

Indian Council of Agricultural Research
Krishi Bhavan
New Delhi, 110001, Delhi, India
21 November 2016

Preface

The tremendous rise in demand for energy has led to scarcity of conventional sources of energy like fossil fuels, thereby pushing us to search for alternative sources of energy. With the sun being the ultimate source of energy, we need to harness its energy to sustain the growth of mankind. Solar drying has been in practice since ages to preserve different kinds of agricultural produce. Due to advancement in science and technology, we have developed inexpensive and efficient solar drying devices for drying different agricultural and marine products using solar power. Using solar dryer, the amount of moisture can be reduced tremendously, thus preserving the products for a longer time. It reduces product wastage and enhances the productivity of farmers.

This book is divided in five parts. The first part deals about the concept of solar drying. In this part, there are five chapters (1, 2, 3, 4, and 5). In *Chap*. 1, the authors discussed the fundamental concepts of drying such as water activity and its significance, the important properties of air and its products, drying mechanism, drying curves and the performance indicators of a dryer. The fundamental knowledge in drying will enable a better understanding of any solar drying system.

In *Chap*. 2, the author discusses the general classification of solar drying systems. Numerous types of solar dryers have been designed and developed in various parts of the world. A solar dryer can be operated based on either natural or forced convection of heat transfer. Based on the mode of heating source, a solar dryer is classified broadly in three types, namely, direct, indirect and mixed mode solar dryer. The most typical solar dryers for agricultural produce based on their construction designs were described. The selection of solar drying systems should consider the available insolation rate in the target region, kind of product that will be dried, production throughput and operational and investment costs. Most studies consider solar drying as a good alternative to traditional open air drying and/or conventional drying systems operated by fossil fuels.

In *Chap*. 3, the author deals with the characteristics of the different systems for solar drying of crops. The fundamental concepts and contexts of their use to dry crops are discussed in the chapter. It is shown that solar drying is the outcome of complex interactions between the intensity and duration of solar energy, the prevailing ambient relative humidity and temperature, the characteristics of a particular crop and its pre-preparation and the design and operation of the solar dryer.

In *Chap*. 4, the authors discuss the fundamental mathematical relations of solar drying systems. Basic mathematical relations and theories of the drying process involving simultaneous heat and mass transfer models as well as those of the simplified thin layer and deep bed models are given. An overview of solar drying methods (in both thin layer and deep bed dryers) along with the principal solar drying systems (direct-sun dryers and passive and active dryers) is briefly provided, discussing the respective fields of application and analysing their advantages and disadvantages. Finally, the basic mathematic equations used for describing and modelling the various physical processes within the most common drying systems and devices are reported. A brief discussion of the recent advances in modelling is presented where pertinent.

In *Chap*. 5, the authors discuss the advancement in greenhouse drying system. Greenhouse drying system is one of the most popular solar drying systems. The state-of-the-art advancement in the field of greenhouse drying is also discussed.

Part II deals with the design and testing of the solar drying systems. In this part, there are three chapters (6, 7, and 8).

In *Chap*. 6, design procedures for solar drying systems including the use of rules of thumb of psychrometric charts and design equations are discussed. The economic aspects of solar drying systems are also deliberated. Various case studies, relating to the application of direct mode, indirect mode and mixed mode types of solar drying systems, have been presented. Although direct mode dryers are economic to construct, they have major drawbacks such as their drying temperatures cannot be regulated, leading to over- or under-drying. Well-designed solar crop drying systems are capable of drastically reducing losses of agricultural products occasioned by postharvest spoilage.

Chapter 7 deals with the thermal testing methods for solar dryers. The standard testing method not only provides better performance management of the dryer system but allows manufacturers to achieve competitive efficiency and good product quality by comparing the available designs. In this chapter, an extensive review of solar dryer performance evaluation has been presented. Furthermore, the chapter describes existing testing procedures for most common designs of solar dryers and related practices used in the measurement, evaluation and description of overall performance, including a variety of food products dried in scientific investigations.

Chapter 8 deals with the exergy analysis of solar dryers. Exergy analysis corrects existing inefficiencies at its sources and contributes more meaningful in solar dryer designs. Increased efficiency can often contribute in an environmentally acceptable way by direct reduction of irreversibility that might otherwise have

occurred. Exergy analysis is one of the most powerful mechanisms in order to design an optimum solar dryer.

Part III deals with the modelling of the solar dryers. Mathematical and soft computing modelling techniques are discussed. There are six chapters (9, 10, 11, 12, 13, and 14) in this part.

In *Chap*. 9, mathematical modelling of solar drying systems is presented. This chapter begins with a broad appraisal of the basic concepts and essential theories for the mathematical modelling of solar drying. Next, the common modelling approaches and developmental steps (model conceptualization, mathematical formulation, determination of model parameters, method of solution and experimental validation) implicated in solar drying were outlined. Then the sequential progress of thin layer drying models (semi-theoretical, theoretical and empirical models) was discussed briefly. The subsequent section of the chapter reviews the application of the above models by different researchers in the last decade. Afterwards, newly developed or commonly used thin layer drying mathematical equations related to the solar collector models and drying cabinet models for different solar drying systems and food products were shown. Finally, the chapter concludes with future directions and the need for more investigations on solar drying.

Chapter 10 deals with the drying kinetics of solar drying systems. This chapter presents the heat and mass transfer mechanisms that regulate the drying rate, the conditions in direct and indirect solar drying, the drying curves and the mathematical modelling of the solar drying processes, with application examples in various dominions.

Chapter 11 deals with mathematical and computational modelling simulation of solar drying systems. In mathematical modelling, both fundamental (Fickian diffusion) and semiempirical drying models have been applied to the solar drying of a variety of agricultural commodities in several different dryer types (direct, indirect and mixed mode with both forced and natural convection). Computational modelling (i.e. computational fluid dynamics or CFD), both in 2-dimensional and 3-dimensional modes, affords insights on geometry-specific solar drying issues, such as airflow patterns within the drying cabinet. Both mathematical and computational modelling have recently been brought to bear on solar drying innovations such as thermal storage, use of desiccants during drying and dynamic feedback control of the drying process. Robust models are also necessary for the performance evaluation and comparison of different dryer designs and configurations. The outputs of mathematical and computational models are compared with measured drying data (whether performed outdoors or with a solar simulator) to ensure the accuracy and efficacy of the model.

Chapter 12 describes the different numerical methods that can be utilized for the performance evaluation of the solar drying system. Numerical techniques help in developing a solar dryer to increase drying effectiveness and analyses and forecast the performance of dissimilar types of a solar dryer. Numerical analysis is essential for forecasting the relevant parameters, which are highly required in a solar drying system. Computational fluid dynamics (CFD) can be used to analyse and investigate the heat and mass transfer inside the solar dryer. Adaptive-network-based

fuzzy inference system (ANFIS) is able to predict the performance of the solar drying system. The artificial neural network can be applied to estimate the quantity of the dehydrated product. FUZZY logic is an essential tool to precisely forecast the results with least inaccuracy. Numerical techniques are applied for testing the drying behaviour of products in the laboratory as well as commercial level.

Chapter 13 deals with simulation of food solar drying. This chapter covers the application of different software in the design and development of solar dryers. This comprehensive and extensive analysis of the different software will be very useful to the research community, academicians and solar dryer designers.

Chapter 14 discusses the simulation process of food solar drying, presenting the basic issues of mass and heat transfer under time-varying conditions. Food drying embraces several phenomena, and scientists do not completely understand its underlying mechanisms. However, mathematical simulation and modelling provide comprehension to improve knowledge on drying mechanisms, allow the prediction of the drying behaviour, and are essential tools in the design of solar drying equipment. The major difficulty in simulating solar food drying arises from variable meteorological conditions that change air temperature, moisture and velocity inside the solar equipment, during the drying process. Therefore, an integrated heat and mass transfer model under dynamic conditions is presented, and appropriate assumptions are discussed. A meteorological model and desorption isotherms are taken into consideration as well. The integrated model includes food shrinkage, changing boundary conditions and variable thermal properties and water diffusivity with time and space (non-isotropic characteristics).

In Part IV, the environomical impact of solar drying systems is discussed. In this part, there are five chapters (15, 16, 17, 18, and 19).

Chapter 15 deals with the economics of solar drying systems. Various methodologies to evaluate the economics of the solar dryer are highlighted. Cost effective drying systems will have great impact on marketing and publicity.

Chapter 16 presents the importance of economic consideration of solar dryers and a review of techno-economic study of solar dryers developed over the years with economic and energy analysis. In the present context, this study is important because many types of solar dryers were invented, namely, hybrid solar dryer, direct solar dryer and indirect solar dryer, for various drying applications. However, the availability of a suitable solar drying system which is technically and cost-effectively feasible is limited. As of now, only some solar dryers which meet the valued parameters like economical, technical and socio-economical requirements commercially exist.

Chapter 17 discusses the holistic approach to the economic analysis of various developed solar dryers. Various important economic analysis parameters are being discussed like annualized cost, capital cost, savings earned in its entire working life and the time required to recover capital investments, payback period with interest and without interest, etc.

Chapter 18 presents the economic analysis of hybrid photovoltaic-thermal (PV-T) integrated indirect-type solar dryer. A solar dryer integrating with photovoltaic (PV)-powered DC fan has been developed for forced air circulation without

the use of external power supplies like grid electricity. This dryer has also been coupled to a solar air heater having a sun-tracking facility and blackened surface as absorber for improved energy collection efficiency. A new PV-T integrated solar dryer consists of a solar air heater and a drying chamber with chimney. This system can be used for drying various agricultural products like fruits and vegetables. Experimental studies have been conducted for the forced mode under no load and load conditions. Energy analysis and techno-economic analysis of hybrid PV-T dryer have also been carried out.

Chapter 19 presents the energy analysis of the direct and indirect solar drying system. Various important energy analysis parameters such as CO_2 discharges per year, embodied energy, energy payback time, carbon mitigation and carbon credit have been considered. This analysis helps to protect the environment from pollution and encourages the use of solar energy. The embodied energy of the greenhouse dryer is calculated.

In the last part, various innovations in the solar drying system are discussed. It includes four chapters (20, 21, 22, and 23).

Chapter 20 presents energy conservation through recirculation of hot air in a solar dryer. The experiment was conducted in a system where the pneumatic conveyor is applied in the solar drying system. The drying efficiency and the specific energy of the solar dryer with inclined drying chamber were on an average less than the vertical type. The drying capacity (initial load) of the inclined drying chamber was larger than the vertical chamber type.

Chapter 21 discusses the development and performance study of solar air heater for solar drying applications. It explores general theoretical thermodynamic performance studies of some improved solar air heater for drying applications, followed with detailed thermal performance studies of an improved hemispherical protruded solar air heater. Economic analysis estimated that if 400 m^2 of galvanized roof of black tea processing factory were converted into a solar air heater by using black painting, plywood insulation and tempered glass enclosure, then an average 20 % of conventional thermal energy for black tea drying may be saved. The annual carbon-dioxide reduction of 2189 tonnes is achievable by using improved solar air heater. The payback period of the hybrid renewable thermal energy-based system is less than 15 months, and benefit to cost ratio is 1:1.

Chapter 22 includes recent and past research on different thermal storage systems for solar dryers like latent heat storage, sensible heat storage and thermos-chemical storage commonly used for domestic and industrial applications.

Chapter 23 provides an idea about the methodology of the promising phase change material (PCM) development through proper mixing and simultaneous measurement of their thermo-physical properties by the differential scanning calorimeter (DSC) thermal analysis technique. Based on the DSC analysis, it may be concluded that the developed binary mixtures were in the melting range of 40–60^{o}C with an adequate amount of latent heat of fusion which can be utilized for the application of solar dryers as well as for other relevant TES applications.

It is hoped that this book is complete in all respects of solar drying technology and can serve as a useful tool to learners, faculty members, practising engineers and students. Despite our best of efforts, we regret if some errors are in the manuscript due to inadvertent mistake. We will greatly appreciate being informed about errors and receiving constructive criticism for the improvement of the book.

Ranchi, Jharkhand, India — Om Prakash
Bhopal, Madhya Pradesh, India — Anil Kumar

Acknowledgements

This book is tribute to the engineers and scientists who continue to push forwards the practice and technologies of solar drying. These advances continue to reduce postharvest crop/fruit losses and promote sustainable crop/food drying technology. This book could not have been written without the efforts of numerous individuals including the primary writers, contributing authors, technical reviewers and practitioners who contribute real-life experience. Our first and foremost gratitude goes to the God Almighty for giving us the opportunity and strength to do our part of service to the society.

We express our heartfelt gratitude to the president of Prince of Songkla University, Hat Yai, Songkhla, Thailand; the director of Maulana Azad National Institute of Technology Bhopal, India; and the vice chancellor of the Birla Institute of Technology, Mesra, Ranchi, India, for their kind encouragement.

We would like to thank our teachers Prof. G. N. Tiwari, Centre for Energy Studies, Indian Institute of Technology Delhi, India, and Prof. Perapong Tekasakul, Vice President (Research System and Graduate Studies) of Prince of Songkla University, Hat Yai, Songkhla, Thailand, for building up our academic and research career.

We are indebted to Dr. Trilochan Mohapatra, Secretary and Director General of the Department of Agricultural Research and Education, Indian Council of Agricultural Research, Ministry of Agriculture & Farmers Welfare, Krishi Bhavan, New Delhi, India, for his constant encouragement.

We gratefully acknowledge Dr. D. P. Kothari, former Director i/c Indian Institute of Technology, Delhi, for his guidance and utmost support at every step.

We also appreciatively acknowledge the help provided by Dr. Akhatar Kalam, Head of Engineering and Leader of Smart Energy Research Unit College of Engineering and Science (D524 or D332), Victoria University, Ballarat Road, Footscray 3011, Victoria, Australia. He is an enthusiastic academician and researcher.

We appreciate our spouses, Mrs. Poonam Pandey and Mrs. Abhilasha, and our beloved children, Ms. Shravani Pandey, Master Tijil Kumar and Ms. Idika Kumar.

They are the great source of support and inspiration, and their patience and sympathetic understanding throughout this project have been most valued.

Our heartfelt special thanks go towards Springer for publishing this book. We would also like to thank those who were directly or indirectly involved in bringing up this book successfully.

Last but not least, we wish to express our warmest gratitude to our respected parents Sh. Krishna Nandan Pandey and Smt. Indu Devi and the late Sh. Tara Chand and Smt. Vimlesh and our siblings for their unselfish efforts to help in all fields of life.

Contents

Contributors

Kamaruddin Abdullah Universitas Darma Persada (UNSADA), Jakarta Timur, Indonesia

Fatima Sierre Alleyne United States Department of Agriculture – Agricultural Research Service, Healthy Processed Foods Research Unit, Albany, CA, USA

Cosmas Ngozichukwu Anyanwu Department of Agricultural and Bioresources Engineering, University of Nigeria, Enugu State, Nigeria

T.V. Arjunan Department of Mechanical Engineering, Coimbatore Institute of Engineering and Technology, Coimbatore, India

Deepali Atheaya School of Engineering and Sciences, Mechanical Engineering Department, Bennett University, Greater Noida, Uttar Pradesh, India

Stamatios Babalis National Center for Scientific Research "DEMOKRITOS", Solar & Energy Systems Laboratory, Athens, Greece

Jan Banout Faculty of Tropical AgriSciences, Department of Sustainable Technologies, Czech University of Life Sciences Prague, Suchdol, Czech Republic

Maria João Barroca Molecular Physical-Chemistry Group, Coimbra University Research Center, Coimbra, Portugal

Vassilios Belessiotis National Center for Scientific Research "DEMOKRITOS", Solar & Energy Systems Laboratory, Athens, Greece

Teresa R.S. Brandão CBQF- Centro de Biotecnologia e Química Fina, Escola Superior de Biotecnologia, Centro Regional do Porto da Universidade Católica Portuguesa, Porto, Portugal

Prashant Singh Chauhan Department of Energy (Energy Centre), Maulana Azad National Institute of Technology, Bhopal, India

Raquel de Pinho Ferreira Guiné CI&DETS Research Centre and Department of Food Industry, Polytechnic Institute of Viseu, ESAV, Viseu, Portugal

CERNAS Research Centre, Polytechnic Institute of Coimbra, ESAC, Coimbra, Portugal

Harsh Deep Department of Mechanical Engineering, Birla Institute of Technology, Mesra, Ranchi, India

Partha Pratim Dutta Department of Mechanical Engineering, Tezpur University, Tezpur, India

O.V. Ekechukwu Department of Mechanical Engineering, University of Nigeria, Nsukka, Nigeria

Rupesh R. Gawande Mechanical Engineering Department, Rashtrasant Tukadoji Maharaj Nagpur University, Nagpur, Maharashtra, India

Ravi Gupta Department of Agricultural Engineering, Rajmata Vijayaraje Scindia Krishi Vishwavidyalaya, Gwalior, India

Anand Jain Department of Energy (Energy Centre), Maulana Azad National Institute of Technology, Bhopal, India

Karunesh Kant Non-Conventional Energy Laboratory, Rajiv Gandhi Institute of Petroleum Technology, Rae Bareli, India

Ajay Kumar Kaviti Department of Mechanical Engineering, Vallurupalli Nageswara Rao Vignana Jyothi Institute of Engineering and Technology, Hyderabad, India

Anil Kumar Department of Energy (Energy Centre), Maulana Azad National Institute of Technology, Bhopal, Madhya Pradesh, India

Rebecca Rose Milczarek United States Department of Agriculture – Agricultural Research Service, Healthy Processed Foods Research Unit, Albany, CA, USA

Kapil Narwal Department of Mechanical Engineering, Manav Rachna University, Faridabad, India

Sujata Nayak Department of Mechanical Engineering, Manav Rachna University, Faridabad, India

Brian Norton Dublin Energy Lab, Dublin Institute of Technology, Dublin 7, Ireland

Daniel I. Onwude Department of Agricultural and Food Engineering, Faculty of Engineering, University of Uyo, Uyo, Nigeria

Elias Papanicolaou National Center for Scientific Research “DEMOKRITOS”, Solar & Energy Systems Laboratory, Athens, Greece

Rajendra C. Patil Mechanical Engineering Department, Bapurao Deshmukh College of Engineering, Wardha, Nagpur, Maharashtra, India

Om Prakash Department of Mechanical Engineering, Birla Institute of Technology, Mesra, Ranchi, Jharkhand, India

Inês N. Ramos CBQF- Centro de Biotecnologia e Química Fina, Escola Superior de Biotecnologia, Centro Regional do Porto da Universidade Católica Portuguesa, Porto, Portugal

Saurabh Ranjan Centre for Energy Engineering, Central University of Jharkhand, Ranchi, India

K. Sampathkumar Department of Mechanical Engineering, Tamilnadu College of Engineering, Coimbatore, India

S. Selvanayaki Department of Agricultural and Rural Management, TamilNadu Agricultural University, Coimbatore, India

Atul Sharma Non-Conventional Energy Laboratory, Rajiv Gandhi Institute of Petroleum Technology, Jais, India

Vinod Kumar Sharma Department of Energy, Division for Bioenergy, Biorefinery and Green Chemistry (DTE-BBC), Italian National Agency for New Technologies, Energy and Sustainable Economic Development (ENEA) Research Centre, Rotondella (MT), Italy

Amritanshu Shukla Non-Conventional Energy Laboratory, Rajiv Gandhi Institute of Petroleum Technology, Rae Bareli, India

Ashish Shukla School of Energy, Construction and Environment, Coventry University, Coventry, UK

Cristina L.M. Silva CBQF- Centro de Biotecnologia e Química Fina, Escola Superior de Biotecnologia, Centro Regional do Porto da Universidade Católica Portuguesa, Porto, Portugal

Shobhana Singh Department of Energy Technology, Aalborg University, Aalborg East, Denmark

P.P. Tripathy Department of Agricultural & Food Engineering, Indian Institute of Technology, Kharagpur, West Bengal, India

S. Vijayan Department of Mechanical Engineering, Coimbatore Institute of Engineering and Technology, Coimbatore, India

About the Editors

Om Prakash received his doctorate in energy from the Maulana Azad National Institute of Technology Bhopal, India, in 2015. He was awarded scholarship during his postgraduate and doctorate programmes. Presently, he is working as Assistant Professor in the Department of Mechanical Engineering at the Birla Institute of Technology, Mesra, Ranchi, India. He has published 20 research papers in international journals and 08 papers in international conferences. He has also contributed four book chapters. He is reviewer of many reputed international journals such as the *International Journal of Green Energy*, *Renewable and Sustainable Energy Reviews* and *International Journal of Ambient Energy* and projects such as *The Energy Report*. He is working in the fields of renewable energy, energy and environment, solar energy applications, heat transfer and energy economics.

Anil Kumar is presently working as Assistant Professor, Dept. of Energy (Energy Centre), Maulana Azad National Institute of Technology (MANIT), Bhopal (India) and he was researcher in the Energy Technology Research Center, Department of Mechanical Engineering, Faculty of Engineering, Prince of Songkla University, Hat Yai, Songkhla, Thailand from June 2015 to May 2017. He completed his B.Tech. in Mechanical Engineering followed by an M.Tech. in Energy Technology and a Ph.D. in 'Thermal Modelling of Greenhouse Dryer' from the Centre for Energy Studies (CES), Indian Institute of Technology Delhi, India. He has 11 years of experience in teaching and research at International/National institutes. His main areas of research interest are: solar thermal technology, distribution of energy generation, clean energy technologies, renewable energy application in buildings and energy economics. He has published four books, namely, Energy, Environment, Ecology, and Society; Fundamentals of Mechanical Engineering; Environmental Science: Fundamental, Ethics & Laws; and Advanced Internal Combustion Engine, and holds two patents. He has also published more than 105 research articles in journals and at international conferences. Presently, he is reviewer of various journals of repute. In his tenure at the MANIT Bhopal, he has supervised 05 Ph.D. and 19 master's students. He is recipient of "Research Excellence Award 2016": The researcher has Top 20 Publications from the Web of Science database, honoured by President, Prince of Songkla University, Hat Yai, Thailand.

Part I
Concept of Solar Drying

Fundamental Concepts of Drying

S. Vijayan, T.V. Arjunan, and Anil Kumar

Abstract In recent years, the postharvest losses of food and agricultural products have been reduced with the advanced preservation methods. Drying is one of the oldest preservation methods used by human for industrial and agricultural products. This is the simplest and most cost-effective method among other preservation methods. This chapter discusses about the fundamental concepts of drying such as water activity and its significance, important properties of air and the product, drying mechanism, drying curves and the performance indicators of dryer. The fundamental knowledge in drying will enable the better understanding of any drying systems.

Keywords Drying • Water activity • Drying mechanism • Drying kinetics • Thin layer drying • Deep bed drying

1 Introduction

Drying is one of the most commonly followed methods of preservation, for fruits, vegetables and food products. The word preservation indicates the process of extending the storage period of any product with desired quality. Food preservation is adopted mainly due to inappropriate planning in agriculture, adding value to the products and variation in nutritional values. The spoilage of the products usually occurs at various stages like harvesting, transport, storage and processing due to handling and physical, chemical or microbial damages. But most of the food products such as grains, fruits and vegetables deteriorate due to chemical or

S. Vijayan • T.V. Arjunan
Department of Mechanical Engineering, Coimbatore Institute of Engineering and Technology, Coimbatore 641109, India

A. Kumar (✉)
Department of Energy (Energy Centre), Maulana Azad National Institute of Technology, Bhopal 462003, Madhya Pradesh, India
e-mail: anilkumar76@gmail.com

© Springer Nature Singapore Pte Ltd. 2017

O. Prakash, A. Kumar (eds.), *Solar Drying Technology*, Green Energy and Technology, DOI 10.1007/978-981-10-3833-4_1

microbial reasons. The spoilage or deterioration of food products is encountered mostly in processing and storage periods. The process of avoiding or reducing the spoilage or deterioration of the quality of the product is known as preservation. Preservation plays an important role in agriculture as well as in industries. Many preservation technologies like drying, freezing, salting, canning, vacuum packaging, etc. have been employed over the years, but still drying is followed for economic reasons (Jangam 2011).

Preservation is performed not only for grains, food and vegetables; it is also used for marine products, meat products and other industrial products having high moisture content. The main reason for the deterioration is high moisture content of the product, which must be reduced in order to reduce the microbial growth or chemical enzymatic reactions. The safe value of the moisture content varies from product to product.

Drying or dehydration may be defined as a process of removing excessive moisture from a product to its safe or desired level of moisture content to store it for a longer time period without spoilage. This drying operation is carried out for the following reasons: to extend the shelf life, to improve the quality and to reduce the volume which results in reduced packaging and transportation cost. But, drying is mainly being performed for food products as it contains very high moisture content (25–95%) rather than industrial products. Normally, the deterioration of food due to chemical and biological activities occurs due to the presence of more moisture content (Sharma et al. 1991).

In most of the cases, drying is achieved by supplying thermal energy and to cause evaporation of water from the product, but in freeze-drying process, the water is removed by reducing the product temperature less than triple point (all three phases exist) temperature and through sublimation. Drying or dehydration is a complex process involved with heat and mass transfer processes. The thermal energy is transferred to the product as sensible and latent heat to increase the temperature of the product, thereby causing water to evaporate. Basically the drying process is known as an energy-intensive process, and in industries, the drying process consumes 10–25% of total energy consumption in well-developed countries (Mujumdar and Huang 2007; Erbay and Hepbasli 2013). With the suitable pre- and/or post-processing steps, the energy requirement for drying could be reduced, and the improvement in product quality is also achieved. The preprocessing techniques are used to enhance the moisture transport during the drying process such as blanching, salting, osmotic dehydration and soaking. Further, the quality of the dried product is maintained with proper post-processing techniques like packaging, coating, blending, etc. (Jangam 2011).

Many researchers from all the over the world have contributed their part, in order to reduce the energy consumption in drying by introducing new type of dryers. As reported by Mujumdar (Mujumdar and Law 2010), there are about 100 types of dryers that are commercially employed among 500 types of dryers. The different designs of dryers are available due to specific conditions of the products, operating conditions (temperature, pressure) and various modes of heat input. The dryers are generally classified as follows:

Classification of dryers based on the method of operation:

(a) Batch dryer
(b) Continuous dryer

Classification based on mode of heat supply to the drying process:

(a) Convection dryer
(b) Conduction dryer
(c) Radiation dryer
(d) Combined dryer

The dryers may also be categorized in other ways like based on the drying medium (air, gas or steam), based on the physical nature of the product (solid, slurry, liquid) and operating pressure (high pressure, atmospheric, vacuum), based on the method of material handling involved (tray, tunnel, rotary, vibratory, gravity, dispersion), etc. The main challenging task is the selection of appropriate dryer for the application; otherwise, it leads to poor-quality dried products, loss of energy, etc.

1.1 Batch Dryer

Batch dryers are mainly suitable for small-scale drying operations, in which the products are loaded in batches. A batch of wet products is loaded and the dryer is allowed to operate till the product reaches its desired moisture level, and the dryer operation is stopped, and then the dried products are unloaded. Again the next batch will be loaded for drying operation. Batch dryers are very simple in design, construction and operation, but the efficiency of batch dryers is less due to the loading and unloading periods of dryers. Examples for batch dryers are kiln dryers, tray dryers, solar dryers, etc.

1.2 Continuous Dryer

Continuous dryers are used for mass production, in which the drying operation is a continuous process and the loading and unloading of the wet products are being carried out during the operation. The products are loaded in a conveyor which passes through the drying region, and the dried products are unloaded at the other side.

1.3 Convection Dryers

Convection dryers are another type of dryers, in which the main mode of heat supply to the process is of convective. The thermal energy required to the drying process is supplied through any one convective medium like air, inert gas or superheated steam. The convective medium is heated by means of heated surface, and the heated medium is passed over or through the product to be dried, where the thermal energy is transferred by means of convection. The convective medium has two activities: first is to transfer the heat for evaporation of moisture from the wet product through convective mode and second is to carry away the evaporated moisture content. The convective dryer has many advantages like high drying rate and high moisture removal compared with all other types. Most of the industrial dryers are of convective dryers.

1.4 Conduction Dryers

In conduction dryers, the heat is supplied to the wet product by means of a heated surface, which is in contact with the product, causing boiling. This type of dryers is called conduction dryer or contact-type dryer. Conduction is the principal mode of heat transfer to the boiling drying. Normally, this boiling drying is used for the products in liquid or in slurry form. During boiling drying process, the product temperature is maintained to equal or higher than that of the boiling point of the liquid at vapour pressure. Because of this reason, the process is called boiling drying. In the case of boiling drying, the final moisture content can be reduced to very low level, whereas in convective drying, it depends on the parameters of the hot gas or air medium.

1.5 Radiation Dryers

In radiation dryers, the method by which heat is transmitted to the product is radiation from a hot body or from the sun. This radiation energy increases the temperature of the product and causes the evaporation of moisture. Example for the radiation dryer is of sun drying or solar dryers.

1.6 Combined Dryers

The method of heat supply may be from more than one method to achieve reduced drying time, like in mixed-mode solar (radiation as well as convective).

2 Water Activity and Its Significance

In day-to-day life, we might have noticed the deterioration of fresh vegetables, fruits and food products rather than the preserved ones. The main reason behind this is of water activity. This water activity is the important parameter which can be correlated with the quality and safe storage period of food products. Normally the food materials that have high moisture content are very prone to spoilage. In wet products, the presence of water can be observed in two forms as either free water or as bound moisture. The free-water content takes part in chemical reactions and biological processes, which mainly deteriorate the food quality. Water activity in a wet product influences much on the chemical reactions (enzymatic and non-enzymatic reactions), spore germinations and growth of microorganisms such as bacteria, moulds, yeasts and fungi, and the rate of reactions could be reduced by maintaining the water activity below 0.6. This water activity in a product can be controlled either by reducing moisture content or by adding chemicals (salts, sugars and glycerol) which control the available water content for reaction. But the addition of chemicals slightly alters the taste of the product (Leistner 1992).

Water activity, a_w, is the term which indicates the availability of free water in a product for chemical reactions, growth of microorganisms and spore germinations. It may be defined as the ratio of partial pressure of water vapour just above the wet product to that of the partial pressure of pure water at the same temperature. The water activity increases with increase in temperature and pressure. Normally, the value varies from 0 to 1. The water activity a_w can also be expressed as (Scott 1957)

$$a_w = \frac{p}{p_o} \tag{1}$$

where:

p – partial pressure of water vapour over wet product at specific temperature
p_o – partial pressure of pure water at saturation and the same temperature

Knowing the information about the availability of water for microbial, enzymatic or chemical activity helps in predicting the stability and control of the water activity for extending the shelf life. The rate of deterioration of the product and the water activity were given in Fig. 1, which was suggested by Labuza (1977) as stability maps. In this stability diagram, the reaction rates of oxidation, browning and enzymatic reactions are represented. It shows that the quality of food products is mainly affected by moulds, yeasts, bacteria and other microorganisms if the water activity is more than 0.7. At lower water activity region, the quality of the product is affected by the chemical reactions like browning, oxidation, enzymatic reactions, etc. rather than microorganisms. The microorganism growth is not only depending upon the water activity; it is also influenced by other factors like temperature, nutritional contents, pH value, preservatives, other food components and oxygen content (Chirife et al. 1996).

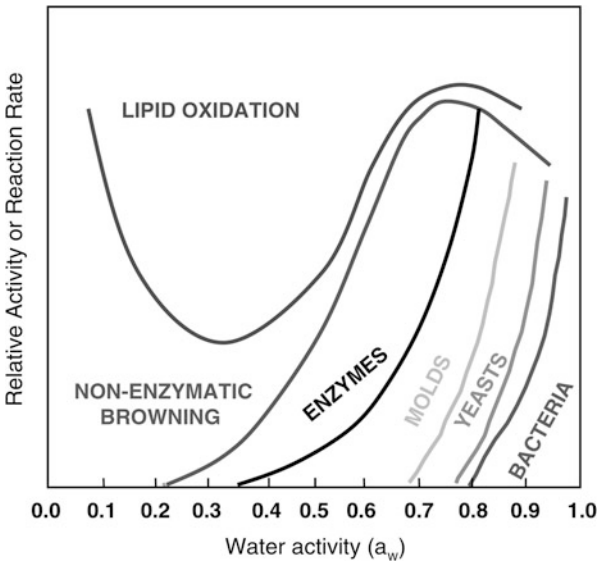

Fig. 1 Water activity–stability diagram (Labuza 1977)

Table 1 Microorganisms growth with respect to water activity in foods (Beuchat 1981)

Range of a_w	Microorganisms generally inhibited by lowest a_w in this range	Foods generally within this range
0.95–1.0	*Pseudomonas*, *Bacillus escherichia*, some yeasts	Fresh and canned fruits, vegetables, meat, fish and other perishable food
0.91–0.95	*Salmonella*, *Vibrio parahaemolyticus*, *Lactobacillus*, moulds, yeasts	Some cheeses, cured meat, some fruit juice concentrates
0.87–0.91	Most yeasts (*Candida*, *Torulopsis*), *Micrococcus*	Fermented sausage (salami), dry cheeses, margarine
0.80–0.87	Most moulds, most *Saccharomyces*, *Staphylococcus*	Most fruit juice concentrates, maple, chocolate and fruit syrups, flour, rice, fruit cake
0.75–0.80	Most *halophilic bacteria*	Jam, marmalade, fruits
0.65–0.75	Xerophilic moulds (*A. chevalieri*), *S. bisporus*	Jelly, nuts, molasses, raw cane, sugar, some dried fruits
0.60–0.65	Osmophilic yeasts (*S. rouxii*), few moulds	Dried fruits containing 15–20% moisture, honey, caramel
Below 0.6	No microbial proliferation	Pasta, food products containing about 10% moisture

The growth and metabolic activity of the microorganisms with respect to water activity in foods are given in Table 1. The water activity is important to determine the microbial stability of any food material (Beuchat 1981).

3 Important Properties of Air for Drying

The drying process is influenced by many parameters based on the type of dryers. Most of the dryers used are convective dryers rather than conductive dryers. In the case of convective dryers, the air is heated by means of any heating source, and the hot air will be supplied to wet products to remove the moisture content. So, it is very important to understand the properties of air (Vega-Mercado et al. 2001). This section discusses about the properties of hot air, which influences the drying process. Usually atmospheric air consists of dry air (mixture of nitrogen and oxygen) and water vapour.

3.1 Dry- and Wet-Bulb Temperatures

The temperature of the air measured by a normal thermometer is known as dry-bulb temperature and usually denoted as T_{db}. If the bulb of thermometer is covered with a wet wick or tissue, then the measured temperature is called as wet-bulb temperature, T_{wb}. In saturated condition of air, the wet-bulb and dry-bulb temperatures will be equal, and in other cases, the dry-bulb temperature is greater than the wet-bulb temperature. The difference between dry-bulb and wet-bulb temperatures is known as wet-bulb depression.

Note The convective drying process is almost similar to the measuring process of wet-bulb temperature. In the case of wet-bulb drying process, the bulb of thermometer is covered with a wet wick and exposed to a moving air, whereas in drying process, the wet product is exposed to heated air.

3.2 Dew Point Temperature

The temperature to which the air is cooled at a constant pressure and humidity will attain a saturation condition, and the water vapour will be condensed as dew. The temperature at which the dew forms is known as dew point temperature. The dew point temperature is denoted as T_{dp}.

3.3 Specific Humidity and Relative Humidity

The atmospheric air contains some amount of water vapour content; the parameters' specific humidity and relative humidity are used to indicate the amount of it. The specific humidity or simply humidity is the mass of water vapour per unit mass of dry air in the mixture of vapour and air. It is generally expressed as grams of

water per kg of dry air. The other important term associated with humidity is relative humidity; it is the ratio of the partial pressure of water vapour in a mixture to partial pressure of the saturated mixture at the same temperature, and it is expressed as percentage. The degree of saturation of moist air is the ratio of the mass of water vapour in a unit mass of dry air to the mass of water vapour in a unit mass of dry air when the air is saturated at same temperature:

$$\text{specific humidity} = \frac{\text{mass of water vapour}}{\text{mass of dry air}}$$

The specific humidity of air can be calculated from the mass of water vapour and from the mass of dry air as follows:

$$H = \frac{m_w}{m_a} \tag{2}$$

$$H = 0.622 \frac{p_w}{p_a} = 0.622 \frac{p_w}{p_t - p_w} \tag{3}$$

where:

p_w – partial pressure of water vapour
p_a – partial pressure of air
p_t – total pressure of air and vapour mixture

$$\text{Degree of saturation} = \frac{\text{mass of water vapour}}{\text{mass of water vapour at saturation}} = \frac{H}{H_s} \tag{4}$$

$$\text{Relative Humiidty (RH)} = \frac{p_w}{p_{ws}} \times 100 \tag{5}$$

where:

p_w – partial pressure of water vapour at a given temperature
p_{ws} – partial pressure of water vapour at saturation at the same temperature

3.4 Psychrometric Charts

The drying process is mainly characterized by the properties of air–water vapour mixture. Psychrometric charts are the chart which indicates the interrelation of all important properties of air–water vapour mixture. The psychrometric chart represents the absolute humidity, dew point temperature and specific volumes with respect to dry-bulb temperature. The dry-bulb temperatures and the mass of

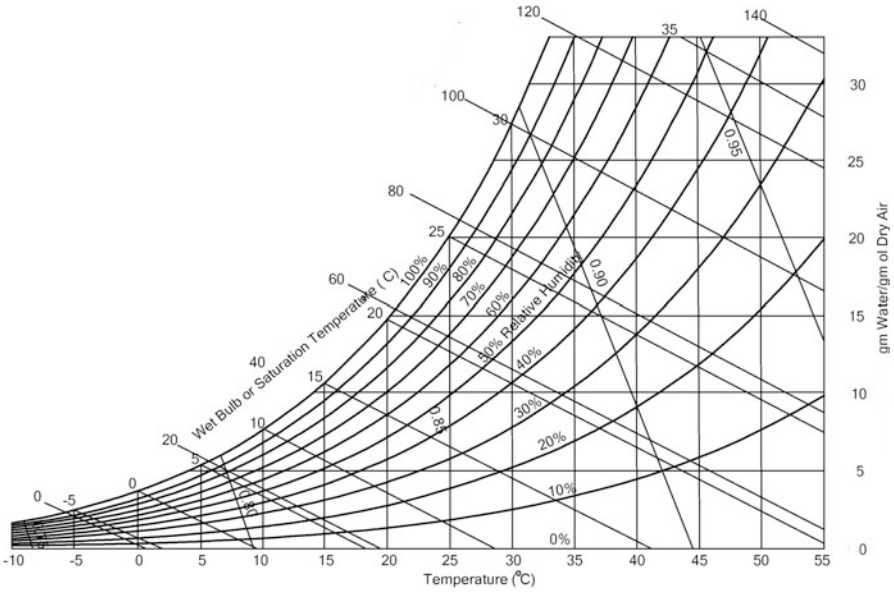

Fig. 2 Psychrometric chart

moisture content per kg of dry air are plotted in horizontal and vertical axes, respectively. The dew point temperatures are marked on the upper curved line, which corresponds to 100% relative humidity. This line is known as saturation line, and the constant relative humidity lines in percent are marked off between saturation line and the base line of the chart. Wet-bulb lines are diagonal lines sloping to the right making an angle of 30° to the horizontal axis. The specific volume, i.e. the volume of air–water vapour mixture per kg of dry air, is another diagonal line steeper at 60 °C. A simple psychrometric chart is shown in Fig. 2. The psychrometric processes of sensible heating or sensible cooling are denoted along the horizontal line, which shows that during the process, the humidity ratio remains constant. The relative humidity decreases with heating and increases with cooling.

Example 1

The atmospheric conditions are 30 °C dry-bulb temperature and 0.015 kg/kg of dry air. Find partial pressure of water vapour and relative humidity.

Solution:

Dry-bulb temperature, $T_{db} = 30$ °C; specific humidity, $H = 0.015$ kg/kg of dry air

The specific humidity of air is given by

$$H = 0.622 \frac{p_w}{p_a} = 0.622 \frac{p_w}{p_t - p_w}$$

$$0.015 = 0.622\,\frac{p_w}{1.013 - p_w}$$

Partial pressure of water vapour, $\boldsymbol{p_w} = 0.02385$ **bar**
The saturation pressure of air at 30 °C is 0.04247 bar (from steam tables)
The relative humidity is

$$\text{Relative Humiidty (RH)} = \frac{p_w}{p_{ws}} \times 100 = \frac{0.02385}{0.04247} = 56.16\boldsymbol{\%}$$

Dew point temperature, $T_{dp} = 20$ °C (from steam tables)

Example 2
Calculate (a) specific humidity and (b) dew point temperature of the air supplied to a heating chamber at 35 °C dry-bulb temperature and 60% relative humidity.

Solution:
Dry-bulb temperature, $T_{db} = 35$ °C; relative humidity, RH = 60%
The saturation pressure of air at 35 °C is 0.05746 bar (from steam tables)
The relative humidity is

$$\text{Relative Humidity (RH)} = \frac{p_w}{p_{ws}} \times 100$$

$$0.60 = \frac{p_w}{0.05746}$$

$$p_w = 0.60 \times 0.05746$$

$$\boldsymbol{p_w = 0.03448\ \text{bar}}$$

The specific humidity of air is given by

$$H = 0.622\,\frac{p_w}{p_a} = 0.622\,\frac{p_w}{p_t - p_w}$$

$$H = 0.622\,\frac{0.03448}{1.01325 - 0.03448}$$

$$\boldsymbol{H = 0.0219\ kg/kg\ of\ dry\ air}$$

Dew point temperature, $\boldsymbol{T_{dp} = 26\ °C}$ (from steam tables)

Example 3
In a convective dryer, atmospheric air at 30 °C and 60% RH is heated to 50 °C and then passed to drying chamber, and the air leaves the chamber at 33 °C and 70% RH. Indicate these on a psychrometric chart.

Solution:
Point 1 – Atmospheric air conditions

Dry-bulb temperature, $T_{db} = 30\ ^{\circ}C$
Relative humidity, $RH = 60\%$

The corresponding moisture content is 16 g of water/g of dry air or 0.016 kg of water/kg of dry air
Point 2 – Heater outlet and drying chamber inlet

Dry-bulb temperature, $T_{db} = 50\ ^{\circ}C$

Point 3 – Drying chamber outlet

Dry-bulb temperature, $T_{db} = 33\ ^{\circ}C$
Relative humidity, $RH = 70\%$

The corresponding moisture content is 24 g of water/g of dry air or 0.024 kg of water/kg of dry air.

The wet bulb for the drying chamber inlet and outlet is 28 °C (Fig. 3).

The heating process from 1 to 2 is a sensible heating process; only heat is added (i.e. no change in moisture content).

The drying process from 2 to 3 is a cooling and humidification process, temperature decreases and the moisture content increases. The process follows a constant wet-bulb temperature.

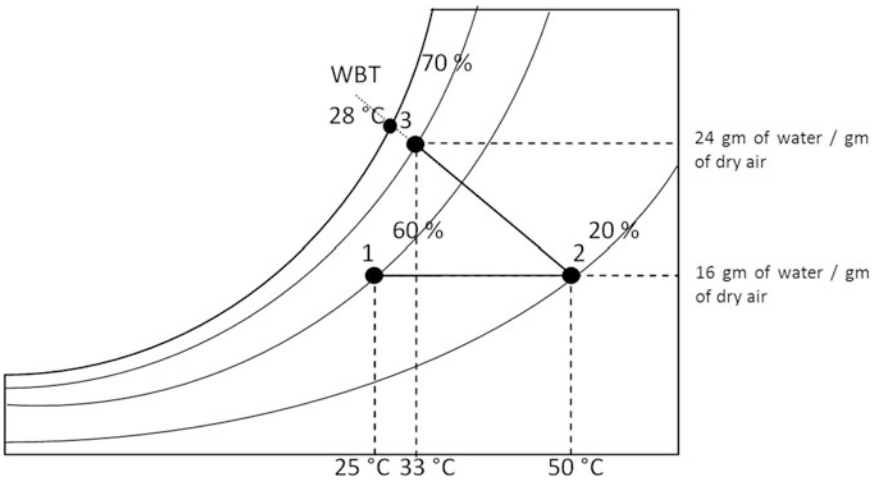

Fig. 3 Drying process

4 Important Properties of Wet Product

The rate of drying process depends upon the properties of air as well as properties of the wet product. This section discusses few properties of the product which are influencing the drying such as moisture content and equilibrium moisture content of a product.

4.1 Moisture Content

Usually, except very few, almost all agricultural as well as industrial products contain moisture content. This moisture content may be indicated as a percent or as a decimal ratio. The amount of moisture content in a product can be expressed in two methods. They are wet basis (% w.b) and dry basis (% d.b).

In wet basis method, the mass of moisture content per unit mass of the product is normally denoted as 'm'. The moisture content in wet basis is calculated as (Belessiotis and Delyannis 2011):

$$m = \frac{m_{\mathrm{w}}}{m_{\mathrm{w}} + m_{\mathrm{d}}} = \frac{m_{\mathrm{w}}}{m_{\mathrm{T}}} \text{ kg of water per kg of material} \tag{6}$$

In dry basis, the mass of moisture content per unit mass of dry product is normally denoted as 'M' and determined as follows:

$$M = \frac{m_{\mathrm{w}}}{m_{\mathrm{d}}} \text{ kg of water per kg of dry material} \tag{7}$$

where:

m = moisture content wet basis (wb)
M = moisture content dry basis (db)
m_{d} = mass of dry material in the product
m_w = mass of water in the product
m_{T} = total mass of the product

If the decimal moisture content is multiplied by 100, the percent moisture content can be obtained. The moisture content of any material is expressed conveniently in dry basis, but for agricultural products, moisture content is indicated in wet basis. Figure 4 shows the variation of moisture content on wet basis with respect to moisture content on dry basis. The moisture contents on the wet (wb) and dry basis (db) are related with each other using the following equations (Ekechukwu 1999):

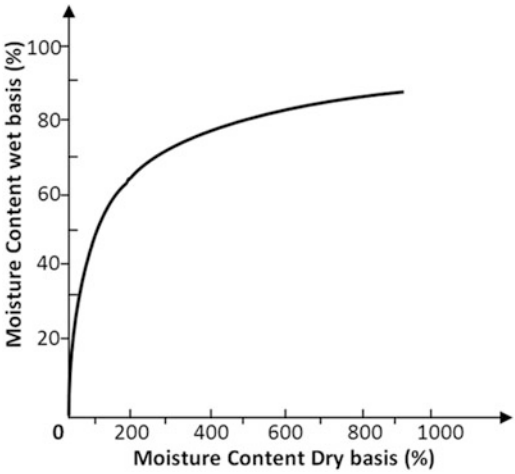

Fig. 4 Variation of moisture content on dry basis with wet basis (Ekechukwu 1999)

$$M = \left[\frac{1}{(1-m)}\right] - 1, \text{in simplified form } M = \frac{m}{1-m} \tag{8}$$

and

$$m = 1 - \left[\frac{1}{(1+M)}\right], \text{in simplified form } m = \frac{M}{1+M} \tag{9}$$

The instantaneous moisture content M_t at any given time 't' on dry basis is determined using the following equation (El-Sebaii et al. 2002; El-Sebaii and Shalaby 2013):

$$M_t = \left[\frac{(M_\mathrm{i}+1)W_t}{W_\mathrm{o}} - 1\right] \tag{10}$$

The moisture ratio (MR) is determined as (Akpinar 2010; Vijayan et al. 2016)

$$\mathrm{MR} = \frac{(M_t - M_\mathrm{e})}{(M_\mathrm{i} - M_\mathrm{e})} \tag{11}$$

The equilibrium moisture content M_e is very less when compared to initial moisture content M_i; the above-mentioned equation can be further reduced as (Akpinar 2006; Vijayan et al. 2016)

$$\mathrm{MR} = \frac{M_t}{M_\mathrm{i}} \tag{12}$$

Based on the nature of moisture content, the materials may be grouped as hygroscopic and nonhygroscopic materials. In nonhygroscopic materials, the moisture content is present as a free or a loosely held form (unbound moisture). This type of moisture content could be removed completely by evaporation during the drying process, whereas hygroscopic materials contain the moisture content in the form of bound moisture which will be available inside of the closed capillaries. Due to this reason, the bound moisture will always remain in the material as residual moisture (Belessiotis and Delyannis 2011). Most of the food materials are of hygroscopic materials. Table 2 gives the initial and final moisture contents of some agricultural products.

4.1.1 Determination of Moisture Content

The amount of moisture content in a material can be measured by many methods, and the commonly used method for measuring the moisture content in the agricultural product is oven-drying method. In this method, a small quantity of the product is taken as sample, and it is heated in an oven at a specific pressure and temperature until the moisture is completely removed. The measured weight is dry weight, and the weight loss is the amount of moisture content. Bennett and Hudson (1954) presented a comprehensive review of the methods commonly used for the determination of moisture content in cereals.

Example 4
A food product sample of 200 g was completely dried to 44 g in a convective oven. Estimate the initial moisture content of the product.

Solution:

Initial weight of the sample, $m_T = 200$ g
Dry solid weight, $m_d = 44$ g
Mass of water removed, $m_w = (200 - 44) = 156$ g

Initial moisture content in a product on wet basis is

$$m = \frac{m_w}{m_w + m_d} = \frac{m_w}{m_T}$$

$$\mathrm{m} = \frac{156}{200} = 0.78 \text{ or } 78\%$$

Initial moisture content (wet basis) = m = 78%
Initial moisture content in a product on dry basis is

$$M = \frac{m_w}{m_d}$$

Table 2 Initial and final moisture content of some agricultural products (Prakash and Kumar 2013)

Product	Initial moisture content %	Final moisture content %
Apples	80	24
Apricots	85	18
Bananas	80	15
Cabbage	80	4
Carrot	70	5
Cassava	62	17
Cauliflower	80	6
Chillies	80	5
Cocoa beans	50	7
Coffee	50	11
Coffee beans	55	12
Copra	30	5
Corn	24	14
Cotton	50	9
Figs	80	24
Fish	75	15
Garlic	80	4
Grapes	80	15–20
Green beans	70	5
Green peas	80	5
Groundnuts	40	9
Guavas	80	7
Maize	35	15
Millet	21	14
Mulberries	80	10
Onions	80	4
Paddy, parboiled	30–35	13
Paddy, raw	22–24	11
Peaches	85	18
Pineapple	80	10
Potatoes	75	13
Rice	24	11
Silk cocoons	68–70	10–12
Spinach	80	10
Sweet potato	75	7
Wheat	20	16

$$M = \frac{0.156}{0.044} = 3.545 \text{ kg of water/kg of dry material}$$

Initial moisture content (dry basis) = M = 3.545 kg of water/kg of dry material

Example 5
Red chilli 80 kg at 74% (w.b), initial moisture content was dried to 29 kg in a tunnel dryer. Determine the amount of moisture removed, final moisture content (wet basis) and the dry solid weight of chilli.

Solution:

Weight of red chilli $= 80$ kg
Final weight of chilli $= 29$ kg
Total amount of moisture removed $= \mathbf{80 - 29 = 51\ kg}$

The initial moisture content of chilli $= 74\%$ (wet basis)

$$\text{Dry solid weight of chilli} = 80 - \frac{74}{100} \times 80$$

$$\textbf{Dry solid weight of chilli} = \mathbf{20.8\ kg\ of\ solid}$$

Final moisture content in kg $= 29–20.8 = 8.2$ kg of water

$$\text{Final moisture content (dry basis)} = \frac{8.2}{20.8} \times 100$$

Final moisture content (dry basis) $\boldsymbol{M = 39.42\%}$

$$\textbf{Final moisture content (wet basis)}\ m = \frac{M}{1+M}$$

$$= \frac{0.3942}{1+0.3942}$$

Final moisture content (wet basis) $= \mathbf{0.2827\ or\ 28.27\%}$

4.2 Equilibrium Moisture Content

When a material is exposed to air at a constant temperature and relative humidity, it will reach a moisture content that is in equilibrium with the surrounding air. The vapour pressure of water in the product equals to the partial pressure of the surrounding air. At this point of time, desorption of moisture from the product is equal to the absorption of moisture by the environmental air. It means that there is no net exchange of moisture between the material and the air. In another way, it is stated that the solids either lose or gain moisture to the surrounding air. This moisture content is known as equilibrium moisture content (EMC). The relative humidity of air at this equilibrium moisture content is known as equilibrium relative humidity (ERH). It is a very important term in drying because the minimum possible moisture content could be obtained under a given set of drying conditions. This equilibrium moisture content will act as a limiting parameter in drying operation. It is denoted by EMC or M_e.

In a product, the moisture content is found as bound moisture, unbound moisture or free water. *Bound moisture* is the moisture that exerts a vapour pressure lower than that of pure water at the same temperature and normally bounds to the solid contents chemically or physically. *Unbound moisture* is the moisture that exerts vapour pressure equal to that of pure water at the same temperature. *Free moisture* is moisture consists of the product in excess of the equilibrium moisture (M-M_e) content at a given relative humidity and temperature. This moisture can be easily removed by supplying heat. The free moisture content can be varied either by increasing or decreasing the equilibrium moisture content (EMC). The EMC can be reduced by reducing the relative humidity of surrounding air, and an additional amount of free moisture can be removed. The equilibrium moisture content of a product decreases with increase in temperature at given relative humidity (Ekechukwu 1999).

4.3 Sorption Isotherms

The variation of equilibrium moisture content with the relative humidity of the surrounding air at a given temperature is called as sorption isotherms. When a porous solid is exposed to an increasing humidity of air stream at a contestant temperature, it results in adsorption, and the curve obtained is adsorption isotherm curve. Similarly, desorption isotherm curve is obtained by exposing the solid to air of decreasing humidity at a constant temperature. During the adsorption process, the partial pressure of water vapour in the solid is less than the surrounding air and vice versa in desorption process. This difference in partial pressure induces the transfer moisture from air to solid and solid to air. The EMC curves obtained during desorption and adsorption processes are not similar, and the phenomenon of the solid is called as moisture hysteresis. This curve varies product to product. The typical sorption isotherm curve is shown in Fig. 5. It consists of three regions indicated as A, B and C, which correspond to different binding mechanisms of water to the solid. In region A, water is tightly bound to solid through adsorption mechanism and is unavailable for reaction. The adsorption isotherm and desorption isotherm are the same in this region due to the monolayer adsorption of water vapour. Region B is known as the transition zone and the water content is more loosely bound. The vapour pressure is less than the equilibrium vapour pressure of water at the same temperature, due to its confinement in smaller capillaries. This water content will take part in reactions. In region C, the water content is more loosely held in larger capillaries which act as a solvent and are available for reactions.

The relationship between the moisture content of a solid and the water activity, a_w, is explained with many mathematical models such as linear, nonlinear and regression models. But only BET and GAB equations are widely accepted mainly for expressing isotherm of crops. They are theoretical models derived based on the forces acting on the material surface and the water absorbed as a monomolecular

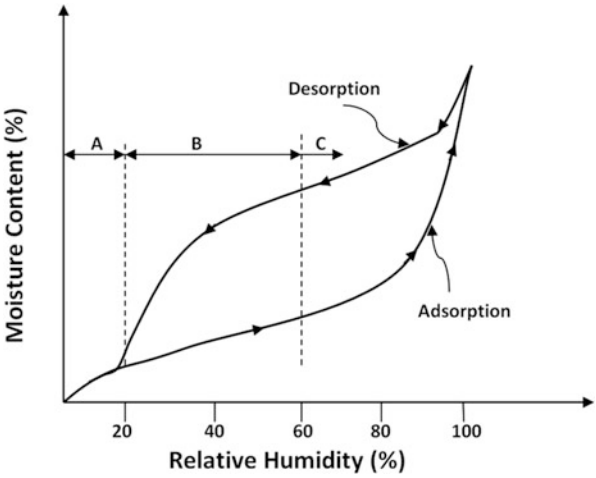

Fig. 5 Typical sorption isotherm showing hysteresis loop (Labuza et al. 1972)

layer and a modification for multilayer absorption of Langmuir's (1918) water molecular monolayer equation:

$$a_w\left(\frac{1}{M}-\frac{1}{M_m}\right)=\frac{1}{C.M} \tag{13}$$

The monolayer moisture content (M_m) is important because at this value the food product is the most stable due to the strongly absorbed water in specific sites.

The Brunauer–Emmett–Teller (BET) equation (Brunauer et al. 1938) is a modification of the previous Langmuir equation, and it is an effective method for calculating the amount of water bound to specific sites in dried food materials. Moreover, it has been accepted widely for food sorption isotherm. The equation can be applied only to the materials which have the water activity value from 0.05 to 0.45:

$$\frac{a_w}{(1-a_w).M}=\frac{1}{M_m.C}+\frac{C-1}{M_m.C}a_w \tag{14}$$

where:

M_m = monolayer moisture content
C = constant related to the net heat of sorption

The BET plot is the graph plotted between a_w and $\frac{1}{(1-a_w).M}$. This resulted graph is a straight line, and the slope and intercept are used to calculate the monolayer moisture content, M_m.

The GAB equation is the most widely accepted and represented isotherm model because it is suitable for all food products that have water activity ranging from 0.1 to 0.9. The GAB equation is written as (Chirife et al. 1992)

$$M = \frac{M_{\mathrm{m}}.\mathrm{C_b}\, K\, a_{\mathrm{w}}}{(1 - K\, a_{\mathrm{w}})(1 - Ka_{\mathrm{w}} + C\, Ka_{\mathrm{w}})} \tag{15}$$

where C_b and K are the model parameters and are related to the temperature. The GAB isotherm equation is an extension of the two-constant BET model, and it considers the properties of the sorbate in the multilayer region and bulk liquid properties through the introduction of a third constant K.

Other sorption isotherm models are also being used; they were reviewed by Chirife and Iglesias (1978) and are given below:

Bradley Equation $$\ln\left(\frac{1}{a_{\mathrm{w}}}\right) = \mathrm{K_2K_1^M} \tag{16}$$

where K_2 is the sorptive polar group constant and K_1 is the dipole moment of sorbed vapour

Caurie Equation $$\ln C = \ln \mathrm{A} - \mathrm{r}\, a_{\mathrm{w}} \tag{17}$$

where A and r are constant and C is the water concentration

Chen Equation $$a_{\mathrm{w}} = \exp[\mathrm{k} + \mathrm{a}.\exp(\mathrm{b}M)] \tag{18}$$

This model was developed based on the drying theory
where k, a and b are constants

Henderson′s Equation $$1 - a_{\mathrm{w}} = \exp - (\mathrm{k}M^{\mathrm{n}}) \tag{19}$$

where k and n are constants

Kuhn Equation $$M = \frac{\mathrm{a}}{\ln a_{\mathrm{w}}} + \mathrm{b} \tag{20}$$

where a and b are constant.

Oswin Equation $$M = \mathrm{a}\left[\frac{a_{\mathrm{w}}}{1 - a_{\mathrm{w}}}\right]^{\mathrm{n}} \tag{21}$$

where a and n are constant

Smith Equation $$M = M_{\mathrm{b}} - M_{\mathrm{a}} \ln(1 - a_{\mathrm{w}}) \tag{22}$$

where M_b and M_a are constant

5 Mechanism of Drying

Drying is a simple process of removing excessive water from an agricultural or industrial product to extend the shelf life by reducing the moisture content to specified value. The moisture removal by drying mechanism is involved with two simultaneous processes: the first is the transfer of heat to the product for the evaporation, and second is the transfer of the mass of moisture from the product surface to air. Because of this reason, the drying process is called as simultaneous heat and mass transfer operation. The process of reducing the moisture results in reduction in water activity of the product. This reduction results in prevention of the product from chemical and biological degradations such as the growth of microorganism. Drying is an energy-intensive process. In this process, the energy required to cause vaporization of the water content present in the food is supplied either directly (convection) or indirectly (conduction). Most of the dryers are convective dryers, in which the hot air or gas is blown over the surface of the product and the heat is transferred to the product. This heat increases the product temperature and thereby the moisture is evaporated as vapour, which increases the vapour pressure of the product. At this condition, the vapour pressure of the product is higher than the vapour pressure of the surrounding air. This pressure difference causes evaporation of moisture from the surface of the product to air. In the drying process, this pressure gradient acts as a driving force for the removal of moisture content from the product surface to air. This evaporation of moisture from the surface of the product is continued till it reaches the equilibrium condition.

In the drying process, moisture transfer takes place at two places:

1. *External mass transfer* – Evaporation of moisture from the product surface to the surrounding air
2. *Internal mass transfer* – Movement of moisture from inside to surface

The moisture movement (mass transfer) from the product surface to convective air is taking place due to the difference in the vapour pressure between them. This external mass transfer is carried out either through convection or diffusion or by both. However, the moisture movement from the interior to the surface is caused by many phenomena like capillary flow, flow caused by vaporization and condensation, flow by gravity and flow caused by temperature difference, vapour diffusion and pressure diffusion. The diffusion in the internal mass transfer is a very important phenomenon, and various diffusion theories are explained by the researchers. The diffusion methods are vapour diffusion, effusion (or Knudsen-type diffusion), thermal diffusion, surface diffusion and Poiseuille flow (Holdsworth 1971). The heat transfer to the product takes place by means of conduction, convection or radiation. The mass transfer and the heat transfer processes are depicted in Fig. 6. The drying process is further explained in the following section.

In the case of convective drying, the air is heated by means of any heating source, and the heated air is passed over the product. The heat from the heated air is transferred to the product through convection, and this heat will have to vaporize

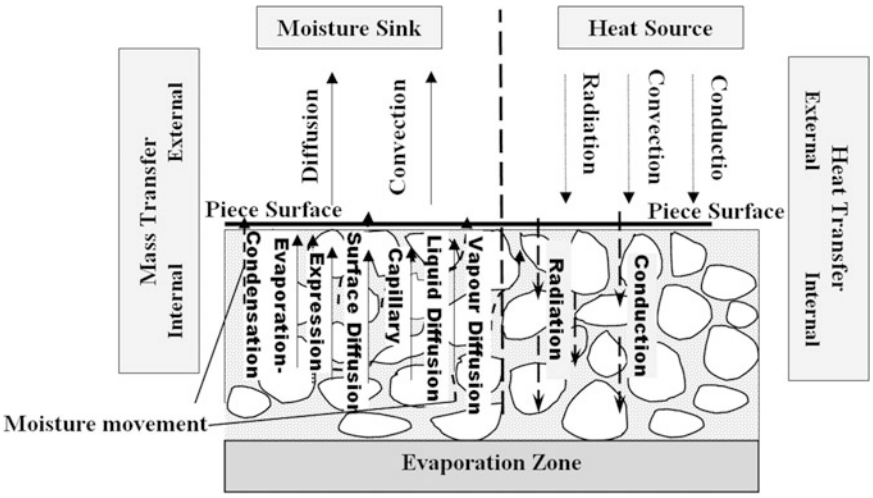

Fig. 6 Rate factors in drying (King 1977)

the liquid water from the surface of the product and to cause migration of internal moisture to the surface. The removal rate of moisture from the surface is depending upon the external parameters of the convective air like temperature, airflow rate, relative humidity and also the contact surface of the product with air and pretreatment method.

5.1 Drying Curves

Further, the drying characteristics of any product can be explained with the use of three curves plotted for:

1. Variation of moisture content vs. time
2. Drying rate vs. time
3. Drying rate vs. moisture content

In a drying process, the variation in moisture content for a product is determined over the period and represented as a curve in Fig. 7. This curve explains the reduction of moisture content in a product, and the corresponding drying rate is calculated. The drying-rate curve differs from product to product because it mainly depends on the type of material and its structure.

The drying rate is defined as the mass of water removed per unit time per unit mass of dry material or the mass of water removed per unit time per unit area. The drying-rate curves are very important quantity for explaining the drying characteristics of a product. Figure 8 shows a typical drying-rate curve and the salient points are mentioned. The period from 1 to 2 is known as constant drying period, in which

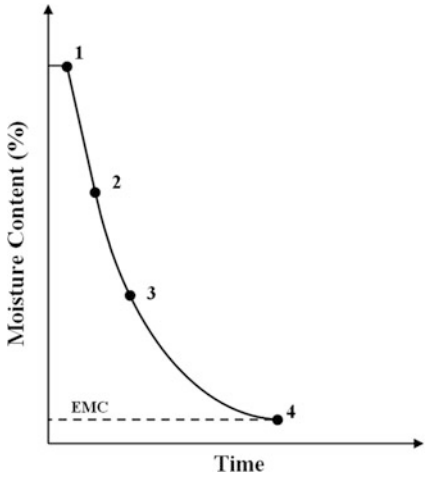

Fig. 7 Moisture content vs time (Ekechukwu 1999)

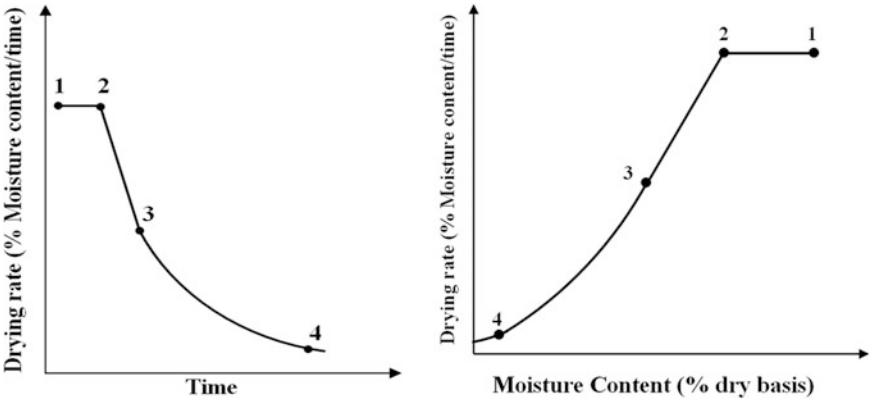

Fig. 8 Drying-rate curves (Ekechukwu 1999)

the drying takes place at a constant rate. The period from 2 to 3 is the first falling-rate period, in which the drying rate is reduced at a steady state (i.e. varies linearly), and the period from 3 to 4 is the second falling-rate period. The following drying periods occur in drying (Belessiotis and Delyannis 2011):

- *Constant-rate period (1–2):* The surface of the product is at saturated condition, and the moisture movement takes place by means of diffusion at a constant rate.
- *First falling-rate period (2–3):* The product moisture reached its critical moisture content, and the surface of the product is not having enough moisture (i.e. unsaturated) to evaporate easily. The drying rate of the product falls continuously as it forms a straight line.
- *Second falling-rate period (3–4):* The surface of the product is almost at dry condition, and the movement of moisture from the interior to its surface takes

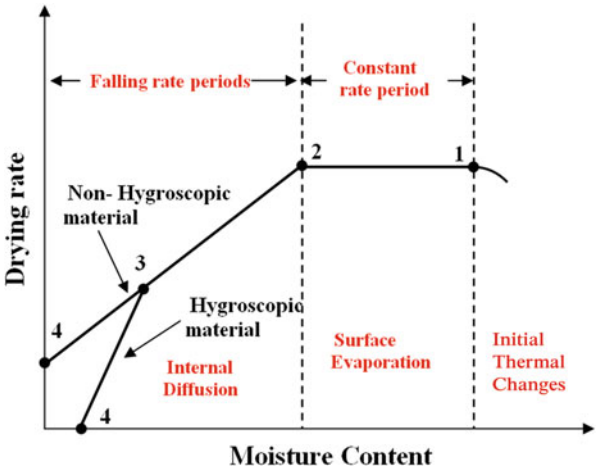

Fig. 9 Idealized curve for drying rate (Holdsworth 1971)

place slowly. The moisture content continues to decrease until equilibrium is achieved and drying stops.

The simple form of drying-rate curve is shown in Fig. 9, which is used to calculate the time for drying. The drying-rate curve for both hygroscopic and nonhygroscopic materials has a constant drying-rate period and a falling-rate period. The constant drying-rate period for both the materials is terminated at critical moisture content, and the falling-rate period begins. The falling-rate period for nonhygroscopic material is continued until it reaches zero moisture content whereas for hygroscopic materials, till it reaches the equilibrium moisture content.

5.1.1 Constant Drying-Rate Period

In constant drying-rate period, drying takes place from the surface of the product and is simply the evaporation of moisture from the free-water surface. In this period, the internal resistance to moisture transfer is much less than the external resistance to water vapour removal from the surface. The evaporation rate of moisture is almost constant during this period, and also it maintains the surface of the product at a constant temperature and approximately equal to the wet-bulb temperature of the surrounding air.

The moisture removal rate in this period is mainly depending upon the difference in partial pressure of water vapour at the surface to the surrounding air. Apart from that, the drying rate may also be affected by other external conditions of the air such as airflow rate, thermodynamic state and transport properties and the surface area of the product exposed for drying. This constant drying period continues till it reaches the critical moisture content of the product. Under dynamic equilibrium conditions, rate of water evaporated is equal to the rate of heat transfer to the surface. The drying rate of the product can be related with the influencing factors such as surface

area of the product exposed for drying air, vapour pressure difference between the drying air and the product surface, drying air velocity and the mass transfer coefficient as follows (Ekechukwu 1999):

$$\frac{\mathrm{d}M}{\mathrm{d}t} = \frac{Ah_{\mathrm{D}}}{R_{\mathrm{v}}T_{\mathrm{abs}}}\left(P_{\mathrm{vwb}} - P_{\mathrm{v}\infty}\right) \tag{23}$$

and

$$\frac{\mathrm{d}M}{\mathrm{d}t} = \frac{Ah_{\mathrm{c}}}{L}\left(T_{\infty} - T_{\mathrm{wb}}\right) \tag{24}$$

where:

A – the surface area of the product
h_{D} – mass transfer coefficient
h_{c} – convective heat transfer coefficient
L – latent heat of vaporization of water
P_{vwb} – the vapour pressure of water in air at temperature T_{∞}
$P_{\mathrm{v}\infty}$ – the vapour pressure of water at the surface of material
T_{wb} – the wet-bulb temperature of air

The drying time t_{c} for constant drying period is given by

$$t_{\mathrm{c}} = \int_{M_{\mathrm{e}}}^{M_0} \frac{R_{\mathrm{v}}T_{\mathrm{abs}}dM}{Ah_{\mathrm{D}}(P_{\mathrm{vwb}} - P_{\mathrm{v}\infty})} = \int_{M_{\mathrm{e}}}^{M_0} \frac{L\,dM}{Ah_{\mathrm{C}}(T_{\infty} - T_{\mathrm{wb}})} \tag{25}$$

In the constant drying-rate drying period, the driving forces ($(T_{\infty} - T_{\mathrm{wb}})$ and $(P_{\mathrm{vwb}} - P_{\mathrm{v}\infty})$) are constant and then the equation becomes

$$t_{\mathrm{c}} = \frac{(M_{\mathrm{o}} - M_{\mathrm{e}})R_{\mathrm{v}}T_{\mathrm{abs}}dM}{Ah_{\mathrm{D}}(P_{\mathrm{vwb}} - P_{\mathrm{v}\infty})} = \frac{L\,(M_{\mathrm{o}} - M_{\mathrm{e}})}{Ah_{\mathrm{C}}(T_{\infty} - T_{\mathrm{wb}})} \tag{26}$$

The drying rate is depending upon many parameters like surface area of the product, inlet air temperature to drying with respect to wet-bulb temperature, the heat transfer and mass transfer coefficients, atmospheric air temperature and difference in vapour pressure of the drying air and the product to be dried, and the drying rate can be accelerated by increasing those parameters. The drying process is a simultaneous heat and mass transfer process, and it mainly depends on its heat and mass transfer coefficients. The coefficients are complex functions of many variables such as airflow conditions, geometry of air–material interface, temperatures, etc.

5.1.2 Falling-Rate Drying Period

The falling-rate period begins at the critical moisture content of the product or the end of constant drying-rate period. The critical moisture content refers that the minimum moisture content at which the minimum rate of free moisture migration from the interior to the surface of the product equals the maximum rate of moisture evaporation from the surface. The drying rate slowly decreases until it reaches the equilibrium moisture content of the product. Usually, the hygroscopic materials have two or more falling-rate periods; on the other hand, nonhygroscopic materials have only one falling-rate period. During the falling-rate period, evaporation rate of moisture from the surface of the product is much lower than the movement of moisture from the interior to its surface. The lower evaporation rate at the surface increases the temperature and results in dry spots (Chung and Chang 1982). The proper drying rate can be achieved by controlling the temperature and humidity of the air. The effect of external parameters on the drying rate (temperature and RH of air) is reducing, and moisture transport from the interior to the surface plays an important role. The falling rate is longer than the constant drying-rate period in most of the products. The movement of moisture from the interior to the surface of the product may be explained with several mechanisms such as liquid movement due to capillary force, diffusion of liquids and vapour diffusion. It is, therefore, not easy to obtain a general expression of drying rate for predicting the drying time in the falling-rate period. Therefore, empirical equations are used in this region.

Example 6
In a dryer, a 150 kg of grain is to be dried from 34 to 18.6% moisture content on wet basis using a current of air at 60 °C. If the critical moisture content of the grain is 18% and the drying takes place at a constant drying rate of 0.00084 kg/s m^2, determine the drying time. The surface area of the grain is 0.024 m^2/kg of dry mass approximately.

Solution:

Mass of grain	W_o	$= 150\ kg$
Initial moisture content percent (wet basis)	M_i	$= 34\%$
Final moisture content percent (wet basis)	M_f	$= 18.6\%$
Critical moisture content percent (wet basis)	M_c	$= 18\%$
Constant drying rate	$\frac{1}{A}\frac{dM}{dt}$	$= 0.00084\ kg/s\ m^2$
Surface area of the grain	A	$= 0.024\ m^2/kg\ of\ dry\ mass$
Mass of water available in grain	$= \frac{34}{100} \times 150$	= 51 kg of water
Dry mass of solid in the grain		= (total mass – mass of water) = 150 – 51 = 99 kg of dry mass

Moisture content in dry basis $= \dfrac{0.186}{1 - 0.186} \times 100 = 0.2285$ kg of water/kg of dry mass

Final mass of water = dry mass × dry basis moisture content
= 99 × 0.2285
= 22.62 kg of water

Mass of water to be removed = (initial mass of water – final mass of water)
= 51–22.62
= 28.38 kg of water

Total surface area of the grain = surface area per kg of dry mass × total dry mass
= 0.024 × 99
= 2.376 m^2

The final moisture content is less than the critical moisture content; hence, the drying can be assumed as constant drying rate, and the drying is

$$\text{Drying time} = \frac{\text{mass of water to be removed}}{\text{drying rate} \times \text{total surface area}}$$
$$= \frac{28.38}{0.00084 \times 2.376} = 14220 \text{ s} = 3.95 \text{ h}$$

Drying time = 3.95 h

6 Drying Kinetics

Drying kinetics explains the changes of average material moisture content and average temperature with time in a drying body, whereas drying dynamics describes changes in the temperature and moisture profiles throughout the drying body. The knowledge in drying kinetics of a product can be applied in calculating the amount of moisture evaporated, drying time, energy consumption and other related parameters, which is considered as a very important parameter as it is used for the design and simulation of dryer (Fontaine and Ratti 1999). Moreover, the drying kinetics completely explains the transport properties such as mass transfer coefficient, moisture diffusion, heat transfer, etc. involved in drying. Drying kinetics may be defined as the dependence of factors affecting drying and drying rate.

The moisture transfer during drying can be described using a first-order kinetic model as mentioned below:

$$-\frac{dM}{dt} = k(M - M_e) \tag{27}$$

where:

M – material moisture content (dry basis) during drying (kg water/kg dry solids)
M_e – equilibrium moisture content of dried material (kg water/kg dry solids)
k – drying rate (min^{-1})
t – time of drying (min)

The drying rate of any material is determined as the slope of the falling-rate drying curve.

At $t = 0$, the material moisture content will be equal to the initial moisture content (i.e. $M = M_i$).

The above equation is integrated to obtain the following expression for moisture content at time 't' and M_t.:

$$M_t = M_e - (M_e - M_i)e^{-kt} \tag{28}$$

This equation is rewritten as

$$MR = \frac{M_t - M_e}{M_i - M_e} = e^{-kt} \tag{29}$$

6.1 Thin-Layer Drying

It means drying of the wet product as a single layer or slices. The temperature distribution can be assumed as uniform due its thin nature. Thin-layer drying equations may be of theoretical, semi-theoretical or empirical equations. The theoretical models were derived by considering the internal resistance to moisture transfer, and they explain the drying behaviour of the product at all conditions. But these models are derived with many assumptions, which cause considerable errors. The most widely used theoretical models are derived from Fick's second law of diffusion. Most of the semi-theoretical models are derived from Fick's second law and Newton's law of cooling. The detailed review of thin-layer drying equations such as theoretical, semi-theoretical and empirical models was presented (Jayas et al. 1991; Erbay and Icier 2009) (Table 3).

Table 3 Thin-layer drying models

Name of the model	Model	References
The models derived from Newton's law of cooling		
Lewis (Newton) model	$MR = \exp(-kt)$	Lewis (1921)
Page model	$MR = \exp(-k\ t^n)$	Diamante and Munro (1993)
Modified page-I models	$MR = \exp(-kt)^n$	Overhults et al. (1973)
Modified page-II model	$MR = \exp\ -(kt)^n$	White et al. (1978)
The models derived from Fick's second law of diffusion		
Henderson and Pabis (single-term) model	$MR = a\ \exp(-kt)$	Henderson and Pabis (1961)
Logarithmic (asymptotic) model	$MR = a\exp(-kt) + c$	Chandra and Singh (1984)
Midilli model	$MR = a\exp(-kt) + b^*\ t$	Midilli et al. (2002)
Modified Midilli model	$MR = \exp(-kt) + b^*\ t$	Ghazanfari et al. (2006)
Demir et al. model	$MR = a\exp[(-kt)] + b$	Demir et al. (2007)
Two-term model	$MR = a\exp(-k_1\ t) + b\exp(-k_2\ t)$	Henderson (1974)
Two-term exponential model	$MR = a\exp(-k\ t) + (1-a)\exp(-ka\ t)$	Sharaf-Eldeen et al. (1980)
Modified two-term exponential models – Verma model	$MR = a\exp(-k\ t) + (1-a)\exp(-g\ t)$	Verma et al. (1985)
Modified Henderson and Pabis (three-term exponential) model	$MR = a\exp(-k\ t) + b\ \exp(-g\ t) + c\ \exp(-ht)$	Karathanos (1999)
Empirical models		
Thompson model	$t = a\ln(MR) + b[\ln(MR)]^2$	Thompson et al. (1968)
Wang and Singh model	$MR = 1 + b^*t + a^*t^2$	Wang and Singh (1978)
Kaleemullah model	$MR = \exp(-c^*T) + b^*t^{(pT+n)}$	Kaleemullah and Kailappan (2006)

6.2 Deep-Bed Drying Analysis

The other type of drying is deep-bed drying, and it is mainly applied for grain drying. Usually, grains are dried either in a stationary bin or continuous bed, in which a bed of grains is dried by passing a stream of air through this bed, wherein the major source of heat transfer is by convection, and there exists a gradient of temperature and moisture content. These gradients vary as a function of position in the bed and time. In convective grain dryers, heat and moisture transfer due to diffusion is very less when compared to convection, and they may be neglected while modelling the drying process. It clearly shows that thin-layer models cannot describe the transfer processes in deep beds, because there are no gradients of temperature or moisture content within a thin layer of grain (Srivastava and John 2002).

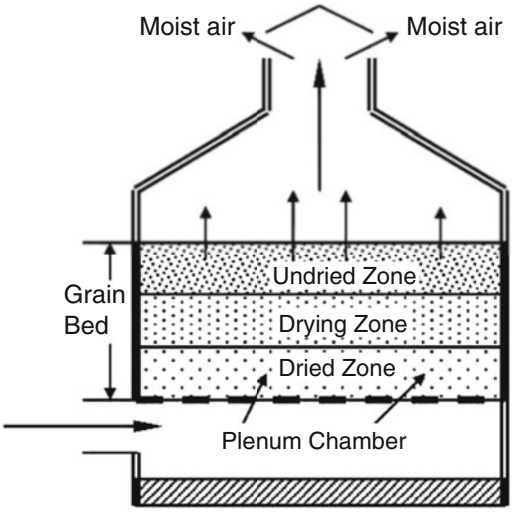

Fig. 10 Schematic layout of deep-bed drying (Belessiotis and Delyannis 2011)

A typical deep-bed drying arrangement is shown in Fig. 10. The drying air is forced by means of fan or blower, and it moves from the bottom to the top of the crop bed. When the drying air passes through the grains, it absorbs moisture from the grains due to the temperature and humidity gradient. Cenkowski et al. (1993) reviewed the deep-bed grain drying theories and classified the drying models as non-equilibrium, equilibrium and logarithmic type.

6.2.1 Non-equilibrium Models

The heat and mass transfer processes in a deep-bed grain drying are expressed using a system of partial differential equations by assuming that there is no heat and mass equilibrium between the drying air and the grain in the bed. The non-equilibrium models are applied to various types of dryers such as stationery and fluidized bed. In fluidized bed dryer, the simulation model is applied for crossflow, concurrent flow and counterflow arrangements. These models are considered as exact theoretical models provided that the above-mentioned assumption is valid. Generally, a set of partial differential equations obtained for deep-bed grain drying process can be solved using numerical integration methods, which require more CPU time and not suitable for optimization purposes (Aregba et al. 2006).

6.2.2 Equilibrium Model

These models are developed based on the assumption that the grain temperature is equal to the temperature of the surrounding air. Thomson et al. (1968) developed a mathematical model by assuming the deep bed is formed by combining many thin

layers, and these models can be used for simulation of drying processes of crossflow, counterflow and concurrent flow. Islam and Jindal (1981) modified Thompson's basic model and proposed equilibrium model for describing the drying of paddy. Further, the model was also applied for wheat and maize; the model was able to predict the position of drying zone with reasonable accuracy. Many other researchers also developed few equilibrium models. These models are able to predict the moisture of grain with reasonable accuracy in short computer time.

6.2.3 Logarithmic Model

The logarithmic models are empirical models developed for simulating the low-temperature drying. Initially, Hukil (1954) developed the first logarithmic model with the following assumption: the amount of sensible heat required to raise the temperature of grains and the moisture removed from grains are negligible when compared to latent heat of vaporization of the water removed. Barre et al. (1971) developed a model by modifying Hukil's model and applied for predicting drying of crossflow deep-bed dryer. Aregba et al. (2006) studied a stationary deep-bed drying process by applying logarithmic model and a non-equilibrium model and compared the results. They concluded that the logarithmic model is very useful to simulate the drying and drier performance.

7 Energy Analysis of Dryers

Energy analysis for a dryer is very important because drying is a highly energy-consuming process. The national industrial energy consumption records 10–25% for thermal dehydration processes in developed countries. Drying industries are keen on reducing the energy consumption for the drying process, in order to reduce the cost per product, thereby competing with others in worldwide market. The major reason for more energy consumption in the convective dryer is removing the moisture content from the product by supplying the latent heat of vaporization. This energy aspect analysis of a dryer will clearly depict the places where the performance of the system could be improved. The energy savings in any process can be achieved through reducing the heat losses in that process. The possible heat losses in the convective drying process can be grouped into heat loss with the exhaust air, heat loss with the product, radiation heat loss from the dryer, heat loss due to leakage of air from the dryer and heat loss due to overdrying of products.

The performance of any dryer could be characterized by its different performance indicators like drying efficiency, specific energy consumption, energy efficiency and specific moisture extraction rate. The specific energy consumption and energy efficiency are considered as important parameters to evaluate a dryer in terms of energy. The following section discusses the energy aspect analysis and efficiencies of the dyer.

The energy or thermal efficiency of a dryer is the ratio of energy required for evaporation to total energy supplied to the drying process (Kudra 2012):

$$\eta = \frac{\text{energy for evaporation}}{\text{total energy supplied}} \tag{30}$$

In convective drying process, the energy efficiency can be approximated by thermal efficiency, if the convective air has low humidity and low temperature during the drying process (Kudra 2012):

$$\eta_T = \frac{\text{inlet air temperature} - \text{outlet air temperature}}{\text{inlet air temperature} - \text{ambient air temperature}} \tag{31}$$

$$\eta_{\mathrm{T}} = \frac{T_{\mathrm{i}} - T_{\mathrm{o}}}{T_{\mathrm{i}} - T_{\mathrm{a}}} \tag{32}$$

From the above equation, it is very clear that the energy efficiency or thermal efficiency depends on the inlet, outlet and ambient temperatures of air. The thermal efficiency can be increased by increasing the inlet air temperature and attaining a nearby saturated condition at outlet.

Another important performance indicator of a drying system is the specific moisture extraction rate (SMER), which is the amount of water evaporated per unit energy consumption. SMER is usually mentioned in kg/kWh (Fudholi et al. 2014; Vijayan et al. 2016):

$$\text{SMER} = \frac{\text{mass of water removed}}{\text{total energy consumption}} \frac{\text{kg}}{\text{kWh}} \tag{33}$$

The reciprocal of SMER is the specific energy consumption (SEC) (Fudholi et al. 2014; Vijayan et al. 2016):

$$\text{SEC} = \frac{\text{total energy consumption}}{\text{mass of water removed}} \frac{\text{kWh}}{\text{kg}} \tag{34}$$

The mass of water evaporated can be calculated as

$$\text{mass of water removed} = \frac{\text{initial weight}(\text{initial moisture content} - \text{final moisture content})}{100 - \text{final moisture content}} \tag{35}$$

$$W_{\mathrm{m}} = \frac{W_{\mathrm{o}}(M_{\mathrm{i}} - M_{\mathrm{f}})}{100 - M_{\mathrm{f}}} \tag{36}$$

There are other performance indicators that are also used to evaluate a dryer (Prakash et al. 2016; Chauhan and Kumar 2016).

7.1 Heat Utilization Factor (HUF)

Heat utilization factor is the ratio of temperature lost by the air during drying to the temperature gained by the air while heating (Chauhan and Kumar 2016):

$$\text{HUF} = \frac{T_1 - T_2}{T_1 - T_a} \tag{37}$$

7.2 Coefficient of Performance (COP)

The coefficient of performance (COP) is the ratio of useful heat output to the corresponding work consumed. It is mainly used for assessing the performance of heat-pump dryers (Prakash et al. 2016):

$$\text{COP} = \frac{Q}{W} = \frac{T_2 - T_a}{T_1 - T_a} \tag{38}$$

The HUF and COP are related as

$$\text{HUF} = 1 - \text{COP} \tag{39}$$

7.3 Drying Effectiveness (DE)

The ratio of outlet relative humidity to the inlet relative humidity of air during the drying process is known as drying effectiveness (Chauhan and Kumar 2016). Drying is basically a humidification process, and the higher drying effectiveness is preferred:

$$\text{DE} = \frac{\text{relative humidity of air at outlet}}{\text{relative humidity of air at inlet}} \tag{40}$$

The performance of the drying units can be improved by reducing the heat losses in the systems. The first and foremost step is to design a suitable drying unit for the particular application. The proper selection of other components like heater, drying chamber, blower or fan, passages, conveyors, etc. will also help to reduce the energy consumption. The methods usually adopted for energy saving are listed below (Kemp 2005):

(a) Reducing energy requirement for drying (e.g. dewatering the feed)
(b) Prevention of heat losses by using better thermal insulations
(c) Adopting suitable heat recovery methods

(d) Using low-cost heat sources
(e) Using heat pumps to recover exhaust waste heat

The main method of improving the energy efficiency of the system is heat recovery. The common heat recovery methods used in industries are heat recovery from the dryer outlet and utilization of heat pumps.

Example 7
A batch dryer holds 10 kg of wet product having an initial moisture content of 86% on wet basis. It is dried to final moisture content of 12% on wet basis in 7 h, by circulating hot air of 320 kg/h at 60 °C, and atmospheric air is at 28 °C, 60% RH. If the energy consumed by the heater and circulation system is 4.2 kWh, calculate the following:

1. Amount of moisture removed
2. Energy efficiency of the dryer
3. Specific moisture extraction rate
4. Specific energy consumption

Solution

Initial mass of the product	W_o	= 10 kg
Initial moisture content	M_i	= 86% (wb)
Final moisture content	M_f	= 12% (wb)
Drying time	t	= 7 h
Mass flow rate of air	$\dot{m}$	= 320 kg/h or 0.0889 kg/s
Inlet temperature of air	T_1	= 48 °C
Outlet temperature of air	T_2	= 30 °C

1. Amount of moisture removed

$$\text{Mass of water removed } W_m = \frac{W_o(M_i - M_f)}{100 - M_f} = \frac{10 \times (86 - 12)}{100 - 12}$$

$$\mathbf{W_m = 8.41\ kg\ of\ water}$$

2. Energy efficiency of the dryer

Energy for evaporation	= mass of water × latent heat of water
	= 8.41 × 2500
	= 21,025 J
Energy supplied per hour	= 3 kWh
Total energy supplied	= energy supplied per hour × drying time
	= 4200 × 7
	= 29,400 J

$$\eta = \frac{\text{energy for evaporation}}{\text{total energy supplied}}$$

$$\eta = \frac{21,025}{29,400} \times 100$$

Energy efficiency $\eta = 71.51\%$

3. Specific moisture extraction rate (SMER)

$$\text{SMER} = \frac{\text{mass of water removed}}{\text{total energy consumption}}$$

$$= \frac{8.41}{29.4}$$

$$\textbf{SMER} = \textbf{0.286 kg of water/kWh}$$

4. Specific energy consumption (SEC)

$$\text{SEC} = \frac{\text{total energy consumption}}{\text{mass of water removed}}$$

$$= \frac{29.4}{8.41}$$

$$\textbf{SEC} = \textbf{3.496 kWh/kg of water}$$

8 Conclusion

In this chapter, the fundamental concepts of drying process are discussed. The microorganism growth and chemical reactions taking part in deterioration of the quality of a product are mainly depending upon the water activity. The water activity can be reduced by removing the available water content for the chemical reactions through drying process. The better understanding of the drying process will help to design an efficient dryer; thereby the energy saving is possible. Further, the performances of drying units are improved using the suitable methods like heat recovery, heat pumps, etc.

References

Akpinar EK (2010) Drying of mint leaves in a solar dryer and under open sun: modelling, performance analyses. Energy Convers Manag 51:2407–2418

Akpinar EK (2006) Mathematical modelling of thin layer drying process under open sun of some aromatic plants. J Food Eng 77(4):864–870

Aregba AW, Sebastian P, Nadeau JP (2006) Stationary deep-bed drying: a comparative study between a logarithmic model and a non-equilibrium model. J Food Eng 77:27–40
Barre HJ, Baughman GR, Hamdy MY (1971) Application of the logarithmic model to cross-flow deep-bed grain drying. Trans ASAE 14(6):1061–1064
Belessiotis V, Delyannis E (2011) Solar Drying. Sol Energy 85:1665–1691
Bennett A, Hudson JR (1954) Determination of moisture in cereals: review of methods in common use. J Inst Brew 60:29–34
Beuchat LR (1981) Microbial stability as affected by water activity. Cereal Foods World 26 (7):345–349
Brunauer S, Emmett PH, Teller E (1938) Adsorption of gases in multi-component layers. Am Chem Soc J 60:309–319
Cenkowski S, Jayas DS, Pabis S (1993) Deep-bed grain drying - a review of particular theories. Dry Technol 110:A53–1581
Chandra PK, Singh P (1984) Thin-layer drying of parboiled rice at elevated temperature. J Food Sci 45:905–909
Chauhan PS, Kumar A (2016) Performance analysis of greenhouse dryer by using insulated north-wall under natural convection mode. Energy Reports 2:107–116
Chirife J, Iglesias HA (1978) Equations for fitting water sorption isotherms of foods: part 1- a review I. J Food Technol 13:159–174
Chirife J, Buera MDP, Labuza TP (1996) Water activity, water glass dynamics, and the control of microbiological growth in foods. Crit Rev Food Sci Nutr 36(5):465–513
Chirife J, Timmermann EO, Iglesias HA, Boquet R (1992) Some features of the parameter k of the GAB equation as applied to sorption isotherms of selected food materials. J Food Eng 15:75–82
Chung DS, Chang DI (1982) Principles of food dehydration. J Food Prot 45(5):475–478
Demir V, Gunhan T, Yagcioglu AK (2007) Mathematical modeling of convection drying of green table olives. Biosyst Eng 98:47–53
Diamante LM, Munro PA (1993) Mathematical modelling of the thin layer solar drying of sweet potato slices. Sol Energy 51(4):271–276
Ekechukwu OV (1999) Review of solar-energy drying systems I: an overview of drying principles and theory. Energy Convers Manag 40:593–613
El-Sebaii AA, Shalaby SM (2013) Experimental investigation of an indirect-mode forced convection solar dryer for drying thymus and mint. Energy Convers Manag 74:109–116
El-Sebaii AA, Aboul-Enein S, Ramadan MRI, El-Gohary HG (2002) Experimental investigation of an indirect type natural convection solar dryer. Energy Convers Manag 43:2251–2266
Erbay Z, Hepbasli A (2013) Advanced exergy analysis of a heat pump drying system used in food drying. Dry Technol 31:802–810
Erbay Z, Icier FA (2009) Review of thin layer drying of foods: theory, modeling, and experimental results, critical reviews. Food Sci Nutr 50:441–464
Fontaine J, Ratti C (1999) Lumped-parameter approach for prediction of drying kinetics in foods. J Food Process Eng 22:287–305
Fudholi A, Sopian K, Yazdi MH, Ruslan MH, Gabbasa M, Kazem HA (2014) Performance analysis of solar drying system for red chili. Sol Energy 99:47–54
Ghazanfari A, Emami S, Tabil LG, Panigrahi S (2006) Thin-layer drying of flax fiber: II. Modeling drying process using semi-theoretical and empirical models. Dry Technol 24:1637–1642
Henderson SM, Pabis S (1961) Grain drying theory I: temperature effect on drying coefficient. J Agric Eng Res 6:169–174
Henderson SM (1974) Progress in developing the thin layer drying equation. Trans ASAE 17:1167–1172
Holdsworth SD (1971) Dehydration of food products a review. Int J Food Sci Technol 6:331–370
Hukil WV (1954) Grain drying. In: Anderson JA, Alcock AW (eds) Storage of cereal grain and their products. American Association of Cereal Chemists, St. Paul
Islam MN, Jindal VK (1981) Simulation of paddy drying under tropical conditions. Agric Mech Asia Afr Lat Am 12(3):37–41

Jangam SV (2011) An overview of recent developments and some R&D challenges related to drying of foods. Dry Technol 29:1343–1357
Jayas DS, Cenkowski S, Pabis S, Muir WE (1991) Review of thin-layer drying and wetting equations. Dry Technol 9(3):551–588
Kaleemullah S, Kailappan R (2006) Modelling of thin-layer drying kinetics of red chillies. J Food Eng 76:531–537
Karathanos VT (1999) Determination of water content of dried fruits by drying kinetics. J Food Eng 39:337–344
Kemp IC (2005) Reducing dryer energy use by process integration and pinch analysis. Dry Technol 23:2089–2104
King CJ (1977) Heat and mass transfer fundamentals applied to food engineering. J Food Process Eng 1:3–14
Kudra T (2012) Energy performance of convective dryers. Dry Technol 30:1190–1198
Labuza TP (1977) The properties of water in relationship to water binding in foods. A review. J Food Process Preserv 1:176–190
Labuza TP, McNally L, GALLAGHER D, Hawkes J, Hurtado F (1972) Stability of intermediate moisture foods. 1. Lipid oxidation. J Food Sci 37(1):154–159
Langmuir I (1918) The adsorption of gases on plane surfaces of glass, mica and platinum. J Am Chem Soc 40:1361–1402
Leistner L (1992) Food preservation by combined methods. Food Res Int 25:151–158
Lewis WK (1921) The rate of drying of solid materials. I & EC-Symp Dry 3(5):42
Midilli A, Kucuk H, Yapar Z (2002) A new model for single-layer drying. Dry Technol 20:1503–1513
Mujumdar AS, Law CL (2010) Drying technology: trends and applications in postharvest processing. Food Bioprocess Technol 3:843–852
Mujumdar AS, Huang LX (2007) Global R&D needs in drying. Dry Technol 25:647–658
Overhults DG, White GM, Hamilton HE, Ross IJ (1973) Drying soybeans with heated air. Trans ASAE 16:112–113
Prakash O, Kumar A (2013) Historical review and recent trends in solar drying systems. Int J Green Energy 10:690–738
Prakash O, Kumar A, Laguri V (2016) Performance of modified greenhouse dryer with thermal energy storage. Energy Rep 2:155–162
Scott WJ (1957) Water relations of food spoilage microorganisms. Adv Food Res 7:83–127
Sharaf-Eldeen YI, Blaisdell JL, Hamdy MY (1980) A model for ear corn drying. Trans ASAE 23:1261–1271
Sharma VK, Sharma TS, Garg HP (1991) Mathematical modelling and experimental evaluation of a natural convection type solar cabinet dryer. Energy Convers Manag 31(1):65–73
Srivastava VK, John J (2002) Deep bed grain drying modeling. Energy Convers Manag 43:1689–1708
Thompson TL, Peart RM, Foster GH (1968) Mathematical simulation of corn drying: a new model. Trans ASAE 11:582–586
Vega-Mercado H, Góngora-Nieto MM, Barbosa-Cánovas GV (2001) Advances in dehydration of foods. J Food Eng 49(4):271–289
Verma LR, Bucklin RA, Ednan JB, Wratten FT (1985) Effects of drying air parameters on rice drying models. Trans ASAE 28:296–301
Vijayan S, Arjunan TV, Kumar A (2016) Mathematical modeling and performance analysis of thin layer drying of bitter gourd in sensible storage based indirect solar dryer. Innovative Food Sci Emerg Technol 36:59–67
Wang CY, Singh RP (1978) A single layer drying equation for rough rice. ASAE Paper No 3001
White GM, Bridges TC, Loewer OJ, Ross IJ (1978) Seed coat damage in thin layer drying of soybeans as affected by drying conditions. ASAE paper no 3052

Solar Drying Systems

Jan Banout

Abstract The open-air drying under the sun is one of the most historical methods of using a solar energy for food preservation. The general classification of solar drying systems is presented in this chapter. A wide range of solar dryers have been designed and constructed in different regions of the world. The solar dryers vary in their capacities and degrees of technical performance. Generally, the solar dryers could be grouped systematically according to drying air circulation to natural and forced convection dryers; according to operational modes to direct, indirect, and mixed-mode dryers; and by their heating sources. The most typical solar dryers for agriculture produce based on their construction designs were described. The final selection of solar drying systems should consider the available insolation rate in the target region, kind of product that will be dried, production throughput, and operational and investment costs. Most studies consider solar drying as good alternative to traditional open-air drying and/or conventional drying systems operated by fossil fuels.

Keywords Forced convection dryers • Natural convection dryers • Hybrid solar dryers • Direct dryers • Indirect dryers • Solar dryer design

1 Introduction

The open-air drying under the sun is one of the most historical methods of using solar energy for food preservation. From the prehistoric times, the people have used the insolation as the thermal energy source to dry a large variety of foods, construction materials such as soil bricks, and animal skins for dressing (Belessiotis and Delyannis 2011). One of the oldest drying facilities (8000 BC) has been discovered in France. It was a stone-paved surface and used for drying of crops. Drying by wind was combined with solar radiation to improve the drying process (Belessiotis and Delyannis 2011).

J. Banout (✉)
Faculty of Tropical AgriSciences, Department of Sustainable Technologies, Czech University of Life Sciences Prague, Kamycka 129, Praha 6, Suchdol 16521, Czech Republic
e-mail: banout@ftz.czu.cz

© Springer Nature Singapore Pte Ltd. 2017

O. Prakash, A. Kumar (eds.), *Solar Drying Technology*, Green Energy and Technology, DOI 10.1007/978-981-10-3833-4_2

Open sun drying is still widely practiced in most developing countries. In the traditional methods of drying mainly used in developing countries, the products are dried on the ground, on concrete, and even on roads under the sun, and these are contaminated by dust and insects and suffer loss by rodents, birds, and other animals (Janjai and Bala 2012). Furthermore, such drying under inappropriate climate conditions leads to losses in the quantity and quality of the final product (Pangavhane et al. 2002). It is estimated that in developing countries, total postharvest losses are equal to 20–50% (Tembo et al. 2008), and almost 10–40% of the crops harvested never reach the final consumers due to postharvest losses along the supply chain (Esper and Muhlbauer 1998).

Solar drying relies on the sun as its primary source of energy. Solar drying differs from open sun drying since some construction has to be used to enhance the effect of the insolation. In many cases, solar drying is a sensible alternative to sun drying. Advantages of solar dryers have been previously reported in the literature by many researchers (Karathanos and Belessiotis 1997; Bala et al. 2003; Hossain and Bala 2007) mainly due to lower investment costs comparing to high-tech drying facilities operated by conventional sources of energy. Further a majority of developing countries can benefit from solar radiation which is higher than the world average of 3.82 kW h m^{-2} a day (Banout and Ehl 2010). In many rural areas of developing countries, the electricity grid and supplies of other conventional energy sources are limited or expensive. Thus, in such areas, crop drying systems with motorized ventilators and/or electrical heating are inappropriate. The high investments and operational costs of conventional drying systems operated by fossil fuels are the main reasons why they are not adopted by small-scale farmers (Ekechukwu and Norton 1999). The small-scale design of most solar dryers can fit the needs of farmers in developing countries since more than 80% of food is produced by small farms (Murthy 2009). Solar dryers can generate higher drying temperatures and lower relative humidity resulting in higher drying rates and lower final moisture contents of the dried products as compared with traditional open sun drying (Belessiotis and Delyannis 2011). Improvement of final product quality and reduction of harvest losses can be achieved by appropriate drying technique. However, the main problem of higher acceptance of improved solar drying systems by the farmers is the fact that in many local markets, there is no or only slight difference in the price for high- and low-quality products (Janjai and Bala 2012).

2 Characteristics of Solar Dryers

In solar drying systems, the solar energy could be used either as the unique source of heat or as a supplemental source of heat. The airflow is generated by natural convection or by forced convection which is ensured by additional equipment such as fans. The drying process could involve the passage of preheated air through the product in closed and dark chamber or by direct exposing of the product to solar radiation or by a combination of both (Ekechukwu and Norton 1999).

When the solar radiation penetrates the material during direct drying, it generates the heat in the interior and surface of the dried product and enhances heat transfer. Important factor in direct solar drying is the solar radiation absorptance of the product. Most agricultural products have relatively high absorptances which may vary through the drying process. The crop thermal conductivity is also an important factor, particularly in the case of deep-layer drying which requires heat conduction between particles. Excessive temperature, which may adversely affect the product qualitative attributes, should be avoided when drying different foods.

3 Classification of Solar Dryers

Solar dryers used in agriculture for food drying are useful device from the energy conservation point of view. However, except energy they save time needed for drying, reduce drying area, improve quality of the product and process effectivity, and finally protect the environment. When the heat sources are diversified, they can be used for supplementing artificial drying systems, and through this fact they can reduce the total amount of fuel energy required (VijayaVenkataRaman et al. 2012).

Different types of solar dryers have been designed, developed, and tested in the different regions (Bala and Janjai 2012). In solar drying process, solar energy is used either as primary source or additional source of heat. The drying airflow can be operated by natural or forced convection, and the preheated air could be passed through the product without exposure to direct insolation or by direct exposure to the insolation. The combination of both modes is also possible (Ekechukwu and Norton 1999). Several criteria such as drying characteristics of the product, quality requirements, and drying expenses influence a final selection of a solar dryer (Augustus Leon et al. 2002; Purohit et al. 2006).

Solar dryers can be classified into two broad categories:

- Passive solar drying systems (conventionally termed natural circulation)
- Active solar drying systems (most types of which are often called forced convection solar dryers)

According to Ekechukwu and Norton (1999), there are three distinct subclasses of either the active or passive solar drying systems. They vary mainly in the design arrangement of system components and mode of utilization of solar heat. These subclasses are:

- Integral-type solar dryers
- Distributed-type solar dryers
- Mixed-mode solar dryers

There are many designs of dryers developed for different purposes of drying agriculture products based on final user needs and available technology level. The general classification of solar drying systems is presented in Fig. 1.

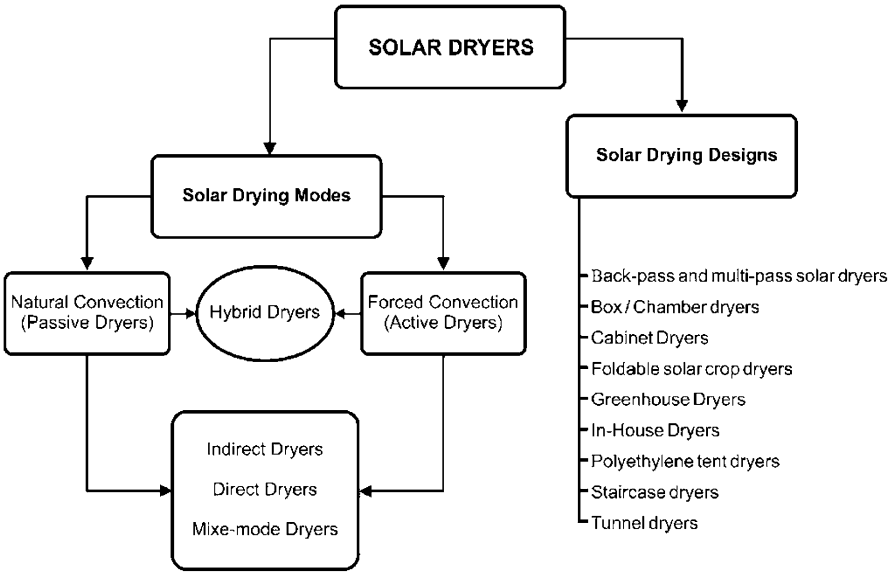

Fig. 1 Classification of solar drying systems (Illustration: J. Banout)

3.1 Natural Convection Solar Dryers

In a natural convection (passive) solar dryers, air is heated and circulated naturally by buoyancy force or as a result of wind pressure or in combination of both. A typical natural convection solar dryer (Fig. 2) consists of the following principal units: an air-heating solar collector, a drying chamber, and a chimney. Passive drying of crops is common practice in many tropical regions and/or developing countries especially in small agricultural farms. Usually they are inexpensive, constructed by locally available materials, and independent to electricity grid. The passive dryers are designed for drying small batches of fruits and vegetables, as the natural convection solar dryers require a smaller area of land to dry similar quantities of crop as compared to open-air drying that enable them to compete with those traditional drying techniques. The drying period is shorter with higher throughput as compared to open-air drying and product, and that is why they yield higher quantity and quality of dried crops (Ekechukwu and Norton 1999).

Numerous types of passive solar dryers have been designed and developed in different regions of the world. Those dryers vary by yielding capacities and technical performance. The simplest passive solar cabinet dryer was reported by Fudholi et al. (2010). It consists of a small wooden box with dimensions of 2 m $\times$ 1 m where the sides and bottom were constructed from wood and metal sheets. A transparent polyethylene sheet was used as cover at the upper surface. On the other hand, Ekechukwu and Norton (1999) described a natural convection solar dryer which is suitable for the drying of different crops. The design comes from a typical greenhouse natural convection solar dryer (Fig. 3). The dryer is constructed by a steel frame forming a cylindrical polyethylene chamber with a surface used as absorber.

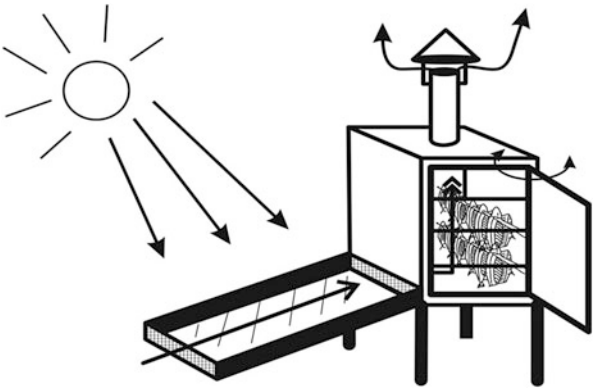

Fig. 2 Natural convection solar dryer (Illustration: J. Banout)

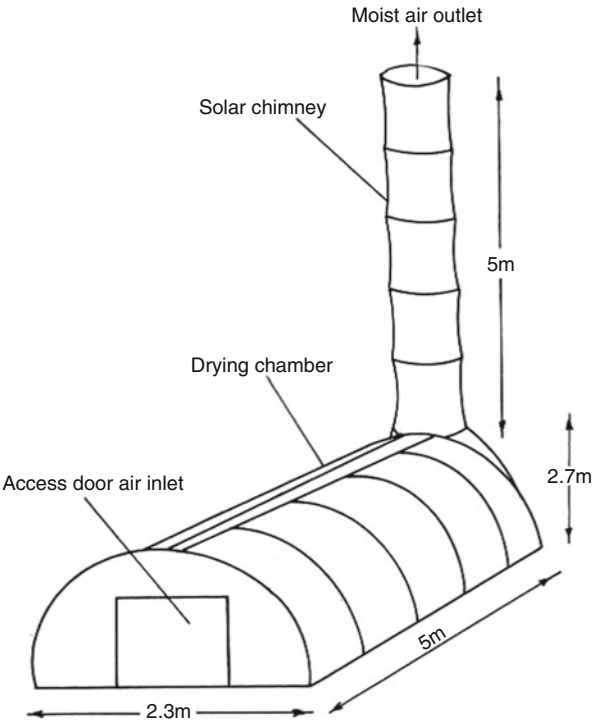

Fig. 3 A greenhouse-type natural circulation solar energy dryer (Ekechukwu and Norton 1999)

3.2 Forced Convection Solar Dryers

A typical forced convection (active) solar dryer depends on solar energy as the primary heat source and employs ventilators to ensure circulation of the air in the drying chamber. Adding a fan improves the airflow and gives much higher drying rates as compared to those achieved by natural convection dryers. The required airflow can be supplied, for example, by an electric fan. However, the electric

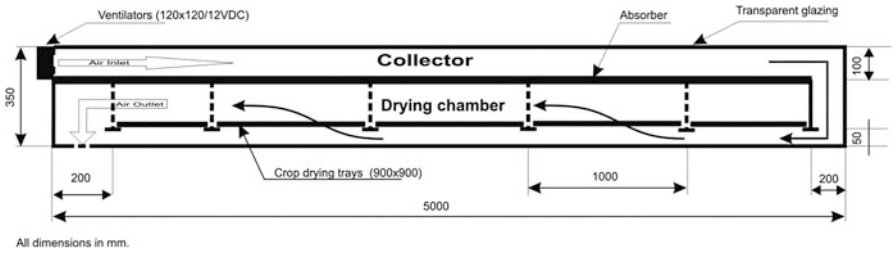

Fig. 4 Forced convection solar dryer (Banout et al. 2012)

power requirement of the fan in case of forced convection solar dryers is very low and can be operated by one photovoltaic module independent of the electric grid (Banout et al. 2011). A typical forced convection solar dryer (Fig. 4) would consist of the following basic units: an air-heating solar energy collector, a drying chamber, and a fan or pump for ensuring the drying air circulation. The active solar dryers are mainly used for commercial purposes and for large-scale drying operations where they have a potential to supplement conventional fossil fuel drying systems as they can significantly reduce the overall energy consumption and drying costs.

Active solar dryers are suitable for drying a higher moisture content agriculture products. Many studies have reported solar dryers equipped by ventilators operated electrically and used for different types of crops such as paddy rice, fruits, and vegetables. The commercial forced convection solar dryers are often equipped by temperature controllers to maintain the safe drying temperature levels (Janjai and Bala 2012). For example, Sharma et al. (2009) reported a large-scale forced convection solar drying system comprising an array of 40 solar collectors and 3 drying cabinets with a blower. It was reported that the drying period was shorter as compared to open sun drying with better quality of dried products. This system was feasible and saves large amounts of fuel compared to industrial large-scale drying system. Janjai and Bala (2012) reported that the daily throughput of the forced convection dryer was 3 times and 14 times higher than those of natural convection and open-air drying, respectively. Further 225 kg of paddy was dried daily from a moisture content of about 21% to below 14% on a good sunny day.

Generally, the overall efficiency of forced convection dryers is higher than in passive solar dryers. As reported by Banout et al. (2011), the measured overall drying efficiency was 24.04% and 11.52% for forced convection and natural convection solar dryer, respectively. It means that the overall dryer efficiency was more than two times higher in case of forced convection dryer. Changes of moisture content with drying time during drying of red chili in different solar dryers and traditional open-air sun drying are presented in Fig. 5.

From the drying curves (Fig. 5), it is evident that the highest drying rate occurred in the case of DPSD where the final moisture content 0.05 ± 0.003 kg kg^{-1} (d.b.) was reached after 23 h of drying followed by CD with 0.09 ± 0.01 kg kg^{-1} (d.b.) after 29 h and open-air sun drying with 0.18 ± 0.09 kg kg^{-1} (d.b.) after 36 h of drying (excluding nights). These results correspond to the fact that DPSD uses

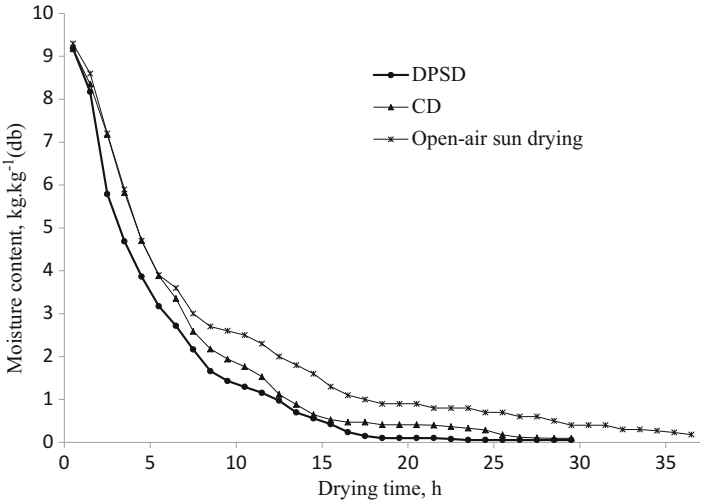

Fig. 5 Changes of moisture content of red chili with drying time. *DPSD* double-pass solar dryer (forced convection dryer); *CD* typical natural convection cabinet dryer (Banout et al. 2011)

forced convection ensuring higher airflow rate which results in higher water removal from the red chili.

3.3 Hybrid Solar Dryers

Hybrid solar drying systems are dryers where the solar energy is just one of more sources of energy used for heating the drying air. They employ solar energy with additional electrical or fossil fuel-based heating systems and ventilators to ensure air circulation. Commonly the hybrid solar dryers operate under forced convection mode. If they are warm enough, the drying air heated by solar energy could be used directly for the drying process; otherwise, the dehydrator operated by fossil fuel is used to achieve required values of drying temperatures (e.g., during nights or during the time with low insolation like rainy seasons). The fossil fuel system is automatically controlled to provide the required drying conditions (Ekechukwu and Norton 1999). Similarly like in the case of natural and forced convection dryers, there are plenty of hybrid dryer designs described in the literature. However, the typical hybrid dryer consists of a solar collector, drying chamber, fan to ensure the air circulation, and auxiliary heat source usually operated by conventional source of energy like LPG as could be seen in Fig. 6. As reported by Fudholi et al. (2010), Fig. 6 represents a hybrid solar drying system for drying bananas. The simulation model was evaluated by comparing the simulation and experimental results. Based on the results obtained, the optimum values of the collector area and recycle factor

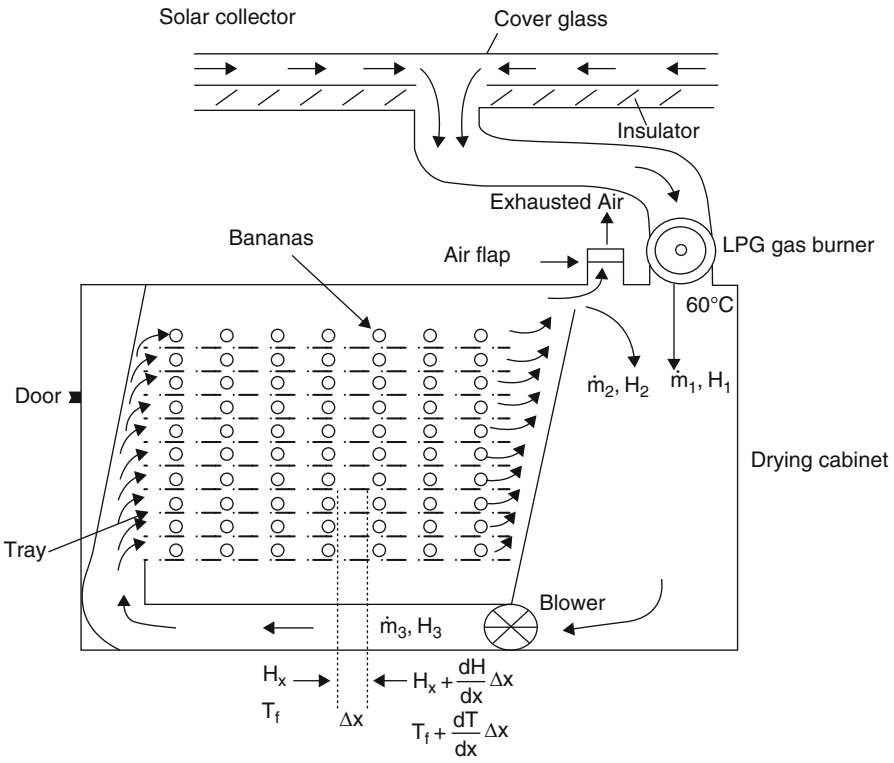

Fig. 6 Typical construction of hybrid solar dryer (Fudholi et al. 2010)

were 26 m^2 and 90%. Based on the optimum values, the minimum drying costs were estimated to be 0.225 USD per kg.

Furthermore, Fudholi et al. (2010) describe in their work different hybrid dryer designs such as:

- Solar drying system with thermal storage
- Solar drying system with auxiliary unit
- Hybrid with geothermal or waste waters
- Solar drying system with heat pump
- Solar drying system with chemical heat pump
- Solar-assisted dehumidification system

As it was reported by Fudholi et al. (2010), the general advantages and disadvantages of natural and forced convection and hybrid dryers could be summarized in Table 1.

Table 1 Advantages and disadvantages of different types of solar dryers

Classification	Advantages	Disadvantages
Passive dryers	Simplest	Low capacity
	Low capital and running costs	
Active dryers	Independent of the ambient climatic conditions	More complex and expensive than passive dryers
	Short drying periods than passive dryers	
Hybrid solar dryers	Allow better control of drying	Expensive and may cause fuel/gas dependence
	Ability to operate without sun reduce of product loss	
	May be faster than passive and active dryers	

Source: Fudholi et al. (2010)

3.4 Direct Solar Dryers

In direct solar dryers (also termed integral-type solar dryers), the crops are situated in a transparent drying chamber or at least a transparent cover that allows the solar radiation to be transmitted during the drying process. Thus, solar radiation strikes directly the product being dried. The heat lowers the relative humidity of the drying air resulted in increased moisture capability and evaporates the water from the product. Further, it expands the air in the drying chamber, ensuring its circulation and moisture removal along with the hot air (Ekechukwu and Norton 1999). The working principle is illustrated in Fig. 7. Direct exposure to sunlight influences the decomposition of residual chlorophyll in the tissue resulting in proper color ripening of greenish crops during the drying process. Direct exposure to sunlight is considered essential for the development of the required color in the dried product for certain varieties of crops such as grapes and dates, cocoa, and coffee. In the case of Arabica coffee, a period of exposure to sunlight is considered indispensable for the development of full flavor of roasted bean. Direct solar dryers are generally simpler in construction since they do not require complicated structures, such as separate air-heating collectors and ducting. That is why they are less expensive as compared to indirect ones for the similar loading capacity. However, the potential drawback of the former is the liability to overheat locally and relatively. In case of combination a direct mode with natural convection principle, a solar chimney can be employed. The solar chimney can increase the buoyancy force of the airstream and provide a greater airflow velocity resulting in more rapid drying rate.

Based on Sharma et al. (2009), a direct solar dryer has the following limitations:

- Discoloration of crop due to direct exposure to solar radiation.
- Moisture condensation inside glass covers sometimes occurs which results in reduced transmissivity.
- Sometimes the insufficient rise in crop temperature affecting moisture removes.
- Limited use of selective coatings on the absorber plate.

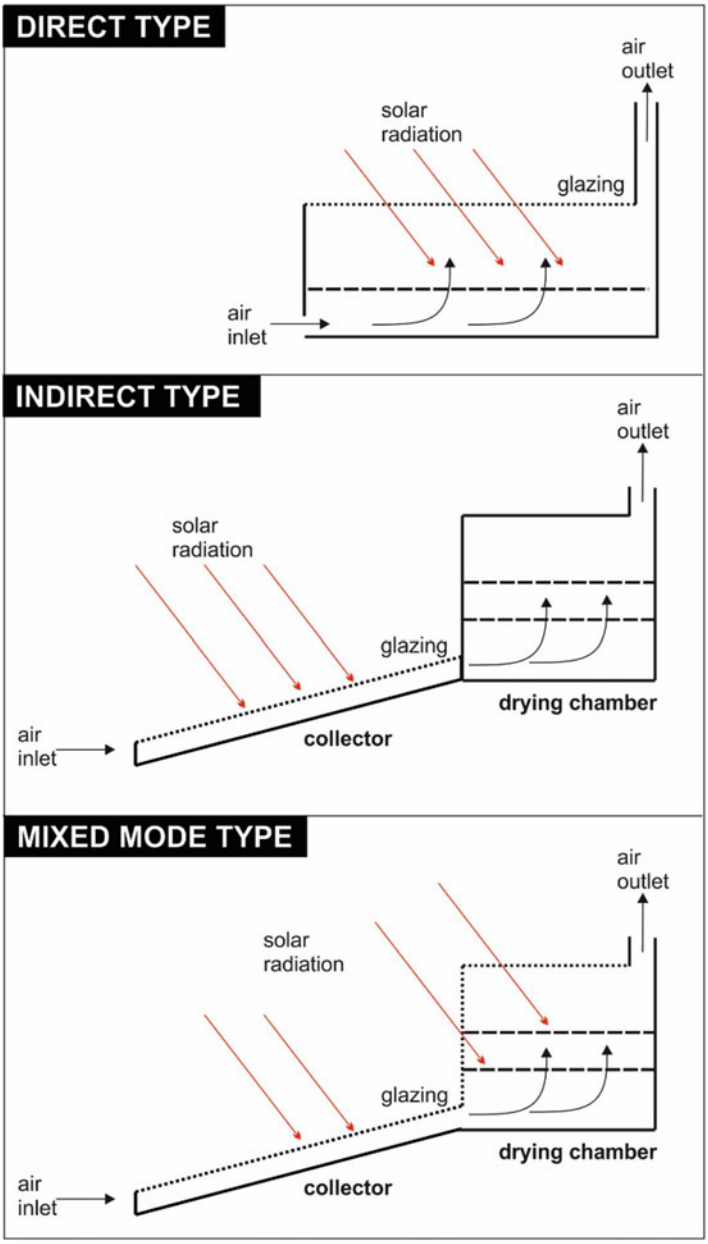

Fig. 7 Working principle of direct, indirect, and mixed-mode solar dryers (Illustration: J. Banout)

3.5 Indirect Solar Dryers

These are often termed distributed-type solar dryers. Here, the crop is located in trays or shelves inside a closed not transparent drying chamber and heated by circulating air, warmed during its flow through a solar collector (Ekechukwu and Norton 1999). The working principle is illustrated in Fig. 7. As the crop is not directly exposed to solar radiation, less discoloration and cracking on the surface of the crop occur during this method (Sharma et al. 2009). Thus, they are recommended for relatively sensitive products such as herbs, spices, and fruits where the vitamin C content could be negatively influenced by the direct exposure of the product to solar radiation. Indirect solar dryers are often relatively complex structures requiring more capital investment in equipment and cause larger running (i.e., maintenance) costs than the direct units (Ekechukwu and Norton 1997).

3.6 Mixed-Mode Solar Dryers

Mixed-mode solar dryers combine the features of the direct (integral)-type and the indirect (distributed)-type solar dryers. The combination of beam solar radiation incident on the product and preheated air in a solar collector is used for the drying process. A typical mixed-mode solar dryer has the same design as the distributed type (i.e., a solar air collector, a separate drying chamber, and a chimney); however, the walls of the drying chamber are transparent, so the solar radiation goes directly on the product as in the case of direct dryers (Ekechukwu and Norton 1999). Their disadvantages come from the variations in temperatures of the air leaving the collector. So maintaining constant operating conditions within the drying chamber becomes difficult especially when they are designed as passive solar dryers (VijayaVenkataRaman et al. 2012).

4 Most Typical Solar Dryer Designs Used in Agriculture

4.1 Back-Pass and Multi-pass Solar Dryers

This group of solar dryers are usually based on the working principle of double-pass solar collectors. The basic types of hot air solar collectors suitable for use in solar drying system are the front duct single-pass collectors, single pass with double duct, and double-pass solar air collectors. The double-pass solar air collectors are more effective than conventional single-pass ones, and it was reported that two-pass designs increased the collector thermal efficiency by 10–15% as compared to single-pass air heaters (Sopian et al. 2007). The typical back-pass solar dryer design is presented in Fig. 4. Fudholi et al. (2015) summarized different solar drying

systems used in Malaysia. In his study he reported a back-pass V-groove collector with dimensions of 1.0 m (width) × 2.3 m (length) × 0.14 m (height). The designed system consists of six set collectors in series that cover a total area of approximately 13.8 m^2. Collector efficiency is approximately 40–65% at solar radiation levels of 400–700 W/m^2. The ambient temperature range was 27–30 °C with airflow rate that ranges from 6.13 to 16.7 m^3/min. Drying system efficiency was approximately 20–30%. The performance of the dryer was tested during chili and tea drying. Jain and Jain (2004) evaluated the performance of a tilted multi-pass solar air heater with thermal storage for deep drying applications. Banout and Ehl (2010) and Banout et al. (2011) developed a new design of double-pass solar dryer (DPSD) which was tested on chili drying and bamboo shoot drying. Results show that the overall drying efficiency was one time higher as compared to a typical cabinet dryer. Further, the highest drying rate was observed during drying in DPSD followed by drying in a cabinet dryer and open-air sun drying.

4.2 Cabinet and Box-Type Dryers

Cabinet and box-type dryers are usually small units designed for preservation of fruit, vegetables, fish, and meat on household or small farm quantities. They are usually insulated boxes with glazed cover and holes at the base and upper parts of the cabinet's walls. The solar radiation is transmitted through the transparent cover and is absorbed on blackened interior absorber as well as on the product. The warm air which is leaving through the upper openings ensures the circulation by buoyancy forces and is replenished by cold air from the base (Ekechukwu and Norton 1999). Cabinet dryers are simple and inexpensive. They are suitable for drying agricultural products, spices, herbs, etc. They normally are constructed with a drying area of 1–2 m^2 and capacities of 10–20 kg (Belessiotis and Delyannis 2011). One of the most known designs of cabinet dryers was reported by the Brace Research Institute, Canada (see Fig. 8). The dryer consists of a container, insulated at both its base and sides and covered with a double-layered transparent roof. Drying temperatures in excess of about 80°C were reported for the dryer (Ekechukwu and Norton 1999). Several other passive cabinet solar dryers similar in construction to the Brace Research Institute dryer have been built and tested for a variety of crops and locations.

Sharma et al. (1990) reported a maximum temperature of 80–85 °C during the noon hours in the case of an unload cabinet dryer, while with 20 kg of wheat, the maximum temperature varied from 45 to 50 °C. As well, Fudholi et al. (2010) reported that temperatures reached in the cabinet dryer were 20–30 °C above the ambient level. The cabinet dryer is recommended to be useful in drying a variety of foodstuff. Very similar design to cabinet dryers is a box-type solar dryer. Box-type solar dryers are often designed as direct solar dryers (Fig. 9). It consists of a quadrilateral box, transparent cover, and trays for the product. Solar radiation is transmitted through the transparent cover and absorbed on a black-painted interior

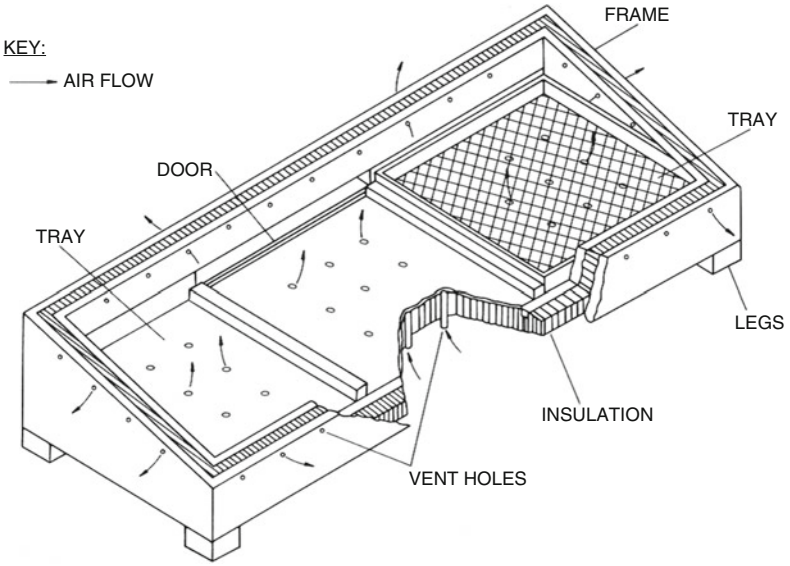

Fig. 8 A typical design of natural convection cabinet dryer (Ekechukwu and Norton 1999)

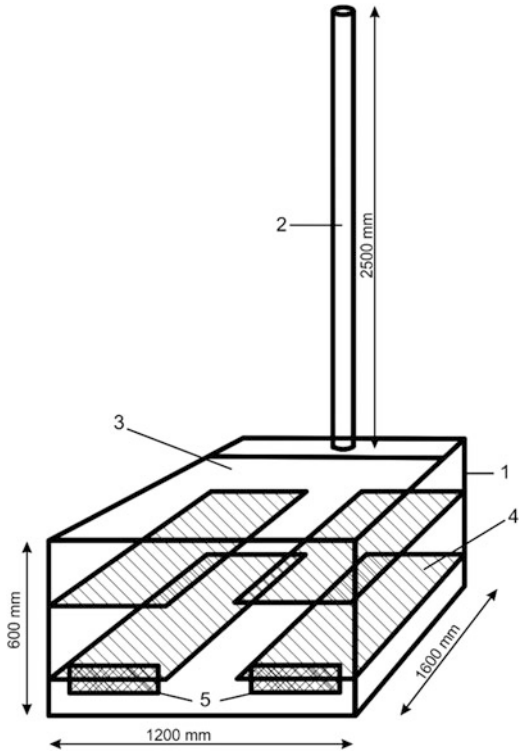

Fig. 9 Schematic diagrams of box-type solar dryer. (*1*) Drying chamber. (*2*) Chimney for ensuring adequate airflow. (*3*) Transparent access door. (*4*) Plastic mesh trays. (*5*) Air inlet (Banout et al. 2008)

absorber. Temperature inside the dryer increases due to accumulation of energy. As the temperature in the dryer rises up, the cold air enters into the dryer through the inlets in the front panel and passes out of the dryer through the outlets due to the buoyancy airflow. This process resulted in a continuous flow of air over the drying product. This type of solar dryer is designed for small quantities of fruits and vegetables from 10 to 15 kg (Janjai and Bala 2012).

4.3 Chamber Dryers

Chamber dryers represent quite wide group of solar dryers where the drying chamber is separated from the solar collector. Based on this fact, they are usually classified as indirect and/or mixed-mode solar dryers. They could be constructed as passive or active dryers with a wide range of capacities from small- to large-scale units. The representative of small-scale application is a solar and wind-ventilated mixed-mode solar dryer illustrated in Fig. 10. Drying air is drawn through the drying chamber by wind-powered blower placed on the top of the chimney. The damper is used to control drying temperature and airflow rate.

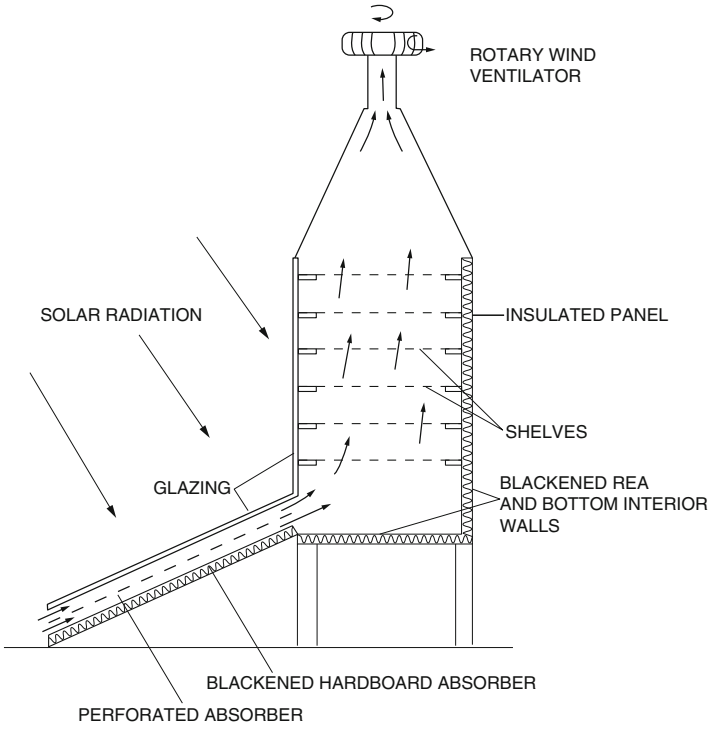

Fig. 10 A wind-ventilated chamber solar dryer (Ekechukwu and Norton 1999)

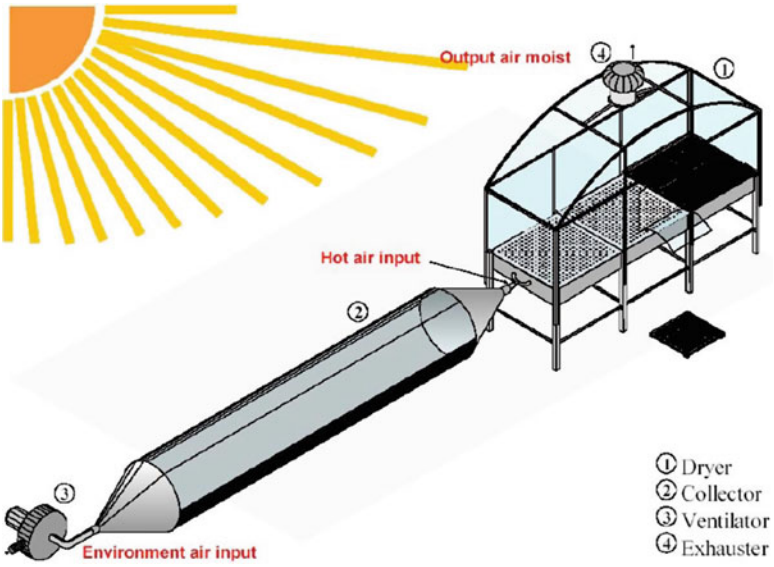

Fig. 11 Brazilian banana dryer with PVC foil collector and transparent chamber (Weiss and Buchinger 2005)

A solar dryer system with a rotating rack drying chamber was reported by Fudholi et al. (2015). The dryer was installed at Green Energy Technology Innovation Park, UKM, Malaysia. The drying system is classified as a forced convection indirect type. The solar dryer consists of an auxiliary heater, blowers, a rotating rack drying chamber, and a back-pass V-groove solar collector. The dryer has been tested on 24 kg of red chilies.

Another type of chamber dryer was described by Weiss and Buchinger (2005). The dryer is operating in mixed mode with forced convection and primarily was used for banana drying in Brazil. The dryer consists of flexible PVC collector with cylinder shape. The collector is connected to transparent drying chamber as it is illustrated on Fig. 11.

4.4 Greenhouse Dryers

Greenhouse dryers could be classified either as direct solar dryers or sometimes as mixed-mode dryers. The greenhouse dryer is low cost, easy to fabricate, and simple in design. This can be used in any part of the world. Based on the mode of air circulation, the greenhouse dryers are classified into two types: (i) greenhouse dryer under passive mode (natural convection) and (ii) greenhouse dryer under active mode (forced convection) (Prakash and Kumar 2014).

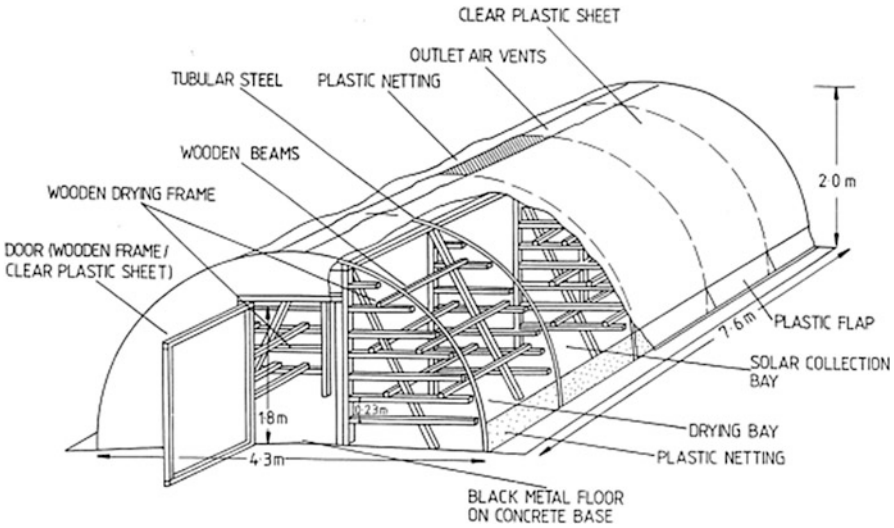

Fig. 12 Natural circulation greenhouse dryer (Ekechukwu and Norton 1999)

The typical design of greenhouse dryer is presented on Fig. 12. The original greenhouse configuration was modified to allow for a black galvanized iron sheet absorber at the floor, air inlets along the whole length of both sides of the dryer, and air outlets along the upper part of the dryer. Both exits are equipped with fine plastic netting to protect the product against insects and dust.

Another type of forced convection greenhouse dryer with transparent polycarbonate cover is visible in Fig. 13. The dryer was installed in the campus of the Royal University of Agriculture in Cambodia. The dryer is approximately 5m wide and 10m long, and it is suitable for drying of different commodities such as fruits, vegetables, and spices. Similar greenhouse dryer of 50m length and constructed as a wooden stack chamber was described by Jairaj et al. (2009). The dryer has trays stacked inside a wooden shed. Trays of size 2 m $\times$ 2 m are fixed in the wooden chamber to spread grapes. The air temperature inside the greenhouse dryer is approximately about 20°C higher than the ambient temperature depending on specific climatic conditions. Heated air passes through the trays placed in the wooden chamber. A blower is placed on the backside of the stack chamber to ensure a regular airflow through the trays. The size of the dryer shed is fixed at 2 $\times$ 3m which ensures easy loading. Fudholi et al. (2010) reported a natural convection greenhouse dryer used for fish drying. The frame is made from metal, and the dryer was covered by clear polyethylene material. Condori et al. (2001) describe a forced convection tunnel greenhouse dryer. The dryer consists of a plastic greenhouse cover containing a drying tunnel made with transparent plastic walls. The air circulation is ensured by an electric fan that moves the hot air from the greenhouse into the tunnel.

Fig. 13 Solar greenhouse dryer installed at the Royal University of Agriculture in Cambodia (Photo: J. Banout)

The main advantages of this dryer are continuous production, lower labor cost since the product handling was partly mechanized, a conventional heater which can be easily installed to keep a constant thermal efficiency, and the installation which can be used as a greenhouse for small production when it is not used as a dryer. Same authors investigated the evaporation rate in two types of forced convection greenhouse dryers, the single- and the double-chamber system. For the same dryer area, the productivity of the double-chamber greenhouse dryer compared to the single-chamber dryer was increased by 87% (Condori and Saravia 1998).

4.5 Polyethylene Tent Dryers

Polyethylene tent dryers on one side represent the most primitive constructions of solar passive dryers. They are easy to construct from locally available materials and unexpansive. Its efficiency is limited as compared to forced convection dryers. The polyethylene tent dryer is illustrated in Fig. 14. The dryer consists of a simple bamboo frame covered with transparent polyethylene sheet on the side facing the sun. The rest siders are covered by black polyethylene sheet which improves absorption of solar radiation. To control airflow in the chamber, the clear plastic cover at the bottom of the front side was rolled around a bamboo stick, and this could be adjusted. The openings at the top of the ends served as outlet for the humid exhaust air (Ekechukwu and Norton 1999).

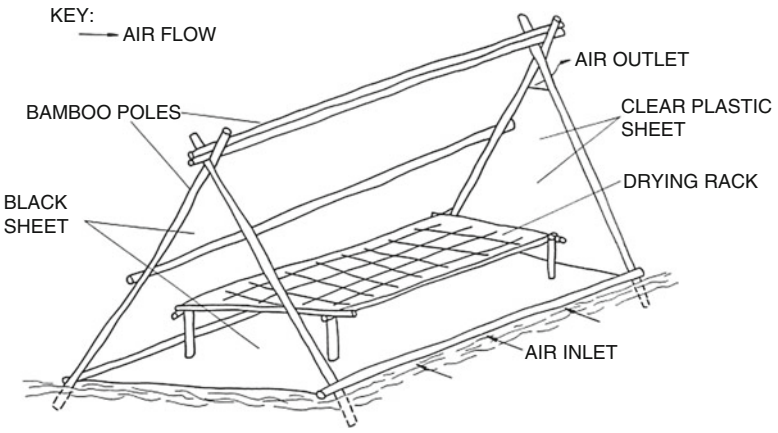

Fig. 14 Polyethylene tent passive solar dryer (Ekechukwu and Norton 1999)

Fudholi et al. (2010) reported in his study three different types of natural convection solar dryers for drying fermented fish in the Gambia. All dryers were made from palm sticks that form a dryer frame covered with transparent polyethylene. The material is low cost and available locally. Solar tent dryer consists of 0.5 m high and 6 m long side openings with triangular shape top vents. The front vent has an area of 0.7 m^2 and the back one is smaller.

Belessiotis and Delyannis (2011) reported a large-capacity polyethylene tent/tunnel solar dryer from Germany. The drying chamber (1.8 m high) consists of a long tunnel-type plastic collector; there are nine tray layers with 1.5 m^2 surface each and they are situated at the top of the plastic tunnel. The solar collector consists of a transparent polyethylene sheet supported by stainless steel bows. The dimensions of the polyethylene collector are 78 m length, 4 m width, and 2.1 m height with 18° of inclination to the south. A black absorbing plastic sheet is used at the bottom of the collector. A blower circulates the heated air up to the dryer. The dryer was used for drying fruits, vegetables, and aromatic herbs.

4.6 Tunnel Dryers

A most recognized model of tunnel dryer is solar tunnel dryer developed at Institute of Agricultural Engineering in Tropics and Subtropics, University of Hohenheim, Germany. The dryer consists of a flat-plate air collector, a tunnel drying chamber, and small fans to provide a regular airflow over the dried product (Schirmer et al. 1996). These are connected in series as shown in Fig. 15. The transparent plastic sheet is used to cover both the collector and the drying chamber. The absorber in the collector part is painted black. The products to be dried are placed in a thin layer on plastic trays in the chamber of the tunnel dryer. To reduce heat loss from the dryer, a glass wool is used as an insulation material. The whole tunnel dryer is installed

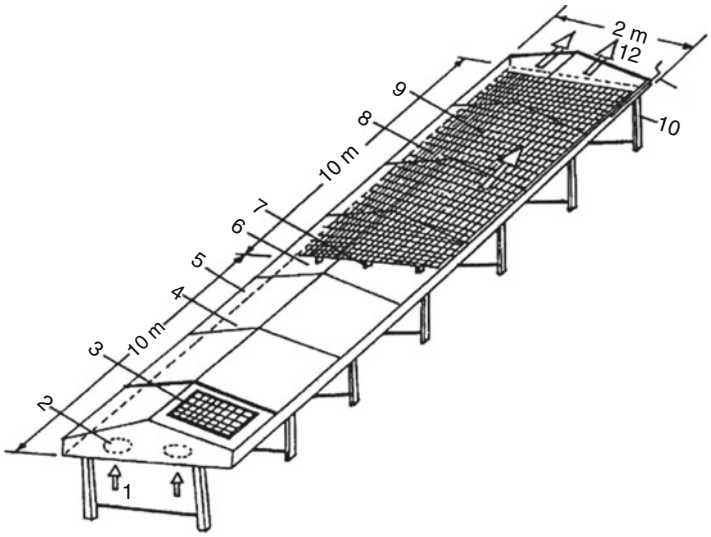

Fig. 15 Solar tunnel dryer: (*1*) air inlet, (*2*) fan, (*3*) solar module, (*4*) solar collector, (*5*) side metal frame, (*6*) outlet of the collector, (*7*) wooden support, (*8*) plastic net, (*9*) roof structure for supporting the plastic cover, (*10*) base structure for supporting the tunnel dryer, (*11*) rolling bar, (*12*) outlet of the drying tunnel (Bala et al. 2003)

horizontally on a raised platform. The air at the required flow rate is provided by two DC fans operated by one photovoltaic panel. The power requirement to drive a fan is equal to 14.4 W. The transparent cover is designed as sloping roof to prevent the entry of water inside the dryer during rainy weather. Solar radiation passes directly through the transparent polyethylene sheet of the collector and heats the absorber. Ambient air is forced through the collector. Heat which is transmitted from the absorber in the collector part passes over the product in the chamber and absorbs moisture from the dried material. The temperature in the dryer varies in the range of 34.1–64.0°C with corresponding solar radiation from 0 to 580 W/m^2 (Bala et al. 2003). The dryer was used for drying of wide agriculture products such as pineapples, bananas, jackfruit, fish meat, and others.

Usub et al. (2008) investigate the performance of a mixed-mode-type forced convection solar tunnel dryer which was used to dry silkworm pupae in Maha Sarakham, Thailand. A transparent glass-covered flat-plate collector and a drying tunnel connected in series were used in this case. Blower was used to ensure the forced circulation of drying air in the tunnel. The dimensions of the dryer were 6.2 m long and 1.8 m width. The drying unit was designed to dry approximately 30 kg of silkworm pupae. Reported drying and overall efficiencies were equal to 30.14% and 19.68%, respectively, corresponding to 0.30 kg/s of airflow rate.

Jairaj et al. (2009) describe in their study a solar tunnel dryer with integral collector. The dryer was designed for large-scale drying operations. As shown in Fig. 16, the solar dryer consists of a solar collector and a tunnel dryer. Grapes to be dried are spread in a thin layer inside the tunnel dryer. As in other cases, the heat is generated in the collector by absorption of solar energy and partly by the dried grapes.

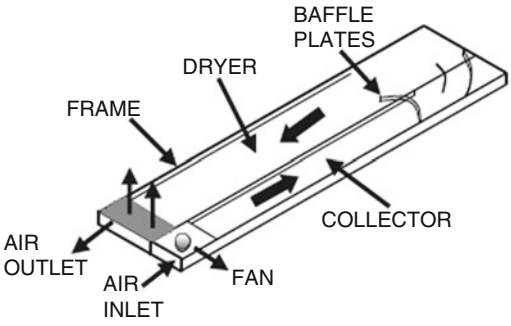

Fig. 16 A solar tunnel dryer with integral collector (Jairaj et al. 2009)

The collector and the dryer chamber are arranged in parallel sections. The solar dryer is 20 m in length and 2 m in width with collector of same length and 1 m wide. The loading capacity of the tunnel dryer is up to 1000 kg of grapes. A transparent polyethylene foil is used as a cover of both the collector and dryer chamber.

Black plastic material is laid out between the walls of collector and dryer. A heat insulation material was used under the absorber to reduce the conductive heat losses. A radial fan integrated into the frame of the collector part is able to blow the drying air through the collector. A 100 W AC motor is used to operate the fan with backwardly curved blades. The drying air is heated in the collector part by solar radiation and passes through its whole length. At the end of the collector, the drying air turns through 180° and enters the tunnel drying chamber. The air outlets can be closed during inappropriate climatic conditions such as rainy season.

The modeling and thermal performance of the collector of a semicylindrical solar tunnel dryer was reported by Garg and Kumar (2000). The performance was estimated for different slopes of the solar tunnel dryer as well as under both natural circulation and forced convection modes, all for Delhi climate. The main parts of a multipurpose solar tunnel dryer are a centrifugal blower, a collector, and a tunnel drying chamber, especially designed for use in arid zones. Authors reported that compared to natural open sun drying method, the drying time for cocoa, coffee, and coconut could be reduced up to 40%. Further, the experiments show that adequate drying which resulted in moisture content suitable for storage was possible even during the rainy season.

4.7 In-House Dryers

In-house solar dryers are usually constructed as large scale for drying of higher capacities of agriculture products as well as for drying of timber. In these designs, very often the solar collector forms an integral part of the roof and/or wall of the drying chamber. Typical design of in-house solar dryer is shown in Fig. 17 which illustrates a solar collector roof dryer.

Janjai et al. (2008) have reported an experimental performance of solar drying of rosella flower and chili by using a roof-integrated solar dryer. The main

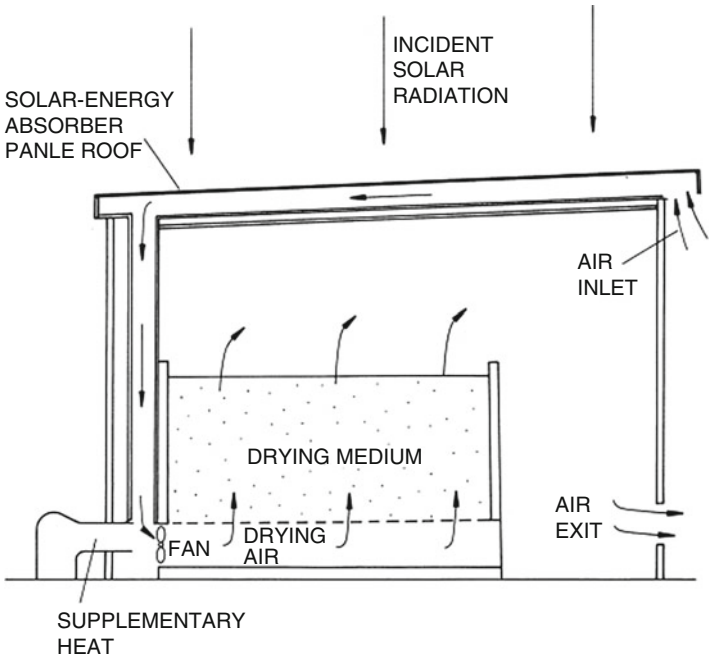

Fig. 17 A roof collector active solar dryer (Ekechukwu and Norton 1999)

components of the dryer are a solar collector integrated directly to the roof of the building and a drying chamber equipped by axial flow blower operated by electric motor (220 V, 1 phase, 0.373 kW) to ensure the required airflow rate. The drying chamber is connected to the collector by a T-type air duct. A roof-integrated collector with total area of 108 m^2 is divided to two parts from which one part is facing the south and other part facing the north.

The dimensions of the dryer chamber are 1.3 m × 2.4 m × 0.8 m, and it is placed inside the building. The in-house dryer was divided in one part with the drying chamber and another two rooms. One room is used as place for the preparation of the products for drying process, and the second room is used for storage of dehydrated products.

5 Using a Double-Pass Solar Dryer for Meat Drying: A Case Study from the Czech Republic

Most nutritional properties of meat, in particular the protein content, remain unchanged through drying. Dried meats are traditional in different parts of the world, and they are known as “cecina” in Spain, “biltong” in South Africa, “bresaola” in Italy, and “jerky” in North America. For instance, in developing

countries the consumption of dried meat as part of total meat consumption has been continuously increasing from a modest average annual per capita consumption of 10 kg in the 1960s to a projected 37 kg around the year 2030 according to the FAO (Hierro et al. 2004). Even though jerky can be made from different animal species, more than 70% of all jerky is produced from beef meat. Nowadays consumers are increasingly becoming concerned about healthy and safe products, and the demand for these products is escalating. According to some studies, game meat and venison meet most of the criteria demanded by the discerning consumer. In general game meat has very low lipid concentrations in the muscles, and these lipids are primarily structural lipids with little contribution from triglycerides, having a very desirable fatty acid profile (Hoffman and Wiklund 2006). One of the perspective venison and/or game animals is eland (*Taurotragus oryx*), a large bovid species with cattle-like appearance recommended for domestication. Eland meat has low (2 g kg^{-1}) total intramuscular fat contents and high proportions of essential fatty acids. That is why it can be considered as a suitable low-fat meat alternative to beef (Barton et al. 2014).

The advantages of solar dryers that enable them to compete with traditional open-air sun drying techniques and/or conventional high-cost drying units operated on fossil fuels have been reported in the literature many times. Thus, the main objective of this study was to use a forced convection solar dryer for drying of eland and beef meat widely recognized as jerky.

The drying of fresh meat slices was carried out in the double-pass solar dryer (DPSD) (Figs. 18 and 19) designed at the Faculty of Tropical AgriSciences, Czech University of Life Sciences Prague (Banout et al. 2011). The DPSD is classified as a forced convection indirect type and is based on the familiar construction of the

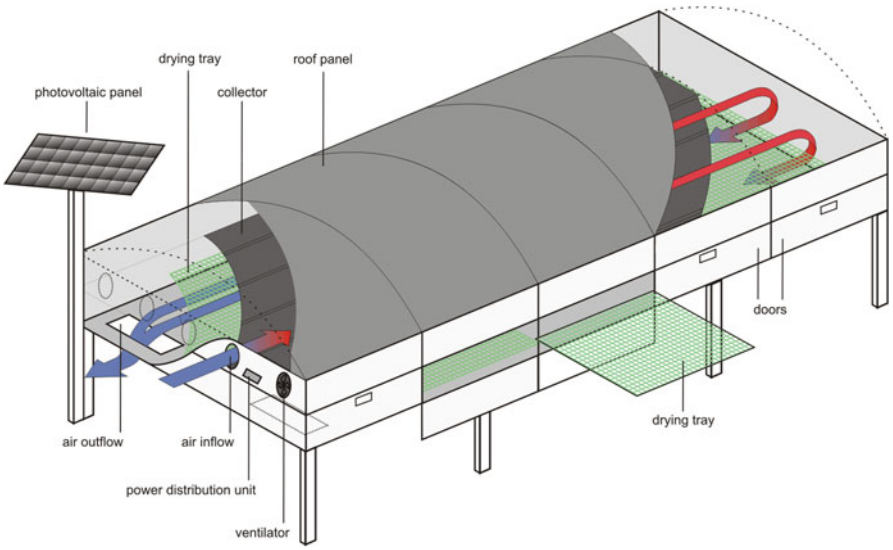

Fig. 18 Illustration of double-pass solar dryer (DPSD) (Banout et al. 2011)

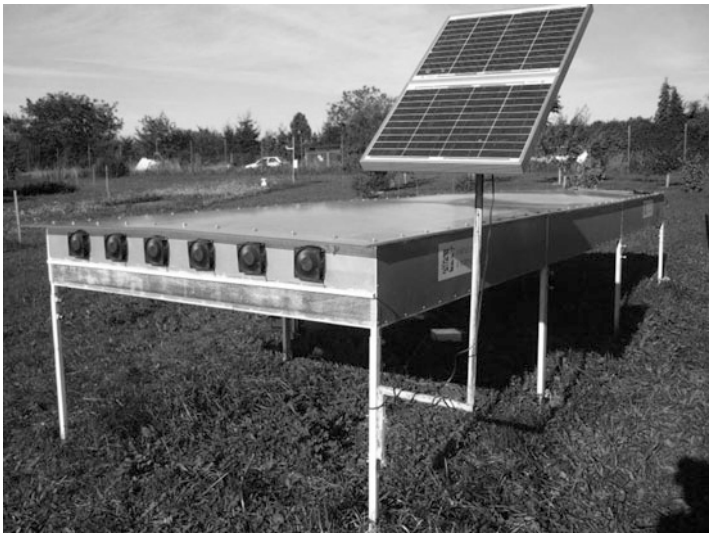

Fig. 19 The double-pass solar dryer installed at the experimental field of Czech University of Life Sciences Prague (Kucerova et al. 2015)

suspended plate air-heating solar collector. The dimensions of the dryer were as follows: length 5 m, width 2 m, and height 0.30 m. The supporting structure was made from square steel rods. The sides were equipped with doors enabling access on each side into the drying chamber. The casing was made from a custom-made sandwich material consisting of four layers. Moving from inside out, these were an aluminum sheet metal (corrosion resistant and odor absorption free), a 2 mm layer of cork (insulation barrier from high heat that could harm the insulation), a 20 mm Styrofoam (insulation), and a galvanized metal sheet (protection from outside influences).

The absorber was made of galvanized metal sheet painted matt black to ensure good absorption of solar radiation. The absorber was provided with axial metal fins that increased the absorber surface. A polycarbonate panel sheet constituted the glazing on the collector part of the dryer. This was made of a UV light stable material with good shatter resistance and transmissivity. At the beginning of the dryer were five DC fans, which provided the necessary airflow through the absorption and drying chamber. The fans were connected directly to a photovoltaic (PV) panel by a parallel connection. No regulatory systems are required as the system regulates the airflow itself due to the position of the sun during the day. The drying chamber was fitted with ten trays, 1x1 m, made from a steel frame and high-density polyethylene (HDPE). This form of plastic is temperature resistant and does not represent any intoxication danger for the product.

The specific climatic and drying conditions of each solar drying experiment at the university campus are presented in Table 2.

Table 2 Climatic and drying conditions of all solar drying experiments (SD – standard deviations)

	Average ambient temperature		Average drying temperature		Average ambient RH		Average RH of drying air		Average insolation		Average airflow speed in a collector	
Experiment	°C	SD	°C	SD	%	SD	%	SD	W.m^{-2}	SD	m.s^{-1}	SD
A	23.4	1.4	46.4	5.7	51.3	8.7	19.7	6.7	525.4	194.1	0.7	0.1
B	24.3	1.7	48.4	6.0	49.2	8.7	18.2	5.7	552.3	219.4	1.0	0.3
C	25.5	2.1	49.3	5.2	46.2	7.7	17.7	5.7	615.3	144.1	1.1	0.1

A solar drying experiment run from June 7, 2012, to June 8, 2012; total drying time, 16 hours excluding nights, *B* solar drying experiment run from August 2,2012, to August 3, 2012; total drying time, 16 hours excluding nights, *C* solar drying experiment run from September 10, 2012, to September 11, 2012; total drying time, 16 hours excluding nights, *RH* relative humidity

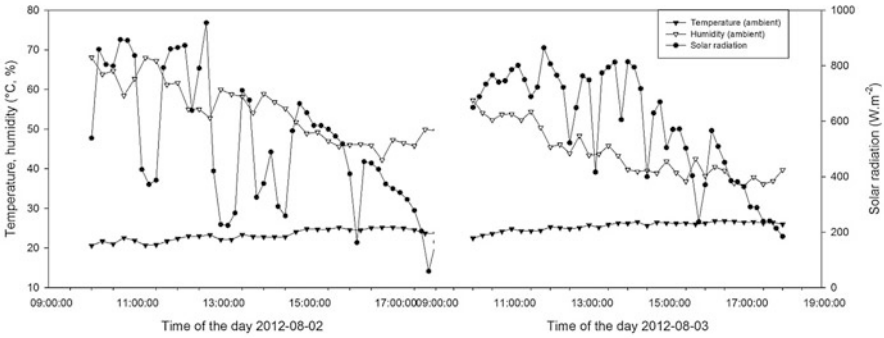

Fig. 20 Variations of ambient temperature, ambient relative humidity, and solar radiation during typical experimental run with standard deviations (Kucerova et al. 2015)

As it is clear from Table 2, the data of all experimental sets show a relative uniformity which is due to similar climatic conditions during each solar drying test. The values of mean ambient temperature, RH, and solar radiation during all experiments were 24.4 ± 1.7 °C, 48.9 ± 8.4%, and 564.3 ± 185.8 W m^{-2}, respectively. Further, the values of mean drying air temperature, drying air RH, and mean drying air velocity during all solar drying experiments were 48.3 ± 5.6 °C, 18.5 ± 6.0%, and 0.9 ± 0.1 m s^{-1}, respectively. For further performance analyses, the data from experiment run B were considered to represent optimal average values. The ambient temperature, ambient RH, and solar radiation curves during the typical solar drying experiment B are presented in Fig. 20, and the daily mean values of the drying air velocity are presented in Fig. 21. From this figure it is evident that high solar radiation corresponds to high drying temperature and low RH of the drying air. The maximum solar radiation on the first day was 954.5 W m^{-2} and the second day 864.3 W m^{-2}. Ambient temperature varied during the whole experimental run between 20.6 °C and 26.8 °C and ambient RH between 35.7 and 64.1%. Corresponding daily mean values of the drying air temperature and RH in the drying chamber of the DPSD varied from 24.5 ± 1.7°C to 60.3 ± 0.9 °C

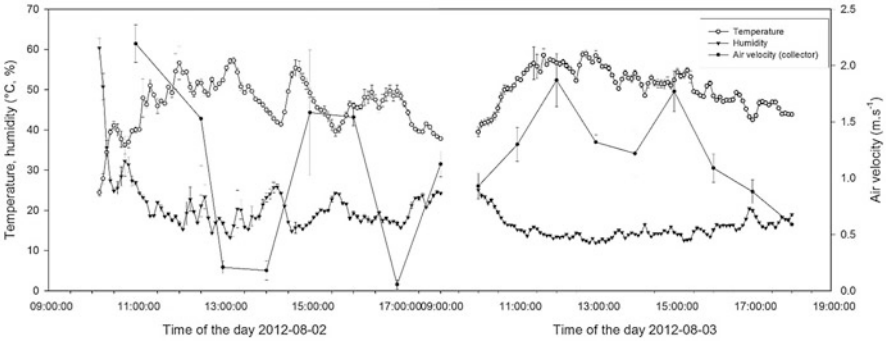

Fig. 21 Variations of drying chamber air temperature, relative humidity, and air velocity during typical solar drying experiment with standard deviations (Kucerova et al. 2015)

and 11.9 ± 0.5% to 60.3±4.9%. Obtained drying temperatures in the DPSD were close to those recommended for the preparation of beef jerky. The daily mean values of the drying air velocity varied from 0.04 to 1.87 m s^{-1}. The relatively large difference between the maximum and minimum drying air velocities was due to the direct connection of the PV module (PV panel) with fans. The fans in the DPSD were connected directly to a PV panel by a parallel connection. No regulatory systems were required as the system regulates the airflow itself due to the position of the sun during the day. However, this disposition makes the airflow rate highly sensitive to actual insolation.

The drying curves (time versus MR) of the eland and beef meat samples with all the used pretreatments TM (traditional marinade), TMH (traditional marinade with honey), and C (control – no marinade used) dried in the DPSD and LO (laboratory oven) are presented in Fig. 22. The MR decreased exponentially with time in both meat samples and all the used pretreatments, which is in agreement with the results reported in previous studies (Perea-Flores et al. 2012). Values of eland and beef MRs were analyzed using the t-test. There was no statistically significant difference (95% confidence level) between eland and beef meat MR dried in the DPSD or between eland and beef meat MR dried in the LO which means that from the statistical point of view, it is possible to conclude that the drying behavior of eland meat and beef meat is the same, even though beef generally contains more lipids, which could affect the drying process. From Fig. 22, it is also evident that the drying rate in the DPSD was higher as compared to the LO mainly in the initial period of drying. This is due to higher maximum drying temperatures in the solar dryer as compared to the LO. Focusing on the overall progress of the drying curves of both meat samples and all pretreatments, we may observe higher drying rates at the initial stages of drying and decreasing drying rates at the latter stages of drying when the process entered the falling rate period. This is typical of all foods, including meats. In the case of meat, it could be caused by denatured proteins being subjected to heat during drying, and therefore a gel matrix is formed, resulting in difficult movement of water from the interior part of the meat. The average initial and final moisture contents of eland meat samples for C, TM, and

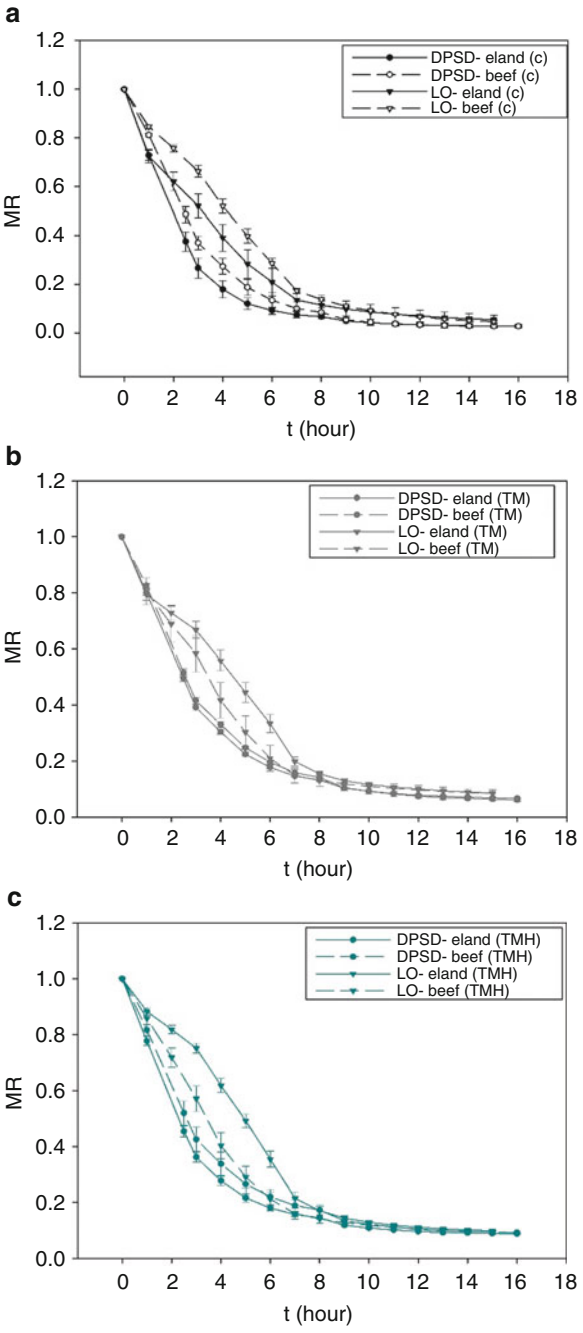

Fig. 22 Experimental moisture ratio of samples of eland meat and beef dried in the DPSD and LO with standard deviations ((**a**) control samples, C; (**b**) traditional marinade samples, TM; (**c**) traditional marinade with honey samples, TMH) (Kucerova et al. 2015)

TMH dried in the solar dryer were 2.79±0.04 kg kg^{-1} (d.b.) and 0.08±0.01 kg kg^{-1} (d.b.), 2.51±0.016 kg kg^{-1} (d.b.) and 0.17±0.01 kg kg^{-1} (d.b.), and 2.39±0.04 kg kg^{-1} (d.b.) and 0.21±0.01 kg kg^{-1} (d.b.), respectively. From these results it is clear that the drying rate was higher in the case of the untreated control sample as compared with the marinated samples.

It was concluded that average temperature and RH in the drying chamber during solar drying were 48.3 ± 5.6 °C, 18.5±6.0%, and 0.9±0.1 m s^{-1}, respectively. Average solar radiation was 564.3_185.8 W m^{-2}. The difference in drying behavior between eland and beef jerky was statistically not significant. In contrast, statistically significant differences in drying behavior were observed between control samples without any treatment and TM samples and TMH samples. Dried meat jerky is one of the important and relatively safe nutrient sources mainly in developing countries. This study brings a new knowledge about the drying behavior of thin-layer drying process of eland jerky which might be important for possible industrial processing. Further the solar drying technology brings compatible results as standard laboratory dryers in terms of drying kinetics.

6 Conclusion

There are no one simple criteria for selecting an appropriate solar dryer for a specific region in the world or a specific product to be dried. The classification of solar drying systems illustrates that the solar dryer designs can be grouped systematically according to drying air circulation to natural and forced convection dryers; according to operational modes to direct, indirect, and mixed-mode dryers; and by their heating sources. The most typical solar dryers for agriculture produce based on their construction designs were summarized and evaluated. The final selection of solar drying systems is generally based on the available insolation rate, kind of product that will be dried, production throughput, operational costs, as well as the experience of the fabricator. Presented case study illustrates the possibility of using a forced convection solar dryer for meat drying. The study brings a new knowledge about the drying behavior of thin-layer drying process of eland jerky which might be important for possible industrial processing. In terms of drying kinetics, the study shows that solar drying technology brings compatible results as standard dryers operated by electricity.

References

Augustus Leon M, Kumar S, Bhattacharya SC (2002) A comprehensive procedure for performance evaluation of solar food dryers. Renew Sust Energ Rev 6:367–393

Bala BK, Janjai S (2012) Solar drying technology: potentials and developments. In: Uqaili MA, Harijan K (eds) Energy. Environment and sustainable development, Springer Vienna, pp 69–98

Bala BK, Mondol MRA, Biswas BK, Das Choudhury BL, Janjai S (2003) Solar drying of pineapple using solar tunnel dryer. Renew Energy 28:183–190
Banout J, Ehl (2010) Using a Double-pass solar dryer for drying of bamboo shoots. J Agric Rural Dev Trop Subtrop 111(2):119–127
Banout J, Havlik J, Kulik M, Kloucek P, Lojka B, Valterova I (2008) Effect of solar drying on the composition of Essential oil of sacha culantro (*Eryngium foetidum L.*) Grown in the Peruvian amazon. J Food Process Eng 33:83–103
Banout J, Ehl P, Havlik J, Lojka B, Polesny Z, Verner V (2011) Design and performance evaluation of a double-pass solar dryer for drying of red chilli (Capsicum annum L.) Sol Energy 85:506–515
Banout J, Kučerová I, Marek Š (2012) Using a double-pass solar dryer for jerky drying. Energy Procedia 30:738–744
Barton L, Bures D, Kotrba R, Sales J (2014) Comparison of meat quality between eland (Taurotragus oryx) and cattle (Bos taurus) raised under similar conditions. Meat Sci 96 (1):346–352
Belessiotis V, Delyannis E (2011) Solar drying. Sol Energy 85:1665–1691
Condori M, Saravia L (1998) The performance of forced convection greenhouse dryers. Renew Energy 13(4):453–469
Condori MR, Echazu L, Saravia (2001) Solar drying of sweet pepper and garlic using the tunnel greenhouse dryer. Renew Energy 22:447–460
Ekechukwu OV, Norton B (1997) Experimental studies of integral-type of natural-circulation solar energy tropical crop dryers. Energy Convers Manag 38:1483–1500
Ekechukwu OV, Norton B (1999) Review of solar-energy drying systems II an overview of solar drying technology. Energy Convers Manag 40:615–655
Esper A, Muhlbauer W (1998) Solar drying – an effective means of food preservation. Renew Energy 15:95–100
Fudholi A, Sopian K, Ruslan MH, Alghoul MA, Sulaiman MY (2010) Review of solar dryers for agricultural and marine products. Renew Sust Energ Rev 14:1–30
Fudholi A, Sopian K, Bakhtyar B, Gabbasa M, Othman MY, Ruslan MH (2015) Review of solar drying systems with air based solar collectors in Malaysia. Renew Sust Energ Rev 51:1191–1204
Garg HP, Kumar R (2000) Studies on semi-cylindrical solar tunnel dryers: thermal performance of collector. Appl Therm Energy 20(2):115–131
Hierro E, De La Hoz L, Ordonez JA (2004) Headspace volatile compounds from salted and occasionally smoked dried meats (cecinas) as affected by animal species. Food Chem 85 (4):649–657
Hoffman LC, Wiklund E (2006) Game and venison – meat for the modern consumer. Meat Sci 74 (1):197–208
Hossain MA, Bala BK (2007) Drying of hot chilli using solar tunnel dryer. Sol Energy 81:85–92
Jain D, Jain RK (2004) Performance evaluation of an inclined multi-pass solar air heater with built-in thermal storage on deep-bed drying application. J Food Eng 65(4):497–509
Jairaj KS, Singh SP, Srikant K (2009) A review of solar dryers developed for grape drying. Sol Energy 83:1698–1712
Janjai S, Bala BK (2012) Solar drying technology. Food Eng Rev 4:16–54
Janjai S, Srisittipokakun N, Bala BK (2008) Experimental and modeling performance of a roof-integrated solar drying system for drying herb and spices. Energy 33:91–103
Karathanos VT, Belessiotis VG (1997) Sun and artificial air drying kinetics of some agricultural products. J Food Eng 31:35–46
Kucerova I, Hubackova A, Rohlik B, Banout J (2015) Mathematical modeling of thin-layer solar drying of Eland (Taurotragus oryx) Jerky. Int J Food Eng 11(2):229–242
Murthy MVR (2009) A review of new technologies, models and experimental investigations of solar dryers. Renew Sust Energ Rev 13:835–844

Pangavhane DR, Sawhney RL, Sarsavadia PN (2002) Design, development and performance testing of a new natural convection solar dryer. Energy 27:579–590

Perea-Flores MJ, Garibay-Febles V, Chanona-Perez JJ, Calderon-Dominguez G, Mendez-Mendez JV, Palacios-Gonzalez E (2012) Mathematical modelling of castor oil seeds (Ricinus communis) drying kinetics in fluidized bed at high temperatures. Ind Crop Prod 38:64–71

Prakash O, Kumar A (2014) Solar greenhouse drying: a review. Renew Sust Energ Rev 29:905–910

Purohit P, Kumar A, Kandpal TC (2006) Solar drying vs. open sun drying: a framework for financial evaluation. Sol Energy 80:1568–1579

Schirmer P, Janjai S, Esper A, Smitabhindu R, Muhlbauer W (1996) Experimental investigation of the performance of the solar dryer for drying bananas. Renew Energy 7(2):119–129

Sharma SJ, Sharma VK, Ranjana JHA, Ray RA (1990) Evaluation of the performance of a cabinet type solar dryer. Energy Convers Manage 30(2):75–80

Sharma A, Chen CR, Vu Lan N (2009) Solar-energy drying systems: a review. Renew Sust Energ Rev 13:1185–1210

Sopian K, Supranto, Othman MY, Daud WRW, Yatim B (2007) Double-pass solar collectors with porous media suitable for higher-temperature solar-assisted drying systems. J Energy Eng 133 (1):1–18

Tembo L, Chiteka ZA, Kadzere I, Akinnifesi FK, Tagwira F (2008) Blanching and drying period affect moisture loss and vitamin C content in Ziziphus mauritiana (Lamk.) Afr J Biotechnol 7 (8):3100–3106

Usub T, Lertsatithanakorn C, Poomsa-ad N, Yang L, Siriamornpun S (2008) Experimental performance of a solar tunnel dryer for drying silkworm pupae. Biosyst Eng 101:209–216

VijayaVenkataRaman S, Iniyan S, Goic R (2012) A review of solar drying technologies. Renew Sustain Energy Rev 16:2652–2670

Weiss W, Buchinger J (2005) Solar drying – Austrian Development Cooperation. AEE INTEC, Gleisdorf, p 110

Characteristics of Different Systems for the Solar Drying of Crops

Brian Norton

Abstract Solar dryers are used to enable the preservation of agricultural crops, food processing industries for dehydration of fruits and vegetables, fish and meat drying, production of milk powder for dairy industries, seasoning of wood and timber and drying of textile materials for textile industries. The fundamental concepts and contexts of their use to dry crops are discussed in the chapter. It is shown that solar drying is the outcome of complex interactions particular between the intensity and duration of solar energy, the prevailing ambient relative humidity and temperature, the characteristics of the particular crop and its pre-preparation and the design and operation of the solar dryer.

Keywords Solar drying • Psychometry • Moisture content • Postharvest technology

1 Introduction

Drying agricultural crops enables:

- Lower postharvest crop losses
- Production of high-quality food products
- Long-term storage without deterioration
- Securing higher prices for crops at times after harvest
- Planning of early harvests
- Maintenance of seed availability

Traditional open-sun drying has, since ancient times, been accomplished by simply placing the crop outdoors, often on a prepared surface or mat, to receive insolation. This causes the crop to heat up and release moisture to the warm relatively dry adjacent air (Jain and Tiwari 2003). Open-sun drying remains widely used for postharvest crop preservation in locations where appropriately sunny and dry conditions prevail with predictability reliably very soon after the crop has been

B. Norton (✉)
Dublin Energy Lab, Dublin Institute of Technology, Grangegorman, Dublin 7, Ireland
e-mail: president@dit.ie

© Springer Nature Singapore Pte Ltd. 2017

O. Prakash, A. Kumar (eds.), *Solar Drying Technology*, Green Energy and Technology, DOI 10.1007/978-981-10-3833-4_3

harvested. If a sufficiently large land area is readily available, then open-sun drying can be used to dry single, or very shallow, crop depths without further capital investment. Open-sun drying entails limited specialist expertise, though some skill is required to optimally cut a crop into pieces whose size and shape meet consumer expectations whilst also achieving reasonably rapid drying. Open-sun drying can be labour intensive as, in addition to crop preparation, the crop usually must be turned and, if it rains, moved to storage. Open-sun drying also is prone to contamination and damage by birds, rats and insects. Open-sun drying can proceed slowly and intermittently with the crop finally being overdried or, more commonly, underdried to a relatively high final moisture content. As there is no protection from rain or dew, the crop can suffer mould growth during drying.

The key strategic drivers to the greater use of solar energy in crop processing are (a) global greenhouse gas emissions (Kumar and Kandpal 2005), (b) local pollution caused by the use of fossil fuels, (c) the desire for security of energy supply and (d) certainty of life cycle system costs. By providing a contained drying environment in which air has been heated by between 10 and 30 °C above ambient temperature, solar dryers dry a crop more rapidly than an open-sun dryer. This faster drying (a) improves dried crop quality and (b) enables a higher crop throughput, and (c) the drying area required is thus much smaller than open-sun drying. However, careful design and operation are required to avoid drying a crop too rapidly as case hardening with subsequent internal mould growth may ensue. Solar dryers also protect foods from dust, insects, birds and animals. They can be constructed from locally available materials at a relatively low capital cost, and there are usually no fuel costs.

The key objectives of drying crops are to remove moisture as quickly as possible at a temperature that does not seriously affect the flavour, texture and colour of the ensuing food product. If the drying temperature is maintained too low, microorganisms may grow before the moist conditions for their development have reduced to the safe storage moisture content. After drying for a specific range of temperature for a particular crop, moisture content must be maintained within specified limits to minimise deterioration.

Temperatures from −37 °C to 71 °C kill bacteria and inactivate enzymes, although, as such temperatures are also likely to cause crop surface hardening, lower operating temperatures in the range 40–45 °C as shown in Table 1 are generally more commonplace in solar dryers.

For many crops pretreatment is recommended such as washing, blanching and cutting into thin slices. Crops are generally harvested at moisture contents ranging from 16 to 30% wet basis and must be dried to a safe storage moisture contents given in Table 1. In grain drying, fissures that can arise from excessive moisture and temperature gradients lead to broken grains during milling reducing the milled cereal yield. Prompt packing in hermetically sealed containers is essential if for consumer acceptability higher safe storage moisture is used, for example, as is the case for some dried fruits.

Table 1 Drying requirements for common crops (Forkas 2003)

Material	Moisture content		Maximum temperature for drying (°C)	Water to be removed (kg/t)	Energy required (kJ/t × 10^6)
	Initial (%)	Final (%)			
Apples	80	24	70	736.8	1.502
Apricots	85	18	65	817.1	1.666
Bananas	80	15	70	823.5	1.679
Cabbage	80	4	55	791.7	1.614
Carrots	70	5	75	684.2	1.365
Cassava	62	17		542.2	1.105
Cauliflower	80	6	65	787.2	1.605
Chillies	80	5	65	789.5	1.610
Cocoa beans	50	7		462.4	0.943
Coffee beans	55	12		488.6	0.996
Coffee	50	11		438.6	0.695
Conifers	30–40	10–15	50	222.2–294.1	0.453–0.600
Corn	24	14	50	116.3	0.237
Figs	80	24		736.8	1.502
Fish, raw	75	15	30	705.9	1.439
Fish, water	75	15	50	705.9	1.439
Foliage trees	25–35	17–20	50	96.4–187.5	0.197–0.382
Garlic	80	4	55	791.7	1.674
Grapes	80	15–20	70	750.0–623.5	1.529–1.679
Green beans	70	5	75	664.2	1.395
Green peas	80	5	65	789.5	1.610
Groundnuts	40	9	50	340.6	0.694
Guavas	80	7	65	784.9	1.600
Maize	35	15	60	235.3	0.480
Onions	80	4	55	791.7	1.614
Peaches	85	18	65	817.1	1.666
Pineapple	80	10	65	777.8	1.586
Potatoes	75	13	75	712.6	1.453
Prunes	85	15	55	823.5	1.679
Rice	24	11	50	146.1	0.298
Spinach	80	10		777.8	1.566
Sweet potato	75	7	75	731.2	1.491
Wheat	20	16	45	47.6	0.097

2 Drying Processes

Solar drying is a natural or an intentional solar energy-induced mass transfer process resulting in the removal of water by evaporation; successful drying requires (a) sufficient solar heat to withdraw moisture, (b) sufficient dry air to absorb released moisture, (c) appropriate control of solar heat gain to avoid cooking the crop and (d) adequate air circulation to remove the moisture. The rate of removal of moisture from a product is proportional to the difference between the average moisture content and the crop's equilibrium moisture content, with the latter in equilibrium with air at a particular mean dry-bulb temperature and relative humidity at particular constant values of air relative humidity and temperature. The drying process takes place at a temperature that is between the temperatures of the air when entering the crop bed and when leaving the dryer. These processes can be summarised on a psychometric chart as shown in Fig. 1. Air is heated at constant humidity ratio in the solar collector from point A to point B to pass through the drying crop isoenthalpically from point B to point C. The equilibrium temperature of drying air can be calculated by establishing a heat balance between molecules in moist air; this becomes the saturated vapour pressure when air cannot take up additional moisture. Pressure equalisation causes moisture to migrate from a region of high to low vapour pressure.

Relative humidity is defined as the ratio of the mole fractions of water vapour in a present in the air to the maximum amount of vapour that the air can hold at a given temperature. Relative humidity is the ratio of the mass of water vapour to the mass of water vapour required to saturate air at that temperature. A dry-bulb temperature is the temperature at an ordinary thermometer. When a thermometer with a water-moistened wick-covered bulb is placed in a stream of unsaturated air, evaporation of water from the wick occurs that cools the bulb; the cooling is proportional to the evaporation rate, which is inversely proportional to the amount of water in the air. The final equilibrium steady-state temperature reached when the temperature of the thermometer remains unchanged is called the wet-bulb temperature. The psychometric wet-bulb temperature is close to but does not precisely correspond to the thermodynamic wet-bulb temperature reached by moist air and water when air is adiabatically saturated by evaporating water. The greater the differences between the amounts of water in the air and the saturation water capacity, the greater the temperature depression between the dry-bulb and wet-bulb temperatures. The dew point temperature is the temperature at which water vapour, being cooled at a constant mixture pressure and humidity ratio, begins to condense. Enthalpy is the relative heat content of moist air per unit mass of dry air above a chosen datum temperature. The enthalpy of moist air per unit mass is the sum of the enthalpies per unit mass of dry air and of superheated water vapour chosen. The humidity ratio is the rate of the vapour pressure of a given moist air sample to that in a saturated air sample at the same temperature and pressure.

A crop drying rate is determined by the temperature and moisture content of the crop, the temperature, the relative humidity and the velocity of the drying air, and,

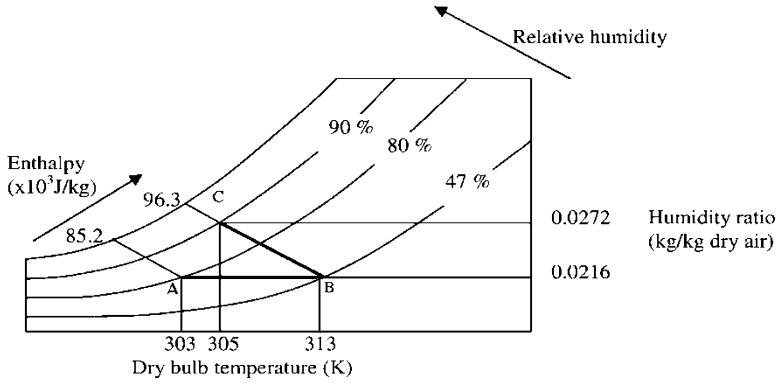

Fig. 1 A psychometric chart showing an illustrative example of a drying process (Adapted from Munira et al. 2013)

thus, drying rate is of main importance. The drying time of each period depends on the nature of the product and the drying conditions. For hygroscopic agricultural products, typical drying rates exhibit up to four distinct periods as shown in Fig. 2.

These are:

- Initially, the crop heats until the drying temperature is achieved; at that juncture, a constant drying rate ensues.
- Constant-rate period during which the crop surface is saturated with water vapour and evaporation takes place continuously as the material's surface has enough water to evaporate. A constant-rate period is not exhibited distinctly by many crop products as their initial moisture content allows the falling rate to be reached almost immediately as dry commences.
- Falling-rate period, when surface is not vapour saturated. Moisture diffusion is controlled by internal liquid movement, whilst surface becomes continuously depleted.
- A concluding falling-rate period, where the moisture content continues to decrease until equilibrium is achieved. For many crops drying is completed before the onset of a concluding falling-rate period is reached.

Figure 2 shows the four drying rate periods. This is followed by a falling drying rate caused by a continuous reduction in the rate of transfer of moisture from the crop's interior which decreases until the crop surface is no longer saturated. Water activity limit is defined by a relationship between the prevailing partial pressure of water; the partial pressure of pure water, at the same temperature; and the relative humidity of the crop at the same temperature. Below the water activity limit, microorganisms stop growing (Beuchat 1981).

Exergetic analyses of dryers have been undertaken (Onyegegbu et al. 1994; Celma and Cuadros 2009). The inclusion of a solar chimney to maintain the air enclosed in the chimney at a higher temperature than ambient enhances buoyant airflow in natural circulation dryers (Bassey et al. 1994; Ferreira et al. 2008; Afriyie

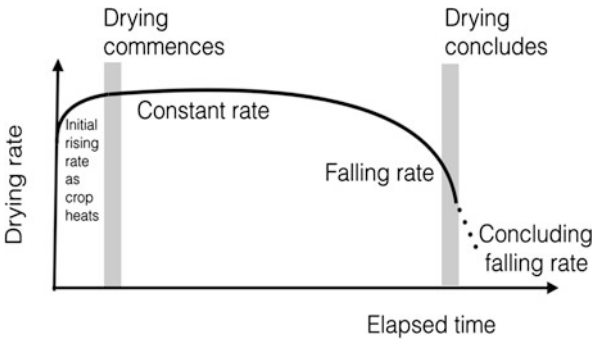

Fig. 2 Drying progression (Tomar et al. 2017)

et al. 2009; Das and Kumar 1989), and PV-powered fans have also been used (Mumba 1996; Barnwal and Tiwari 2008; Punlek et al. 2009). Roof-integrated air-heating solar collectors have been used for solar dryers (Roman et al. 2009) in temperate climates; their output of heated air can also be used to heat farm buildings when not required for drying (Henricksson and Gustafsson 1986).

Dryers that include a biomass backup heater (Bena and Fuller 2002; Chavan et al. 2008), energy storage (Ayensu and Asiedu Bondzie 1986) or both (Madhlopa and Ngwalo 2007) can continue the drying process from the day into the evening and night (Akyurt and Selcuk 1973). Energy storage has been accomplished by including sensible heat storage, for example, in rock beds (Chauhan et al. 1996; Jain 2005, 2007), and by the use of phase change materials (Enibe 2002). Heat pumps have been employed to increase drying air temperature (Best et al. 1994; Fadhel et al. 2011), and desiccants have been used to aid moisture removal (Thoruwa et al. 1996a, b; Mahmouda and Ball 1991; Hodali and Bougard 2001).

The very extensive previous literature available on different types of solar dryers and their performance in particular climates with specific crops have been brought together in several reviews (Sodha and Chandra 1994; Ekechukwu 1999; Ekechukwu and Norton 1999a, b; Ramana Murthy 2009; Sharma et al. 2009; Fudholi et al. 2010; Venkataraman et al. 2012). Solar drying has been employed to dry grain (Radajewski et al. 1987; Mahmouda and Ball 1991; Tiwari et al. 1994; Fraser and Muir 1980; Tayeb 1986; Roa and Macedo 1976) and rice (Basunia and Abe 2001; Zaman and Bala 1989; Bala and Wood 1994; Janjai et al. 1994). A very broad range of dried fruits have been produced using a variety of solar dryers. Some examples of solar-dried fruits include bananas (Schirmer et al. 1996; Amer et al. 2010; Smitabhindu et al. 2008; Koua et al. 2009; Janjai et al. 2009); papaya (Narinesingh and Mohammed-Maraj 1988); mangos (Koua et al. 2009); apricots (Sarsilmaz et al. 2000; Togrul and Pehlivan 2002); figs (Doymaz 2005); pumpkins (Sacilik 2007); apples (Aktas et al. 2009); pineapples (Bala et al. 2003); plums (Tarhan 2007); strawberries (El-Beltagy et al. 2007); grapes (Yaldiz et al. 2001; Jairaj et al. 2009; Pangavhane and Sawhney 2002; Fadhel et al. 2005; Barnwal and Tiwari 2008); mulberries (Akbulut and Durmus 2010); lemons, usually sliced (Chen et al. 2005); and the peel of prickly pears (Lahsasni et al. 2004). In multiple locations, many herbs and spices are, as a matter of course, dried in the sun or in

solar dryers (Muller et al. 1989; Janjai and Tung 2005; Prasad et al. 2006; Janjai et al. 2008; Kumar and Tiwari 2006; Arslan and Ozcan 2008) as are chillis (Hossain et al. 2005; Hossain and Bala 2007; Banout et al. 2011) and green (Akpinar and Bicer 2008) and red (Kooli et al. 2007) peppers. Among the dried vegetables produced using solar dryers are cauliflowers (Kadam and Samuel 2006), coriander (Chauhan et al. 1996), onion flakes (Kumar and Tiwari 2007) and tomatoes (Sacilik et al. 2006). Solar drying has been used to dry root crops, usually cut into slices, including cassava (Ekechukwu and Norton 1997, 1998; Olufayo and Ogunkunle 1996; Koua et al. 2009) and sweet potatoes (Diamante and Munro 1993; Hatamipour et al. 2007; Bechoff et al. 2009). Dried seeds have been produced using solar dryers (Patil and Ward 1989; Williamson et al. 2008). Solar dryers have also been used successfully for specialist high-value products such as coffee beans (Phillips 1965) and pistachio nuts (Midilli and Kucuk 2003). In addition to drying crops, solar drying has also been adopted for drying products as diverse as timber (Headley 1998, 2000; Luna et al. 2009; Taylor and Weir 1985), fermented dairy products (Bahnasawy and Shenana 2004) and fish (Belessiotis and Delyannis 2011; Fudholi 2010).

Typical drying times in solar dryers range from 1 to 3 days depending on the dryer type, intensity and duration of solar radiation incident, airflow rates, drying chamber humidity, ambient humidity and temperature-dependent mass transfer coefficients that determine the drying kinetics of the crop to be dried (Tripathy and Kumar 2009). An airflow will continue to take up moisture that is available at the moist surface of a crop until the airflow is fully saturated. The latter is determined by a temperature-dependent absolute maximum humidity. At higher temperatures, the absolute humidity is higher. So, when an airflow is heated by solar energy, the moisture content remains unchanged, but the relative humidity is lower so that the airflow is now able to take up more moisture from a crop once it flows in the drying chamber.

The optimal drying time is a trade-off in achieving:

- Sufficiently fast crop throughput to make best economic use of the dryer and to, where possible, complete drying, preferably in 1 day, to obviate the need for nocturnal crop storage
- High-quality product without excessive heating degrading the crop to give a lower market price

Drying time can be hastened by:

- Heating the crop directly by solar heating and/or indirectly, via a solar-heated airflow, so that the moisture can be vaporised more readily.
- Crop pre-preparation, including slicing to allow a larger crop surface area to be available to release moisture, breaks into long moisture migration paths and/or dense hydrophobic crop skin layers. As can be seen in Fig. 3, the effect of slicing can reduce drying times significantly.

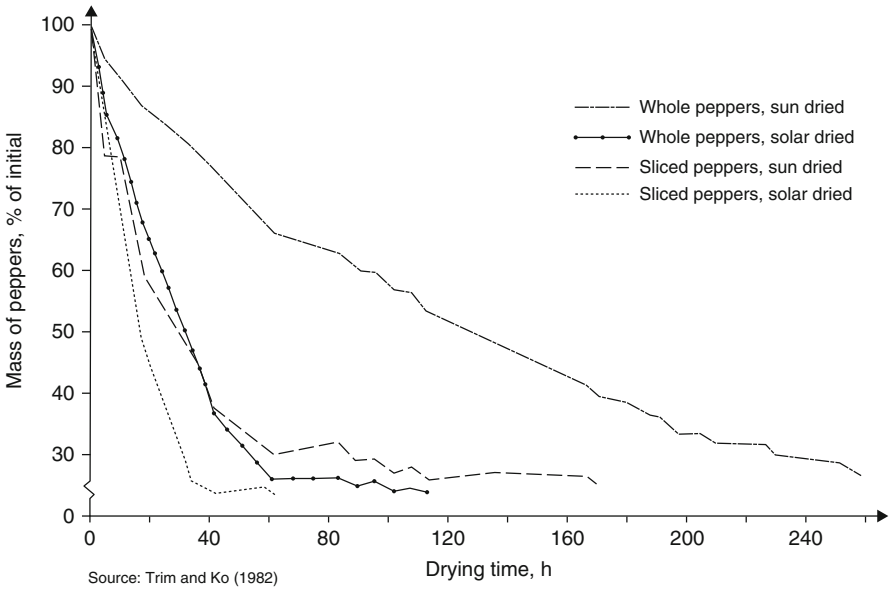

Fig. 3 Effect of pre-preparation on drying times for solar drying and open-sea dryers of red peppers (Tron and Ko 1982)

2.1 Types of Solar Thermal Dryer

The types of solar thermal dryers commonly available are illustrated in Figs. 4 and 5.

Dryers in which crops are directly exposed to solar radiation are termed direct solar dryers. A crop is directly heated by the sun in most cabinet solar dryers (Singh et al. 2006; Datta et al. 1988; Sharma et al. 1990) though indirectly heated cabinet dryers have been realised (Sreekumar et al. 2008; Goyal and Tiwari 1999).

In an indirect solar dryer, the crop is exposed to warm air from an air-heating solar collector and not directly to the sun. Indirect and direct solar dryers are, broadly speaking, applicable to different, but overlapping, ambient conditions as shown indicatively in Fig. 6. It is important to note that for a given location, conditions are changeable (El-Sebaii et al. 2002; Sharma et al. 1992; Singh et al. 2004).

In a mixed mode dryer (Forson et al. 2007a, b), a crop is simultaneously exposed directly to incident solar heat gain and a flow of solar-heated air. As fruit and vegetable crops are dried in an airflow, browning ensues due to a combination of enzymatic and nonenzymatic browning reactions (Krokida et al. 1998). For different dryers, operational conditions and initial crop parameters drying method significant differences have been observed in the browning reactions that crop undergoes during drying.

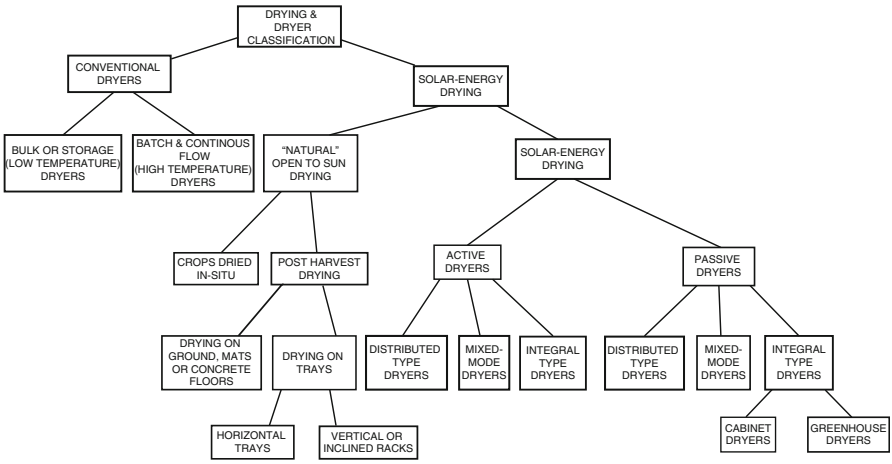

Fig. 4 Taxonomy of solar drying (Ekechukwu and Norton 1999b)

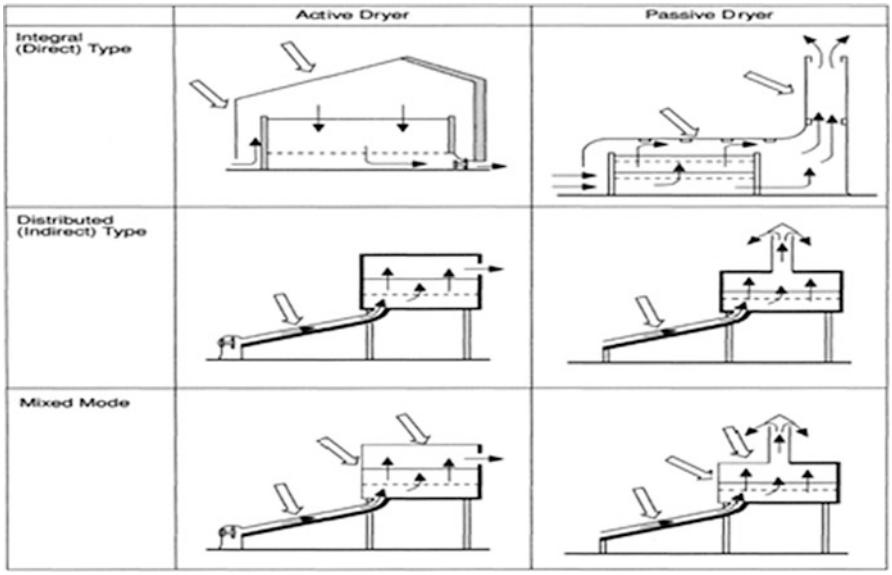

Fig. 5 Solar dryer's classification (Ekechukwu and Norton 1999a)

A direct solar dryer consists of an enclosure with a transparent cover and/or side panels. To enhance solar energy collection efficiency, the internal surfaces of the enclosure are often dark in colour. Heat generated from the absorption of the solar radiation within the crops as well as at the surfaces of the enclosure causes the removal of moisture. Direct dryers are simple to construct. Compared to open-sun drying, direct solar dryers are more hygienic and can heat the crops to higher

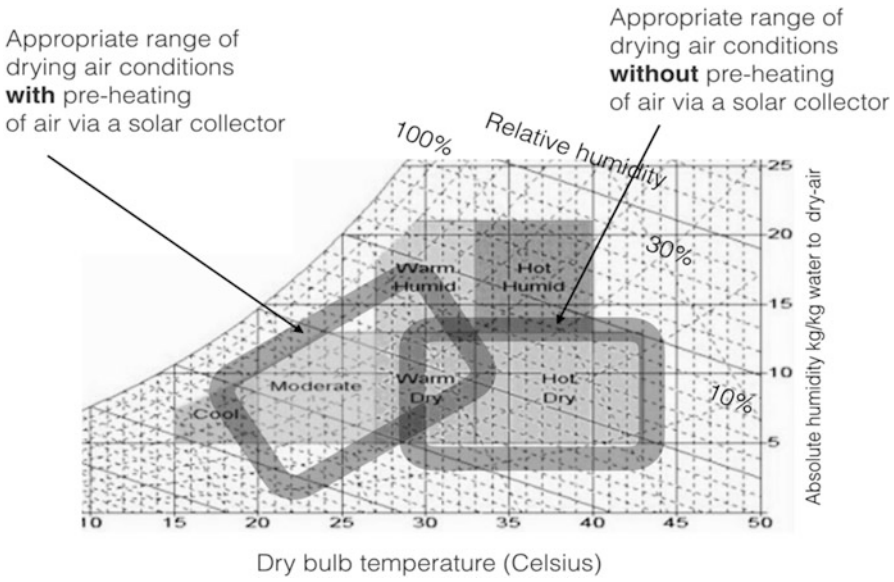

Fig. 6 Indicative ambient conditions for direct and indirect solar dryers

temperatures. As they are normally built in quite small sizes, direct dryers are only intended to dry small quantities of, often high value, crops. However, without knowledgeable and experienced operation, slow drying rates, overheating and changes in crop colour and flavour can ensue due to the direct exposure to the sun. In direct dryers, it can be difficult to control effectively the rate of moisture removal. At the start of the drying process, it is often necessary to close the outlet air holes to allow the temperature of air in the dryer to rise. Water evaporates from the crop and condenses on the inside of the transparent cover and thus reducing the amount of solar radiation transmitted to the dryer interior. This condition is subsequently improved by opening the outlet vents, but in turn it causes temperature inside the dryer to fall. A chimney as shown in Fig. 7 is usually incorporated in natural convection direct dryers to increase the airflow through the crop bed.

Indirect solar dryers are those in which the crops are placed in an enclosed drying cabinet, thereby being shielded from direct exposure to solar radiation. An indirect solar dryer basically consists of three major components: an air heater, which is used to raise the temperature of the drying air, a drying chamber which is the enclosure that accommodates the crops and a fan to convey air between them. Large-scale forced indirect convection solar dryers, such as that shown in Fig. 8, generate the high airflow rates required to overcome pressure drops through deep drying crop beds which make them suitable for drying very large crop volumes. Higher solar energy collection efficiency also results generally from the consistently controlled higher air velocities in the solar collector.

An alternative to the installation of specialist air-heating solar collectors as shown in Fig. 6 is the lower-cost fabrication of roof-integrated collectors as

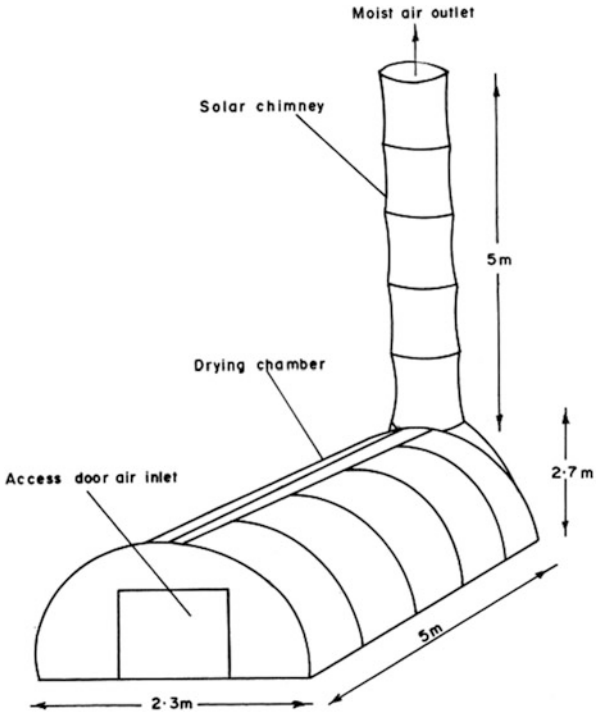

Fig. 7 A greenhouse solar dryer incorporating a chimney (Ekechukwu and Norton 1995)

Fig. 8 A large-scale forced convection solar dryer

shown in Fig. 9 or the use of roof-mounted transpired air-heating collectors as shown in Fig. 10.

Drying is a continuous process where the moisture content, air and crop temperature and the humidity of the air all change simultaneously. The introduction of

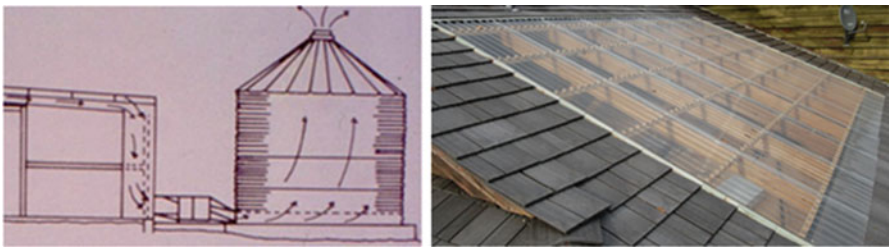

Fig. 9 A roof-mounted air-heating solar collector and the integration of airflow to a drying silo

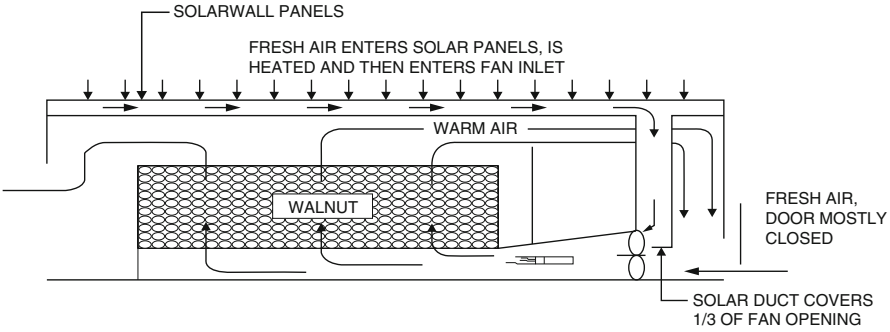

Fig. 10 A walnut dryer constructed in California using transpired air-heating solar collector (Hollick 1999)

a fan enables more direct control of the flow rate to archive optimal drying, particularly in the transition from initial falling to constant drying rates, than can usually be achieved by the operation of flaps and louvres in natural circulation dryers. Forced convection dryers require an electrical or fossil fuel source of power to operate the fan. This is the most significant obstacle to their deployment in remote rural areas where such power has been either rarely available, unreliable or expensive. With the continuing reductions in the cost of photovoltaics, the use of a photovoltaic array to power a fan has become practicable. Where drying takes place over several days, the dryer needs to be designed to avoid nocturnal reabsorption of moisture. This can be accomplished by closing off all air ducts with dampers. An alternative is to continue drying using stored energy or other fuel sources.

Air heated in the collector passes through the drying chamber where the crop to be dried is placed on one or more porous trays. The air passes through the wet crop bed and becomes nearly saturated, thus lowering its temperature to nearly that of the ambient air, before it exits via a chimney. This type of dryer is used when the crop being dried can be damaged if it is exposed to the direct solar radiation. Many crops can be dried in deeper layers, therefore requiring a smaller installation area. However, natural convection indirect solar dryers are prone to poor performance. Since the air above the crop bed is not substantially different in temperature from that of the ambient air, which is also damp in humid regions, the resulting buoyancy forces, which are proportional to the temperature difference, are very small and in

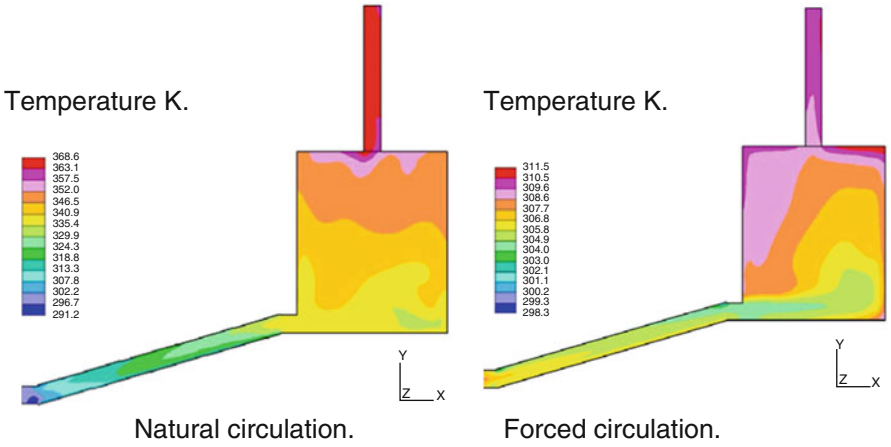

Fig. 11 Predicted temperatures in cabinet solar dryers with natural and forced circulation (Ghaffari and Mehdipour 2015)

turn often low airflow rates. A combination of direct and indirect solar dryers is termed mixed mode dryers. They normally comprise indirect dryers with transparent drying chamber tops and/or sides.

Mixed mode dryers are also suitable to drying crops to which the exposure to sunlight is considered essential for the required colour or flavour development in the dried product such as Arabia coffee beans. A solar dryer with transparent or translucent walls is designed to transmit the greatest amount of incident solar energy into the dryer. Surfaces inside the dryer are dark in colour to absorb that transmitted energy to heat internal surfaces. Energy is then transferred from the heated surfaces to the air in the dryer, primarily by convection. Circulated by natural or forced convection, air then transfers energy to the crop where it removes water from the crop to the air.

Typical drying durations to safe storage moisture content can range from 1 to 3 days, again depending on solar radiation intensity and duration, air movement, the prevalence of lower ambient humidities and the quantity and type of food. As can be seen from Fig. 11, forced circulations lead to less thermal stratification in the dryer and generally archive uniform drying without additional operational interventions. To achieve similarly uniform drying in natural circulation dryers, crop trays need to usually rotate daily, whilst drier crops in upper parts of the drying chamber are often moved to continue drying on lower racks. The crop is allowed to cool completely before it is stored in airtight containers.

2.2 Solar Dryers with Fans Powered by Photovoltaic Modules

The capital cost of photovoltaic installations has reduced globally. In certain jurisdictions, their various market interventions have been made to encourage the

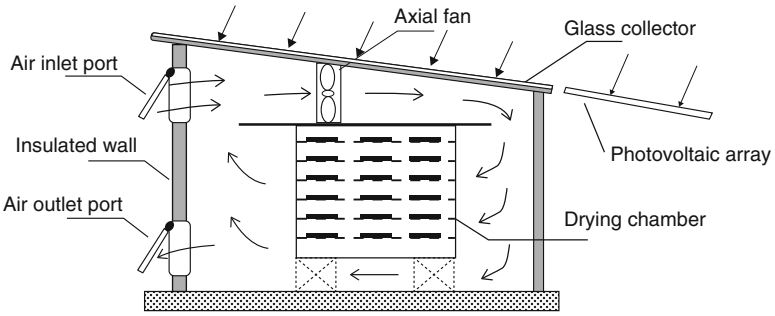

Fig. 12 A forced circulation dryer with a photovoltaic powered fan

use of photovoltaics as a contribution to the decarbonisation of electricity production. A photovoltaic array can be used to power the fan in a forced circulation solar dryer as shown in Fig. 12 enabling (a) autonomy in use that avoids external recurrent energy costs and (b) the extension of the use of forced circulation dryers to remote or portable uses.

Electricity provided by a photovoltaic array can be used to power vacuum dryers where heat is supplied by contact conduction, radiation or microwaves and the vapour produced removed by a vacuum system. Similarly, electricity from a photovoltaic array can be used to provide the refrigeration required for the drying technique where the solvent is frozen prior to drying to be subsequently sublimed (i.e. passed to the gas phase directly from the solid phase) below the melting point of the solvent. Such freeze-drying is often carried out under high vacuum to allow drying to proceed swiftly. As this process maintains complex internal solid structures, low density and highly porous products are produced able to regain moisture rapidly. Freeze-drying is one of the best methods of retaining the initial properties of biological materials such as foods. Freeze-drying is becoming used increasingly to preserve foods for which it is important to keep intact protein quality, vitamins and other bioactive compounds.

3 Conclusion

Solar dryers can include a wide range of modes of airflow, arrangement via which solar energy is harvested to accommodate the distinctive process optimisations required for the production of high-quality different crops. There are, however, a generic set of attributes that are distinctive of specific generic solar dryer types as illustrated in Fig. 13.

Unlike water heating and electricity generation, drying crops is a direct and long-standing use of solar energy. Nevertheless, as shown in Fig. 14, careful

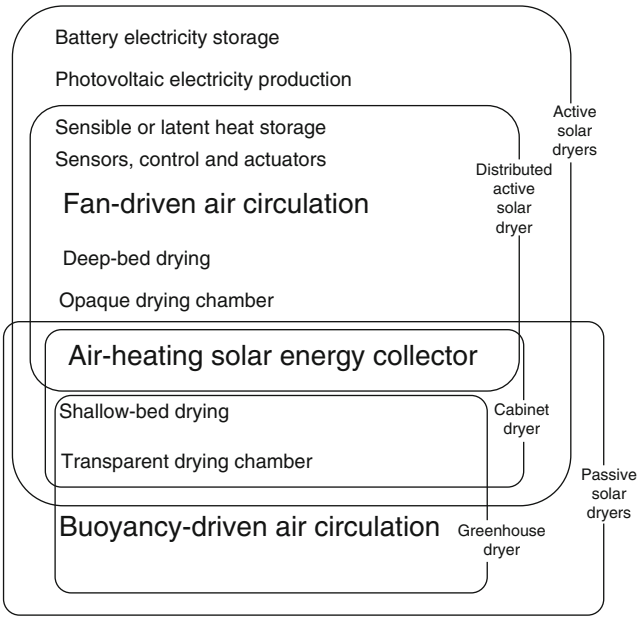

Fig. 13 Groupings of dryer attributes with generic dryer type

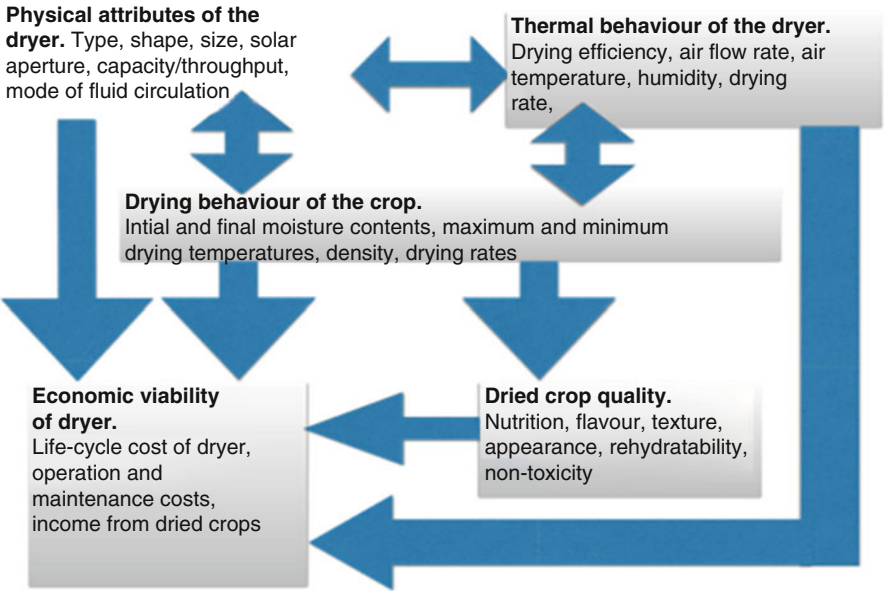

Fig. 14 Factors determining the economic viability of a solar dryer (Tomar et al. 2017)

consideration of the crop characteristics and ambient conditions must inform dryer design to achieve economic viability. Extensive examples of the use of solar drying now exist each with a distinct characteristic depending of the crop and climate. New developments are informed increasingly by the experience of operational practice.

References

Afriyie JK, Nazha MAA, Rajakaruna H, Forson FK (2009) Experimental investigations of a chimney-dependent solar crop dryer. Renew Energy 34:217–222

Akbulut A, Durmus A (2010) Energy and exergy analyses of thin layer drying of mulberry in a forced solar dryer. Energy 35:1754–1763

Akpinar EK, Bicer Y (2008) Mathematical modelling of thin layer drying process of long green pepper in solar dryer and under open sun. Energy Convers Manag 49:1367–1375

Aktas M, Ceylan I, Yilmaz S (2009) Determination of drying characteristics of apples in a heat pump and solar dryer. Desalination 239:266–275

Akyurt M, Selcuk MK (1973) A solar drier supplemented with auxiliary heating systems for continuous operation. Sol Energy 14:313–3320

Amer BMA, Hossain MA, Gottschalk K (2010) Design and performance evaluation of a new hybrid solar dryer for banana. Energy Convers Manag 51:813–820

Arslan D, Ozcan MM (2008) Evaluation of drying methods with respect to drying kinetics, mineral content and colour characteristics of rosemary leaves. Energy Convers Manag 49:1258–1264

Ayensu A, Asiedu Bondzie V (1986) Solar drying with convective self-flow and energy storage. Solar Wind Technol 3:273–279

Bahnasawy AH, Shenana ME (2004) A mathematical model of direct sun and solar drying of some fermented dairy products (Kishk). J Food Eng 61:309–319

Bala BK, Wood JL (1994) Simulation of the indirect natural convection solar drying of rough rice. Sol Energy 53:259–266

Bala BK, Mondol MRA, Biswas BK, Das Chowdury BL, Janjai S (2003) Solar drying of pineapple using solar tunnel drier. Renew Energy 28:183–190

Banout J, Ehl P, Havlik J, Lojka B, Polesny Z, Verner V (2011) Design and performance evaluation of a double-pass solar drier for drying of red chilli (Capsicum annum L.) Sol Energy 85:506–515

Barnwal P, Tiwari GN (2008) Grape drying by using hybrid photovoltaic-thermal (PV/T) green-house dryer: an experimental study. Sol Energy 82:1131–1144

Bassey MW, Oosthuizen PH, Sarr J (1994) Using heated chimneys and reduced collector air gap height to improve the performance of indirect passive solar dryers. Renew Energy 4:169–178

Basunia MA, Abe T (2001) Thin-layer solar drying characteristics of rough rice under natural convection. J Food Eng 47:295–301

Bechoff A, Dufour D, Dhuique-Mayer C, Marouze C, Reynes M, Westby A (2009) Effect of hot air, solar and sun drying treatments on provitamin A retention in orange-fleshed sweet potato. J Food Eng 92:164–171

Belessiotis V, Delyannis E (2011) Solar drying. Sol Energy 85(8):1665–1691

Bena B, Fuller RJ (2002) Natural convection solar dryer with biomass back-up heater. Sol Energy 72:75–83

Best R, Soto W, Pilatowsky I, Gutierrez LJ (1994) Evaluation of a rice drying system using a solar assisted heat pump. Renew Energy 5:465–468

Beuchat LR (1981) Microbial stability as affected by water activity. Cereal Foods World 26:345–349

Celma AR, Cuadros F (2009) Energy and energy analysis of OMV solar drying process. Renew Energy 34:660–666

Chauhan PM, Choudhury C, Garg HP (1996) Comparative performance of coriander dryer coupled to solar air heater and solar air-heater-cum-rock bed storage. Appl Therm Eng 16:475–486
Chavan BR, Yakupitiyage A, Kumar S (2008) Mathematical modelling of drying characteristics of Indian mackerel (rastrilliger kangurta) in solar-biomass hybrid cabinet dryer. Drying Technol Int J 26:1552–1562
Chen H-H, Hernandez CE, Huang T-C (2005) A study of the drying effect on lemon slices using a closed-type solar dryer. Sol Energy 78:97–103
Das SK, Kumar Y (1989) Design and performance of a solar dryer with vertical collector chimney suitable for rural application. Energy Convers Manag 29(1):29–135
Datta G, Garg HP, Ray RA, Prakash J (1988) Performance prediction of a cabinet-type solar drier. Solar Wind Technol 5:289–292
Diamante LM, Munro PA (1993) Mathematical modelling of the thin layer solar drying of sweet potato slices. Sol Energy 51:271–276
Doymaz I (2005) Sun drying of figs: an experimental study. J Food Eng 71:403–407
Ekechukwu OV (1999) Review of solar energy drying I: an overview of drying principles and theory. Energy Convers Manag 40:593–613
Ekechukwu OV, Norton B (1995) Design and measured performance of a solar chimney for natural circulation solar dryers. J Solar Energy Eng 118:69–71
Ekechukwn OV, Norton B (1997) Experimental studies of intergral type natural circulation solar energy tropical crop dryers. Energy Convers Manag 380:1483–1500
Ekechulewu OV, Norton B (1998) Effects of seasonal weather variations on the measured performance of a natural-circulation solar-energy tropical crop dryer. Energy Convers Manag 39:1265–1276
Ekechukwu OV, Norton B (1999a) Review of solar energy drying II: an overview of drying technology. Energy Convers Manag 40:615–655
Ekechukwu OV, Norton B (1999b) Review of solar energy drying III: low temperature air-heating solar collectors for crop drying applications. Energy Convers Manag 40:657–667
El-Beltagy A, Gamea GR, Amer Essa AH (2007) Solar drying characteristics of strawberry. J Food Eng 78:456–464
El-Sebaii AA, Aboul-Enein S, Ramadan MRI, El-Gohary HG (2002) Experimental investigation of an indirect type natural convection solar dryer. Energy Convers Manag 43:2251–2266
Enibe SO (2002) Performance of a natural circulation solar air heating system with phase change material energy storage. Renew Energy 27:69–86
Fadhel A, Kooli S, Farhat A, Bellghith A (2005) Study of the solar drying of grapes by three different processes. Desalination 185:535–541
Fadhel MI, Sopian K, David WRW, Alghoul MA (2011) Review on advance of solar assisted chemical heat pump dryer for agriculturla produce. Renewable and Solar Energy Rev 15:1152–1168
Ferreira AG, Cristina VM, Marcio FBC, Ramon MV (2008) Technical feasibility assessment of a solar chimney for food drying. Sol Energy 82:198–205
Forkas I (2003) Control aspects of post harvest technologies, handbook of post harvest technology. Marcel Dehker Inc, New York, pp 845–866
Forson FK, Nazha MAA, Akuffo FO, Rajakaruna H (2007a) Design of mixed-mode natural convection solar crop dryers: application of principles and rules of thumb. Renew Energy 32:2306–2319
Forson FK, Nazha MAA, Rajakaruna H (2007b) Modelling and experimental studies on a mixed-mode natural convection solar crop-dryer. Sol Energy 81:346–357
Fraser BM, Muir WE (1980) Energy consumptions predicted for drying grain with ambient and solar -heated air in Canada. J Agric Eng Res 25:325–331
Fudholi A, Sopian K, Ruslan MH, Alghoul MA, Sulaiman MY (2010) Review of solar dryers for agricultural and marine products. Renew Sust Energ Rev 14:1–30

Ghaffari A, Mehdipour R (2015) Modelling and improving the performance of a cabinet dryer using computational fluid dynamics. Int J Food Eng 11:157–172
Goyal RK, Tiwari GN (1999) Performance of a reverse flat plate absorber cabinet dryer: a new concept. Energy Convers Manag 40:385–392
Hatamipour MS, Kazemi HH, Nooralivand A, Nozarpoor A (2007) Drying characteristics of six varieties of sweet potatoes in different dryers. Food Bioprod Process 85:171–177
Headley OSC (1998) Solar thermal applications in the West Indies. Renew Energy 15:257–263
Headley OSC (2000) Solar crop drying in the West Indies. World Renew Energy Congr VI:934–939.
Henricksson R, Gustafsson G (1986) Use of solar collectors for drying agricultural crops and for heating farm buildings. Energy Agric 5:139–150
Hodali R, Bougard J (2001) Integration of a desiccant unit in crops solar drying installation: optimisation by numerical simulation. Energy Convers Manag 42:1543–1558
Hossain MA, Bala BK (2007) Drying of hot chilli using solar tunnel dryer. Sol Energy 81:85–92
Hossain MA, Woods JL, Bala BK (2005) Optimisation of solar tunnel drier for drying of chilli without colour loss. Renew Energy 30:729–742
Jain D (2005) Modelling the performance of greenhouse with packed bed thermal storage on crop drying application. J Food Eng 71:170–178
Jain D (2007) Modelling the performance of the reversed absorber with packed bed thermal storage natural convection solar crop dryer. J Food Eng 78:637–647
Jain D, Tiwari GN (2003) Thermal aspects of open sun drying of various crops. Energy 28:37–54
Jairaj KS, Singh SP, Srikant K (2009) A review of solar dryers developed for grape drying. Sol Energy 83:1698–1712
Janjai S, Tung P (2005) Performance of a solar dryer using hot air from roof-integrated solar collectors for drying herbs and spices. Renew Energy 30:2085–2095
Janjai S, Esper A, Muhlbauer W (1994) A procedure for determining the optimum collector area for a solar paddy drying system. Renew Energy 4:409–416
Janjai S, Srisittipokakun N, Bala BK (2008) Experimental and modelling performances of a roof-integrated solar drying system for drying herbs and spices. Energy 33:91–103
Janjai S, Lamlert N, Intawee P, Mahayothee B, Bala BK, Nagle M et al (2009) Experimental and simulated performance of a PV-ventilated solar greenhouse dryer for drying of peeled longan and banana. Sol Energy 83:1550–1565
Kadam DM, Samuel DVK (2006) Convective flat-plate solar heat collector for cauliflower drying. Biosyst Eng 93:189–198
Kooli S, Fadhel A, Farhat A, Belghith A (2007) Drying of red pepper in open sun and greenhouse conditions: mathematical modelling and experimental validation. J Food Eng 79:1094–1103
Koua KB, Fassinou WF, Gbaha P, Toure S (2009) Mathematical modelling of the thin layer solar drying of banana, mango and cassava. Energy 34:1594–1602
Krokida MK, Tsami E, Maroulis ZB (1998) Kinetics on colour changes during drying of fruits and vegetables. Dry Technol 16:667–685
Kumar A, Kandpal TC (2005) Solar drying and CO_2 emission mitigation: potential for selected cash crops in India. Sol Energy 78:321–329
Kumar A, Tiwari GN (2006) Thermal modelling of a natural convection greenhouse drying system for jaggery: an experimental validation. Sol Energy 80:1135–1144
Kumar A, Tiwari GN (2007) Effect of mass on convective mass transfer coefficient during open sun and greenhouse drying of onion flakes. J Food Eng 79:1337–1350
Lahsasni S, Kouhila M, Mahrouz M, Idlimam A, Jamali A (2004) Thin layer convective solar drying and mathematical modelling of prickly pear peel (Opuntia ficus indica). Energy 29:211–224
Luna D, Nadeau JP, Jannot Y (2009) Solar timber kilns: state of the art and foreseeable developments. Renew Sust Energ Rev 13:1446–1455
Madhlopa A, Ngwalo G (2007) Solar dryer with thermal storage and biomass-backup heater. Sol Energy 81:449–462

Mahmouda KG, Ball HD (1991) Solar desiccant systems for grain drying. Energy Convers Manag 31:595–598
Midilli A, Kucuk H (2003) Mathematical modelling of thin layer drying of pistachio by using solar energy. Energy Convers Manag 44:1111–1122
Muller J, Reisinger G, Kisgeci J, Kotta E, Tesic M, Muhlbauer W (1989) Development of a greenhouse-type solar dryer for medicinal plants and herbs. Solar Wind Technol 6:523–530
Mumba J (1996) Design and development of a solar grain dryer incorporating photovoltaic powered air circulation. Energy Convers Manag 37:615–621
Munira A, Sultan U, Iqbal M (2013) Development and performance evaluation of a locally fabricated portable solar tunnel dryer for drying of fruits, vegetables and medicinal plants. Pak J Agric Sci 50:493–498
Narinesingh D, Mohammed-Maraj R (1988) Solar drying characteristics of papaya (Carica papaya) latex. J Sci Food Agric 46:175–186
Olufayo AA, Ogunkunle OJ (1996) Natural drying of cassava chips in the humid zone of Nigeria. Bioresour Technol 58:89–91
Onyegegbu SO, Morhenne J, Norton B (1994) Second law optimisation of integral type natural circulation solar energy crop dryers. Energy Convers Manag 35:973–983
Pangavhane DR, Sawhney RL (2002) Review of research and development work on solar dryers for grape drying. Energy Convers Manag 43:45–61
Patil BG, Ward GT (1989) Simulation of solar air drying of rapeseed. Sol Energy 43:305–320
Phillips AL (1965) Drying coffee with solar-heated air. Sol Energy 9:213–216
Prasad J, Vijay VK, Tiwari GN, Sorayan VPS (2006) Study on performance evaluation of hybrid drier for turmeric (Curcuma Longa L.) drying at village scale. J Food Eng 75:497–502
Punlek C, Pairintra R, Chindaraksa S, Maneewan S (2009) Simulation design and evaluation of hybrid PV/T assisted desiccant integrated HA-IR drying system (HPIRD). Food Bioprod Process 87:77–86
Radajewski W, Jolly P, Abawi GY (1987) Optimisation of solar grain drying in a continuous flow dryer. J Agric Eng Res 38:127–144
Ramana Murthy MV (2009) A review of new technologies, models and experimental investigations of solar driers. Renew Sust Energ Rev 13:835–844
Roa G, Macedo IC (1976) Grain drying in stationary bins with solar heated air. Sol Energy 18:445–449
Roman F, Nagle M, Leis H, Janjai S, Mahayothee B, Haewsungcharoen M, Muller J (2009) Potential of roof-integrated solar collectors for preheating air at drying facilities in northern Thailand. Renew Energy 34:1661–1667
Sacilik K (2007) Effect of drying methods on thin-layer drying characteristics of hull-less seed pumpkin (Cucurbita Pepo L.) J Food Eng 79:23–30
Sacilik K, Keskin R, Elicin AK (2006) Mathematical modelling of solar tunnel drying of thin layer organic tomato. J Food Eng 73:231–238
Sarsilmaz C, Yildiz C, Pehlivan D (2000) Drying of apricots in a rotary column cylindrical dryer (RCCD) supported with solar energy. Renew Energy 21:117–127
Schirmer P, Janjai S, Esper A, Smitabhindu R, Mühlbauer W (1996) Experimental investigation of the performance of the solar tunnel dryer for drying bananas. Renew Energy 7:119–129
Sharma S, Sharma VK, Jha R, Ray RA (1990) Evaluation of the performance of a cabinet type solar dryer. Energy Convers Manag 30:75–80
Sharma VK, Colangelo A, Spagna G (1992) Investigation of an indirect type multi-shelf solar fruit and vegetable dryer. Renew Energy 2:577–586
Sharma A, Chen CR, Lan NV (2009) Solar energy drying systems: a review. Renew Sust Energ Rev 13:1185–1210
Singh S, Singh PP, Dhaliwal SS (2004) Multi-shelf portable solar dryer. Renew Energy 29:753–765
Singh PP, Singh S, Dhaliwal SS (2006) Multi-shelf domestic solar dryer. Energy Convers Manag 47:1799–1815

Smitabhindu R, Janjai S, Chankong V (2008) Optimisation of a solar-assisted drying system for drying bananas. Renew Energy 33:1523–1531
Sodha MS, Chandra R (1994) Solar drying systems and their testing procedures: a review. Energy Convers Manag 35:219–267
Sreekumar A, Manikantan PE, Vijayakumar KP (2008) Performance of indirect solar cabinet dryer. Energy Convers Manag 49:1388–1395
Tarhan S (2007) Selection of chemical and thermal pretreatment combination for plum drying at low and moderate drying air temperatures. J Food Eng 79:255–260
Tayeb AM (1986) Modern solar grain dryer. Solar Wind Technol 13:211–214
Taylor KJ, Weir AD (1985) Simulation of a solar timber drier. Sol Energy 34:249–255
Thoruwa TFN, Johnstone CM, Grant AD, Smith JE (1996a) Novel, low cost $CaCl_2$ based desiccants for solar crop drying applications. Renew Energy 9:686–689
Thoruwa TFN, Smith JE, Grant AD, Johnstone CM (1996b) Developments in solar drying using forced ventilation and solar regenerated desiccant materials. Renew Energy 9:686–689
Tiwari GN, Singh AK, Bhatia PS (1994) Experimental simulation of a grain drying system. Energy Convers Manag 35:453–458
Togrul IT, Pehlivan D (2002) Mathematical modelling of solar drying of apricots in thin layers. J Food Eng 55:209–216
Tomar V, Tiwari GN, Norton B (2017) Thermophysics of crops, systems and components of solar dryers for tropical food preservation. Solar Energy, in press
Tripathy PP, Kumar S (2009) A methodology for determination of temperature dependent mass transfer coefficients from drying kinetics: application to solar drying. J Food Eng 90:212–218
Tron DS, Ko MY (1982) Development of a forced convection solar dyes for red peppers. Tropical Agric (Trinidad) 59:319–323
Venkataraman SV, Iniyan S, Goic R (2012) A review of solar drying technologies. Renew Sust Energ Rev 16:2652–2670
Williamson J, Williamson T, Callahan C (2008) Solar seed dryer and storage bin at state line farm, Bennington, VT; feasibility analysis. Callahan Engineering, Cambridge/New York
Yaldiz O, Ertekin C, Uzun HI (2001) Mathematical modelling of thin layer solar drying of sultana grapes. Energy 26:457–465
Zaman MA, Bala BK (1989) Thin layer solar drying of rough rice. Sol Energy 42:167–171

Fundamental Mathematical Relations of Solar Drying Systems

Stamatios Babalis, Elias Papanicolaou, and Vassilios Belessiotis

Abstract Drying of agricultural products is a widely spread method achieving a physiochemical stabilization of the material by removing part of the moisture content, producing therefore products with new qualitative properties and different nutritional and economical value. Significant amounts of agricultural crops are dried artificially in mechanical drying systems using heated air. Simulation models of the drying process are used either for designing new or improving existing drying systems or for the control of the drying process. All parameters (transfer coefficients, drying constants, etc.) used by the simulation models are directly related to the drying conditions, i.e., temperature and velocity of the drying medium inside the mechanical dryer. As a consequence, the drying conditions, as directly related to the drying time, are affecting the energy demands.

The drying process principles, describing the periods of drying and their modeling (constant and falling-rate periods), are first reported and analyzed, giving the fundamental mathematical relations describing the drying process and the driving forces involved. The concepts of water activity and equilibrium moisture content are therefore introduced, in order to describe the fundamental concept of sorption-desorption isotherms which are the curves that fundamentally determine the way the particular solid can be dehydrated.

In the subsequent chapter, the basic mathematical relations and theories of the drying process involving simultaneous heat and mass transfer models as well as those of the simplified thin-layer and deep-bed models are given.

An overview of solar drying methods (in both thin-layer and deep-bed dryers) along with the principal solar drying systems (direct sun dryers, passive and active dryers) will then be briefly introduced, discussing the respective fields of application and analyzing their advantages and disadvantages. Finally, the basic mathematic equations used for describing and modeling the various physical processes within the most common drying systems and devices are reported. A brief discussion of the recent advances in modeling is finally presented where pertinent.

Keywords Drying dryers • Drying modeling • Thin-layer drying

S. Babalis • E. Papanicolaou • V. Belessiotis (✉)
National Center for Scientific Research "DEMOKRITOS", Solar & Energy Systems Laboratory, Patriarchou Gregoriou & Neapoleos st., 15310 Aghia Paraskevi, Athens, Greece
e-mail: sbabalis@ipta.demokritos.gr; elpapa@ipta.demokritos.gr; beles@ipta.demokritos.gr

© Springer Nature Singapore Pte Ltd. 2017

O. Prakash, A. Kumar (eds.), *Solar Drying Technology*, Green Energy and Technology, DOI 10.1007/978-981-10-3833-4_4

1 The Drying Process Principles

1.1 Introduction

Drying is the phenomenon of removal of a liquid (usually water) contained in a solid (natural product or product obtained by an industrial process), by using natural or mechanical means. This water, in liquid or gaseous phase, is characterized as "moisture." In a broader sense, apart from water, drying comprises the removal of various other liquids, usually solvents, also contained in small quantities in solid, liquid, or gaseous materials, such as alcohol, gasoline, benzene, etc. In this work, we will only consider the drying of solid materials containing moisture, which is the most frequent case of drying.

Drying is classified as a basic separation method of chemical engineering science (unit operation) and is mainly achieved by supplying thermal energy to the material to be dried through a stream of hot air. The moisture is removed from the solid and carried away by this airstream. It is analyzed by dealing with simultaneous heat, mass, and momentum transfer processes that cause changes in the different water phases inside the structure of the composite system. Phenomena in which the heat and mass transfer occur by contact of the porous solid surface with a liquid (osmosis) or a solid medium (contact drying) are not taken into consideration. Procedures such as mechanical methods (compression, centrifugation) that often precede the drying process itself are also not considered. Those procedures are usually less expensive and often simpler in their application, in comparison with thermal ones. The core subject of the food drying is, therefore, the removal of the moisture content, by thermal methods alone, up to the point where the quality degradation of the finally obtained product is minimized during storage.

It should be clarified that the drying process comprises evaporation as a natural process only and not as a process of chemical engineering. It is an extremely complicated procedure with many factors that are changing simultaneously and involving a number of ancillary processes that inevitably follow, directly or indirectly, the course of removal of the moisture until the final dry product is obtained. Apart from the introduction of hot air already mentioned, moisture removal is also achieved by heat radiation on the surface of the material, by heat conduction, or by applying vacuum. In the hot air drying, the free water is converted into vapor in two ways, *evaporation* or *vaporization* (Belessiotis and Delyannis 2006).

Evaporation is a natural process that occurs when the saturation vapor pressure at the solid surface is equal to the surrounding atmospheric pressure. This procedure, applied to certain dryers, is accomplished by raising the temperature of the material to the temperature of boiling water. If the material is sensitive to high temperatures, the method of reducing the boiling point of water is applied instead, e.g., application of vacuum.

Vaporization is achieved when hot air is flowing over the surface or within the mass of the raw material, at a temperature lower than the boiling point of water. The moisture is transferred to the air from the surface of the material by diffusion, and

the saturation pressure at the surface is lower than the surrounding atmospheric pressure.

In practice, because of the minimum differences, no distinction is made between evaporation and vaporization, and both terms are usually employed to simply indicate the removal of moisture from the surface of a material.

Three main types of drying are generally distinguished, namely osmotic dehydration, physicochemical drying, and thermal drying (Belessiotis and Delyannis 2006).

Osmotic Dehydration This is a special method used to remove large quantities of water and is mainly applied in food and agricultural products to which the technique of the preliminary mechanical dewatering cannot be applied.

Physicochemical Drying This technique of drying consists of the absorption of moisture with hygroscopic substances, such as potassium chloride (KCl), calcium chloride ($CaCl_2$), silica gel, etc. The process is usually complicated and expensive and is primarily used to remove a small amount of moisture from various gases. It is not used for food applications.

Thermal Drying This is the most widespread drying technique. During thermal drying, the moisture content on the surface or within the mass of the solid material is first transformed into water vapor by evaporation or vaporization and then diffused into the surrounding air. When a material is subjected to thermal drying, two parallel processes occur simultaneously (Fig. 1), which are (Belessiotis and Delyannis 2006):

– *Energy transfer* (in the form of heat) from the surroundings to the body in order to evaporate moisture. The heat transfer can take place by conduction, convection, radiation, or any of their combination (see Fig. 1). In most cases, the heat is transferred from the surface to the interior, but there are cases (dielectric drying, microwave, etc.) whereby the heat is generated internally and transferred to the surface.
– *Transfer of moisture* from the interior to the surface of the body and from the solid-gas interface to the drying medium (hot air). The internal humidity content is transferred in all three forms in which it may be present in the solid, namely, the bound moisture, the free moisture, and the vapor form.

The first process (energy transfer) depends only on external factors such as humidity, airflow speed, ambient pressure, and the surface area exposed to drying. The second process (moisture transfer) is a function of the physical state of the solid and the moisture content inside the mass of the product only and will be described in the paragraph on drying kinetics.

Thermal drying as a method is expensive, because it is an extremely energy-intensive procedure, due to the high amount of heat energy required and consumed mainly as enthalpy of evaporation. Therefore, in cases where water is present in greater amounts, drying is preceded by a preliminary partial removal of the moisture by using mechanical separation methods. The mechanical dehydration

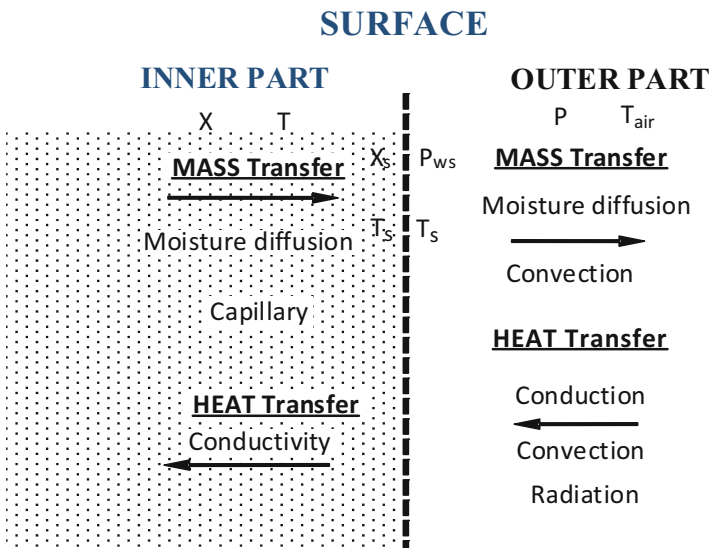

Fig. 1 Internal and external heat and mass transfer processes occurring during drying (Babalis 2006)

techniques involve one or more of the following mechanical separation processes: compression, absorption, filtration, and centrifugation. Those processes are not real drying methods. They can be considered as a pretreatment in order to remove the large quantities of water up to the point where the moisture content can no more be removed mechanically but requires thermal drying methods.

In the case of solar drying, it is assumed that heat is transferred exclusively by convection from the hot airstream flowing parallel to the surface of the product and (or) radiation (sun drying) and moisture is diffused into the product from the interior to the surface from where it is discharged into the hot airstream. The rate at which these phenomena develop is generally conditioning the overall rate of drying.

The drying rate is difficult to be evaluated, because the moisture evaporation rate depends on both internal transport mechanisms and external parameters. Those mechanisms and parameters determine the flow of moisture and therefore control the drying rate. For example, in the large majority of cases of food drying with hot air, the drying rate is controlled within the fruit by the liquid diffusion mechanism, while on its surface by the vapor diffusion mechanism.

Hot air at low relative humidity provides the material with the energy required to evaporate the water and extract water vapor from the surface. In case an adiabatic process is assumed, the temperature of a drying material (being always lower than the air temperature) increases until at a certain time it exceeds the wet-bulb temperature and tends to the dry-bulb temperature of the drying air. This temperature increase cannot be contained within certain values (which are different from

product to product) and when these are exceeded chemical mechanisms appear, acting in parallel, which may lead to the degradation of the product.

From the brief phenomenological description of the drying kinetics discussed above, it is evident that the development of a broad and generic model would require (a) the determination of all moisture transfer mechanisms and (b) the knowledge of the structure and the behavior of the solid. This modeling would take into account both the internal processes and mechanisms of liquid or vapor flow inside the product, as well as the influence of the external conditions on drying rate. These external conditions include temperature, humidity and airflow, the quality attributes of the product, the placing, and eventually the contact between the surfaces of the solids. They significantly affect both the duration of the drying process and the quality of the dried product. The knowledge or the determination of heat and mass transfer coefficients for the particular configuration, the moisture diffusion rate into the product, the thermophysical properties of the drying solid and the sorption isotherms thereof are also necessary. When these are further combined with the ability to accurately forecast the phenomenon of shrinkage, all the major parameters involved in the process would have been identified (Belessiotis and Delyannis 2006).

The investigation of the process and the development of physical and mathematical models, which allow the identification of key characteristics, ensure the quality of dried products. Furthermore, they lay the foundation for the development of optimal design criteria and the dryer evaluation, with emphasis on product quality and energy savings. These, however, will arise only if the mechanical means used for drying follow certain rules and standards. Although the basic operation of the dryer is "just" the removal of part of the moisture from the drying product without deterioration of its quality, a precise determination of the dryer features is required. Thus, high drying efficiency requires (Belessiotis and Delyannis 2006):

- Good knowledge of the flow field inside the dryer and other devices involved (dependence on geometric factors)
- Optimal placement of the product inside the trays and drying conditions (drying kinetics)
- Favorable factors related to the physical texture of the product, its physicochemical characteristics, the geometry, and the external conditions

The drying techniques, i.e., the methods available for removing the water vapor from a solid are distinguished into *natural* and *artificial* ones (Belessiotis and Delyannis 2006):

- *Natural drying* is applied under a free, high-temperature environment, e.g., under the influence of the heat of solar radiation, without movement of the surrounding air but only with the natural flow due to density difference. It is a very slow process, which prevents not only the intermediate control of drying but also the control of the final moisture content and the quality of the material.

The natural drying technique is still used nowadays in some areas for drying agricultural products, e.g., raisins, figs, tomatoes, etc.

– *Artificial or mechanical drying*, depending on the method of removal of the water vapor, is divided into vacuum drying, steam drying, and finally hot-air drying. The latter is the most commonly and widely applied method. The choice of the most appropriate method, and therefore the relevant drying system, requires a detailed knowledge of both the physical, thermal, chemical, and biological properties of the product to be dried and the desired characteristics of the final dry product.

For a good understanding of the characteristics of the material to be dried in a systematic manner, a profound knowledge of the characteristics of the water retained in the material, the conveying mechanisms of water and vapor, as well as the mass and heat transfer properties of the vapor is necessary (Belessiotis and Delyannis 2006).

1.2 Water Bound in Solids

Fresh solid bodies typically contain moisture, either in the form of pure water or as an aqueous salty solution, e.g., natural water or juices. Of great importance, for the course of drying, is the manner in which the water is bound to the solid body. Water may be free, connected, and strongly or moderately bound. In most cases, water is present in the solid mass in one of the following forms (Belessiotis and Delyannis 2006).

Free Water It is the water form in which the molecules are loosely held together and are easily replaced by other water molecules. It is the free moisture which forms, on the outer surface of the solid body, a continuous thin film of water. The water vapor pressure is equal to the water saturation pressure.

Naturally Retained Water It is the form of water contained in the interior of the solid and permanently retained in the pores by means of capillary forces. During drying, this is transferred to the solid surface. The water in the capillary pores is divided into two types: one that is held by the largest pores or open channels, as described above, and the water held within very thin capillaries, whose removal requires increased amounts of energy. The forces retaining water in the larger pores are loose and generally of very small magnitude, thus causing no decrease in water pressure. The water retained in fine capillaries is released the hardest and has a significantly lower pressure than that of free water for the same temperature. In naturally retained water, the moisture molecules are in a relatively loose state within the mass of material or adhere to the molecules of moisture retained in the pore surface. When water is inside the thin capillaries or held by absorption forces, the respective material is characterized as “hygroscopic.” For a hygroscopic body, the pressure is always greater than a minimum value, named the “critical pressure.”

When the capillary pressure is equal to the saturation pressure of the solid, then the body is characterized as "nonhygroscopic." The hygroscopic materials behave as a nonhygroscopic when containing large quantities of water.

Swelling Water It is the water contained in the mass of the solid causing swelling of the solid body. This effect has been observed only in certain materials, e.g., in clay.

Crystalline Water It consists of water molecules which are built into the crystal lattice of the solid material. The crystalline water is strongly bonded to the solid material and requires high temperatures for decomposition and removal. Generally, this decomposition process does not include drying, unless the crystals decompose at low temperature during drying.

Chemically Combined Water It is the water formed during the chemical reactions inside the mass of the solid material, if and when chemical reactions occur during drying at the process temperature. Generally, this is observed in a few, very specific cases of drying.

1.3 Preliminary Definitions

1.3.1 The Moisture Content

Energy is consumed during the drying process mainly in order to transform moisture content (liquid water) into its vapor (2258 kJ/kg at 101.3 kPa). Different formulations for the moisture content can be shown in literature, based either on a dry or on a wet basis, e.g., moisture content in wet (W) basis is the weight of moisture per unit of wet material:

$$W = \frac{m_w}{m_w + m_d} \text{ expressed in kg of water per kg of wet matter} \quad (1)$$

whereas on a dry basis (X), it is respectively expressed as the ratio of water content to the weight of dry material:

$$X = \frac{m_w}{m_d} \text{ expressed in kg of water per kg of dry matter} \quad (2)$$

where m_w is the mass of water and m_d is the mass of dry solid.

The most convenient way to express moisture for mathematical calculations is on a dry basis. For agricultural applications in particular, moisture content normally is expressed on a wet basis.

A more convenient form to express the moisture content both in wet or in dry reference conditions and in nondimensional form is the moisture ratio:

$$MR = \frac{X(t) - X_{eq}}{X_O - X_{eq}} \tag{3}$$

1.3.2 The Water Activity, α_w

Water activity a_w is of great importance for food preservation as it is a measure and a criterion of microorganism growth and probably toxin release, of enzymatic and nonenzymatic browning development, etc. For every food or agricultural product, there exists an activity limit below which microorganisms stop growing. Beuchat (1981) reports that the vast majority of bacteria will grow at around $\alpha_w = 0.85$, mold and yeast at around $\alpha_w = 0.61$, fungi at $\alpha_w < 0.70$, etc. In these cases, water activity is more precisely regulated by means of drying with the addition of some solutions of sugars, starch, etc. Water in food and agricultural crops is in the form of a solution which contains salts, sugars, carbohydrates, proteins, etc. and which is in thermodynamic equilibrium at constant temperature. The water activity is then given by the following equation:

$$\alpha_w = \left(\frac{p_w}{p_w{}^*}\right)_T \approx \varphi \tag{4}$$

where p_w is the partial pressure of water solution and $p_w{}^*$ is the partial pressure of pure water, at the same temperature. φ is the relative humidity of the material at the same temperature.

1.3.3 The Equilibrium Moisture Content

The equilibrium moisture content is the expression of the moisture content when the vapor pressure exerted by the moisture of product equals the vapor pressure of the adjacent ambient air. This means that moisture desorption from the product and the absorption of the ambient-air moisture content is in dynamic equilibrium between them. Relative humidity at this point is therefore known as the *equilibrium relative humidity* and is characterized by the moisture content curves with respect to the equilibrium humidity (known as moisture equilibrium isotherms).

1.4 The Drying Rate Curves

The mechanism of drying, i.e., the complex processes within the mass and on the surface of the material, generally depends on the properties of the material and the

behavior during drying. The moisture loss with respect to time gives the rate or drying, which differs considerably not only from product to product but even for one and the same product at different periods of the drying process. The vapor and water transfer rate in the z direction of evaporation, i.e., the mass transfer rate from the interior of the wet pores, to the surface is given by the following general mass transfer equation (Belessiotis and Delyannis 2006):

$$\rho_{\mathrm{w}}\psi_{\mathrm{T}}\frac{\partial X_V}{\partial t}=\rho_{\mathrm{w}}\psi_{\mathrm{T}}\frac{\partial}{\partial z}\left(\beta\frac{\partial X}{\partial z}\right)+\frac{\partial \dot{m}_v}{\partial z}-\frac{\psi_{\mathrm{T}}(1-X_V)M_v}{R_vT}\left(\frac{\partial p_v}{\partial t}\right) \tag{5}$$

where: X_V	Water content inside the empty space (void) of the entire pores, m^3 water per m^3 of empty pores	[$m^3\ m^{-3}$]
ψ_{T}	Total porosity	[–]
z	Distance, from the surface	[m]
$\dot{m}_v$	Density of the moisture mass flow rate	[$kg\ s^{-1}\ m^{-2}$]
β	Mass transfer coefficient	[$m^2 s^{-1}$]

In the above equation, the term on the left-hand side gives the rate of drying. On the right-hand side, the first term represents the mass transfer rate of water, and the second one represents the mass transfer rate of water vapor (which in dry zones is zero, $\partial mv/\partial z = 0$), while the third term gives the quantity of vapor accumulated within the empty pores. Since the purpose of drying is to determine the moisture reduction rate in a solid, it is assumed that the driving force is the slope of the moisture content $\partial X/\partial z$ (kg moisture per kg of dry material and m). According to Fick's law of diffusion, the moisture flow and the water diffusivity are directly related and their dependence is given as:

$$\dot{m}_v=\rho_{\mathrm{s}}D_{\mathrm{w}}\left(\frac{\partial X}{\partial z}\right) \tag{6}$$

The local moisture reduction rate $\partial X/\partial t$ is given by the equation**:**

$$\frac{\partial X}{\partial t}=\frac{\partial}{\partial z}\left(D_{\mathrm{w}}\frac{\partial X}{\partial t}\right) \tag{7}$$

where:

$\dot{m}_v$	Moisture flow density	[$kg\ m^2\ s^{-1}$]
D_{w}	Diffusivity of water	[$m^2\ s^{-1}$]
ρ_{s}	Density of the solid	[$kg\ m^3$]
X	Water content of the product	[$kg\ kg^{-1}$]
z	Flow direction	[m]

The system of the two relations Eqs. (6 and 7) constitutes the *drying equations*. The above relations are valid for nonhygroscopic materials, for water flow inside

the mass of the material, and for moisture contents $X > X_c$ (moisture at the critical point). The same relations are also valid for hygroscopic materials when moisture content is above the critical value. In case $X < X_c$, simultaneous transfer of water and vapor occurs, by means of diffusion. In parallel with the mass transfer of water and vapor, heat transfer in the z- direction also takes place.

The process of drying is characterized by different time periods where the drying rate is different. In general, three stages or "phases" can be distinguished where the drying rate exhibits significant variations owing to the internal process mechanisms. The first phase (Phase I) is the one of constant drying rate, whereby the surface of the material remains saturated with water and the water flows through the mass smoothly to the surface. At the end of the first phase, the moisture reaches the critical point X_c where the surface begins to no longer be saturated with humidity, and then Phase II begins. Phase II is the phase of decreasing drying rate or of the unsaturated surface drying zone, wherein no sufficient quantity of moisture is transferred from the interior of the mass to the surface, where it can be evaporated; hence, the surface is gradually dried. Finally, Phase III is the phase during which moisture flows from the interior of the solid mass to the unsaturated surface at a decreased rate. This phase mainly refers to hygroscopic materials (Chung and Prost 1967).

In the first curve of Fig. 2, the variation of the material moisture X versus time is given. The segment AB is the time necessary for the material to be heated up to the drying temperature. The segment BC refers to the constant rate of drying, in which the flow of moisture from the interior of the material to the surface is constant, indicating a progressive pressure reduction with the simultaneous emptying of the larger pores. The segment CE refers to the moisture flow rate reduction from the interior to the surface, and it relates to Phase II (first falling-rate period). The internal pressure continues to decrease, and the removal of moisture occurs through the capillaries. Starting from point D and beyond, and despite the fact that there is still enough moisture inside the mass of the material, the flow occurs slowly by diffusion.

The equilibrium is achieved after practically infinite time. The second curve of Fig. 2 depicts the curve of drying rate $(\mathrm{d}X/\mathrm{d}t) = m_v$, versus time t, whereby the difference between constant drying rate (Phase I) and Phase II (falling-rate of drying) becomes evident. The third curve gives the variation of the drying rate with respect to the change of moisture content of the material.

1.4.1 Phase I, Constant Drying Rate

Considering a porous hygroscopic material with high initial moisture content, during drying, as the surface of the solid comes into contact with hot air and heated, a thin layer of free moisture covering the entire surface is initially formed. Due to the concentration difference established between the surface and the interior of the mass, moisture is transferred from the mass to the surface. In case there is sufficient moisture inside the mass, the transfer rate at the surface is equal to the vaporization

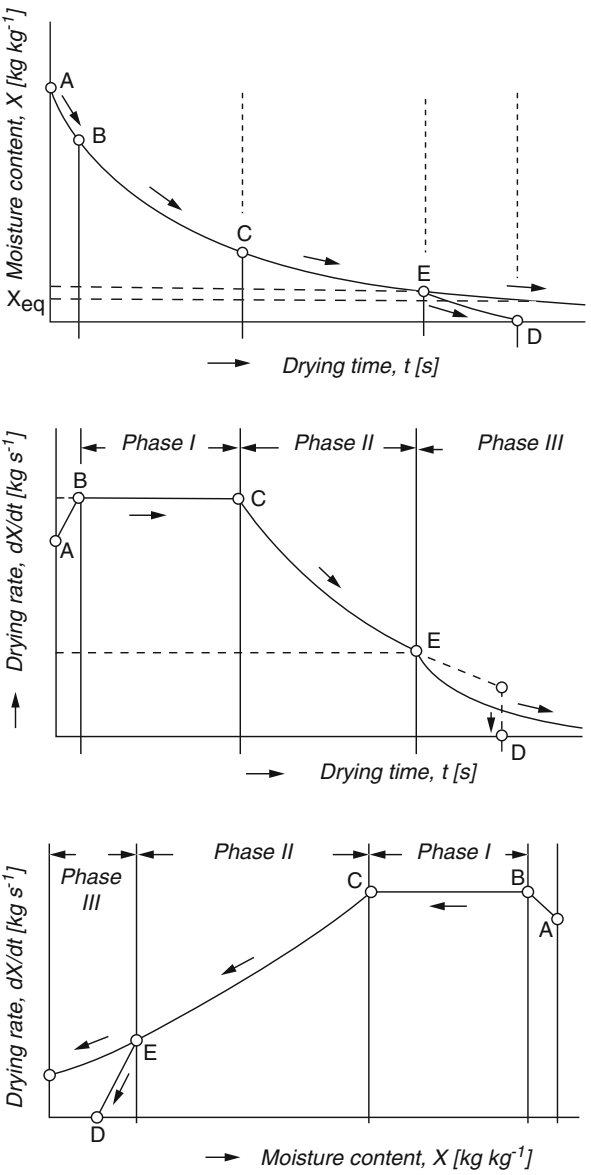

Fig. 2 The drying curves (Belessiotis and Delyannis 2006)

rate from the interface to the air and is stable ($dX/dt = m_v = \text{const}$), provided of course that the inlet velocity, the temperature, and the initial moisture content of the air remain constant. In this phase, the drying rate is controlled by the diffusion of water vapor in the air-humidity interface, and the humidity at the surface remains constant.

During the constant drying period, the vaporization is only a function of the external conditions, and the rate of vaporization is controlled by the diffusion rate

through the thin film of moisture on the surface of the material, i.e., from the humidity difference dX and the thickness of the liquid film s. On the surface, the saturation conditions prevail, and both temperature and drying rate are calculated from the familiar equations of heat (radiation, conduction, and convection) and mass transfer. Inside the mass of the material, only the distribution of moisture changes and during the first phase $X = X_{\max}$ applies (Belessiotis and Delyannis 2006).

1.4.2 Phase II, First Falling-Rate Period

At the end of the constant drying rate, at point C, the surface is no longer saturated with water vapor. The humidity of the material therefore begins to decrease, and moisture is transferred from the interior of the mass of the material to the surface under the action of capillary forces. When the average moisture content reaches a concentration wherein the moisture flow rate from the interior to the surface begins to decrease (with respect to what could have theoretically been vaporized), then the decrease in drying rate begins. The value of the moisture at this point (point C) is called "critical moisture content $X_{\mathbf{c}}$," and the point C is called "turning point." At this point, the thin film is greatly reduced by the vaporization, and on the surface of the material, dry areas are formed. From the critical moisture point C begins the first part of the decreasing drying rate period, i.e., the Phase II, where the drying rate gradually decreases over time (CE segment).

1.4.3 Phase III, Second Falling-Rate Period

From the turning point C and thereafter, drying is no longer dependent on external conditions. It depends only on the capillary properties of the material, since the transfer from the interior of the material occurs only through the capillaries. When all the liquid film on the surface of the material has vaporized, the second part of the decreasing-drying-rate or third phase (Phase III) begins, and a point of inflection E appears. For a hygroscopic material, the point of inflection E occurs when the surface of the material exhibits the maximum hygroscopic moisture $X_{\max}$. This happens for a certain air humidity content that corresponds to the respective point on the sorption isotherm curve. In this second period of decreasing drying rate, for a hygroscopic material, the rate decreases asymptotically with time, and it becomes zero when it reaches the equilibrium point X_{eq}, after infinite time. For nonhygroscopic materials, the drying rate reaches a point wherein the moisture motion becomes zero ($m_{\mathrm{vIII}} = 0$) when $X = 0$, whereby the drying is terminated (point D).

During the third period, the drying rate is controlled by the moisture transfer rate from the deeper layers of the material to its surface, due to the concentration difference. At this point, a particular role is played by the heat transferred from the hot air, which occurs both by convection and by conduction. As the average depth of the moisture front inside the mass increases and the thermal conductivity

of the overlying layers of the dry material are too low, the drying rate is controlled by the heat conduction phenomena. For the nonporous bodies or materials with few or very small pores, the drying rate in Phase III is not controlled by heat conduction but by the increasing resistance to moisture diffusion, both inside the mass and the surface of the material (Belessiotis and Delyannis 2006).

1.5 Sorption Isotherm Curves

The *sorption isotherm curves or moisture sorption isotherms* are those curves that describe the hygroscopic behavior of the product at a certain temperature. A dry product is hygroscopic when containing bound water, with correspondent reduction of the vapor pressure. This property is due to the molecular structure of the material and the extension of its active surface, which differs significantly from one material to the other. The isothermal curves are determined in equilibrium point (equilibrium moisture content) that is the point at which moisture remains unaltered on a dry matter when the drying rate is zero. At this point, the moisture is in equilibrium with the vapor of the surrounding drying air. It is a property of the material that concerns only the hygroscopic material and is independent of the drying process. When a dry material is wetted up to the equilibrium point (water sorption), that is called "sorption," whereas in drying, wherein water is removed from the material, this process is called "desorption." The corresponding isothermal curves that give the variation of moisture content of the material X, with respect to the relative humidity $\varphi = p_v / p_s$ of the material (Fig. 3), for various temperatures are the "sorption isothermal curves" (Belessiotis and Delyannis 2006).

For foods, the drawing of those curves is expressed by the variation of activity α_w (Eq. 4), with respect to the moisture X or W. From the isothermal curves, the equilibrium point during desorption of moisture in the course of drying is verified as well as the respective point during moistening (sorption). Those curves determine the point where, both from an economical as well as material-property of the final product viewpoint, one can or should stop the drying.

In food, sorption isotherms give additional useful information for the dehydration and condensation:

- Describe the ease or difficulty of water removal that is a function of the partial pressure on the surface of the food and of the water binding energy
- Provide the activity to which a product should be after drying the food

1.5.1 The Sorption Equations

The sorption phenomena can be described theoretically by mathematical relations. Most equations do not include the temperature in the sorption properties. Especially for food, a wider application has been found by the BET equation and the GAB equation. The latter, although having a semiempirical form, gives the best results,

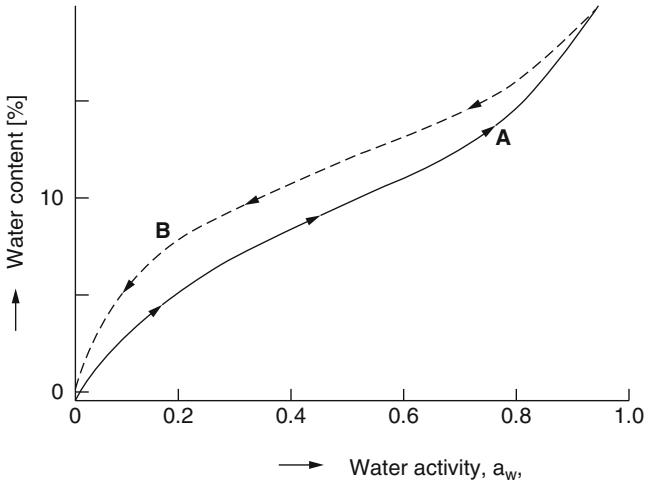

Fig. 3 Sorption isotherms. (**a**): Absorption curve. (**b**): Desorption curve (Belessiotis and Delyannis 2011)

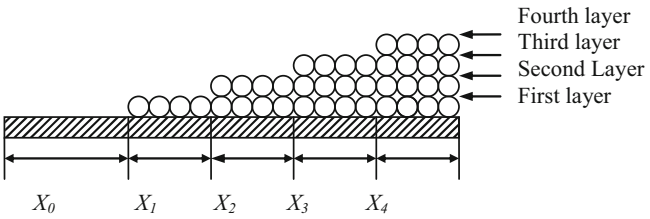

Fig. 4 Schematic model of BET theory (Toei 1996)

and has the widest application. Both these equations are based on the theory of molecular layers of water absorbed onto the materials surface, which is a modification for multilayer absorption of Langmuir's (1918) water molecular monolayer equation:

$$a_w\left(\frac{1}{X}-\frac{1}{X_{mon}}\right)=\frac{1}{C\cdot X} \tag{8}$$

where X is the moisture content at the observation time period, X_{mon} is the monolayer moisture content, and C is Langmuir's constant.

As shown in the schematic model of Fig. 4 (Toei 1996), it is assumed that, with respect to the externally exposed molecules on each layer within the multilayer arrangement, a dynamic equilibrium between Langmuir's adsorption-desorption rates still holds for the exposed molecules on each layer. In the paragraphs below the most commonly used models are presented.

1.5.2 The BET Equation

The BET isotherm equation (Brunauer et al. 1938) is related to the characteristics of sorption curves and is widely accepted for foods. It is assumed that at the internal surface of the hygroscopic pores, upon increase of the pressure, layers of adsorbed water molecules are formed, the thickness of which, s_m, increases. This adsorption theory is called BET (Brunauer-Emmett-Teller) theory. The model of the theory is given in Fig. 21 in chapter "Design Analysis and Studies on Some Solar Drying Systems" and involves four layers of molecules. The BET theory is an extension for multiple molecule layers of the Langmuir theory for single layer of molecules (monolayer).

The equation has the form:

$$\frac{a_w}{(1-a_w)\cdot X} = \frac{1}{X_{mon}\cdot C} + \frac{C-1}{X_{mon}\cdot C}\cdot a_w \tag{9}$$

Chirife and Inglesias (1978) found that for a variety of food, this equation has reliable application over the region of water activity $0.45 < \alpha_w < 0.50$. A modification of the previous equation assuming a number of n layers of absorption and was proposed by Brunauer et al. (1938):

$$X = \left[\frac{X_{mon}\cdot C\cdot a_w}{(1-a_w)}\right]\cdot\left[\frac{1-[n+1]\cdot a_w^n + n\cdot a_w^{n+1}}{1-(C-1)\cdot a_w - C\cdot a_w^{n+1}}\right] \tag{10}$$

1.5.3 The GAB Equation

The GAB (Guggenheim-Anderson-de Boer) equation is the most widely accepted isotherm model as it fits isotherms of products in a range of water activities from $\alpha_w = 0$ up to $\alpha_w = 0.99$ (Belessiotis and Delyannis 2006). It is a variant of the Langmuir-BET theory, specially elaborated for foods. It applies both on fresh products and in dried or modified foods. The GAB equation is considered as the most accepted and well-documented theory for foods and has a wide application in Europe. The biggest advantages of the method may be summarized as follows:

- It has a sound theoretical base.
- It is applicable to sorption curves of all materials having water activity from 0 up to 0.9.
- It has a simple mathematical form with only three parameters and is reliable for calculations.
- Its parameters have a physical meaning.
- It describes the influence of temperature on the sorption curves by an Arrhenius equation.

The three factors of the GAB equation arose independently by the three previously mentioned researchers. It is essentially an extension of the theory of Langmuir and BET and contains three parameters with physical meaning. Mathematically, it is expressed by the following equation:

$$\frac{X}{X_{\text{mon}}} = \frac{C_b \cdot K \cdot a_w}{(1 - K \cdot a_w) \cdot (1 - K \cdot a_w + C_b \cdot K \cdot a_w)} \tag{11}$$

where C_b and K are constants related to the sorption enthalpies. When K is equal to one, Eq. (11) becomes the BET equation.

Singh and Singh (1996) analyzed in detail the validity of the GAB model for isotherms of a variety of food products. They have tabulated the estimated parameters for the GAB model obtained by various authors and compared them with model prediction values from the literature. The values of the coefficients for the GAB equation can be found in literature for several food and other materials (Madamba et al. 1996).

1.5.4 The Bonding Energy

As the temperature increases by keeping the relative humidity constant, the moisture bonding forces are reduced, and at higher temperatures the absorption becomes less intensive. When the material reaches the point of hygroscopicity, the bonding enthalpy of water h_b should be also considered along with the evaporation enthalpy Δh_v. In general, for high moisture contents, the bonding enthalpy is very small (Belessiotis and Delyannis 2006).

The average enthalpy of humidification of the materials, for hygroscopically retained water, ranges from 200 to 370 kJ kg^{-1}, but in general, the bonding enthalpy is not essential to the balance of drying because of its low magnitude. The bonding enthalpy for natural cotton, for instance, is 40–45 kJ kg^{-1}, for wood cellulose is 50–59, and for synthetic fibers is 92–100 kJkg^{-1} of dry material (Belessiotis and Delyannis 2006).

If the sorption isotherms for different temperatures are known, then it is possible to obtain the bonding enthalpy, h_b, or the sorption enthalpy ($h_v + dh_{hb}$) in association with the moisture content of the product. The vapor pressure reduction in the hygroscopic area is achieved by the action of traction stresses in the water:

$$\frac{p_v}{p_s} = \varphi_{eq} = \exp\left(\frac{p_w \upsilon_w}{R_v T}\right) \tag{12}$$

It is therefore possible for any vapor pressure reduction to set a path in the water, whereby the pressure p_w results negative. The previous Eq. (12) is then written as:

$$\ln \frac{p_v}{p_{v-s}} = -\left(\frac{p_w \upsilon_w}{R_v T}\right) \tag{13}$$

h_b	Bonding enthalpy	[kJ kg^{-1}]
p_v	Vapor pressure over the water	[Pa]
p_{v-s}	Pressure of saturated vapor	[Pa]
p_w	Pressure over the water	[Pa]
υ_w	Specific volume of water	[m^3 kg^{-1}]

The differentiation of this equation with respect to temperature, when $p_w \upsilon_w$ depends on temperature, i.e., when X is constant, gives:

$$\left[\frac{d\left(\ln \frac{p_v}{p_{v-s}}\right)}{p\left(\frac{1}{T}\right)}\right]_{X\ =\ \text{const}} = -\frac{p_w \upsilon_w}{R_v} = \frac{h_b}{R_v} \tag{14}$$

From the value of bonding enthalpy, the sorption enthalpy can be estimated if in Eq. (14) the saturated enthalpy of vaporization is added, and therefore:

$$\left[\frac{\partial \ln p_v}{\partial (1/T)}\right]_{X\ =\ \text{const}} = \frac{d \ln p_{v-s}}{d(1/T)} = \frac{p_w \upsilon_w}{R_v} = -\frac{\Delta h_v + h_b}{R_v} \tag{15}$$

Thus, the product $p_w \upsilon_w$ gives the bonding enthalpy of water h_b in kJ kg^{-1}. When plotting the variation $\ln(p_v/p_s) = \ln\varphi$,, with respect to the inverse temperature $1/T$, for constant moisture content, the curves of Fig. 5 are obtained. The lines are drawn for wood and potatoes which are two products with very different properties. Figure 6 gives, for the same materials, the curves of change of bonding energy with the moisture content at different temperatures.

Therefore, if the calculation of the heat of sorption from the curves is required, the bonding heat value must be added to the heat of evaporation of the saturated vapor (Belessiotis and Delyannis 2006).

1.6 Psychrometry in Drying

Air-water vapor data can be translated into a convenient and useful graphic form through the psychrometric charts. There exist some forms of psychrometric charts for air-water vapor mixtures, at equilibrium, especially modified for drying purposes. In Europe and countries following the SI system, the charts are based on humidity-enthalpy coordinates with relative humidity and temperature as parameters. They are known as Mollier charts and are very useful for the prediction of drying. Even though in large conventional drying systems the psychrometric charts have been replaced by direct computer calculations, their use nevertheless still provides a quick and reliable estimation as well as a check for small and medium

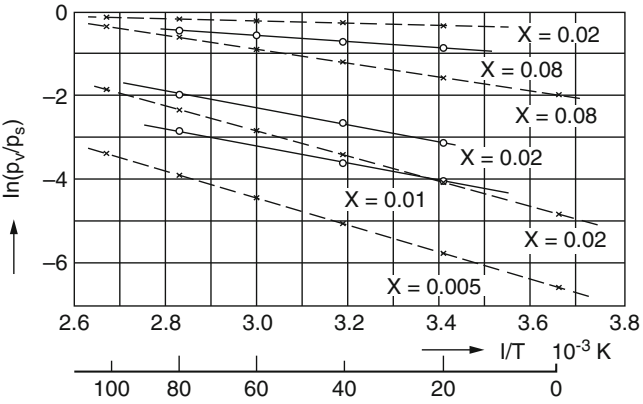

Fig. 5 Determination of the bonding enthalpy using the sorption isotherms. —— Wood. — — Potato (Belessiotis and Delyannis 2006)

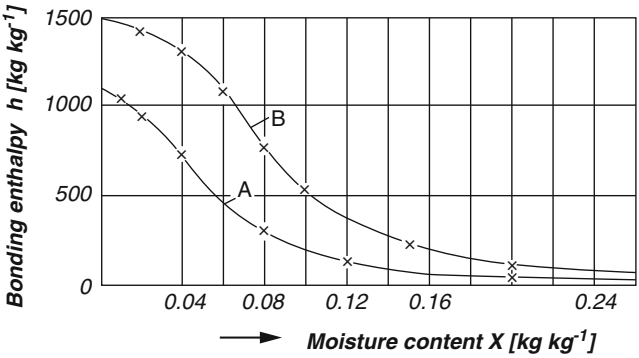

Fig. 6 Curves of variation of bonding enthalpy with respect to the moisture content. (**a**) Wood. (**b**) Potatoes (Belessiotis and Delyannis 2006)

drying installations. They rely on the fact that in drying processes the rate at which water evaporation occurs depends on vapor concentration (humidity) in the surrounding air (Belessiotis and Delyannis 2011).

In drying phenomena particularly, psychrometry is of great importance as it refers to the properties of air-vapor mixture that controls the rate of drying. In any drying process, if an adequate amount of heat is supplied, the temperature and rate at which liquid vaporization occurs will depend on the vapor concentration in the surrounding atmosphere. When a free liquid or wetted surface is present, drying will occur at the saturation temperature, and when accumulated vapor is purged from the dryer environment by using a second gas, the temperature at which vaporization occurs will depend on the concentration of vapor in the surrounding gas.

In effect, the liquid must be heated to a temperature at which its vapor pressure equals or exceeds the partial pressure of vapor in the purge gas. In the reverse situation, condensation will occur. In drying operations, water is the liquid evaporated, and air is the normally employed purge gas. For drying purposes, a psychrometric chart which has been found very useful is the one reproduced in Fig. 7.

Referring to this chart (Belessiotis and Delyannis 2006), the wet-bulb or saturation temperature line gives the maximum weight of water vapor that 1 kg of dry air can carry at the intersecting dry-bulb temperature shown on the abscissa and at saturation humidity.

Enthalpy data are given in terms of kilojoules per kilogram of dry air. Enthalpy at saturation data is accurate only at the saturation temperature and humidity. A given humidity chart is precise only at the pressure for which it is evaluated. Most air-water-vapor charts are based on a pressure of 1 atm. Humidities read from these charts for given values of wet- and dry-bulb temperature apply only at this atmospheric pressure. More detailed presentation could be found in any specialized text for drying or psychrometry, such as in Belessiotis and Delyannis (2006).

2 Mathematical Relations and Modeling of the Drying Processes

2.1 Introduction

A mathematical model is a mathematical analog of the physical reality, describing the properties and features of a real system in terms of mathematical variables and operations. Mathematical models can be classified somewhat loosely, depending on the starting point in making a model, into physics-based and observation-based models. In observation-based models, the starting point is the experimental data from which a model is built. They are primarily empirical in nature. In contrast, the starting point for physics-based models is the universal physical laws that should describe the presumed physical phenomena. Physics-based models are also validated against experimental data, but in physics-based models, the experimental data do not have to exist before the model (Datta 2008). Most of the commonly used physics-based models in food are discussed in Datta (2008), and observation-based models in Sablani (2008).

At an industrial scale, drying is realized in installations – known as dryers – of various types, characterized by either continuous or discontinuous operation. For the design of these apparatuses, it is necessary to know the variation of the drying rate, moisture content, and drying temperature with respect to time. For foodstuffs, like for other materials (e.g., ceramics), it is necessary to know the temperature and moisture distributions over time inside the material. This information is very useful in order to be able to prevent unwanted degradation of the product. The theoretical models simulating drying kinetics and developed in order to face up these

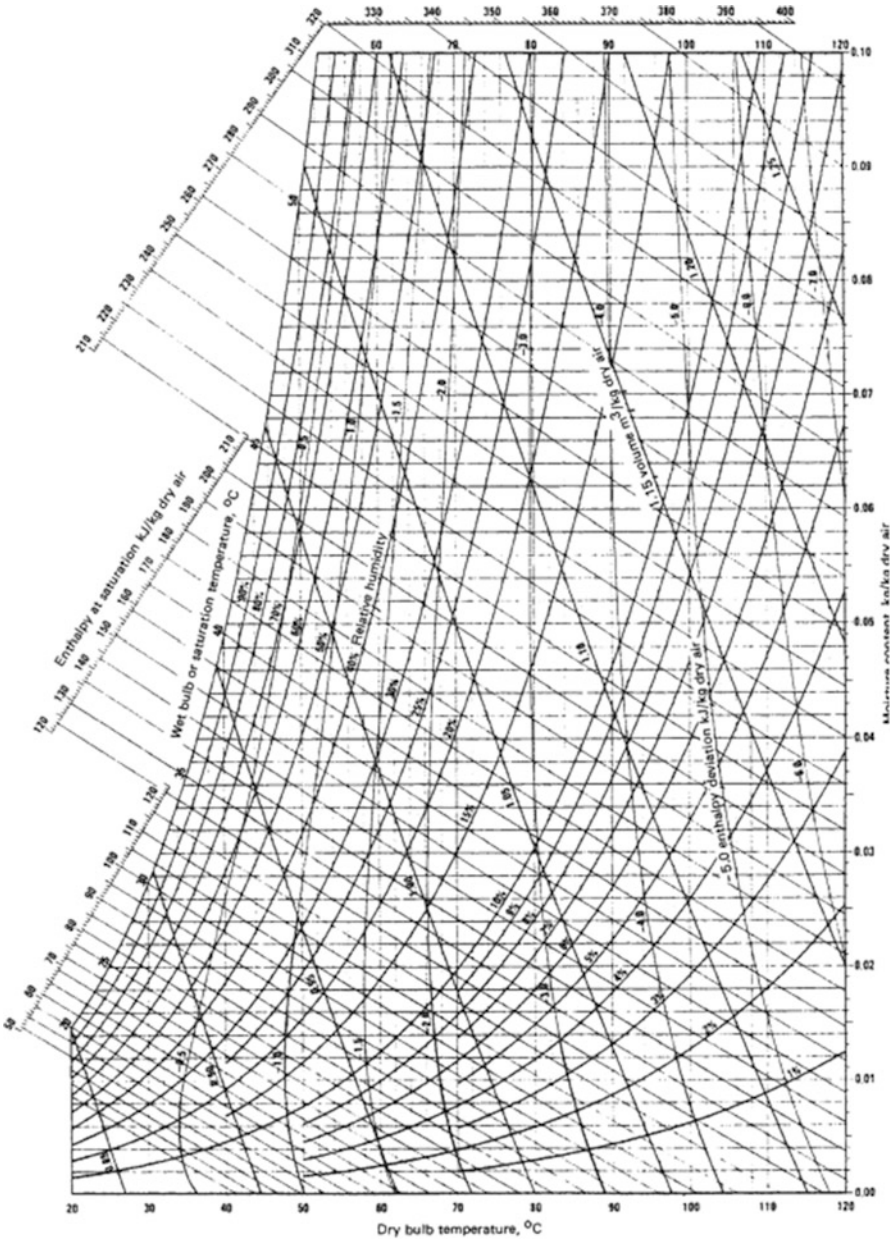

Fig. 7 Psychrometric chart: properties of air and vapor mixtures from 20 °C to 120 °C (Belessiotis and Delyannis 2006)

requirements are focused on the understanding of the mechanisms which act on the material during drying and the prediction of the behavior of the design parameters. They also allow the design of efficient processes ensuring the quality of the final product, as well as the energy planning and economic optimization of equipment and facilities.

The analysis of the process of drying can be done either experimentally or theoretically, assuming a prevailing moisture transport mechanism. In the experimental approach, the drying rate is correlated with the external conditions such as temperature, speed, and relative humidity of drying air. This approach combines the advantage of simplicity with the disadvantages of not allowing extension of the results to other conditions and products as well as the unpredictability of possible qualitative changes. On the other hand, the theoretical approach enables the formulation of heat and mass balance equations inside the material along with the conditions of interaction with the environment (boundary conditions). This approach, although promising, has not yet found a wide application, because of the complexity of the mathematical models on one hand (usually no analytical solutions are possible and the corresponding numerical ones are time consuming and complicated in their implementation), while on the other hand, the parameters of the equations are either not available in the literature or can be determined only experimentally. Moreover, the determination of the physical properties of products is subject to considerable uncertainty due to both the complex structure of the food and the considerable diversification they exhibit, even for one and the same product (Babalis 2006).

Initially, the theoretical models were based on the experimental observation that a large part of biological materials including foodstuffs (also called biopolymers) exhibit a constant drying rate behavior in the early phase, which is then constantly decreasing (Belessiotis and Delyannis 2006). On the contrary, most of the low-initial-moisture agricultural products, such as cereals, are dried with a drying rate that follows a continuously descending curve. In general, the products having medium and high initial moisture content exhibit a drying rate which is constant and then gradually decreasing. The prediction of the drying kinetics is therefore essentially reduced to solving a problem of simultaneous heat and mass transfer in non-steady-state conditions, in order to determine the temperature and moisture distribution within a hygroscopic porous solid exchanging heat and moisture with the environment and with temperature and humidity that are either constant or changing over time. An ideal solution to the problem would involve the general relationship of temperature and humidity with time and position within the solid, along with the relationships describing the thermophysical properties in the product. These theoretical relationships arising from the basic principles of fluid mechanics (as opposed to semiempirical and relationships obtained from experimental results) are generally preferable, since they are applicable to any product with the only requirement of knowledge of its thermophysical characteristics (Babalis 2006).

The theoretical approach to this subject, aiming at successfully predicting the transfer properties inside the product by considering simultaneous heat and mass

transfer processes in porous solids, is extremely diversified. This is mainly due to the large choice of possible internal moisture transfer mechanisms. The transport mechanisms in porous materials most widely found in the literature, as given by Waananen et al. (1993) and Srikiatden and Roberts (2007), are:

- Interdiffusion
- Liquid or gas diffusion
- Knudsen diffusion
- Molecular diffusion (effusion)
- Creeping flows
- Stefan diffusion
- Poiseuille flow
- Evaporation-condensation in the vapor phase for the capillary flow
- Surface diffusion
- Hydrodynamic flow of the liquid phase

The selection of one model is hence complicated, since more than one mechanisms affect and contribute to the process, and, in addition, the relative contribution of each of them may vary during the process. The development of a broad and generic model would require to identify and take into account all of these possible mechanisms. In theoretical descriptions of the phenomenon in which the mechanism of the internal mass diffusion is considered, it is common to distinguish among liquid diffusion, water vapor diffusion, and surface diffusion. For example, the surface diffusion seems to best describe the diffusion of water in solids containing starch.

The majority of perishable foods are dried by arranging the product in the dryer either in a thin layer (single or thin layer) or in deep bed (cereals) which is normally the manner of their storage also. The behavior of the products during drying in each of these two cases is different and delimits the differences in their theoretical approach, therefore also the form of the respective models.

From the form of the equations for each mechanism used to describe the drying process, the models can be distinguished in four main categories (Vagenas 1988):

- Models which make use of *equations of simultaneous heat*, *mass*, *and momentum transfer*, for some specific components (phases) used in thermodynamic phenomena. The models of this most complex category require information which is not always available and when it is, this is based on approximate data adversely affecting the accuracy of the mathematical models.
- Models which include *only mass transfer* and are either based on the mechanism of molecular diffusion in the liquid phase or on the capillary mechanism.
- Models which use *experimental*, *empirical*, *semiempirical*, *or theoretical relationships* (Lewis equations, Page, White, etc.), namely, thin-layer drying models. Usually obtained from experimental results and applying only to the specific case of foodstuff and to the conditions to which they relate.
- *Deep-bed drying models*, used for specific applications of drying.

Several review efforts on various specific and more general issues related to drying have appeared in the literature. Waananen et al. (1993) described the historical development of drying theories and analyzes the mass transfer in the process of drying by convection. In the same work, the basic mechanisms by which the process takes place along with the respective models are also described, giving theoretically their mathematical description. Vagenas (1988) and Vagenas et al. (1990) make a critical review of drying theories as applied to food, while Rossen and Hayakawa (1977) and Katekawa and Silva (2006) presented a review of the different strategies used in the literature to model drying processes in which material shrinkage occurs. Datta (2007) investigating the transport in porous media has synthesized in a systematic and comprehensive way the heat and mass transfer formulations appearing in the food processing literature covering the entire range of formulations starting from the most fundamental to the semiempirical ones.

In the subsequent section, the main aspects of the literature are given, emphasizing on the limitations and shortcomings in respect mainly to food drying.

2.2 *Models Using Equations of Simultaneous Heat and Mass Transfer*

2.2.1 Models Based on Evaporation-Condensation Mechanism

Henry (1948), while investigating the uptake of moisture in cotton, studied the phenomenon of diffusion of a substance through another within the solid pores, which may absorb or desorb part of the diffusing substance. Although this theory was not limited to vapor as an exclusive diffusing substance, in his work and also in all models based on it, moisture is considered being transferred entirely in the gaseous phase. In Henry's theory, simultaneous heat and mass transfer was taken into consideration, assuming that the pores of the solid constitute a continuous free space network within the solid and also that the amount of vapor in the solid varies linearly with concentration of vapor and temperature. The diffusion coefficient was considered to be constant. The relevant relationships were derived from the mass and energy balances, and finally the following form was obtained:

$$\gamma \frac{\partial X}{\partial t} = K_{\mathrm{v}}^{1} \nabla^2 X_{\mathrm{v}} - \frac{\partial X_{\mathrm{v}}}{\partial t} \tag{16}$$

$$\varepsilon \frac{\partial X}{\partial t} = K_{\mathrm{v}}^{11} \nabla^2 T - \frac{\partial T}{\partial t} \tag{17}$$

where $\gamma = \frac{1-w_\alpha}{w_\alpha}\rho_{\mathrm{s}}$, $K_{\mathrm{v}}^{1} = \varepsilon K_{\mathrm{v}}$, $\delta = \frac{h_{\mathrm{fg}}}{\rho_{\mathrm{s}} c_{\mathrm{p,s}}}$, $K_{\mathrm{v}}^{11} = \frac{\lambda_T}{w_\alpha \rho_{\mathrm{s}} c_{\mathrm{p,s}}}$, $\varepsilon = \delta/\alpha$

K_{v} is the vapor diffusion coefficient, X_{v} is the vapor concentration inside the pores, X is the moisture content of the solid, w_α is the volume fraction of air inside

pores, ε is the tortuosity coefficient of the diffusion path, ρ_s is the density of the solid skeleton and $c_{p,s}$ is the specific heat capacity of the solid skeleton, λ_T is the overall thermal conductivity, and h_{fg} the specific evaporation enthalpy of water.

Further enhancement of Henry's scheme was obtained by Harmathy (1969) who developed the theory for the simultaneous heat and mass transfer in a porous solid. The model was based on the evaporation-condensation concept and on the assumption that the various phases inside a porous solid are so finely distributed that macroscopically the whole system can be considered as a single phase. This led to a final system of differential equations that fully describe moisture concentration, temperature, and pressure within the solid during drying and where the capillary flow is not the only mechanism at the beginning of the falling-rate period but coexists with the transfer of vapor by diffusion. The evaporation-condensation mechanism was further developed and used for the solution of problems of drying by Harmathy (1969), Cho (1975), Raj and Emmons (1975), Mikhailov (1975), Willits et al. (1976), Gibson et al. (1979) among others.

The moisture transfer in vapor phase was confirmed by Kuzmak and Sereda (1957a, b) who demonstrated experimentally that in a porous solid, unsaturated in moisture just as in the case of soil, during the moisture transfer caused by a temperature gradient, transfer does not occur in the liquid phase but the flow takes place only in the vapor phase. In case a pressure gradient is present, transfer does also occur in the liquid phase.

2.2.2 Models Based on the Receding Evaporation Front Theory

Evaporation of the moisture during drying of a solid body takes place inside the solid and within a certain depth from the external surface, forming a surface which advances like a moving front. This phenomenon occurs even in the case of the constant evaporation rate, having a significant impact on the heat and mass transfer rate. The phenomenon of the variable evaporation front during drying is extremely important, owing to the internal stresses developed in the dried area and, therefore, an increasing probability of causing cracks in the solid (Handley 1982).

According to this theory, the dried solid is divided internally into two independent regions (Fig. 8). In one of these, the moisture is present in the vapor phase while, in the other, either in the liquid phase alone or in a mixed form (vapor and liquid) (Handley 1982; Chou et al. 1997).

In a porous region ($x > 0$), in which the surface $x = 0$ is at a temperature T_1, wherein T_1 is greater than the evaporation temperature of moisture, the phenomenon is expressed by the following relations:

$$\frac{\partial T_1}{\partial t} = \alpha \frac{\partial^2 T_1}{\partial x^2} \quad X_1 = X_v, \quad \text{with } 0 < x < S, \quad t > 0 \tag{18}$$

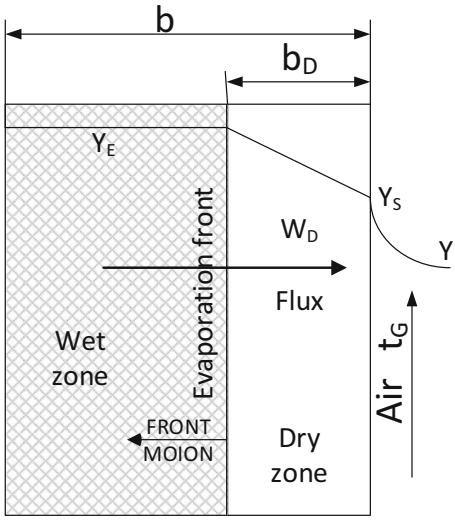

Fig. 8 Diagram of the receding evaporation front (Handley 1982)

where the index 1 denotes the first region and S is the position of the evaporation front. For the second region (denoted with index 2) the following heat and mass transfer relations of apply.

$$\begin{aligned} \frac{\partial T_2}{\partial t} &= \frac{\partial^2 T_2}{\partial x_2^2} + \frac{\varepsilon h_{\mathrm{fg}} c_{\mathrm{p,p}}}{C_{\mathrm{p,b}}} \frac{\partial X}{\partial t} \quad \text{with } S < x < \infty, \quad t > 0 \\ \frac{\partial X_2}{\partial t} &= K_{\mathrm{m}} \frac{\partial^2 T_2}{\partial x_2^2} + K_{\mathrm{m}} \delta \frac{\partial^2 X_2}{\partial x_2^2} \end{aligned} \tag{19}$$

The phenomenon of the moving front was studied by Luikov (1975) and Mikhailov (1975) who obtained solutions for several drying problems using these equations, by applying different boundary and initial conditions and by Handley (1982) who gave the theoretical treatment of evaporation front drying. This phenomenon, referred to as the problem of Stefan, has been studied and applied mainly to inorganic nonhygroscopic bulk porous materials (Handley 1982). In this form, the model does not take into consideration the phenomenon of shrinkage, and the values of the coefficients introduced are difficult to define.

It was proposed (Pakowski 1991, 1999) that the humidity inside a drying solid should not be considered as bonded with the solid structure. With reference to the Fig. 8, moisture in the dry region can be present in a mixed form (vapor and liquid) and in the other region only in the liquid phase. By introducing modified mass transfer coefficients, they assumed that the drying rate on the solid surface is proportional to the difference of the humidities between the surface and air ($Y_{\mathrm{S}} - Y$) and on the evaporation front it is proportional to the difference of the humidities between the dry solid and the surface ($Y_{\mathrm{E}} - Y_{\mathrm{S}}$).

From the above mass transfer relations, the drying rate can be calculated, by taking into consideration that the ratio between the Biot number referred to the total thickness of the body Bi_{mt} and the Biot number referred to the thickness of the dry solid Bi_m is equal to the ratio of the dry solid thickness to the total thickness of the solid. Therefore, and after elaboration, the thickness of the evaporation zone in relation to the moisture content can be expressed in terms of the moisture content of the solid, the equilibrium moisture content, and the moisture content at the critical point as:

$$\frac{X - X_{eq}}{X_{cr} - X_{eq}} = 1 - \frac{b_D}{b} \tag{20}$$

From the above analysis and further elaboration, a relation for the drying rate during the falling-rate period can be finally obtained.

Based on the model presented above, Ratti and Crapiste (1992) proposed and experimentally proved that the position of the moving evaporation front is independent of the drying conditions, the particular geometry of the solid, and the type of solid under drying but it depends only on the moisture content of the solid. They called the ratio b_D/b a "generalized drying parameter" Φ. It is therefore possible to determine the moisture content of the product during drying, by applying Eq. (5), when Φ is known. Based on experimental data for different agricultural products, they suggested the following relation for the determination of the position of the moving receding evaporation front:

$$\Phi \approx C_1 \times \left(\frac{X}{X_0}\right)^{C_2} \tag{21}$$

where the coefficients were determined by applying methods of nonlinear analysis and found to have the values 5.32×10^{-3} and -1.079, respectively.

2.2.3 Models Based on the Principles of Irreversible Thermodynamics (Luikov)

A large part of the theoretical methods approach the simultaneous heat and mass transfer phenomenon considering a predominant driving mechanism for the transport of moisture inside the solid. This hypothesis, apart from the fact that it is completely arbitrary, presents further complications when applied. For foodstuffs, considered as a biological system having a complex structure, the moisture transport can be achieved by many different mechanisms depending on the type of product, the type of bond of moisture, the moisture content, the temperature, the pressure within the pores, etc. Therefore, the assumption that a sole mechanism prevails over all others is, particularly for food, extremely restrictive.

Luikov (1961) first introduced a system of differential equations that describe the simultaneous heat and mass transfer in porous materials and which avoid the limitation of a single driving mechanism being predominant during the mass transfer within the solid. The analysis was based on the principles of thermodynamics of irreversible processes which not only allowed to avoid the idea of some overriding driving mechanism but also introduced the concept of the coupling of the interacting phenomena during the simultaneous heat and mass transfer. The thermodynamics of the irreversible processes was developed on the principles of linearity and Onsager's relation of reciprocity (Osnager 1931a, b; Luikov 1961, 1966).

The principle of linearity, as opposed to the classical theory of molecular transport, accepts that simultaneous heat and mass transfer is determined not only by the action of the respective driving force but also by the action of all the thermodynamic forces acting.

The basic equation of the thermodynamics of irreversible processes

$$\sigma = \frac{\mathrm{d}_i S}{\mathrm{d}t} = \sum_i \mathbf{J}_i \cdot \mathbf{X}_i \geq 0 \tag{22}$$

connects the entropy production rate $\mathrm{d}_i S/\mathrm{d}t$ with the flows $\mathbf{J}_i$ (heat, mass flows, etc.) and the thermodynamic forces $\mathbf{X}_i$ which cause these flows (temperature gradient, concentration gradient, etc.). This relationship results from the known relationship of Gibbs which shows that the entropy of a system which is not in equilibrium is determined by the same independent variables as in equilibrium. Of course, this fact is valid for small deviations from equilibrium. In the case of heat and mass transfer in a capillary porous solid, the vapor and liquid diffusion flows were considered to occur due to both the concentration and the temperature gradients.

The Luikov model is based on the following assumptions:

- The transport of vapor, air, and water takes place simultaneously. (The vapor and air transfer takes place by diffusion and molecular diffusion whereas, when a pressure gradient exists, by filtration). The liquid transport is considered to be achieved by means of the mechanisms of diffusion, capillary absorption, and filtration. All these transfer mechanisms, known under the generic term diffusion, are expressed by relations analogous to Fick's law.
- The phenomena of shrinkage, contraction, and deformation of the solid are not considered.
- No relation between the equations and the sorption isotherms is taken into account.
- The solid is considered to be isotropic.
- The relaxation term is negligible.

After further elaboration by using the mass balance equations, Onsager's relations (Osnager 1931a, b), and by taking into account the filtration flows which occur in the case of intensive heating (above 100 °C) and described by Darcy's law, the

equations known as Luikov's were developed, comprising the following general relations which describe the drying phenomenon:

$$\frac{\partial X}{\partial t} = \nabla^2 K_{11} X + \nabla^2 K_{12} T + \nabla^2 K_{13} P \tag{23}$$

$$\frac{\partial T}{\partial t} = \nabla^2 K_{21} X + \nabla^2 K_{22} T + \nabla^2 K_{23} P \tag{24}$$

$$\frac{\partial P}{\partial t} = \nabla^2 K_{31} X + \nabla^2 K_{32} T + \nabla^2 K_{33} P \tag{25}$$

Here K_{11}, K_{22}, and K_{33} are phenomenological coefficients, whereas the rest are the correlation coefficients. Although moisture content X, temperature T, and pressure P all affect the flow of moisture inside the product, it has been observed that the moisture transfer due to pressure difference becomes important only at high temperatures, which are not of interest for the drying of foods. Therefore, the abovementioned relationships are simplified to:

$$\frac{\partial X}{\partial t} = \nabla^2 K_{11} X + \nabla^2 K_{12} T \tag{26}$$

$$\frac{\partial T}{\partial t} = \nabla^2 K_{21} X + \nabla^2 K_{22} T \tag{27}$$

which find application in many cases of food drying.

From experimental results, it has been observed that temperature and humidity coupling phenomena, for most of the foods, are not significant and considering that even the thermal diffusion effects are insignificant for relatively low moisture content and for temperatures up to 120 °C, Luikov's equations are converted to the relationship:

$$\frac{\partial X}{\partial t} = \nabla^2 K_{11} X \tag{28}$$

In this relation, coefficient K_{11} is no other than the diffusion coefficient D, and, if considered as constant, the above relation can be written as:

$$\frac{\partial X}{\partial t} = D\left(\frac{\partial^2 X}{\partial r^2} + \frac{C}{r}\frac{\partial X}{\partial r}\right) \tag{29}$$

where r is a spatial coordinate within the solid and C is a constant having the value of 0 for a plane symmetry solid, 1 for cylindrical symmetry, and 2 for spherical symmetry of the solid body.

The above relationship can be solved for any regular solid body with the following boundary conditions:

$$X(r,0) = X_{\text{in}} \tag{30}$$

and

$$X(r_0,t) = X_{\text{eq}} \tag{31}$$

where X_{in} is the initial moisture content and X_{eq} is the equilibrium moisture content.

By resolving the above equation with the boundary conditions, the moisture ratio $\text{MR} = (X - X_{\text{eq}})/(X_{\text{in}} - X_{\text{eq}})$ can be expressed analytically for the cases of plane, cylindrical, and spherical symmetry.

For an infinite plane sheet the moisture ratio is given by:

$$MR = \frac{8}{\pi^2}\sum_{n=1}^{\infty}\frac{1}{(2n-1)^2}\exp\left[-\pi^2\frac{(2n-1)^2 Dt}{4x^2}\right] \tag{32}$$

For a cylinder of infinite length:

$$MR = \sum_{n=1}^{\infty}\frac{4}{\lambda_n^2}\exp\left[-\frac{\lambda_n^2 Dt}{4x^2}\right] \tag{33}$$

And for a sphere:

$$MR = \frac{6}{\pi^2}\sum_{n=1}^{\infty}\frac{1}{n^2}\exp\left[-\pi^2\frac{n^2 Dt}{x^2}\right] \tag{34}$$

where λ_n is the roots of the zero order Bessel function, A is the surface, and V is the volume of the solid.

On the contrary, for products of high moisture content (fruits and vegetables), the K_{11} coefficient (diffusion coefficient D) does not have a constant value. The drying of products with high moisture content can be described by expressing the diffusion coefficient as an exponential function of moisture content.

$$D(M) = D_0\exp(\text{p}X), \quad \text{where p is a constant.} \tag{35}$$

When drying products with high moisture content, as discussed in the previous section, a constant-drying-rate period (more or less extended) is preceding the falling-rate one. For the drying process in these cases, it has been proven that this can be divided into three different stages: a first constant-rate period, a first falling-rate period, and a second falling-rate period. Therefore, for each drying period, a different model, based on the above exposed Luikov relations, can be applied. These equations can be solved by taking into account the initial and boundary conditions.

The approach of the thermodynamics of irreversible processes and Luikov's relations have been used in the drying of the products by various researchers, such

as Wang and Brennan (1995), Parti (1990), Sereno and Medeiros (1990), Balaban and Pigott (1988), Mikhailov and Shishedjiev (1975), Luikov (1975), Furuta and Hayakawa (1992), Furuta et al. (1992), Tripathi et al. (1977), Liu and Cheng (1991), Ribeiro et al. (1993), Fortes and Okos (1981a, b, c).

2.2.4 Philip and De Vries' Theory

Philip and De Vries (Philip 1957a, b, c; De Vries 1987) developed, independently of Luikov, a theory to describe the simultaneous heat and mass transfer in porous solids where temperature and humidity gradients are present. Their approach assumed that the water moves inside the solid by the vapor diffusion mechanism and the capillary phenomenon.

Considering the expression for the vapor transfer, including and separating the effects of thermal and isothermal transfer of the vapor and after mathematical elaboration and substitutions, the expression for the total flow of water as the sum of the effects of liquid flow and vapor flow is obtained:

$$\mathbf{J}_{\mathrm{M}} = -K_{\mathrm{m}} \nabla X - K_{\mathrm{mT}} \nabla T - \mathbf{K}_i \tag{36}$$

where

$$K_{\mathrm{mT}} = K_{\mathrm{lT}} + K_{\mathrm{vT}} = \text{total vapour thermal diffusivity, and}$$
$$K_{\mathrm{m}} = K_{\mathrm{l}} + K_{\mathrm{v}} = \text{total moisture isothermal diffusivity}$$

From this equation and applying the continuity equation, a general partial differential equation is obtained, describing the moisture transport in porous solids under the influence of temperature and humidity gradients:

$$\frac{\partial X}{\partial t} = \nabla \cdot (K_{\mathrm{mT}} \nabla T) + \nabla \cdot (K_{\mathrm{m}} \nabla X) + \frac{\partial K}{\partial Z} \tag{37}$$

From the energy balance, the following relation is obtained:

$$\rho_b c_{\mathrm{p,b}} \frac{\partial T}{\partial t} = \nabla \cdot (K_T \nabla T) + h_{\mathrm{fg}} \nabla \cdot (K_v \nabla X) \tag{38}$$

Major limitations in the theory lie in the use of relations which apply only to the region where the capillary phenomenon is present, because only there the assumption of fluid continuity (mass conservation) in the pores is valid. A further disadvantage is also the assumption of negligible shrinkage which is not valid for food products. Generally liquid diffusivities (K_{l} και K_{lT}) become significant at high moisture contents, whereas vapor diffusivities (K_{v} και K_{vT}) become significant at low moisture contents. The Philip and De Vries approach is not used in food materials.

2.2.5 Berger and Pei's Theory

Berger and Pei (1973) expanded the model developed in an earlier work by Krischer. Krischer (Belessiotis and Delyannis 2006) analyzed the heat and mass transfer phenomena for various porous materials. The basic theory of Krischer accepted that during drying, moisture is transferred in the liquid form due to the capillary phenomenon and in the vapor form due to a concentration gradient. The relations describing the theory are:

$$\begin{aligned} \mathbf{J}_{\mathrm{l}} &= -K_{\mathrm{l}}\rho_{\mathrm{l}}\nabla X \\ \mathbf{J}_{\mathrm{v}} &= -K_{\mathrm{v}}\nabla P_{\mathrm{v}} \end{aligned} \tag{39}$$

where K_{l} and K_{v} are the diffusivities of the liquid phase and of the vapor. The term ∇P_{v} is obtained from the equation of the isothermal variation or graphically.

This model has not been applied to biological materials, while Krischer's model was used for various food products by Krischer (Belessiotis and Delyannis 2006).

2.2.6 Whitaker's Theory

Whitaker (Crapiste et al. 1988a, b) developed a theory of heat and mass transfer in porous solids which is based on the expression of heat, mass, and momentum transfer equations for each fluid phase of the material (solid, liquid, and gaseous), by setting boundary conditions at the interfaces between phases.

These phenomena are therefore described by taking into account the internal structure of the product. Thus, transport equations are derived for each phase in the cellular space, the intracellular space, the cell walls, and the air gaps inside the material, applying the continuity conditions at the interfaces and therefore resulting in a system of differential equations for heat and mass transfer.

This approach gives useful information on the moisture and heat transfer mechanisms inside the complex structure of the food, but it is extremely difficult to apply because of the huge number of transfer coefficients and thermodynamic properties absolutely necessary for the full description of the system. The values for the required properties are not only extremely difficult to determine experimentally but also to find them in the literature. Furthermore, this model is based solely on the cellular structure of the food, it neither applies to the case of food products with low moisture content, nor it takes into account the shrinkage of the product.

2.3 Models Involving Mass Transfer Mechanisms Only

2.3.1 Models Based on the Molecular Diffusion of Liquid

Several investigators have proposed the liquid diffusion as the main effective mechanism for moisture transfer into the solid during drying. The relationship describing the liquid diffusion in a solid is the familiar Fick equation:

$$\frac{\partial X}{\partial t} = \nabla(K_1 \nabla X) \tag{40}$$

This relationship has been used extensively to solve the moisture transport problems by making various assumptions about the values of key parameters involved (such as fixed or variable diffusion coefficient, isotropy or not for the solid, various boundary conditions, etc.). The analytical solution of the moisture diffusion equation, because of the simplicity of its form, has been met with the preference of most scholars and has been widely used in mass transfer problems in various foodstuffs and cereals.

An extensive analysis of the diffusion equation for drying of solids of different geometry (spherical, cylindrical and parallelepiped shape), providing analytical and numerical solutions with different boundary conditions and for various problems, can be found in all classic works on heat and mass transfer (f.e. Mikhailov 1973).

The principle of diffusion as the one and only moisture transport mechanism has received severe criticism. In practice, when using a diffusion coefficient corresponding to the average measured value of the moisture content significant discrepancies do often arise between the calculated and the experimental values. For this reason, a variable diffusion coefficient is proposed, the results of which are significantly improved when used. The diffusion coefficient can take either the form of a relation linearly dependent of the temperature (or even of the concentration) or the form of the Arrhenius equation:

$$K_1 = K_{10} \exp\left(-\frac{E}{RT}\right) \tag{41}$$

Even when the results of the diffusion equation might agree well with the experimental values for the drying of some solid, the problem of physical interpretation may still remain. Answers to the problem of the physical interpretation of the observed deviations from Fick's relationship (dependence of the drying rate on the thickness of a drying solid) have been given by Vaccarezza and Chirife (1978), who took into account the heat transfer accompanying mass transfer and by Vaccarezza and Chirife (1975) who considered the dependence of the diffusion coefficient on the concentration of the dissolved sugars (Saravakos and Charm 1962).

The view of diffusion as the only moisture transfer mechanism during drying is considered by many researchers as erroneous and misleading, as it quite often gives

inconsistent results. The only reason for its relative acceptance is that the solution of the diffusion equation yields a logarithmic behavior which is similar to that of the experimental drying. The same approach and the same problems in the prediction of drying kinetics were followed by Ben Mabrook and Belghith (1995), Walton and Casada (1986), Sokhansanj and Bruce (1987), Walton et al. (1988), Cordova-Quiroz et al. (1996), Simal et al. (1996), Sakai and Hayakawa (1992), Jun Wan and Langrish (1995), Alvarez and Legues (1986), Shusheng et al. (1993), Dutta et al. (1988), Parti and Dugmanics (1990), Dincer and Dost (1995), Lago et al. (1971), van der Zanden et al. (1996), and Kumar et al. (1982). Babbit (1949) considers pressure as the driving mechanism of moisture diffusion during the drying of a solid rather than the moisture concentration. The relationship between pressure and humidity is rarely linear due to the adsorption and desorption phenomena. The models based solely on the concentration gradient should be avoided because they do not separate the diffusion from the other driving mechanisms that act simultaneously. Sherwood has demonstrated experimentally that moisture transport is possible even against the concentration gradient. However, it is not possible for anybody to deny the existence of the liquid diffusion phenomenon. More recent theories consider Fick's law of diffusion as a representative only when moisture and vapor transport are both present. Therefore, liquid diffusion should not be considered as the sole mechanism for transporting moisture at all stages of drying. In such a case, it would have been as if we considered the liquid diffusion as an isothermal process having very small temperature differences within the solid. Besides that, theories making use only of the diffusion mechanism do not take into account phenomena such as shrinkage, hardening, and sorption isotherms. In this case, the physical meaning of the diffusion coefficient is either nonexistent or interpreted as a value encompassing all phenomena and depending on both temperature and concentration.

2.3.2 Models Based on the Capillary Mechanism

The capillary phenomenon refers to the flow of a liquid into the interstices and on the surface of a solid due to the molecular attraction between the liquid and solid. The analysis of this phenomenon was made by Buckingham who also introduced the concept of "capillary force" as the driving force of capillary flow.

The capillary potential Ψ is the pressure difference between the water and air in the water-air interfaces within the capillaries or pores. The curvature of the interface is caused by the surface tension of water. The relationship for capillary liquid flow is given as:

$$J_l = -\lambda_H \nabla \Psi \tag{42}$$

where λ_H is the unsaturated hydraulic conductivity and Ψ is the capillary potential.

In isothermal conditions, the capillary potential is usually considered to be proportional to the moisture concentration gradient. During drying of granular

solids, water flow is totally dependent on the capillary forces developed and is thus independent of the moisture concentration. It was shown experimentally that moisture flow is possible even in a direction opposing the concentration gradient. Miller explains the phenomenon by considering the vapor pressure gradient as the driving force, given that both the surface tension and the flow of a fluid are dependent on the pressure. The vapor pressure is then proportional to the moisture content in the case of homogeneous material only when considering shrinking and hardening forces of the solid as negligible. The water inside the interstices of the solid, as a liquid which wets the surface and as free water inside cells, is transferred both by gravity and by capillarity through continuous passages present in this solid. Therefore, the above relationship of capillary fluid flow may be applied during drying only for the water that is not related to the solution, for water over its saturation point, and for water over the moisture equilibrium point in a saturated atmosphere.

Practically, it has been shown that capillary flow is not the main moisture transport mechanism for food products (Saravakos and Charm 1962). In the drying of food, capillary flow, along with molecular diffusion, is considered by many researchers to be one of the main moisture transport mechanisms only at the phase where the moisture content is high. This is true for the early phases, but it is doubtful if this mechanism has a significant contribution at the later phases of drying as well.

The capillary flow phenomenon has been adopted successfully by Philip (1957a, b), Luikov et al. (1974), Schadler and Kast (1987), Dietl et al. (1995), Yu et al. (1993), Berger and Pei (1973), Chen and Pei (1989), Fortes and Okos (1981a, b, c).

2.4 Models Based on Theoretical, Semi-theoretical, or Empirical Relations (Thin-Layer Drying Models)

Simulation models of the drying process based on semi-theoretical or even fully empirical relationships have been widely used for designing new and improving existing drying systems predicting the airflow over the product or even for the control of the process (Karathanos and Belessiotis 1997; Mathioulakis et al. 1998; Karathanos and Belessiotis 1999; Xia and Sun 2002). Besides that, a deep knowledge of the transfer parameters (heat and mass transfer, diffusion and thermal conductivity coefficients) and the drying behavior of the particular product to be dried are considered indispensable for the optimization of the drying performance achieved through simulation models. For this purpose, a sufficiently accurate model is required, capable of predicting the water removal rates and describing the drying performance of each particular product under the common conditions used in normal commercial relevant facilities. The parameters of the model used by the simulation algorithms (transfer coefficients, drying constants, etc.) are directly

related to the drying conditions, i.e., temperature and velocity of the drying medium inside the mechanical dryer.

Several researchers have investigated the drying kinetics of various agricultural products in order to evaluate different mathematical models for describing the thin-layer drying characteristics of specific products. Chhinnan (1984) evaluated mathematical models for drying of in-shell pecans. Byler et al. (1987) applied statistical methods in thin-layer parboiled rice, drying models, and the two-component thin-layer model was applied for unshelled peanuts (Colson and Young 1990). Muhidong et al. (1992) have studied the thin-layer drying of kenaf, while the low-temperature moisture transfer characteristics of wheat in thin layers was reported by Sun and Woods (1994). The thin-layer drying characteristics of rough rice at low and high temperatures were investigated by Basunia and Abe (2001), while those of Taxus clippings by Hansen et al. (1993) and of grapes by Tulasidas et al. (1993). Recently Rapusas and Driscoll (1995) investigated the thin-layer drying characteristics of onion, and Sawhney et al. (1999b) determined the relevant drying constants. Other researchers investigated the thin-layer drying characteristics of garlic (Madamba et al. 1996, and Vasquez et al. 1999), Thompson seedless grapes (Sawhney et al. 1999a), sultana grapes (Yaldiz et al. 2001), black tea (Panchariya et al. 2002), red pepper (Doymaz and Pala 2002), prickly pear fruit (Lahsasni et al. 2004), and figs (Babalis and Belessiotis 2004, Babalis et al. 2006). Finally, Chukwunonye et al. (2016), Ertekin and Firat (2015), Kumar pandey et al. (2015), Kucuk et al. (2014), Erbay and Icier (2009), Sander (2007), and Jayas et al. (1991) gave comprehensive reviews of experimental and empirical relationships routinely used to describe the behavior of certain foods during drying by means of the form of the drying curve.

The transport of water during the food dehydration process takes place predominately in the falling-rate period (Sharaf-Eldeen et al. 1979). This is controlled by the liquid diffusion mechanism and can be described by Fick's second law, when radial diffusion is considered. The analytical solution of Fick's equation for various geometries (sphere, cylinder, rectangular plate) was used by many researchers for describing the drying phenomena of various foodstuffs.

The thin-layer drying models, describing the drying process, can be distinguished in three main categories, namely, the *theoretical*, the *semi-theoretical*, and the *fully empirical* ones (Sharaf-Eldeen et al. 1979). The major difference between these groups is that while the theoretical models suggest that the moisture transport is controlled mainly by internal resistance mechanisms, the other two consider only external resistance.

The *semi-theoretical models* are derived directly from the general solution of Fick's law by simplification. The *empirical models* are derived from statistical relations, and they directly correlate moisture content with time, having no physical connection with the drying process itself. These types of models (empirical and semiempirical) are valid in the specific ranges of temperature, air velocity, and humidity for which they are developed.

The basic equation, most commonly used to describe the thin-layer drying process, is similar to Newton's law for cooling, incorporating a single drying

constant (k) for the combined effect of the various transport phenomena present. It was first suggested by Lewis (1921) and has the general form:

$$\frac{\mathrm{d}X}{\mathrm{d}t} = -k\left(X - X_{\mathrm{eq}}\right) \tag{43}$$

Assuming that the bulk moisture content (X) depends only on time and the resistance to the flow of moisture is concentrated only on the superficial layer of the product, the solution of Eq. (1), called *the Lewis equation*, is obtained by integration (Sawhney et al. 1999a, b; Pahlavanzadeh et al. 2001; Azzouz et al. 2002) as:

$$MR = \frac{\bar{X}(t) - X_{eq}}{X_0 - X_{eq}} = \exp(-k \cdot t) \tag{44}$$

In this equation and in what follows, the moisture ratio (MR) is introduced, as the dimensionless form of moisture content. X_0 is the initial moisture content. The moisture ratio determines the unaccomplished moisture change, defined as the ratio of the free water still to be removed, at time t over the initial total free water. The term X_{eq} determines the *equilibrium moisture content*, being the value of the drying curve to be asymptotic, and is also known as *dynamic equilibrium moisture content* or *effective surface moisture content*. This has typically a value which is higher than the value encountered in praxis, but it yields good modeling results, and, for this reason, it is used by many researchers.

Various researchers (Hustrulid 1963; Becker and Sallans 1955) demonstrated that for large drying periods and for spherical objects, the higher-order terms of the above equation can be neglected and the moisture diffusion relation is then transformed into:

$$MR = \frac{6}{\pi^2}\exp(-\pi^2 Fo_{\mathrm{m}}) \tag{45}$$

where $Fo_{\mathrm{m}} = \frac{D \cdot \mathrm{t}}{R^2}$ is the nondimensional Fourier number for the mass transfer.

The accuracy of the solution of the liquid diffusion equation is:

$$\frac{\partial X}{\partial t} = D \cdot \left[\frac{\partial^2 X}{\partial r^2} + \frac{2}{r}\frac{\partial X}{\partial r}\right] \tag{46}$$

as given by the classical relation:

$$MR = \frac{\bar{X}(t) - X_{eq}}{X_0 - X_{eq}} = \frac{6}{\pi^2}\sum_{n=1}^{\infty}\frac{1}{n^2}\exp\left(-n^2\pi^2\frac{D \cdot t}{r_o^2}\right) \tag{47}$$

which is good enough only for products having spherical form. Therefore, when considering the possible errors in the measurement of the dimensions of the

"spherical" material, the diffusion coefficient, and the equilibrium moisture content, the total error when using this equation as a solution to the diffusion equation depends on the number of terms retained in Eq. (46). Jaros et al. (1992) presented a method for determining the number of terms required in order to minimize these errors when calculating the average moisture content by means of this relation.

A similar approach is the one reported by Henderson and Pabis (1961):

$$MR = a \cdot \exp(-k \cdot t) \tag{48}$$

demonstrating that it is possible for the drying coefficient k to be related with a coefficient of effective diffusion D and an equivalent radius of the product R, through the relation:

$$k = D \cdot \frac{\pi^2}{R^2} \tag{49}$$

and therefore the relation is transformed in:

$$MR = \frac{6}{\pi}\exp(-Kt) \tag{50}$$

The same researchers developed the following Arrhenius type equation between the drying coefficient k and the drying air temperature:

$$K = f_0 \exp\left(-\frac{f_1}{T_{\text{abs}}}\right) \tag{51}$$

where f_0 and f_1 are coefficients depending on the product and T_{abs} is the absolute temperature.

Due to its simple form, relation Eq. (44) is widely used for drying simulation purposes even if it cannot describe all three phases of drying. Noomhorm and Verma (1986) used only two terms of the equation to describe the drying of rice, whereas Sharaf-Eldeen et al. (1980) presented the two-term exponential model for the drying of corn seeds:

$$MR = a \cdot \exp(-k_0 \cdot t) + b \cdot \exp(-k_1 \cdot t) \tag{52}$$

Page (1949) introduced the homonymous thin-layer drying equation for shelled corn:

$$MR = \exp(-k \cdot t^n) \tag{53}$$

with k and n being drying-air-temperature and dew-point depended parameters. In this equation, the parameter n is time dependent in order to simulate the experimental data, and K and n were expressed as functions of drying temperature and wet-bulb temperature. The same equation was also used for other grains by many

researchers (White et al. 1981; Jayas and Sokhansanj 1989; Singh et al. 1983a, b, Bruce and Sykes (1983). Misra and Brooker (1980) collected a large amount of thin-layer drying data in order to determine the value of the Page equation parameters for different products. They found that k is strongly dependent on the drying air temperature and speed, whereas n respectively on the relative humidity of air and the initial moisture content of the product.

The Page Eq. (53) describes more accurately drying data compared to Lewis Eq. (43), as demonstrated by Bruce and Sykes (1983). When differentiating the Page equation with respect to time, the following equation is obtained:

$$dX = -nKt^{n-1}\left(X - X_{eq}\right) \tag{54}$$

Here it is clear that the drying rate is not only dependent on the moisture content, as stated by Lewis, but also on the drying time.

Overhults et al. (1973) demonstrated that the following relation, derived from the basic Page relation, is more appropriate for describing drying data in comparison to the very similar Page equation:

$$MR = \exp[-(k \cdot t)^n] \tag{55}$$

where k και n are obtained by the following relations:

$$n = \beta_3 + \beta_4 T_a \quad \text{and} \quad \ln K = b_0 + \frac{b}{T_a} \tag{56}$$

White et al. (1981) used this model for soy beans with initial moisture varying from 24% up to 30%, air temperature from 30 up to 70 °C, and wet-bulb temperature from 8 °C up to 38 °C. From this study, it was demonstrated that in a large number of tasks, the drying simulations using this model a very good agreement with the experimental drying data was obtained.

A number of variations of the basic equation (Eq. 43) are also reported. Togrul and Pehlivan (2004) introduced the logarithmic model for fruits:

$$MR = a \cdot \exp(-k \cdot t) + c \tag{57}$$

where α and c are constants which depend on the model. Page (1949), introduced a modified Page equation:

$$MR = a \cdot \exp[-(k \cdot t^n)] \tag{58}$$

All the above relations Eqs. (53, 55, 57, and 58) are of the exponential form and have a certain theoretical foundation. Besides those, a number of purely empirical relations for the modeling of the behavior of products during drying have been proposed (Paulsen and Thompson 1973; Wang and Singh 1978; Troeger and Hukil

1971; Roa et al. 1977; Pabis 1967; Byler et al. 1987). Wang and Singh (1978) suggested the following relation for the intermittent drying of rough rice:

$$MR = 1 + a \cdot t + b \cdot t^2 \tag{59}$$

Purely empirical models, directly relating moisture ratio and drying time but incorporating parameters with no physical meaning, are also reported by Thompson et al. (1968) for shelled corn:

$$t = a \cdot \ln MR + b \cdot (\ln MR)^2 \tag{60}$$

where a and b are coefficients related to the air temperature and have different values for each product, being evaluated only experimentally.

Finally, model based on the Weibull distribution has also been introduced and evaluated (Babalis 2006; Babalis et al. 2006):

$$\mathrm{MR} = a \cdot b \cdot \exp[-(k \cdot t^n)] \tag{61}$$

The main drawback of these relations is the fact that although they provide an accurate description of the kinetics of drying, even if empirical, they do not provide any information about the internal temperature of a material during drying because they consider that the temperature of the material is equal to the air temperature right from the beginning of the process. In case this assumption is used in dryer design, it is likely to lead to product deterioration. Nevertheless, a wide use of relations of this type is still being made, due to their simplicity.

On the contrary, for the description of the temperature variation with respect to time, Newton's law is widely used:

$$\frac{\mathrm{d}T_\mathrm{p}}{\mathrm{d}t} = \frac{h_\mathrm{g}\alpha\left(T_\mathrm{a} - T_\mathrm{g}\right) + \rho_\mathrm{p}\frac{\mathrm{d}X}{\mathrm{d}t}\left[h_\mathrm{fg} + c_{\mathrm{p,v}}\left(T_\mathrm{a} - T_\mathrm{p}\right)\right]}{\rho_\mathrm{p}\left(c_{\mathrm{p,p}} + c_\mathrm{pw}X\right)} \tag{62}$$

The specific surface α is the surface of the product contained in a unitary volume and is calculated considering the geometric form of the material or even experimentally. For the mass transfer coefficient h_g, several empirical relations have been proposed (Pabis 1967). Sokhansanj and Bruce (1987) compared six of those relations and concluded that the one proposed by Gamson et al. (1943) gives the best results:

$$h_\mathrm{g} = 0.00327G/\left(\mathrm{Re}^{0.65}\mathrm{Pr}^{2/3}\right) \tag{63}$$

where $\mathrm{Re} = \mathrm{G\ L}/\mu$ and $\mathrm{Pr} = \mathrm{C_{p,a}}\ \mu/\lambda$ are the well-known nondimensional numbers. Many alternative relations have been suggested but all of the same form of the Eq. (62) (Parry 1985).

Many other relations, most of them based on the above reported models, have been used by researchers and applied in different solids and agricultural products. Sharaf-Eldeen et al. (1979) reported an extensive list of the relations used in drying, and Jayas et al. (1991) presented relationships commonly applied in practice, reporting the values of the coefficients for each product. An extensive review of those models used in agricultural products was reported by Ertekin and Firat (2015). The most frequently used of the newly developed mathematical models for thin-layer drying of fruits and vegetables in the past 10 years are reported by Onwude et al. (2016), giving also relationships between model constants and process conditions.

Kucuk et al. (2014) reviewed a total of 67 models, selected and classified under 28 performance assessment criteria for comparison purposes. These models are then evaluated by considering the following parameters: (1) product type; (2) pretreatment type; (3) drying parameters, such as temperature, air velocity, layer thickness, microwave power levels, amount of solar radiation, vacuum pressure, frequency of sound wave, excitation amplitude, relative humidity, bed depth, product shape, pH, salt content, absolute pressure, etc.; and (4) drying method employed. Furthermore, the best models obtained are employed for product drying applications and compared for different drying methods, drying parameters, and dried products.

Erbay and Icier (2009) studied the general modeling approaches for food drying and reported the most widely used or newly developed thin-layer drying equations. Chukwunonye et al. (2016) gave a review of the thin-layer drying models with particular application to some farm products in Nigeria. Hedayatizadeh and Chaji (2016) gave a review of thin-layer drying models for plum drying, while Pereira da Silva et al. (2014) gave the mathematical models to describe thin-layer drying and to determine drying rate of whole bananas.

2.5 Deep-Bed Drying Models

Mathematical models investigated so far were related to drying of individual products fully exposed to air or arranged in a thin layer. This method of drying is applied only to a product when initial moisture content is high. On the contrary, products having low initial moisture content, including most of grains, are usually dried in large quantities, and it is therefore preferable to dry them in the form of a deep bed, which usually takes place directly inside the storage silo (Parry 1985).

2.5.1 Logarithmic Models

The first logarithmic model proposed, basically being an empirical method for modeling drying at low temperatures, was suggested by Hukill (1954). In this model, the following assumptions were adopted: (1) the enthalpy of evaporation

of moisture of the product is much larger than the sensible heat required for the heating of product and the removal of moisture; (2) during the drying process, when moisture is transferred to the air, the increase of sensible heat is negligible; (3) the density of the product is constant; and (4) during the process, the temperature of the drying air and the product are in equilibrium.

Based on these hypotheses, Hukill (1954) proposed the following relations (Parry 1985):

$$G_{\mathrm{a}} c_{\mathrm{p,a}} \frac{\partial T}{\partial y} = \rho_{\mathrm{p}} h_{\mathrm{fg}} \frac{\partial X}{\partial t} \tag{64}$$

where G_{a} is the airflow rate. The solution of this equation is given by (Parry 1985):

$$MR = \frac{2^{D'}}{2^{D'} + 2^{Y'} - 1} \tag{65}$$

where D' and Y' are nondimensional variables representing the depth and the time and are given by (Parry 1985):

$$\begin{aligned} D &= \frac{h_{\mathrm{fg}} K \rho_{\mathrm{g}} (X_0 - X_{\mathrm{eq}}) y}{G_{\mathrm{a}} c_{\mathrm{p,a}} (T_{\mathrm{a}} - T_{\mathrm{p}})} = D' \ln 2 \\ Y &= K \cdot t = Y' \ln 2 \end{aligned} \tag{66}$$

where T_{a} is the air temperature inside the drying chamber (plenum) and T_{g} is the air temperature at the exit. Using this logarithmic scheme and applying the boundary conditions, Barre proposed the following relation for the moisture ratio:

$$MR = \frac{1}{D} \ln \left(\frac{\mathrm{e}^{D} + \mathrm{e}^{Y} + 1}{\mathrm{e}^{Y}} \right) \tag{67}$$

The above mentioned models were subjected to thorough investigation by many researchers, who compared their results with experimental ones, and it was concluded that logarithmic models fail to describe the kinetics of the variable evaporation front inside of the solid.

2.5.2 The Partial Differential Equations Model

The models of partial differential equations are simply a set of equations used to describe the process of drying. These models, initially developed for high temperatures, when applied to low temperatures, gave more accurate results in comparison with the logarithmic ones.

For the development of the model, the following assumptions were adopted:

(1) During drying, the phenomenon of shrinkage is negligible.
(2) Heat transfer by conduction is negligible.
(3) Inside the solid body the temperature gradient is negligible.
(4) The airflow field around the dried product is considered to be representative of a bluff body flow.
(5) The side walls of the chamber are adiabatic and have negligible heat capacity.
(6) For short intervals the thermal conductivity of the product and of the moist air remain constant.
(7) Isothermal moisture equilibrium curves and drying curves in a thin layer are known (Parry 1985).

By applying the principles of heat and mass transfer, four partial differential equations are generated, considering the heat and mass exchange in an incremental layer which is located anywhere on the drying bed and having a unit cross-sectional area and depth (x, x + δx) by a time interval (t, t + δt).

Mass Balance
The moisture loss of the product is equal to the sum of the moisture extracted by the airflow, plus the change of the humidity of the air which is still present in the elementary layer void volume (Parry 1985):

$$G\frac{\partial Y}{\partial x} = -\rho_p \frac{\partial X}{\partial t} - \varepsilon\rho_{\mathrm{a}} \frac{\partial Y}{\partial t} \tag{68}$$

Energy Balance of the Air
The heat transferred by convection to the product is equal to the sum of the enthalpy transferred from the airflow outside the elementary layer and the variation in time of the air enthalpy which lies inside the void space of the elementary layer (Parry 1985):

$$\begin{aligned} G\left(c_{\mathrm{p,a}} + c_{\mathrm{p,v}}Y\right)\frac{\partial T}{\partial x} = {} & \rho_{\mathrm{p}} c_{\mathrm{p,v}}\left(T - T_{\mathrm{p}}\right)\frac{\partial X}{\partial t} - h_{\mathrm{a}}\left(T - T_{\mathrm{p}}\right) \\ & - \rho_{\mathrm{a}}\varepsilon\left(c_{\mathrm{p,a}} + c_{\mathrm{p,v}}Y\right)\frac{\partial T}{\partial t} \end{aligned} \tag{69}$$

Energy Balance of the Product
The transferred energy by convection from the heated air to the product is the sum of the sensible heat needed to raise the product temperature of the dry product, plus the moisture and enthalpy of vaporization of the product moisture. Therefore, from the balance of enthalpy on the product (Parry 1985):

$$\rho_{\mathrm{p}}\left(c_{\mathrm{p,p}} + c_{\mathrm{p,w}}X\right)\frac{\partial T}{\partial t} = h_{\mathrm{a}}\left(T - T_{\mathrm{p}}\right) + h_{\mathrm{fg}}\frac{\partial X}{\partial t}\rho_{\mathrm{p}} \tag{70}$$

Drying Kinetics Equation of the Product

In order to determine the drying rate as a function of the air and product temperature as well as of the absolute humidity, any thin-layer drying relation can be used:

$$\frac{\mathrm{d}X}{\mathrm{d}t} = -k\left(X - X_{\mathrm{eq}}\right) \tag{71}$$

In any case, however, the adoption of this relation is a point of uncertainty that complicates the solution of the model.

In the abovementioned four partial differential equations, it was shown by Spencer (1969) and Bakker-Arkema et al. (1967) that the terms containing $\partial T/\partial t$ and $\partial H/\partial t$ can be considered negligible. This approach simplifies the solution of the four simultaneous PDE. The deep-bed drying simulation can be achieved by dividing the bed in layers. The output conditions of a layer are used as input conditions of the next layer. Each layer is considered to have a uniform temperature and moisture content. The time interval for the integration should be sufficiently short, so that the conditions of air may be considered practically constant at the inlet and the outlet of each layer.

2.6 Principles for the Selection of a Simulation Model

From a thorough investigation conducted in the preceding paragraphs, it becomes evident that in order to properly take into account and describe the heat and moisture transport phenomena which occur during drying, it is necessary to adopt a model which includes relations in which the two independent variables (concentration and temperature) are coupled to one another. This fact increases the complexity of the mathematical solution of the problem and the description of the phenomenon. Equations that describe heat and mass transfer as a function of drying time only are considered as *lumped* models, while those describing heat and mass transfer as a function of drying time and position within the product are considered as *distributed* models.

In determining the relations describing the behavior of the solid during drying, relations that also permit a good understanding of the phenomenon, an important role is played by the dimensionless Biot numbers for heat and mass transfer (Parti 1993). From the investigation of the values received by these dimensionless numbers and the physical properties of the solid, the form of the simulation model relations of the process becomes more specific. The Biot dimensionless numbers are defined as follows:

$$Bi_{\mathrm{m}} = \frac{k_{\mathrm{g}}\mathrm{L}_0}{\rho_{\mathrm{p}} D_{\mathrm{eff}}} \tag{72}$$

and

$$Bi_{\mathrm{h}} = \frac{h_{\mathrm{g}}\mathrm{L}}{\lambda} \tag{73}$$

The magnitude of these dimensionless numbers depends on the values selected for the properties of the solid and of the drying medium (air in our case) as well as on the conditions of the fluid (air) during the process.

In order to determine and minimize the number of relations to be used, after an analysis of the drying conditions and of the physical properties of the parameters involved, various simplifications have been introduced to the full and general description of the process models. In selecting, thus, a particular model, an isothermal behavior of the solid and a distributed or cumulative or homogenized (lumped) behavior of any of the dependent variables in relation to the independent variables of time and position within the solid, may be adopted.

A typical simplification hypothesis, which is applied to the thin-layer models and analyzed in the previous paragraph, is the one in which the whole process is considered as isothermal and thus a single parameter, the moisture diffusion, is sufficient to determine the drying kinetics. According to this hypothesis, the dried solid acquires immediately the temperature of hot drying air, and throughout the whole duration of the drying, it is in this constant and uniform temperature. This assumption is generally acceptable when the product $Bi_{\mathrm{h}}Le$ (where $Le = a/D$) is less than 100 and becomes true particularly for an infinite value of the Biot Bi_{m} number for mass (Sun and Meunier 1987). It is practically true when solids are dried in fluidized beds, in pneumatic conveyors, or by spray drying and generally where the drying solid consists of small parts or is in powder form. It has been widely applied to biological products under the name of thin-layer drying with its major disadvantage being that no information about the internal temperature of the drying solid is provided, which initially is considered equal to the drying air temperature.

Unlike the case of isothermal drying, models that take into account the simultaneous heat and mass transfer have been proposed. They are combining the internal kinetics of moisture by means of Fick's law along with heat transfer by convection from the hot air in the solid.

When Bi_{h} is very small (less than 0.2), the solid temperature is essentially uniform. The assumption underlying this uniform temperature model is generally valid when the Le number is greater than 10 (Sun and Meunier 1987). This condition is satisfied in the case where the thermal conductivity λ is sufficiently high, which allows the heat to be rapidly diffused throughout the body. The same applies in the case where the coefficient of convection h_{g} takes small values, i.e., when the resistance to heat transfer from the environment to the body through the surface is increased, allowing therefore the solid to maintain the uniform temperature. The same phenomenon may occur in the case of small solids wherein the heat has a small path to cover which is substantially contributing to maintain uniform temperature throughout the solid (thin-layer drying) (Fig. 9).

In the case where the Bi_{h} number attains high values, e.g., greater than 10, the temperature difference between the ambient and the solid surface is negligible, and a temperature distribution develops, from the surface toward the center of the solid

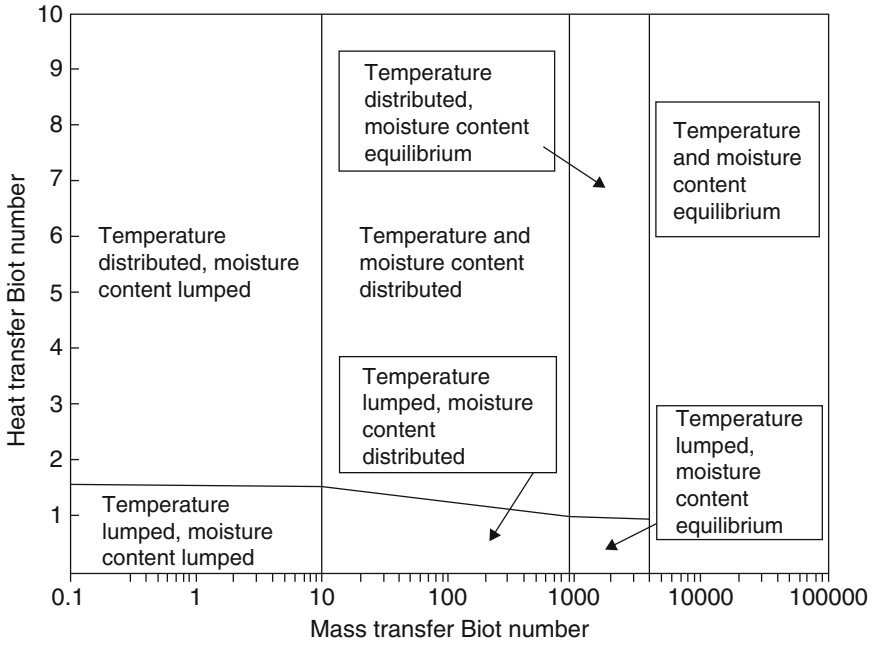

Fig. 9 Ranges of applicability of different drying models and theoretical assumptions (Parti 1993)

body only. This case is particularly valid for a solid of relatively large dimensions, when dried within a well miscible fluid which is the case where the convection coefficient h_g takes very large values. This is the case when the thermal conductivity λ of the solid is very low.

In the intermediate region, wherein the Bi_h number takes values between 10 and 0.2, the temperature gradients from the environment to the surface of the solid, as well as inside the solid, are significant and therefore cannot be ignored.

A similar behavior arises also in the case of the Biot number for the mass. In the case where Bi_m is less than 10, the solid does not present an internal moisture distribution and can be regarded as a body having a moisture equal to the average value. On the other hand, when the Biot number is greater than 10, the moisture of solid shows a distribution of increasing intensity up to the number 1000.

For values of the Bi_m number greater than 1000, it may be considered that the difference in moisture content between the environment and the solid surface is negligible and in this case only a moisture gradient from the surface to the center of the rigid body develops (state of surface equilibrium) (Parti 1993). The smaller the value of Biot mass number, the longer the time necessary to heat the solid. This fact radically modifies the shape of the rise of the temperature curves. For values greater than 4000, the drying solid behaves like temperature-homogeneous and in equilibrium with its environment.

For distributed models, Fick's diffusion law can be applied to the moisture transfer and Fourier's law to the heat transfer, as below:

$$\frac{\partial X}{\partial t} = D\frac{\partial^2 X}{\partial x^2} \tag{74}$$

and

$$\frac{\partial T}{\partial t} = a\frac{\partial^2 T}{\partial x^2} \tag{75}$$

with the respective boundary conditions.

The approach considering the lumped behavior of the solid ignores the internal resistance to heat and mass transfer, while the corresponding distributed behavior takes into account internal as well as external resistances. For the lumped models, $(\partial T/\partial t) = (\partial X/\partial t) = 0$ is always valid, along with the boundary conditions. The majority of these models were derived from the simplification of the distributed models.

As emerged from the investigation of the literature, the drying of inorganic porous material has been covered adequately. This is unlike the drying of organic products and especially food, which still contains ambiguities and difficulties in the application parameters. More specifically, the main difficulty is in the definition of transfer factors and thermophysical and technical properties of the products. The transfer rates depend on the geometric characteristics of the product and of the drying chamber, on the arrangement of the product inside trays and the preparation of the product. Physical properties and technical choices exhibit a strong dependence on humidity and temperature, and therefore, they cannot be considered constant during drying. Furthermore, although in most of the approaches, the shrinkage of the solid is not taken into account when developing the models, this parameter often cannot be neglected. The absence of reliable values for the various necessary parameters involved in the literature makes their immediate implementation impossible.

After all information reported in the preceding paragraphs regarding the advantages and disadvantages of the different models describing the drying process, these can be summarized as follows (Babalis 2006):

– The models based on empirical and semi-theoretical relationships as well as those providing mass transfer only (molecular diffusion and capillary transport) presuppose the uniformity of temperature within the solid throughout the duration of drying (isothermal process), and they do not take into account shrinking. The result is that the diffusion coefficient obtained includes the influence of all factors and is a complex function of temperature and humidity. In addition, the capillary phenomenon has been shown to have small influence, and it is of less importance for foodstuffs.

- In evaporation-condensation theory, although the moisture transfer by means of vapor diffusion has been experimentally demonstrated (especially in the last stages of drying), only in a few cases is it the predominant mechanism, and thus should be combined with other mechanisms to fully describe the phenomenon. On the other hand, the assumptions of linear sorption isotherms and constant transfer rates are arbitrary and have been nowadays abandoned.
- Despite the relative success of Luikov's approach, whose theory combines all possible modes of transport, the main disadvantage of the method is the assumption of negligible shrinkage which does not apply to food. When combined with the lack of data for the combined transfer coefficients (K_{11}, K_{22}, K_{12}, etc.) and the thermophysical properties, this model has limited application in food materials.
- Philip and De Vries' and Berger and Pei's theories are practically simplifications of the general approach of Luikov where some terms of this general relationship are omitted or broken down into individual components. All the advantages and disadvantages of Luikov approach apply here also.
- Whitaker approach is extremely difficult to apply in practice because of the large number of transfer coefficients and of the thermodynamic properties which are relevant for the full description of the system. The values for these properties are extremely difficult to quantify experimentally, and they are not available in the literature. Furthermore, the model is based only on the cellular structure of food and does not take into account the shrinkage of the product.
- The deep-bed models apply only to applications of such kind.
- On the contrary, the model of the moving front describes quite realistically the phenomenon of drying, as found experimentally, considering in advance the shrinkage phenomenon which is an important factor in the drying of food. It does not assume a dominant transport mechanism, nor it imposes thermodynamic constraints to the development of the model. It has only been applied to inorganic solids in bulk materials and products, and it has not been tested in the modeling of food and particularly those placed in a thin-layer arrangement.

3 Simulation and Modeling of Solar Drying Systems

3.1 Introduction

Solar radiation, in the form of solar thermal energy, is an alternative source of energy, particularly for drying fruits, vegetables, agricultural grains, and other types of materials. It is also frequently used to assist in convective drying of several materials, such as various foodstuffs, wastewater sludge, wood, hay, or ceramic bricks. Solar drying implies the use of solar radiation to dry the product directly or to preheat the drying air or a combination of both. In regions where the intensity of solar radiation is high and sunshine duration is long (the so-called sunny belt), this procedure is commonly used. It is estimated that in developing countries, a

significant amount of postharvest losses of agricultural products (mainly due to lack of preservation means) can be saved by using solar dryers. Food materials and crops are very sensitive to the drying conditions. Drying must be performed in a way that does not seriously affect their color, flavor, or texture. Thus the selection of drying conditions, such as temperature, is of major importance. Many products need pretreatment, similar to pretreatment applied to conventional drying systems. For solar drying, some products are pretreated to facilitate drying or to keep their flavor and texture. Outdoor sun-air heating is well suited to fruits. Their high sugar and acid content makes the direct sun drying safe. On the contrary, vegetables have low sugar and acid content, increasing therefore the risk of spoilage during open-air sun drying (Belessiotis and Delyannis 2011).

In order to preserve the excess of production, especially for medium to small amounts of agricultural products, drying by using solar energy consists of a procedure that is and economical and environment friendly. It is still used for domestic and up to small-commercial-sized drying of crops, agricultural products, and foodstuff, such as fruits, vegetables, aromatic herbs, wood, etc., contributing thus significantly to the economy of small agricultural communities and farms. As of today, neither standardized nor widely commercialized technology has become available, and in many cases, the relevant systems are constructed on an empirical basis rather than as the product of scientific design and technical calculations. Drying by solar radiation can be divided into two main categories (Belessiotis and Delyannis 2006):

– Direct or open-air sun drying, the direct exposure to the sun
– Indirect solar drying or convective solar drying

Research on solar drying has increased exponentially during the past decade, as reflected in multiple review papers (Bal et al. 2010; Belessiotis and Delyannis 2011; El-Sebaii and Shalaby 2012; Murthy Ramana 2009; Vijaya Venkata Raman et al. 2012). This technology is a convenient way of saving process energy but also enables drying of materials in regions where access to conventional energy sources is scarce. For food, solar drying will become one of the key technologies to help mitigate the large amount of food losses and resulting food insecurity in developing countries and to increase their access to international markets by providing better product quality (Müller and Mühlbauer 2012). Foods also comprise an important share of all materials to be dried (Defraeye 2014), and roughly 35% in weight of the world's fresh produce requires drying at some stage during processing (Dev and Raghavan 2012).

Before the various modeling approaches and relevant mathematical expressions are presented, it is necessary to outline briefly some of the major types of solar dryers and their structural and operational features, since this will allow for a better understanding of the modeling of the various processes taking place within the dryers.

3.2 The Drying Mode (Thin-Layer and Deep-Bed Drying)

Drying rate is affected and controlled by the external factors of the process, the internal mechanisms as well as the type and size of the product. Thus many products, such as fruits, vegetables, sliced fruits, are better to be dried in thin layers. Grains (corn, beans, wheat, etc.) can be dried in deep beds, in mechanical dryers, or into bins (Belessiotis and Delyannis 2011).

3.2.1 Thin-Layer Solar Drying

In Fig. 10, an example of direct solar drying of black Corinthian seedless grapes on an outdoor concrete surface is depicted. There exist many theoretical and empirical equations for thin-layer drying that predict the drying characteristics for a variety of agricultural products. In general, they are based on the assumption that the ratio of air volume to the crop volume is infinitely large. Considering this assumption, drying rate depends only on the properties of the material to be dried, its size, the drying air temperature, and the moisture content (Belessiotis and Delyannis 2011). A model for the prediction of the performance of dryers where the crop was arranged in thin layer was presented by Jain and Tiwari (2003) and will be presented in the next chapter.

3.2.2 Deep-Bed Solar Drying

Figure 11 presents a schematic of a deep-bed dryer, where drying takes place in zones (Ekechukwu 1999). It is obvious that the lower zone dries rapidly. As the air moves up to the upper zones, it cools down due to evaporation, while its moisture content increases. Thus, a gradient of temperature and relative humidity is formed between the lower and the upper zone, constituting a measure of the drying rate. Final moisture content is the mean moisture of the zones. The critical drying factors are airflow rate (the most important factor), drying air temperature, and the bed's depth. By adjusting these parameters, a moderate drying operation can be achieved without overdrying in the lower material zone (Belessiotis and Delyannis 2011). Jain (2005) presents a transient analytical model for packed bed thermal storage in crop drying applications.

3.2.3 Pretreatment of Crops for Solar Drying

Many crops, fruits, and vegetables are grown near the soil and are susceptible to various activities of microorganisms. They must, if possible, immediately after harvest, be treated and dried. This applies for all methods, direct and indirect, open-air, or mechanical drying. Pretreatment helps to slow down the activity of

Fig. 10 Direct solar drying of black Corinthian seedless grapes on an outdoor concrete surface (Belessiotis and Delyannis 2011)

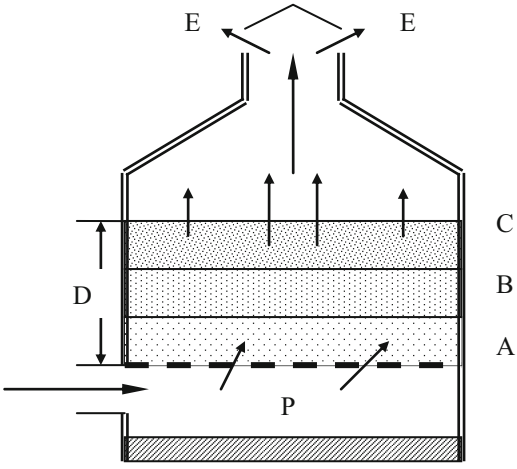

Fig. 11 Deep-bed drying zones of grains. *D* bed height, *P* Plenum chamber, *A* dried zone ($X = X_{eq}$, $T = T_{in}$), *B* drying zone, *C* not dried zone ($X = X_{in}$, $T = T_{out}$) (Ekechukwu 1999)

microorganisms as well as to soften the product skin, etc, and concerns, in general, simple methods based on experience (Belessiotis and Delyannis 2011).

3.3 Solar Drying Technology

Solar dryers are more or less simple devices. They range from very primitive ones used in small, desert, or remote communities up to more sophisticated industrial installations, although the latter are still very few and under development.

It is not an easy task to classify, reliably, solar drying equipment, as there are a lot of configurations many of which are empirical constructions. They can be classified in terms of various modes, such as based on the type of dryer; the operation temperature or the material to be dried; the mode of operation, e.g., batch or continuous; etc. Leon et al. (2002) give a systematic classification based on design and mode of utilization of solar energy (Fig. 10). In this classification, a

new mode of solar dryers may be added, the hybrid solar dryers that combine solar energy with an auxiliary energy source, mainly a gas, propane, conventional fuels, or biomass (Belessiotis and Delyannis 2011).

A comprehensive review on various designs, construction, and operation principles of a wide variety of solar energy dryers is given by Ekechukwu and Norton (1999a). They also present a complete classification according partly to the type of dryers. According to the drying process (direct or indirect) dryers may be classified as (a) *passive dryers*, those heated directly from the sun's radiation with or without natural air circulation, and (b) *active (or forced convection) solar dryers*, where hot drying air circulates by means of a ventilator (Belessiotis et al. 2006).

Despite the numerous configurations, especially of the forced circulation dryers, they consist almost of the same individual parts which are (Belessiotis and Delyannis 2011):

- A space for the material to be dried, such as a chamber, tunnel, etc.
- A heating system to heat the drying air, e.g., a solar collector.
- An air circulation system, e.g., ventilators, fans, etc.
- Pipes, velocity measurement sensors, and auxiliary parts.
- A control and measurement system.
- When water is used as heating medium, a heat exchanger is needed and for larger drying systems eventually a storage device.

Review works have been presented by Belessiotis and Delyannis (2011), Fudholi et al. (2010), Sontakke and Salve (2015), VijayaVenkataRamana et al. (2012), Ekechukwu and Norton (1999a, b), Sharma et al. (2009), Mustayen Billah et al. (2014), Umesh Toshniwal and Karale (2013), and El-Sebaii and Shalaby (2012). Phadke et al. (2015) presented a review on indirect solar dryers, meanwhile several researchers presented review works for specific applications. Jairaj et al. (2009) presented a review of solar dryers developed for grape drying; Reyes et al. (2014) presented a hybrid solar dryer for mushrooms dehydration using phase-change materials.

Some of the most common types of dryers are presented below, representative of each of the major types, namely, natural or forced convection types, for which mathematical and numerical models will be discussed in more detail in the subsequent section.

3.3.1 Passive Solar Dryers

Direct or passive drying of crops is still in common practice in many tropical and subtropical regions especially in Africa and Asia or in small communities for agricultural products. Passive solar dryers are "hot box" units where the product in the hot box is exposed to the solar radiation through a transparent cover. Heating takes place by natural convection, through the dryer transparent cover or in a solar air heater. The passive-type solar dryers are primitive, inexpensive constructions,

and easy to install and to operate, especially at sites where no electrical grid exists (Belessiotis and Delyannis 2011).

The chamber (or cabinet) greenhouse type constitutes the simplest solar dryers. They are passive systems where the product is heated up by means of the direct solar radiation and the natural convection induced to the surrounding air. The solar radiation passes through the transparent plastic or glass cover of the dryer. Cabinet dryers are simple and inexpensive. They are suitable for drying agricultural products, spices, herbs, etc. Normally, they are constructed with a drying area of 1–2 m^2 and capacities of 10–20 kg. A typical cabinet dryer is presented in Fig. 12. It resembles an asymmetric solar still unit oriented north-south. The cover (*a*) is made of glass or transparent plastic. The material (*m*) is spread on perforated plates, through which air circulates, by natural convection, leaving the drying chamber from the upper north side (*n*). Bottom and side walls (*w*) are opaque and well insulated.

Other types of greenhouse-type chamber dryers have been presented which are a dual purpose tool; used as a fruit dryer at summer and beginning of autumn, while in winter and spring, acting as a greenhouse for vegetable growing and seedlings. The transparent surface faces southward and consists of a single layer of glass during drying period. In winter, it is covered with a second layer of polyethylene on the side, to reduce heat loss. Most of the dryers described above are of low capacities because they can only handle one layer of product. To increase capacity for certain fixed area, the trays containing the material must be accommodated in more independent layers, one above the other. This creates an increased resistance to the natural movement of the air through the bed of multilayer products. Thus the vertical flow of air must be increased without use

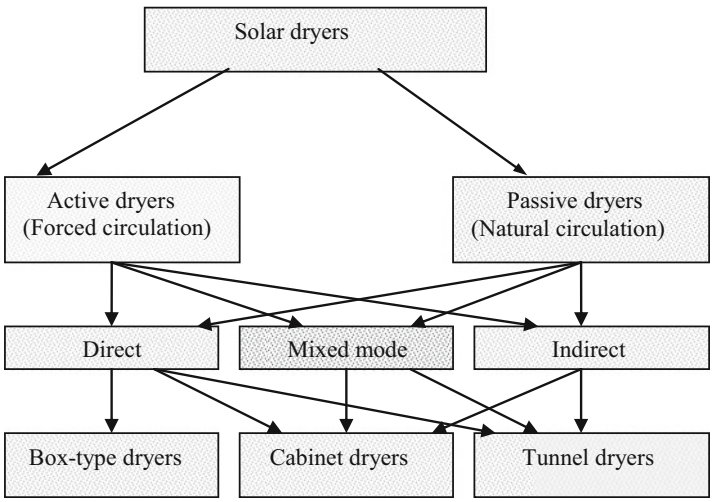

Fig. 12 Classification of dryers and solar heating modes according to Leon et al. (2002)

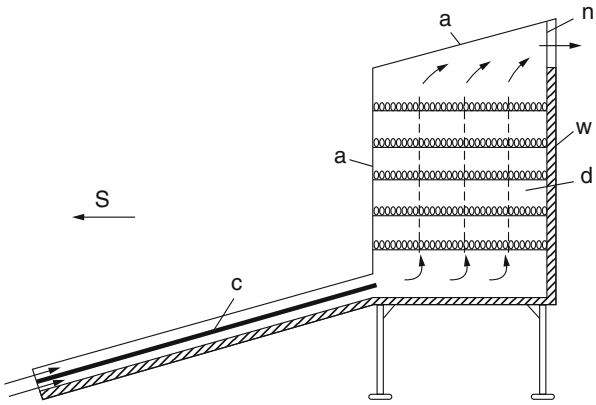

Fig. 13 A shelf-type solar dryer (Belessiotis and Delyannis 2011)

of a ventilator. To achieve this, the so-called chimney effect may be used (Belessiotis and Delyannis 2011).

Figure 13 presents a multilayer dryer (Selçuk et al. 1974) which is called "shelf-type solar dryer." It is oriented southward with the top and south wall covered with a transparent material (a). The thermal effect is increased by the use of an air heater (c), which helps the chimney effect to be produced. Humid air is exhausted from the northern wall (n) of the dryer. North wall (w) is well insulated. The material is spread in the trays inside the dryer (d). They also give a detail "quasi-steady-state" analysis and a performance evaluation for shelf-type solar dryers. For increased amounts of material to be dried, up to 1000 kg, chimney has to be taller for proper air circulation. Figure 14 presents a typical chimney solar dryer (Belessiotis and Delyannis 2011).

3.3.2 Forced Convection Solar Dryers

Forced convection solar dryers (or active solar dryers) are suitable for larger amounts of material. They use either a direct absorption system through transparent covers or are connected to solar collectors using indirect solar heat. Hybrid systems use, in cases where available, auxiliary sources of energy such as conventional fuels, biomass, gas, etc., to avoid some disadvantages of the passive solar dryers. Forced convection solar drying systems are more complicated and more expensive than passive systems as they need fans, ventilators for air circulation, and piping loops. Belghit et al. (1997) give a mathematical model for simulating the behavior of solar crop dryers in forced-mode operation (Belessiotis and Delyannis 2011).

Tunnel solar dryers are used for larger amounts of material and are almost near to be commercialized. They consist of a transparent roof and transparent side walls, mainly in hemispherical mode. Inside the tunnel are moving chariots with several stacked trays containing the material to be dried. Hot air flows through the trays

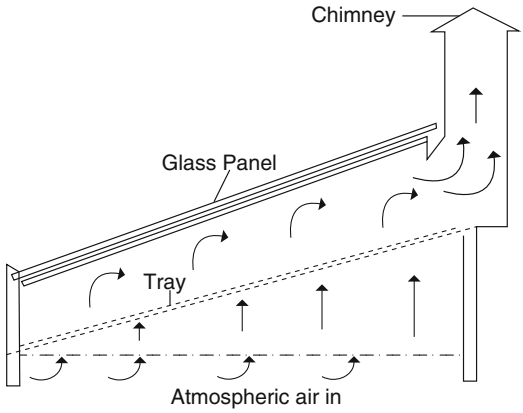

Fig. 14 A cabinet solar dryer with chimney (Belessiotis and Delyannis 2011)

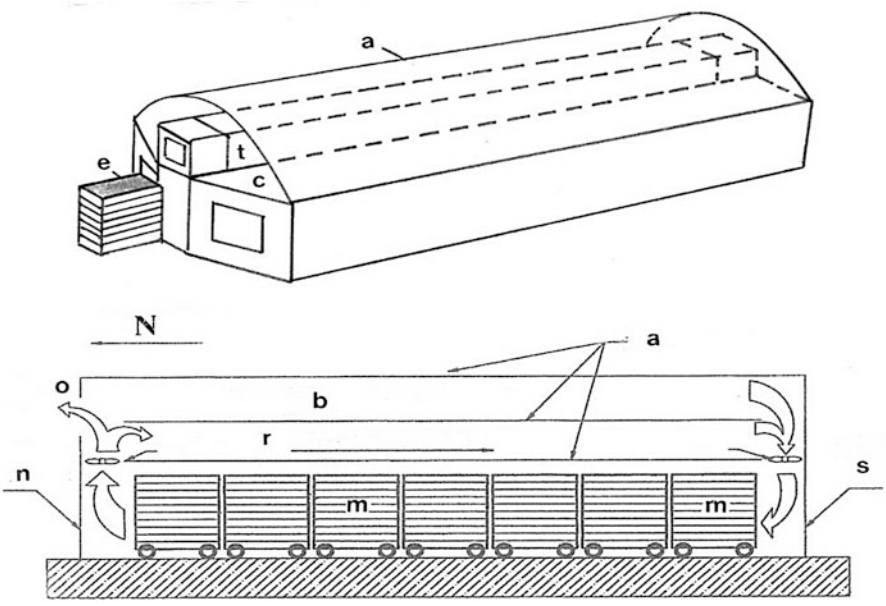

Fig. 15 (**a**) Tunnel dryer covered by transparent plastic sheet, with chariots for the material. (**b**) Cross section of the tunnel dryer (Belessiotis and Delyannis 2011)

containing the material. The chariots are either stable during the drying cycle, or they are beeing moved manually. They operate similarly as the conventional batch chamber dryers. A tunnel dryer of greenhouse type is presented in Fig. 15a, whereas Fig. 15b shows a schematic view of the tunnel inside of the solar dryer (Belessiotis and Delyannis 2006).

3.4 Simulation and Modeling of Solar Drying Systems

From all perspectives, solar drying is a much more complex procedure, compared to the conventional hot-air drying. The operation of solar dryers is complicated because of (1) fluctuations in incident radiation (day-night cycle, the presence of clouds) and ambient conditions (temperature, relative humidity), (2) the associated partial rehydration of the product during the night, and (3) the use of auxiliary heating or airflow and thermal energy storage systems, which aim to dampen fluctuations in environmental conditions and to enable continuous operation (Chua and Chou 2003; Müller and Mühlbauer 2012). A critical role is also played by the heat and mass exchange with the turbulent airflow via the boundary layer, in addition to the transport processes within the dried material. Also the heterogeneity in drying kinetics at different locations in the dryer is virtually uncharted. This lack of understanding of the solar drying process makes that losses are still very large compared to hot-air drying, combined with inferior product quality and stability. Little is yet understood on the product drying process under such complex environmental and operational conditions.

Besides that, the convective drying of soft cellular materials (as the foodstuffs are) is complicated by the large changes in fruit tissue microstructure which alter the macroscopic material properties (Halder et al. 2011). Within the tissue, cells shrink and can rupture. Near the air-material interface, drastic cell collapse occurs during dehydration, which leads to a very thin layer of dried cellular tissue (Lewicki and Pawlak 2003). Next to mechanical effects such as crust formation (case hardening), recent measurements unveiled large moisture gradients near this surface layer, where the underlying fruit tissue remains at high moisture content (Aregawi et al. 2013; Defraeye et al. 2012). Hence, this layer induces a significant resistance to moisture removal and plays a key role in the drying process, where this new "skin" protects the fruit from further dehydration.

Little is known on how these microstructural changes affect the material properties of the tissue and what is the role of the dried surface layer on the moisture removal from the tissue below. Convective drying of soft cellular materials using solar energy is affected by (1) the impact of the complex environmental and operational boundary conditions inherent to solar drying, (2) the interaction of the drying kinetics of the material with the turbulent airflow and the associated heterogeneity between dried materials, and (3) the impact of microstructural changes of the bulk fruit tissue and of the surface layer of dried cells. For these reasons, drying of foodstuffs requires a multiscale modeling approach, closely complemented by experiments. Multiscale models are essentially a hierarchy of sub-models which describe the material behavior at different spatial scales in such a way that the sub-models are interconnected. Given that the dried materials are inherently multiscale assemblies, the drying process within a solar dryer should be sought by explicitly accounting for the relevant transport processes within the fruit and the exchange at the air-product interface down to the lower scales, as depicted in Fig. 16 (Defraeye 2014). An overview of applications of multiscale modeling in food engineering and the respective future prospects were given by Ho et al. (2013).

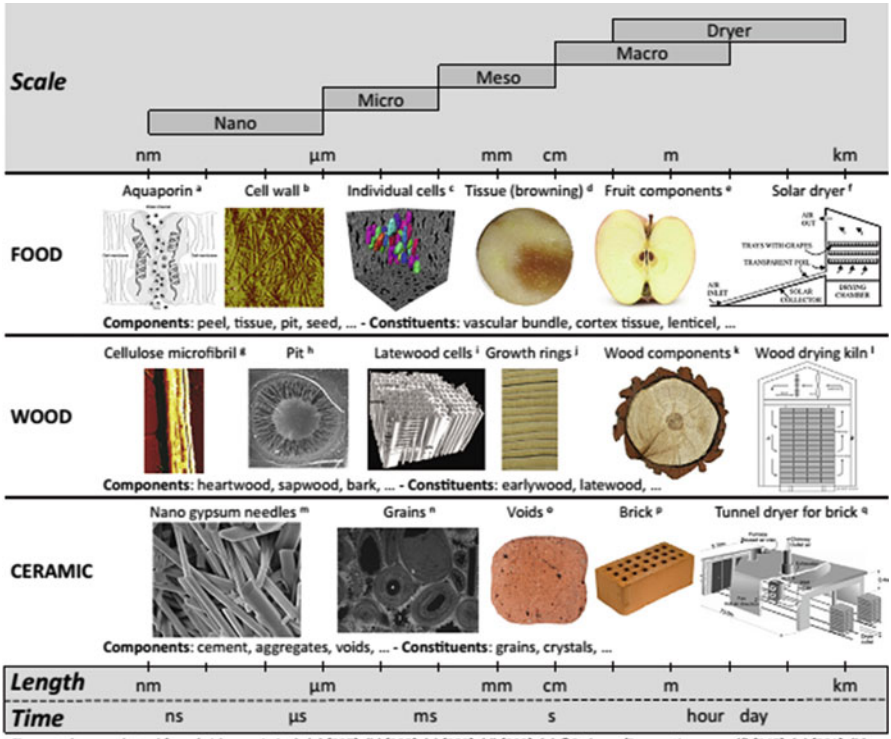

Fig. 16 Multiscale nature of some products relevant to the drying (Defraeye 2014)

Research on solar dryers has been mainly technology oriented and predominantly based on full-scale experiments (Murthy Ramana 2009). The bulk of the previous modeling work aimed to improve dryer design, operational parameters and control, in relation to the complex environmental conditions. To this end, energy and mass balances are solved over the different parts of the dryer (e.g., air heater/collector, dryer chamber (Janjai et al. 2009; Sami et al. 2011a, b)). Airflow and product dehydration behavior are however accounted for in a very simplified way, for example, by using semiempirical drying kinetics models, which is commonplace in drying process engineering.

More advanced mechanistic modeling of solar dryers is much scarcer. Computational fluid dynamics (CFD) is predominantly used to target the airflow and temperatures inside the solar dryer and the radiative exchange (Adeniyi et al. 2012; Hughes and Oates 2011), but only few works include the drying of the product explicitly (Krawczyk and Badyda 2011). The complex product drying behavior is often not the prime focus due to the challenges faced with capturing the hygrothermo-mechanical processes in the material, linking them to the airflow exchange and modeling the large amount of products in a dryer. Product-focused

approach is also considered for convective drying of other materials (Perré 2010; Perré et al. 2012; Shokouhmand et al. 2011).

In addition, modeling solar drying, in particular, faces specific difficulties at the dryer scale: (1) mixed and natural convective airflow regimes that have to be captured in a transient way with CFD; (2) complex and rapidly varying environmental boundary conditions; (3) large shrinkage of the materials, which leads to decreasing coverage ratio of the trays in the dryer and which requires remeshing in both material and airflow domain; (4) occurrence of both solar and longwave radiation; and (5) complex drying kinetics compared to forced convective drying, including partial rehydration, which affects the implementation of adaptive time-stepping procedures.

Generally, different approaches in modeling and analyzing of solar dryer systems can be categorized into four groups: thermodynamic modeling, differential-equation-based modeling, statistics-based modeling, and reacting engineering approach method (Ghaffari and Mehdipour (2015)).

1. Thermodynamic modeling: In this method, a state equation is solved for all parts of the dryer, and temperature, pressure, and velocity are determined. This method is fast, and if semiempirical equations are used, more accurate results can be achieved, although effects of many parameters like geometric complexity are being neglected. This method was employed by Sami et al. (2011a, b) and Bolaji and Olalusi (2008).
2. Solving differential equations method: In this method, the governing equations are solved using CFD method, and temperature, velocity, and humidity profiles are obtained for all parts of the system. Among the advantages of this method, the possibility of considering complex geometries can be noted; although the large number of calculations restricts the analysis. This method is employed for cabin dryer in Shokouhmand et al. (2011). Some innovative methods are proposed for more efficiently solving the governing equations (Gallesty and Paice 1996).
3. Statistical methods: This method is mostly used to derive the equations based on a series of experimental data. Then statistical methods and criteria such as root of mean square error (RMSE), reduced Chi-square and coefficient of determination are used to find an equation capable of describing the system in the best manner. Zomorodian and Moradi (2010) and Singh (2011) have applied this method on forced convection cabinet dryer.
4. Reacting engineering approach (REA) proposed by Chen and Xie (1997) for explaining different challenging drying processes. This method follows the basic rules of chemical reaction engineering to model the kinetics of drying. It is proven that the REA method is a simple, precise, and robust way of modeling the convective drying of edible and nonedible materials under constant environmental conditions. The method is also employed for modeling intermittent drying.

Choosing the dryer type depends on the product to be dried and the area in which the dryer will be employed. The five common categories of solar dryers that

mostly attract the attention of the researchers and consumers are as follows (Ghaffari 2015):

1. Indirect forced convection cabinet dryers (Sami et al. 2011a, b; Singh 2011; Benhamoua and Fazouane 2014; Sreekumar et al. 2008; Akbulut and Durmus 2010; Chirarattananon and Chinporncharoenpong 1998)
2. Direct natural convection cabinet dryers (Zomorodian and Moradi 2010; Ogheneruona and Yusuf 2011);
3. Mixed-mode cabinet dryers (Bolaji and Olalusi 2008; Forson and Nazha 2007, 2008)
4. Direct forced convection cabinet dryers
5. Indirect natural convection cabinet dryers

In the next paragraphs, the general concepts for the modeling of the main types of agricultural product dryers, i.e., direct (open air, greenhouse natural convection, and forced convection) and indirect (passive solar dryer with collector and chimney and tunnel dryers), will be outlined.

3.4.1 Direct Solar Drying

Open-air solar drying uses solar radiation to directly heat the material. It is a process used for millennia to preserve food, a natural convection drying procedure, as the air movement is due to density differences. It is accomplished by two methods: (a) by using the outdoor direct incidence solar radiation onto the surface of the material and (b) through a transparent cover which protects partly the foodstuff from rain and other natural phenomena, i.e., a passive solar drying method.

The technique of direct solar drying involves the spread out of the product to be dried (Fig. 10), in a thin layer, if possible, on large outdoor free threshing surfaces, where it is left until has been dried up to the desired moisture content. From time to time, during the day, the material has to be turned over to accelerate drying permitting trapped moisture to escape. The drying surface is made, generally, from concrete-paved floors lined with polyethylene nets, but sensitive food material is put on perforated trays, mostly made of wood. It is extensively applied for grapes, figs, and various fruits. As is obvious, the drying rate is very slow. The crops must remain outdoors for long periods of time, usually 10–30 days, depending on its nature and the weather conditions of the site (Belessiotis and Delyannis 2006).

During drying treatment, solar radiation falls on the crop surface and simultaneously moisture is transferred from the material to the ambient air. A part of the solar radiation is lost to the atmosphere and to the surrounding soil. Heat and moisture transfer take place by natural convection and diffusion, respectively, and both depend on weather conditions and solar radiation intensity as well as on the wind velocity, which at low flow rates accelerates drying. Due to these factors, direct solar drying is an unsteady state operation. Most of the time, the material must remain for a long time outdoors. During this time period, the agricultural products are subject to any weather changes and natural attacks, such as insects, rain, or even hail. If rain is expected, the crops can be protected by removable

plastic covers (Fig. 10). There do exist, however, cases of complete or partial degradation of crops due to sudden storms, heavy rains, or hail that might harm even the plastic cover. Very sensitive crops are spread on trays covered with transparent material and are dried by the sun's radiation and natural air circulation (Belessiotis and Delyannis 2011).

Another type of direct solar drying is that where the material (Sultana grapes) is not on direct exposure to the sun's rays but is rather dried in part, in the shadow. The grapes are hanged on wires forming shelves in scaffoldings open to all sides except the roof. They are dried by free air circulation and indirect solar heating. Pangavhane and Sawhney (2002) present a similar way of shadow drying of sultana seedless-type grapes in Australia and for Thompson seedless type in India where drying takes place in scaffolds. They are called "rack-type solar dryers." A similar type of solar grape drying is applied in Afghanistan to dry local type grapes. The shadows are put inside rectangular houses with flat roofs. The walls have holes to promote hot-air circulation.

The working principle of crop drying under open sun is illustrated in Fig. 13a (Jain and Tiwari 2004).

The solar radiation falling on the crop surface is partly absorbed and partly reflected. The absorbed radiation heats the crop surface. A part of this heat is utilized to evaporate the moisture from the crop surface to the surrounding air. The portion that is absorbed and the corresponding wavelength depend mostly on the color of the product. The remaining part of this heat is conducted into the interior of the crop or lost through radiation (long wavelength) to the atmosphere and through the bottom loss (through conduction to the ground if the crop is laid on the ground). The rate of moisture evaporation depends on the vapor pressure difference between the crop and the environment air surrounding the crop (Jain and Tiwari 2004).

Placing a plastic cover over the crop produces a greenhouse effect. It traps the solar energy in the form of thermal heat within the cover since the plastic cover acts essentially as opaque to the thermal heat radiation radiated by the crop and reduces the convective heat loss. The fraction of trapped energy will be received partly by the crop and partly by the floor and exposed tray area. Furthermore, the remaining solar radiation heats up the enclosed air inside the greenhouse. The principle of crop drying inside a greenhouse under natural convection is shown in Fig. 13b. The natural draft takes place due to the temperature difference between the greenhouse air and ambient air. The rate of moisture evaporation depends on the vapor pressure difference between the crop and the greenhouse air. A greenhouse with the forced mode of drying reduces the relative humidity inside the greenhouse and increases the vapor pressure difference, resulting in a faster rate of moisture removal (Fig. 13c).

Thermal models for prediction of crop temperature and moisture evaporation have been developed using energy balance equations for open sun drying and greenhouse drying under both natural and forced modes. Jain and Tiwari (2003) present a sketch of the working principles of open solar drying and a mathematical model which predicts the crop temperature, the moisture removal rate, and the

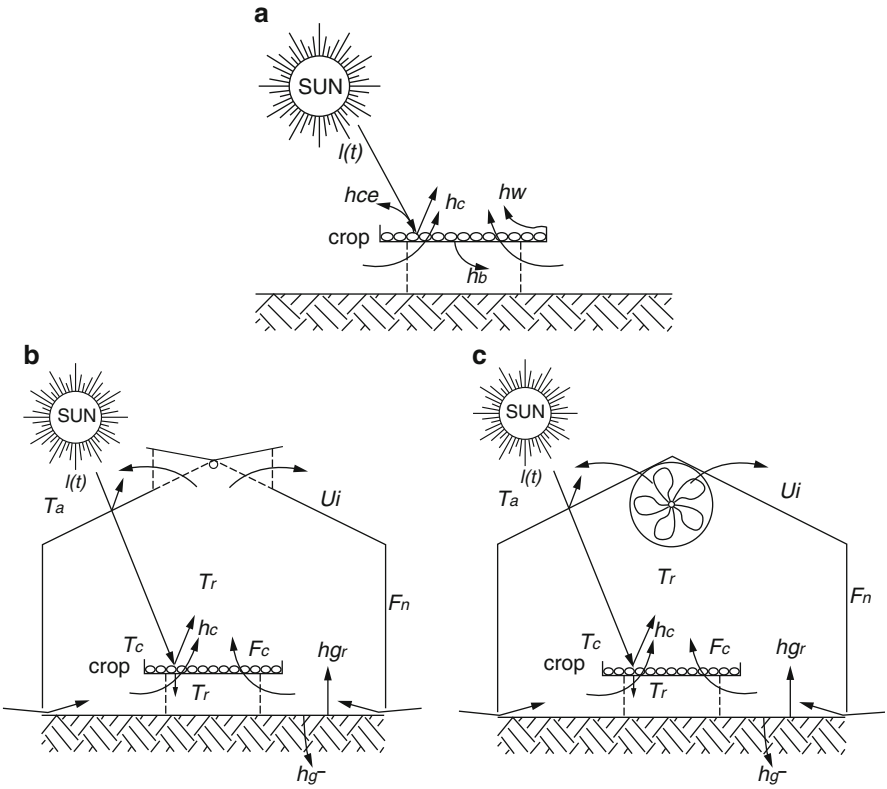

Fig. 17 The principle of solar drying: (**a**) open sun drying, (**b**) greenhouse drying under natural convection, and (**c**) greenhouse drying under forced convection (Jain and Tiwari 2004)

equivalent solar temperature. Figure 13 gives the energy balance during open door drying. The energy balance equations are presented in the next paragraphs, with the following assumptions: (a) thin-layer (single layer) drying is adopted, (b) heat capacity of cover and wall material is neglected, (c) no stratification in greenhouse air temperature, (d) absorptivity of air is negligible, and (e) greenhouse is east-west oriented (Jain and Tiwari 2004).

Thermal Modeling of Open Sun Drying (OSD) (Fig. 17a)

(a) Energy balance equation on crop surface for moisture evaporation (Jain and Tiwari 2004):

$$a_c I(t) A_c - h_{ce}(T_c - T_e)A_c - 0.016 h_c[P(T_c) - \gamma_e P(T_e)]A_c - \\ - h_b(T_c - T_a)A_c = M_c C_c \frac{dT_c}{dt} \tag{76}$$

(b) Energy balance equation of moist air above the crop (Jain and Tiwari 2004):

$$h_{ce}(T_c - T_e)A_c + 0.016 h_c[P(T_c) - \gamma_e P(T_e)]A_c = h_w(T_e - T_a)A_c \tag{77}$$

(c) Moisture evaporated can be evaluated as (Jain and Tiwari 2004):

$$m_{ev} = 0.016 \frac{h_c}{\lambda}[P(T_c) - \gamma_c P(T_e)]A_c t \tag{78}$$

Thermal Modeling of Greenhouse Drying Under Natural Mode (Fig. 17b)

(a) Energy balance equation at crop surface (Jain and Tiwari 2004):

$$(1 - F_n)F a_c \Sigma I_i A_i \tau_i = M_c C_c \frac{dT_c}{dt} + h_c(T_c - T_r)A_c \\ + 0.016 h_c[P(T_c) - \gamma_r P(T_r)]A_c \tag{79}$$

(b) Energy balance equation at ground surface (Jain and Tiwari 2004):

$$(1 - F_n)(1 - F_c)a_g \Sigma I_i A_i \tau_i = h_{g\infty}\left(T|_{x=0} - T_\infty\right)A_g \\ + h_{gr}\left(T|_{x=0} - T_r\right)\left(A_g - A_c\right) \tag{80}$$

(c) Energy balance equation at greenhouse chamber, using the coefficient of diffusion and difference in partial pressure due to the temperature difference of the greenhouse chamber air and ambient air (Jain and Tiwari 2004):

$$(1 - F_n)(1 - F_c)(1 - a_g)\Sigma I_i A_i \tau_i + h_c(T_c - T_r)A_c + 0.016 h_c[P(T_c) - \gamma_r P(T_r)]A_c \\ + h_{gr}(T|_{x=0} - T_r)(A_g - A_c) = C_d A_v \sqrt{2g\Delta H \Delta P} + \Sigma U_i A_i (T_r - T_a) \tag{81}$$

Thermal Modeling of Greenhouse Drying Under Forced Mode (Fig. 17c)

(a) Energy balance equation on crop surface for moisture evaporation (Jain and Tiwari 2004):

$$(1-F_n)Fa_c\Sigma I_i A_i \tau_i = M_c C_c \frac{dT_c}{dt} + h_c(T_c - T_r)A_c + 0.016h_c[P(T_c) - \gamma_r P(T_r)]A_c \quad (82)$$

(b) Energy balance at greenhouse chamber (Jain and Tiwari 2004):

$$(1-F_n)(1-F_c)a_g\Sigma I_i A_i \tau_i = h_{g\infty}\left(T|_{x=0} - T_\infty\right)A_g + h_{gr}\left(T|_{x=0} - T_r\right)\left(A_g - A_c\right) \quad (83)$$

(c) Energy balance equation at greenhouse chamber, using the coefficient of diffusion and difference in partial pressure due to the temperature difference of the greenhouse chamber air and ambient air (Jain and Tiwari 2004):

$$\begin{aligned}&(1-F_n)(1-F_c)\left(1-a_g\right)\Sigma I_i A_i \tau_i + h_c(T_c - T_r)A_c \\ &+ 0.016h_c[P(T_c) - \gamma_r P(T_r)]A_c + h_{gr}\left(T|_{x=0} - T_r\right)\left(A_g - A_c\right) \\ &= 0.33NV(T_r - {}_aT) + \Sigma U_i A_i (T_r - T_a)\end{aligned} \quad (84)$$

3.4.2 Indirect Solar Drying

Indirect solar drying is a rather new technique, not yet standardized or widely commercialized, that involves some thermal energy collecting devices and dryers of special construction. There exist several dryer sizes, the construction technique of which meets the special drying requirements of food products. Many of them still operate based on experience rather than on scientific basis.

Indirect solar drying technique has almost only advantages. Its only disadvantage is the high initial capital cost for the dryer, the collector field, and all necessary auxiliary equipment, such as ducts, pipes, blowers, control and measurement instruments. It also requires more or less skilled personnel to supervise the drying process. The advantages are as follows (Belessiotis and Delyannis 2011):

1. Drying rate is high. Agricultural products are dried within 15–30 h instead of, e.g., few days.
2. Drying can be controlled, ensuring the proper moister content of the final product, according to the specifications. Thus, the dried product can be stored for long times.
3. No losses at all, as the product is not subject to any natural phenomena.
4. For the same quantity of material, they need smaller surface areas due to trays accommodation in series one upon the other inside the dryers.

5. Since the products are not exposed to direct sunlight during drying, they have better color and more vitamins.
6. Increased productivity, as dryers can be loaded again within few hours.
7. Flexibility of the dryer to accept similar seasonal crops, thus expanding operation of the system almost around the year.
8. The high initial capital and operating cost counterbalance, partly, the direct sun drying.
9. In the mechanical drying, the most important parameter which is temperature can be controlled accurately and therefore a product of controlled and high quality is obtained.

Passive Through Solar Dryer with Collector and Chimney (Fig. 14)

The main difference between direct and indirect dryers is that in direct dryers the air is heated in the same chamber where the products are located whereas in indirect dryers the air adjacent to the collector is heated in an individual chamber containing the collector and then carried over into the storage chamber. The air can be either moved naturally by buoyancy or be sucked using a fan. Though dryers are made in different types, they mostly consist of some of the following three components (drying chamber is evidently always required):

1. Solar collector which collects the sunrays and delivers it to the air inside the collector. This causes buoyancy and, therefore, a natural flow of air inside the collector.
2. Drying chamber with walls made of glass and a few rectangular trays inside which the product dries. This part of the dryer is the most complex one regarding heat and fluid flow analyses.
3. Chimney located at the end of the system, which enhances the buoyancy force and consequently increases the convective flow of the air.

Choosing the dryer type depends on the to-be-dried product and the area in which the dryer will be employed. In the following, an indirect natural convection cabinet dryer model is outlined as depicted in Fig. 18. According to this figure, the air enters the collector comprising a transparent cover (the upper plate in the picture), an absorbent plate (the middle plate), and an isolator (the lower plate), where it is heated up. The air is then driven into the drying chamber where it passes through the layers of to-be-dried products. During this step, it absorbs the humidity of the products and enhances their drying. Afterward, the air moves toward the exit hatch and exits through the chimney.

In the relevant study (Ghaffari and Mehdipour 2015), each part of the dryer is modeled individually. The collector and the chimney are modeled using one-dimensional thermodynamic equations, and the drying chamber is by using CFD methods.

Modeling of the Collector Components

(a) Energy balance in the collector cover (Ghaffari and Mehdipour 2015):

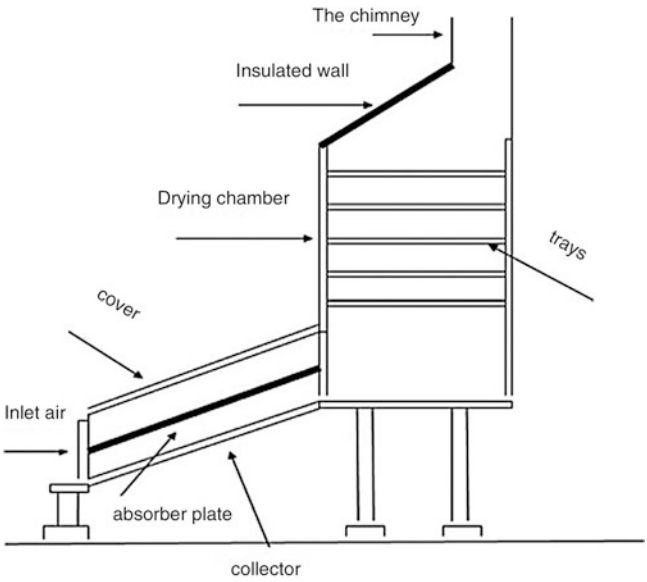

Fig. 18 Schematic of an indirect passive solar dryer with collector and chimney (Ghaffari and Mehdipour 2015)

$$h_{af}(T_c - T) + h_{ca}(T_c - T_a) + h_{re}(T_c - T_s) + h_{rp}(T_c - T_p) = \left[a_{cs}(1 + \rho_{ps}\tau_{cs}) - \tau_{cs} - \rho_{cs}\right]I \tag{85}$$

(b) Energy balance for the absorber plate (Ghaffari and Mehdipour 2015):

$$h_{rp}(T_c - T_p) + h_{af}(T_p - T) = \left[\tau_{cs}(a_{ps} - \rho_{ps} - \tau_{ps})\right] \tag{86}$$

(c) Energy balance of the airflow inside the collector (Ghaffari and Mehdipour 2015):

$$mc_p \frac{dT}{w} = h_{af}(T_c - T)dy + h_{af}(T_p - T)dy \tag{87}$$

(d) Pressure drop inside the collector (Ghaffari and Mehdipour 2015):

$$\Delta P = f\frac{lV^2}{d_h 2g} \tag{88}$$

Modeling of the Drying Chamber

Drying chamber is the most important component of the dryer. In this part, the airflow causes the products to dry by passing through the trays. The flow in this area is completely three or two dimensional, and modeling it one dimensionally may introduce large amounts of errors in the model. In this study, the drying chamber is simulated using CFD methods. In order to calculate the velocity, pressure, and temperature fields, it is important to solve the conservation of mass and the Navier-Stokes equations in the turbulent form. These equations are expressed as follows (Ghaffari and Mehdipour 2015):

$$\begin{aligned} \frac{\mathrm{d}\rho}{\mathrm{d}t} + \nabla \cdot (\rho \vec{v}) &= 0 \\ \frac{d}{\mathrm{d}t}(\rho \vec{v}) + \vec{v} \cdot (\rho \vec{v} \vec{v}) &= -\nabla P + \nabla \cdot (\vec{\tau}) + \rho \vec{g} + \vec{F} \end{aligned} \tag{89}$$

where $\vec{v}$ is the velocity vector and $\vec{\tau}$ is the stress tensor with:

$$\vec{\tau} = \mu\left(\nabla \vec{v} + \nabla \vec{v}^T\right) - \left(\frac{2}{3}\right) \nabla \cdot \vec{v} \cdot I \tag{90}$$

where μ denotes the dynamic viscosity coefficient of the fluid and I is the identity matrix.

The energy equation is as follows (Ghaffari and Mehdipour 2015):

$$\frac{d}{dt}(\rho E) = \nabla \cdot \left(K_{eff} \nabla T - \sum_j h_j \vec{J}_j + \tau_{eff} \vec{V} \right) + S_h \tag{91}$$

where K_{eff} is the effective coefficient of heat transfer, J_{j} is the heat flow diffusion coefficient, the first term on the right side is related to conductivity, the second term is related to species diffusion, and the third term is related to the viscous loss. S_{h} is related to the chemical reaction heat and other enthalpy sources. Based on the governing conditions on the dryer, the flow should be considered turbulent. For modeling, the turbulence dynamic viscosity, the $\varepsilon - k$ method is employed. Therefore, two more equations for determining the viscosity are added to the equation set above.

Modeling the Chimney

The length of the chimney is usually small and does not have significant effect on temperature reduction through the chimney; but as the chimney's length directly influences the dryer's outlet temperature, in this part, the appropriate equations are presented for modeling the chimney component.

Writing energy balance for an element of length dy at a distance of y from the chimney's inlet, the following equation is obtained (Ghaffari and Mehdipour 2015):

$$mc_{\mathrm{p}}\mathrm{d}T = Up\mathrm{d}y(T - T_{\mathrm{a}}) \tag{92}$$

where p is the chimney's base perimeter and U is the chimney's general heat transfer coefficient. U is obtained from the following equation:

$$U = \left(\frac{1}{h_i} + \frac{k_{\text{ch}}}{t_{\text{ch}}} + \frac{1}{h_{\text{o}}}\right)^{-1} \tag{93}$$

By solving the equations above, the chimney outlet air temperature is obtained:

$$T_{\text{e}} = T_{\text{a}} + (T_{\text{i}} - T_{\text{a}})\text{e}^{-Upl/mc_p} \tag{94}$$

where T_i and T_e are the chimney inlet and outlet air temperatures, respectively.

The pressure drop equations in the chimney are similar to those presented for the collector. Detailed description of the solution method, the flowchart, the values of the parameters and results obtained can be found in Ghaffari and Mehdipour (2015).

Bennamou and Belhamri (2003) presented a model of a simple efficient and inexpensive passive solar batch dryer with collector and chimney for agricultural products. The application of heat and mass balances leads to two sets of differential equations completed by an empirical model, which represents the drying kinetics. Onion was chosen as the dried product because of its swift deterioration property. The results showed that drying is affected by the surface of the collector, the air temperature, and the product characteristics.

Sami et al. (2011a, b) presented a dynamic mathematical model for drying of agricultural products in an indirect cabinet solar dryer of the type considered above. This model describes the heat and mass transfer in the drying chamber and also considers the heat transfer and temperature distribution in a solar collector under transient conditions. For this purpose, using conservation laws of heat and mass transfer and considering the physical phenomena occurring in a solar dryer, the governing equations are derived and solved numerically. The predicted results are compared with available experimental data. It is shown that the model can predict the performance of the cabinet solar dryer in unsteady-state operating conditions as well.

Tunnel Dryer

Oueslati et al. (2012) presented a study of convective drying for wet agricultural product by hot air. The system studied was a tunnel dryer, working with different sources of energy (solar, gas, electric) and conceived to dry several agricultural products. This system operates in open loop for adjustable air in temperature and velocity. The objective of this work is to establish a mathematical model describing the phenomena of heat and mass transfer at the product layer and in the air. The drying process is simulated under real operating conditions based on a thin-layer model and experimental drying kinetics.

The system studied is a tunnel dryer with partially solar heating. For the modeling, several assumptions are made in order to obtain the macroscopic scale governing equations:

- Air density is constant.
- Air velocity distribution in the dryer is uniform.
- Air and water vapor are considered as perfect gases.
- The shrinkage of the product during the drying is neglected, and the product can be considered as a thin layer of water.
- The phenomenon of water condensation on the inner metal walls of the drying chamber is neglected, and so is the radiative transfer phenomenon inside and outside the drying chamber.
- Hot air is provided by two sources, the solar module and the auxiliary heating unit for a combined operation or by the solar module for only solar drying.
- The room is assumed to be waterproof, and soil losses are neglected.
- The exchange at the air-product interface has a constant rate during drying.
- All the products are considered homogeneous, characterized by their superficial temperature.
- The studied system is described with lumped parameters, thus having an evenly distributed temperature.

The various transport processes retained are those between the air and the product (convection and vaporization of water), between the air and walls (heat convection), and between internal air and outside air through the walls (thermal loses by conduction).

(a) Mass Balance in the Product

The mass conservation of water in the agricultural product is the change in the amount of water in the product, which is equal to the water evaporated from the product (Oueslati et al. 2012):

$$m_{\mathrm{pr}} \frac{\mathrm{d}X}{\mathrm{d}t} = -h_{\mathrm{m}} A_{\mathrm{pr}} \left(P_{\mathrm{vs}} - P_{\mathrm{v}}^{\mathrm{i}} \right) \tag{95}$$

(b) Mass Balance in the Air

The balance of water masses in the air exchanged during drying is the change in the amount of water in the air which is equal to the moisture of the outside air entering the dryer plus the moisture evaporated from the product minus the moisture of the exhaust air from the dryer (Oueslati et al. 2012):

$$m_{\mathrm{a}} \frac{\mathrm{d}Y}{\mathrm{d}t} = \dot{m}_{\mathrm{a,in}} Y_{\mathrm{in}} + \dot{m}_{\mathrm{v}} - \dot{m}_{\mathrm{a,out}} Y \tag{96}$$

(c) Energy Balance in the Product

The energy balance in the product is the change in internal energy of the product which is equal to the energy of evaporation of the water from the product plus the heat exchanges by convection between the air and the product (Oueslati et al. 2012):

$$m_{\mathrm{pr}} c_{\mathrm{p,pr}} \frac{\mathrm{d}T_{\mathrm{pr}}}{\mathrm{d}t} = -\dot{m}_{\mathrm{v}} L_{\mathrm{v}} + A_{\mathrm{pr}} h_{\mathrm{cl}} \left(T_{\mathrm{a}} - T_{\mathrm{pr}}\right) \tag{97}$$

where L_{v} is the latent heat of vaporization and h_{c1} is the convective heat transfer coefficient between the hot air and the agricultural product.

(d) Energy Balance in the Air

The equation for the energy balance in the air is the change in internal energy of the air inside the dryer. This is the enthalpy of the air entering the dryer minus the enthalpy of the air leaving the dryer plus the enthalpy of the moisture evaporated from the product, minus the heat exchanges by convection between the air and the product, minus the convective heat flow between the air and the inner wall (Oueslati et al. 2012):

$$\begin{aligned} \rho_{\mathrm{a}} V_{\mathrm{a}} c_{\mathrm{p,a}} \frac{\mathrm{d}T_{\mathrm{a}}}{\mathrm{d}t} = {} & \dot{m}_{\mathrm{a,in}} c_{\mathrm{p,a}} T_{\mathrm{a,in}} - \dot{m}_{\mathrm{a,out}} c_{\mathrm{p,a}} T_{\mathrm{a,out}} + \dot{m}_{\mathrm{v}} c_{\mathrm{p,v}} T_{\mathrm{a,out}} - \\ & - h_{\mathrm{cl}} (T_{\mathrm{a}} - T_{\mathrm{pr}}) A_{\mathrm{pr}} - h_{\mathrm{c2}} (T_{\mathrm{a}} - T_{\mathrm{wa}}) A_{\mathrm{wa}} \end{aligned} \tag{98}$$

where A_{wa} is the area of the wall and $h_{2\mathrm{c}}$ is the convective heat transfer coefficient between the moist air and the inner wall.

(e) The Energy Balance of the Wall of the Drying Chamber

This is the change in internal energy of the inner wall which is equal to the convective heat flow between the air and the inner wall minus the heat flow by conduction between internal air and outside air through the walls (Oueslati et al. 2012):

$$\rho_{\mathrm{wa}} V_{\mathrm{wa}} c_{\mathrm{p,wa}} \frac{\mathrm{d}T_{\mathrm{wa}}}{\mathrm{d}t} = h_{\mathrm{c3}} (T_{\mathrm{a}} - T_{\mathrm{wa}}) A_{\mathrm{wa}} - h_{\mathrm{d}} (T_{\mathrm{wa}} - T_{\mathrm{am}}) A_{\mathrm{wa}} \tag{99}$$

where $h_{\mathrm{d}} = \lambda / d_{\mathrm{i}}$ [W/m^2 °C] is the conductive heat transfer coefficient across the insulation.

The system of the above equations can be resolved along with the drying rate equation obtained from an experimental study on a thin product layer:

$$\left(-\frac{\mathrm{d}X}{\mathrm{d}t}\right) = \left(-\frac{\mathrm{d}X}{\mathrm{d}t}\right)_m F(X_r) \tag{100}$$

where the functional dependence $F(X)$ used in this study has been deduced from an experimental analysis in a thin product layer. For grapes, the functional dependence is given by the following expression:

$$F(X_{\mathrm{r}}) = X_{\mathrm{r}} + X_{\mathrm{r}}(1 - X_{\mathrm{r}})[1.1697 X_{\mathrm{r}} - 0.8415] \tag{101}$$

This modeling allows to describe the heat and mass transfer phenomena involved in food drying, showing that air temperature is an influential external parameter which is not the case with the air velocity. The developed model has the capability to describe the different drying periods and the evolution of the profiles of temperature and moisture content.

Condori and Saravia (2003) presented an analytical study describing the performance of a tunnel greenhouse dryer. In this study, the greenhouse is considered as a solar collector which is analyzed separately, and a linear function between the incident solar radiation and the greenhouse output temperature is obtained. A simple model for the tunnel behavior is presented using two energy balance equations, a water mass balance and a semiempirical equation for the drying kinetics of a given product. Using the dryer characteristic function, the dryer performance is evaluated as a function of the drying potentials. The results show that an almost constant production is obtained each day. The generalized drying curve concept is applied to the first tunnel cart, obtaining a result that is similar to the single chamber dryer case.

Recent Works on Indirect Dryers

Norton et al. (2013) have presented a review of recent advances in CFD in the design and analysis of thermal processes. This paper discusses the fundamental aspects involved in developing CFD solutions and forms a state-of-the-art review on various CFD applications in conventional as well as novel thermal processes. From this review, it is evident that present-day CFD software, with its rich tapestries of mathematical physics, numerical methods, and visualization techniques, is currently recognized as a formidable and pervasive technology which can permit comprehensive analyses of thermal processing and especially in drying problems.

A review of applications of software in solar drying systems can be found in (Chauhan et al. 2015). In this paper, applications of software in solar drying systems are investigated and reported. All recent employed software and their utility in solar drying systems are emphasized. Patil and Gawande (2016) presented a comprehensive review on solar tunnel greenhouse drying systems while Prakash and Kumar (2013) gave a historical review and recent trends in solar drying systems and Prakash et al. (2016) gave a review on various modelling techniques for solar dryers.

Jamaleddine and Ray (2010) presented a comprehensive review of the current literature on the use of CFD models in both industrial and lab-scale drying applications. The use of Eulerian-Eulerian and Eulerian-Lagrangian models in the study of the drying kinetics for gas-solid multiphase flow systems is fully discussed. Recent advancements in mathematical techniques and computer hardware, CFD has been found to be successful in predicting the drying phenomenon in various types of industrial dryers, which utilize all forms of drying operations including spray, freeze, and thermal drying techniques. Merits and disadvantages of using various CFD models in the design of industrial dryers are illustrated, and the scope of their applicability is also discussed.

Lemus-Mondac et al. (2011) presented the computational simulation and developments applied to food thermal processing. Mathematical conjugated and nonconjugated models used along with suitable numerical methods such as finite differences, finite elements, and finite volumes in predicting food freezing, dehydration, and sterilization are discussed in this review. In this work, a review including mathematical modeling, computer-based finite numerical methods, fluid mechanics, heat and mass transfer results, discussions, and examples related to the formulation of two mathematical models, nonconjugated cases and conjugated studies applied to food dehydration, freezing, and sterilization processes, are presented.

Defraeye (2014) presented a review of the advanced computational modeling for drying processes. This review deals with rapidly emerging advanced computational methods for modeling dehydration of porous materials, particularly for foods. Drying is approached as a combined multiphysics, multiscale, and multiphase problem. These advanced methods include computational fluid dynamics, several multiphysics modeling methods (e.g., conjugate modeling), multiscale modeling and modeling of material properties, and the associated propagation of material property variability. Development of more user-friendly, specialized software is paramount to bridge the current gap between modeling in research and industry by making it more attractive. These advanced computational methods show promising perspectives to aid developing next-generation sustainable and green drying technology, tailored to the new requirements for the future society, and are expected to play an increasingly important role in drying technology R&D.

Flow Simulation Coupled with Conjugate Heat and Mass Transfer Models

A literature survey reveals that very few studies are available whereby flow simulations in dryers have been carried out in combination with a drying model (Caccavale et al. 2016). Such a study, based on a finite-volume methodology was presented by Lamnatou et al. (2010) who analyzed the unsteady, conjugate heat/mass transfer phenomena during convective drying of a porous solid, by taking into account the effect of slab thickness on heat/mass transfer. The drying model developed considered a domain for the simulation, encompassing both the solid body (drying product) and the airflow in the chamber.

The solution for the flow field was obtained along with that for a conjugate heat/mass transfer problem and with phase change (evaporation) also taken into account. The methodology developed is applicable to the analysis of drying of either slabs of construction materials or trays containing agricultural products in chambers such as the experimental facility shown in Fig. 20, where solar heat is provided by an evacuated-tube solar collector using air as the working fluid. This methodology is certainly of interest to researchers involved in the design of solar dryers, since the treatment of the heat/mass transport phenomena is particularly suited to these types of dryers which are generally convective dryers.

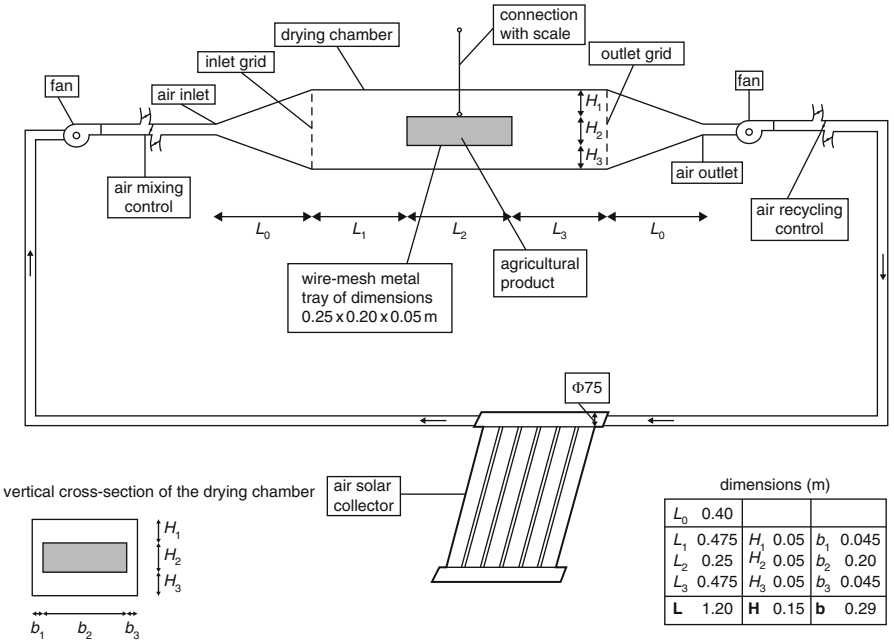

Fig. 19 Experimental solar dryer with a tray of agricultural product (Lamnatou et al. 2010)

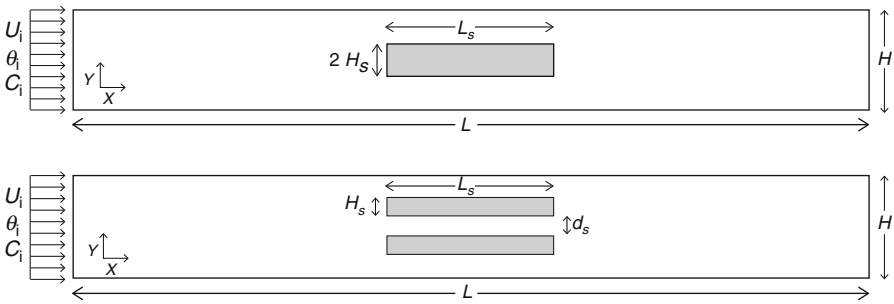

Fig. 20 Schematic of a drying chamber configuration for the flow and heat/mass transport simulation with (*i*) one a single tray and (*ii*) two trays in a side-by-side arrangement (Lamnatou et al. 2010)

The mathematical model comprised the two-dimensional equations for the flow field, which include the Poisson-type equation for stream function Ψ:

$$\nabla^2 \Psi = -\Omega \tag{102}$$

while for the remaining dimensionless variables (vorticity Ω, temperature θ, concentration C (humidity) in the air and moisture content w^* in the solid), the equation of transport has the general (convection-diffusion) form:

Table 1 Coefficients of the terms for each variable that follows Eq. (103)

Φ	Γ_φ	S_φ
Ω	1/Re	0
θ (fluid)	1/(Re *Pr*)	0
C	1/(*Re Pr Le*)	0
θ (solid)	R_{df} /(Re *Pr*)	$\nabla^2(K_1-\Gamma_\phi)\theta+\nabla^2(K_2 w^*)$
w^*	K_3	$\nabla^2(K_4\theta)$

Table 2 Coefficients that appear in Eqs. (104a) and (104b)

K_1	$\frac{R_{\mathrm{df}}}{\mathrm{RePr}}\left(1+LuKoPnD_{\mathrm{T}}^*\right)$	K_4	$\frac{R_{\mathrm{df}}}{\mathrm{RePr}}LuPn$
K_2	$\frac{R_{\mathrm{df}}}{\mathrm{RePr}}\left(LuKoD_{\mathrm{T}}^*\right)$	K_5	$B\cdot\frac{1}{Le}\cdot\frac{1}{\mathrm{RePr}}$
K_3	$\frac{R_{\mathrm{df}}}{\mathrm{RePr}}Lu$	K_6	$\frac{1}{R_{\mathrm{cp}}}\cdot\frac{1}{\mathrm{RePr}}$

$$\frac{\partial\phi}{\partial\tau}+\frac{\partial(U\phi)}{\partial X}+\frac{\partial(V\phi)}{\partial Y}=\frac{\partial}{\partial X}\left(\Gamma_\phi\frac{\partial\phi}{\partial X}\right)+\frac{\partial}{\partial Y}\left(\Gamma_\phi\frac{\partial\phi}{\partial Y}\right)+S_\phi \tag{103}$$

In Table 1, the diffusion coefficients Γ_φ and the source terms S_φ for each variable φ are given. The equations for temperature and moisture content in the solid have been developed based on the Luikov theory and involve a number of coefficients K_1–K_4 which are given in Table 2.

At the solid-fluid interface, the conditions $\theta_{\mathrm{fluid}}=\theta_{\mathrm{solid}}$, $C_{\mathrm{fluid}}=C(\theta, w^*)_{\mathrm{solid}}$ must be satisfied along with the continuity equations for heat and mass fluxes, written, respectively, as:

$$K_1\nabla\theta+K_2\nabla w^*=K_6\nabla\theta+(KoK_5)\nabla C \tag{104a}$$

$$K_3\nabla w^*+K_4\nabla\theta=K_5\nabla C \tag{104b}$$

The nonslip condition is imposed at the walls and the solid-fluid interface, whereby in the latter case the thermodynamic equilibrium equation is also applied:

$$\frac{c}{\rho_\alpha-c}=0.62198\frac{\varphi P_{\mathrm{ws}}}{P-\varphi P_{\mathrm{ws}}} \tag{105}$$

The coefficients K_5 and K_6 are also given in Table 2.

In the above tables, a number of dimensionless numbers are included and these are defined as follows:

R_{df}	Thermal diffusivity ratio (solid-fluid),	$R_{\mathrm{df}}=\alpha_{\mathrm{s}}/\alpha_{\mathrm{f}}$
R_{cp}	Thermal capacity ratio (solid-fluid),	$R_{\mathrm{cp}}=(\rho_{\mathrm{s}}C_{\mathrm{ps}})/(\rho_{\mathrm{f}}C_{\mathrm{pf}})$
Re	Reynolds number,	$\mathrm{Re}=(u\,L)/\nu$
Pr	Prandtl number,	$\mathrm{Pr}=\nu/\alpha_{\mathrm{f}}$
Lu	Luikov number,	$\mathrm{Lu}=D_{\mathrm{m}}/\alpha_{\mathrm{s}}$
Ko	Kossovitch number,	$\mathrm{Ko}=(\Delta H\ \Delta W)/(C_{\mathrm{ps}}\ \Delta T)$

Pn	Posnov number,	$\mathrm{Pn} = (\delta\ \Delta\mathrm{T})/\Delta W$
Le	Lewis number,	$\mathrm{Le} = \alpha_f/D_f$
D_T^*	Diffusion coefficient ratio for temperature in the solid (gas phase/total value),	$D_T^* = D_T/D$
D_M^*	Diffusion coefficient ratio for moisture in the solid (gas phase/total value),	$D_M^* = D_M/D$
B	Coupling parameter,	$B = \Delta c/(\Delta W\ \rho_s)$

In the above definitions the following variables are involved:

D Moisture diffusivity ($m^2\ s^{-1}$)
D_m Isothermal moisture diffusivity ($m^2\ s^{-1}$)
δ Thermal gradient coefficient (K^{-1})
ΔH Latent heat of evaporation ($J\ kg^{-1}$)
ΔT $= T_{max} - T_{min}$, where T_{max} and T_{min} are the incoming air dry and wet-bulb temperature, respectively
ΔW $= W_{max} - W_{min}$, where W_{max} is the initial and W_{min} is the final solid moisture content, respectively
Δc $= c_{max} - c_{min}$, where c_{max} is the saturation value of concentration at ambient temperature and $c_{min\ i9s}$ the concentration at wet-bulb temperature

Also, according to Luikov, the ratios of the diffusion coefficients D_T^*, D_M^* are replaced by a coefficient of phase conversion ε (typically $\varepsilon = 0.3$) when their values are not available. The Reynolds number is defined in terms of a characteristic velocity u (e.g., inlet mean velocity) and length L (e.g., half the chamber height).

In Eq. (105), φ is the relative humidity of air; P and P_{ws} are the total pressure and saturation vapor pressure of air, respectively; c is the dimensional concentration (kg/m^3) of humidity; and ρ_a is the density of air.

Thermodynamic Analysis

Torres-Reyes et al. (2001, 2002) applied methods derived from the second law of thermodynamics for solar thermal systems which may be used in a design procedure. Torres-Reyes et al. (2002) in particular, applied such a method in a solar drying system using energetic quantities of the drying process. The main formulas used in such an analysis are described below.

At the first, the solar collector is considered, whereby the solution of the entropy balance for the maximal temperature of collector plate, known as sun-air temperature (Torres-Reyes 2001), is given by:

$$\theta_{max} = 1 + \frac{GA_C(\tau\alpha)}{U_L A_P T} \tag{106}$$

where θ_{max} ($=T_{max}/T_a$) is the maximum temperature reached by the collector and depends on factors such as geographic location, climatic conditions, and collector

physical characteristics. By using Eq. (106) and once the physical characteristics of the collector are known, the plate surface temperature can be determined. The second stage of the design procedure is based on the second law and refers to the graphical determination of the entropy generation number N_s (Torres Reyes et al. 2001):

$$N_S = MF\left(\ln\frac{\theta_o}{\theta_i} - \theta_o + \theta_i\right) - \frac{1}{\theta'} + 1 \tag{107}$$

N_s represents the generated entropy during thermal conversion of solar energy while MF is a parameter known as mass flow number (Eq. 109) and θ' the apparent sun temperature (dimensionless).

This procedure was applied to the experimental dryer shown in Fig. 19 above by Lamnatou et al. (2012) with the aim of obtaining estimates for the optimum collecting surface of an evacuated-tube air collector for various drying tasks. In Fig. 21, N_s is shown as a function of the plate maximum temperature θ_{max} (these temperatures refer to collector stagnation temperature and depend on T_a and G), at different outlet temperatures θ_o of the working fluid. The analysis was applied to the data of apple drying experiments for three different air velocities (0.3; 0.6; 0.9 m/s), and the results show that the increase of air velocity leads to a decrease of N_s. The minimum value of N_s corresponds to the desirable operation conditions. For this optimal design, the working fluid outlet temperature is taken equal to the optimal operating temperature of the collector θ_{opt}, which is a function of its maximum temperature and obtained by (Torres-Reyes et al. 2001]:

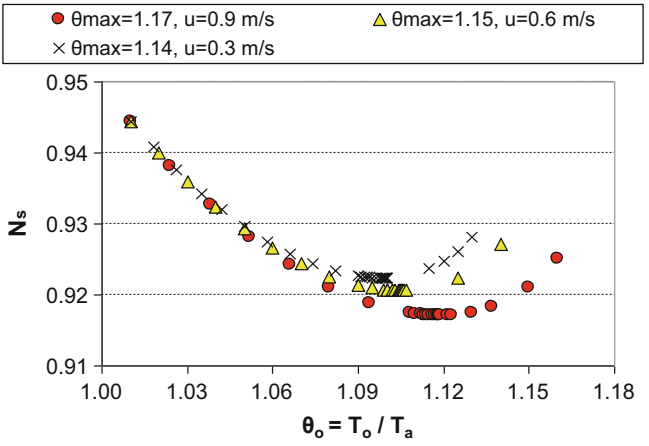

Fig. 21 Apple drying experiments in the experimental dryer shown in Fig. 14: entropy generation number N_s (Eq. 6) of the solar collector as a function of the dimensionless outlet fluid temperature θ_o, for different dimensionless maximum temperatures θ_{max} of the collector plate (Lamnatou et al. 2012)

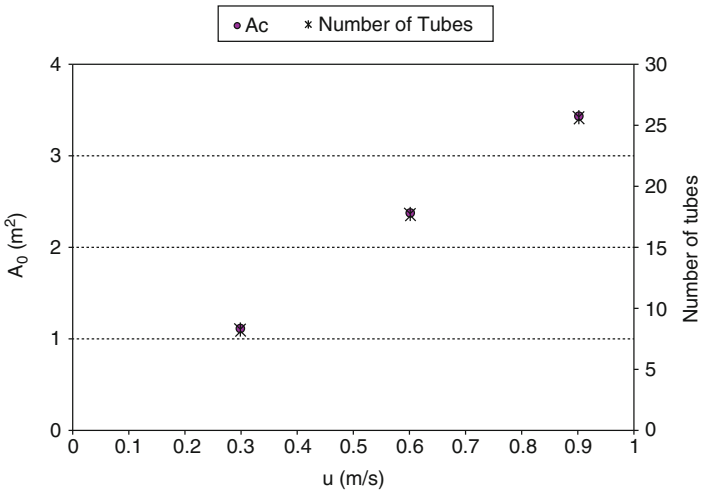

Fig. 22 Apple drying experiments in the experimental dryer of Fig. 14: collector optimal design based on minimum entropy generation N_s. Collection area of the evacuated-tube air solar collector (A_c) and number of tubes as a function of drying air velocity (u). (Lamnatou et al. 2012)

$$\theta_{\text{opt}} = \theta_{\text{max}}^{0.7} \tag{108}$$

Furthermore, MF is calculated for the collector maximum temperature and the fluid exit temperature, which minimize the generated entropy. MF represents the thermal energy of the fluid at the ambient temperature related to the solar energy absorbed and is given by:

$$MF = \frac{\dot{m} C_P T_a}{G A_c (\tau\alpha)} \tag{109}$$

The collector absorber area, when it operates at the minimum loss of available work, can be found from Eq. (109). The results of the study of Lamnatou et al. (2012) are presented in Fig. 22 as a function of the drying air velocity for a fixed mass flow rate. It is obvious that the increase in air velocity leads to an increase of collection area A_c and thus of the tube number. Thus, 8, 18, and 26 tubes are required for 0.3, 0.6, and 0.9 m/s velocity, respectively. The opposite approach may also be considered, i.e., to obtain the optimum flow rate for a given, fixed collector area.

4 Conclusions

Drying is a complex procedure to describe mathematically, given that the relevant phenomena take place at different scales and the characteristic parameters such as material properties exhibit strong variations in space and time. However, the availability of mathematical formulas that are as accurate as possible and easy to implement is a key factor in developing simulation models that can be used in designing drying processes and equipment, combined with experimental methods.

Central part in the modeling procedure occupy the heat and mass (moisture) transport mechanisms in the porous solid material undergoing drying, and these are generally considered at the macroscopic level, often combined with phase-change formulas (evaporation-condensation). Phenomenological laws such as Fick's, Fourier's, and Darcy's laws are involved to express momentum, heat, and moisture transfer, and the relevant equations require a number of transport coefficients which are not always readily available and need to be approximated in an empirical manner. More recently, more realistic conjugate heat-mass transfer models have been introduced, coupling the drying modeling to an external fluid flow.

Regarding solar drying technologies and applications in particular, the diversity of the present state of the art shows that there have not been generally acceptable and workable solutions so far. All available solar drying technologies, both of passive and active type, can satisfy only partially the energy demands (load) of drying, while a part of the load is covered from a conventional power source (electricity or fossil fuel). Thus, the relevant research activity continues today with a twofold objective: to improve first the modeling tools of the drying process (drying kinetics) and second the design of both the drying chamber and the air solar collector. The objectives are, in the first case, to achieve uniform drying conditions and, in the second case, to improve the efficiency of flat plate collectors used in drying applications so far.

In order to achieve the abovementioned objectives, the implementation of efficient algorithms based on models able to accurately describe the drying process for any material becomes obligatory. The continuous improvement in computing power offers scientists the capability to resolve, even in real time, problems involving complicate mathematical models and patterns. Those algorithms and mathematical models require the availability of the values of several parameters, constants, and properties of the materials that suitably describe the real behavior of the material to be dried. The problem is that the various natural, artificial, or by-product materials exhibit strong variability in behavior during drying, even in the case where they constitute members of the same family, group, or subgroup. The determination of the values of those parameters, physical or mathematical, constitutes nowadays the major challenge for the scientists as this is a crucial factor in the accurate characterization of the drying process, the quality of the final product, and the efficient operation of the dryer.

Nomenclature

a_w	Water activity	–
a, b, c, n	Constants	–
A	Area	m^2
A_p	Area of a drying product	m^2
Bi_m	Biot number for mass	–
Bi_h	Biot number for heat	–
$c_{p,p}$	Specific thermal capacity of a product	$kJ \cdot kg^{-1} \cdot K^{-1}$
$c_{p,a}$	Specific thermal capacity of air	$kJ \cdot kg^{-1} \cdot K^{-1}$
C, c_o, K, k_o	Constants in GAB equation	–
D	Moisture diffusion coefficient	$m^2 \cdot s^{-1}$
D_o	Constant in the Arrhenius equation for diffusion	–
D_{eff}	Effective value of diffusivity	$m^2 \cdot s^{-1}$
$D_{eff,ref}$	Reference value for effective diffusivity	$m^2 \cdot s^{-1}$
DR	Drying rate	$kg \cdot kg^{-1}$ dry mater $\cdot s^{-1}$
Fo	Nondimensional Fourier number	–
h_g	Heat transfer coefficient	$W \cdot m^{-2} \cdot {}^\circ C^{-1}$
h_{fg}	Latent heat of evaporation of water	$kJ \cdot kg^{-1}$
J_m	Mass flow	$kg \cdot m^{-2} \cdot s^{-1}$
j_h	Chilton-Colburn coefficient for heat	–
j_m	Chilton-Colburn coefficient for mass	–
k_g	Mass transfer coefficients	$kg \cdot m^{-2} \cdot s^{-1}$
k, k_o, k_1	Constants	–
K_v	Vapor diffusion coefficient	$m^2 \cdot s^{-1}$
K	Drying constant	h^{-1}
L	Characteristic length	m
m	Mass	kg
m_p	Mass of product	kg
m_d	Mass of dry material	kg
M	Moisture content, wet basis	kg $H_2O \cdot kg^{-1}$ prod.
M_o	Initial moisture content, wet basis	kg $H_2O \cdot kg^{-1}$ prod.
M_{eq}	Equilibrium moisture content, wet basis	kg $H_2O \cdot kg^{-1}$ prod.
MR	Moisture ratio	–
M_v	Vapor molecular weight	kg
M_g	Drying air molecular weight	kg
Nu	Nusselt number	–
Pr	Prandtl number	–
P_v	Vapor pressure	Pa
$P_{v,sat}$	Saturated vapor pressure	Pa
P_t	Total pressure of vapor	Pa
P_w	Pressure of vapor over water	Pa
q	Heat flow	$W \cdot m^{-2}$
Re	Reynolds number	–
R	Σταθερά αερίων	$8.3143\ J \cdot mol^{-1} \cdot K^{-1}$
t	Time	h
T, θ	Temperature	°C
T_{abs}	Absolute air temperature	K
T_{air}	Air temperature	°C
T_p	Product temperature	°C
T_{wb}	Wet-bulb temperature	°C
Y	Moisture content of air	kg $H_2O \cdot kg^{-1}$ dry air

V	Volume	m^3
V_b	Apparent volume	m^3
V_{ref}	Reference volume	m^3
v_{air}	Velocity	$m \cdot s^{-1}$
W	Weight	kg
W_o	Initial weight	kg
W_d	Weight of dry matter	kg
X	Moisture content, dry basis	kg $H_2O \cdot kg^{-1}$ dry matter
X_o	Initial moisture content, dry basis	kg $H_2O \cdot kg^{-1}$ dry matter
X_{eq}	Equilibrium moisture content, dry basis	kg $H_2O \cdot kg^{-1}$ dry matter
X_{cr}	Moisture content at critical point	kg $H_2O \cdot kg^{-1}$ dry matter
X_s	Moisture content, dB, at the surface	kg $H_2O \cdot kg^{-1}$ dry matter

Greek Symbols

α	Air or thermal diffusivity of a fluid	$m^2 \cdot s^{-1}$
ε	Porosity of a solid	–
λ	Thermal conductivity	$W \cdot m^{-1} \cdot {}^oC^{-1}$
μ	Dynamic viscosity	$kg \cdot m^{-1} \cdot s^{-1}$
ν	Kinematic viscosity	$m^2 \cdot s^{-1}$
ρ	Density	$kg \cdot m^{-3}$
φ	Relative humidity	%
Φ	Drying parameter	–

Indices

air	Air
b	Bulk
cr	Critical
d	Dry matter
eff	Effective value
eq	Equilibrium value
h	Heat
in	Initial value
l	Liquid
m	Mass
o	Initial value
p	Product
ref	Reference value
sat	Saturated value
v	Vapor
ή vap	
w	Water

References

Adeniyi AA, Mohammed A, Aladeniyi K (2012) Analysis of a solar dryer box with ray tracing CFD technique. Int J Sci Eng Res 3:1–5

Akbulut A, Durmus A (2010) Energy and exergy analyses of thin layer drying of mulberry in a forced solar dryer. Energy 35:1754–1763

Alvarez PI, Legues P (1986) A semi-theoretical model for the drying of Thompson seedless grapes. Dry Technol 4(1):1–17

Aregawi W, Defraeye T, Saneinejad S, Vontobel P, Lehmann E, Carmeliet J, Derome D, Verboven P, Nicolai B (2013) Dehydration of apple tissue: intercomparison of neutron tomography with numerical modelling. Int J Heat Mass Transf 67:173–182

Azzouz S, Guizani A, Lomaa W, Belgith A (2002) Moisture diffusivity and drying kinetic equation of convective drying of grapes. J Food Eng 55:323–330

Babalis S (2006) Theoretical and experimental investigation of the heat and mass transfer phenomena during the drying of foods in hot air stream. PhD thesis, (In Greek) University of Thessaloniki

Babalis SJ, Belessiotis VG (2004) Influence of the drying conditions on the drying constants and moisture diffusivity during thin-layer drying of figs. J Food Eng 65(3):449–458

Babalis S, Papanikolaou E, Kyriakis N, Belessiotis V (2006) Evaluation of thin-layer drying models for describing drying kinetics of Figs (ficus carica). J Food Eng 75(2):205–214

Babbitt JD (1949) Observations on the adsorption of water vapour by wheat. Can J Res Sec F 27:55–72

Bakker-Arkema FW, Bickert WG, Patterson RJ (1967) Simultaneous heat and mass transfer during the cooling of a deep bed of biological products under varying inlet air conditions. Agric Eng Res 12:297–307

Bal LM, Satya S, Naik SN (2010) Solar dryer with thermal energy storage systems for drying agricultural food products: a review. Renew Sust Energ Rev 14:2298–2314

Balaban M, Pigott GM (1988) Mathematical model of simultaneous heat and mass transfer in food with dimensional changes and variable transport parameters. J Food Sci 53(3):935–939

Basunia MA, Abe T (2001) Thin-layer solar drying characteristics of rough rice under natural convection. J Food Eng 47:295–301

Becker HA, Sallans HR (1955) A study of internal moisture movement in the drying of wheat kernel. Cereal Chem 32:212–226

Belghit A, Belahmidi M. et. al. (1997) Étude numérique d'un séchoir solaire fonctionnant en convectionforcée, Revue Général de Thermique 36, No 11, 837–850

Belessiotis V, Delyannis E (2006) Drying: methods and systems – principles of drying procedures. [in Greek], Athens

Belessiotis VG, Delyannis E (2011) Solar Drying. Sol Energy 85:1665–1691

Ben Mabrook S, Belghith A (1995) Numerical simulation of the drying of a deformable material: Evaluation of the diffusion coefficient. Dry Technol 13(8&9):1789–1805

Benhamoua A, Fazouane F (2014) Simulation of solar dryer performances with forced convection experimentally proved. Physics Proc 55:96–105

Bennamou L, Belhamri A (2003) Design and simulation of a solar dryer for agriculture products. J Food Eng 59:259–266

Berger D, Pei DCT (1973) Drying of hygroscopic capillary porous solids – a theoretical approach. Int J Heat Mass Transf 16:293–302

Beuchat LR (1981) Microbial stability as affected by water activity. Cereal Foods World 26(7):345–349

Bolaji BO, Olalusi AP (2008) Performance evaluation of a mixed-mode solar dryer. AU J T 11:225–231

Bruce DM, Sykes RA (1983) Apparatus for determining mass transfer coefficients at high temperatures for exposed paniculate crops with initial results for wheat and hops. JAgric Eng Res 28:385–400

Brunauer S, Emmett PH, Teller E (1938) Adsorption of gases in multicomponent layers. Am Chem Soc J 60:309–319

Byler RK, Anderson CR, Brook RC (1987) Statistical methods in thin-layer parboiled rice drying models. Trans ASAE 30(2):533–538

Caccavale P, De Bonis MV, Ruocco G (2016) Conjugate heat and mass transfer in drying: a modeling review. J Food Eng 176:28–35
Chauhan PS, Kumar A, Tekasakul P (2015) Applications of software in solar drying systems: a review. Renew Sust Energ Rev 51:1326–1337
Chen P, Pei DCT (1989) A mathematical model of drying processes. Int J Heat Mass Transf 18 (2):297–310
Chen XD, Xie GZ (1997) Fingerprints of the drying behaviour of particulate or thin layer food materials established using a reaction engineering model. Trans I Chem E Part C Food Bioprod Process 75:213–222
Chhinnan MS (1984) Evaluation of selected mathematical models for describing thin-layer drying of in-shell pecans. Trans ASAE 84:610–615
Chirarattananon S, Chinporncharoenpong C (1998) A steady-state model for the forced convection solar cabinet dryer. Sol Energy 41(4):349–360
Chirife J, Inglesias HA (1978) Equations for fitting water sorption isotherms of food. Part I. A review. J Food Technol 13:159–174
Cho SH (1975) An exact solution of the coupled phase change problem in a porous medium. Int J Heat Mass Transf 18:1139–1142
Chou SK, Hawlander MNA, Chua KJ (1997) Identification of the receding evaporation front in convective food drying. Dry Technol 15(5):1353–1367
Chua KJ, Chou SK (2003) Low cost drying for developing countries. Food Sci Technol 14:519–528
Chukwunonye CD, Nnaemeka NR, Chijioke OV, Obiora NC (2016) Thin layer drying modelling for some selected products: a review. Am J Food Sci Nutr Res 3(1):1–15
Chung DS, Pfost HB (1967) Adsorption and Desorption of Water Vapor by Cereal Grains and Their Products Part III: A Hypothesis for Explaining the Hysteresis Effect. Transactions of the ASAE 10 (4):0556–0557
Colson KH, Young JH (1990) Two-component thin-layer drying model for unshelled peanuts. Trans ASAE 33(1):241–246
Condori M, Saravia L (2003) Analytical model for the performance of the tunnel-type greenhouse dryer. Renew Energy 28(3):467–485
Cordova-Quiroz AV, Ruiz-Cabrera MA, Garcia-Alvarado MA (1996) Analytical solution of mass transfer equation with interfacial resistance in food drying. Dry Technol 14(7&8):1815–1826
Crapiste GH, Whitaker S, Rotstein E (1988a) Drying of cellular material – I. Mass transfer theory. Chem Eng Sci 43(11):2919–2928
Crapiste GH, Whitaker S, Rotstein E (1988b) Drying of cellular material – II. Experimental and numerical results. Chem Eng Sci 43(11):2929–2936
Datta AK (2007) Porous media approaches to studying simultaneous heat and mass transfer in food processes. I: Problem formulations. J Food Eng 80:80–95
Datta AK (2008) Status of physics-based models in the design of food products, processes, and equipment. Compr Rev Food Sci Food Saf 7:121–129
De Vries DA (1987) The theory of heat and moisture transfer in porous media revisited. Int J Heat Mass Transf 30:1343–1350
Defraeye T (2014) Advanced computational modelling for drying processes – a review. Appl Energy 131:323–344
Defraeye T, Aregawi W, Saneinejad S, Vontobel P, Lehmann E, Carmeliet J, Verboven P, Derome D, Nicolai B (2012) Novel application of neutron radiography to forced convective drying of fruit tissue. Food Bioprocess Technol 6:3353–3367
Dev SRS, Raghavan VGS (2012) Advancements in drying techniques for food, fiber, and fuel. Dry Technol 30:1147–1159
Dietl C, George OP, Bansal NK (1995) Modeling of diffusion in capillary porous materials during the drying process. Dry Technol 13(1&2):267–293
Dincer I, Dost S (1995) An analytical model for moisture diffusion in solid objects during drying. Dry Technol 13(1&2):425–435

Doymaz I, Pala M (2002) Hot-air drying characteristics of red pepper. J Food Eng 55:331–335
Dutta SK, Nema VK, Bhardwaj RK (1988) Drying behaviour of spherical grains. Int J Heat Mass Transf 31(4):855–861
Ekechukwu OV (1999) Review of solar-energy drying systems I: an overview of drying principles and theory. Energy Convers Manag 40:593–613
Ekechukwu OV, Norton B (1999a) Review of solar-energy drying systems II: an overview of solar drying technology. Energy Convers Manage 40(6):615–655
Ekechukwu OV, Norton B (1999b) Review of solar-energy drying systems III: low temperature air-heating solar collectors for crop drying applications. Energy Convers Manag 40 (6):657–667
El-Sebaii AA, Shalaby SM (2012) Solar drying of agricultural products: a review. Renew Sust Energ Rev 16:37–43
Erbay Z, Icier F (2009) A review of thin layer drying of foods: theory, modeling, and experimental results. Crit Rev Food Sci Nutr 50:441–464
Ertekin CM, Ziya Firat MZ (2015) A comprehensive review of thin layer drying models used in agricultural products. Crit Rev Food Sci Nutr 57:701–717
Forson FK, Nazha MA (2007) Design of mixed-mode natural convection solar crop dryers: application of principles and rules of thumb. Renew Energy 32:2306–2319
Forson FK, Nazha MA (2008) Modelling and experimental studies on a mixed-mode natural convection solar crop-dryer. Sol Energy 81:346–357
Fortes M, Okos MR (1981a) A non-equilibrium thermodynamics approach to transport phenomena in capillary porous media. Trans ASAE 24(3):756–760
Fortes M, Okos MR (1981b) Heat and mass transfer in hygroscopic capillary extruded products. AIChE J 27(2):255–262
Fortes M, Okos MR (1981c) Non-equilibrium thermodynamics approach to heat and mass transfer in corn cernels. Trans ASAE 24(3):761–769
Fudholi A, Sopian K, Ruslan MH, Alghoul MA, Sulaiman MY (2010) Review of solar dryers for agricultural and marine products. Renew Sust Energ Rev 14:1–30
Furuta T, Hayakawa K-I (1992) Heat and moisture transfer with thermodynamically interactive fluxes. I Mathematical model development and numerical solution. Trans ASAE 35 (5):1537–1546
Furuta T, Tsukada T, Hayakawa K-I (1992) Heat and moisture transfer with thermodynamically interactive fluxes and volumetric changes. III. Computer simulation. Trans ASAE 35 (5):1553–1557
Gallesty E, Paice AD (1996) Mathematical modeling and optimal control of solar dryers. J Math Model Syst 1:27–54
Gamson BW, Thodos G, Hougen OA (1943) Heat, mass and momentum transfer in the flow of gases through granular solids. Trans Am Inst Chem Engrs 39:l–25
Ghaffari A, Mehdipour R (2015) Modeling and improving the performance of cabinet solar dryer using computational fluid dynamics. Int J Food Eng 11(2):157–172
Gibson RD, Cross M, Young RW (1979) Pressure gradients generated during the drying of porous shapes. Int J Heat Mass Transf 22:827–830
Halder A, Datta AK, Spanswick RM (2011) Water transport in cellular tissues during thermal processing. AICHE J 57:2574–2588
Handley RG (1982) Theoretical treatment of evaporation front drying. Int J Heat Mass Transf 25 (10):1511–1522
Hansen RC, Keener HM, ElSohly HN (1993) Thin-layer drying of cultivated Taxus clippings. Trans ASAE 36(5):1387–1391
Harmathy TZ (1969) Simultaneous moisture and heat transfer in porous systems with particular reference to drying. Ind Eng Chem Fundam 8(1):92–103
Hedayatizadeh M, Chaji H (2016) A review on plum drying. Renew Sustain Energy Rev 56:362–367

Henderson SM, Pabis S (1961) Grain drying theory. 1 Temperature effect on drying coefficient. J Agric Eng Res 6:169–174
Henry PH (1948) The diffusion of moisture and heat through textiles. Discussions of the Faraday Society 3:243
Ho QT, Carmelie J, Datta AK, Defraeye D, Delele MA, Herremans E, Opara L, Ramon H, Tijskens E, van der Sman R, Van Liedekerke P, Verboven P, Nicolaï BM (2013) Multiscale modeling in food engineering. J Food Eng 114:279–291
Hukill WV (1954) In: Anderson JA, Alcock AW (eds) Grain dying in storage of cereal grains and their products. American Association of Cereal Chemistry, St. Paul
Hughes BR, Oates M (2011) Performance investigation of a passive solar-assisted kiln in the United Kingdom. Sol Energy 85:1488–1498
Hustrulid A (1963) Comparative drying rates of naturally moist, re-moistened and frozen wheat. Trans ASAE 6:304–308
Jain D (2005) Modelling the performance of greenhouse with packed bed thermal storage on crop drying applications. J Food Eng 71(2):170–178
Jain D, Tiwari GN (2003) Thermal aspects of open sun drying of various crops. Energy 28:37–54
Jain D, Tiwari GN (2004) Effect of greenhouse on crop drying under natural and forced convection. II. Thermal modeling and experimental validation. Energy Convers Manage 45:2777–2793
Jairaj KS, Singh SP, Srikant K (2009) A review of solar dryers developed for grape drying. Sol Energy 83:1698–1712
Jamaleddine TJ, Ray MB (2010) Application of computational fluid dynamics for simulation of drying processes: a review. Dry Technol 28:120–154
Janjai S, Lamlert N, Intawee P, Mahayothee B, Boonrod Y, Haewsungcharern M, Bala BK, Nagle M, Müller J (2009) Solar drying of peeled longan using a side loading type solar tunnel dryer: experimental and simulated performance. Dry Technol 27:595–605
Jaros M, Cenkowski S, Jayas DS, Pabis S (1992) A method of determination of the diffusion coefficient based on kernel moisture content and its temperature. Dry Technol 10(1):213–222
Jayas DS, Sokhansanj S (1989) Thin-layer drying of barley at low temperatures. Can Agric Eng 31:21–23
Jayas DS, Cenkowski S, Pabis S, Muir WE (1991) Review of the thin-layer drying and wetting equations. Dry Technol 9(3):551–588
Karathanos VT, Belessiotis VG (1997) Sun and artificial air-drying kinetics of some agricultural products. J Food Eng 31(1):35–46
Karathanos VT, Belessiotis VG (1999) Application of a thin-layer equation to drying data of fresh and semi-dried fruits. J Agric Eng Res 74(4):355–362
Katekawa ME, Silva MA (2006) A review of drying models including shrinkage effects. Dry Technol 24:5–20
Krawczyk P, Badyda K (2011) Two-dimensional CFD modeling of the heat and mass transfer process during sewage sludge drying in a solar dryer. Arch Thermodyn 32:3–16
Kucuk H, Midilli A, Kilic A, Dincer D (2014) A review on thin-layer drying-curve equations. Dry Technol 32:757–773
Kumar pandey S, Diwan S, Soni R (2015) Review of mathematical modelling of thin layer drying process. Int J Curr Eng Sci Res 2(11):96–107
Kumar A, Blaisdell JL, Herum FL (1982) Generalized analytical model for moisture diffusion in a composite cylindrical body. Trans ASAE 25(3):752–758
Kuzmak JM, Sereda PJ (1957a) The mechanism by which water moves through a porous material subjected to a temperature gradient.: I. Introduction of a vapour gap into a saturated system. Soil Sci 84:291–299
Kuzmak JM, Sereda PJ (1957b) The mechanism by which water moves through a porous material subjected to a temperature gradient.: II. Salt tracer and streaming potential to detect flow in the liquid phase. Soil Sci 84:419–422

Lago ME, Bohm U, Plachco F (1971) Diffusional mass transfer through porous media. Int J Heat Mass Transf 14:813–823
Lahsasni S, Kouhila M, Mahrouz M, Jouhari JT (2004) Drying kinetics of prickly pear fruit (Opuntia ficus indica). J Food Eng 61:173–179
Lamnatou C, Papanicolaou E, Belessiotis V, Kyriakis N (2010) Finite-volume modeling of heat and mass transfer during convective drying of porous bodies – non-conjugate and conjugate formulations involving the aerodynamic effects. Renew Energy 35(7):1391–1402
Lamnatou C, Papanicolaou E, Belessiotis V, Kyriakis N (2012) Experimental investigation and thermodynamic performance analysis of a solar dryer using an evacuated-tube air collector. Appl Energy 94(2):232–243
Langmuir I (1918) The adsorption of gases on plane surfaces of glass, mica and platinum. J Am Chem Soc 40:1361–1402
Lemus-Mondac R, Vega-Galvez A, Moraga NO (2011) Computational simulation and developments applied to food thermal processing. Food Eng Rev 3:121–135
Leon MA, Kumar S, Bhattachaya SC (2002) A comprehensive procedure for performance evaluation of solar dryers. Renew Sustain Energy Rev 6:367–393
Lewicki PP, Pawlak G (2003) Effect of drying on microstructure of plant tissue. Dry Technol 21:657–683
Lewis WK (1921) The rate of drying of solid materials. Ind Eng Chem 13:427–432
Liu JY, Cheng S (1991) Solutions of Luikov equations of heat and mass transfer in capillary-porous bodies. Int J Heat Mass Transf 34(7):1747–1753
Luikov AV (1961) Application of methods of thermodynamics of irreversible processes to investigation of heat and mass transfer in a boundary layer. Int J Heat Mass Transf 3:167–174
Luikov AV (1966) Application of irreversible thermodynamics methods to investigation of heat and mass transfer. Int J Heat Mass Transf 9(1):139–152
Luikov AV (1975) Systems of differential equations of heat and mass transfer in capillary porous bodies (review). Int J Heat Mass Transf 18:1–14
Luikov AV, Perelman TL, Levdansky VV, Leitsina VG, Pavlyukevich NV (1974) Theoretical investigation of vapour transfer through a capillary – porous body. Int J Heat Mass Transf 17:961–970
Madamba PS, Driscoll RH, Buckle KA (1996) The thin-layer drying characteristics of garlic slices. J Food Eng 29:75–97
Mathioulakis E, Karathanos VT, Belessiotis VG (1998) Simulation of air movement in a dryer by computational fluid dynamics: application for the drying of fruits. J Food Eng 36:182–200
Mikhailov MD (1973) General solutions of the diffusion equations coupled at boundary conditions. Int J Heat Mass Transf 16:2155–2164
Mikhailov MD (1975) Exact solution of temperature and moisture distribution in a porous half-space with moving evaporation front. Int J Heat Mass Transf 18:797–804
Mikhailov MD, Shishedjiev BK (1975) Temperature and moisture distributions during contact drying of a moist porous sheet. Int J Heat Mass Transf 18:15–24
Misra MK, Brooker DB (1980) Thin-layer drying and rewetting equations for shelled yellow corn. Trans ASAE 23:1254–1260
Muhidong J, Chen LH, Smith DB (1992) Thin-layer drying of kenaf. Trans ASAE 35 (6):1941–1944
Murthy Ramana MV (2009) A review of new technologies, modes and experimental investigations of solar driers. Renew Sust Energ Rev 13:835–844
Mustayen AGMB, Mekhilef S, Saidur R (2014) Performance study of different solar dryers: a review. Renew Sust Energ Rev 34:463–470
Noomhorm A, Verma LR (1986) Generalized single-layer rice drying models. Trans ASAE 29 (2):587–591
Norton T, Tiwari B, Sun D-W (2013) Computational fluid dynamics in the design and analysis of thermal processes: a review of recent advances. Crit Rev Food Sci Nutr 53:251–275

Ogheneruona D, Yusuf MOL (2011) Design and fabrication of a direct natural convection solar dryer for Tapioka. Leonardo Electron J Pract Technol 18:95–104
Onwude DI, Hashim N, Janius RB, Nawi NM, Abdan K (2016) Modeling the thin-layer drying of fruits and vegetables: a review. Compr Rev Food Sci Food Saf 15
Osnager L (1931a) Reciprocal relations in irreversible processes. I. Phys Rev 37:405–426
Osnager L (1931b) Reciprocal relations in irreversible processes. II. Phys Rev 38:2265–2279
Oueslati H, Ben Mabrouk S, Mami A (2012) System design, mathematical modelling and simulation of process drying in a solar-gas convective tunnel dryer. Int J Sci Eng Res 3(5):1–8
Overhults DG, White HE, Hamilton HE, Ross IJ (1973) Drying soybean with heated air. Trans ASAE 16:112–113
Pabis S (1967) Grain drying in thin layers. Paper No. 1lCl4. Presented in Silsoe, England, Symposium 12 Aug 1967
Page GE (1949) Factors influencing the maximum rates of air drying shelled corn in thin layers. M. Sc. thesis, Purdue University
Pahlavanzadeh H, Basiri A, Zarrabi M (2001) Determination of parameters and pretreatment solution for grape drying. Dry Technol 19(1):217–226
Pakowski Z (1991) Evaluation of equations approximating thermodynamic and transport properties of water, steam and air for use in CAD for drying processes. Dry Technol 9(3):753–773
Pakowski Z (1999) Simulation of the process of convective drying: identification of generic computation routines and their implementation in a computer code dryPAK. Comput Chem Eng 23(Suppl):S719–S722
Panchariya PC, Popovic D, Sharma AL (2002) Thin layer modeling of black tea drying process. J Food Eng 52:349–357
Pangavhane DR, Sawhney RL (2002) Review of research and developing work on solar dryers for grape drying. Energy Conversion & Management 43(1):45–61
Parry L (1985) Mathematical modelling and computer simulation of heat and mass transfer in agricultural grain drying: a review. J Agric Eng Res 32:1–29
Parti M (1990) A theoretical model for thin-layer grain drying. Dry Technol 8(1):101–122
Parti M, Dugmanics I (1990) Diffusion coefficient for Corn drying. Trans ASAE 33(5):1652–1656
Parti M (1993) Selection of Mathematical Models for Drying Grain in Thin-Layers. Journal of Agricultural Engineering Research 54 (4):339–352
Patil R, Gawande R (2016) A review on solar tunnel greenhouse drying system. Renew Sust Energ Rev 56:196–214
Paulscn MR, Thompson TL (1973) Drying analysis of grain sorghum. Trans ASAE 16:537–540
Pereira da Silva W, Cleide MDPSe S, Gama FJA, Palmeira Gomes J (2014) Mathematical models to describe thin-layer drying and to determine drying rate of whole bananas. J Saudi Soc Agric Sci 13:67–74
Perré P (2010) Multiscale modeling of drying as a powerful extension of the macroscopic approach: application to solid wood and biomass processing. Dry Technol 28:944–959
Perré P, Rémond R, Colin J, Mougel E, Almeida G (2012) Energy consumption in the convective drying of timber analyzed by a multiscale computational model. Dry Technol 30:1136–1146
Phadke PC, Walke PV, Kriplani VM (2015) A review on indirect solar dryers. ARPN J Eng Appl Sci 10(8):3360–3371
Philip JR (1957a) The theory of infiltration: I. The infiltration equation and its solution. Soil Sci 83:345–347
Philip JR (1957b) The theory of infiltration: I. The profile of infinity. Soil Sci 83:435–448
Prakash O, Kumar A (2013) Historical review and recent trends in solar drying systems. Int J of Green Energy 10(7):690–738
Prakash O, Laguri V, Pandey A, Kumar A, Kumar A (2016) Review on various modelling techniques for the solar dryers. Renew Sust Energ Rev 62:396–417
Raj PPK, Emmons HW (1975) Transpiration drying of porous hygroscopic materials. Int J Heat Mass Transf 18:635–648

Rapusas RS, Driscoll RH (1995) The thin layer drying characteristics of white onion slices. Dry Technol 13(8&9):1905–1931
Ratti C, Crapiste GH (1992). A generalized drying curve for shrinking food materials. Paper presented at IDS'92, Montreal, 2–5 August 1992
Reyes A, Mahn A, Vásquez F (2014) Mushrooms dehydration in a hybrid-solar dryer, using a phase change material. Energy Convers Manag 83:241–248
Ribeiro JW, Cotta RM, Mikhailov MD (1993) Integral transform solution of Luikov's equations for heat and mass transfer in capillary porous media. Int J Heat Mass Transf 36(18):4467–4475
Roa G, Fioreze R, Rossi, JS, Villa LG (1977) Dynamic estimation of thin-layer drying parameters. ASAE Paper 77-3530
Rossen JL, Hayakawa K (1977) Simultaneous heat and moisture transfer in dehydrated food. A review of theoretical models. AIChE Symp Ser 73(163):71–81
Sablani S (2008) Status of observational models in design and control of food processes. Compr Rev Food Sci Food Saf 7:130–136
Sakai N, Hayakawa K-I (1992) Two dimensional simultaneous heat and moisture transfer in composite food. J Food Sci 57(2):475–480
Sami S, Etesami N, Rahimi A (2011a) Energy and exergy analysis of an indirect solar cabinet dryer based on mathematical modelling results. Int J Energy 36:2847–2855
Sami S, Rahimi A, Etesami N (2011b) Dynamic modeling and a parametric study of an indirect solar cabinet dryer. Dry Technol 29:825–835
Sander A (2007) Thin-layer drying of porous materials: selection of the appropriate mathematical model and relationships between thin-layer models parameters. Chem Eng Process 46:1324–1331
Saravakos GD, Charm SE (1962) A study of the mechanism of fruit and vegetable dehydration. Food Technol 26(1):78–81
Sawhney RL, Pangavhane DR, Sarsavadia PN (1999a) Drying kinetics of single layer Thompson seedless grapes under heated ambient air conditions. Dry Technol 17(1&2):215–236
Sawhney RL, Sarsavadia PN, Pangavhane DR, Singh SP (1999b) Determination of drying constants and their dependence on drying air parameters for the thin layer onion drying. Dry Technol 17(1&2):299–315
Schadler N, Kast W (1987) A complete model of the drying curve for porous bodies – experimental and theoretical studies. Int J Heat Mass Transf 30:2031–2044
Sereno AM, Medeiros GL (1990) A simplified model for the prediction of drying rates for foods. J Food Eng 12:1–11
Sharaf-Eldeen YI, Hamdy MY, Blaisdell JL (1979) Falling rate drying of fully exposed biological materials: a review of mathematical models. ASAE Paper No. 79-6622. Winter Meeting of ASAE
Sharaf-Eldeen YI, Blaisdell JL, Hamdy MY (1980) A model for ear corn drying. Trans ASAE 23:1261–1265
Sharma A, Chen CR, Lan NV (2009) Solar-energy drying systems: a review. Renew Sust Energ Rev 13:1185–1210
Shokouhmand H, Abdollahi V, Hosseini S, Vahidkhah K (2011) Performance optimization of a brick dryer using porous simulation approach. Dry Technol 29:360–370
Shusheng P, Langrish TAG, Keey RB (1993) The heat of sorption of timber. Dry Technol 11 (5):1071–1080
Simal S, Mulet A, Catala PJ et al (1996) Moving Boundary model for simulating moisture movement in grapes. J Food Sci 61:157–160
Singh PL (2011) Silk cocoon drying in forced convection type solar dryer. Appl Energy 88:1720–1726
Singh PC, Singh RK (1996) Application of GAB model for water sorption isotherms of food products. J Food Process Preserv 20:203–220
Singh RK, Lund DB, Buelow FH (1983a) Application of solar energy in food processing. II Food dehydration. Trans ASAE 26(5):1569–1574

Singh RK, Lund DB, Buelow FH (1983b) Application of solar energy in food processing. III Economic performance evaluation. Trans ASAE 26(5):1575–1579
Sokhansanj S, Bruce DM (1987) A conduction model to predict grain drying temperatures in grain drying simulation. Trans ASAE 30(4):1181–1184
Sontakke MS, Salve SP (2015) Solar drying technologies: a review. Int Referee J Eng Sci (IRJES) 4(4):29–35
Spencer HB (1969) A mathematical simulation of grain drying. Journal of Agricultural Engineering Research 14 (3):226–235
Sreekumar A, Manikantan PE, Vijayakumar KP (2008) Performance of indirect solar cabinet dryer. Energy Convers Manag 49(1):388–395
Srikiatden J, Roberts JS (2007) Moisture transfer in solid food materials: a review of mechanisms, models, and measurements. Int J Food Prop 10(4):739–777
Sun LM, Meunier F (1987) A detailed model for nonisothermal sorption in porous absorbents. Chemical Engineering Science 42(7), 1585–1593.
Sun D-W, Woods JL (1994) Low temperature moisture transfer characteristics of wheat in thin-layers. Trans ASAE 37(6):1919–1926
Thompson TL, Peart RM, Foster GH (1968) Mathematical simulation of corn drying – a new model. Trans ASAE 11:582–586
Troeger JM, Hukill WV (1971) Mathematical description of the drying rate of fully exposed corn. Trans ASAE 14:1153–1156, 1162.
Toei R (1996) Theoretical fundamentals of drying operation. Dry Technol 14(1):1–194
Togrul IT, Pehlivan D (2004) Modelling of thin-layer drying kinetics of some fruits under open-air sun drying process. J Food Eng 65(3):413–425
Torres-Reyes E, Cervantes-de Gortari JG, Ibarra-Salazar BA, Picon-Nuρez MA (2001) Design method of flat-plate solar collectors based on minimum entropy generation. Energy Int J 1(1):46–52
Torres-Reyes E, Navarrete-Gonzalez JJ, Ibarra-Salazar BA (2002) Thermodynamic method for designing dryers operated by flat-plate solar collectors. Renew Energy 26:649–660
Toshniwal U, Karale SR (2013) A review paper on Solar Dryer. Int J Eng Res Appl (IJERA) 3(2):896–902
Tripathi G, Shukla KN, Pandey RN (1977) Intensive Drying of an Infinite Plate. Int J Heat Mass Transf 20:451–458
Tulasidas TN, Raghavan GSV, Norris ER (1993) Microwave and convective drying of grapes. Trans ASAE 36(6):1861–1865
Vaccarezza LM, Chirife J (1975) On the mechanism of moisture transport during air drying of sugar beet root. J Food Sci 40:1286–1289
Vaccarezza LM, Chirife J (1978) On the application of Fick's law for the kinetic analysis of air drying of foods. J Food Sci 43:236–238
Vagenas GK (1988) Application of heat and mass transfer in air-drying of foods. PhD thesis (in Greek), National Technical University of Athens
Vagenas GK, Marinos-Kouris D, Saravakos GD (1990) An analysis of mass transfer in air-drying of foods. Dry Technol 8(2):323–342
Van der Zanden AJJ, Coumans WJ, Kerkhof PJAM, Schoenmakers AME (1996) Isothermal moisture transport in partially saturated porous media. Dry Technol 14(7&8):1525–1542
Vazquez G, Chenlo F, Moreira R, Costoyas A (1999) The dehydration of garlic. 1. Desorption isotherms and modelling of drying kinetics. Dry Technol 17(6):1095–1108
Vijaya Venkata Ramana S, Iniyanb S, Goicc R (2012) A review of solar drying technologies. Renew Sust Energ Rev 16:2652–2670
Waananen KM, Litchfield JB, Okos MR (1993) Classification of drying models for porous solids. Dry Technol 11(1):1–40
Walton LR, Casada ME (1986) A new diffusion model for drying burley tobacco. Trans ASAE 29(1):271–275

Walton LR, White GM, Ross IJ (1988) A cellular diffusion-based drying model for corn. Trans ASAE 31(1):279–283
Wan J, Langrish TAG (1995) A numerical simulation for solving the diffusion equation in the drying of hardwood timber. Dry Technol 13(3):783–799
Wang N, Brennan JG (1995) A mathematical model of simultaneous transfer during drying of potato. J Food Eng 24:47–60
Wang CN, Singh RP (1978) A single layer drying equation for rough rice. ASAE Paper 78-3001
White GM, Bridges TC, Loewer OJ, Ross IJ (1981) Thin-layer drying model for soybeans. Trans ASAE 24:1643–1646
Willits DH, Ross IJ, White GM, Hamilton HE (1976) A mathematical drying model for porous materials: Part I – theory. Trans ASAE 19:556–561
Xia B, Sun D-W (2002) Application of Computational Fluid Dynamics (CFD) in the food industry: a review. Comput Electron Agric 34:5–24
Yaldiz O, Ertekin C, Uzun HB (2001) Mathematical modelling of thin-layer solar drying of sultana grapes. Energy 26:457–465
Yu W-P, Wang B-X, Shi M-H (1993) Modeling of heat and mass transfer in unsaturated wet porous media with consideration of capillary hysteresis. Int J Heat Mass Transf 36:3671–3676
Zomorodian A, Moradi M (2010) Mathematical modeling of forced convection thin layer solar drying for Cuminum cyminum. Int J Agr Sci Tech 12:401–408

Advancement in Greenhouse Drying System

Anil Kumar, Harsh Deep, Om Prakash, and O.V. Ekechukwu

Abstract Greenhouses are extensively glazed (typically of glass or plastic) buildings which are thermally conditioned within desired range, used for cultivating tender plants or growing plants out of season: short-wavelength visible light passes through the transparent glazing and is absorbed by interior surfaces which heat up and emit long-wave infrared radiation. Air warmed by the heat emitted from warmed interior surfaces is retained within the enclosure by the roof and walls. Greenhouse dryers are essentially modified greenhouses. They are equipped with vents sized and positioned appropriately to control the airflow. Practically realized greenhouse dryers are typically of the integral- or direct-type solar dryers and sometimes of the mixed mode. They are predominantly passive and in some cases active. Comprehensive description and application of the greenhouse as a dryer is present in this chapter.

Keywords Greenhouse dryer • Greenhouse effect • Passive mode • Active mode • Direct mode • Indirect mode • Mixed mode

1 Introduction

Open sun drying or natural drying is being frequently used from generation in the developing countries. This is mainly because it practically does not involve any technology and capital investment except labor cost. It takes advantage of the local

A. Kumar
Department of Energy (Energy Centre), Maulana Azad National Institute of Technology, Bhopal 462003, Madhya Pradesh, India

H. Deep • O. Prakash (✉)
Department of Mechanical Engineering, Birla Institute of Technology, Mesra, Ranchi 835215, India
e-mail: omprakash@bitmesra.ac.in

O.V. Ekechukwu
Department of Mechanical Engineering, University of Nigeria, Nsukka 410001, Nigeria

© Springer Nature Singapore Pte Ltd. 2017

O. Prakash, A. Kumar (eds.), *Solar Drying Technology*, Green Energy and Technology, DOI 10.1007/978-981-10-3833-4_5

atmosphere (Ekechukwu and Norton 1999). Although it is a widely used method for drying, however it has certain very serious limitations such as overdrying, underdrying, spoilage by the bird and beast, sudden change of the weather, etc. The quality of the dried product is of low quality (Prakash and Kumar 2013a; Kumar et al. 2014). In this situation, solar dryer emerges as the alternative solution for the drying. It removes all disadvantages of the open sun drying. It can be operated based on natural convection mode (passive mode) and forced convection mode (active mode) of heat transfer. A solar dryer under passive mode depends for their operation entirely on solar energy. In such systems, solar-heated air is circulated through the crop by buoyancy forces. These dryers are often called "passive" in order to distinguish them from "active" solar dryers that employ fans to convey the air through the crop (Prakash et al. 2016a).

Comprehensive reviews of solar dryer types exist in literature (Prakash et al. 2016b). Solar energy drying systems are classified primarily per their heating modes and the manner in which the solar heat is utilized. In broad terms, they can be classified into two major groups, namely, active solar energy drying systems (most types of which are often termed hybrid solar dryers) and passive solar energy drying systems (conventionally termed natural-circulation solar drying systems). Three distinct subclasses of either the active or passive solar drying systems can be identified which vary mainly in the design arrangement of system components and the mode of utilization of the solar heat, namely, integral-type (often referred to as direct) solar dryers, distributed-type (usually referred to as indirect) solar dryers, and the mixed-mode solar dryers.

Drying process is the least costly method of preserving foods as compared to all other methods of postharvest preservation. Furthermore, the suitable drying methodology is applied in each food using suitable pre- and post-processing and suitable dryers (Mujumdar 2008). It is very important to select the proper pre- and post-processing steps in order to reduce the drying load and drying time and to make good quality of dried food product. These are the preprocessing steps applied depending on foods—osmotic dehydration, blanching, salting, and soaking. In addition, various post-processing steps— coating and packaging—had the immense impact on dried food.

1.1 Definition of Greenhouse

Greenhouses are extensively glazed (typically of glass or plastic) buildings which are thermally conditioned within desired range, used for cultivating tender plants or growing plants out of season: short-wavelength visible light passes through the transparent glazing and is absorbed by interior surfaces which heat up and emit long-wave infrared radiation. Air warmed by the heat emitted from warmed interior surfaces is retained within the enclosure by the roof and walls.

The "greenhouse effect" is thus extended to the role the atmosphere plays in insulating and warming the earth's surface. The atmosphere is largely transparent to

incoming solar radiation. When this radiation strikes the earth's surface, some of it is absorbed, thereby warming the earth's surface. The surface of the earth emits some of its energy back out in the form of infrared radiation. As this infrared radiation travels through the atmosphere, much of it is absorbed by atmospheric gases such as carbon dioxide, methane, nitrous oxide, and water vapor. These gases then reemit infrared radiation, some of which is absorbed by the earth. The absorption of infrared energy by the atmosphere and the earth is called the greenhouse effect, which maintains a temperature range on the earth that is hospitable to life. Without the greenhouse effect, the earth would be a frozen planet with an average temperature of about -18 °C (0 °F) (Prakash 2015).

1.2 Greenhouse Dryers

The greenhouse dryer is being operated in two different modes of heat transfer. When it is operated under natural convection mode of heat transfer, then it is called a greenhouse dryer under passive mode. When it is operated under forced convection based on heat transfer, then it is called a greenhouse dryer under active mode. Greenhouse dryer under passive mode is also known as tent dryer. By proper design of this system, it provided better control of the overdrying process as compared to the solar cabinet dryer. It is more appropriate for large-scale drying of the agricultural produce (Prakash and Kumar 2014a). In the greenhouse dryer under passive mode, crop is placed inside the drying chamber over the drying tray. The drying air removes the moisture due to thermosyphon effect. Hence, hot exhaust air takes away the moisture and crop gets dried up (Chauhan et al. 2015). The moist air removal could be achieved by forced convection, in which case such greenhouse dryers would be active.

A greenhouse dryer under passive mode is found to be cheaper and easy to fabricate as compared to the greenhouse dryer under active mode. The only shortcoming of this is the slow drying rate and local overheat.

To overcome these limitations, a solar chimney can be employed, which increases the buoyancy force imposed on the airstream, to provide a greater airflow velocity and, thus, a more rapid rate of moisture removal.

Greenhouses are traditionally used for the cultivation of crops. It can also be used for space heating, soil solarization, poultry, and aquaculture. This creates an ideal atmosphere for the cultivation. Greenhouse dryers are adaptations of the traditional greenhouse for drying. Therefore, the greenhouse structure can be used throughout the year for a variety of purposes, for example, for cultivation and for drying purposes. This easy adaptability makes the greenhouse structure more economically feasible. It has little capital cost or no capital cost is required, and running costs are low: often labor only (Kumar et al. 2006).

1.3 Application of Greenhouse

The greenhouse is used in five different ways.

1.3.1 Crop Cultivation

Light energy is indispensable for most of living organism. Photosynthesis enables the utilization of solar energy for crop production. Visible light is the major source of energy for plants. Solar radiation, along with water and carbon dioxide, participates in the process of photosynthesis. It leads to the growth of the plant. Variation in any of these parameters adversely influences the growth of the plant. When plant is cultivated in the open field, there were no provisions to control any of these parameters. Plants are subject to variability in ambient conditions. Unsteady wind and untimely rain adversely affect the plant growth. India, for example, has a large scope to apply the greenhouse for cultivation purpose (Cakmakçi et al. 2006).

1.3.2 Crop Drying

The basic principles of solar energy drying have been discussed comprehensively previously in literature. In the greenhouse, there is collection of solar energy and its conversion into thermal form of energy: short-wavelength visible light passes through the transparent glazing and is absorbed by both the crop and the interior surfaces which heat up and emit long-wave infrared radiation. Air warmed by the heat emitted from warmed interior surfaces is retained within the enclosure by the roof and walls acting as an envelope by minimizing convective heat losses (Prakash and Kumar 2014a).

1.3.3 Soil Solarization

Soil solarization is the most efficient process of controlling damage due to soil borne and plant pathogens. In this process, solar energy is used to heat the soil to the certain temperature, which is fatal to these organisms. Soil solarization works on the principle of passive solar heating process. It happened by covering moist soil with transparent plastic film in clear sky condition with plenty of sunlight, for a 2- to 8-week period. Most of the pest gets killed at a temperature in between 40 and 60 °C. Loannou (2000) has done a detailed study in the field of greenhouse soil solarization.

1.3.4 Aquaculture

The greenhouse pond system is an alternative for maintaining water temperature. A shallow solar pond covered with transparent plastic cover maintains required temperature due to greenhouse effect causing ideal atmosphere for the growth of living organism residing in the water. Silva et al. (2011) have applied a geographic information system (GIS) and farm-scale model for site selection of shellfish aquaculture.

2 Types of Greenhouse Drying System

A broad classification of the greenhouse applications is presented in the Fig. 1 (Kumar et al. 2006). There are various shapes and sizes of the solar greenhouse dryer based on the requirements (Tiwari and Goyal 1998). Greenhouse dryers can

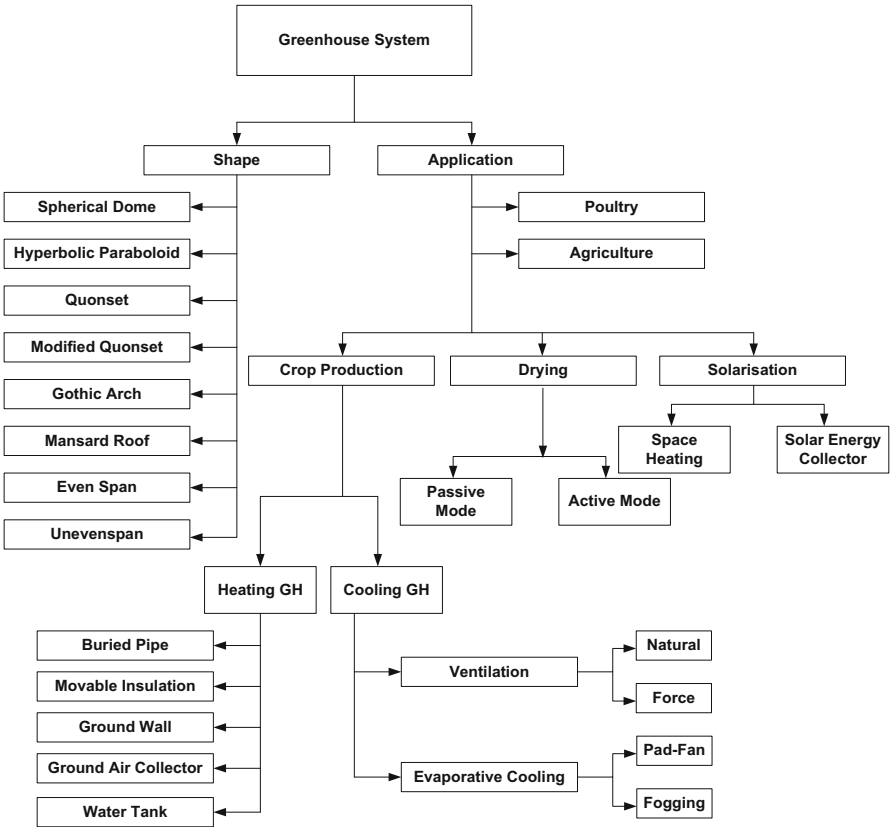

Fig. 1 Classification of greenhouse (Kumar et al. 2006)

be classified into two main types based on structure, namely: dome shape and roof even type. The objective of the dome-type greenhouse dryer is to enhance solar radiation utilization, while the roof even span type improves air circulation within the dryer. Greenhouse dryer is also classified based on heating of drying air. Based on that it is classified into two groups, namely, active and passive mode of a greenhouse dryer. The greenhouse dryer under passive mode operates based on natural convection of heat transfer. Its drying performance can be enhanced by attaching a chimney at the air outlet of the system. The greenhouse dryer under active mode operates based on forced convection of heat transfer. Here pump or exhaust fan is applied at the air outlet of the drying air. The moist air gets drawn out through an exhaust fan/ventilator.

3 State-of-the-Art Research Work on Minimization of Thermal Losses in Greenhouse

Researchers and scientists have done extensive research work in area of minimization of the thermal losses in the greenhouse dryer. Gupta et al. (2012) have done detailed calculation of total solar fraction for all different orientations of greenhouse. They have used 3D shadow analysis in the AutoCAD software. Based on detailed study, it is being concluded that there is a very significant loss of incident solar radiation through the north wall as compared to the other walls in the greenhouse in the northern hemisphere of the globe. It has attracted attention of the researchers in recent years. Santamouris et al. (1994) evaluated the performance of the north wall and observed that inside temperature of the greenhouse is 10 °C higher than ambient temperature. There is no contribution toward the heating of the greenhouse by the transmitted global solar radiation incident on the transparent north wall in the northern hemisphere (Tiwari et al. 2002). The distribution of the transmitted solar intensity was calculated by an experiment inside the greenhouse. In the northern hemisphere, the orientation of solar greenhouse is kept east-west to evaluate the solar fraction for the north wall. Researchers used an AutoCAD model to evaluate the solar fraction (Tiwari et al. 2003; Gupta and Tiwari 2004; Gupta and Tiwari 2005). Some researchers have used solar fraction for north wall in writing an energy balance equation for thermal modeling and crops drying (Ghosal and Tiwari 2004). The solar fraction for the north wall cannot help in examining the distribution of the transmitted global solar radiation on the other walls. There is a radiation loss from other walls too and not only from the north wall of the greenhouse, so the overall solar fraction should be evaluated in order to formulate the energy balance equation.

Sethi and Arora (2009) have used an inclined north wall reflector and hence have modified the even span east-west-oriented greenhouse dryer (GHD). The inclined north wall checked the incident solar radiation. It leads to raise the inside temperature of the GHD due to absorption of direct global radiation along with reflected

Fig. 2 Pictorial view of (**a**) outside and (**b**, **c**) inside of the improved GHD (Sethi and Arora 2009)

radiation. The angle of the reflective north wall vertical can be fine-tuned depending upon the zenith angle, width of the tray, and height of the erect north wall as shown in Fig. 2.

Jain (2005) has proposed a greenhouse dryer having a packed bed thermal storage in the north wall for onion drying. The proposed system is shown in Fig. 3. The length, breadth, and inside airflow rate of the greenhouse dryer are responsible for crop temperature. The fluctuation of temperature in off-sunshine hours is reduced by the application of thermal energy storage.

Berrouga et al. (2011) have presented thermal performance of the greenhouse where phase change material ($CaCl_2 \cdot 6H_2O$) is used in the north wall when it is kept in east-west orientation. The proposed system is shown in Fig. 4. Due to phase change material, it leads to rise of 6–12 °C inside temperature and 4–5 °C cover temperature at off-sunshine hours, and relative humidity is decreased by 10–15%.

To check the solar fraction through the north wall from the roof even span-type greenhouse dryer under passive mode, there are two modifications being done in the classical model (Prakash and Kumar 2014a, b, c, d, e, f). First modification is in the north wall material. The reflective mirror is replacing the transparent cover of the north wall. The second modification is the covering of the inside floor of the greenhouse dryer. The proposed system is being presented in Fig. 5. During the daytime, some portion of inside thermal energy is being stored in the ground thermal storage. And at night time, this stored energy is released for heating purpose in the greenhouse. Due to this, it substantially decreases the heat loss of the greenhouse dryer. This will minimize the thermal loss from the inside ground of the dryer. Black PVC sheet is being covered the inside concrete floor of the dryer. Authors have done experimentation in the two floor conditions. In the first condition, the modified greenhouse dryer is being kept in the barren concrete floor. In the next condition, the modified greenhouse dryer is being kept in the concrete floor covered with the black PVC sheet. In order to evaluate the effect of the black polyvinyl chloride (PVC), experiment is being conducted in 2 consecutive days under similar ambient conditions. The experimental result reveals that the covered floor provides 14.46 % higher inside temperature as compared to the without

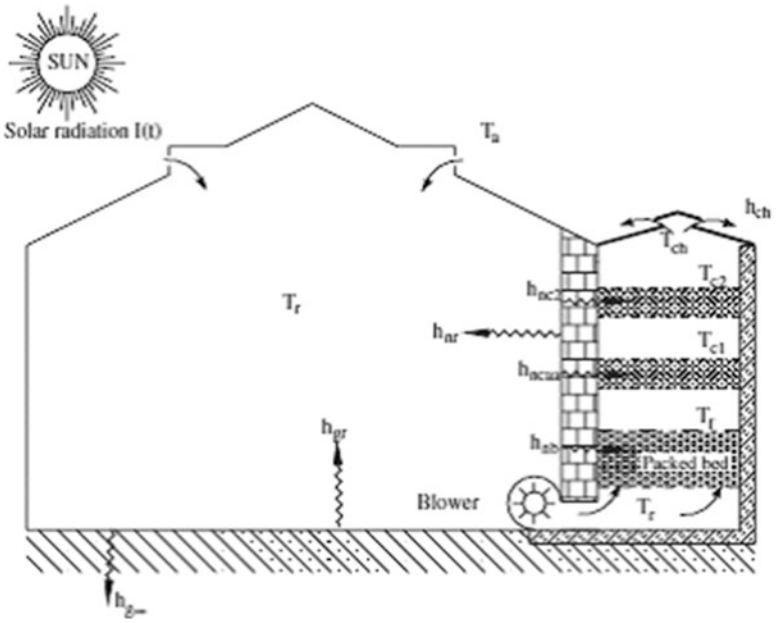

Fig. 3 Schematic view of greenhouse having north wall made of packed bed thermal storage (Jain 2005)

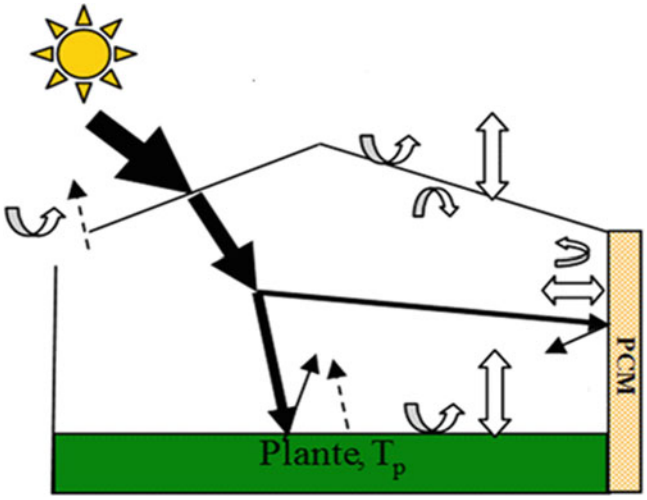

Fig. 4 Schematic view of greenhouse having north wall made of PCM material (Berrouga et al. 2011)

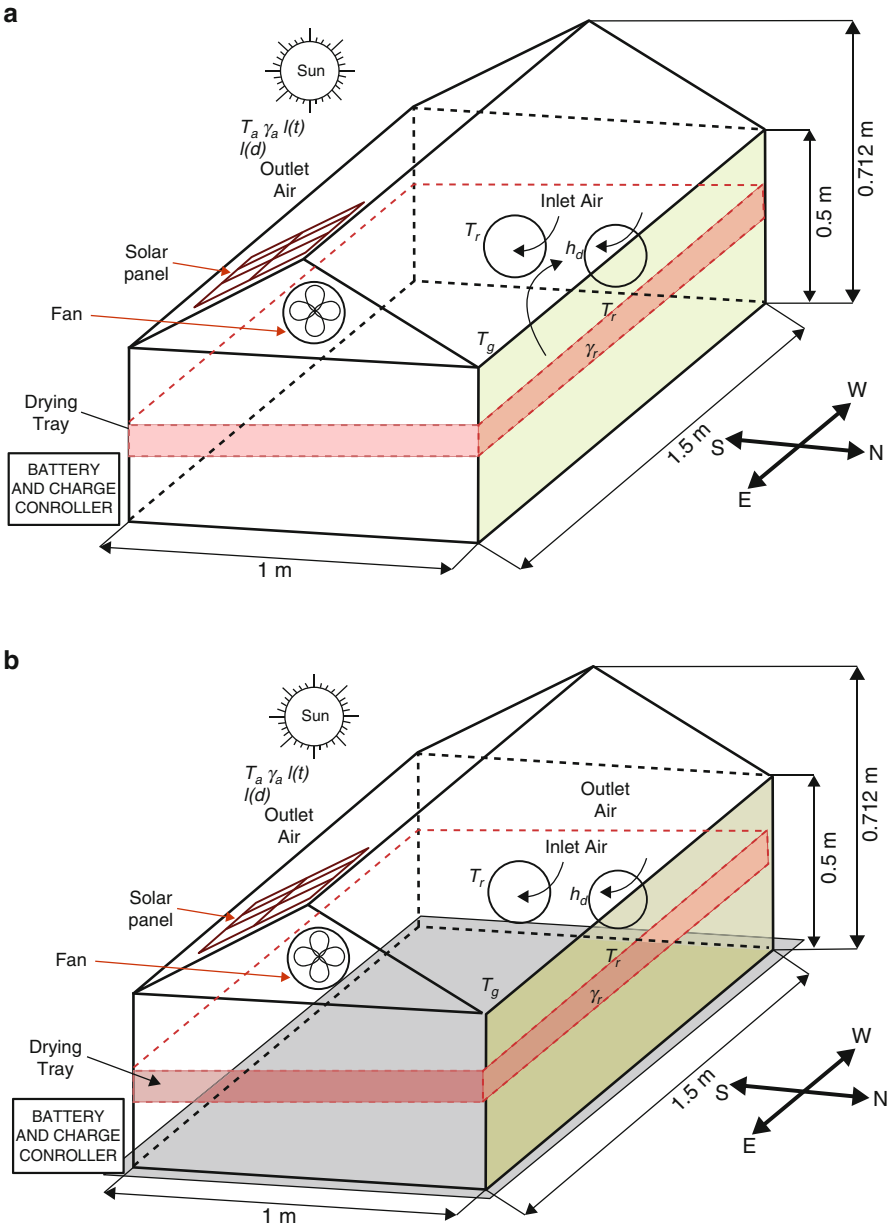

Fig. 5 Schematic diagram of modified greenhouse dryer a) without covered inside floor and b) with covered inside floor (Prakash and Kumar 2014b)

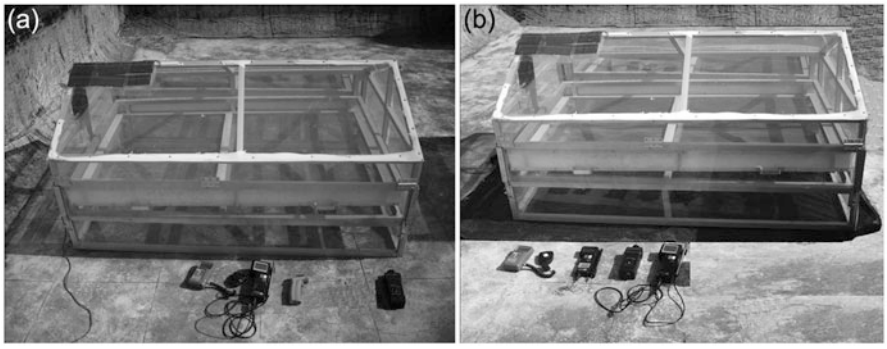

Fig. 6 (**a**) Experimental setup of modified active greenhouse dryer (a) without covered floor conditions and (**b**) with covered inside floor (Prakash and Kumar 2014c)

covered floor greenhouse dryer. On the peak hour, the difference is being increased up to 17.59%.

The same above-discussed concept is being applied for the greenhouse dryer under active mode (Prakash and Kumar 2014c). The peak global radiation on days 1 and 2 was 1061 and 978 W/m^2, respectively. The average ambient temperature on the first day and second day was 28.2 °C and 27.6 °C, respectively. In the covered floor conditions, inside temperature is always higher (0–5 °C) than the uncovered floor. The Fig. 6 shows the modified active greenhouse dryer with and without covered floor conditions.

In order to further enhance the performance of the modified greenhouse dryer under passive mode, Chauhan and Kumar (2016a) have done further modification in it. There are two major modifications in this. First, concrete floor is painted with black paint, and then it is covered with the double layer of the black PVC sheet with holes in the upper layer. And the radiation losses through the north wall can be reduced with the help of reflectors such as mirrors or by insulating the north wall with thermocol sheet. Experimentation is being conducted in two different floor conditions in the similar ambient conditions. In the first condition, the proposed dryer is being *placed* on the covered concrete floor (with collector), and in the second condition, the dryer was *placed* on the barren floor (without collector). The convective heat transfer coefficient of the modified greenhouse dryer from the ground to the inside air was 40.29 W/m$^{2\circ}$C, whereas for the north wall insulated greenhouse dryer, it was 46.62 W/m$^{2\circ}$C, which is 13.65% higher than the modified greenhouse dryer without a collector. This is showing the effectiveness of insulated north wall and solar collector of north wall insulated greenhouse dryer. Fig. 7 shows the view of the north wall insulated greenhouse dryer with and without a solar collector (Chauhan and Kumar 2016a, b).

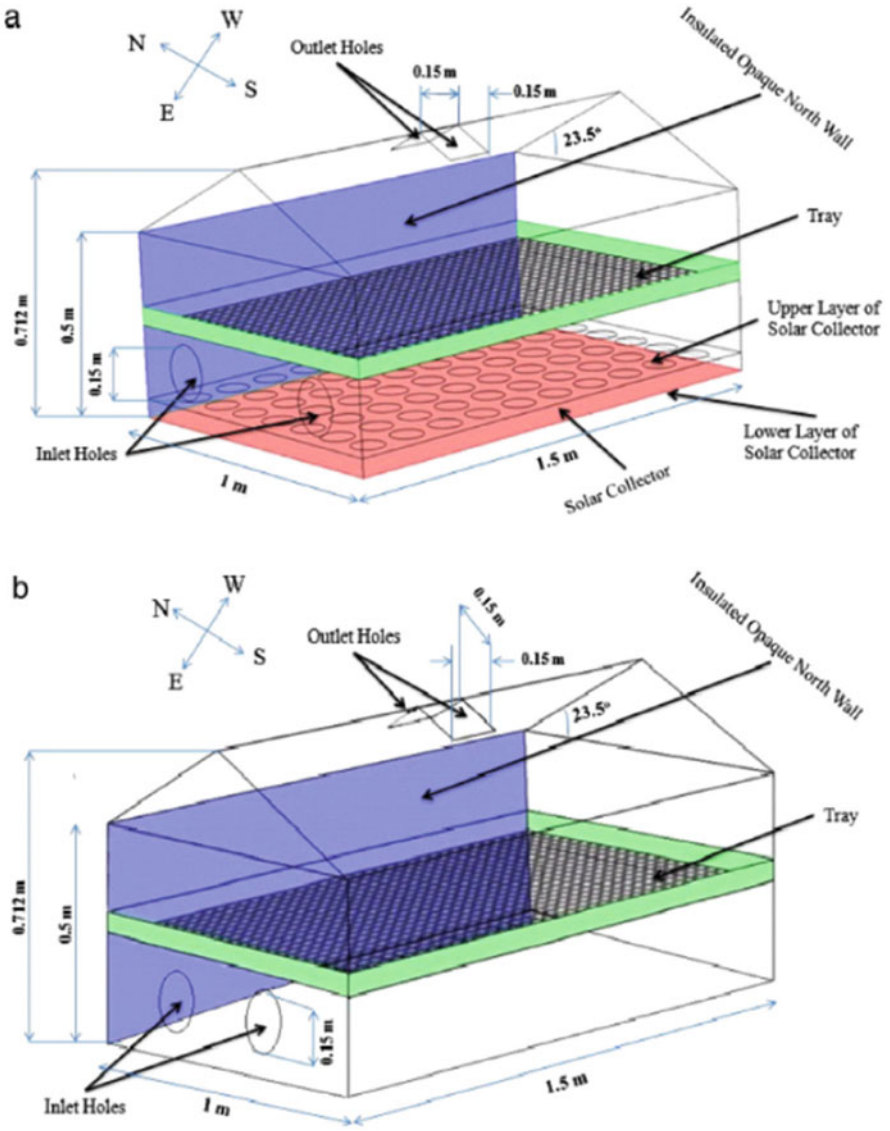

Fig. 7 (**a**) Schematic view of north wall insulated greenhouse dryer with solar collector. (**b**) Schematic view of north wall insulated greenhouse dryer without solar collector (Chauhan and Kumar 2016a)

4 State-of-the-Art Review on Various Types of Greenhouse Dryer

4.1 Greenhouse Dryer Under Active Mode

The solar greenhouse dryer is a big solar collector in which drying of crops takes place inside the chamber. It can be operated in either passive or active mode. In the greenhouse dryer under active mode, humid air is exhausted through the exhaust fan. This fan is operated either by renewable or nonrenewable energy. By this methodology, inside humid air is removed in a regulated manner, and fresh air is sucked through inlet holes. Greenhouse dryer under active mode is good for high moisture content crop. It also reduces the drying time and gives better quality products thus more preferred in food and chemical industries (Prakash and Kumar 2013b).

Condori and Saravia (1998) have studied two types of greenhouse dryers under active mode. One dryer has single chamber and another one has double chamber system. The study reveals that double-chamber is more effective than single-chamber greenhouse dryer. Condori et al. (2001) have designed, developed, and tested a forced convection tunnel-based greenhouse dryer. This dryer consists of a transparent plastic cover to cover the tunnel, an exhaust electric fan and manually driven carts with several stacked trays. Inside solar radiation is absorbed by the product to be dried, which is kept on the tray. Heat loss from this dryer is low as compared to others. The hot air distribution through the tray gets enhanced by the forced airflow. The main *benefits* of the tunnel greenhouse dryer are continuous drying production, minimum expenditure in labor wages, lower energy consumption, and used as a greenhouse for plant cultivation when drying assignment is not there. In the north of Argentina, the laboratory scale of such dryer was constructed and was tested on the red sweet pepper and garlic. The performance of the greenhouse dryer tunnel type is being studied (Condori and Saravia 2003). The study shows that steady production takes place during each day of drying process.

Convective mass transfer coefficient (h_c) and rate of moisture removal of cabbage and peas have been done experimentally found for open sun drying and greenhouse drying under active and passive mode (Jain and Tiwari 2004). Result reveals that h_c was lower for passive mode greenhouse drying as compared to open sun drying. The value of h_c is double in the case of active mode as compared to passive in the initial stage of the greenhouse drying. In the initial phase of drying time, the moisture evaporation rate is highest, and mass transfer rate gets stagnated after 20 h of drying time. Tiwari et al. (2004) have calculated the value of h_c during the drying of jaggery in the roof even span-type GHD under AM and PM. It was observed that the convective mass transfer coefficient is strongly dependent upon jaggery mass, temperature, and relative humidity for a given size of a greenhouse dryer. Thermal modeling for jaggery drying in a greenhouse dryer under active mode (AM) is being proposed to predict the jaggery temperature, mass of jaggery, and greenhouse room temperature during drying (Kumar and Tiwari 2006a). The

predicted values were validated with experimental values. The study reveals that there is a fair agreement between them. The effect of sizes of jaggery in GHD under AM and passive mode (PM) on the convective mass transfer coefficient (h_c) is being studied (Kumar and Tiwari 2006a, b). The three different dimensions of jaggery are used for experimentation, namely, $0.03 \times 0.03 \times 0.01$ m^3, $0.03 \times 0.03 \times 0.02$ m^3, and $0.03 \times 0.03 \times 0.03$ m^3. Result shows that the value of h_c for the size of $0.03 \times 0.03 \times 0.02$ m^3 is high in GHD under PM. However, the value of h_c of GHD under active for the size of $0.03 \times 0.03 \times 0.01$ m^3 is higher. The floor area of 1.20×0.78 m^2 was used to dry the jaggery in a roof even span-type greenhouse.

Kumar and Tiwari (2007) have studied the effect of different masses (300 gm, 600 gm, and 900 gm) of onion flakes on the value of h_c in natural and active modes GHD. Drying experiments have been performed in the months of October–December at IIT Delhi, India. The value of constant "C," "n," and convective mass transfer coefficient was calculated by regression analysis with the help of experimental data. The study revealed that the rate of moisture evaporation under greenhouse drying is more as compared to natural or open sun drying. The mode of drying and mass of onion flakes are two important parameters of which convective mass transfer coefficient depends on. Sami et al. (2007) have studied indoor greenhouse drying and natural drying of red pepper. Experimentations have been conducted inside the wind tunnel. One thousand-watt lamp is used as the sun. Both modes of drying were validated by the drying models. Nayak and Tiwari (2008) have studied energy and exergy analysis of the photovoltaic-thermal-integrated greenhouse dryer. Predicted value shows fair agreement with experimental result.

Barnwal and Tiwari (2008) have proposed a large-size hybrid photovoltaic-thermal (PV/T) GHD of 100 kg capacity. In the month of April 2007, under two conditions, i.e., in proposed dryer and in natural shade drying of Thompson, seedless grapes (mutant: Sonaka) of GR-I and GR-II were dried. Linear and multilinear expression is being developed to predict the moisture evaporation of the grapes. It is found that the multilinear expression model was able to predict the moisture evaporation with high-level accuracy in the case of force convection mode dryer. However, the linear expression model was able to predict with high-level accuracy for the natural drying. It is found that GR-II grapes have higher convective heat transfer coefficient than GR-I. Janjai et al. (2009) have studied the experimental and simulated drying performance of banana and peeled longan in PV-ventilated greenhouse dryer. The roof of the dryer is in parabolic shape and it was kept on the concrete floor. Three exhaust fans were used which are powered by 50 W PV module. Drying of crop took place simultaneously in the dryer and open sun. For peeled longan, 2–3 days is saved when it is dried in the sdryer; however, for banana, 1–2 drying days is saved as compared to the open sun drying. To simulate the data, a program is written in Compaq Visual Fortran version 6.5. Simulated and experimental results show fair agreement. Rathore and Panwar (2010) have designed and developed a solar tunnel dryer under AM which is hemicylindrical walk-in type. Dryer was experimented to dry grapes. The temperature gradient inside the tunnel was 10–28 °C in clear sky conditions, which is quite good for medium-temperature drying. Nayak et al. (2011) have studied the drying of mint in hybrid PV/T

greenhouse dryer and tested the dried sample of mint. The quality of the dried mint shows that the nutrient and calorific value is retained as compared to fresh mint along with reduction of moisture content, which will increase the shelf life of dried product. The authors also did the energy analysis of the dryer.

A large scale up to 1000 kg crop drying capacity of the greenhouse dryer under active mode has been proposed by Janjai et al. (2011). The dryer is in parabolic shape and the inside floor is black painted concrete. Polycarbonate sheet is used to cover the dryer. The three 50 Wp solar cell modules are used to operate nine DC fans. One thousand kilograms of banana with 68% (w.b.) moisture content get dried up in this dryer within 5 days, while natural drying takes 7 days to dry with the same ambient conditions.

Prakash and Kumar (2013b) have developed ANFIS prediction model for the modified greenhouse dryer under active mode in the no-load condition. The experimentation is being conducted in the month of January. The model was developed to predict the inside room temperature and relative humidity. The predicted result was validated with the experimental result. It is concluded that the model is able to predict with high level of accuracy.

Prakash and Kumar (2014d) have done an analysis on the tomato flakes drying in the modified greenhouse dryer in active mode and found that the nutrition content of tomato dried in active mode is more than the open sun drying. Prakash et al. (2015) have developed the fuzzy prediction model to predict the moisture evaporation rate for jaggery drying in the greenhouse dryer under active mode. Fuzzy prediction model was developed in the MATLAB software version no. 7. The model was validated with experimental result. It is found that there is fair agreement between simulated result and experimental result.

4.2 Passive Mode

In the greenhouse dryer under passive mode, humid air is exhausted due to thermosyphon effect through the outlet vent. It is advantageous as compared to active mode due to lower investment and simplicity in operation and maintenance. Hence, it can be used in family scale more effectively (Janjai and Bala 2012).

The inside air temperature of the greenhouse dryer under passive mode is being predicted by a mathematical model proposed by the Rachmat and Horibe (1999). The drying of pineapple slices in the solar tunnel dryer is proposed by Bala et al. (2003). Proximate analysis of the dried pineapple slices revealed that it is very good for the consumption of the human being. Abdelhamid et al. (2004) have proposed pepper drying in polyethylene greenhouse under passive mode. Dried pepper is found to be hygienic with sufficient nutrient contents, which is good for consumption of the human being. Turhan (2006) had studied to improve the performance of the greenhouse dryer for agricultural produce. The two different types of greenhouse dryers under passive mode are designed, fabricated, and tested. Experimentation was conducted in the summer month. Pepper was used to dry in the designed

dryer and open sun drying (OSD) simultaneously. The experimental study showed that the greenhouse dryer is 2.5 times more effective than OSD.

A roof even span-type GHD has been proposed for jaggery drying under active mode (AM) and passive mode (PM) by Kumar and Tiwari (2006b). The two different masses of jaggery, namely, 0.75 kg and 2.0 kg, having dimension of $0.03 \times 0.03 \times 0.01$ m^3 have been used for experimentation. For predicting hourly jaggery temperature, greenhouse air temperature, and evaporated moisture, a thermal model is used. It was seen that at the beginning of the drying process, the value of the convective mass transfer coefficient was higher and then decreased with time. Products were dried continuously for 4 days in the clear sky conditions. The final moisture content of jaggery was 7% (wet basis) at the end of the fourth day of the drying. Temperature inside the dryer varies from 31.2 to 54.71 °C and its relative humidity ranges from 22 to 34%. A good agreement is found between the predicted results by thermal modeling and experimental observations. Kumar and Tiwari (2007) have studied the effect of convective mass transfer coefficient for the different masses (300 g, 600 g, and 900 g) of onion flakes. Experimentations were done in open sun drying and GHD under AM and PM simultaneously. The drying time of the onion was 33 h. The study revealed that the rate of moisture evaporation in the case of the greenhouse dryer in off-sunshine hour is more than the natural mode of the drying. Convective mass transfer coefficient increases with the increase of the mass of the onion.

Ronoh et al. (2010) have presented an experimental study of a solar tent dryer under natural convection for thin layer drying of amaranth (*Amaranthus cruentus*) grains. This drying system has two layers—top and bottom—for drying of grains. Amaranth grain having initial moisture content (d.b.) of 64% gets dried up within the 7 h till 7% of moisture content (d.b.). Rathore and Panwar (2011) have conducted experimentation of tomato flakes drying in a dryer. The experimental data were modeled by the help of seven standard mathematical models and artificial neural network (ANN) model. ANN model can predict better than mathematical equations. Prakash and Kumar (2014e) have developed the adaptive neuro-fuzzy inference system (ANFIS) model for the greenhouse dryer for the jaggery drying. The model was developed in the MATLAB software in version 7. It was used to predict the three important drying parameters, namely, jaggery temperature, greenhouse room temperature, and rate of moisture evaporation during jaggery drying. Models were validated with experimental results. Results show the model was able to predict very well. Prakash and Kumar (2014f) have developed ANN model for the greenhouse dryer. The ANN model was able to predict 8–9% better than the thermal model.

Prakash and Kumar (2015) have done a detailed study in the modified greenhouse dryer under passive mode. Experiment was conducted in no-load condition in the Energy Centre, Maulana Azad National Institute of Technology Bhopal, India, from January 2013 to May 2013. The study was conducted in the dryer with different floor conditions showing difference in performance. It was conducted between 15th and 17th of each month, and the floor was put under different conditions as such barren floor, floor covered with black PVC sheets, and black-

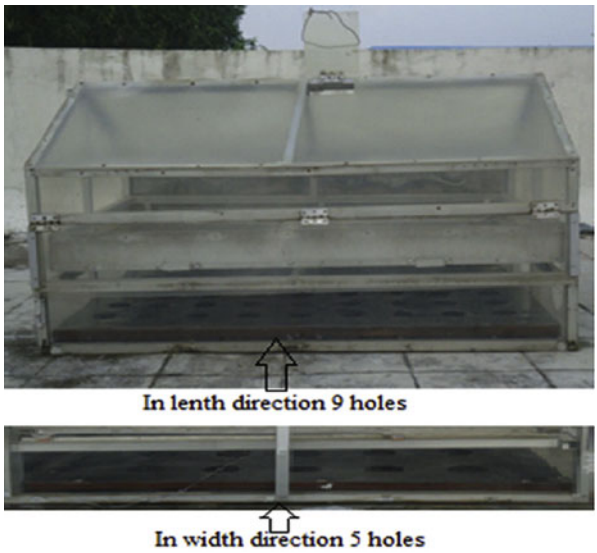

Fig. 8 Photograph of the north wall insulated greenhouse dryer under passive mode with solar collector Chauhan and Kumar (2016b)

painted floor. Out of these, the floor covered with black PVC sheet showed the superior performance than the other two conditions. The rise in inside temperature with respect to ambient temperature under black PVC conditions varies from 22.3 to 28.9 °C. Chauhan and Kumar (2016b) have done a detailed study on the greenhouse dryer under passive mode with insulated north wall. Experiment was conducted with and without ground solar collector. They have designed, developed, and tested in Bhopal, India, the climatic condition as presented in the Fig. 8. The following important parameters are being calculated in both conditions, namely, convective heat transfer coefficient, coefficient of diffusivity, heat loss factor, heat utilization factor, and coefficient of performance. The study reveals that the dryer with solar collector shows the superior performance as compared to the dryer without solar collector.

4.3 Innovative Greenhouse Dryer

Elkhadraoui et al. (2015) have applied new concept in the greenhouse dryer. The solar air heater is being attached to the greenhouse dryer. By this concept, greenhouse dryer gets thermal energy both direct and indirect ways. The even span greenhouse drying experimental setup had a flat-plate solar collector as shown in Fig. 8. Experiments were carried out to dry red pepper and sultana grapes. The moisture removal rate was much higher than the OSD. The analysis of this dryer showed that the time for drying was reduced by 7 and 17 h for red pepper and grapes, respectively. The estimated life of the system is 20 years, which is much higher, and the 1.6-year payback period is estimated.

Fig. 8 Photograph of mixed-mode-type solar greenhouse dryer (Elkhadraoui et al. 2015)

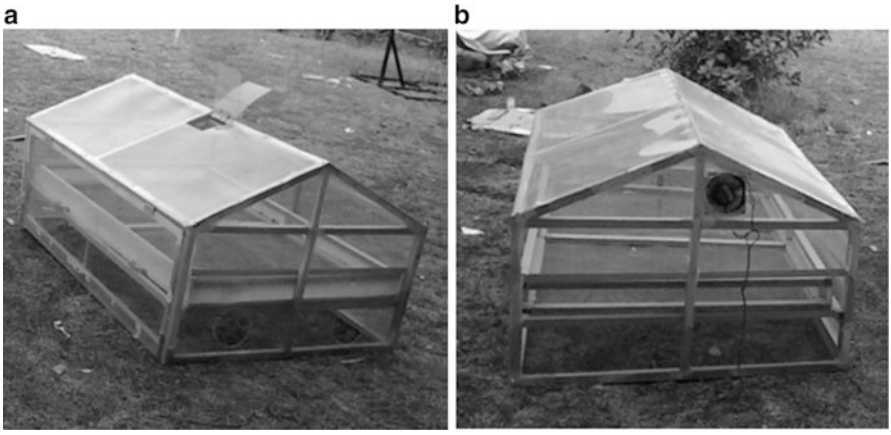

Fig. 9 Photograph of the experimental setup: (**a**) passive mode and (**b**) active mode

5 Case Study of Greenhouse Dryer in No-Load Condition

Kumar et al. (2013) have done experimental thermal analysis of the greenhouse dryer in no-load condition. The experimental setup is shown in Fig. 9.

The greenhouse dryer under active and passive mode is being experimented in the Department of Energy (Energy Centre), Maulana Azad National Institute of Technology, Bhopal-462036 (India), in monsoon season. Ambient temperature, wind velocity, relative humidity, and solar radiation were recorded on an hourly basis for 2 consecutive days from 10 am to 3 pm. Experimental data analysis shows

that drying conditions in passive mode of greenhouse drying are not favorable due to high relative humidity inside the dyer. Though, drying in active mode is encouraging because relative humidity can be maintained by exhaust fan.

6 Conclusion

All over the world, a lot of research has been undertaken on the solar greenhouse dryer in both natural and forced convection mode type. Forced convection or active mode was found more suitable for high moisture content crops, while natural convection or passive mode was found to be the best for the low moisture content crops/fruits/vegetables. The greenhouse dryer is much more superior than open sun drying in terms of quality, texture, and color of the product. The PV-integrated solar greenhouse dryers are recommended to use in remote areas as it does not require any grid-connected electricity to dry the high moisture content crop. In Southeast Asian countries, it has the maximum application. The researchers have given developed various simulation models These models are highly useful in obtaining the required data without conducting the tedious experiments, which can save a lot of time.

References

Abdelhamid F, Sami K, Chakib K, Mohamed M, Abdelhamid F, Ali B (2004) Validation of a pepper drying model in a polyethylene tunnel greenhouse. Int J Therm Sci 43:53–58

Bala BK, Mondol MRRA, Biswas BK, Das Chowdury BL, Janjai S (2003) Solar drying of pineapple using solar tunnel drier. Renew Energy 28:183–190

Barnwal P, Tiwari GN (2008) Grape drying by using hybrid photovoltaic-thermal (PV/T) greenhouse dryer: an experimental study. Sol Energy 82:1131–1144

Berrouga F, Lakhal EK, Omari M El, Faraji M, Qarnia H El (2011) Thermal performance of a greenhouse with a phase change material north wall. Energ Buildings 43:3027–3035.

Cakmakçi R, Dönmez F, Aydın A, Şahin F (2006) Growth promotion of plants by plant growth-promoting rhizobacteria under greenhouse and two different field soil conditions. Soil Biol Biochem 38(6):1482–1487

Chauhan PS, Kumar A, Tekasakul P (2015) Applications of software in solar drying systems: a review. Renew Sust Energ Rev 51:1326–1337

Chauhan PS, Kumar A (2016a) Performance analysis of greenhouse dryer by using insulated north-wall under natural convection mode. Energy Reports 2:107–116

Chauhan PS, Kumar A (2016b) Heat transfer analysis of north wall insulated greenhouse dryer under natural convection mode. Energy. In Press

Condori M, Saravia L (1998) The performance of forced convection greenhouse driers. Renew Energy 13(4):453–469

Condori M, Saravia L (2003) Analytical model for the performance of the tunnel-type greenhouse drier. Renew Energy 28:467–485

Condori M, Echazu R, Saravia L (2001) Solar drying of sweet pepper and garlic using the tunnel greenhouse drier. Renew Energy 22:447–460

Ekechukwua OV, Norton B (1999) Review of solar-energy drying systems II: an overview of solar drying technology. Energy Convers Manag 40:615–655
ELkhadraoui A, Kooli S, Hamdi I, Farhat A (2015) Experimental investigation and economic evaluation of a new mixed-mode solar greenhouse dryer for drying of red pepper and grape. Renew Energy 77:1–8
Ghosal MK, Tiwari GN (2004) Mathematical modelling for greenhouse heating by using thermal curtain and geothermal energy. Sol Energy 76:603–613
Gupta R, Tiwari GN (2004) Effect of latitude on weighted solar fraction of north partition wall for various shapes of solarium. Build Environ 39:547–556
Gupta R, Tiwari GN (2005) Modeling of energy distribution inside greenhouse using concept of solar fraction with and without reflecting surface on north wall. Build Environ 40:63–71
Gupta R, Tiwari GN, Kumar A, Gupta Y (2012) Calculation of total solar fraction for different orientation of greenhouse using 3d-shadow analysis in auto-CAD. Energ Buildings 47:27–34
Jain D (2005) Modeling the performance of greenhouse with packed bed thermal storage on crop drying application. J Food Eng 71:170–178
Jain D, Tiwari GN (2004) Effect of greenhouse on crop drying under natural and forced convection I: evaluation of convective mass transfer coefficient. Energy Convers Manag 455:765–783
Janjai S, Bala BK (2012) Solar drying technology. Food Eng Rev 4:16–54
Janjai S, Lamlert N, Intawee P, Mahayothee B, Bala BK, Nagle M, Muller J (2009) Experimental and simulated performance of A PV-ventilated solar greenhouse dryer for drying of peeled longan and banana. Sol Energy 83:1550–1565
Janjai S, Poolsak I, Jinda K, Chanoke S, Vathsana K (2011) A large-scale solar greenhouse dryer using polycarbonate cover: modeling and testing in a tropical environment of lao people's democratic republic. Renew Energy 36:1053–1062
Kumar A, Tiwari GN (2006a) Thermal modeling and parametric study of a forced convection greenhouse drying system for jaggery: an experimental validation. Int J Agric Res 1 (3):265–279
Kumar A, Tiwari GN (2006b) Effect of shapes and size on convective mass transfer coefficient during greenhouse drying (GHD) of jaggery. J Food Eng 73:121–134
Kumar A, Tiwari GN (2007) Effect of mass on convective mass transfer coefficient during open sun and greenhouse drying of onion flakes. J Food Eng 79:1337–1350
Kumar A, Tiwari GN, Kumar S, Pandey M (2006) Role of greenhouse technology in agricultural engineering. Int J Agric Res 1:364–372
Kumar A, Prakash O, Kaviti A, Tomar A (2013) Experimental analysis of greenhouse dryer in no-load condition. J Environ Res Develop 7(4):1399–1406
Kumar A, Singh R, Prakash O, Ashutosh (2014) Review on global solar drying status. Agric Eng Int CIGR 16(4):161–177
Loannou N (2000) Soil solarization as a substitute for methyl bromide fumigation in greenhouse tomato production in Cyprus. Phytoparasitica 28(3):248–256
Mujumdar AS (2008) "Guide to industrial drying principles", equipments & new developments, 3rd edn. Three S Colors Publications, Hyderabad
Nayak S, Tiwari GN (2008) Energy and exergy analysis of photovoltaic/thermal integrated with a solar greenhouse. Energy Build 40:2015–2021
Nayak S, Kumar A, Mishra J, Tiwari GN (2011) Drying and testing of mint (Mentha Piperita) by a Hybrid Photovoltaic-Thermal (PVT)-based greenhouse dryer. Dry Technol 29:1002–1009
Prakash O (2015) Design and performance analysis of modified greenhouse dryer. Ph.D. Thesis in the Department of Energy, Maulana Azad National Institute of Technology, Bhopal (India)
Prakash O, Kumar A (2013a) Historical and recent trend of solar drying system: a review. Int J Green Energy J 10(7):690–738
Prakash O, Kumar A (2013b) ANFIS prediction model of a modified active greenhouse dryer in no-load conditions in the month of january. Int J Adv Comp Res 3(1):220–223
Prakash O, Kumar A (2014a) Solar greenhouse drying: a review. Renew Sust Energ Rev 29:905–910

Prakash O, Kumar A (2014b) Design, development and testing of modified greenhouse dryer under natural convection. Heat Trans Res 45(5):433–451
Prakash O, Kumar A (2014c) Thermal performance evaluation of modified active greenhouse dryer. J Build Phys 37(4):395–402
Prakash O, Kumar A (2014d) Environomical analysis and mathematical modeling for tomato flakes drying in modified greenhouse dryer under active mode. Int J Food Eng 10(4):669–681
Prakash O, Kumar A (2014e) ANFIS modeling of a natural convection greenhouse drying system for jaggery: an experimental validation. Int J Sustain Energy 33(02):316–335
Prakash O, Kumar A (2014f) Application of artificial neural network for prediction of jaggery mass during drying inside natural convection greenhouse dryer. Int J Amb Energy 35 (4):186–192
Prakash O, Kumar A (2015) Annual performance of modified greenhouse dryer under passive mode in no-load conditions. Int J Green Energy 12:1091–1099
Prakash O, Kumar O, Kaviti A, Vishwanatha P (2015) Prediction of moisture evaporation rate from jaggery in green house drying using fuzzy logic. Heat Trans Res 46(10):923–935
Prakash O, Kumar A, Sharaf-Eldeen Y (2016a) Review of indian solar drying status. Current Sustainable/Renewable Energy Reports by Springer Press. doi:10.1007/s40518-016-0058-9
Prakash O, Laguri V, Pandey A, Kumar A, Kumar A (2016b) Review on various modelling techniques for the solar dryers. Renew Sust Energ Rev 62:396–417
Rachmat R, Horibe K (1999) Solar heat collector characteristics of a fibre reinforce plastic drying house. Trans ASAE 42(1):149–157
Rathore NS, Panwar NL (2010) Experimental studies on hemi cylindrical walk-in type solar tunnel dryer for grape drying. Appl Energy 87:2764–2767
Rathore NS, Panwar NL (2011) Design and development of energy efficient solar tunnel dryer for industrial drying. Clean Techn Environ Policy 13:125–132
Ronoh EK, Kanali CL, Mailutha JT, Shitanda D (2010) Thin layer drying kinetics of amaranth (amaranthus cruentus) grains in a natural convection solar tent dryer. Afr J Food Agric Nutr Dev 10(33)
Sami K, Abdelhamid F, Ali B (2007) Drying of red pepper in open sun and greenhouse conditions mathematical modeling and experimental validation. J Food Eng 79:1094–1103
Santamouris M, Argiriou A, Vallindras M (1994) Design and operation of a low energy consumption passive solar agricultural greenhouse. Solar Energy 52(5):371–378
Sethi VP, Arora S (2009) Improvement in greenhouse solar drying using inclined north wall reflection. Sol Energy 83:1472–1484
Silva C, Ferreira JG, Bricker SB, Delvalls TA, Martín-Diaz ML, Yanez E (2011) Site selection for shellfish aquaculture by means of GIS and farm-scale models, with an emphasis on data-poor environments. Aquaculture 318(3–4):444–4578
Tiwari GN, Goyal RK (1998) Greenhouse technology. Narosa Publishing House, New Delhi, pp 117–187
Tiwari GN, Din M, Shrivastava NSL, Jain D, Sodha MS (2002) Evaluation of solar fraction (Fn) for north wall of a controlled environment greenhouse: an experimental validation. Int J Energy Res 26:203–215
Tiwari GN, Gupta A, Gupta R (2003) Evaluation of solar fraction on north partition wall for various shapes of solarium by Auto-CAD. Energ Buildings 35:507–514
Tiwari GN, Kumar S, Prakash O (2004) Evaluation of convective mass transfer coefficient during drying of jaggery. J Food Eng 63:219–227
Turhan K (2006) An investigation on the performance improvement of greenhouse-type agricultural dryers. Renew Energy 31:1055–1071

Part II
Design and Testing of Solar Drying Systems

Design Analysis and Studies on Some Solar Drying Systems

Vinod Kumar Sharma and Cosmas Ngozichukwu Anyanwu

Abstract Solar drying is an unsophisticated, yet very ancient technology. It is one of the most accessible and, hence, the most common preservation techniques applied to agricultural products, mainly in tropical regions of the world where the intensity of solar radiation justifies its use. Different types of solar dryers exist and find suitable applications in the preservation of different agro-produce as a proven means of reducing postharvest losses. The present chapter discusses extensively the design procedures for solar drying systems, including the use of rules of thumb, psychrometric charts and design equations. Economic aspects of solar drying systems are also considered. Various case studies, relating to the application of direct-mode, indirect-mode and mixed-mode types of solar drying systems, have been presented. Although direct-mode dryers are generally cheaper to construct, a major drawback in their application is the fact that drying temperatures cannot be regulated, leading to over- or under-drying. It is concluded that well-designed solar crop drying systems are capable of drastically reducing losses of agricultural products occasioned by postharvest spoilage and preservation challenges.

Keywords Drying • Moisture content • Design • Insolation • Convection • Direct-mode dryers • Mixed-mode dryers

1 Introduction

Drying has been described as a process of moisture removal owing to simultaneous heat and mass transfer (El-Sebaii and Shalaby 2012). It is an excellent way to preserve foods. The main purpose of drying is to reduce moisture content and, thus,

V.K. Sharma (✉)
Department of Energy, Division for Bioenergy, Biorefinery and Green Chemistry (DTE-BBC), Italian National Agency for New Technologies, Energy and Sustainable Economic Development (ENEA) Research Centre, Trisaia, 75026 Rotondella (MT), Italy
e-mail: sharma@enea.it

C.N. Anyanwu
Department of Agricultural and Bioresources Engineering, University of Nigeria, Nsukka, 410001 Enugu State, Nigeria

© Springer Nature Singapore Pte Ltd. 2017

O. Prakash, A. Kumar (eds.), *Solar Drying Technology*, Green Energy and Technology, DOI 10.1007/978-981-10-3833-4_6

reduce or eliminate microbial activities, which are capable of leading to spoilage. Drying is a very easy-to-accomplish, yet an ancient, technology. It is one of the most accessible and, hence, the most common processing technologies practiced mainly in tropical regions of the world (Belessiotis and Delyannis 2011). Open-air sun drying takes place when the products are kept under direct solar radiation. It is a well-known fact that the capacity of the air to absorb moisture depends on ambient temperature. At higher temperatures, air has lower humidity ratio and is therefore able to absorb larger amount of moisture. If air is heated (typically, in a solar drying system), the quantity of water vapour in it remains somewhat the same, but the relative humidity drops, and the air, in this way, takes up more moisture from its surroundings.

1.1 Solar Drying

Solar drying involves the use of well-designed and/or constructed contrivances capable of trapping solar radiation and maximizing its efficient use for dying materials, usually agricultural products. According to Anon. (2016), solar dryers, when correctly designed, have significant merits over sun drying. They produce faster drying rates by heating the air to 10–30 °C above ambient, which leads to faster air movement through the dryer as well as reduction in its humidity. Dryers also eliminate easy access for insects and rodents. Faster drying rates reduce, and in some cases eliminate the risk of microbial spoilage, while improving the quality and product throughput. This helps to reduce the required drying area. However, care must be taken to avoid rapid drying in the case of fruits as this is capable of causing case hardening and subsequent mould growth. Solar dryers also offer protection from dust and rodents attacks on foods. They can be fabricated from local engineering materials at a very low capital cost. Since there are no fuel costs, they are most useful in places with high fuel or electricity costs, scarcity of land for sun drying and high intensity of solar radiation, but high air humidity. They are also quite useful as a means of air preheating for artificial dryers to reduce fuel costs. Typical drying times for most solar dryers range from 1 to 3 days depending on the intensity of solar radiation, air speed, relative humidity and the type of food/crop targeted for drying.

1.2 Open-Air Sun Drying Versus Use of Solar Dryers

Drying of fruits and vegetables under the sun is still practised largely unchanged from ancient times. Traditional open-air sun drying takes place when products are stored under direct sunlight (Anon. 2016). Little expertise is required for sun drying, but its major merits include low capital and operating costs. However, its demerits are numerous, ranging from contamination, damage by animals, to slow or

uncontrolled drying rates and lack of protection from rain or dew. Another major challenge is that it tends to encourage mould growth which may result in low and variable final products quality owing to over- or under-drying. A large expanse of land is required to spread the shallow layers of food, and drying is labour intensive, since the crop must be turned or moved in case of rain or other adverse weather conditions. Direct open-air sun drying actually affects the quality (colour and vitamin content) of certain fruits and vegetables negatively (Anon 2016). Umogbai and Iorter (2013), who compared open-air sun drying with solar drying, concluded that solar dryers are more effective since they produce higher temperatures, lower RH and lower final product moisture content. These culminate in reduced spoilage during the drying process than in the case of sun drying.

2 Types of Solar Drying Systems

Drying systems are be classified in a number of ways. According to Hii et al. (2012), there are two very important classifications, which are based either on the method of heat transfer to the wet solids or the characteristics and physical properties of the wet material. Based on heat transfer method, there are differences in dryer design and operation, whereas the second method is most useful in the selection of a group of dryers for preliminary consideration in a given drying problem. Ekechukwu and Norton (1999) recognized direct and indirect types of dryers, with subclasses of continuous or batch-wise operation.

2.1 Classification Based on Dryer Architecture

On the basis of dryer architecture, some authors (Szulmayer 1971; Anon. 2016) have identified three main types of solar dryers, namely:

2.1.1 Direct (Integral) Dryers

These are also known as absorption or hot box-type dryers, whereby the product is heated directly by the sun. Integral solar dryers appear to be better suited for fruits, vegetables, medicinal herbs such as *Moringa oleifera*, etc., which require mild temperatures for their preservation.

2.1.2 Indirect (Distributed) Dryers

They are known as indirect or convection dryers since the product is dried using warm air, which is heated by letting it pass through a solar collector, air heater or

heat exchanger before entering the drying chamber. These dryers can operate at higher temperatures and are better suited for tubers and such materials.

2.1.3 Mixed-Mode Systems

These are drying systems, which function on the basis of the above two principles, whereby the product is dried partly by the sun as well as a stream of preheated air at the same time.

2.2 Classification Based on Operating Temperature

2.2.1 Low Temperature Systems

In such drying systems, constant ventilation is applied to establish equilibrium between the product moisture content and that of the working fluid (drying air). Thus, they are able to withstand intermittent, as well as variable heat input. Drying at low temperatures is quite suitable when considering bulk processing for long-term storage. Hence, they are often referred to as bulk or storage dryers (Ekechukwu and Norton 1999).

2.2.2 High Temperature Systems

These dryers are required when fast drying is desirable. High temperature systems are used when the handled products require a minimum contact with the drying air, since over drying is likely to occur if the working fluid remains in contact with the product until equilibrium moisture content is reached. Therefore, the products are dehydrated to the required moisture contents and then cooled (Ekechukwu and Norton 1999). Batch and continuous flow dryers are the main types of high temperature dryers commonly encountered (Reddy and Chakraverty 2004; Lalit et al. 2010).

2.3 Classification Based on Heating Mode and Utilization of Heat

2.3.1 Passive (Natural Draft) Drying Systems

Passive drying systems generally are not equipped with moving parts to facilitate draft, such as fans or blowers. They rely on natural convection to supply air draft to

the drying materials. As such the drying times are usually longer, but they are well adapted for certain drying operations.

2.3.2 Active (Forced Convection) Drying Systems

Active dryers are employed when commercial-scale drying operation must be accomplished within a short duration. They rely on fans or blowers to furnish air draft through the system. Active dryers are becoming increasingly important, especially when using DC fans powered by photovoltaic systems in remote locations, where power supply issues are often a challenge. Anyanwu et al. (2012) reported the experimental investigation of a photovoltaic-powered active cassava chips dryer in Nigeria. In India, several rural-based crop drying projects have been accomplished using active drying systems. Passive and active solar dryers can, in turn, be classified as direct, indirect and mixed-mode types.

3 Design Considerations for Solar Drying Systems

The procedure for designing drying systems involves the collection of climatic data, such as solar radiation, wind speed and relative and absolute humidity, of the study location. Typically, the following are evaluated (Tonui et al. 2014): the quantity of moisture to be expelled from a given amount of crop, harvesting time during which the drying is needed, the intensity of solar radiation and daily sunshine hours (for determining the total drying time and energy received by the dryer per day), the quantity of air needed for drying, wind velocity for determination of minimum air vent dimensions, etc.

The most important data being the insolation is usually studied more carefully and calculated for the given collector architecture. For the conceptual stage of dryer design, many existing configurations could be studied and some of the design parameters determined. During this phase, some physical parameters of the material to be dried may be studied alongside, for instance, thickness of the slices or drying layers, other dimensions of the sliced chips etc. Construction materials such as wood, stainless steel, clear glass, galvanized iron sheet, etc. are also considered.

3.1 Rules of Thumb Approach

Experienced designers of solar crop drying systems sometimes apply some tested rules of thumb, without necessarily understanding the mathematical formulae. Using this approach, important parameters such as air flow rate, required collector area, dryer area, etc. can be estimated easily without the use of rigorous

mathematical approach or numerical computations. For instance, the following (A-E) are some design rules of thumb, according to Peace Corps (1980).

(A) *Considerations for solar dryer designs*

At normal pressure, 1 kg air at 35 °C occupies about 0.9 m^3.

For grain drying, bed thickness should not exceed 15 cm. This translates to a maximum loading rate of about 90 kg/m^2, to be stirred occasionally (Peace Corps 1980). The energy supplied as heated air to the drying crop or food is approximately 25% of the solar energy striking a horizontal surface of equivalent area to the dryer's collector (Peace Corps 1980).

(B) *Size of collector*

Making the collector equal to three times the tray area increases the drying rate significantly.

(C) *Dryer capacity*

In tropical conditions, assume that approximately 180 m^3 of air is required to expel 1 kg of water (Peace Corps 1980), whereas approximately 0.75 m^2 of collector area is needed to remove every kg of water per day. This is equivalent to the amount of water to be expelled from 1.5 kg fresh fruits or 5.25 kg grain per day (Peace Corps 1980).

(D) *Dryer temperature*

1. To a great extent, reducing the area of vents by 50% increases ΔT threefold
2. Increasing the dryer temperature from 20 to 35 °C can triple the moisture absorption capacity of the air.

(E) *Dryer air flow rate*

1. Increasing vent area by 100% doubles the air flow rate (but leads to 75% drop in ΔT).
2. Increasing the height by 100% increases air flow by 40%.
3. Increasing collector area by 100% increases air flow by about 40% (Peace Corps 1980).

It is pertinent to mention that the rules of thumb are not always valid for all drying systems. Therefore, it is necessary to use proper design equations which are more accurate.

3.2 Design Equations

1. The following design considerations are usually taken into account when developing crop drying systems (Tonui et al. 2014): the quantity of moisture to be expelled from a given quantity of crop, daily sunshine hours to determine the

total drying time, daily insolation to calculate energy received by the dryer per day, quantity of air needed for drying and wind speed for the determination of air vent area.

3.2.1 Design Procedure and Calculations

The size of the dryer is usually based on the total area needed for drying each kilogram of crop. The drying temperature is usually estimated based on the maximum temperature the crop can withstand. From the historical climatic data of the study area, the mean diurnal temperature and relative humidity are obtained. Hence, the humidity ratio is determined from the psychometric chart. The maximum allowable drying temperature for the crop, as well as its safe storage moisture content, is also obtained from literature data.

3.2.2 Design Algorithm

The Concept of Moisture Content

Moisture content is a constantly encountered terminology whenever drying process is considered. Moisture content is calculated either in wet or dry basis. Suppose we denote the initial (wet) and final (dry) masses of the substance to be dried as M_i and M_f, respectively. Then moisture content wet basis is given by Eq. 1, while Eq. 2 gives dry basis moisture content.

$$\mathrm{MC_{wb}} = \frac{100\left(M_i - M_f\right)}{M_i} \tag{1}$$

$$\mathrm{MC_{db}} = \frac{100\left(M_i - M_f\right)}{M_f} \tag{2}$$

Applying simple mathematical rearrangements, it can be shown that $\mathrm{MC_{wb}}$ and $\mathrm{MC_{db}}$ are related via Eqs. 3a and 3b as follows:

$$\mathrm{MC_{db}} = 100\left(\frac{\mathrm{MC_{wb}}}{100 - \mathrm{MC_{wb}}}\right) \tag{3a}$$

$$\mathrm{MC_{wb}} = 100\left(\frac{\mathrm{MC_{db}}}{100 + \mathrm{MC_{db}}}\right) \tag{3b}$$

(a) *Amount of Moisture to Be Expelled*

Consider 20 kg of freshly harvested cassava tubers with moisture content of 75%. It means that each kg of the cassava contains 750 g of water and 250 g pure cassava. Thus, the 20 kg would contain 15 kg of water (i.e. 20*0.75 kg) and 5 kg of

pure cassava. Suppose then that we need to dry the cassava from 75% initial moisture content down to 10% for safe storage. The amount of moisture to be expelled is given by Eq. 4, thus:

$$M_w = M_p \frac{(M_i - M_f)}{(100 - M_f)} \tag{4}$$

where:

Mp = Initial mass of product (kg).
M_i, M_f = Initial and final moisture contents, respectively (%).

Once the mass of moisture to be expelled has been determined, it is possible to calculate the average drying rate, m_{dr} (kg/h) according to Eq. 5. The drying time t_d is usually estimated based on previous experience, or when using computer programming, an iterative approach is used to arrive at its final value.

$$m_{dr} = \frac{M_w}{t_d} \tag{5}$$

(b) *Quantity of Air Needed for Drying*

Prior to calculating the amount of air required for drying, some researchers recommend that the equilibrium relative humidity (ERH) be determined. In that case, it is calculated from the water activity, a_w as follows:

$$\text{ERH} = 100\ a_w \tag{6}$$

The water activity may be calculated from absorption isotherms presented elsewhere (Tonui et al. 2014). In order to obtain the amount of air necessary for drying, it is necessary to determine the humidity ratio using the psychrometric charts at the ambient dry bulb temperature and relative humidity values. Thus, suppose the dry bulb temperature is 30 °C, while the relative humidity is 70%. Then, tracing the lines using the psychometric chart, we obtain a humidity ratio of 0.019 kg water/kg dry air. When the incoming air is heated by the solar collector to an optimum drying temperature (taken as the highest allowable product temperature or temperature at the exit of collector for distributed type dryers) of say 45 °C (dry bulb), the humidity ratio remains unchanged. If, while passing through the crop, the air absorbs moisture until its RH equals ERH (calculated above), e.g. 56%, the psychometric chart indicates that the humidity ratio is 0.015 kg water/kg dry air and the corresponding dry bulb temperature is 37.6 °C. Therefore, the change in humidity ratio is 0.019–0.015 = 0.004.

Then, using the gas laws Eq. (7):

$$PV = M_A RT \tag{7}$$

where:

P = Atmospheric pressure (101.3 KPa).
T = Absolute temperature, Kelvin.
V = Volume of air, m^3.
R = Universal gas constant (0.291 kPa m^3/kg K).
M_A = Mass of the air, kg.

Therefore, for an increase in humidity ratio of 0.004 kg water/kg dry air, each kilogram of water will require 1/0.004 = 250.00 kg dry air. Applying Eq. 7 while taking the absolute temperature as 37.6 + 273 = 310.6 K, the volume of air needed to expel a kilogram of water is 223.06 m^3. Hence, Mw (from Eq. 4) will require (Mw*223.06) m^3 of air for effective drying. The volumetric flow rate of air V_a (m^3/h) may be calculated using Eq. 8 (Tonui et al. 2014):

$$V_a = \frac{W_a}{t_d} \tag{8}$$

where:

W_a = Quantity of air required, m^3.
t_d = Total drying time, hours.

The product of the volumetric flow rate (m^3/h) and the air density (approx. 1.2 kg/m^3) gives the value of the mass flow rate of air, m_a, kg/h. This is a needed input in item (c). When the volumetric air flow rate is appreciably higher than what can be achieved by natural draft, a blower may be recommended. Otherwise, longer drying times will be expected.

(c) *Quantity of Heat Energy Required for Drying, E*

The heat energy, E (kJ), required for a drying process is usually calculated using Eq. 9 as follows:

$$E = m_a(h_f - h_t)t_d \tag{9}$$

where:

m_a = Mass flow rate of air.
kg/h h_f and h_i = final and initial enthalpy of drying and ambient air, respectively, kJ/kg_{da} (obtained from psychometric charts).
t_d = Drying time, h

(d) *Total Collector Area, Ac*

Dryer collector area is directly proportional to the amount of heat energy required for drying and inversely proportional to the collector efficiency. Applying the energy balance equation, we obtain the following:

Input Energy = Output Energy.

$$\mathrm{A_c}I\eta = E = \mathrm{m_a}\left(h_f - h_i\right)t_d \tag{10}$$

Hence, collector area, Ac (m^2), is given by Eq. 11:

$$A_c = \frac{m_a\left(h_f - h_i\right)}{I\eta} \tag{11}$$

where:

I = Total global solar radiation during the period, kJ/m^2.

η = Collector efficiency (usually in the range of 30–50% (Barley and Winn 1978; Tonui et al. 2014; Om and Kumar 2013).

(e) *Determining the Size of the Dryer Chamber*

The drying chamber breadth, B, is usually made to match the width (W) of the solar air heater (collector) (Anyanwu et al. 2012; Tonui et al. 2014). Thus, its length, L_{dc}, is calculated as the area to width ratio.

(f) *Air Vent Dimensions*

The area of the air vent, A_v, may then be determined by dividing the volumetric air flow rate by the average wind speed, while the length of air vent, L, will be equal to the length of the dryer:

$$A_v = \frac{V_a}{v_w} \tag{12}$$

where:

V_w = Wind speed, m/s.

The width of the air vent can then be obtained as the ratio of the area to the length.

(g) *Pressure Drop Through the Drying Bed*

A number of approaches exist for calculating the resistance to air flow through a packed bed of agricultural produce (Anyanwu et al. 2012; Tonui et al. 2014; Jindal and Gunasekaran 1982; Forson et al. 2007). The superficial air velocity, u (m/s), is given by Eq. 13:

$$u = a\left(\Delta\frac{p_b}{h_L}\right) \tag{13}$$

where:

h_L = Thickness drying bed, m.
a = Constant.
Δp_b = Pressure drop across crop bed, Pa.

The value of the constant, a, is usually evaluated experimentally. However, for natural circulation of air through a thin layer of crop ($h \leq 0.20$ m), it is taken as 0.465 m3 s/kg (Tonui et al. 2014; Forson et al. 2007). The same figure may be used for small-scale active drying systems. Forson et al. 2007, proposed a value of 0.4 m/s for the air velocity (u). It is usually taken as the maximum speed at the exit of the solar air heater, if measured. Pressure drop across the bed (ΔP_B) is usually determined using 0.2 m as the optimum drying bed thickness. According to Forson et al. 2007, when all components of pressure drop are taken into account, the gross pressure drop is about six times ΔP_B as shown in Eq. 14:

$$\Delta P_T = 6 \times (2\Delta P_B) \tag{14}$$

(h) *Height of the Hot Air Column (H)*

This is the minimum required height of the exit vents above the inlet of the collector, which is provided to allow escape of moist air to the ambient under natural convection air circulation (Tonui et al. 2014). In order to arrive at the height of the air column, steady-state conditions inside the dryer are assumed. In addition, the following assumptions are usually made: (a) the depth of the drying bed, $h_L < H$; (b) the entire structure is airtight; ambient air enters through the inlet while wet warm air leaves through the exit vent (s); and (c) T_{dryer} is the average value of the temperature under steady-state conditions, whereas density of the hot air inside the dryer is denoted as ρ^*. Then, using Bernoulli's equation within the relevant dryer sections leads to Eq. 15:

$$H = \frac{\Delta P_T}{g(\rho_a - \rho^*)} = \frac{\Delta P_T R}{g\left(\frac{1}{T_{amb}} - \frac{1}{T_{dryer}}\right)P_a} \tag{15}$$

where:

$\Delta^P{}_T$ = Total pressure drop through the dryer, Pa
g = Acceleration due to gravity (9.81 m/s^2).

In fabricating the dryer, an allowance is usually made for the clearance height of the solar collector air inlet above the ground. In order to allow for natural air flow, Tonui et al. 2014, recommended a clearance height of at least 0.40 m.

4 Performance Evaluation of Solar Drying Systems

The performance evaluation of solar drying systems is usually carried out using the same crops or products for which they have been designed. The objective of performance evaluation is usually twofold: firstly, it serves as a measure of functionality but also enables the calculation of actual efficiency of the realized system. Results of performance evaluation of solar drying systems can also be used for design enhancement.

5 Economic Considerations

An economic appraisal of solar air heaters applied in solar drying systems is well detailed by Sharma et al. (1993a). The authors considered and explained the relationship between direct and indirect investment costs. Costs related to plant construction are usually captured under direct costs. These include cost of land and its preparation, plant components, electrical and mechanical works, etc. They are generally subdivided into plant components and civil works (Sharma et al. 1993a). Indirect costs, on the other hand, cover plant design and testing costs. According to Sharma et al. 1993a, engineering and supervision costs constitute about 10–20% of the total direct investment costs, C. If C_1 denotes the cost of equipment or a plant with output M_1, then the cost of a similar plant with output M_2 can be estimated using the similitude relationship described by Sharma et al. 1993a:

$$C_2 = C_1 . \left(\frac{M_2}{M_1} \right)^s \tag{16}$$

Here, S is a factor dependent on the type of plant. Using the above analogy, the cost of solar drying systems is usually estimated on the basis of the cost of a pilot plant as well as on literature data (Sharma et al. 1993a). O&M costs capture all other costs necessary for the normal functioning of the plant. These include the cost of fuels (if needed), electric energy, chemicals, different consumables, personnel costs, etc.

6 Applications of Solar Drying Systems: Case Studies

Solar drying systems find useful application in the preservation of fruits, vegetables, grains, tubers and many other agricultural produce. It is believed that massive deployment of solar drying systems in agricultural production could drastically reduce the incidence of postharvest losses, especially in the tropical countries of the world. Sharma et al. (1995) carried out drying experiments to compare a cabinet-

type natural convection solar dryer with a multi-stacked natural convection solar dryer and an indirect-type multi-shelf forced convection solar dryer. They concluded that the cabinet-type natural convection solar dryer is suitable for drying small quantities of fruit and vegetables on the domestic/household scale. The indirect-type multi-shelf dryer, on the other hand, is suitable for large-scale industrial applications.

6.1 Direct-Mode Solar Dryers

Using weather conditions for Warri (lat. 5°30′N, long. 5°41′E), Nigeria, Diemuodeke and Momoh (2011) designed and fabricated a direct, natural convection solar dryer suitable for preserving tapioca in rural areas. A minimum collector area of 7.56 m^2 was needed to dry a batch of 100 kg of tapioca in 20 h (i.e. 2 days drying period). Initial and final moisture contents were 79% and 10% wet basis, respectively. The prevailing ambient conditions were 32 °C air temperatures and 74% RH. The daily global solar radiation was 13 MJ/m^2/day.

6.2 Indirect-Mode Solar Dryers

The development and testing of an indirect-mode, active solar drying system was reported by Sharma et al. (1993b). The dryer, which consists of an air heater and a drying chamber, was used by the authors to dry grapes, brinjals, apricots and tomatoes. Outlet air from the collector is made to pass through a thermally and acoustically well-insulated rectangular air ducts measuring 30 x 30 cm, before being sucked through the collector by an electrically driven ventilator. According to Sharma et al. (1995), the indirect, multi-tray dryers are suitable for use in large-scale industries.

6.3 Mixed-Mode Solar Dryers

Schirmer et al. (1996) designed and developed an active solar tunnel drying system capable of handling 300 kg of bananas per batch. The payback period of the dryer is estimated to be about 3 years when the dryer is produced locally. Using a direct-mode and a mixed-mode solar crop dryers they constructed, Sharma et al. (1986) successfully dried whole peas, grapes and potatoes within 3 days, under ambient conditions of 50% average relative humidity and 20 MJ/m^2 solar radiation. The average dryer efficiency was put at 40%. Although, the performance of mixed-mode dryers is usually better than the direct-mode and indirect-mode dryers (Sharma et al. 1995), the former are slightly more expensive.

7 Conclusions

Drying is a process of moisture removal occasioned by simultaneous heat and mass transfer. It is an excellent way to preserve foods and reduce postharvest losses, especially in the tropics. The main purpose of drying is to reduce moisture content and, thus, reduce or eliminate microbial activities, which are capable of leading to spoilage. The major merits of open-air sun drying are low capital and operating costs and the fact that little expertise is required. Solar dryers have a number of advantages over traditional open-air sun drying. The design of solar drying systems can be accomplished using a set of rules of thumb. However, in order to achieve higher accuracy and performance of the dryers, it is necessary to adopt proper design procedures, which involve the use of data from psychrometric charts to calculate the required drying area and time. Solar drying systems find application in the preservation of fruits, vegetables meats, fish, tubers, etc.

Nomenclature

Av	*Area of air vent,* m^2
a_w	*Water activity*
$C_{1/2}$	*Cost of equipment*
E	*Total useful heat energy, KJ,*
ERH	*Equilibrium relative humidity, %*
g	*Acceleration due to gravity (9.81* m/s^2*)*
H	*Height of air column, m*
h	*Drying bed thickness, m*
hi/f	*Initial/final enthalpy, kJ/kg*
I	*Total global solar radiation,* kJ/m^2
L_{dc}	*Length of the drying chamber, m*
$M_{1/2}$	*Plant output*
M_A	*Mass of air, kg*
MC	*Moisture content, %*
Mi/f	*Initial/final mass, kg*
Mp	*Initial mass of product, kg*
Mw	*Mass of moisture to be expelled, kg*
mdr	*Drying rate, kg/hr*
P	*Atmospheric pressure, kPa*
Δp_b	*Pressure drop across crop bed, Pa*
ΔP_T	*Pressure drop through the dryer, Pa*
R	*Universal gas constant, 0.291 kPa* $m^3/kg\ K$
t_d	*Total drying time, hrs*
U	*Superficial air velocity, m/s*
V	*Volume of air,* m^3
Vw	*Wind speed, m/s*
Va	*Volumetric airflow rate,* m^3/h
Wa	*Quantity of air required,* m^3
η	*Efficiency*

References

Anon (2016) Sun and solar drying, techniques and equipment. Paper no. 33. Accessed from the Worldwide web on 14th October, 2016 http://www.unido.org/fileadmin/import/32146_33SUNANDSOLARDRYING.16.pdf

Anyanwu CN, Oparaku OU, Onyegegbu SO, Egwuatu U, Edem NI, Egbuka K, Nwosu PN, Sharma VK (2012) Experimental investigation of a photovoltaic-powered solar cassava dryer. Taylor & Francis J Dry Technol 30:398–403

Barley CD, Winn CB (1978) Optimal sizing of solar collectors by the method of relative areas. Sol Energy 21:279

Belessiotis V, Delyannis E (2011) Solar drying. Sol Energy 85:1665–1691

Diemuodeke EO, Yusuf MOL (2011) Design and fabrication of a direct natural convection solar dryer for Tapioca. Leonardo Elect J Pract Technol Issue 18:95–104; ISSN 1583–1078

Ekechukwu OV, Norton B (1999) Review of solar-energy drying systems II: an overview of solar drying technology. Energy Convers Manag 40(6):615–655

El-Sebaii AA, Shalaby SM (2012) Solar drying of agricultural products: a review. Renew Sust Energ Rev 16:37–43

Forson FK, Nazha MAA, Akuffo FO, Rajakaruna H (2007) Design of mixed-mode natural convection solar crop dryers: application of principles and rules of thumb. Renew. Energy J 32:1–14

Hii CK, Jangam SV, Ong SP, Mujumdar AS (eds) (2012) Solar drying: fundamentals, applications and innovations. ISBN: 978-987-07-3336-0

Jindal VK, Gunasekaran S (1982) Estimating air flow and drying rate due to natural convection in solar rice dryers. Renew Energ Rev 4(2):1–9

Lalit MB, Satya S, Naik SN (2010) Solar dryer with thermal energy storage systems for drying agricultural food products: a review. Renew Sustain Energy Rev 14(8):2298–2314

Om P, Kumar A (2013) Historical review and recent trends in solar drying systems. Int J Green Energy 10(7)

Peace Corps (1980) Appropriate community technology: a training manual. Information collection and exchange. ISES Sunworld 1(6):18081

Reddy BS, Chakraverty A (2004) Equilibrium moisture characteristics of raw and parboiled paddy, brown rice, and bran. Dry Technol 22(4):837–851

Schirmer P, Janjai S, Esper A, Smitabhundu R, Mulbauer W (1996) Experimental investigation of the performance of the solar tunnel dryer for drying bananas. Renew Energy 7(2):119–129

Sharma VK, Sharma S, Ray RA, Garg HP (1986) Design and performance studies of a solar dryer suitable for rural applications. Energy Convers Manag 26(1):111–119

Sharma VK, Colangelo A, Spagna G, Pistochi F (1993a) Preliminary economic appraisal of solar air heating systems used for drying of agricultural products. Energy Convers Manag 34

Sharma VK, Colangelo A, Spagna G (1993b) Experimental performance of an indirect type solar fruit and vegetable dryer. Energy Convers Mgmt 34(4):293–308

Sharma VK, Colangelo A, Spagna G (1995) Experimental investigation of different solar dryers suitable for fruit and vegetable drying. Renew Energy 6(4):413–424

Szulmayer W (1971) From sun-drying to solar dehydration I and II. Food Technology in Australia, pp 440–501

Tonui KS, Mutai EBK, Mutuli DA, Mbuge DO, Too KV (2014) Design and evaluation of solar grain dryer with a back-up heater. Res J Appl Sci Eng Technol 7(15):3036–3043

Umogbai VI, Iorter HA (2013) Design, construction and performance evaluation of a passive solar dryer for maize cobs. Afr J Food Sci Technol 4(5):110–115

Thermal Testing Methods for Solar Dryers

Shobhana Singh

Abstract Solar food drying is a complex heat and mass transfer phenomena which depend on a number of drying process-dependent parameters such as operating conditions and characteristics of the food product to be dried. The variation in these parameters significantly affects the overall performance of the dryer system. Since commercial growth and acceptance of any solar dryer system momentously depend on its performance guarantee, the development of a standard methodology for their thermal testing has become necessary. The standard testing method not only provides better performance management of the dryer system but allows the manufacturers to achieve competitive efficiency and good product quality by comparing the available designs. In this chapter, an extensive review of solar dryer performance evaluation has been carried out. Furthermore, the chapter describes the existing testing procedures for the most common designs of solar dryers and the related practices used in the measurement, evaluation, and description of overall performance, including a variety of food product dried in scientific investigations.

Keywords Solar dryer • Heat and mass transfer • Performance • Thermal testing method

1 Introduction

Performance evaluation or prediction is an important part of manufacturers and design engineers' strategy. Manufacturing industries are encouraged to reach the highest possible energy efficiency and product quality by certification from various national and international standards. These objectives are often achieved by formulation and implementation of established test methods by standardizing agencies and research institution. Standard test procedure provides a guaranteed equipment of best quality to the end user for the safe and reliable operation. It also helps in comparing different equipment designs under certain similar conditions.

S. Singh (✉)
Department of Energy Technology, Aalborg University, Pontoppidanstræde, 9220 Aalborg East, Denmark
e-mail: ssi@et.aau.dk

© Springer Nature Singapore Pte Ltd. 2017

O. Prakash, A. Kumar (eds.), *Solar Drying Technology*, Green Energy and Technology, DOI 10.1007/978-981-10-3833-4_7

Standard test procedures for and certification of several solar thermal systems, such as solar cookers, solar collectors, solar water heaters, etc., have already been developed and utilized to evaluate the thermal performance around the world. Development of a testing procedure to evaluate the thermal performance of a box-type solar cooker is first initiated by Vaishya et al. (1985). A testing parameter based on outdoor experiments under no-load is classified and defined as the ratio of solar radiation intensity on a horizontal surface to the temperature difference between absorber plate and ambient air for stagnation condition. For performance evaluation of box-type solar cooker, two figures of merit, F1 and F2 with no-load and load conditions, respectively, are proposed by Mullick et al. (1987). It is important to note that the recommended test parameters are measured independent of the climatic conditions, which therefore can be used to compare various box-type solar cooker designs on an equitable basis. Furthermore, to test and characterize thermal performance of paraboloid concentrator solar cookers under load condition, Mullick et al. (1991) suggested F'UL and F'ηo as two design test parameters. Soltau (1992) proposed standard test model to determine the performance of uncovered solar collector under unsteady conditions. Amer et al. (1997) conducted a detailed review on various test methods of flat-plate solar collectors and calculated two characteristic parameters such as optical efficiency (F_R) and overall heat loss factor ($F_R U_l$) for an extensive comparative study between dynamic testing methods (Amer et al. 1998). Furthermore, thermal performance of flat-plate collectors is critically evaluated and presented using transient methods by Nayak and Amer (2000). However, the tests are independent of frequently changing weather characteristics during the year. Thermal performance of flat-plate collectors is critically evaluated and presented using transient methods by Nayak and Amer (2000). However, the tests are independent of frequently changing weather characteristics during the year. In addition, other important test parameters were identified for various solar thermal systems such as field focus concentrator for the industrial oven (Bhirud and Tandale 2006), a compound parabolic concentrator with the spherical absorber (Senthilkumar et al. 2009) to evaluate their thermal performance.

2 Testing of Solar Dryers

With increased attention on the utilization of renewable energy, numerous studies have been directed toward the development of standardized testing methods in order to evaluate the thermal performance of various designs of solar dryer system. For instance, Sodha and Chandra (1994) reviewed several designs of solar air collector and presented various testing methods for their evaluation, considering them the critical and important component of a solar dryer. Similarly, Grupp et al. (1995) presented a method of evaluating and comparing solar dryers by conducting tests on various designs of dryers such as a circular box-type dryer, a shell dryer, a cabinet dryer, a tunnel dryer, and a chimney dryer. An overall grading is assigned to the tested dryer on the basis of tests. The term "evaporative index" is proposed by

Jannot and Coulibaly (1998) to rate the performance of the solar air heater connected in series through a solar drying chamber. Leon et al. (2002) presented a more detailed review of testing procedures, very often used for reporting thermal performance evaluation results. With an objective of finding more rational test parameters for performance evaluation of solar dryer alone or integrated with air collector, the investigators proposed an overall heat loss coefficient (U_L) under stagnant no-load condition (Singh et al. 2006; Sreekumar et al. 2008) and drying efficiency (η_d) (Pande and Thanvi 1991; Bena and Fuller 2002; El-Sebaii et al. 2002) under load condition.

Due to complex nature of physical phenomena involved during drying, there exists a significant number of drying process-dependent variables. There are multiple operating conditions and characteristics of a food product which can critically affect moisture removal rate and therefore overall performance of drying process. As a consequence, the dryer performance results reported in the literature deviate significantly. It can be noticed from the literature that U_L and η_d have been utilized as test parameters at stagnation no-load and load conditions, respectively, for performance evaluation and comparison of various solar dryer designs. Recently, a recirculation-type integrated collector drying chamber (ICDC) solar dryer for drying rough rice has been designed and tested (Chan et al. 2015). In another study, solar crop dryer with thermal energy storage is developed to maintain color and flavor during drying of herbs (Jain and Tewari 2015). In both studies, the performance of the solar dryer is evaluated by drying efficiency in different load conditions. However, these parameters are found to be highly dependent on climatic condition and other operating variables. The drying efficiency, η_d, in fact, also depends on food product characteristics in addition to these variables. Thus, the results based on such parameters may not reflect the true indication of dryer performance and hence cannot be applied for reliable comparison of the thermal performance of different solar dryer designs. Hence, it becomes imperative to develop such methodology for thermal testing of dryers that is independent of climatic and operating conditions as well as food product characteristics.

Numerous experimental studies on diverse solar dryer designs and their performance evaluation are available (Condori et al. 2001; Leon et al. 2002; Murthy 2009; Stiling et al. 2012; Jain and Tewari 2015); nevertheless, there is lack of attention to develop a standard test that can be utilized to compare different designs on a common foot. Most often, complex dryer system geometries, coupled heat and moisture transfer, and nonuniform airflow pattern make the analysis even more challenging to undertake. Moreover, the thermal performance of a given dryer cannot be compared in a meaningful way because the results obtained are strongly dependent on drying process variables. A number of experiments are required under a variety of test conditions and to predict the performance of a solar independent of any process-dependent parameters. However, the development of procedure identifying a test parameter that can demonstrate the effectiveness of any dryer design in a convincing manner is impending. Singh and Kumar (2012a, b) conducted several experiments on the cabinet, indirect, and mixed-mode solar dryers under natural and forced airflow and identified suitable dimensionless parameters which can be

used for thermal performance-based rating of solar dryers under no-load and load conditions. The proposed testing methods for load and no-load conditions are described in detail in the following section.

3 Performance Index

3.1 No-Load Performance Index (NLPI)

Singh and Kumar (2012a) proposed a mathematical framework of a testing method for the conventional solar air heater-dryer designs which includes cabinet, mixed-mode, and indirect solar dryers. The test method is simple and easy to implement under both natural and forced convection operation of dryers to evaluate and predict the thermal performance in a no-load condition.

3.1.1 Experimental Methodology

The designs selected in the study are the most common solar dryers that are widely used in drying applications of food products (El-Sebaii et al. 2002; Simate 2003; Forson et al. 2007; Boughali et al. 2009). The laboratory models of the cabinet, mixed-mode, and indirect dryers are fabricated and used to conduct no-load experiments. The schematic diagrams of laboratory scale dryer systems used in the experimentation can be seen in Figs.1, 2, 3 and 4. The experiments are performed in a simulated environment with a wide range of input power 300–800 W/m^2 of dryer/air heater absorber plate and airflow rate varying from 0.009 to 0.026 kg/s. Different levels of absorbed energy flux levels are maintained by independently regulating the wattage of electric heaters fitted underneath of air heater and drying chamber absorber plates. In the thermal analysis, it is assumed that 100% of supplied electric energy is converted to the thermal energy to be absorbed by a plate of air heater-dryer assembly. The desired absorbed thermal energy flux level is calculated by dividing supplied electric energy by absorber area of the dryer system assembly. For experimentation under forced convection, desired airflow rate is set by using AC drive coupled to the motor-fan arrangement. On reaching the steady state for a given level of absorbed energy flux and airflow rate, the temperatures of all components of an air heater and drying chamber along including ambient air are measured by pre-calibrated thermocouples. Each temperature data point is determined in 4–6 h to get a very good steady state.

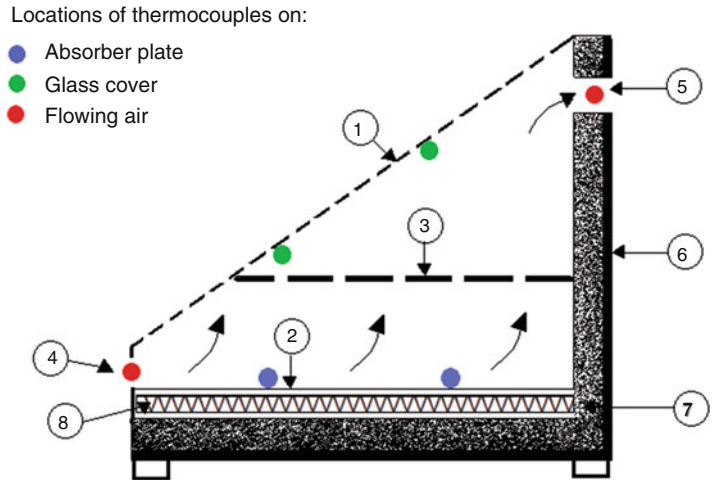

Fig. 1 Schematic diagram of cabinet solar dryer with indicated thermocouple locations and dryer components (*1* glass cover, *2* absorber plate, *3* wire mesh, *4* inlet vent, *5* outlet vent, *6* wooden case, *7* insulation, *8* electric heating plate) (Singh and Kumar 2012a)

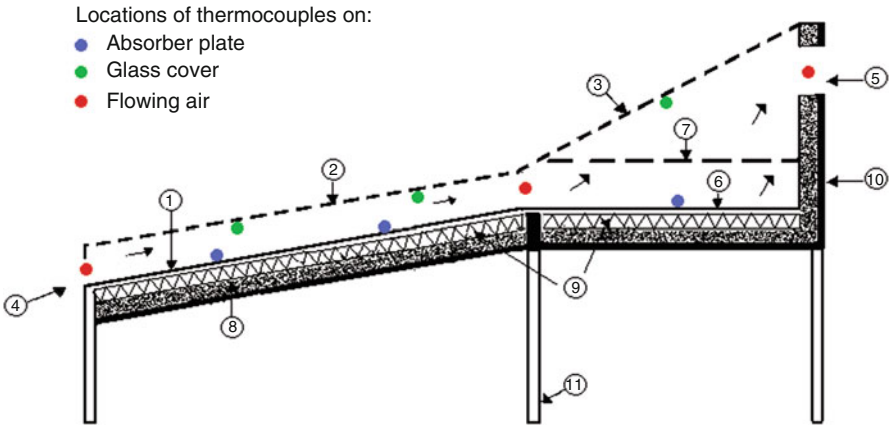

Fig. 2 Schematic diagram of mixed-mode solar dryer with indicated thermocouple locations and dryer components (*1* collector absorber plate, *2* collector glass cover, *3* drying chamber glass cover, *4* inlet vent, *5* outlet vent, *6* drying chamber absorber plate, *7* wire mesh, *8* insulation, *9* electric heating plates, *10* wooden case, *11* angle iron stand) (Singh and Kumar 2012a)

3.1.2 Mathematical Formulation

Under steady-state condition, the heat balance of solar air heater-dryer assembly is given as follows (Singh and Kumar 2012a):

Heat balance on the absorber plate air collector-dryer chamber,

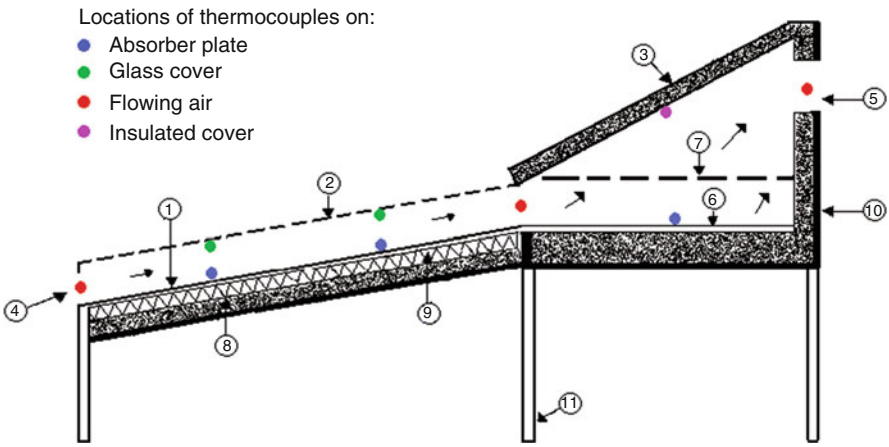

Fig. 3 Schematic diagram of indirect solar dryer with indicated thermocouple locations and dryer components (*1* air heater absorber plate, *2* air heater glass cover, *3* insulated opaque cover, *4* inlet vent, *5* outlet vent, *6* drying chamber absorber plate, *7* wire mesh, *8* insulation, *9* electric heating plate, *10* wooden case, *11* angle iron stand) (Singh and Kumar 2012a)

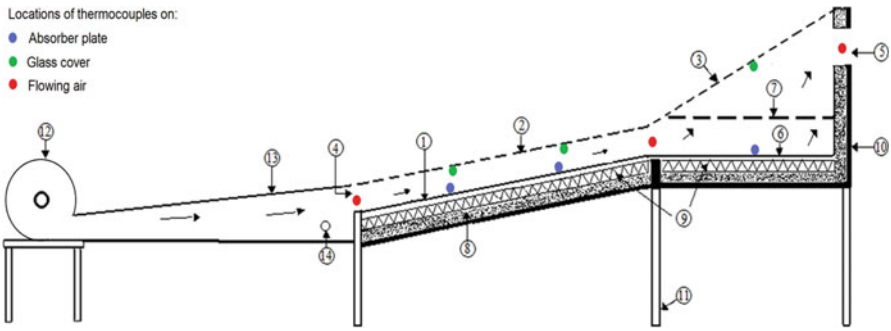

Fig. 4 Schematic diagram of mixed-mode solar dryer operated under forced convection with indicated thermocouple locations and dryer components (*1* air heater absorber plate, *2* air heater glass cover, *3* drying chamber glass cover, *4* inlet vent, *5* outlet vent, *6* drying chamber absorber plate, *7* wire mesh, *8* insulation, *9* electric heating plates, *10* wooden case, *11* angle iron stand, *12* air blower, *13* divergent duct, *14* small hole to measure air flow rate) (Singh and Kumar 2012a)

$$S = U_b\left(\bar{T}_p - \bar{T}_{am}\right) + h_{cpf}\left(\bar{T}_p - \bar{T}_f\right) + h_{rpg}\left(\bar{T}_p - \bar{T}_g\right) \tag{1}$$

Heat balance on glass cover,

$$h_{cfg}\left(\bar{T}_f - \bar{T}_g\right) + h_{rpg}\left(\bar{T}_p - \bar{T}_g\right) = U_t\left(\bar{T}_g - \bar{T}_{am}\right) \tag{2}$$

Heat balance on flowing air in the passage between absorber plate and glass cover,

$$\dot{m}\,C_{\mathrm{p}}(\bar{T}_{\mathrm{fo}}-\bar{T}_{\mathrm{f}i})=A_{\mathrm{abs}}\left[h_{\mathrm{cpf}}\left(\bar{T}_{\mathrm{p}}-\bar{T}_{\mathrm{f}}\right)-h_{\mathrm{cfg}}\left(\bar{T}_{\mathrm{f}}-\bar{T}_{\mathrm{g}}\right)\right] \tag{3}$$

where S is the absorbed thermal energy flux. U_{b} is the bottom heat loss coefficient, and h_{rpg} is the radiative heat transfer coefficient between absorber plate and glass cover of collector-dryer assembly. $\bar{T}_{\mathrm{p}}, \bar{T}_{\mathrm{g}}$, and $\bar{T}_{\mathrm{f}}$ are the average temperatures of the plate, glass cover, and hot air of solar air heater-dryer assembly, respectively, at the steady state. $\bar{T}_{\mathrm{am}}$ is the average ambient air temperature at that time. $\dot{m}$ and C_{p} is the airflow rate and specific heat of air, respectively. $\bar{T}_{\mathrm{fo}}$ and $\bar{T}_{\mathrm{fi}}$ represent the average temperatures of air at dryer outlet and collector inlet, respectively. A_{abs} is the surface area of absorber plate of the dryer system.

The radiative heat transfer coefficient between absorber plate and glass cover is determined as (Singh and Kumar 2012a):

$$h_{\mathrm{rpg}}=\frac{\sigma\left[\left(\bar{T}_{\mathrm{p}}+273\right)^2+\left(\bar{T}_{\mathrm{g}}+273\right)^2\right]\left[\left(\bar{T}_{\mathrm{p}}+273\right)+\left(\bar{T}_{\mathrm{g}}+273\right)\right]}{\left[\frac{1}{\varepsilon_{\mathrm{p}}}+\frac{1}{\varepsilon_{\mathrm{g}}}-1\right]} \tag{4}$$

where ε_{p} and ε_{g} are the emissivities of dryer absorber plate and glass cover, respectively, which is taken equal to 0.90 for each parameter.

The bottom heat transfer coefficient is obtained as:

$$U_{\mathrm{b}}=\frac{k_{\mathrm{b}}}{L_{\mathrm{b}}} \tag{5}$$

where k_{b} and L_{b} represent the conductivity and thickness of thermal insulation, respectively.

Total heat loss coefficient is expressed as the sum of radiative and convective heat transfer coefficients between the glass cover and the surrounding ambient air.

$$U_t=h_{\mathrm{rga}}+h_{\mathrm{cga}} \tag{6}$$

where h_{rga} is the radiative heat transfer coefficient between the glass cover and the ambient air and is given as (Singh and Kumar 2012a):

$$h_{\mathrm{rga}}=\frac{\sigma\cdot\varepsilon_{\mathrm{g}}\left[\left(\bar{T}_{\mathrm{g}}+273\right)^4-\left(\bar{T}_{\mathrm{am}}+273\right)^4\right]}{\left(\bar{T}_{\mathrm{g}}-\bar{T}_{\mathrm{am}}\right)}. \tag{7}$$

The convective heat transfer coefficient (h_{cga}) between the glass cover and the ambient air under natural convection is given as:

$$Nu=h_{\mathrm{cga}}\frac{L}{k_{\mathrm{a}}}=0.54(\mathrm{Ra})^{0.25} \tag{8}$$

$$h_{\mathrm{cga}} = 0.54(\mathrm{Ra})^{0.25}\left[\frac{k_{\mathrm{a}}}{L}\right] \tag{9}$$

where k_{a} is the conductivity of air and L represents the characteristic length.

Rearrangement of Eqs. (1), (2) and (3) gives:

$$\frac{h_{\mathrm{cfg}}}{h_{\mathrm{cpf}}} = \left[\frac{U_{\mathrm{t}}\left(\bar{T}_{\mathrm{g}} - \bar{T}_{\mathrm{am}}\right) - h_{\mathrm{rpg}}\left(\bar{T}_{\mathrm{p}} - \bar{T}_{\mathrm{g}}\right)}{S - U_{\mathrm{b}}\left(\bar{T}_{\mathrm{p}} - \bar{T}_{\mathrm{am}}\right) - h_{\mathrm{rpg}}\left(\bar{T}_{\mathrm{p}} - \bar{T}_{\mathrm{g}}\right)}\right] \cdot \left[\frac{\left(\bar{T}_{\mathrm{p}} - \bar{T}_{\mathrm{f}}\right)}{\left(\bar{T}_{\mathrm{f}} - \bar{T}_{\mathrm{g}}\right)}\right] \tag{10}$$

$$\dot{m}\, C_{\mathrm{p}}(\bar{T}_{\mathrm{fo}} - \bar{T}_{\mathrm{f}i}) = A_{\mathrm{abs}} h_{\mathrm{cpf}}\left[\left(\bar{T}_{\mathrm{p}} - \bar{T}_{\mathrm{f}}\right) - \frac{h_{\mathrm{cfg}}}{h_{\mathrm{cpf}}}\left(\bar{T}_{\mathrm{f}} - \bar{T}_{\mathrm{g}}\right)\right] \tag{11}$$

On simplification, one can get:

$$\frac{\dot{m}\, C_{\mathrm{p}}}{A_{\mathrm{abs}} h_{\mathrm{cpf}}} = \frac{\left(\bar{T}_{\mathrm{p}} - \bar{T}_{\mathrm{f}}\right)}{\left(\bar{T}_{\mathrm{fo}} - \bar{T}_{\mathrm{fi}}\right)}\left[\frac{S - U_{\mathrm{b}}\left(\bar{T}_{\mathrm{p}} - \bar{T}_{\mathrm{am}}\right) - U_{\mathrm{t}}\left(\bar{T}_{\mathrm{g}} - \bar{T}_{\mathrm{am}}\right)}{S - U_{\mathrm{b}}\left(\bar{T}_{\mathrm{p}} - \bar{T}_{\mathrm{am}}\right) - h_{\mathrm{rpg}}\left(\bar{T}_{\mathrm{p}} - \bar{T}_{\mathrm{g}}\right)}\right] \tag{12}$$

where $\dot{m}\, C_{\mathrm{p}}/A_{\mathrm{abs}} h_{\mathrm{cpf}}$ represents the *no-load performance index*, *NLPI*, which is defined as the ratio of heat capacity rate of working fluid to remove energy from the absorber surface of solar dryer system to convective heat transfer coefficient describing the performance characteristic of a given dryer design. In other words, it is a measure of the heat transfer effectiveness of a solar dryer. The value of *NLPI* depends on the relative values of heat capacity rate through the dryer, collector area, and heat transfer coefficient. It can range from zero to a large value. However, higher values are always desired for better performance of solar collector-dryer assembly (Singh and Kumar 2012a).

3.1.3 Results

The temperature data for no-load steady-state indoor experiments on the cabinet, indirect, and mixed-mode type is analyzed under natural and forced air circulation and is utilized to compute *NLPI* with the help of Eq. (12). The computed *NLPI* of the cabinet, mixed, and indirect-type dryers for different absorbed energy flux levels (300–800 W/m^2) for natural and forced air circulation is presented in Tables 1, 2, 3, 4, 5. It can be noticed from Tables 1, 2, 3 that the mean *NLPI* values obtained under the natural convection for the cabinet, mixed-mode, and indirect dryers are 0.442, 0.524, and 0.633, respectively. The results depict that the highest *NLPI* value is exhibited by the mixed-mode dryer followed by indirect and cabinet dryers. However, solar dryers operated under natural air circulation show lower *NLPI* values due to low buoyancy-induced airflow inside the natural convection dryers (Bala and Woods 1994).

The computed results of *NLPI* of mixed- and indirect-type dryery flux levels are also given in Tables 4 and 5. It is observed that *NLPI* value improves with the increase in airflow rate for each of the dryer design. In addition, higher values of

Table 1 Observational temperatures data of different components and calculated *NLPI* for cabinet dryer operated in natural convection (Singh and Kumar 2012a)

Absorbed thermal energy flux levels (W/m^2)	Plate $\bar{T}_p$ v (°C)	Hot air, $\bar{T}_f$ (°C)	Glass cover, $\bar{T}_g$ (°C)	Ambient air, $\bar{T}_{am}$ (°C)	No-load performance index (*NLPI*)
286	46.94	24.82	30.32	14.67	0.385
403	55.75	26.77	33.50	13.94	0.441
504	64.30	29.95	36.68	14.67	0.465
571	70.17	32.03	40.34	14.67	0.433
588	77.02	38.51	46.46	20.78	0.425
605	71.64	32.52	39.85	14.67	0.452
672	77.75	34.84	42.79	15.40	0.461
756	89.98	42.79	54.52	22.01	0.453
806	86.06	36.43	46.46	13.94	0.459

NLPI are obtained for mixed-mode dryer in comparison with the indirect dryer due to improved design characteristics; mixed-mode dryer shows better heat transfer effectiveness under given test conditions. For instance, at the airflow rates of 0.009, 0.017, and 0.026 kg/s, mean *NPLI* values of the mixed-mode dryer are 1.078, 1.495, and 1.602, respectively, and 0.923, 1.353, and 1.476 for indirect, respectively. Furthermore, it is observed that for a given airflow condition, quite consistent values of *NLPI* can be achieved by any dryer design over a wide range of ambient air temperature (14–34 °C) and absorbed thermal energy flux level (300–800 W/m^2).

3.1.4 Validation of the Test Method

Singh and Kumar (2012a) verified the experimental results of *NLPI* for a given dryer by conducting a statistical analysis. A number of parameters, namely, arithmetic mean $\bar{x}$, standard deviation (SD), standard error of mean (SE), and confidence interval (E), are used in the analysis to determine the inconsistencies and are defined as:

$$\bar{x} = \frac{\sum_{i=1}^{n} x_i}{N} \tag{13}$$

$$\mathrm{SD} = \sqrt{\frac{1}{(N-1)} \sum (x_i - \bar{x})^2} \tag{14}$$

$$\mathrm{SE} = \frac{\mathrm{SD}}{\sqrt{N}} \tag{15}$$

$$\bar{x} - 1.96\left[\frac{\mathrm{SD}}{\sqrt{N}}\right] \leq E \leq \bar{x} + 1.96\left[\frac{\mathrm{SD}}{\sqrt{N}}\right] \tag{16}$$

where x_i is the value obtained in the ith test result and N is the total number of experimental observations.

Table 2 Observational temperatures data of different components and calculated *NLPI* for indirect dryer operated in natural convection (Singh and Kumar 2012a)

Absorbed thermal energy flux levels (W/m^2)	Ambient air, $\bar{T}_{am}$, (°C)	Air heater			Drying chamber			No-load performance index (*NLPI*)
		Plate, $\bar{T}_{cp}$, (°C)	Hot air, $\bar{T}_{cf}$, (°C)	Glass cover, $\bar{T}_{cg}$, (°C)	Plate, $\bar{T}_{dp}$, (°C)	Hot air, $\bar{T}_{df}$ (°C)	Insulated cover, $\bar{T}_{dg}$, (°C)	
300	24.69	53.91	35.57	34.96	44.01	44.62	39.85	0.483
450	24.94	64.67	38.51	36.80	45.23	49.88	42.30	0.476
550	24.69	68.34	38.88	37.04	48.41	51.59	43.28	0.523
600	25.43	71.27	40.22	38.14	50.12	53.18	44.25	0.546
650	25.43	74.21	41.81	39.12	53.79	55.99	48.17	0.541
700	25.43	77.38	43.03	41.69	56.24	57.82	48.66	0.553
750	24.94	79.46	44.25	43.89	61.13	61.13	53.06	0.519
800	26.16	82.40	46.09	44.99	65.04	63.33	54.52	0.553

Table 3 Observational temperatures data of different components and calculated *NLPI* for mixed-mode dryer operated in natural convection (Singh and Kumar 2012a)

Absorbed thermal energy flux levels (W/m^2)	Ambient air, $\bar{T}_{am}$, (°C)	Air heater			Drying chamber			No-load performance index (*NLPI*)
		Plate, $\bar{T}_{cp}$, (°C)	Hot air, $\bar{T}_{cf}$, (°C)	Glass cover, $\bar{T}_{cg}$, (°C)	Plate, $\bar{T}_{dp}$, (°C)	Hot air, $\bar{T}_{df}$, (°C)	Glass cover,$\bar{T}_{dg}$, (°C)	
300	24.45	53.30	34.35	32.15	59.41	45.72	36.19	0.654
375	24.45	59.17	36.31	33.37	66.02	50.12	39.61	0.638
450	24.45	62.47	37.78	33.74	73.35	53.79	42.79	0.643
550	24.69	70.78	40.34	36.06	80.69	59.41	46.46	0.635
650	24.69	76.90	42.79	37.90	89.24	64.79	51.35	0.611
700	25.18	80.32	44.38	39.49	94.13	68.22	52.81	0.607
750	24.69	82.89	45.84	39.49	97.80	68.95	54.28	0.632
800	26.65	86.68	48.17	40.34	102.69	72.13	59.90	0.641

Table 4 Observational temperatures data of different components and calculated *NLPI* for mixed-mode dryer operated in forced convection (Singh and Kumar 2012a)

Absorbed thermal energy flux levels (W/m^2)	Ambient air, $\bar{T}_{am}$, (°C)	Air heater			Drying chamber			No-load performance index (*NLPI*)
		Plate, $\bar{T}_{cp}$, (°C)	Hot air, $\bar{T}_{cf}$, (°C)	Glass cover, $\bar{T}_{cg}$, (°C)	Plate, $\bar{T}_{dp}$, (°C)	Hot air, $\bar{T}_{df}$, (°C)	Glass cover,$\bar{T}_{dg}$, (°C)	
(a) Airflow rate: 0.009 kg/s								
250	33.01	54.89	38.75	37.65	59.41	45.97	41.08	1.053
300	33.01	56.60	39.73	38.88	62.59	46.94	42.05	1.062
450	31.05	61.49	41.93	40.10	73.11	48.90	44.74	1.086
600	31.79	72.25	46.33	42.30	84.60	55.01	48.90	1.088
750	31.05	77.87	46.70	43.64	93.40	58.68	51.10	1.094
800	32.27	81.30	49.02	44.01	99.51	62.35	53.06	1.085
(b) Airflow rate: 0.017 kg/s								
300	32.76	54.40	36.31	34.72	51.35	42.05	38.88	1.478
450	33.74	57.46	37.65	36.92	64.30	46.46	41.57	1.486
600	32.52	62.35	39.24	37.90	69.44	47.19	42.30	1.527
750	33.50	67.97	41.20	39.24	76.77	50.61	45.23	1.534
800	34.72	70.66	42.42	40.71	80.93	53.79	46.46	1.451
(c) Airflow rate: 0.026 kg/s								
250	29.34	40.83	31.91	30.93	45.97	35.45	33.01	1.604
300	33.01	44.62	34.47	33.01	52.57	40.34	36.68	1.603
450	32.27	51.83	35.45	33.99	55.01	41.57	37.90	1.633
600	31.30	57.34	36.68	35.09	59.66	42.79	39.61	1.619
750	32.76	61.25	38.63	36.19	66.99	46.21	42.30	1.616
800	34.47	65.40	40.46	39.98	70.42	49.39	43.52	1.536

Table 5 Observational temperatures data of different components and calculated *NLPI* for indirect dryer operated in forced convection (Singh and Kumar 2012a)

Absorbed thermal energy flux levels (W/m^2)	Ambient air, T_{am}^{-}, (°C)	Air heater			Drying chamber			No-load performance index (*NLPI*)
		Plate, T_{cp}^{-}, (°C)	Hot air, T_{cf}^{-}, (°C)	Glass cover, T_{cg}^{-}, (°C)	Plate, T_{dp}^{-}, (°C)	Hot air, T_{df}^{-} (°C)	Insulated cover, T_{dg}^{-}, (°C)	
(a) Airflow rate: 0.009 kg/s								
300	29.34	54.16	36.43	35.82	42.05	41.07	39.12	0.918
450	30.07	62.47	38.26	37.65	45.48	44.98	44.01	0.900
600	30.07	69.07	39.85	38.88	48.66	48.04	46.94	0.899
750	29.34	75.06	40.71	40.10	50.86	49.62	48.17	0.959
800	30.07	78.73	42.54	41.69	53.30	52.06	50.61	0.939
(b) Airflow rate: 0.017 kg/s								
300	28.85	47.19	32.64	31.79	36.19	35.32	34.72	1.323
450	28.61	52.32	33.13	32.76	37.41	36.67	36.19	1.331
600	28.61	57.95	34.60	34.23	39.12	38.37	37.65	1.375
750	29.58	63.94	37.16	36.06	42.30	41.17	40.59	1.388
810	30.81	65.65	38.63	37.65	46.46	43.38	42.30	1.349
(c) Airflow rate: 0.026 kg/s								
300	27.63	43.15	30.93	32.15	34.96	33.00	32.27	1.432
450	26.90	47.31	31.54	30.93	34.72	35.72	32.76	1.432
600	27.87	51.96	32.52	32.03	35.70	35.30	33.74	1.486
750	27.87	55.50	33.25	32.52	38.63	36.67	35.21	1.518
800	30.07	59.78	36.31	35.70	40.34	39.36	36.19	1.509

The analysis shows lower *SE* values ranging from 0.005 to 0.019 for all solar dryer designs investigated which demonstrate respectable consistency in *NLPI*. Moreover, *E* is estimated to be 95% which indicates insignificant variation in *NLPI* values about mean value for all dryers under different test conditions (Singh and Kumar 2012a). Results from statistical analysis represent more or less independence of *NLPI* on climatic variables (i.e., absorbed energy flux and ambient air temperature); therefore, *NLPI* can be recommended as an index for equitable comparison between the solar dryer's designs.

3.2 *Dryer Performance Index (*DPI*)*

For an even hand performance comparison of solar dryers, the performance index should not only be independent of operational conditions but also of food product characteristics specifically initial moisture content, amount of product to be dried, product shape and size, etc. This section describes a new concept of such a testing procedure as formulated and proposed by Singh and Kumar (2012b).

3.2.1 Experimental Methodology

This performance test is based on the condition when solar dryers are loaded with the food product to be dried. In the investigation, cylindrical pieces of potatoes are used as a test food product. The cylindrical samples of length 50 mm and varied thickness are dried as a thin layer on a stainless steel wire mesh tray inside the drying chamber of the solar dryer. The mixed-mode dryer is chosen since it performs the best in terms of drying time (Zaman and Bala 1989; Simate 2003).

Sixteen indoor experiments are conducted over a wide range of drying process-dependent variables until the final moisture content of food product reached 12% (w.b.). The investigated variables and the baseline values are given in Table 6.

3.2.2 Characteristic Drying Curve

In a thin layer drying modeling, experimental dimensionless moisture content (ϕ) of the food product and drying time (t) generates a drying characteristic curve

Table 6 List of variables investigated in the experiments (Singh and Kumar 2012b)

Variable	Investigated value	Baseline value
Absorbed thermal energy flux (W/m^2)	150, 350, 550, 750	750
Airflow rate (kg/s)	0.009, 0.011, 0.017, 0.022	0.011
Loading density (kg/m^2)	1.08, 2.16, 3.24, 4.33	2.16
Sample thickness (mm)	5, 8, 11, 18	8

(Dincer and Dost 1996) for a particular combination of the food product and the dryer system which is expressed as:

$$\phi = \frac{M_t}{M_o} = k_o \exp(-k \cdot t) \tag{17}$$

where t is the drying time and k is the drying constant which indicates the drying capability of that food product-dryer system. In addition, it depends on many drying process variables such as operational conditions, food product characteristics, and dryer design resulting in a different value for each set of the process variable. The impact of different process-dependent variables (Sect. 2.1 of chapter "Fundamental Mathematical Relations of Solar Drying Systems") on the dimensionless moisture content of food product (potato) can be seen in Figs. 5, 6, 7, and 8.

Due to the well-established correlation between k and t, performance comparison of different dryer designs based on k determination cannot be justified. However, the product of drying constant and time, i.e., $(k.\ t)$, is found to be more or less constant for each test condition and, therefore, can be defined in terms of a new dimensionless parameter as drying process time (τ):

$$k_1 \cdot t_1 = k_2 \cdot t_2 = k_3 \cdot t_3 = \ldots = k_i \cdot t_i = \tau \tag{18}$$

where $i = 1, 2, 3 \ldots 16$ represents different test conditions studied as described in Sect. 2.1.

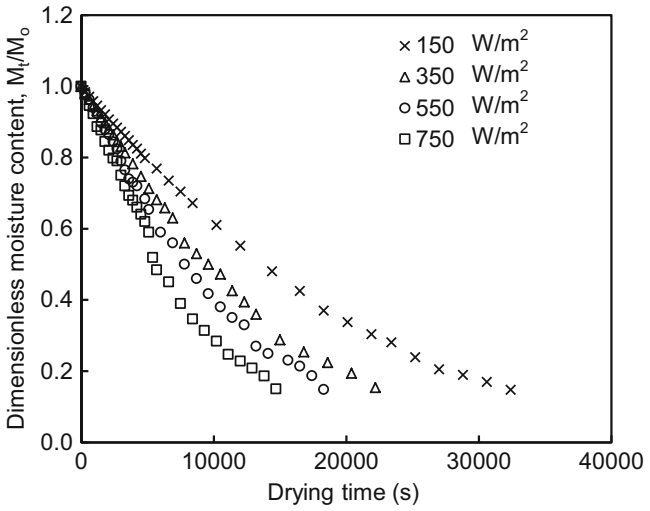

Fig. 5 Variation of dimensionless moisture content with respect to drying time at different absorbed energy flux level (Singh and Kumar 2012b)

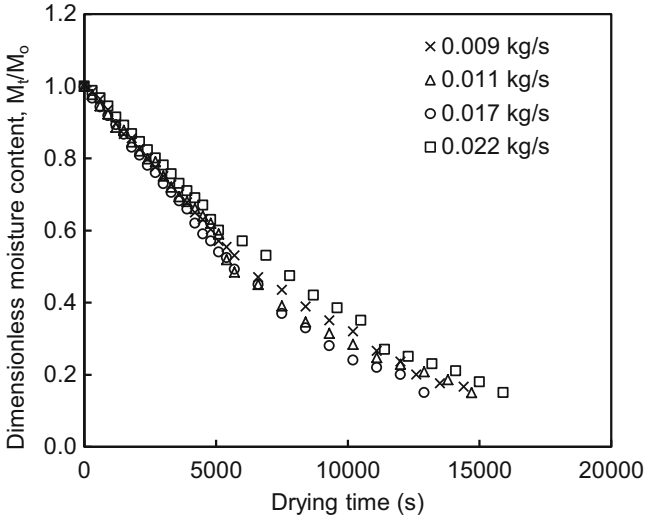

Fig. 6 Variation of dimensionless moisture content with respect to drying time at different airflow rates (Singh and Kumar 2012b)

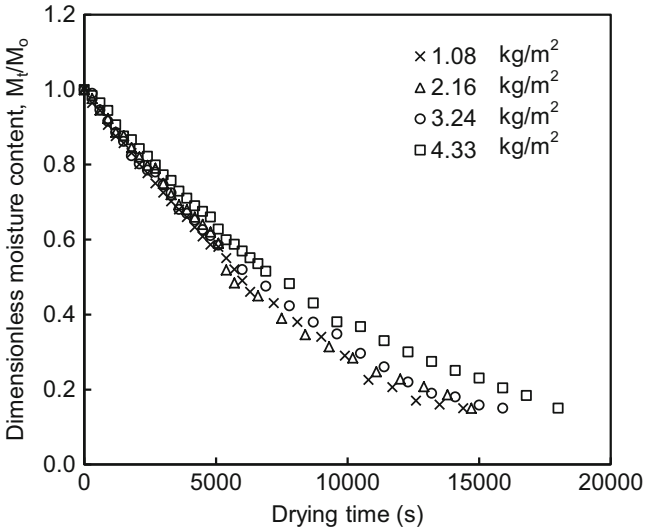

Fig. 7 Variation of dimensionless moisture content with respect to drying time at different sample loading density (Singh and Kumar 2012b)

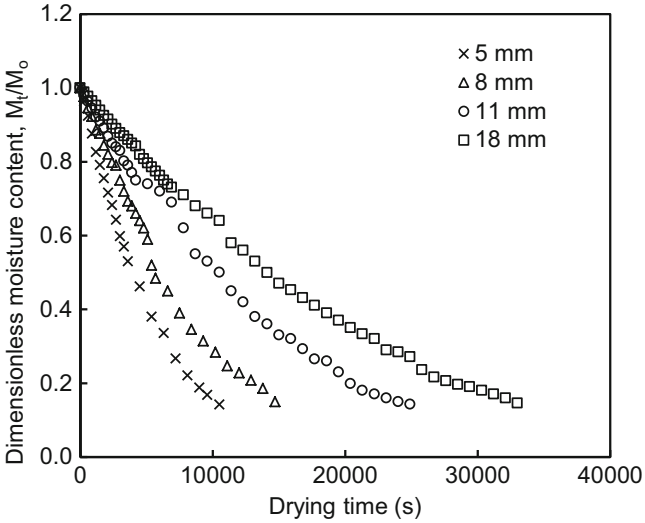

Fig. 8 Variation of dimensionless moisture content with respect to drying time at different sample thickness (Singh and Kumar 2012b)

To incorporate the impact of different safe storage moisture content values of food products in the solar dryer performance, two dimensionless parameters, ϕ and τ, are plotted individually by modifying the coordinate system from classical $\phi = f(t)$ to the universal dimensionless system $\phi = f(\tau)$ for each test condition. Figures 9, 10, 11 and 12 show the generalized curve for a wide range of absorbed thermal energy flux levels, airflow rate, food product loading density, and size, respectively. The single curve obtained from fitting of experimental data is known as *generalized drying characteristic curve* of a given dryer design. The overlapped normalized moisture content-drying time data in each generalized drying curve of the investigated variable signifies its unconventional independence from that specific test variable.

Following the similar methodology, the normalized moisture content-drying time data for each testing variable representing 16 drying test conditions is plotted and analyzed in Fig. 13. Significant overlapping of the 16 drying test data further demonstrates that the proposed concept can effectively evaluate the performance of a solar dryer design irrespective of different testing conditions. However, to achieve an objective of determining a single parameter that characterizes the effectiveness of a dryer system in a rational manner, the generalized experimental data shown in Figs. 9, 10, 11, 12 and 13 is individually regressed and expressed as:

$$\phi = \frac{M_t}{M_o} = \exp\left(-DPI \cdot \tau\right) \tag{19}$$

where *DPI* is referred as *dryer performance index* representing the drying capability of a given solar dryer. *DPI* is a dimensionless parameter which is a measure of the

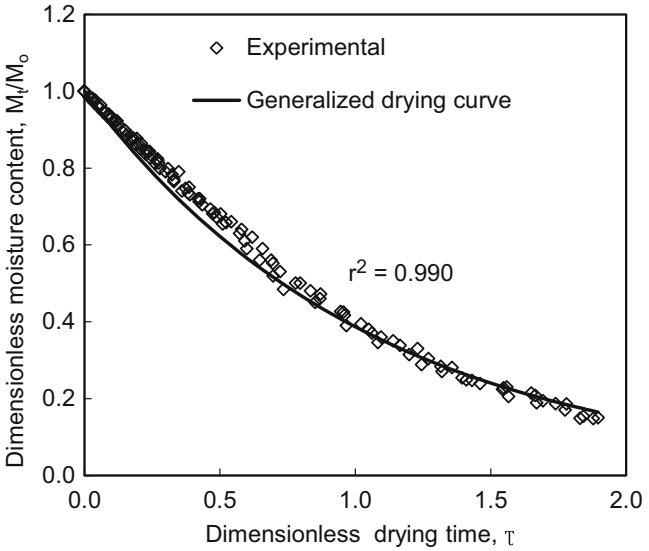

Fig. 9 Generalized drying characteristic curve for different absorbed thermal energy flux level (Singh and Kumar 2012b)

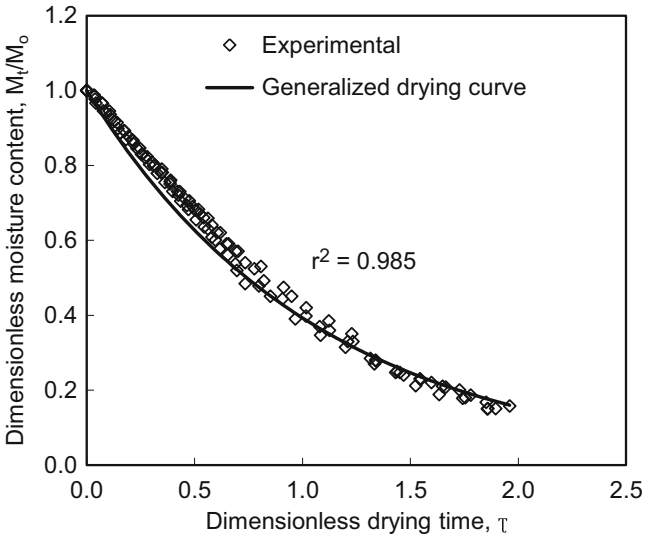

Fig. 10 Generalized drying characteristic curve for different airflow rates (Singh and Kumar 2012b)

effectiveness of a given dryer system and is solely dependent on the characteristic design of the dryer. In fact, a higher value of *DPI* indicating more efficient system design is always desirable.

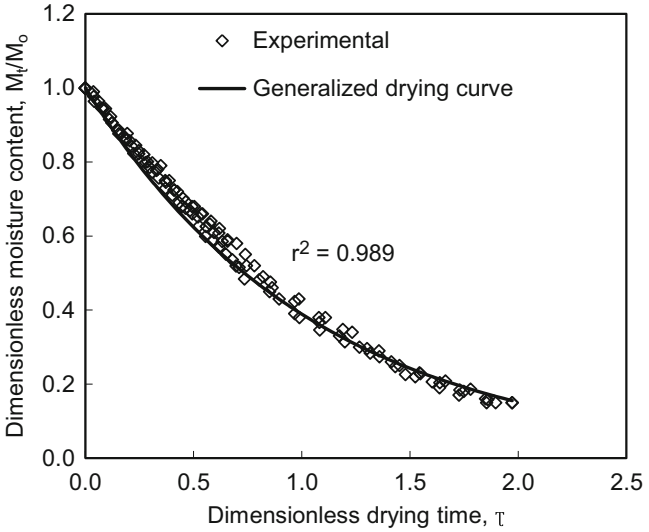

Fig. 11 Generalized drying characteristic curve for different values of loading density (Singh and Kumar 2012b)

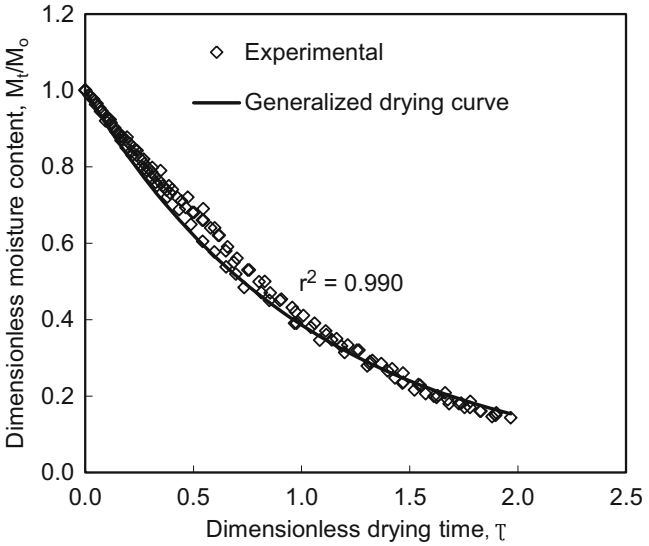

Fig. 12 Generalized drying characteristic curve for different sample thickness (Singh and Kumar 2012b)

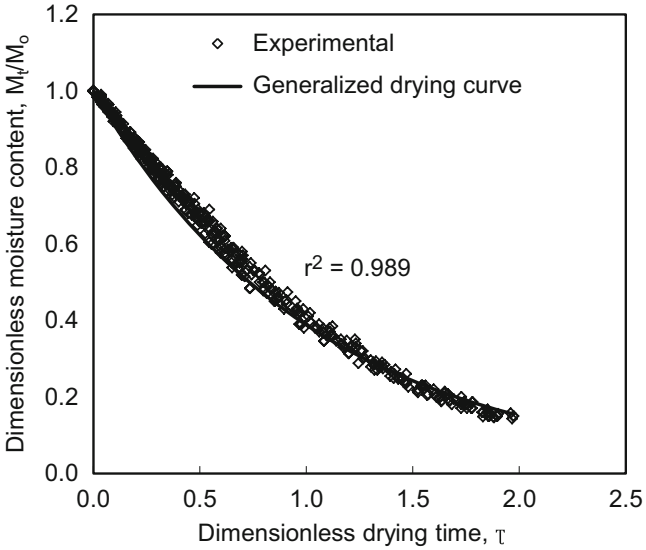

Fig. 13 Generalized drying characteristic curve for all drying process variables (Singh and Kumar 2012b)

3.2.3 Results

Table 7 shows the *DPI* values calculated from indoor experiments on the mixed-mode solar dryer at different drying process variables and final safe storage moisture contents. The values of *DPI* are found extremely consistent and invariable for a wide range of process variables studied with respect to the final safe storage moisture content of dried food product (Singh and Kumar 2012b).

3.2.4 Validation of the Test Method

Experimental Validation

The proposed testing method is validated by comparing the *DPI* results of indoor experimentation with the results in real climatic conditions. For the purpose, outdoor experiments with a variety of food products from vegetables, fruits, and grains such as potato, banana, and wheat on typical sunny days of March are performed on mixed-mode and cabinet solar dryers to test the reliability and applicability of the proposed method. A set of experimental parameters such as potato samples of length 50 mm and thickness 8.0 mm, circular slices of freshly ripe bananas of thickness 8.0 ± 2.0 mm and diameter 30.0 ± 2.0 mm, and 100 g wheat sample soaked at 30 °C for 8 h in a constant temperature water bath are used. The samples of potato, banana, and rehydrated wheat of weight 200, 200, and 142 g and initial moisture contents of 81.5, 75.5, and 33.61% (w.b.), respectively, are used.

Table 7 Calculated *DPI* of the mixed-mode solar dryer for different drying variables (Singh and Kumar 2012b)

Variable	No. of tests	Range of values	Final moisture content =12% Dryer performance index (*DPI*)	Final moisture content = 19% Dryer performance index (*DPI*)
Absorbed thermal energy flux (W/m^2)	4	150–750	0.949	0.944
Airflow rate (kg/s)	4	0.009–0.022	0.934	0.923
Loading density (kg/m^2)	4	1.08–4.33	0.944	0.943
Sample thickness (mm)	4	5–18	0.952	0.928
All variables are taken together	16	All ranges of variables	0.945	0.934

The *DPI* for each test is calculated following the proposed test method described above in Sect. 2.2 of chapter "Fundamental Mathematical Relations of Solar Drying Systems" using Eq. (19).

The comparative *DPI* results of mixed-mode and cabinet solar dryer operated under real outdoor test conditions are given in Table 8. Results show the consistent *DPI* values are obtained for different food products investigated (potato, banana, and wheat) irrespective of dryer design tested, indicating its independent nature from food product characteristics (Singh and Kumar 2012b). However, for the same food product, mixed-mode solar dryer exhibits higher *DPI* values as compared to that of cabinet solar dryer. The reason is attributed to effective heat transfer in the mixed-mode dryer because of its better design features. This close consistency in *DPI* results for different operating conditions and food product characteristics implies that the proposed parameter can be employed as the performance index to assess the solar dryer performance on an equitable basis.

Statistical Analysis

The accuracy and the prediction capability of the testing method given by Eq. (19) are determined by statistical error analysis (Singh and Kumar 2012b). The most commonly used parameters, namely, root mean square error (*RMSE*), standard error of mean (*SE),* and correlation coefficient (*R*), are defined in Eqs. 20, 21, 22 and 23 and are evaluated for dimensionless moisture content of food product, ϕ:

$$\mathrm{RMSE} = \left[\frac{1}{N}\sum_{i=1}^{N}\left(\phi_{\mathrm{exp},i} - \phi_{\mathrm{cal},i}\right)^2\right]^{1/2} \tag{20}$$

Table 8 Comparison of *DPI* values of different dryer designs for a variety of food products in real climatic conditions (Singh and Kumar 2012b)

Range of ambient temperature (°C)	Range of solar radiation intensity (W/m^2)	Food product	Dryer performance index, *DPI*	
			Mixed-mode dryer	Cabinet dryer
24.5–29.8	627.9–820.3	Potato	0.962	0.893
24.9–33.4	539.7–813.2	Banana	0.972	--*--
30.8–33.5	652.6–827.5	Wheat	0.975	0.905

$$\mathrm{SD} = \sqrt{\frac{\sum_{i=1}^{N}\left(\phi_{\mathrm{exp},i} - \phi_{\mathrm{cal},i}\right)^2}{N-1}} \tag{21}$$

$$\mathrm{SE} = \frac{SD}{\sqrt{N}} \tag{22}$$

$$R = \frac{\mathrm{N}\sum_{i=1}^{N}\phi_{\mathrm{exp},i}\phi_{\mathrm{cal},i} - \left(\sum_{i=1}^{N}\phi_{\mathrm{exp},i}\right)\left(\sum_{i=1}^{N}\phi_{\mathrm{cal},i}\right)}{\left[N\sum_{i=1}^{N}\left(\phi_{\mathrm{exp},i}\right)^2 - \left(\sum_{i=1}^{N}\phi_{\mathrm{exp},i}\right)^2\right]^{1/2}\left[N\sum_{i=1}^{N}\left(\phi_{\mathrm{cal},i}\right)^2 - \left(\sum_{i=1}^{N}\phi_{\mathrm{cal},i}\right)^2\right]^{1/2}} \tag{23}$$

where $\phi_{\mathrm{exp},i}$ and $\phi_{\mathrm{cal},i}$ are experimental and calculated dimensionless moisture content for the ith observation, respectively. The computed *DPI* value of each generalized curve in Figs. 9, 10, 11, 12 and 13 is used to calculate dimensionless moisture content. Equations 20, 21, 22, and 23 are then used to evaluate RMSE, SE, and R between experimental and calculated dimensionless moisture contents for safe storage moisture content values of 12 and 19%. The values of RMSE and SE are found in the range of 0.0303–0.0367 and 0.0014–0.0033 for final moisture content of 12% and 0.0259–0.0311 and 0.0013–0.0030 for 19%, respectively. The values of correlation coefficient (R) is found greater than 0.97 which further demonstrate that the proposed *DPI* parameter can accurately provide dimensionless moisture content data and therefore can be utilized to predict the solar dryer performance.

4 Conclusion

This chapter reviewed and addressed the thermal test methods that are available to evaluate the most common dryer designs used for solar drying. The need of developing a test methodology to predict and improve the thermal performance is clarified in the chapter. To be able to compare the different dryer designs, two separate test parameters, namely, *NLPI* and *DPI*, based on loading condition are

presented. The parameters are mathematically deduced and validated experimentally to confirm the reliability of the method. Moreover, the results from the test methods inferred ability of both parameters to demonstrate how well the solar dryer design will work in a given operating conditions. Hence, they can be treated a useful tool by design engineers and manufacturers in developing a solar dryer for different applications of required thermal performance.

References

Amer EH, Nayak JK, Sharma GK (1997) Transient test methods for flat-plate collectors: review and experimental evaluation. Sol Energy 60(5):229–243

Amer EH, Jadeja P, Nayak JK, Sharma GK (1998) Comparison of two dynamic test methods for solar flat-plate collectors. Energy Convers Manag 39(3/4):285–293

Bala BK, Woods JL (1994) Simulation of the indirect natural convection solar drying of rough rice. Sol Energy 53:259–266

Bena B, Fuller RJ (2002) Natural convection solar dryer with biomass back-up heater. Sol Energy 72(1):75–83

Bhirud N, Tandale MS (2006) Field evaluation of a fixed-focus concentrators for industrial oven. In: Proceedings of national conference on advances in energy research, December, 2006, IIT-Bombay (India), pp 364–370

Boughali S, Benmoussa H, Bouchekima B, Mennouche DH, Bouguettaia H, Bechki D (2009) Crop drying by indirect active hybrid solar - electrical dryer in the eastern Algerian Septentrional Sahara. Sol Energy 83:2223–2232

Chan Y, Dyah N, Abdullah K (2015) Performance of a recirculation type integrated collector drying chamber (ICDC) solar dryer. Energy Procedia 68:53–59

Condori M, Echazu R, Saravia L (2001) Solar drying of sweet pepper and garlic using the tunnel greenhouse drier. Renew Energy 22:447–460

Dincer I, Dost S (1996) A modeling study for moisture diffusivities and moisture transfer coefficients in drying of solid objects. Int J Energy Res 20:531–539

El-Sebaii AA, Aboul-Enein S, Ramadan MRI, El-Gohary HG (2002) Experimental investigation of an indirect type natural convection solar dryer. Energy Convers Manag 43(16):2251–2266

Forson FK, Nazha MAA, Rajakaruna H (2007) Modeling and experimental studies on a mixed-mode natural convection solar crop dryer. Sol Energy 81(3):346–357

Grupp M, Bergler, Maria O, Schroder G 1995 Comparative tests of solar dryers. Technology Demonstration Center (TDC) Serial Report 2/95, Plataforma Solar de Almeria (PSA), Spain

Jain D, Tewari P (2015) Performance of indirect through pass natural convective solar crop dryer with phase change thermal energy storage. Renew Energy 80:244–250

Jannot Y, Coulibaly Y (1998) The “evaporative capacity” as a performance index for a solar-drier air-heater. Sol Energy 63(6):387–391

Leon MA, Kumar S, Bhattacharya SC (2002) A comprehensive procedure for performance evaluation of solar food dryers. Renew Sust Energ Rev 6:367–393

Mullick SC, Kandpal TC, Saxena AK (1987) Thermal test procedure for box-type solar cooker. Sol Energy 39(4):353–360

Mullick SC, Kandpal TC, Kumar S (1991) Thermal test procedure for a parabolloid concentrator solar cooker. Sol Energy 46(3):139–144

Murthy MVR (2009) A review of new technologies, models and experimental investigations of solar driers. Renew Sust Energ Rev 13:835–844

Nayak JK, Amer EH (2000) Experimental and theoretical evaluation of dynamic test procedures for solar flat-plate collectors. Sol Energy 69(5):377–401

Pande PC, Thanvi KP (1991) Design and development of a solar dryer cum water heater. Energy Convers Manag 31(5):419–424
Senthilkumar S, Perumal K, Srinivasan PSS (2009) Optical and thermal performance of a three-dimensional compound parabolic concentrator for spherical absorber. Sadhana 34(3):369–380
Simate IN (2003) Optimization of mixed mode and indirect mode natural convection solar dryers. Renew Energy 28(3):435–453
Singh S, Kumar S (2012a) Testing method for thermal performance based rating of various solar dryer designs. Sol Energy 86(1):87–98
Singh S, Kumar S (2012b) New approach for thermal testing of solar dryer: development of generalized drying characteristic curve. Sol Energy 86(7):1981–1991
Singh PP, Singh S, Dhaliwal SS (2006) Multi-shelf domestic solar dryer. Energy Convers Manag 47:1799–1815
Sodha MS, Chandra R (1994) Solar drying systems and their testing procedures: a review. Energy Convers Manag 35(3):219–267
Soltau H (1992) Testing the thermal performance of uncovered solar collectors. Sol Energy 49 (4):263–272
Sreekumar A, Manikantan PE, Vijayakumar KP (2008) Performance of indirect solar cabinet dryer. Energy Convers Manag 49:1388–1395
Stiling J, Li S, Stroeve P, Thompson J, Mjawa B, Kornbluth K, Barrett DM (2012) Performance evaluation of an enhanced fruit solar dryer using concentrating panels. Energy Sustain Dev 16:224–230
Vaishya JS, Tripathi TC, Singh D, Bhawalkar RH, Hegde MS (1985) A hot box solar cooker performance analysis and testing. Energy Convers Manag 25(3):373–379
Zaman MA, Bala BK (1989) Thin layer solar drying of rough rice. Sol Energy 42:167–171

Exergy Analysis of Solar Dryers

Anil Kumar, Saurabh Ranjan, Om Prakash, and Ashish Shukla

Abstract In order to find out the energy interactions and thermodynamic behaviour of drying air throughout a drying chamber, the energy and exergy analysis of the drying process needs to be informed. Exergy of a solar dryer is the maximum useful work possible during a drying process that brings the dryer into equilibrium with a heat reservoir. The exergy method can help further in maximizing efficient energy resource use because it is applied at component level and enables to determine losses for their magnitude at the point of origin. By using exergy method, it is possible to correct existing inefficiencies at its sources and design more efficient thermal system, and in the current case, it is solar dryer. Increased efficiency can often contribute in an environmentally acceptable way by the direct reduction of irreversibility that might otherwise have occurred.

Keywords Solar dryer • Exergy analysis • Exergetic efficiency • Energy analysis

1 Introduction

Modern world sees the process of change and innovation in technology in order to improve the standard of living. Amid the development, still today, hunger is a challenge for mankind. In India, 10 million people die every year of hunger or

A. Kumar
Department of Energy (Energy Centre), Maulana Azad National Institute of Technology, Bhopal 462003, Madhya Pradesh, India

S. Ranjan
Centre for Energy Engineering, Central University of Jharkhand, Ranchi 835205, India

O. Prakash (✉)
Department of Mechanical Engineering, Birla Institute of Technology, Mesra, Ranchi 835215, India
e-mail: omprakash@bitmesra.ac.in

A. Shukla
School of Energy, Construction and Environment, Coventry University, Coventry CV1 2HF, UK

© Springer Nature Singapore Pte Ltd. 2017

O. Prakash, A. Kumar (eds.), *Solar Drying Technology*, Green Energy and Technology, DOI 10.1007/978-981-10-3833-4_8

related disease, and over 20 crore people sleep hungry every night. According to the United Nations, about 21,000 people in the world die everyday of hunger and hunger-related disease. Every nation witnesses the development, but many of us died due to food scarcity, and on the other side, tonnes of food are wasted due to poor preservation (Prakash 2015). The Swedish Institute for Food and Biotechnology (SIK) published a report on 2011 that global food loss per year is 1.3 billion tonnes which is one third of the total edible food produced. In developing countries, the 40% food losses occur during postharvest period. Drying is an effective method for food preservation which protects food and inhibits bacteria and yeasts through removal of water (Gustavsson et al. 2011). High-energy input required for drying process of high-moisture content products such as oilseed, tomato, meats, etc. Over 2000 kJ/kg heat required to provide latent heat of evaporation for removal of moisture. For example, if a drying process required evaporation of 1 kg s^{-1}, approximately 2400 kW of energy is required to conduct the drying process. Electrical heaters required over 3 kW of primary energy for supplying 1Kw of evaporation (Kemp 2012). In present scenario, engineers and researcher focus on to design and manufacture efficient systems or devices in order to harness renewable energy for drying products. Solar energy is clean, abundant and environmental friendly energy resource, and it is gaining more importance in global platform regarding climate change. Fossil fuel is quite responsible for greenhouse gas emission from its mining to combustion process (Saidur et al. 2012). Solar dryer is an efficient device for drying of agricultural products and its allied material. Non-polluting character of solar energy, its energy effectiveness, the quality of solar dried products and its economy all justify the adoption and application of solar dryer for drying of fruits, vegetables and spices (Prakash et al. 2016). In order to find out the energy interactions and thermodynamic behaviour of drying air throughout a drying chamber, the energy and exergy analyses of the drying process should be performed. The exergy method can help further the goal of more efficient energy resource use, because it enables the locations, types and true magnitudes of losses to be determined. As a result, exergy analyses can reveal where and by how much it is possible to design more efficient thermal systems by reducing the sources of existing inefficiencies (Kalogirou et al. 2016). Increased efficiency can often contribute in an environmentally acceptable way by the direct reduction of irreversibility where exergy is destroyed that might otherwise have occurred. This makes the concept of exergy one of the most powerful tools to provide optimum drying conditions. The thermal efficiencies of different design of solar dryer are governed by the first law of thermodynamics. The first law of thermodynamics states that energy can neither be created nor destroyed, although energy can be changed from one form to another. It follows the principle of conservation of energy. Details regarding non-possibility of conversion of heat into mechanical work in any thermodynamic process are not given by the first law of thermodynamics (FLT). It gives quantitative study of losses in solar drying system. However,

energy-based analysis lags for providing some information, or it has many limitations such as (Dincer and Rosen 2007):

- Energy losses do not mean actual losses which persist for required product's generation.
- Incomplete information of storage duration.
- Energy analysis cannot deal complete system performance approach to ideal.
- It does not provide information about the reversibility or irreversibility aspects of thermodynamics process.

Exergy means available energy or heat availability in system. Exergy analysis is very important for any thermal system and alternative of comparing thermal system. It helps in reducing losses and achieving the maximum resources utilization and economic benefits. These analyses are based on the second law of thermodynamics. Exergy utilizes the second law of thermodynamics (SLT) balance for the analysis and design of thermal system. Entropy is defined by SLT as a distributed state of energy not available for transformation into work. It overcomes the limitation of an energy-based analysis (Dincer and Rosen 2007). In solar dryer, the transfer of exergy occurs along with the flow of mass and thermal interaction. Engineers/researcher gets clear view of the quantitative and qualitative assessment of losses in exergetic analysis that provides a lucid view regarding the losses of energy in a system. In fire, the exothermic reaction takes place between fuel and oxygen that gives heat and waste product. Heat can be utilized for many purposes but what about waste. Waste product should have potential for usefulness or potential to do work. Exergy is a quantification of the potential for usefulness. It is somehow like entropy which is not conserved due to irreversibility. Exergy is the maximum theoretical work that a body can do before coming to equilibrium with its surroundings. In order to perform exergy analysis, we need to define an exergy reference, i.e. environment or surrounding. It means large enough of heat transfer in system without making any measurable difference in surrounding such as temperature, pressure, etc. The dead state is reference temperature and pressure. The dead state has no potential of doing work (Querol et al. 2011; Querol 2013).

1.1 Some Important Facts About Exergy

Here, the concept of exergy is given in the following points that would provide basic idea about exergy:

(i) Exergy is a measure of the departure of state of the system from that of the environment.
(ii) The value of exergy cannot be negative. It is zero at dead state.
(iii) Exergy is not be conserved but is destroyed by irreversibility.

Table 1 Difference between energy and exergy

Energy	Exergy
Depends on characteristics of matter or flow of energy whereas independent of surrounding characteristics	Dependent on characteristics of flow of energy as well as environment
Can neither be demolished nor created	Can neither be demolished nor created only in reversible process; destroyed in irreversible process
Conserved for all process	Not conserved for real process and conserved for only in reversible process
Non-zero values when in equilibrium with environment	Zero at dead state
Appears in different forms such as kinetic energy, potential energy, work, heat	Apparent in different forms such as kinetic energy, potential energy, work, thermal energy
Measure in quantity only	Measure in quantity as well as quality
It exists as a simple mechanism	It exists as a lengthy and complex mechanism

(iv) Exergy can be viewed as either the maximum theoretical work obtainable from an overall system and environment to bring the system to the dead state.
(v) A system at the dead state is at both thermal and mechanical equilibrium with the environment. Mechanical equilibrium happens when pressure no longer changes, so no forces are at work (Panwar et al. 2012).

1.2 Difference Between Energy and Exergy

Table 1 helps to eliminate confusion with energy-based analysis and exergy-based analysis. The FLT deals with energy utilization on quantity basis, and SLT deals with exergy which refers to the quality of energy.

2 The First Law Analysis: Energy Utilization

Generally solar drying process was assumed as a steady-state flow process. The first law analysis, i.e. energy analysis of solar dryer, was performed to determine the best utilization of solar energy in solar dryer. There are three balance equations such as mass, energy and exergy balance equation needed to find out the heat supplied to system, the rate of destruction of available energy and energy and exergy efficiencies. The mass conservation of moisture can be written as (Darvishi et al. 2014)

$$\sum m_{\text{in}} = \sum m_{\text{out}} \tag{1}$$

$$m_{\text{initial}} = m_{\text{evw}} + m_p \tag{2}$$

The energy conservation equation can be written as in Eq. 3:

$$\sum E_{\text{in}} = \sum E_{\text{out}} \tag{3}$$

The Eq. 3 can be elaborated as given in Eq. 4:

$$\left(mC_p \times T\right)_{\text{in}} + P \times t = \left(mC_p \times T\right)_p + m_{\text{evw}} \iota_{hp} + E_L \tag{4}$$

Here, the total energy supplied to solar dryer will be equal to the energy required in drying processes, water evaporation and energy loss.

Latent heat and specific heat capacity of drying product were calculated on the base of Eq. 5 and Eq. 6, respectively (Darvishi et al. 2014):

$$\frac{\iota_{hp}}{\iota_{fw}} = 1 + 23\exp(-0.4\text{M}) \tag{5}$$

$$C_p = 1.675 + 2.5W_{ws} \tag{6}$$

The specific energy loss is obtained by Eq. 7:

$$E_L = \left(1 - \eta_{\text{energy}}\right) \times \frac{P \times t}{m_{\text{evw}}} \tag{7}$$

3 The Second Law Analysis: Exergetic Analysis

Exergy analysis followed the second law of thermodynamics. It is not possible to convert heat completely into work. Some part of the heat supplied always rejected to sink. The amount of thermal energy which is convertible to work out of total input energy is called available energy or exergy. The energy that rejects heat to surrounding is called unavailable energy (Tiwari et al. 2009). In exergy analysis, the total exergy inflow, the total exergy outflow and the exergy losses of the drying chamber were estimated. Exergy analysis of a system involves some basic process such as to determine exergy values at steady-state regime, exergy variation during the thermodynamic process, etc. The total exergy of a system is physical exergy (E_P), chemical exergy (E_C), kinetic exergy (E_K) and potential exergy (E_{PT}) (Celma and Cuadros 2009):

- Physical exergy (E_P): Variation in temperature and pressure of the system reference from surrounding.
- Chemical exergy (E_C): Change in chemical composition of the system reference from surrounding.

- Kinetic exergy (E_K): It is due to system velocity reference to surrounding.
- Potential exergy (E_{PT}): It is due to system height reference to surrounding.

Total exergy form system in general equation is written as

$$Ex_T = Ex_P + Ex_C + Ex_K + Ex_{PT} \tag{8}$$

By expanding above equation,

$$Ex_T = (U - U_0) + P_0(V - V_0) - T_0(S - S_0) + \frac{1}{2}mv^2 + mgz + \left(E^R + E^N\right) \tag{9}$$

where '0' denotes the thermodynamic environment and E^R and E^N represent the reactive and non-reactive exergy. $P_0(V - V_0)$ works pressure at dead state, and $T_0(S - S_0)$ means reversible heat transfer at temperature of dead state. There is no value difference in kinetic energy and potential energy because of absence of dead state of velocity and height. The second law of thermodynamics uses an exergy balance for the analysis and the design of thermal systems. In the analysis of many systems, some terms in Eq. 9 may be neglected. Equation 9 also operated in the condition in which kinetic terms and gravitational terms are ignored. In addition, if pressure change in the system is also neglected when $V = V_0$, the Eq. 9 will be written as

$$\dot{E}x = \dot{m}_{da}\,\overleftarrow{c_p}\left\{(T - T_0) - T_0 \ln\frac{T}{T_0}\right. \tag{10}$$

where $\overleftarrow{c_p}$ is average drying air's mean specific heat.

Balance equation of exergy is written as

$$\begin{aligned}\text{Exergy} = {} & \text{internal energy} - \text{entropy} + \text{work} + \text{momentum} + \text{gravity} \\ & + \text{radiation emission}\end{aligned} \tag{11}$$

Exergy balance equation has the form of

$$\sum Ex_{\text{in}} = \sum Ex_{\text{out}} + \sum Ex_{\text{dest}} + \sum Ex_{\text{loss}} - \sum Ex_{\text{evap}} \tag{12}$$

Inflow exergy to dryer, outflow exergy from dryer and exergy flow due to evaporation and exergy loss in dryer can be expressed in Eqs. 13, 14, 15 and 16, respectively (Erbay and Icier 2011). Figure 1 shows the schematic diagram of the flow of the energy in the drying chamber of the solar dryer.

$$Ex_{\text{in}} = m_{\text{air}}ex_1 + m_{\text{product}}\left(ex_{\text{product}}\right)_2 + (m_{\text{water}})_2(ex_{\text{water}})_2 \tag{13}$$

$$Ex_{\text{out}} = m_{\text{air}}ex_3 + m_{\text{product}}\left(ex_{\text{product}}\right)_4 + (m_{\text{water}})_4(ex_{\text{water}})_4 \tag{14}$$

$$Ex_{\text{evap}} = \left(1 - \frac{T_0}{T_{\text{product,surface}}}\right)Q_{\text{evap}} \tag{15}$$

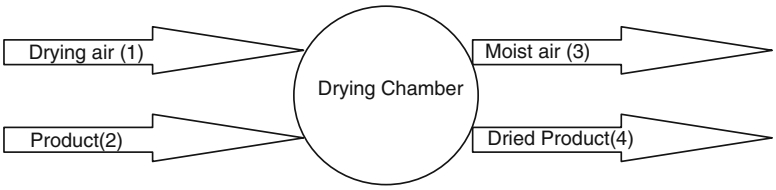

Fig. 1 Schematic diagram of the energy flow from the drying chamber

$$Ex_L = \left(1 - \frac{T_0}{T_{\text{boundary}}}\right) Q_L \tag{16}$$

The specific exergy for input and output terms at different points can be obtained by these following Eqs. 17, 18, 19 and 20. Equation 17 is for drying air, Eq. 18 is for moist air, Eq. 19 is for product (material used for drying) and Eq. 20 is for moisture content (Erbay and Icier 2011):

$$\begin{aligned} ex_1 = \; & \left(Cp_{\text{air}} + \delta_1 Cp_{\text{vapour}}\right)(T_1 - T_0) \\ & - T_0 \left[\left(Cp_a + \delta_1 Cp_{\text{vapour}}\right) \ln\left(\frac{T_1}{T_0}\right) - \left(R_{\text{air}} + \phi_1 R_{\text{vapour}}\right) \ln\left(\frac{P_1}{P_0}\right)\right] \\ & + T_0 \left[\left(R_{\text{air}} + \delta_1 R_{\text{vapour}}\right) \ln\left(\frac{1 + 1,6078\phi_0}{1 + 1,6078\phi_1}\right) + 1,6078\delta_1 R_{\text{air}} \ln\left(\frac{\delta_1}{\delta_0}\right)\right] \end{aligned} \tag{17}$$

$$\begin{aligned} ex_3 = \; & \left(Cp_{\text{air}} + \delta_3 Cp_{\text{vapour}}\right)(T_3 - T_0) \\ & - T_0 \left[\left(Cp_{\text{air}} + \delta_3 Cp_{\text{vapour}}\right) \ln\left(\frac{T_3}{T_0}\right) - \left(R_{\text{air}} + \delta_3 R_{\text{vapour}}\right) \ln\left(\frac{P_3}{P_0}\right)\right] \\ & + T_0 \left[\left(R_{\text{air}} + \delta_3 R_{\text{vapour}}\right) \ln\left(\frac{1 + 1,6078\delta_0}{1 + 1,6078\delta_1}\right) + 1,6078\delta_3 R_{\text{air}} \ln\left(\frac{\delta_3}{\delta_0}\right)\right] \end{aligned} \tag{18}$$

$$ex_{\text{product}} = \left[h_{\text{product}}(T,P) - h_{\text{product}}(T_0,P_0)\right] - T_0\left[s_{\text{product}}(T,P) - s_{\text{product}}(T_0,P_0)\right] \tag{19}$$

$$\begin{aligned} ex_{\text{water}} = \; & \left[h_f(T) - h_{\text{gas}}(T_0)\right] + v_f\left[P - P_{\text{gas}}(T)\right] - T_0\left[s_f(T) - s_{\text{gas}}(T_0)\right] \\ & + T_0 R_{\text{vapour}} \ln\left[\frac{P_{\text{gas}}(T_0)}{x_{\text{vapour}} P_0}\right] \end{aligned} \tag{20}$$

The entropy change in dried product can be calculated as

$$s_{\text{product}} - s_0 = \left(\frac{C_{p,\text{product}} + C_{p,0}}{2}\right) \times \ln\frac{T_{\text{product}}}{T_0} \tag{21}$$

Exergy inflow and outflow for solar drying chamber can be calculated by Eqs. 22 and 23 based on inlet and outlet temperature of the drying chamber. The equation of exergy inflow and outflow for drying chamber under steady flow system are expressed as (Fudholi et al. 2014):

Exergy inflow for solar drying chamber (Fudholi et al. 2014):

$$\dot{E}x_{\text{dchi}} = m_{da}\overleftarrow{c}_{pda}\left[(T_{\text{dchi}} - T_0) - T_0 \ln\frac{T_{\text{dchi}}}{T_0}\right] \tag{22}$$

Exergy outlet for solar drying chamber (Fudholi et al. 2014):

$$\dot{E}x_{\text{dcho}} = m_{da}\overleftarrow{c}_{pda}\left[(T_{\text{dcho}} - T_0) - T_0 \ln\frac{T_{\text{dcho}}}{T_0}\right] \tag{23}$$

Exergy loss can be calculated by equation (Fudholi et al. 2014):

$$Ex_L = \dot{E}x_{\text{dchi}} - \dot{E}x_{\text{dcho}} \tag{24}$$

4 Exergetic Efficiencies

The exergy efficiency is an important tool for analysing performance of thermodynamic systems being recognized by various researchers. The exergy analysis of system which includes exergy input, exergy output, exergy losses and exergy destruction is based on SLT.

Energy and exergy balance equation can be written as:

$$\text{Energy input} = \text{Energy output in product} + \text{Energy emitted with waste} \tag{25}$$

$$\text{Exergy inflow} = \text{Exergy outflow in product} + \text{Exergy emitted with waste} + \text{Exergy destruction} \tag{26}$$

These equations comprise the term product means shaft work, electricity, a certain heat transfer. In exergy balance equation exergy mission with waste and destruction refers to exergy losses. The exergy destruction caused by internal irreversibility.

The energy efficiency η is written as

$$\begin{aligned}\eta &= \text{Energy output in products/Energy input} \\ &= 1 - [\text{Energy loss/Energy input}]\end{aligned} \tag{27}$$

Exergy efficiency ε is the ratio of output exergy to input exergy (Kuzgunkaya and Hepbasli 2007). Exergy output refers to product exergy.

$$\begin{aligned}\varepsilon &= \text{ Exergy outflow in product/Exergy inflow} \\ &= 1 - [\text{Exergy loss/Exergy inflow}] \\ &= 1 - [(\text{Exergy waste emission} + \text{Exergy destruction})/\text{Exergy input}]\end{aligned} \tag{28}$$

$$\varepsilon = \frac{Ex_o}{Ex_i} = 1 - \frac{Ex_L}{Ex_i} \tag{29}$$

Referring Eqs. 22 and 23,

$$\varepsilon = \frac{Ex_{\text{dcho}}}{Ex_{\text{dchi}}} \tag{30}$$

In case of solar dryer, it is defined as exergy input in the moisture evaporation from crop produce to the exergy of drying air supplied (i.e. entering the drying chamber):

$$\varepsilon = \frac{Ex_{evap}}{Ex_{das}} \tag{31}$$

Exergetic efficiency of drying chamber can be calculated by (Prakash et al. 2016)

$$\text{Exergetic efficiency} = \frac{\text{Exergyinflow} - \text{Exergyloss}}{\text{Exergyinflow}} \tag{32}$$

5 Exergetic Analysis of Solar Dryer

Solar dryer's exergy balance applied in drying process is written as

$$Ex_{sr} - \left(Ex_{\text{evap}} + Ex_{\text{work}}\right) = Ex_L \tag{33}$$

Ex_{sr} is exergy input to the solar dryer.

The exergy factor of solar radiation from any source of geometrical factor f can be expressed as (Badescu 2015; Kalogirou et al. 2016)

$$\psi = \left[1 - \frac{4}{3} \times \left(\frac{T_e}{T_s}\right) + \frac{11}{f3} \times \left(\frac{T_e}{T_s}\right)^4\right]$$

where geometrical factor $f \supseteq \left(\frac{T_e}{T_s}\right)^3$.

Solar intensity insulated, i.e. solar energy falling on surface area A of solar dryer on Earth, is $I(t)_{sr}$. The thermal radiation energy (E_{tr}) is the product of incident solar intensity and surface area of system ($I(t)_{sr} \times A$). Thus, radiation exergy, i.e. conversion of radiation to work, is written as given in Eq. 34:

$$Ex_{sr} = \left\{A \times I(t)_{sr}\right\} \times \psi = \left\{A \times I(t)_{sr}\right\} \times \left[1 - \frac{4}{3} \times \left(\frac{T_e}{T_s}\right) + \frac{1}{3} \times \left(\frac{T_e}{T_s}\right)^4\right] \quad (34)$$

Similarly, influx of exergy to greenhouse is expressed as

$$Ex_{sr} = \sum \left(A_i \times I(t)_{sr_i}\right) \times \left[1 - \frac{4}{3} \times \left(\frac{T_e}{T_s}\right) + \frac{1}{3} \times \left(\frac{T_e}{T_s}\right)^4\right] \quad (35)$$

where $A_i \times I(t)_{sr_i}$ is gross insulated solar energy (W) at ith surface of greenhouse total incident solar, and T_e is environment temperature equal to ambient air temperature T_a. Sun surface temperature T_s is 6000 K (Petela 2003). The comparative analysis of the previous selected research work is being presented in Table 2.

5.1 Exergy Analysis of Passive Solar Dryer

The exergy of work rate is zero in passive solar dryer:

$$Ex_{\text{work}} = W(t) = 0 \quad (36)$$

Now, the product exergy or output exergy is the rate of exergy (heat) utilized for moisture evaporation or moisture transfer (Ex_{evap}) which can be expressed as

$$Ex_{\text{evap}} = \sum \left(1 - \frac{T_e}{T_{\text{dch}}}\right) \times Q_e \quad (37)$$

T_{dch} is drying air temperature in drying chamber.

The rate of heat utilized for moisture evaporation or moisture transfer can be expressed as

$$Q_e = m_{ev} \times \iota = h_{ev}(T_c - T_e) \times A_t \quad (38)$$

Table 2 Some previous research based on exergy analysis of solar dryer

S. no.	Author	Concluding remarks
1.	Tiwari et al. (2009)	The exergy analysis for drying of fish in greenhouse drying system has been studied. The predicted value matched well with experimental value
2.	Celma and Cuadros (2009)	The drying process of olive mill waste water in an indirect-type solar dryer has been investigated by means of exergy analysis. The exergetic efficiencies ranged from 53.24 to 100% during the first day and from 34.0 to 100% during the second day of drying processes
3.	Midilli and Kucuk (2003)	An experiment was conducted to analyse the drying process of dry shelled and unshelled pistachios in multi-shelf (16 shelf) solar dryer. An exergy analysis has been proposed to investigate the drying process. The maximum exergy inflow to solar dryer was 3.718 kJ kg^{-1}. The more important parameter to decrease exergy loss was product's order, structure and its moisture content
4.	Akbulut and Durmus (2010)	Exergy analysis of thin layer drying process of mulberry in forced solar dryer has been investigated. It was observed that with increase in drying mass flow rate, the exergy loss and energy utilization decreased
5.	Nayak and Tiwari (2008)	The study of exergy analysis of PV/T integrated greenhouse system based on quasi-static condition has been done. The predicted value holds good agreement with measured data of solar cell, tedlar back surface and greenhouse air temperature
6.	Chowdhury et al. (2011)	An experiment was conducted to analyse the drying process of jackfruit leather in tunnel-based solar dryer. The exergetic efficiency of solar dryer was obtained 32.69%, while mean value was 41.2%. Author concluded that with increasing solar radiation, the exergy loss and exergy input increased
7.	Akpinar et al. (2005)	The study of single layer drying process of potato chips in cyclone-type dryer was conducted. The experiment concluded that in the first tray of dryer, the available energy was less utilized; hence exergy loss was more in the first tray of cyclone-type dryer
8.	Kurtbas and Durmus (2004)	In order to save energy, author designed five different types of solar air dryer. It was suggested that collector efficiency, heat transfer coefficient and pressure loss may be taken into consideration in order to decrease exergy loss and increase system efficiency

where ι is latent heat of vaporization, h_{ev} is evaporative heat transfer coefficient and A_t is tray area where crop is kept.

In Table 3, the total solar radiation for drying purpose can be expressed with parts accessibility.

5.2 *Exergy Analysis of Active Solar Dryer*

Active solar dryer consists of a fan which can alternatively be driven with or without generated electricity by PV module.

Table 3 Total solar radiation expression as per dryer parts availability for passive solar dryer

Flat-plate air collector (FPC)	Drying chamber (dch)	Chimney	Total solar radiation
Transparent	Transparent	Transparent	$\sum \left(I(t)_{sr_i} A_i\right) = \left(I(t)_{sr_i} A_i\right)_{\text{FPC}} + \left(I(t)_{sr_i} A_i\right)_{\text{dch}} + \left(I(t)_{sr_i} A_i\right)_{\text{chimney}}$ (39)
Transparent	Opaque	Transparent	$\sum \left(I(t)_{sr_i} A_i\right) = \left(I(t)_{sr_i} A_i\right)_{\text{FPC}} + \left(I(t)_{sr_i} A_i\right)_{\text{chimney}}$ (40)

5.2.1 Active Solar Dryer Without PV Module

The exergy inflow to solar dryer of active type is expressed as

$$Ex_{\text{in}} = U_{ee} \sum \left(I(t)_{sr_i} A_i\right) + Ex_{\text{PV}} \tag{41}$$

where $\sum \left(I(t)_{sr_i} A_i\right) = \left(I(t)_{sr_i} A_i\right)_{\text{FPC}} + \left(I(t)_{sr_i} A_i\right)_{\text{dch}}$, and fan work done ($W_{\text{fan}}$) is electrical energy used in driving fan.

Exergy input to active solar dryer can be expressed as

$$Ex_{\text{in}} = Ex_{sr} + Q_{te}\left(1 - \frac{T_e + 273}{T_{\text{dch}} + 273}\right) + W_{\text{fan}} \tag{42}$$

Here exergy input (Ex_{in}) from flat-plate collector and radiation exergy inflow (Ex_{sr}) are combined, and thermal energy is supplied to drying chamber from flat-plate collector. The exergetic efficiency of active solar dryer can be expressed as

$$\varepsilon = \frac{Ex_o}{Ex_i} = \frac{Ex_{\text{evap}}}{Ex_i} \tag{43}$$

5.2.2 Active Solar Dryer with PV Module

DC electricity is supplied by PV module; the exergy input can be expressed as

$$Ex_{\text{in}} = U_{ee} \sum \left(I(t)_{sr_i} A_i\right) + Ex_{\text{PV}} \tag{44}$$

The exergy of PV module is written as given in Eq. 45:

$$Ex_{\text{PV}} = \eta_{\text{PVmodule}} \times \left(I(t)_{sr_i} A_i\right)_{\text{PVmodule}} \tag{45}$$

η_{PVmodule} is PV module efficiency which calculated from Eq. 46:

$$\eta_{\text{PVmodule}} = \left(\frac{FF \times I_{SC} \times V_{OC}}{A_M \times I_{sr}}\right) \tag{46}$$

Generally, the fill factor value of good quality Si is 0.88.

Combining exergy input from flat-plate collector and radiation exergy input to drying chamber, then exergy input will be expressed as

$$Ex_{\text{in}} = Ex_{sr} + Q_{te}\left(1 - \frac{T_e + 273}{T_{\text{dch}} + 273}\right) + Ex_{\text{PV}} \tag{47}$$

Q_{te} is thermal energy derived from flat-plate collector and supplied to drying chamber. If PV module is integrated in collector, the exergy of PV module (Ex_{PV}) is zero.

The exergy of work rate including PV module and fan work in active solar dryer is expressed as

$$Ex_{wh} = P_{\text{PV}} - P_e = (0.8 \times I_{sc} \times V_{oc}) - (I_{\text{load}} \times V_{\text{load}}) \tag{48}$$

where P_{PV} (W) is PV module's power output from PV module, P_e (W) power required to run fan, I_{sc} (A) is short circuit current, V_{oc} (V) is open circuit voltage, I_{load}(A) is load current and V_{load} (V) is load voltage.

The gross output of exergy is extracted from active solar dryer including consumed DC power output from PV module, and fan work, i.e. hybrid active solar dryer, is calculated by Eq. 49:

$$Ex_o = Ex_{ev} + Ex_{wh} \tag{49}$$

Exergetic efficiency can be calculated from given Eq. 50:

$$\varepsilon = \frac{Ex_{ev} + Ex_{wh}}{Ex_i} \tag{50}$$

Saidur et al. (2012) have studied the exergy analysis of various solar collectors, and it is presented in Table 4.

Table 5 shows the comparative analysis of the various solar thermal systems.

Table 4 Exergy efficiency of different solar collector system (Saidur et al. 2012)

S. no.	Solar collector system	Exergetic efficiency
1	The PV/T water collector with glazing	13.30%
2	The coverless PV/T water collector	11–12.87%
3	The unglazed PV/T air collector	10.75%
4	The (glass-to-glass) PV/T air collector	10.45%
5	The PV/T water collector with glazing	8–13%
6	The PV array	3–9%
7	The unglazed PV/T air collector integrated greenhouse with earth air heat exchanger	5.50%
8	The unglazed PV/T air collector integrated greenhouse	4%
9	The flat-plate water collector with double glazing	3.90%
10	The BIPV/T air collector	2.12%
11	The air heater with double glazing	2%

Table 5 Comparative analysis of different solar heating system based on previous research

S. no.	Solar heating system	Exergy efficiency	Concluded remarks	References
1.	Flat-plate solar heaters	44%	The exergy efficiency increases with increase in time and air mass flow rate	Akpinar and Kocyigit (2010)
2.	Solar-assisted heat pump	23.81%	Compressor comprises maximum exergy losses than condenser and solar collector	Kara et al. (2008)
3.	Solar-assisted heat pump	30.80%	Solar collector's exergy loss was obtained as 1.92 kW	Dikici and Akbulut (2008)
4.	Solar water heater	16.17%	The maximum exergy destruction occurred in solar collector	Gunerhan and Hepbasli (2007)
5.	Flat-plate solar air heater	–	The efficiency of solar air heaters with fins is higher than without fins	Alta et al. (2010)

6 Case Studies

In this chapter, there are three case studies being presented. These three types of case study deal with three different types of the solar dryer, namely, direct, indirect and mixed solar dryer.

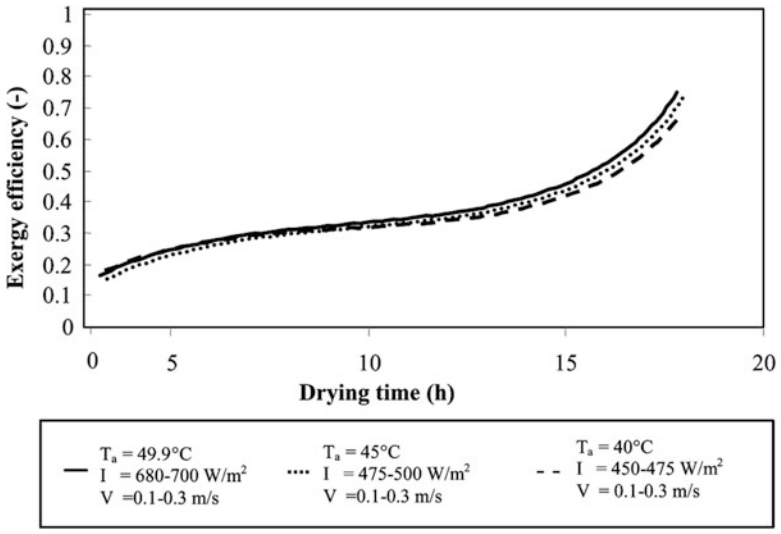

Fig. 2 Variation of exergy efficiency with respect to time

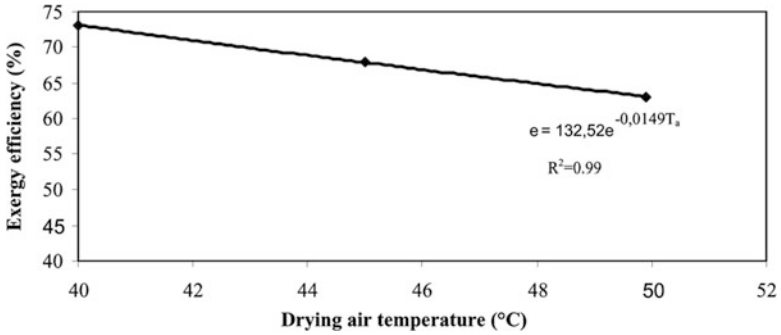

Fig. 3 Variation of exergy efficiency and inside room air temperature during experimentation

6.1 Direct Solar Dryer

Ozgener and Ozgener (2009) investigated the exergy properties related to drying process of solar greenhouse. Experimental results demonstrate that such drying application is better choice for saving electricity, oil and gas in the Turkey's Aegean region. Mean efficiency of exergy was obtained as 63–73%. The variation of the exergy efficiency with time is being shown in Fig. 2. Figure 3 shows the variation of the exergy efficiency with respect to the inside room air temperature during the process of experimentation. It was concluded that passively solar-heated greenhouse can be implied for product's drying when solar energy gain is low.

6.2 *Indirect Solar Dryer*

Celma and Cuadros (2009) investigated analysis of exergy in drying process of olive mill's waste water. Indirect-type natural convection solar dryer is being used in the process of drying of olive mill waste water. Using the second law of thermodynamics, exergy analysis was carried out during solar drying process. It determines the magnitude of exergy losses during drying process. The exergy losses varied in range from 0 kJ/kg to 0.125 kJ/kg for the first day; in the second day, it was found that available energy (exergy) was less used. Exergy losses mainly took place in the second day of solar drying process varied from 0 kJ/kg to 0.168 kJ/kg. The exergetic efficiencies ranged from 53.24 to 100% during the first day and from 34.0 to 100% during the second day of drying processes. As the name exists, olive mill wastewater comes from the fresh water used in the production process of olive oil extraction plants. Olive mill waste water (OMW) contains olive pulp, mucilage, pectin, residual oil, different dissolved mineral salt, etc. The drying chamber's exergetic efficiency, exergy loss in the drying chamber and the dependence of exergy with drying time were analysed. It was observed that the exergy inflow, exergy outflow and exergy loss in the drying chamber increased during the first 3 h of experiment. These variations occur due to the changes in the solar radiation with respect to time (in h). The variation of the exergy in the first and second day of experimentation is being shown in Figs. 4 and 5. Peak exergy inflow to the system

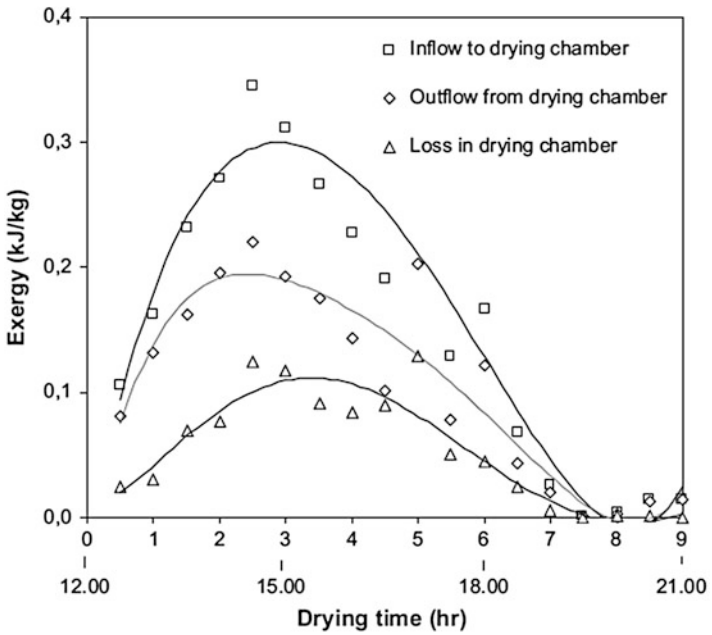

Fig. 4 Exergy as a function of drying time during the first day (Celma and Cuadros 2009)

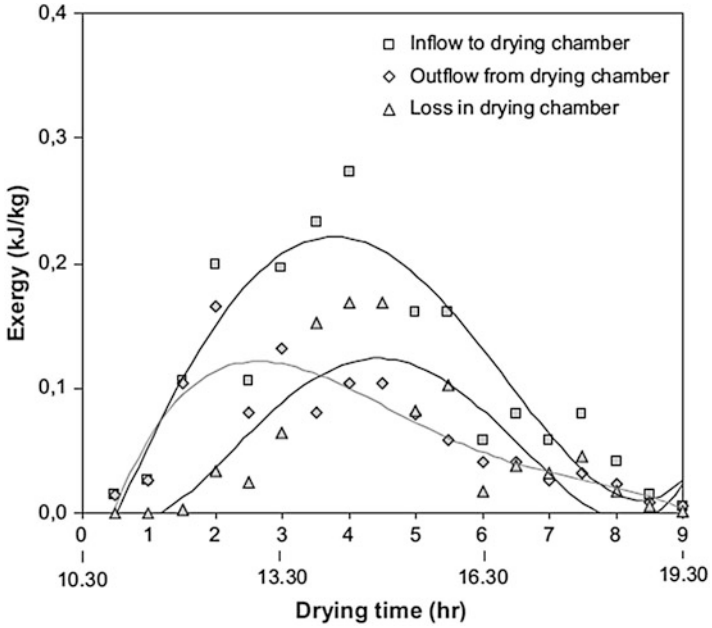

Fig. 5 Exergy variation during second day of experimentation (Celma and Cuadros 2009)

was obtained as 0.345 kJ/kg. In the second day of operation, inflow of exergy had a maximum value of 0.272 kJ/kg. In particular, exergy inflow is increasing in the first 4 h. The exergy inflow decreased rapidly after such interval.

Figure 6 shows the exergy loss in drying chamber per energy utilization during both days of experimentation. The exergy losses in drying chamber increased linearly as energy utilization also increased. It shows exergy loss as the function of energy utilization. The maximum value of exergy losses during the first and second day of operation were 0.125 kJ/kg and 0.168 kJ/kg.

The exergetic efficiency was calculated by Eq. 19 based on the calculated value of exergy inflow, exergy outflow and exergy loss. As the inlet temperature of dryer increased, the exergetic efficiencies of drying chamber decreased as a result exergy losses increased. Note that when exergy efficiency is evaluated as 100%, therefore, exergy loss is nil at particular operating point, provided the drying process in the chamber is discontinued. The exergetic efficiencies were 53.24–100% during the first day and 34.40–100% during the second operating day. In relation to this, indirect-type solar dryer is used for solar drying process of OMW more efficiently during the first day.

Figure 7 shows the exergetic efficiencies of the drying chamber as a function of drying time. In function of drying time, the exergetic efficiencies were decreased during the first 4.5 h; after that it increased in the next 4.5 h forming parabolic curve.

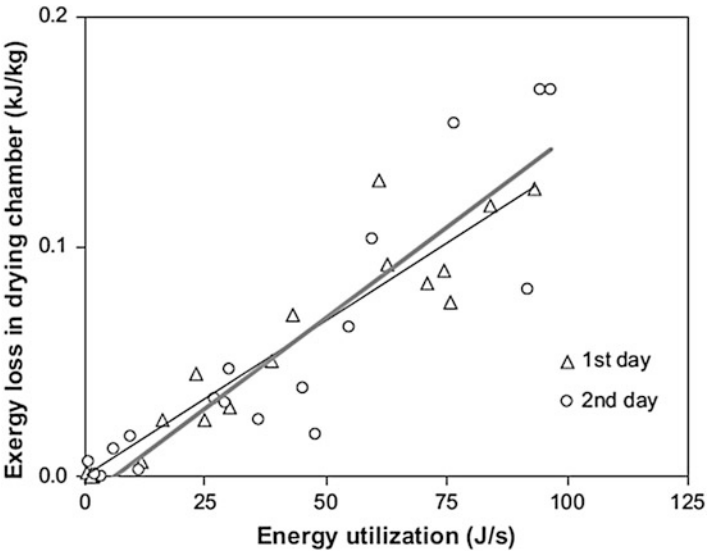

Fig. 6 Exergy loss as a function of energy utilization (Celma and Cuadros 2009)

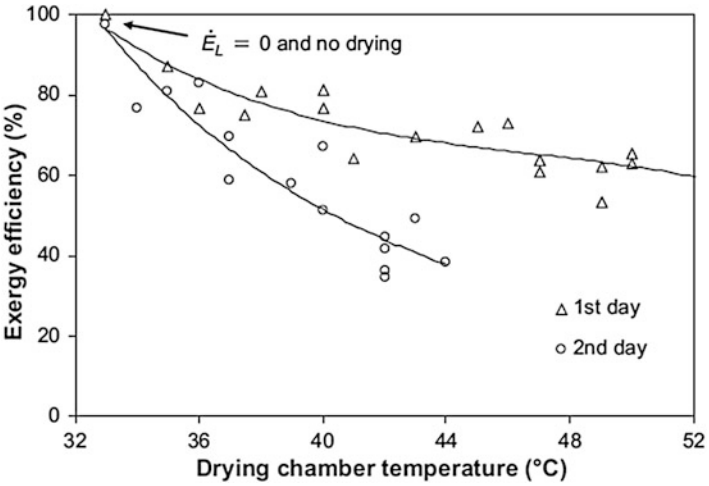

Fig. 7 Exergetic efficiency in function of drying time (Celma and Cuadros 2009)

6.3 Mixed-Mode Solar Dryer

An experiment was conducted by Akinola and Fapetu (2006) for accessing the analysis of exergy in drying process of crop in mixed-mode solar dryer. The following parameters were measured during experiments:

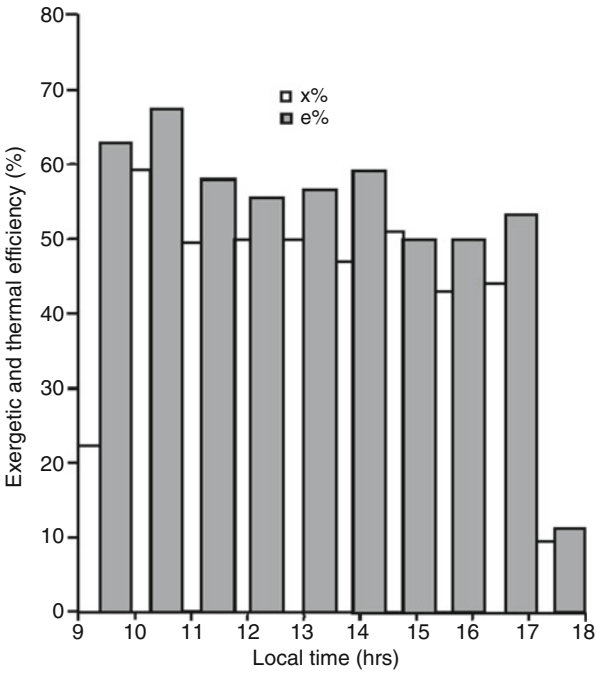

Fig. 8 Variation of exergetic and thermal efficiency during experimentation in the no-load condition

- Incident solar radiation intensity
- Relative humidity and ambient temperature
- The collector plate and drying temperature

Appropriate measuring tools were used for measuring these parameters such as solarimeter, hygrometer and mercury glass thermometer, respectively. The first system was tested in no-load condition and then in load condition. The crop material used for drying was pepper, sliced yam, waterleaf and okra. The variation of exergy and thermal efficiency during experimentation in no-load condition and load condition is being shown in Figs. 8, 9, 10, 11 and 12. The total duration of operation was 15 days per day 9 h (9 a.m. to 6 p.m.) in local time of Nigeria. The exergy losses were 44%, and average exergetic efficiency was calculated as 56%. The dryer was also tested under no-load condition for the first 5 days. In zero-load condition, no product was dried as the name suggests. There were no exergy losses exist; hence the exergetic efficiencies were assumed as 100% (Akinola and Fapetu 2006).

The concluding remark of these dryers is being presented in Table 6.

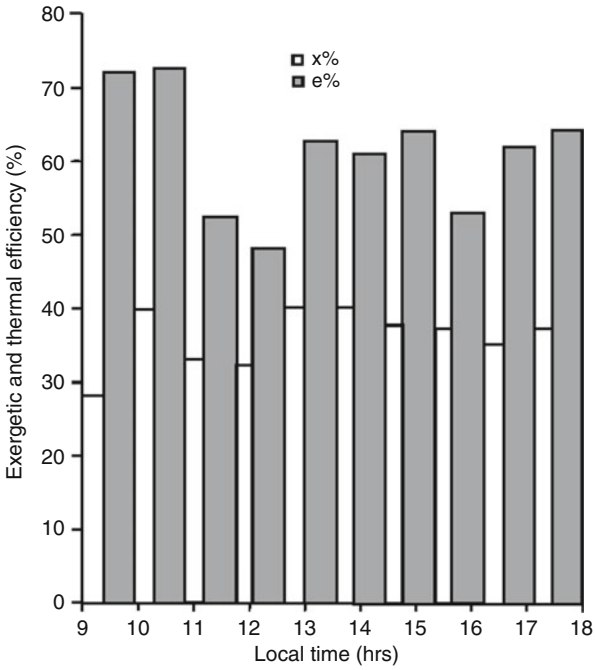

Fig. 9 Variation of exergetic and thermal efficiency during experimentation for drying of yam

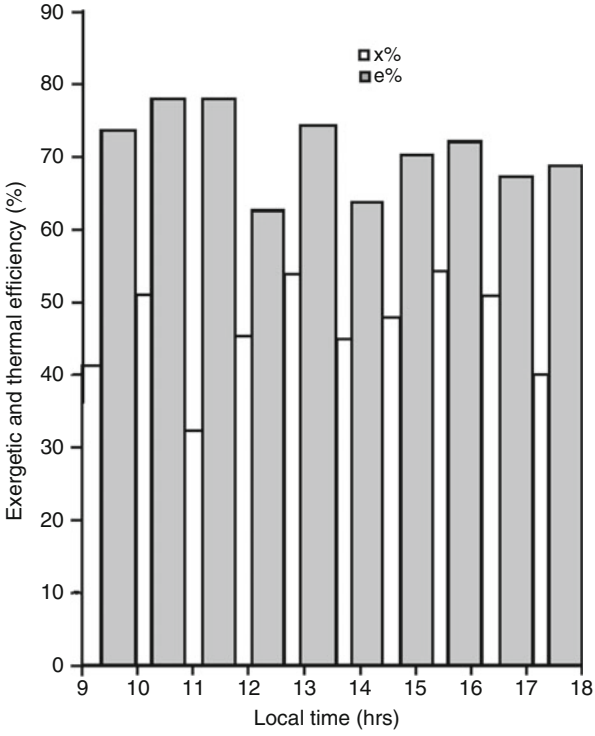

Fig. 10 Variation of exergetic and thermal efficiency during experimentation for drying of pepper

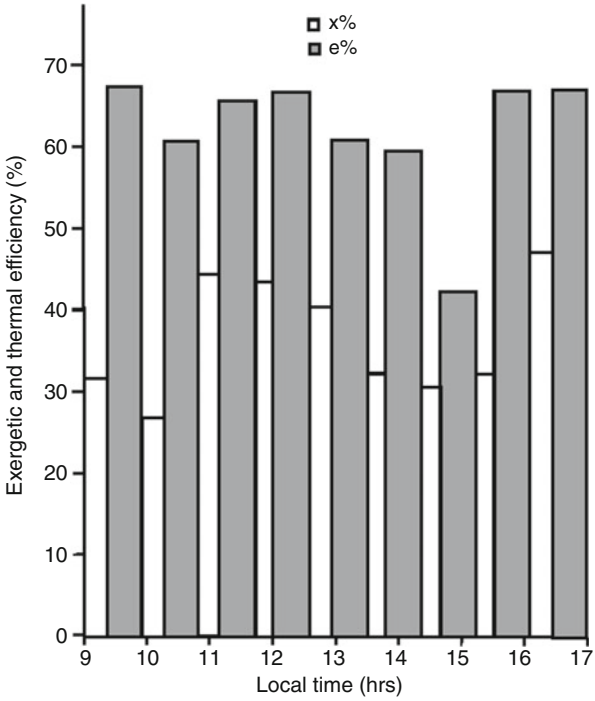

Fig. 11 Variation of exergetic and thermal efficiency during experimentation for drying of waterleaf

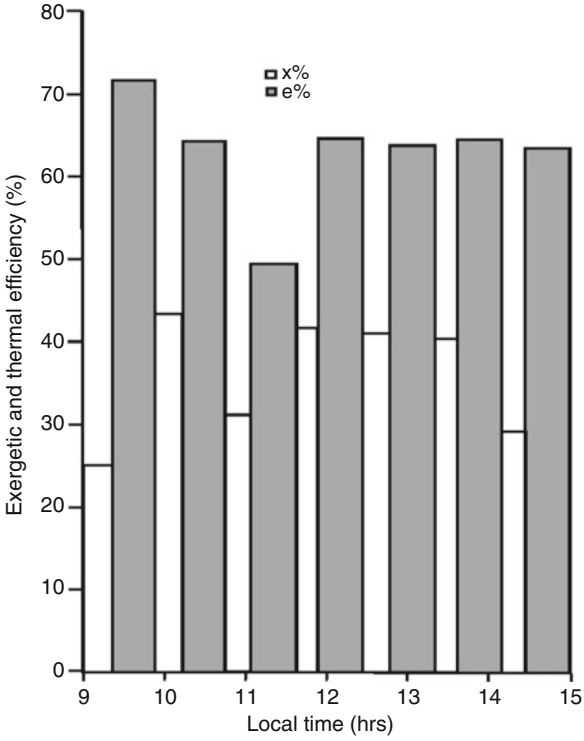

Fig. 12 Variation of exergetic and thermal efficiency during experimentation for drying of okra

Table 6 Concluding remarks of the case study

S. no.	Author	Solar dryer	Concluded remarks
1.	Ozgener and Ozgener (2009)	Direct solar dryer	Mean efficiency of exergy was obtained as 63–73%
2.	Celma and Cuadros (2009)	Indirect solar dryer	On the first day, the exergetic efficiencies was over 53.2%; during the second day of operation, the exergetic efficiency was over 34%
3.	Akinola and Fapetu (2006)	Mixed-mode solar dryer	The average exergetic efficiency was obtained as 56%

7 Conclusion

In this chapter exergy analysis of different solar dryers is being presented. It is concluded from study that exergy analysis gives better performance evaluation of solar dryer system. It was found from the case studies that the average exergy efficiency of direct-mode solar dryer was 63–73%, whereas exergy efficiency of mixed-mode solar dryer was only 56%.

The main highlight from the present research follows:

- Without exergy analysis, thermal analysis is not the only option to choose and design optimal dryer.
- The exergy efficiency increases with increase in air mass flow rate in photovoltaic thermal system.
- The maximum exergy destruction occurred in solar collector.
- In solar-assisted heat pump, higher exergy losses occurred in compressor.
- Solar radiation and radiation intensity affects the exergy efficiency of solar dryer.
- The product's order and moisture content in product should always be considered in order to decrease exergy loss before drying process.

Exergy analysis gives important information regarding processes, losses occurred, sources, causes of destruction, identity of system, etc., and it would make the system more efficient and help to choose desired system. This study will be helpful for selection of the optimal dryer and further development.

Nomenclature

Symbol	Meaning
U	Internal energy (kJ)
V	Volume (m^3)
S	Entropy (kJ/kg k)
E_{in}	Energy input
E_{out}	Energy output

Ex	Exergy (kJ/kg)
$\dot{E}x$	Exergy rate (kJ/s)
ex	Specific exergy
E_L	Specific energy loss (J/kg water)
ι_{hp}	Latent heat of product
W_{ws}	Weight fraction of water in a sample
v	Velocity (m/s)
m	Mass (kg)
z	Coordinate
g	Gravitational force(m/s^2)
M	Moisture content
da	Drying air
dch	Drying chamber
dest	Destruction (irreversibility)
sr	Solar radiation
PV	Photovoltaic
V_{oc}	Output voltage
I_{sc}	Short circuit current
V_{load}	Load voltage
SLT	Second law of thermodynamics
FLT	First law of thermodynamics

Greek Symbol

η	Energy efficiency
ε	Exergy efficiency
δ	Air absolute humidity

Subscript

o	Outlet, outflow
0	Ambient
i	Inlet
L	Loss

References

Akinola AO, Fapetu OP (2006) Exergetic analysis of a mixed mode solar dryer. J Eng Appl Sci 1 (3):205–210

Alta D, Bilgili E, Ertekin C, Yaldiz O (2010) Experimental investigation of three different solar air heaters: energy and exergy analyses. Appl Energy 87:2953–2973

Akpinar E, Kavak AM, Bicer Y (2005) Energy and exergy of potato drying process via cyclone type dryer. Energy Convers Manag 46(15):2530–2552

Akpinar EK, Kocyigit F (2010) Energy and exergy analysis of a new flat-plate solar air heater having different obstacles on absorber plates. Appl Energy 87(11):3438–3450
Akbulut A, Durmus A (2010) Energy and exergy analyses of thin layer drying of mulberry in a forced solar dryer. Energy 35:1754–1763
Badescu V (2015) Maximum reversible work extraction from a blackbody radiation reservoir. Way to closing the old controversy. Europhys Lett 109:40008
Celma AR, Cuadros F (2009) Energy and exergy analyses of OMW solar drying process. Renew Energy 34(2009):660–666
Chowdhury MMI, Bala BK, Haque MA (2011) Energy and exergy analysis of the solar drying of jackfruit leather. Biosyst Eng 110:222–229
Darvishi H, Zarein M, Minaei S, Khafajeh H (2014) Exergy and energy analysis, drying kinetics and mathematical modeling of white mulberry drying process. Int J Food Eng 10(2):269–280
Dikici A, Akbulut A (2008) Performance characteristics and energy–exergy analysis of solar-assisted heat pump system. Build Environ 43(11):1961–1972
Dincer I, Rosen MA (2007) Exergy: energy, environment and sustainable development. Elsevier, Newnes
Erbay Z, Icier F (2011) Energy and exergy analysis on drying of olive leaves (Olea Europaea L.) in tray drier. J Food Process Eng 34(2011):2105–2123
Fudholi A, Sopian K, Othman MY, Ruslan MH (2014) Energy and exergy analyses of solar drying system of red seaweed. Energ Buildings 68:121–129
Gustavsson J, Cederberg C, Sonesson U, Otterdijk R, Meybeck A (2011) Global food losses and food waste – extent, causes and prevention. SIK/FAO, Sweden/Rome
Gunerhan H, Hepbasli A (2007) Exergetic modeling and performance evaluation of solar water heating systems for building applications. Energ Buildings 39(5):509–516
Kalogirou SA, Karellas S, Badescu V, Braimakis K (2016) Exergy analysis on solar thermal systems: a better understanding of their sustainability. Renew Energy 85(2016):1328–1333
Kurtbas I, Durmus A (2004) Efficiency and exergy analysis of a new solar air heater. Renew Energy 29:1489–1501
Kara O, Ulgen K, Hepbasli A (2008) Exergetic assessment of direct-expansion solar assisted heat pump systems: review and modeling. Renew Sustain Energy Rev 12(5):1383–1401
Kemp IC (2012) Modern drying technology volume 4: energy savings, 1st edn. Wiley-VCH Verlag GmbH & Co. KGaA, Weinheim
Kuzgunkaya EH, Hepbasli A (2007) Exergetic performance assessment of a ground-source heat pump drying system. Int J Energy Res 31(8):760–777
Midilli A, Kucuk H (2003) Energy and exergy analyses of solar drying process of pistachio. Energy 28:539–556
Nayak S, Tiwari GN (2008) Energy and exergy analysis of photovoltaic/thermal integrated with a solar greenhouse. Energ Buildings 40:2015–2021
Ozgener L, Ozgener O (2009) Exergy analysis of drying process: an experimental study in solar greenhouse. Dry Technol 27:580–586
Petela R (2003) Exergy of undiluted thermal radiation. Sol Energy 74(6):469–488
Prakash O, Laguri V, Pandey A, Kumar A, Kumar A (2016) Review on various modelling techniques for the solar dryers. Renew Sust Energ Rev 62(2016):396–417
Prakash O (2015) Design and performance analysis of modified greenhouse dryer. Phd thesis from department of Energy, Maulana Azad Natiional Institute of Technology, Bhopal, India
Panwar NL, Kaushik SC, Kothari S (2012) A review on energy and exergy analysis of solar dying systems. Renew Sust Energ Rev 16:2812–2819
Querol E, Gonzalez-Regueral B, Perez-Benedito JL (2011) Novel application for exergy and thermos economic analysis of processes simulated with aspen plus®. Energy 36:964–974
Querol E. (2013) Practical approach to exergy and thermoeconomic analyses of industrial processes. Springer Briefs in Energy, doi:10.1007/978-1-4471-4622-3_2
Saidur R, Boroumand JG, Mekhlif S, Jameel M (2012) Exergy analysis of solar energy applications. Renew Sust Energ Rev 16:350–356
Tiwari GN, Das T, Chen CR, Barnwal P (2009) Energy and exergy analyses of greenhouse fish drying. Int J Exergy 6(5):620–636

Part III
Modeling of Solar Drying Systems

Mathematical Modeling of Solar Drying Systems

Rajendra C. Patil and Rupesh R. Gawande

Abstract Mathematical modeling appears to be valuable utensils for the forecasting of drying kinetics of agro-commodities. Numerous mathematical models like heat and mass balance models, thin-layer models, and equilibrium moisture content models have been used to illustrate the thin-layer and deep bed drying of agro-products. This chapter begins with a broad appraisal of the basic concepts and theories essential for the mathematical modeling of solar drying. Next, the common modeling approaches and developmental steps (model conceptualization, mathematical formulation, determination of model parameters, method of solution, and experimental validation) implicated in solar drying were outlined. Then a sequential progress of thin-layer drying models (semi-theoretical, theoretical, and empirical models) has been discussed briefly. The subsequent section reviews the application of above models by different researchers in the last decade. Afterward newly developed or commonly used thin-layer drying mathematical equations related to the solar collector models and drying cabinet models for different solar drying systems and food products were shown. Finally, we conclude this chapter with future directions and need for more investigations on solar drying. It is estimated that this chapter will be valuable to persons concerned with mathematical modeling and investigation of solar drying.

Keywords Drying kinetics • Mathematical modeling • Moisture content • Solar dryer • Thin-layer drying models

R.C. Patil (✉)
Mechanical Engineering Department, Bapurao Deshmukh College of Engineering, Wardha, Nagpur, Maharashtra, India
e-mail: rcp_296@rediffmail.com

R.R. Gawande
Mechanical Engineering Department, Rashtrasant Tukadoji Maharaj Nagpur University, Nagpur, Maharashtra, India

© Springer Nature Singapore Pte Ltd. 2017

O. Prakash, A. Kumar (eds.), *Solar Drying Technology*, Green Energy and Technology, DOI 10.1007/978-981-10-3833-4_9

1 Introduction

Drying is a method of elimination of moisture from the commodity to a precise value due to the use of thermal energy. In other words, drying is an amalgamation of heat and mass transport process (Patil and Gawande 2016). Solar drying is a technical process having its own vocabulary with it, so accurate definitions of basic concepts, fundamental principles governing the drying process and modeling form the sound foundation for growth of knowledge and prevent probable misunderstandings. A careful study of these concepts related to solar drying and mathematical modeling is essential for good understanding. An inclusive assessment of basic concepts and theories leading the drying process was presented by Ekechukwu O.V (1999).

1.1 Basic Definitions and Laws Related to Solar Drying Process

(a) Moisture Content

The most important ingredient of energy utilization throughout drying is meant for the vaporization of water into its vapor. The moisture content of the commodity to be dried is a significant aspect for determining the quality of the product and by this means the market worth. The moisture content within a product can be articulated either on wet or dry basis. Moisture content on dry basis (d.b.) is meant for engineering investigations, whereas the concept of wet basis (w.b.) has tended to be engaged for commercial purposes.

The weight of moisture in a product per unit weight of the undried matter is referred to as moisture content on wet basis and represented by Eq. (1):

$$M_{\mathrm{wb}} = \frac{W_{\mathrm{o}} - W_{\mathrm{d}}}{W_{\mathrm{o}}} \tag{1}$$

where W_{o} is the initial weight of undried produce and W_{d} the is weight of dry matter in produce.

The weight of moisture present in a product per unit weight of the dry matter product is referred to as moisture content on dry basis and expressed by Eq. (2):

$$M_{\mathrm{db}} = \frac{W_{\mathrm{o}} - W_{\mathrm{d}}}{W_{\mathrm{d}}} \tag{2}$$

Also the relationship between moisture (water) content on dry and wet basis is specified by means of Eqs. (3, 4):

$$M_{\mathrm{db}} = \left(\frac{1}{1 - M_{\mathrm{wb}}}\right) - 1 \tag{3}$$

$$M_{\mathrm{wb}} = 1 - \left(\frac{1}{M_{\mathrm{db}} + 1}\right) \tag{4}$$

where M_{db} and M_{wb} are the moisture content on dry and wet basis, respectively.

During experimentation, weight losses are recorded; hence, instantaneous moisture contents at any given time can be determined by using Eqs. (5, 6):

$$M_{\mathrm{tdb}} = \left[\frac{(M_{\mathrm{odb}} + 1) \times W_{\mathrm{o}}}{W_{\mathrm{t}}}\right] - 1 \tag{5}$$

$$M_{\mathrm{twb}} = 1 - \left[\frac{(1 - M_{\mathrm{owb}}) \times W_{\mathrm{o}}}{W_{\mathrm{t}}}\right] \tag{6}$$

where M_{o} is the initial moisture content, M_{t} is the moisture content, and W_{t} is the weight of product at specified time, respectively.

(b) Equilibrium Moisture Content (EMC)

It is the restraining moisture to which a certain product can be dried in definite conditions of humidity and air temperature. At this condition, the relative humidity of the instantaneous surrounding air is well known as the equilibrium relative humidity.

EMC may be determined experimentally by making use of an evacuated container, which is more accurate and expensive. The moisture equilibrium isotherms (sigmoid curves) can be obtained by plotting EMC against *RH* (relative humidity) at unvarying temperature (Ekechukwu 1999).

(c) Moisture Ratio

Moisture ratio is one of the significant criteria to establish the drying characteristics of biological product. When the *RH* of the drying air remains stable throughout the drying operation, moisture equilibrium also remains steady. The moisture ratio (*MR*) equation is given by

$$MR = \frac{M_{\mathrm{t}} - M_{\mathrm{e}}}{M_0 - M_{\mathrm{e}}} \tag{7}$$

Diamante and Munro (1993) presented Eq. (8) in support of determination of moisture ratio (*MR*), when relative humidity of drying air goes on changing incessantly during the drying process:

$$MR = \frac{M_t}{M_0} \tag{8}$$

where MR represents the moisture ratio, M_0 is the initial moisture content, M_t is the moisture content at time t, and M_e indicates the equilibrium moisture content in % dry basis.

(d) Latent Heat of Vaporization

The amount of energy required to vaporize the moisture from the product to be dried is referred to as latent heat of vaporization, and it depends on the moisture content of product and temperature.

(e) Safe Storage Period

It is the instant of exposure for the commodity at a particular moisture content to a particular temperature and RH under which the deterioration of commodity may arise.

(f) Drying Rate

It is subjected to variation of moisture content with time and has first the stable drying rate and second the falling drying rate period. During stable or constant drying rate period, moisture subtraction rate per unit drying surface remains steady, while in falling drying rate phase, the instant drying speed constantly decreases. The details about drying regime are discussed in earlier chapter. Equation (9) indicates the expression for drying rate:

$$DR = \frac{M_{t+\mathrm{d}t} - M_t}{\mathrm{d}t} \tag{9}$$

where DR shows drying rate and $M_{t+\mathrm{d}t}$ represents moisture content at $t + \mathrm{d}t$ in % dry basis.

(g) Principles Used in Solar Drying Systems

In solar drying processes, various principles like first and second law of thermodynamics, law of conduction (Fourier's law), law of convection (Newton's cooling law), and Fick's law of diffusion were involved in drying of numerous agricultural products. So in this section an effort is made to give a short and snappy overview of above crucial laws for better understanding of the physics of solar drying processes.

The *first law of thermodynamics* is also referred to as law of conservation of energy and deals with energy as a property and states that the quantity of energy remains constant during a process.

In solar drying systems, energy investigation is performed to determine the amount of energy gained from solar air collector and the ratio of energy consumption of the drying chamber. Energy analysis of drying process for many agricultural

products is carried out on the base of mass and energy conservation in steady state and can be expressed by Eqs. (10, 11) and Eq. (12), respectively:

Mass conservation equation for drying air

$$\sum m_{\mathrm{i}} = \sum m_{\mathrm{o}} \tag{10}$$

where m_{i} and m_{o} are mass flow rate of air at inlet and outlet, respectively.

Moisture conservation equation for drying air

$$\begin{aligned} \sum \left(m_{\mathrm{wi}} + m_{\mathrm{mp}}\right) &= \sum m_{\mathrm{wo}} \\ \sum \left(m_{\mathrm{i}} w_{\mathrm{i}} + m_{\mathrm{mp}}\right) &= \sum m_{\mathrm{i}} w_{\mathrm{o}} \end{aligned} \tag{11}$$

where m_{wi} and m_{wo} are the inlet and the outlet mass flows of humidity, respectively, m_{mp} is the mass flow of moisture of the product, and w_{i} and w_{o} are the inflow and outflow specific humidity, respectively.

And the energy conservation equation by

$$Q - W = \sum m_{\mathrm{o}} \left(h_{\mathrm{o}} + \frac{v_0^2}{2}\right) - \sum m_{\mathrm{i}} \left(h_{\mathrm{i}} + \frac{v_{\mathrm{i}}^2}{2}\right) \tag{12}$$

where Q is the net heat rate, W is the energy utilization rate, h means enthalpy, and v is the velocity of drying media.

The *second law of thermodynamics* deals with quality as well as quantity of energy and asserts that the actual process takes place in the direction of decreasing quality of energy.

In second falling drying rate period, moisture movement commencing from the commodity core to the exterior side is typically by way of molecular diffusion, i.e., the moisture flux is directly proportionate to the moisture content gradient. In other words, moisture moves from higher moisture content region to lower moisture content region, and this phenomenon is explained with the help of second law of thermodynamics. The handy concept of exergy in the investigation of thermal systems is also explained by the second law of thermodynamics, and it states that the fraction of exergy inflowing a thermal system with flowing streams of matter, fuel, electricity, etc., is smashed within the system due to irreversibility (Chowdhury et al. 2011; Midilli and Kucuk 2003a, b).

The general form for total exergy equation of a system is given by Eq. (13):

$$E_{\mathrm{X}} = E^{\mathrm{PT}} + E^{\mathrm{KN}} + E^{\mathrm{PH}} + E^{\mathrm{CH}} \tag{13}$$

where E_{X} = exergy of total system, while E^{PT}, E^{KN}, E^{PH}, and E^{CH} represent potential, kinetic, physical, and chemical exergy, respectively.

During heat transport between drying media and product, knowledge of *Fourier's law of heat conduction* and *Newton's law of cooling* is a must. Fourier's law is an empirical law, made important contribution to the analytical treatment of conduction heat flow, and states that the rate of flow of heat per unit area through a

homogeneous solid is proportional to the normal temperature gradient. Mathematically, Fourier's law is represented by Eq. (14):

$$\frac{Q}{A} = -k\frac{\mathrm{dT}}{\mathrm{dx}} \tag{14}$$

where Q is the conductive heat flow rate in J/s and A is the surface area of heat flow in m^2.

The fundamental law for convection is Newton's law of cooling (Eq. 15) and states that heat transfer per unit area is proportional to the temperature difference between a fluid and surface of product:

$$Q = h \times A \times \Delta T \tag{15}$$

where Q is the convective heat flow rate in J/s, A is the surface area of heat flow in m^2, and ΔT is the temperature difference between fluid and surface.

In modeling of solar dryers for drying of agro-products, the knowledge of convective mass transfer coefficient and moisture diffusion is essential. **Fick's law of diffusion** is used for determination of diffusion coefficient (Eq. 16) and states that the mass flux of constituents per unit area (molar flux) is proportional to the concentration gradient:

$$\frac{m_\mathrm{A}}{A} = -D\frac{\partial C_\mathrm{A}}{\partial \mathrm{x}} \tag{16}$$

where m_A is the mass flux per unit area in kg/s, D is the diffusion constant in m^2/s, and C_A is the mass concentration of component A per unit volume in kg/m^3.

Convective mass transfer coefficient (Eq. 17) can be defined in the analogous manner that is used for defining convective heat transfer coefficient:

$$m_\mathrm{conv.} = h_\mathrm{m} \times A \times \Delta C \tag{17}$$

where $m_\mathrm{conv.}$ = the rate of mass convection across the boundary, h_m is the average mass transfer coefficient, A is the surface area, and ΔC is the mass concentration difference.

1.2 Basics and Principles of Mathematical Modeling

A model is an illustration or an idea of a system or process. Mathematical modeling represents the real system or process in terms of mathematical equations and works to be the most efficient technique to realize the profundity of drying in postharvest operation of agro-products. In model-building endeavor, a lucid depiction of why the model is required or wanted is of major significance. Now we will illustrate the principles of mathematical modeling; likewise in next headings we will briefly

Table 1 Phrased questions in mathematical modeling

Phrased question	Question	Answer
Why	Why are we looking for?	Recognize the need for the model
Find	What do we want to know?	List the data we are in search of
Given	What do we be familiar with?	Identify the available significant data
Assume	What can we presume?	Make out the situations that apply
How	How should we seem at this model?	Name the governing physical principles
Predict	What will our model envisage?	Identify and solve the equations that will be used
Valid	Are the predictions valid?	Identify tests that can be consistent with its principles and assumptions
Verified	Are the predictions good?	Identify tests to authenticate the model
Improve	Can we improve the model?	Identify parameter values that could be lifted Put into action the iterative loop "model-validate-verify-improve-predict"
Use	How will we exercise the model?	Use the model for which it is meant

assess the approach and steps involved in it for solar drying. The mathematical modeling is a principled activity based on principles of overarching or meta-principle phrased as questions regarding the objective and rationale of mathematical modeling. The following questions and directions are not an algorithm for developing a high-quality arithmetical model, but they act as an important key in formulation of a problem (Maria 1997). Table 1 represents how the questions raised in a principled approach for constructing the model.

2 Modeling Approaches and Steps in Mathematical Modeling

This segment presents the approaches for modeling of solar drying process and can be classified into models those based on the fundamental physics of drying process as well as thin layer and equilibrium moisture content models. Later on various steps involved in mathematical modeling for solar drying process were discussed in detail.

2.1 Modeling Approaches

Modelers frequently categorized their models as differential equation models, disaggregated models, matrix models, individual-based models, object-oriented models, spatial models, modular models, and so on.

The first modeling approach is generally based on the models employing the fundamental laws of conservation of mass, momentum, and energy. In this approach the physics implicated in the drying process is largely represented by fundamental transport equations (classical models) as well as heat and mass transfer equations. The classical models involve high mathematical complexity due to involvement of too many parameters. Natural and forced convection solar drying processes are strongly dependent on heat and mass transfer rates at the air-produce interface which is mainly controlled by air velocity through the drying chamber. Hence, to get better predictive accuracy of the model, it should be coupled with momentum transport dynamics of drying process. Further, fluid dynamics in solar drying system plays a vital role for characterizing the effect of heat and mass transfer from product to drying air (equipment models). In this model, the inconsistency of airflow around the produce is also considered. Such model not only describes the mass and energy transfer during the process but also forecasts the instantly varying drying conditions of air in the drying chamber. In short a more extensive modeling approach involves the mathematical computation of a theoretical model describing the transport of air impulsion, heat energy, and mass exchange between drying media and produce under transitory conditions of solar drying.

In drying systems, drying processes are often modeled by (1) distributed elemental model and (2) lumped element model.

(a) Distributed Element Model

This model depends on the interaction among time and spatial variables (minimum one variable) on behalf of all of its dependent variables. In addition to this, such model considers the simultaneous heat and mass transport phenomena during drying processes. According to the different researchers, the temperature and moisture effects are more dominant than the pressure effects.

(b) Lumped Element Model

It takes in account the consequence of time only over the reliant variables. However, such model assumes an even supply of drying air temperature into the produce, i.e., constant temperature along with negligible pressure variable (Luikov 1975). The model is publicized by Eq. (18):

$$\frac{\delta M}{\delta t} = \nabla^2 K_1 \quad \text{and} \qquad \frac{\delta T}{\delta t} = \nabla^2 K_{12} \tag{18}$$

where K_1 and K_{12} show thermal (α) and effective diffusivity (D), respectively.

For the invariable values of thermal (α) and effective diffusivity (D), Eq. (18) can further be written as Eq. (19):

$$\frac{\delta M}{\delta t} = D\left[\frac{\delta^2 M}{\delta X^2} + \frac{b_1}{X}\frac{\delta M}{\delta X}\right] \quad \text{and} \qquad \frac{\delta T}{\delta t} = \alpha\left[\frac{\delta^2 T}{\delta X^2} + \frac{b_1}{X}\frac{\delta T}{\delta X}\right] \tag{19}$$

In the assessment of Ekechukwu (1999), for plate or slab geometry ($b = 0$), for cylindrical geometry ($b = 1$), and for spherical geometry ($b = 2$) are reported. Nevertheless, these assumptions give error in temperature at the start of the drying process.

Thin layer and equilibrium moisture content models in solar drying are sometimes referred to as characteristics of drying rate curves. These models are further classified into three categories, namely, theoretical, semi-theoretical, and empirical models. These models are usually based on simplifying hypothesis which may not be relevant for complex geometries of agro-commodities and for altering working conditions during drying process. Such models consider resistance (internal or external) to mass exchange only and express the drying curves for the situation of the experimentation. Empirical model not only neglects the fundamentals of the drying process but also neglects heat transfer and product shrinkage phenomenon.

However, a comprehensive analysis of transient phenomena such as heat, mass, momentum, as well as deformation in drying process increases the model complexity which in turn increases the computational time. Therefore, it is essential to have meaningful, simple, precise, and robust mathematical model.

2.2 *Steps in Mathematical Modeling*

The mathematical modeling is an effort to explain some part of actual system in mathematical language. The basic steps used for modeling a drying process include model conceptualization, mathematical formulation, determination of model parameters, methods of solution, and experimental validation.

(a) Model Conceptualization

It is the most significant step in the growth of a mathematical modeling. During this step of the modeling, the critical decisions should be taken by the modeler on what component of realism to study and how to express it. In short modeler must be

familiar among the fundamental problem area and identify the most important questions to be raised, along with the time horizon of the problem of attention. Conceptualization is the most significant and least unspoken of all modeling activities. The limitation of conceptualization is the data gathering method which is an intricate interface between the conceptual process and the actual observation (Frejd 2013).

(b) Mathematical Formulation

In building of mathematical model, conceptualization of model is followed by mathematical formulation, manipulation, and evaluation. Mathematical formulation of interested system starts with the questions which may be too big or indistinct. If questions are too big, then split it into manageable parts. Afterward formulation of model proceeds with identification of the relevant factors. These factors help modeler to decide the quantities, and relationship should be considered related to your questions as well which may be neglected. Finally, mathematical formulation ends with mathematical description showing the physics of process. Every quantity related to the questions may be represented by an appropriate mathematical entity like a function, a variable, or a geometric figure. Also the relationship between quantities should be described by suitable assumptions, inequality, or an equation.

In solar drying process of various agro-commodities, two discrete transfer mechanisms take place concurrently, regarding heat (product and air) and mass transfer from the inside of the commodity to its exterior along with drying media through evaporation. The heat along with water transport between the drying air and product depends on air velocity, temperature, and on concentration difference. The partial differential equations are used for explaining the instantaneous heat, mass, and momentum transport between drying media and product. PDEs illustrate the healthy and precise physics of the drying process (heat, mass, and momentum). For describing the transient heat transfer in the solid product, Fourier's law of heat conduction may be the best choice. The various coefficients related to the heat and mass transport depend on the drying parameters like product type, size, air velocity, etc.

In solid products, mass exchange phenomenon depends on the effective diffusion coefficient. However, diffusion coefficient strongly depends on product type and size, temperature, water content, as well as on drying conditions. In regard to diffusion coefficient, a lumped model or parameter can be employed. However, a proper care should be taken during application of diffusion coefficient correlations to intricate geometries of product, which may lead to inaccurate calculated outcome.

(c) Model Parameters

For precise prediction of drying kinetics, it is assumed that many drying parameters (density, specific heat, conductivity, heat and mass transfer coefficients, etc.) do not remain constant throughout the drying process but largely depend upon the moisture content of product (commodity) to be dried and temperature of air inside

Table 2 Thermophysical and transport properties

Sr. no.	Thermophysical properties	Transport properties
1	Density = f(temperature)	Heat transfer coefficient = f(Nu, Re, Pr, shape, velocity)
2	Specific heat capacity = f (temperature)	Mass transfer coefficient = f(Sh, Re, Sc, shape, velocity)
3	Thermal conductivity = f (temperature)	Diffusion coefficient = f(moisture content, temperature)

the solar dryer. The comprehension of transport as well as thermophysical properties of commodity to be dried along with drying media is a must for solving the partial differential equations. The main model parameters for solar drying processes are shown in Table 2.

The empirical equations having various dimensionless numbers are used to determine the heat and mass transport coefficients in the boundary conditions. The free and forced convective heat transfer coefficients are estimated by using Nusselt-Reynolds and Prandtl correlations, whereas convection mass transfer coefficients on exterior shell of the commodity are computed by Sherwood-Reynolds and Schmidt correlations for a particular shape of product.

(d) Method of Solution

Various tools are available for solving the mathematical models, but mostly analytical and numerical methods of solution are preferred for solving the models associated with solar drying system. The analytical approach for normal-shaped geometries of product with simplified assumptions and accurate boundary conditions is able to generate the general solutions. On the other hand, for complex models and shapes of product, numerical computational approach provides fairly accurate solutions for the drying system under study. It includes finite volume, finite element, and finite difference methods. In numerical method of solution, complex governing mathematical equations were abridged to a set of uncomplicated polynomial or linear equations by employing correct approximation techniques. Numerical method creates answer in steps, with each step providing the solution for one set of situation and computation repeated to enlarge the range of solutions. Also the spatial discretization techniques (nonlinear partial differential equations with proper boundary conditions) were used for the models dealing with deformation of drying material. Mesh-free, Arbitrary Lagrange Eulerian (ALE), Lagrange, and Euler methods are usually used in spatial discretization techniques. During development of mathematical modeling, certain assumptions were made by different researchers and few of them listed below:

Assumptions in mathematical modeling for solar drying system

1. Drying calculation depends on a thin-layer solar drying model.
2. Specific heat capacity of cover, drying air, and commodity are stable.
3. One-dimensional heat and moisture movement.

4. During drying properties of air, moisture and commodity for the specified temperature remain steady.
5. A shrinkage phenomenon is considered throughout drying.
6. Uniform circulation of drying air inside the dryer.

Modeling the drying attitude of unlike agro-commodities frequently needs the statistical techniques of regression as well as correlation analysis. Linear and nonlinear regression models are vital utensils to discover the connection among different variables, mostly for which no reputable empirical connection subsists. Also the interaction of the unchanging factor of the most excellent model through the drying air velocity is also found out by multiple regression method with simple, linear, logarithmic, exponential, and power regression models.

At present, much viable modeling software (MATLAB, COMSOL Multiphysics) and programs (TRNSYS, WATSUN, Polysun, and F-Chart) are available for solving the linear and nonlinear equations using suitable solver. Further various programming languages like FORTRAN, C++, and Delphi are used for developing computer programs. This program helps the modeler to iteratively resolve the equations representing the system (Akpinar et al. 2003, Akpinar and Bicer 2005, 2008; Akpinar 2006, 2008, 2010; Bala et al. 2011; Chukwunonye et al. 2016; Kalogirou 2004; Karim and Hawlader 2005; Kucuk et al. 2014; Midilli et al. 2002, 2003a, b; Onwude et al. 2016; Yaldiz et al. 2001).

(e) Model Validation

It is the most significant and overlooked step in the model building progression. The excellence of real performance is established during this validation segment of mathematical modeling. The difference in information gathered from real system and model output shows the level of validity of the selected model. There are various statistical utensils for model validation, but the prime tool for the majority of processes modeling application is a graphical residual analysis. The different types of graphs of the residuals offer the information on the competence of various aspects of the model.

In solar drying, all mathematical models are validated and verified by comparing the measured data obtained from the experimentation with predicted values such as moisture content, temperature, etc. Several researchers (Madamba et al. 1996; Palipane and Driscoll 1994) recommend the mean relative percentage deviation ($\%P$) parameter for validating the drying models, as shown by Eq. (20), and reported that a model is good enough or having a fine fit, when $P < 10\%$. Ismail and Ibn Idriss (2013) and many more investigators reported that a precise model must have an average AME (average model error), AAD (average absolute difference) near the zero, and a little SEE (standard error of estimate). Midilli et al. (2002), Togrul and Pehlivan (2004), Akpinar et al. (2003), and Yaldiz and Ertekin (2001) claimed that coefficient of determination(R^2), reduced chi-square (χ^2), root mean square error (RMSE), residual sum of square (RSS or SSR), mean bias error (MBE), and t-test are the crucial parameters for validation of solar drying models and are

given in Eqs. (21, 22, 23, 24, 25, and 26), respectively. The model is said to be the best model when it shows the least values for chi-square, RMSE, MBE, t-test, and maximum value of R^2:

$$\text{MRPE} \quad \text{or} \quad P = \frac{100}{N}\left[\sum_{i=1}^{N}\left(\frac{|MR_{\text{E}}\text{-}MR_{\text{P}}|}{MR_{\text{E}}}\right)\right] \tag{20}$$

$$R^2 \quad \text{or} \quad r^2 = 1 - \left\{\frac{\left[\sum_{\text{i}=1}^{N} MR_{\text{P,i}} - MR_{\text{E,i}}\right]^2}{\left[\sum_{i=1}^{N} MR_P - MR_{E,i}\right]^2}\right\} \tag{21}$$

$$\chi^2 = \left[\frac{\sum_{i=1}^{N}\left(MR_{\text{E,i}} - MR_{\text{P,i}}\right)^2}{N-n}\right] \tag{22}$$

$$E_{\text{RMS}} \quad \text{or} \quad \text{RMSE} = \left[\sqrt{\frac{\sum_{i=1}^{N}\left(MR_{\text{P,i}} - MR_{\text{E,i}}\right)^2}{N}}\right] \tag{23}$$

$$\text{RSS} \quad \text{or} \quad \text{SSR} = \sum_{i=1}^{N}\left[MR_{\text{E,i}} - MR_{\text{P,i}}\right]^2 \tag{24}$$

$$E_{\text{MB}} \quad \text{or} \quad \text{MBE} = \left[\frac{\sum_{i=1}^{N}\left(MR_{\text{P,i}} - MR_{\text{E,i}}\right)}{N}\right] \tag{25}$$

$$t = \left[\sqrt{\frac{(n-1)\times(\text{MBE})^2}{(\text{RMSE})^2 - (\text{MBE})^2}}\right] \tag{26}$$

where $MR_{\text{E, i}}$ is ith experimental value of MR, $MR_{\text{P, i}}$ is ith predicted value of MR, MR_{P} is the mean value of MR, N is the number of observations, and n is the number of constants.

3 Thin-Layer Drying Curve Models

A consistent dryer model, showing the exact drying kinetics of the agro-commodities with drying behavior of air as well as the matter to be dried, is frequently required (Karim and Hawlder 2005). A number of mathematical models for solar drying systems have been used to illustrate the deep bed and thin-layer drying of agro-products. In this segment, the advantages and limitations of each type of thin-layer models have been discussed briefly. Further, we recognize a numerous thin- layer solar drying models and tried to review the commonly used models from the literature.

Drying tempo is controlled through the exterior and interior factors of the process in conjunction with type and size of the product. Therefore, several products like fruits and vegetables are well to be dried in thin layers; however, cereal crops can be dried in deep beds into the solar dryers.

3.1 Deep Bed Drying

According to Ekechukwu (1999), in deep bed drying, agro-product is kept stationary while air progresses from lower end to upper end through the entire bed of drying chamber. Thus, it is obvious that air removes the moisture from lower zone and it goes on increasing as air moves toward upper ending. This indicates that final moisture content in deep bed drying is the mean moisture of zones. Hence, in deep bed drying, all products are not subjected to the identical condition of drying air. In deep bed drying, airflow rate, bed's depth, and drying air temperatures are the most critical factors.

3.2 Thin-Layer Drying

Many authors commented on the definition of thin layer. Menzies et al. (1971) stated that a layer is said to be a thin layer when the effect of changes in state of drying air moving through the product layer on the rate of heat and mass transport is ignored. If the thickness of product bed is up to 200 mm, it is treated as a thin layer. In general, thin-layer drying refers to the drying process in which all product slices are wholly exposed to the air under stable conditions. Numerous thin-layer drying models are existing and extensively used for showing the physics of solar drying process. These models usually classified into three categories as theoretical, semi-theoretical, and empirical (Panchariya et al. 2002; Akpinar and Bicer 2005; Akpinar E K 2006). A thin-layer equation explains the drying behavior in a unified manner regardless of the controlling means and to generalize the drying curves (Togrul and

Pehlivan 2004). Hence, experimental studies are vital, and in consequence thin-layer drying terms are imperative utensils in the modeling of solar drying.

(a) Theoretical Thin-Layer Models

Theoretical model is concerned with concurrent heat and mass transfer or diffusion equations, which provide a better indulgent of the transport processes involved. Theoretical equations were found to give inexact results in first and last stages of drying because they tend to ignore the temperature changes and moisture content dependence of the diffusion coefficient.

(b) Semi-theoretical Thin-Layer Models

Akpinar and Bicer (2005) showed that semi-theoretical models are related to approximated theoretical equations and resulting via simplifying general series solution of Fick's second law. These models require not as much of time as compared to the theoretical models and are valid only for temperature, air velocity, moisture content, and relative humidity. Parry (1985) reported that such models do not depend on assumption of geometry of product, its conductivity, and mass diffusivity. Nevertheless, the semi-theoretical equations have been successfully applied by many researchers to describe drying rates for various agricultural products. In this category, Henderson and Pabis model, Page model, and Lewis model are extensively used.

(c) Empirical Thin-Layer Models

Like semi-theoretical models, empirical model also neglects the basics of solar drying process and considers only external resistance to the moisture transport between drying air and the product to be dried (Usub et al. 2010). Empirical model provides a straight connection among the average moisture content and drying period. Afzal and Abe (2000) and Akpinar and Bicer (2005) study reveals that even though empirical models are easy to apply, they cannot offer obvious correct view of the significant drying processes, whereas they describe the drying curve for the conditions of the experimentation. In other words, empirical equation provides a better fit to the experimental data exclusive of any indulgent of the transport processes involved.

During expansion of thin-layer solar drying models for farming products, the moisture content of the product at any time is usually recorded and interrelated to the various drying parameters (Kashaninejad et al. 2005, Midilli et al. 2002). In open literature, abundant models illustrating the rate of moisture loss have been identified, while only a few of it were discussed underneath on the basis of Newton's law of cooling together with Fick's law of diffusion. Moreover, commonly used empirical models were highlighted.

3.2.1 Models Resulting from Newton's Law of Cooling

Now we will discuss the thin-layer drying models derived from Newton's law of cooling.

(a) Lewis Model

In this model, the alter in moisture content during the falling rate period is directly proportional to the instant difference among the moisture content and the anticipated moisture content as soon as it comes into equilibrium with drying air (Black 2014). He proposed the following relation (Eq. 27) on the basis of assumptions that material is thin as much as needed: adequate velocity of drying air and the constant drying conditions.

$$\text{Lewis model}: \quad \frac{\mathrm{d}M}{\mathrm{d}t} = (-K[M - M_{\mathrm{e}}]) \tag{27}$$

where K is the drying constant (includes concurrent heat and mass transport, thermal conductivity, and moisture diffusivity).

If drying constant K does not depend on the moisture content, at that moment Eq. (27) becomes

$$\text{Lewis model}: \quad \left[\frac{M_{\mathrm{t}} - M_{\mathrm{e}}}{M_{\mathrm{i}} - M_{\mathrm{e}}}\right] = MR = \exp[-Kt] \tag{28}$$

The drying constant K can be obtained from experimental information. The Eq. (28) is recognized as the Lewis equation or Newton model.

(b) Newton's Model

The Newton model is one of the simplest and commonly used drying models due to only single model constant. Sometimes it is also referred to as exponential (single exponential) or Lewis' model, as shown by Eq. (29). It neglects the interior resistance to the moisture progress. However, by correlating this fact with Newton's law of cooling, the drying tempo is directly proportional to the variation of water content among the product to be dried and EMC of drying air.

$$\text{Newton's model}: \quad MR = \exp[-kt] \tag{29}$$

where k represents drying constant in s^{-1}, MR means moisture ratio, and t is drying time.

In the earlier period, Newton's model has been extensively used for showing the drying performance of numerous agricultural and food matter. In recent times, it has rarely been found appropriate for explaining the drying kinetics of various vegetables and fruits due to underestimation as well as overestimation of drying behavior at the commencement and later stages of drying curve.

(c) Page Model

The Page model is a new modified form of Newton's model, where shortcomings linked with Newton's model are reduced with accumulation of dimensionless empirical constant (n). Due to this, Page model with two constants has been frequently used by a lot of researchers and found to be the second-best appropriate model on the basis of certain evaluation criterion used. It is commonly used in a following form shown by:

$$\text{Page model}: \quad MR = \exp\left(-kt^{\text{n}}\right) \tag{30}$$

where k and n represent drying rate and model constant (varies for each productl), respectively.

The Page model (Eq. 30) has formed fine fits for explaining the drying of lots of agricultural products and is too convenient to use (Yadollahinia et al. 2008).

(d) Modified Page Model

Modified Page model is the modification of page model and can be referred to as modified Page models I, II, and III. The model contains two constants and has been acknowledged to be eight-best solar drying model after Henderson and Pabis. The Page equation is modified and written in the following form:

$$\text{Modified Page model II}: \quad MR = \exp\left[-(kt)^{\text{n}}\right] \tag{31}$$

$$\text{Modified Page model III}: \quad MR = k\exp\left[\left(-\frac{t}{d^2}\right)^{\text{n}}\right] \tag{32}$$

where d is an investigational constant (dimensionless).

Modified Page model can also be expressed by Overhults et al. model.

3.2.2 Models Resulting from Fick's Second Law of Diffusion

Following models are derived from Fick's law and can be effectively used during drying of various agro-products.

(e) Henderson and Pabis Model

It is the first term of the universal solution of Fick's second law of diffusion and hence also referred to as a single-term exponential model. Sometimes this model can also be known as single term (Eq. 33), Brooker et al. (Eq. 34) or McCormick (Eq. 35), and approximation of diffusion model (Eq.36) and is cited as the ninth-best suitable solar drying model in the literature. In this, two model constants are used and have been successfully used in the drying of cereal crops (Meisamiasl et al. 2010). However, it has not been so successful in drying of vegetables and fruits.

$$\text{Henderson and Pabis equation}: \quad MR = a\exp(-kt) \tag{33}$$

$$\text{Brooker et al.model}: \quad X_{\mathrm{r}} = c\exp(-Kt) \tag{34}$$

$$\text{McCormick model}: \quad RU = a\exp[(-k)t] \tag{35}$$

$$\text{Approximation of diffusion equation}: \quad MR = Be^{-\mathrm{At}} \tag{36}$$

where RU and X_{r} are the mean moisture ratio, while a, b, c, and B represent shape of material (drying constants).

(f) Modified Henderson and Pabis Model

For overcoming the shortcomings of Henderson and Pabis model, it is modified by adding few constants for getting better predictions and also called as asymptotic model. It is a third term common solution of Fick's second law of diffusion. The first term of the equation shows the final part of drying process, which arises in the falling rate period, whereas the second and third term explains halfway part and first water (moisture) loss of the drying process.

The model contains six constants and third-best suitable model in drying of several agricultural materials. However, the involvement of six constants makes it complex.

$$\text{Modified Henderson and Pabis model}: \quad MR = [a\exp(-kt) + b\exp(-gt) + c\exp(-ht)] \tag{37}$$

where a, b, and c are model constants, while g and h show drying constants (1/s).

Such model finds application in drying of mushrooms, pistachios, pollen, and laurel leaves (Midilli et al. 2002; Yagcioglu et al. 1999).

(g) Midilli and Modified Midilli Model

Henderson and Pabis model was modified by Midilli by adding extra "t" with "a" coefficient. The equation shows a linear as well as an exponential term. The Midilli-Kucuk model is developed in 2012 and nowadays treated as a best model by the various researchers due to consideration of almost all parameters of drying. Hence, it is cited as a first-best appropriate model for showing best drying behavior of products and represented by the following equation. It has four drying constants and sometimes called as Midilli et al. model, as shown in Eq. (38):

$$\text{Midilli model}: \quad MR = [a \times \exp[-k(t)^{\mathrm{n}}] + (b \times t)] \tag{38}$$

Further the modified Midilli model has been used for prediction of drying kinetic of jackfruit only, expressed by Eq. (39):

$$\text{Modified Midilli model}: \quad MR = [a \times \exp(-kt) + b] \tag{39}$$

The Midilli model was recognized as the most appropriate model in more than 24% of the open journalism source assessment. It has been found to be more proper in explaining the drying behavior of chili, jackfruits, apples, ginger, mango, pepper, pineapple, and pumpkin.

(h) Logarithmic Model

It is another customized type of Henderson and Pabis model and sometimes called as an asymptotic model. It contains three model constants and in fact has a logarithmic character of the Henderson and Pabis model through accumulation of an empirical expression. It is the fourth-best drying model for describing the drying kinetic of beetroot, apple, stone apple, basil leaves, and pumpkin. The frequently used logarithmic model with three model constants is given in Eq. (40):

$$\text{Logarithmic model}: \quad MR = a\exp(-kt) + c \tag{40}$$

(i) Two-Term and Other Models

This model is a second-term universal resolution of Fick's second law of diffusion. Two-term model has four drying model constants (two model constants along with two empirical constants) and appears as the fourth-best solar drying model in the literature. The foremost term explains the final element of the drying process, whereas the second term tells information during commencement of the drying process. This model assumes the uniform material temperature and diffusivity during the drying process. We can write this equation as:

$$\text{Two-term model}: \quad MR = [a \times \exp(-k_1 t) + b \times \exp(-k_2 t)] \tag{41}$$

where K_1 and K_2 are drying constants, (1/s) while a and b are empirical constants.

This model is established to be outstanding in explaining the drying character of stuffed pepper, onion, fig, pumpkin, plum, and beetroot.

The other two-term models like Sharma et al. (Eq. 42), Sharaf-Eldeen et al. (Eq. 43), double logarithmic (Eq. 44), Henderson (Eq. 45), and two-factor models (Eq. 46) can be expressed in the following forms, respectively:

$$\text{Sharma et al. model}: \quad MR = a\exp(-bt) + c\exp(-dt) \tag{42}$$

$$\text{Sharaf-Eldeen et al. model}: \quad MR = A_0\exp(-k_1 t) + A_1\exp(-k_2 t) \tag{43}$$

$$\text{Double logarithmic model}: \quad MR = a\exp(-kt) + b\exp(-k_1 t) \tag{44}$$

$$\text{Henderson model}: \quad X_R = ae^{-k_1 t} + be^{-k_2 t} \tag{45}$$

$$\text{Two-factor model}: \quad MR = a\exp(-k\tau) + b\exp(-k_1\tau) \tag{46}$$

(j) Three-Term Model

This model is developed to further diminish the errors involved; thus, a third expression in the common solution of Fick's second law of diffusion is added. The added third expression indicates the commencement part of the drying curve, as shown in Eq. (47):

$$\begin{aligned} &\text{Three-term model}: \\ &MR = [a \times \exp(-k_1 t) + b \times \exp(-k_2 t) + c \times \exp(-k_3 t)] \end{aligned} \tag{47}$$

where a, b, and c are termed as geometric constants, while the K's are drying constants.

(k) Hii Model

The Hii model (Eq. 48) may be referred to as a modified Page or, more suitably, a modified two-term model. This model is an amalgamation of two-term with Page model. This model can be called as a complex model due to involvement of five constants. This model has been implemented effectively in describing the drying kinetics of commodities like carrot and pumpkin. Hii model can be written in the subsequent compact form:

$$\begin{aligned} &\text{Hii model}: \\ &MR = [a \times \exp(-k_1 (t)^n) + b \times \exp(-k_2 (t)^n)] \end{aligned} \tag{48}$$

(l) Two-Term Exponential Model

The two-term expression is modified by reducing the number of unchanged factors and improving the indication of shape constant of the second exponential term. The two-term exponential model (Eq. 49) is also used by few researchers during drying of agricultural products and is renowned to be the ninth excellent model. The model has three constants and found to be admirable in showing the drying behavior of just star fruit.

$$\begin{aligned} &\text{Two-term exponential model}: \\ &MR = [a \times \exp(-kt) + [(1 - a) \times (\exp(-kat))]] \end{aligned} \tag{49}$$

(m) Verma Model

Verma model is also developed by modifying two-term model, which contains four model constants and found to be the eleventh-appropriate model in drying of pumpkin along with parsley.

$$\text{Verma model}: \quad MR = a\exp(-kt) + (1-a)\exp(-gt) \tag{50}$$

(n) Approximate Diffusion Model

The approximate diffusion model is occasionally known as simplified diffusion model. It includes four constants and has found to be sixth-best model in solar drying. It is a supplementary revision of term model with constant "b" in the second fraction of the model along with (k and t) drying constant. Equation (51) represents the diffusion model:

$$\begin{aligned}&\text{Approximate diffusion model}:\\ &\text{RU} = [a \times \exp(-kt) + (1-a) \times (\exp(-kbt))]\end{aligned} \tag{51}$$

From the literature, we can say that the drying behavior of pumpkin, tomato, and green pepper has been successfully expressed by approximate diffusion model.

3.2.3 Empirical Models

The commonly used empirical models to describe the drying characteristics of several produces were discussed.

(o) Wang and Singh Model

Wang and Singh projected an innovative empirical model intended for alternating drying of rice. It includes two constants and is well known as the fifth-appropriate model; however, it does not have any physical or theoretical understanding. Equation (52) shows the expression of Wang and Singh model:

$$\text{Wang and Singh model}: \quad MR = 1 + at + bt^2 \tag{52}$$

where a, b = drying constants which can be obtained from the experimentation.

This expression has been established as an excellent model in explaining the drying kinetic of banana.

(p) Diamante Model

Diamante utilizes polynomial regression study to find out the values of the constants involved in the model. Similar to the Wang and Singh model, this model is also unable to give the exact physical and theoretical knowledge of the drying phenomenon.

From the literature, we can say that drying phenomenon of kiwifruit with apricot has been fruitfully uttered by Diamante et al. model as expressed by Eq. (53):

$$\text{Diamante et al.model}: \quad [n \times (-\ln MR)] = \left(1 + \boldsymbol{b} \times (\ln\ \boldsymbol{t}) + \mathrm{c} \times (\ln\ \boldsymbol{t})^2\right) \tag{53}$$

(q) Weibull Model

It is the twelfth-appropriate drying curve fitting model having two constants only. This model can be expressed by Eqs. (54 and 55). Literature of mathematical modeling shows that Weibull model was effectively used for describing the drying behavior of quinces, garlic, etc.:

$$\text{Weibull model}: \quad M_{\mathrm{R}} = [\mathrm{a} - \mathrm{b} \times \exp(-\mathrm{k}(t)^n)] \tag{54}$$

$$\text{Weibull model}: \quad \mathrm{MR} = [\mathrm{A} - (\mathrm{B} \times \exp(-\mathrm{K}(t)^n))] \tag{55}$$

Corzo et al. (2010) projected the use of a statistical model for the explanation of drying and employed the Weibull distribution which had merely been applied for osmotic dehydration plus rehydration characteristics, as shown by Eq. (56):

$$\mathrm{MR} = \exp\left[-\left(\frac{t}{\mathrm{a}}\right)^{\mathrm{b}}\right] \tag{56}$$

where a, b and A, B are constants (dimensionless), while k and K represent drying constant.

(r) Thompson Model

Thompson developed an empirical expression from the investigational data via correlating the time as a function of the logarithm of MR. The model was unable to show the drying kinetics of nearly all fruits and vegetables since it has no hypothetical base and lacks substantial explanation of the process involved. Still, the model has been found to be appropriate in favor of drying behavior of blueberries and green peas. The model has two constants and is cited as first-best appropriate drying model through literature. Equation (57) represents the expression for Thompson model:

$$\text{Thompson model}: \quad t = \left[(\times \ln\ (MR)) + b \times [\ln\ (MR)]^2\right] \tag{57}$$

(s) Da Silva Model

Da Silva presented an expression for showing moisture movement phenomenon inside the grains of chickpea. The expression for Da Silva model is given by Eq. (58):

$$\text{DaSilva et al. model}: \quad MR = \exp\left(-at - b\sqrt{t}\right) \tag{58}$$

(t) Peleg Model

Peleg expression has no material understanding and theoretical knowledge. Nevertheless, it has been used fruitfully just in explaining the drying kinetics of banana, as shown by Eq. (59):

$$\text{Peleg model}: \quad M_R = \left(1 - \frac{t}{a + bt}\right) \tag{59}$$

The Wang and Singh, Diamante, and Thompson model shows the polynomial or second-order quadratic expressions indicating highest moisture ratio at the beginning; later on it reduces and finally yet again increases with regard to time. But in actual practice, such situations are not viable in solar drying processes.

Hence, it is easy to understand that the complications of the thin-layer model are largely based on the quantity of constants involved in it. The thin-layer drying models have constants varying between one constant and six constants. From the revision of above models, it is not possible to choose the model explaining the thin-layer curve in view of the number of model constants. In short, the constants involved in the models are not a decisive factor for choosing the outstanding model. Nevertheless, it is anticipated that the drying model should provide precise outcome for optimization of drying conditions of the agro-commodities.

4 Applications of Thin-Layer Drying Curve Models

In solar drying, the drying kinetics of product and the drying period being studied are anticipated to be most significant areas of drying. Hence, there is a need of time to recognize, categorize, assess, and compare thin-layer drying curve models. A review editorial on various thin-layer drying models projected by different researchers for diverse types of solar drying systems, agricultural materials, type of product, pretreatment of material, and different drying variables was presented by Kucuk H. et al. (2014). The study revealed that uncertainty analysis should be used not only in the analysis with modeling of the thin-layer drying but also in designing and performing cost analysis of solar dryers. A comprehensive review for modeling of thin-layer drying for selected Nigerian produce has been recently offered by Chukwunonye et al. (2016) and reported that the Page and Midilli et al. models are the dominating models. They suggest that the statistical approach is the most appropriate method of investigation for the performance of all thin-layer drying models available in literature. Recently, an endeavor was made by Onwude et al. (2016) illustrating an extensive outline of the thin-layer drying theories,

expressions, implication, activation energy, and effectual wetness diffusivity with outcome of modeling thin-layer drying of foodstuffs. The study revealed that temperature and thickness of commodity are mainly responsible for altering the thin-layer drying behavior of vegetables along with fruits. Further, facts from the journalism indicate that drying of fruits along with vegetables occurs just in the falling rate period, and in relation to this, 22 thin-layer models were found to be relevant in illuminating the drying kinetics of vegetables and fruits.

This heading mainly deals with assessment of thin-layer drying models existing in the text during the last decade. In this view the models are examined by considering different variables like drying method engaged, type of product, and drying variables such as air velocity, temperature, shape of product, etc. In addition, the coefficient of determination R^2, chi-square, mean bias error (MBE), and root mean square error (RMSE) are the most important criteria for selecting the best curve equation. Researchers reported that the best suitable model should have higher values of R^2 and lower values of chi-square, MBE, and RMSE. The author hoped that this review effort may be precious and suitable for future improvement of work.

Yaldiz et al. (2001) constructed a forced convection solar dryer for the development of a mathematical thin-layer drying model meant for sultana grapes and few vegetables like onion, pumpkin, green beans, green pepper, and stuffed pepper. Initially, during development of thin-layer solar drying model for grapes, they used eight semi-theoretical models and tried to find out the connection of the coefficients and constants of the most excellent model among the drying variables like drying air velocity and temperature. All these models were compared with the statistical parameters and reported two-term drying model as a satisfactory model for the produce having correlation coefficient of $R = 0.979$. The constants and coefficients involved in two-term model were regressed beside those of drying air velocity and temperature via multiple regression analysis. Further result shows that the grapes of 3 kg water per kg dry matter of initial moisture content were dried to 0.16 kg water per kg dry matter in solar dryer. Later on Yaldiz and Ertekin (2001) worked on the same dryer for drying a few vegetables as mentioned above. During this investigation, drying curves for every vegetable under study were uttered by the effect of drying air velocity. Three unlike drying air velocities were used in drying process for investigating its effect with drying period. The obtained drying curves then fitted with 12 diverse moisture ratio equations and regression analysis (logarithmic, linear, exponential, and power regression models) were finished by means of statistical computer program. Result of regression analysis shows the values of *MR* by high R^2 stuck between 0.9972 and 0.9999. With solar dryer under consideration, it is possible to accomplish drying air temperature in the range of 38.56–45.82 °C for different drying air velocities.

Numerous studies have been presented on natural and forced convection dryer by Akpinar et al. in a period of 2003–2010. Akpinar et al. (2003) also work on the convective cyclone dryer to examine the lone-layer drying phenomenon of potato as well as to perform mathematical modeling by using thin-layer drying models

available in literature. This type of dryer does not work on solar energy, hence not discussed here.

An indirect forced convection solar dryer was developed by Akpinar and Bicer (2008) to compare the slim-layer drying behavior of green pepper (1.7 mm thickness) under open sun (natural convection) and forced convection mode. Consecutively to clarify the drying performance and to build up mathematical model for pepper, 13 models were selected from articles published and then applied for both free and forced convective solar drying. The thin-layer equations were tested to select most appropriate model by statistical computer program. The performance of all models was also determined by comparing the coefficient of determination, reduced chi-square, and RMSE among the experimental and predicted *MR*. Result shows that Midilli model ($R = 0.99656$, RMSE = 0.02404129) and logarithmic model ($R = 0.98815$, RMSE = 0.040998285) for natural sun and forced convection drying were found to be most appropriate models to clarify the slim-layer aeration characteristics of long peppers. Later on Akpinar E. (2008) tested the same dryer under same conditions (natural open and forced convection mode) for drying of white mulberry. The experimental data was fitted to the earlier 13 models for explaining the drying kinetics of white mulberry and found that instead of Midilli model, Verma et al. model shows the best fit in open sun drying, while for forced convection mode, logarithmic model shows the best conformity between the results. In this study the author also found out the effective moisture diffusivity estimated to be 3.560×10^{-9} m^2/s in forced convection and 2.4×10^{-9} m^2/s in natural convection mode of drying. Further he tested the same solar dryer for describing the drying kinetics of mint leaves in natural and forced convection mode. The energy analysis on the basis of first law of thermodynamics was done for energy utilization ratio (EUR) and found out to be in the range of 7.826–46.285%. Nevertheless, exergy analysis by using second law of thermodynamics for drying of mint leaves was also performed to determine exergetic efficiency (34.8–87.72%). The moisture content of mint leaves was reduced from 6.14 to 0.05 gram of water/gram of dry matter in 3.5 h of drying in solar cabinet, whereas it took 6.5 h to trim down the water content to 0.09 gram of water/gram of dry stuff during natural open sun drying. The moisture content data at the different experimental mode were transformed to the main handy moisture ratio expression, and after that, curve fitting computations with the drying time were done on the ten drying models by Akpinar E. K. (2010). The results of statistical analysis undertaken show that drying data was best fitted to the Wang and Singh model for both forced convection ($R = 0.99918$, RMSE = 0.01361781) and open sun ($R = 0.99883$, RMSE = 0.01744519) drying mode.

A mathematical modeling of slim layer natural (open sun) and forced convective aeration of shelled along with unshelled pistachio was presented by Midilli A. and Kucuk H. (2003a, b). From available semi-theoretical and empirical models, eight drying models were selected, then applied to the data (obtained from experimentation), and solved by numerical program (statistica) for determination of R^2 (coefficient of determination). As per the results of multiple linear regression investigation, out of eight drying models selected, the logarithmic model as well

as two-term model effectively shows the thin-film drying behavior of pistachio in forced and natural convective mode, respectively. When the effect of drying air temperature on the coefficients and constants of the logarithmic drying model was examined, the subsequent model gave an $R^2 = 1$, $\chi^2 = 4.041 \times 10^{-9}$ for unshelled pistachios, and $R^2 = 1$, $\chi^2 = 5.914 \times 10^{-10}$ for shelled pistachios (forced convection mode). Moreover, two-term model gave an $R^2 = 1$, $\chi^2 = 9.775 \times 10^{-10}$ for unshelled pistachios, and $R^2 = 1$, $\chi^2 = 4.378 \times 10^{-9}$ for shelled pistachios (natural sun drying). The temperature in the dryer varies from 40 to 60 °C (for velocity of 1.23 m/s) in forced convection and 21–32 °C (for velocity of 0.8 m/s) in open sun drying mode.

El-Sabaii et al. (2002) conducted experiments for drying of vegetables as well as fruits like peas, figs, onions, tomatoes, and seedless grapes in an indirect natural convective solar dryer. The constants and coefficients of Henderson's model were calculated on the basis of mass and energy balance equations. Result showed that the linear correlations among drying product temperature T_{dp} and drying constant k were estimated satisfactory to illustrate the drying trend of fruits and vegetables under inspection.

Bahnasawy and Shenana (2004) developed a mathematical model of open sun (natural convection) and solar drying of Kashk (dairy product). Authors considered the various parameters like solar insolation, amount of heat energy received as well as lost from the solar dryer bin wall, and the latent heat of water vaporization for developing equations to describe the drying kinetics of system. Result showed that the model is competent to forecast moisture loss and drying air temperature for different values of *RH*. From experimentation authors conclude that the model is most excellent to utilize air at high velocity with less temperature at the start of drying, while air at high temperature should be utilized in the later stages of drying.

Sacilik K. et al. (2006) developed and tested STD (solar tunnel dryer) for aeration of organic tomato in the environment of Ankara, Turkey. The study was undertaken to explore the thin-layer drying behavior of tomato and to fit the experimental data to ten semi-theoretical models. The nonlinear least squares regression method was used to fit the experimental data. The statistical parameters like R^2 (coefficient of determination), P (MRPE), RMSE, and reduced chi-square (χ^2) were considered to compare best fit. Result shows that values of R^2, P, RMSE, and chi-square (χ^2) for all ten models vary in the range of 0.9350–0.9809, 10.01–26.48%, 7.77×10^{-3}–13.98×10^{-3}, and 1.96×10^{-3}–6.31×10^{-3}, respectively. An approximation of diffusion model was considered to be the most excellent model due to the highest values for R^2. The water content was reduced from 93.35 to 11.50% (w.b.) within 4 days in STD, while the open sun drying takes 5 days for the same moisture reduction. Further, investigational study was performed by Sacilik K. (2007) for illustrating the drying behavior of pumpkin in STD (solar tunnel dryer) as well as in open sun (natural convection) drying. The experimental data obtained from the testing has been used to fit the Henderson and Pabis, two-term, and Page along with logarithmic model. A nonlinear regression analysis was used to determine the drying and model constants. All the models were compared on the basis of statistical indicators for determining the best suitable

model for describing the drying kinetics of pumpkin. During experimentation, hot air flows at a consistent rate of 0.8 m/s over the pumpkin; in addition to this, the temperature of air in the range of 40–60 °C was noted.

Forson et al. (2007) offered a mathematical modeling (collector model, drying chamber model, and technical concert criterion model) meant for drying of farming products under mixed mode natural convection dryer. Authors considered SPDDSAH (single pass double duct solar air heater) for investigation and derived the governing equations for product temperature with its moisture content, drying air temperature along with absolute humidity, and various performance-decisive factors. The predicted and experimental data describes the performance of natural dryer for drying of farming products.

A forced convection dryer was developed by Zomorodian A. and Moradi M. (2010) for drying of *Cuminum cyminum* through mixed and indirect drying methods. In this study, they also tried to report best-suitable thin-layer model for *Cuminum cyminum*. For this purpose, Zomorodian and Moradi selected 11 semi-theoretical and empirical models. A nonlinear regression investigation technique was used to determine the relevant coefficients and constants for each model. To authenticate the integrity of the fit, three statistical criteria were found out by using MSTATC and Excel software. Finally, authors concluded that among 11 thin-layer mathematical models commonly applied, the Midilli and approximation of diffusion model showed the most excellent curve-fitting outcome for the experimental *MR* values in indirect and mixed mode operation, respectively.

Lahsasni et al. (2004) proposed a mathematical model for describing thin-film drying of prickly pear peel in forced convection mode. The solar dryer comprises collector, drying cabinet, and circulating fan for moving the drying air above the produce. The experimental readings were carefully noted and plotted in terms of drying curve, which shows that drying takes place merely in falling rate juncture. The drying curves developed were fitted to the number of semi-theoretical as well as empirical equations and also evaluated by regression analysis. Finally result showed that Midilli-Kucuk drying model was found suitable ($R = 0.9998$ and $\chi^2 = 4.6572 \times 10^{-5}$) for explaining the drying kinetics of the produce.

Basunia and Abe (2001) investigated natural convection mixed mode solar dryer, meant for rough rice at Matsuyama, Japan. Further they tried to describe the drying kinetics of medium grain rice through Page model. The experimental data like drying air temperature and velocity, sample moisture loss, etc. were regularly recorded throughout the drying process. Finally, all experimental data was fitted to Page model. The modeling is based on the difference among opening and concluding moisture contents as well as EMC. Fudholi A. et al. (2013) conducted an investigational analysis for drying of ginger at different mass flow rates 0.06–0.12 kg/s. The moisture content of ginger has been reduced from 89 to 8% (w.b.). Author uses three semi-theoretical drying models (Page; Newton; Henderson & Pabis) in order to demonstrate most excellent model for ginger at dissimilar mass flow rate. The change in moisture content against time was calculated via Excel software; however, graphical method is used for determination of drying constants. The study revealed that the Page model has the maximum value of

R^2 (0.9633), along with the minimum values of RMSE (0.0348) and MBE (0.0012), in comparison to the Newton and Henderson and Pabis model.

The drying kinetics of chili pepper with solar and open sun drying (solar cabinet dryer) was investigated and presented by Tunde-Akintunde T. Y. in 2011 under the environmental conditions of Ogbomosho, Nigeria. He conducted the experiments on both pretreated and untreated chili pepper and found that drying rate of pretreated produce is quicker than untreated one. Fick's diffusion (slab geometry) was applied to the investigational data. The *MR* values were evaluated by using experimental data for predicting the drying behavior of pretreated and untreated samples of chili. Four statistical criteria were used to compute the integrity of fitting, and result showed that the Page model which gave lesser values of MBE, chi-square, and RMSE along with higher values of R^2 was considered as the best appropriate model for predicting the drying kinetics of solar and sun-dried chili pepper.

Ismail and Ibn Idriss (2013) developed a flat plate-type free convective solar dryer for conducting thin- layer drying investigations on the entire okra pods. They selected Newton's and Page models for describing the drying kinetics of okra and observed that drying process takes place in the falling rate period. Further they showed that the moisture movement inside the okra pods is largely due to diffusion phenomenon. During investigation, the drying curve of okra has been set with Page and Lewis drying models; however, result showed that Page model predictions were found to be more precise. This is due to fact that the probability of Page model is less than 0.05. The author also evaluates the integrity of fit between predicted and experimental data by using two sample-independent t-tests. Further few statistical parameters like AAD (average absolute difference), AME (average model error), and RMSE (root mean square error) were compared. MINITAB statistica (Release 13.30) software has been adopted by the author for validation purpose and showed the values for AME, AAD, and SEE as 0.001, 0.125, and 0.160 correspondingly for Page model, 0.128, 0.224, and 0.324, respectively, for Lewis model. The prediction of Page model was found to be more precise as compared to Lewis model. The other observation during experimentation like a maximum temperature difference of 41.9 °C has been noted between collector and ambient air; moisture content of okra was reduced from 84.64 to 13.61% (w.b.).

5 Case Study: Mathematical Modeling for Solar Drying Systems

This section presents characteristics of case study for different types of solar dryer (solar tunnel, greenhouse, indirect, and mixed mode solar dryers) for drying of several agro-commodities (banana, tomato, and potato) to illustrate the application of mathematical modeling approach in determining the optimized design and operating conditions. In the first case study (Karim and Hawlader 2005), a

simulation model considering the concurrent heat and mass transfer processes along with shrinkage effect was proposed for explaining the drying characteristics of banana, while in later studies various energy and mass balance equations were proposed by Janjai (2012) and Smitabhindu et al. (2008) for solar dryer operating in direct and indirect mode, respectively. Finally, the case study proposed by Kumar and Tripathy (2009) for determination of $D_{effective}$ and h_m by using drying coefficients k, k_0 along with lag factor was discussed.

5.1 Mathematical Modeling for Solar Tunnel Dryer

Karim and Hawlader (2005) presented the mathematical model for STD meant for explaining the drying characteristics of banana. During study, shrinkage of material and both material as well as equipment model was considered.

5.1.1 Material Model

To make things easier, few assumptions like 1-D moisture movement and heat transfer rate, no chemical reaction during drying, the material shrinkage effect through drying, and consistent dissemination of air throughout the solar dryer were made. The matter which is to be dried is considered as a thin wall or slab (thickness $L = 2b$) subjected to air at temperature Ta and relative humidity RH. The shrinkage outcome appears plainly in expressions of velocity u(x) into heat and mass transport expressions.

A concept of control volume of thickness dx has been used by the author to determine mass and heat transfer rates.

The conservation of mass equations for CV can be uttered as

(Moisture increase in control volume – Moisture out of CV) + mass generated = mass stored in CV

Net change in moisture due to diffusion in control volume is given by

$$= \left(N''_X \times A - N''_{X+\mathrm{d}X} \times A\right) = \left[\left(N''_X \times A\right) - \left(\left(N''_X \times A\right) + \left(N''_X \times A + \frac{\partial\left(N''_X\right)}{\partial X} A dX\right)\right)\right]$$
$$= \rho A D \frac{\partial^2 M}{\partial X^2} dX \tag{60}$$

Similarly, net change in moisture for shrinkage is

$$= N''_{S,X} A - N''_{S,X+dX} A = \rho u M A - \rho(M + \Delta M) u A = -\rho u \Delta M A \tag{61}$$

Now, moisture storage in CV is

$$= \rho u \mathrm{d}X \frac{\partial M}{\partial t} \tag{62}$$

The generation is taken as zero, since no chemical reaction occurs throughout the drying process.

Combining Eqs. (60 and 62), the conservation of mass equation is expressed by Eq. (63) as

$$\frac{\partial M}{\partial t} + u\frac{\partial M}{\partial X} = D_{\text{effective}} \frac{\partial^2 M}{\partial X^2} \tag{63}$$

Conservation of energy equation can be also written as

(Energy gain in control volume − Energy going away of control volume) + Energy generated = energy storage in control volume

By solving above energy balance, conservation of energy equation is obtained and expressed by Eq. (64) as

$$\frac{\partial T}{\partial t} + u\frac{\partial T}{\partial X} = \alpha \frac{\partial^2 T}{\partial X^2} \tag{64}$$

where $D_{\text{effective}}$, D_{ref} represent effective and reference diffusion coefficient (m^2/s); k is the thermal conductivity (W/m K); N is the moisture flux (kg/m^2s); u is the shrinkage velocity (m/s); x and z indicate distance from the center of the drying sample and inlet of dryer, respectively (m) (kg/kg dry air); and Z means length of dryer (m).

The author uses the following expression (Eq. 65) for effective diffusion coefficient and the thickness ratio:

$$\frac{D_{\text{ref}}}{D_{\text{effective}}} = \left(\frac{b_0}{b}\right)^2 \quad \text{and} \quad b = b_0\left[\frac{\rho_w + \bar{M}\rho_s}{\rho_w + M_0{}^{-}\rho_s}\right] \tag{65}$$

At this time, as the shrinkage rate cannot be predicted and experimentation study is not easy, that is why a linear distribution of shrinkage rate is assumed. Thus, the velocity at any point and at outer surface is given by Eq. (66):

$$u(X) = u(b)\frac{X}{b} \quad \text{and} \quad u(b) = \frac{b - b_{\text{old}}}{\Delta t} \tag{66}$$

The moisture content at the beginning of the drying is assumed to be uniform. Hence, using boundary conditions,

Initial boundary conditions are $M_{\text{t=0}} = M_0$ and $T_{\text{t=0}} = T_0$

$$\text{At} X = 0, \frac{\partial M}{\partial X} = 0 \quad \text{and} \quad \frac{\partial T}{\partial X} = 0$$

At $X = b$, moisture and energy balance becomes

$$\begin{aligned} -\mathrm{D}_{\text{effective}} \frac{\partial M}{\partial X}_{@X=b} + uM_{@X=b} &= h_m (M - M_e)_{@X=b} \quad \text{and} \\ \left(\mathrm{k} \frac{\partial T}{\partial X} - \rho C_P u T\right)_{@X=b} &= h(T_a - T)_{@X=b} - h_m (M - M_e) h_{fg@X=b} \end{aligned} \tag{67}$$

Karim and Hawlader (2005) use the following mass transfer coefficient correlations for laminar and turbulent flow, shown by Eq. (68):

$$\begin{aligned} Sh &= \frac{h_{\mathrm{m}} L}{D_{\mathrm{O}}} = 0.332 \mathrm{Re}^{0.5} Sc^{0.33} \\ Sh &= \frac{h_{\mathrm{m}} L}{D_O} = 0.0296 \mathrm{Re}^{4/5} Sc^{1/3} \end{aligned} \tag{68}$$

Similarly, heat transfer coefficient was determined by using Eq. (69):

$$\begin{aligned} N_{\mathrm{u}} &= \frac{h \times L}{D_{\mathrm{O}}} = 0.332 \times (R_{\mathrm{e}})^{0.5} \times (\mathrm{Pr})^{0.33} \\ N_{\mathrm{u}} &= \frac{h \times L}{D_{\mathrm{O}}} = 0.0296 \times (R_{\mathrm{e}})^{0.5} \times (\mathrm{Pr})^{0.33} \end{aligned} \tag{69}$$

where h_{m} is mass transfer coefficient (m/s); h shows convective heat transfer coefficient (W/m^{2}K); N_{u}, Pr, Re, Sc, and Sh represent dimensionless Nusselt, Prandlt, Reynolds, Smith, and Sherwood number, respectively; and L is the thickness of the product sample (m).

5.1.2 Equipment Model

In formulating a set of differential expressions for showing variation within drying air throughout the drying process, assumptions like 1−D problem, negligible conduction inside the bed and bed porosity, uniform distribution of product in drying chamber, and constant thermal properties of air and moisture were made. Using concept of CV in dryer (thickness dZ on distance Z as of inlet of dryer), energy balance equation for dryer was determined. Therefore, change in energy of air across CV may be written as shown in Eq. (70):

$$G_{\mathrm{o}} C_{\mathrm{Pa}} \frac{\partial T_{\mathrm{a}}}{\partial Z} \mathrm{d}Z \mathrm{d}t = \varepsilon \rho_{\mathrm{a}} \mathrm{d}Z C_{\mathrm{Pa}} \frac{\partial T_a}{\partial Z} \mathrm{d}t - - - - - (\because G_{\mathrm{o}} = \varepsilon \rho_{\mathrm{a}}) \tag{70}$$

The Eq. (71) shows change in sensible heat of product owing to alter in temperature with time:

$$\begin{aligned} &= \left[(1-\varepsilon) \times \rho_S \frac{\partial T_S}{\partial t} \times (c_s + c_w M) \times \mathrm{d}Z\mathrm{d}t\right] \\ &= \varepsilon \rho_a \mathrm{d}Z C_{Pa} \frac{\partial T_a}{\partial Z} \mathrm{d}t - - - - - (\because G_o = \varepsilon \rho_a) \end{aligned} \tag{71}$$

Now, the energy necessary to evaporate the moisture from the material is given by Eq. (72):

$$= h_{fg} \frac{\partial M}{\partial t} \rho_S (1-\varepsilon) \mathrm{d}Z\mathrm{d}t \tag{72}$$

Hence, energy stability Eq. (73) among air and material is

$$\begin{aligned} -G_o C_{Pa} \frac{\partial T_a}{\partial Z} \mathrm{d}Z\mathrm{d}t = \varepsilon \rho_a \mathrm{d}Z C_{Pa} \frac{\partial T_a}{\partial t} \mathrm{d}t + (1-\varepsilon)\rho_S \frac{\partial T_S}{\partial t} (c_s + c_w M)\mathrm{d}Z\mathrm{d}t \\ - h_{fg} \frac{\partial M}{\partial t} \rho_S (1-\varepsilon) \mathrm{d}Z\mathrm{d}t \end{aligned} \tag{73}$$

where $T_o/T_a/T_s$ means initial or air or surface temperature.

Finally, author focuses on the mass equilibrium with variation in humidity of air leaving the control volume and expressed by following Eqs. (74, 75, and 76):

Change in *RH* of air coming out of CV is

$$= G_o \left(\frac{\partial Y}{\partial Z}\right) \mathrm{d}Z\mathrm{d}t \tag{74}$$

Increase in moisture content of air for time dt is

$$= \varepsilon \rho_a \left(\frac{\partial Y}{\partial t}\right) \mathrm{d}t\mathrm{d}Z \tag{75}$$

Water evaporated from product is

$$= \rho_s (1-\varepsilon) \left(\frac{\partial M}{\partial t}\right) \mathrm{d}t\mathrm{d}Z \tag{76}$$

Therefore, moisture balance Eq. (77) is

$$G_o\left(\frac{\partial Y}{\partial Z}\right)\mathrm{d}Z\mathrm{d}t + \varepsilon\rho_a\left(\frac{\partial Y}{\partial t}\right)\mathrm{d}t\mathrm{d}Z = -\rho_s(1-\varepsilon)\left(\frac{\partial M}{\partial t}\right)\mathrm{d}t\mathrm{d}Z$$
$$\therefore G_o\left(\frac{\partial Y}{\partial Z}\right) + \varepsilon\rho_a\left(\frac{\partial Y}{\partial t}\right) = -\rho_s(1-\varepsilon)\left(\frac{\partial M}{\partial t}\right) \tag{77}$$

In actual practice, time derivatives are neglected in comparison with their space derivatives for obtaining the good approximation (Van Meel 1958). Hence, the energy and mass balance equations are

$$-\frac{G_o C_{Pa}}{\rho_S(1-\varepsilon)}\frac{\partial T_a}{\partial Z} = \frac{\partial T_S}{\partial t}(c_s + c_w M)\mathrm{d}Z\mathrm{d}t - h_{fg}\frac{\partial M}{\partial t} \quad \text{and}$$
$$G_o\left(\frac{\partial Y}{\partial Z}\right) = -\rho_s(1-\varepsilon)\left(\frac{\partial M}{\partial t}\right) \tag{78}$$

The initial and final boundary conditions are

$$\mathrm{At\,X} = 0, \mathrm{t} = 0; \mathrm{T_a} = T_0, \frac{\mathrm{d}T_a}{\mathrm{d}t} = 0 \quad \text{and} \quad \mathrm{Y} = Y_0, \frac{\mathrm{dY}}{\mathrm{d}t} = 0$$
$$\mathrm{At\,X} > 0, \mathrm{t} = 0; \mathrm{T_a} = T_0, Y = Y_0$$

where G_o= air mass flux (kg/m^2 s), ρ_a or ρ_s means air density or solid/shrinkage/surface density (kg/m^3), ε = bed void portion, b is half thickness of product sample (m), C_s and C_w show specific heat of solid and water (J/kgK), C_{pa} represents specific heat of air (J/kgK), M is moisture content of specimen (g/g dry), t = time (s), Y is air humidity ratio, and h_{fg} shows enthalpy of evaporation (J/kg).

5.1.3 Method of Solution

All governing expressions describing the drying kinetics of material and dryer were solved numerically, while initial and equivalent moisture content along with diffusion coefficient of product (banana) was found out experimentally. To solve the finite differential equations, a processor program in FORTRAN language was prepared by the author.

Eq. (79) can be effectively used for determination of diffusion coefficient:

$$\ln\frac{M}{M_0} = \ln\left(\frac{8}{\pi^2}\right) - \frac{\pi^2 Dt}{L^2} \tag{79}$$

Extensive experimentations on tunnel dryer for drying of banana were conducted by authors, and they conclude that the experimental outcome validates the mathematical model developed. The mathematical model is easy and competent to give the consistent predictions for drying rate, temperature, as well as moisture distributions in both drying air and product to be dried.

5.2 Mathematical Modeling for Greenhouse-Type Dryer

Janjai (2012) developed a greenhouse type of solar dryer (8 m width, 20 m length, and 3.5 m height) at Thailand for drying of 1000 kg of tomatoes. For continual drying process, the author used a LPG burner (capacity: 100 kW) for supplying hot air during hours of darkness plus in showery or overcast days. The author formulated a set of partial differential equations for heat and mass transfer for dried out tomatoes.

The following assumptions were made by Janjai during mathematical modeling of greenhouse dryer:

(I) Drying calculation depends on a thin-film drying model.
(II) No air stratification inside the dryer.
(III) Specific heat of dryer cover, drying air, and product to be dried remains stable.

Figure 1 shows the schematic for energy transport within the solar greenhouse dryer.

5.2.1 Energy Balance of the Cover

Heat energy in cover can be shown by following Eq. (80):

$$Q_C = Q_{ac} + Q_{cam} + Q_{sc} + Q_{solar} + Q_{pc} \tag{80}$$

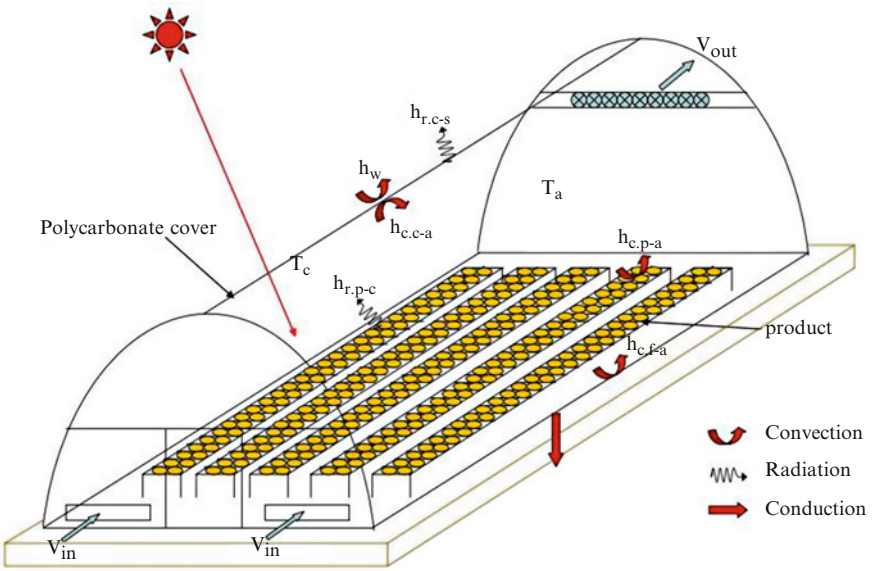

Fig. 1 Energy transfer within the greenhouse dryer

where Q_c is heat energy within drying air and cover due to convection, Q_{cam} is energy transfer between cover and ambient air, Q_{sc} is energy transport among atmosphere and cover owing to radiation, Q_{solar} is heat absorbed by cover from solar insolation, and Q_{pc} is energy exchange between drying product and cover by radiation.

The Eq. (80) can further be presented by Eq. (81) as

$$m_c C_{pc} \frac{dT_C}{dt} = A_C h_c (T_a - T_C) + A_C h_W (T_{am} - T_C) + A_C h_r (T_S - T_C) + A_c \alpha_c I_t + A_P h_r (T_p - T_C) \quad (81)$$

where m_C is mass of cover, A_c is area of cover, C_{pc} is sp. heat of collector, T_a is drying air temperature, T_C is cover temperature, T_S is sky temperature, T_p is product temperature, T_{am} is ambient temperature, h_C is convective heat transfer coefficient, h_r is radiative heat transfer coefficient, h_W is convection heat transfer coefficient between cover and atmosphere, α_c is absorptivity of cover material, and I_t is solar insolation.

5.2.2 Energy Balance of Air Inside the Dryer

Similarly, the gain in heat energy of air can be obtained by doing energy balance as shown in Eq. (82):

$$Q_{ad} = Q_{fa} + Q_{pa} + Q_{produce} + Q_{airflow} + Q_{loss} + Q_{sd} \quad (82)$$

where Q_{ad} is increase in heat energy of air within dryer, Q_{pa} is thermal energy transfer among product and air due to convection, Q_{fa} is energy transfer between floor and air owing to convection, $Q_{produce}$ is increase in heat energy of air by product, $Q_{airflow}$ is heat gain in air chamber due to airflow at inlet and outlet, Q_{loss} is energy loss from drying air to atmosphere, and Q_{sd} is energy absorbed by air in dryer as of solar radiations.

The Eq. (82) can be written as

$$\begin{aligned} m_a C_{pa} \frac{dT_a}{dt} = {} & A_f h_c (T_f - \mathrm{Ta}) + A_P h_c (T_P - \mathrm{Ta}) \\ & + \left[D_P \times A_P \times C_{PV} \times \rho_P \times (T_p - T_a) \frac{dM_P}{dt} \right] \\ & + (\rho_a V_{out} C_{Pa} T_{out} - \rho_a V_{in} C_{Pa} T_{in}) + U_C A_C (T_{am} - T_a) \\ & + [(1 - F_P)(1 - \alpha_f) + (1 - \alpha_P) F_P] A_C \alpha_C I_t \end{aligned} \quad (83)$$

where D_P is product thickness; A_P is area of product; C_{Pa} and C_{PV} are specific heat of air and water vapor, respectively; ρ_a and ρ_p are density of air and product,

respectively; V_{in} and V_{out} are airflow rate at inlet and outlet of dryer, respectively; T_{in} and T_{out} are temperature of air at inlet and outlet of dryer, respectively; U_C is overall heat loss coefficient; F_P is part of solar radiation falling on the product; and α_P and α_f are absorptivity of product and floor, respectively.

5.2.3 Energy Balance of the Product

Equation (84) shows the thermal energy balance for product:

$$Q_P = Q_{ap} + Q_{cp} + Q_{sp} + Q_{P\,loss} \tag{84}$$

where Q_P is gain of heat energy in product, Q_{ap} is thermal energy transfer among air and product due to convection, Q_{cp} is energy transfer between cover and product owing to radiation, Q_{sp} is solar radiations absorbed by product, and $Q_{P\,loss}$ is loss of energy (sensible plus latent) from product.

The Eq. (84) can further written as

$$m_P\left(C_{pg} + C_{PP}M_P\right)\frac{dT_P}{dt} = A_P h_c(T_a - T_P) + A_P h_r(T_C - T_P) + F_P A_C \alpha_P I_t \tau_C + D_P A_P \rho_P [L_P + C_{PV}(T_a - T_P)]\frac{dM_P}{dt} \tag{85}$$

where m_p is mass of product, M_P is moisture content of product, L_P is latent heat of vaporization of moisture from product, and C_{Pl} and C_{PP} are specific heat of liquid and product, respectively.

5.2.4 Energy Balances on the Concrete Floor

Equations (86 and 87) represent the energy balance for floor:

$$Q_f = Q_{af} + Q_{sf} + Q_{fg} \tag{86}$$

where Q_f is gain of heat energy in floor, Q_{af} is thermal energy transfer among drying air and floor due to convection, Q_{sf} is energy gain by floor due to solar radiation, and Q_{fg} is energy exchange between floor and ground.

$$m_f C_{pf}\frac{dT_f}{dt} = A_f h_c(T_a - T_f) + (1 - F_P)A_f \alpha_f I_t + A_f h_D\left(T_g - T_f\right) \tag{87}$$

where m_f and A_f are mass and area of concrete floor, respectively; T_f and T_g are temperature of floor and ground, respectively; h_D is heat transfer coefficient between floor and underground; and C_{Pf} is specific heat of liquid.

5.2.5 Mass Balance Equation

The Eq. (88) shows the moisture balance inside the dryer as

$$Q_{\text{gain}} = Q_{\text{mi}} - Q_{\text{mo}} + Q_{\text{mp}} \tag{88}$$

where Q_{gain} is gain of moisture in drying air, Q_{mi} is moisture present in air at inlet to dryer, Q_{mo} is moisture present in air going out of dryer, and Q_{mp} is rate of moisture separated from the product.

Hence, Eq. (88) can further be expressed by Eq. (89):

$$\rho_{\text{a}} V \frac{\text{d}H}{\text{d}t} = A_{\text{in}} \rho_{\text{a}} H_{\text{in}} V_{\text{in}} - A_{\text{out}} \rho_{\text{a}} H_{\text{out}} V_{\text{out}} + D_{\text{P}} A_{\text{P}} \rho_{\text{d}} \frac{\text{d}M_{\text{P}}}{\text{d}t} \tag{89}$$

where V is volume of drying chamber; H is humidity ratio of air in dryer; H_{in} and H_{out} are humidity ratio of air at inlet and outlet of dryer, respectively; and ρ_{d} is density of dried product.

5.2.6 Heat Transfer and Heat Loss Coefficients

Heat transfer coefficient among cover and sky plus product and cover due to radiation is given by Eqs. (90 and 91), respectively:

$$h_{\text{rcs}} = \varepsilon_{\text{C}} \times \sigma \times \left[T_{\text{C}}^2 + T_{\text{S}}^2\right] \times \left[T_{\text{C}} + T_{\text{S}}\right] \tag{90}$$

$$h_{\text{rpc}} = \varepsilon_{\text{P}} \times \sigma \times \left[T_{\text{P}}^2 + T_{\text{C}}^2\right] \times \left[T_{\text{P}} + T_{\text{C}}\right] \tag{91}$$

where h_{rcs} is radiative heat transfer from cover to sky and h_{rpc} is radiative heat transfer coefficient between product and cover.

Convective heat transfer coefficient from the cover to atmosphere due to wind (h_{w}) is calculated by

$$h_{\text{W}} = 2.8 + 3.0 \times V_{\text{W}} \tag{92}$$

Heat transfer coefficient within the greenhouse dryer used for the cover, product, and floor is found out by using the following correlation:

$$h_{\text{Cfa}} = h_{\text{Cca}} = h_{\text{Cpa}} = h_{\text{C}} = \frac{Nu \times k}{D_{\text{h}}} \tag{93}$$

Equations (94 and 95) describe the relationship for calculating Nusselt number (Nu) and overall heat loss coefficient (U_{c}) from the greenhouse cover, respectively:

$$Nu = 0.0158 \times (\text{Re})^{0.8} \tag{94}$$

$$U_C = \left(\frac{k_C}{\delta_C}\right) \tag{95}$$

where V_W is the wind speed, δ_c is thickness of cover of greenhouse, and K_c refers to thermal conductivity of insulation used.

5.3 Thin-Layer Drying Equation

The experiments intended for describing thin-layer kinetics were conducted on the laboratory dryer under controlled environment of *RH* along with temperature.

For describing thin-layer drying of tomatoes, Eq. (96) was presented:

$$\frac{M - M_e}{M_o - M_e} = \exp\left(-At^B\right) \tag{96}$$

where M is the product moisture content at time t, while M_e and M_0 are equilibrium and initial moisture content on dry basis, respectively.

The drying parameters A and B are given as $A = -(0.276) + 0.00723 \times T + 0.001594 \times RH - 0.000041 \times (RH)^2 B = 1.512073 - 0.04305 \times T + 0.0134277 \times RH - 0.30020655 \times T_{RH} + 0.000533 \times (T)^2 - 0.001355 \times {}^{(RH)2}$ where T is temperature in °C and *RH* is relative humidity in %.

EMC of tomatoes in controlled environment of relative humidity along with temperature was found out by Eq. (97):

$$a_w = \frac{1}{1 + \left[\frac{51.5 - 0.42T}{M_e}\right]^{1.74215}} \tag{97}$$

where a_w is water activity (decimal).

5.3.1 Method of Solution

The developed equations for energy and mass balance were solved numerically by means of the finite difference method. The change in moisture content of tomatoes for a particular time interval can be calculated using Eq. (96).

The equations for energy balance and mass balance were then resolved by Gauss-Jordan elimination method by means of the recorded values for the relative humidity, change in moisture content of the commodity, and drying air temperature for the specified time period. The procedure is repetitive until the concluding time is reached. The numerical explanation was programmed in FORTRAN.

The simulated outcomes are good enough with the tentative data. Continuous as well as quicker rate of drying is the narrative characteristic of greenhouse dryer (parabolic roof type). Furthermore, the tempo of drying was consistent in all trays due to supply of hot air by LPG burner. To pick up the concert of dryer, it is worthwhile to recirculate the exhaust air coming from the dryer.

5.4 *Mathematical Modeling for Indirect Forced Convection Solar Drying System*

Smitabhindu R. et al. (2008) designed and developed forced convection indirect type of solar drying system (Fig. 2) for drying bananas in the metrological conditions of Bangkok (Thailand). The most important objective of the study is to create a mathematical model for the indirect SDS (solar drying system) as well as to optimize the various parameters related to the drying system. LPG burner was meant for supplying additional heat to the drying air. Smitabhindu R. et al. (2008) presented a mathematical model for solar collector as well as drying chamber and discussed in detail as below.

5.4.1 Solar Collector

For analysis, consider a small element of thickness dX at distance X from inlet of solar collector.

Heat balance for cover, absorber, and drying air inside the solar collector for element of width W_c in Δt time interval is expressed by Eqs. (98, 99, and 100), respectively:

$$\rho_c \times \delta_c \times \Delta X \times C_{pc} \times W_c \left[T_c + \left(\frac{dT_c}{dt} \times \Delta t \right) \right] - \rho_c \times \delta_c \times \Delta X \times C_{pc} \times W_c \times T_c$$
$$= h_{cfc} \times \Delta X \times W_c \times (T_f - T_c) \times \Delta t + h_{rcs} \times \Delta X \times W_c \times (T_s - T_c)$$
$$\times \ \Delta t + h_{wca} \times \Delta X \times W_c \times (T_a - T_c) \times \Delta t + h_{rbc} \times \Delta X \times W_c \times (T_b - T_c)$$
$$\times \Delta t + \Delta X \times W_c \times \alpha_c \times I \times \Delta t$$

The above equation can be rearranged as

$$\rho_c \times \delta_c \times C_{Pc} \times \left(\frac{dT_c}{dt} \right) = h_{cfc} \times (T_f - T_c) + h_{rcs} \times (T_s - T_c) + h_{wca} \times (T_a - T_c) + h_{rbc} \times (T_b - T_c) + \alpha_c \times I \qquad (98)$$

where C_{PC} is sp. heat of cover; T_a, T_b, T_c, T_f, and T_P are temperature of ambient air, absorber, cover, air in collector, and product, respectively; h_{wca} is convection heat loss coefficient of cover due to wind; h_{cfc} is convection heat transfer among air in collector-cover of solar collector; h_{rbc} and h_{rcs} are radiation heat transfer coefficient

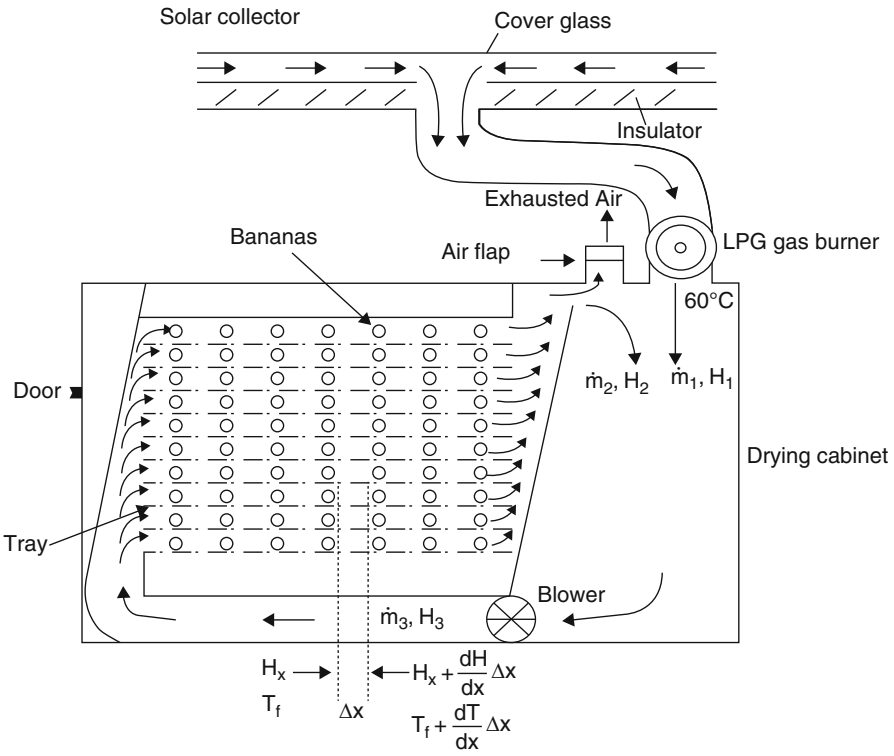

Fig. 2 Indirect forced convection solar drying system

among cover-absorber and cover-sky, respectively; δ_c indicates thickness of cover; W_c is width of collector; α_c is absorptivity of cover; and I is solar insolation received on solar collector.

Heat balance for element of absorber of solar collector can be expressed as

$$\rho_b \times \delta_b \times \Delta X \times C_{pb} \times W_c \left[T_b + \left(\frac{dT_b}{dt} \times \Delta t\right)\right] - \rho_b \times \delta_b \times \Delta X \times C_{pb} \times W_c \times T_b = h_{cfb} \times \Delta X \times W_c \times (T_f - T_b) \times \Delta t + u_b \times \Delta X \times W_c \times (T_a - T_b) \times \Delta t + h_{rbc} \times \Delta X \times W_c \times (T_c - T_b) \times \Delta t + \Delta X \times W_c \times \tau \times \alpha \times I \times \Delta t$$

The above equation can be written as

$$\rho_b \times \delta_b \times C_{pb} \times \left(\frac{dT_b}{dt}\right)_b = h_{cfb} \times (T_f - T_b) + U_b \times (T_a - T_b) + h_{rbc} \times (T_c - T_b) + \tau \times \alpha \times I \quad (99)$$

where C_{Pb} is specific heat of absorber, h_{cfb} is convection heat transfer among air-absorber, U_b is heat loss coefficient through back side of solar collector to surrounding air, and ρ_c, ρ_b, and ρ_a represent density of cover, absorber, and air, respectively.

Heat balance for air within the solar collector gives

$$D_c \times G \times C_{Pa} \times W_c \left[T_f + \left(\frac{dT_f}{dX} \times \Delta X\right)\right] - D_c \times G \times W_c \times [C_{Pa} + (C_{Pa} \times H)] \times T_f \times \Delta t = h_{cfc} \times \Delta X \times W_c \times (T_c - T_f) \times \Delta t + h_{cbf} \times \Delta X \times W_c \times (T_b - T_f) \times \Delta t$$

Equation (100) represents heat balance for air flowing through the solar collector:

$$D_c \times G \times C_{Pa} \times \left(\frac{dT_f}{dX}\right) = h_{cfc} \times (T_c - T_f) + h_{cbf} \times (T_b - T_f) \tag{100}$$

where C_{Pa} is sp. heat of air, D_c is distance among cover and absorber, h_{cbf} is convection heat transfer among absorber-air in solar collector, G is sp. mass flow rate of air in solar collector in kg/s m^2, and H is humidity ratio of drying air.

Convective and Radiative Heat Transfer for Solar Collector

The radiation heat transfer coefficient among collector cover-sky as well as collector cover-absorber and convection heat transfer coefficient among collector cover-surrounding air were calculated as shown by Eqs. (101, 102, and 103), respectively:

$$h_{rcs} = \varepsilon_c \times \sigma \times \left[T_c^2 + T_s^2\right] \times [T_c + T_s] \quad \text{where} \quad T_s = 0.522 \times (T_a)^{1.5} \tag{101}$$

$$h_{rbc} = \frac{\sigma \times \left[T_b^2 + T_c^2\right] \times [T_b + T_c]}{\left(\frac{1}{\varepsilon_b} + \frac{1}{\varepsilon_c} - 1\right)} \tag{102}$$

$$h_{wca} = [5.37 + (3.8 \times V)] \tag{103}$$

The heat transfer coefficient air-cover and absorber-air was assumed to be the same. Equation (104) represents Kays and Crawford correlation for determination of heat transfer coefficient:

$$N_u = 0.0158 \times (R_e)^{0.8} = 0.0158 \times \left(\frac{D_h \times V \times \rho_f}{\nu}\right)$$
$$\therefore \frac{h_{cbf} \times D_h}{k} = 0.0158 \times \left(\frac{D_h \times V \times \rho_f}{\nu}\right) \quad (104)$$
$$\text{where} \quad D_h = \left(\frac{4 \times W_c \times D_c}{2 \times (W_c + D_c)}\right)$$

Solution for Solar Collector

The differential Eqs. (98, 99, and 100) are difficult to solve by analytical method. Hence, finite difference methods have been used and the following set of Eqs. (105, 106 and 107) were obtained:

Cover

$$\rho_c \times \delta_c \times C_{Pc} \times \left(\frac{T_{c,t+\Delta t} - T_{c,t}}{\Delta t}\right) = h_{cfc} \times (T_{f,t+\Delta t} - T_{c,t+\Delta t}) + h_{rcs} \times (T_{s,t+\Delta t} - T_{c,t+\Delta t}) + h_{wca} \times (T_{a,t+\Delta t} - T_{c,t+\Delta t}) + h_{rbc} \times (T_{b,t+\Delta t} - T_{c,t+\Delta t}) + \alpha_c \times I_{t+\Delta t} \quad (105)$$

Absorber

$$\rho_b \times \delta_b \times C_{Pb} \times \left(\frac{T_{b,t+\Delta t} - T_{b,t}}{\Delta t}\right)_b = h_{cfb} \times (T_{f,t+\Delta t} - T_{b,t+\Delta t}) + u_b(T_{a,t+\Delta t} - T_{b,t+\Delta t}) + h_{rbc} \times (T_{c,t+\Delta t} - T_{b,t+\Delta t}) + \tau \times \alpha \times I_{t+\Delta t} \quad (106)$$

Air

$$D_c \times G \times C_{Pa} \times 0.5 \times \left[\frac{T_{f,X+\Delta X,t+\Delta t} - T_{f,X-\Delta X,t+\Delta t}}{2 \times \Delta X} + \frac{T_{f,X+\Delta X,t+\Delta t} - T_{f,X-\Delta X,t+\Delta t}}{2 \times \Delta X}\right] = h_{cbf} \times (T_{b,X,t+\Delta t} - T_{f,X,t+\Delta t}) + h_{cbf} \times (T_{c,X,t+\Delta t} - T_{f,X,t+\Delta t}) \quad (107)$$

The above Eqs. (105, 106, and 107) were uttered in matrix form for time interval Δt for the whole length of solar collector and solved by Gauss-Jordan elimination technique:

$$\begin{bmatrix} a_{11} & a_{12} & a_{13} \\ a_{21} & a_{22} & a_{23} \\ a_{31} & a_{32} & a_{33} \end{bmatrix} \begin{bmatrix} T_{\mathrm{c}} \\ T_{\mathrm{f}} \\ T_{\mathrm{b}} \end{bmatrix} = \begin{bmatrix} b_1 \\ b_2 \\ b_3 \end{bmatrix}$$

5.4.2 Drying Chamber or Cabinet

Bananas are placed in a single layer on the trays of cabinet and also evenly subjected to a consistent temperature.

For drying air, heat exchange to product due to convection is equal to change in energy of air in cabinet and can be written as

$$D_{\mathrm{t}} \times G \times W_{\mathrm{t}} \times (\mathrm{C}_{\mathrm{Pa}} + C_{\mathrm{Pv}} \times H)\left(\mathrm{T}_{\mathrm{f}} + \frac{\mathrm{d}T_{\mathrm{f}}}{\mathrm{d}X}\right) \times \Delta t - D_{\mathrm{t}} \times G \times W_t \times (\mathrm{C}_{\mathrm{Pa}} + C_{\mathrm{Pv}} \times H) \times \mathrm{T}_{\mathrm{f}} \times \Delta t = \Delta X \times W_{\mathrm{t}} \times h_{\mathrm{cpf}} \times \left(\mathrm{T}_{\mathrm{p}} - T_{\mathrm{f}}\right) \times \Delta t$$

Solving and rearranging the terms, we can write

$$D_{\mathrm{t}} \times G \times (\mathrm{C}_{\mathrm{Pa}} + C_{\mathrm{Pv}} \times H) \times \frac{\mathrm{d}T_{\mathrm{f}}}{\mathrm{d}X} = h_{\mathrm{cpf}} \times \left(\mathrm{T}_{\mathrm{p}} - T_{\mathrm{f}}\right) \tag{108}$$

Energy balance for product within the drying chamber can be written as

$$Q_{\mathrm{P}} = Q_{\mathrm{C}} - Q_{\mathrm{S}}$$

where Q_{P} energy in the product, Q_{C} is heat exchange to product due to convection, and Q_{S} is heat required to evaporate moisture:

$$W_{\mathrm{t}} \times \rho_{\mathrm{P}} \times \Delta X \times (\mathrm{C}_{\mathrm{PP}} + C_{\mathrm{PW}} \times M)\left(\mathrm{T}_{\mathrm{P}} + \left(\frac{\mathrm{d}T_{\mathrm{P}}}{\mathrm{d}t}\right)\Delta t\right) + W_{\mathrm{t}} \times \rho_{\mathrm{P}} \times \Delta X \times (\mathrm{C}_{\mathrm{PP}} + C_{\mathrm{PW}} \times M) \times T_{\mathrm{P}} = h_{\mathrm{fg}} \times D_{\mathrm{t}} \times G \times \left(\frac{\mathrm{d}H}{\mathrm{d}X}\right)\Delta X \times \Delta t + C_{\mathrm{v}} \times (\mathrm{T}_{\mathrm{f}} - T_{\mathrm{P}}) \times D_{\mathrm{t}} \times G \times \left(\frac{dH}{dX}\right) \times \Delta t + \Delta X \times W_{\mathrm{t}} \times h_{\mathrm{cpf}} \times (T_{\mathrm{f}} - T_{\mathrm{P}}) \times \Delta t$$

The above expression can be rearranged, as shown in Eq. (109):

$$\rho_{\mathrm{P}} \times (\mathrm{C_P} + C_{\mathrm{W}} \times M) \times \left(\frac{\mathrm{dT_P}}{\mathrm{dt}}\right) = \left(h_{\mathrm{fg}} + C_{\mathrm{W}} \times (\mathrm{T_P} - T_{\mathrm{f}})\right) \times D_{\mathrm{t}} \times G \times \left(\frac{dH}{dX}\right) + h_{\mathrm{cpf}} \times (\mathrm{T_f} - T_{\mathrm{P}}) \quad (109)$$

Now, for moisture balance of the air, we can write
Moisture increase in air = moisture loss from product

$$D_{\mathrm{t}} \times G \times W_t \times \left(\mathrm{H} + \left(\frac{\mathrm{d}H}{\mathrm{d}X}\right)\Delta X\right) \times \Delta t - D_{\mathrm{t}} \times G \times W_{\mathrm{t}} \times H \times \Delta t =$$
$$\rho_{\mathrm{P}} \times \Delta X \times W_{\mathrm{t}} \times M - \rho_{\mathrm{P}} \times \Delta X \times W_{\mathrm{t}} \times \left(M + \left(\frac{\mathrm{d}M}{\mathrm{d}t}\right)\Delta t\right)$$

Solving and rearranging,

$$D_{\mathrm{t}} \times G \times \left(\frac{\mathrm{d}H}{\mathrm{d}X}\right) = -\rho_{\mathrm{P}} \times \left(\frac{\mathrm{d}M}{\mathrm{d}t}\right) \quad (110)$$

where C_{PV} is sp. heat of vapor, C_{PW} is sp. heat of water, D_{t} is height of gap among trays, h_{ccf} is convection heat transfer among cover-air in solar collector, h_{cpf} is convection heat transfer among product-drying air, W_{t} refers to width of trays, and δ_{c} and δ_{b} indicate thickness of cover and absorber, respectively.

Equation (111) shows the moisture content of the produce as

$$\left[\frac{M - M_{\mathrm{e}}}{M_{\mathrm{o}} - M_{\mathrm{e}}}\right] = A \times \exp(-B \times t) \quad (111)$$

The constants A and B are expressed in terms of RH and temperature as

$$A = a_{\mathrm{o}} + a_1 \times \mathrm{RH} + a_2 \times T \times t + a_3 \times (RH)^2 + a_4 \times (T)^2$$
$$B = b_{\mathrm{o}} + b_1 \times \mathrm{RH} + b_2 \times T \times t + b_3 \times (RH)^2 + b_4 \times (T)^2$$

where a and b are empirical constants.

Solution for Drying Chamber

Author divides the banana bed into a number of sections along the length of trays:

$$X = j \times \Delta X \quad \text{where} \quad j = 1, 2, 3, 4, 5 - - - - - - --$$

Similarly, time required for drying the banana is also divided into a number of intervals as

$$t = i \times \Delta t \quad \text{where} \quad i = 1, 2, 3, 4, 5 - - - - - - - -$$

Then drying constants B and M_e have been evaluated by using *RH*, air temperature, and airflow rate at inlet of drying chamber.

The change in moisture content (ΔM) for banana in Δt (time interval) has been determined from Eq. (111).

Finally, the calculations for air temperature (Eq. 108), product temperature (Eq. 109), and air humidity (Eq. 110) for the first section were done by noting the respective value variables involved in respective equations. This procedure was continued section by section and for each time interval.

FORTRAN language was selected by author for getting numerical solution.

5.4.3 Experimental Validation

The developed model was validated by comparing measured values of collector air temperature and moisture content with predicted values and found a close agreement between them.

The presented mathematical model for drying of bananas (indirect forced convection SDS) can be used as a guideline for different solar dryers and commodities.

5.5 Moisture Diffusion Model for Natural Convection Mixed Mode Solar Dryer

In mathematical modeling of solar drying systems, the information of h_m (convection mass transfer coefficient) and $D_{effective}$ (effective moisture diffusion coefficient) is crucial. In this case study, Kumar and Tripathy (2009) presented a method for determination of $D_{effective}$ and h_m by using drying coefficients k, k_0, and lag factor. Authors also tried to propose the variable correlations for k and k_0. Further these correlations help to set up connection among $D_{effective}$ and h_m. Kumar and Tripathy performed the experimentation on mixed mode natural convection solar dryer (Fig. 3) for drying of potato.

5.5.1 Moisture Diffusion Model

Analytical Eq. (112) shows the major expression, describing transitory moisture diffusion through a sample of potato in 1-D Cartesian and cylindrical coordinates (for infinite plate/cylinder) as

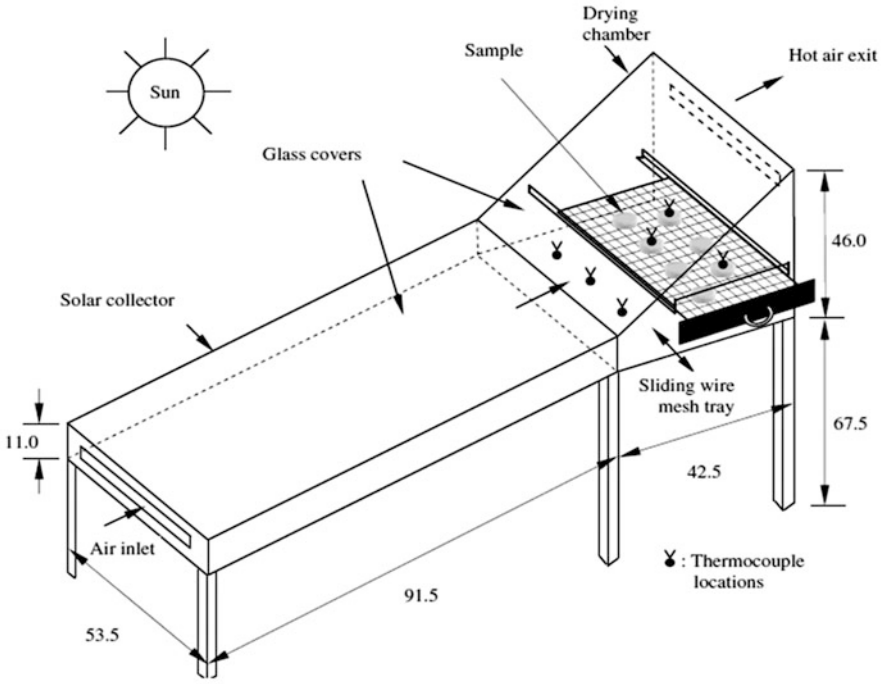

Fig. 3 Mixed mode natural convection solar dryer (Kumar and Tripathy 2009)

$$\left[\frac{\partial M(y,t)}{\partial t}\right] = D_{\text{effective}} \times \left(\frac{1}{y^{\text{n}}}\right)\left\{\left(\frac{\partial}{\partial y}\right)\left[y^{\text{n}} \times \left(\frac{\partial M(y,t)}{\partial y}\right)\right]\right\} \tag{112}$$

For infinite plate: $n = 0$, $y = x$.

For infinite cylinder: $n = 1$, $y = r$

where y and t = space coordinate, n = constant, and $D_{\text{effective}}$ is effective moisture diffusion coefficient.

Authors assume that initial *MR* (moisture content) is equally dispersed within potato and moisture gradient is symmetrical about center.

Equations (113 and 114) represent the boundary conditions of central symmetry along with convection boundary at the surface of potato as

$$\begin{aligned} \mathrm{M}[y,o] &= M_{\text{o}} \\ \left[\frac{\partial M(0,t)}{\partial y}\right] &= 0 \end{aligned} \tag{113}$$

$$\therefore -D_{\text{effective}} \times \left(\frac{\partial M(L_d, t)}{\partial y}\right) = h_m \times (M(L_d, t) - M_\infty) \tag{114}$$

where M is MR of product, M_∞ is MR of atmospheric air, L_d is moisture diffusion path (radius of cylinder/half thickness of slice), and h_m is convection mass transfer coefficient.

During investigation, MR_e (experimental moisture content) of potato was obtained as mean MR (MR_m). In model validation, MR_m obtained from prediction and experimentation is compared. Therefore, volume MR_m can be obtained by integrating Eq. (112). Also for Fourier number greater than 0.2, the answer may be approximated using the first term of series. Equations (115 and 116) show final solution of Fick's diffusion model for MR_m:

$$MR_m = \left[\frac{M_t - M_\infty}{M_0 - M_\infty}\right] = X \times \left[\exp\left(-\mu_1^2 \times \left(\frac{D_{\text{effective}}}{L_d^2} \times t\right)\right)\right] \tag{115}$$

$$X = \left[\frac{4 \times J_1^2(\mu_1)}{\mu_1^2 \times \left[J_0^2(\mu_1) + J_1^2(\mu_1)\right]}\right]$$

$$MR_m = \left[\frac{M_t - M_\infty}{M_0 - M_\infty}\right] = Y \times \left[\exp\left(-\mu_1^2 \times \left(\frac{D_{\text{effective}}}{L_d^2} \times t\right)\right)\right] \tag{116}$$

$$Y = \left[\frac{2 \times \sin^2(\mu_1)}{\mu_1 \times (\mu_1 + \sin\mu_1 \times \cos\mu_1)}\right]$$

where M_t is MR at time t (d.b.), μ is characteristics constant, and $J_1(\mu_1)$ and $J_0(\mu_1)$ refer to first- and zeroth-order Bessel function of first type, respectively.

Author uses Eq. (117) for determining the characteristics constant:

$$\mu_1^2 = [\mu_1]_\infty^2 \times \left[\frac{1}{1 + \frac{A_1}{Bi_m}}\right] \tag{117}$$

Values for following constants are

For Cylinder : $[\mu_1]_\infty = 2.405; P = 1.04$ and $A_1 = 2.45$

For Cylinder : $[\mu_1]_\infty = 1.571; P = 1.02$ and $A_1 = 2.24$

Pflug and Blaisdell (1963) proposed the following expression (Eqs. 118, 119) for Biot number in terms of drying constant k_0 and lag factor as below:

$$\text{For Cylinder}: \qquad Bi_{\mathrm{m}} = \left[\frac{3.356 \times (\ln(k_{\mathrm{o}}))}{1 - 1.974 \times (\ln(k_0))}\right] \tag{118}$$

$$\text{For Slice}: \qquad Bi_{\mathrm{m}} = \left[\frac{5.132 \times (\ln(k_{\mathrm{o}}))}{1 - 3.948 \times (\ln(k_0))}\right] \tag{119}$$

where Bi_{m} is Biot No. for mass transfer and $(\mu_1)_{\infty}$ is value of μ_1 at $Bi_{\mathrm{m}} = \infty$.

The thin-layer drying model is usually expressed by Eq. (120) for determining mean *MR* of potato:

$$MR_{\mathrm{m}} = k_0 \times e^{(-\mathrm{k} \times t)} \tag{120}$$

where k_0 is lag factor and k refers to as drying constant.

Equation (120) is similar to Eqs. (115 and 116). Hence, by comparing, $D_{\text{effective}}$ was obtained and shown by Eq. (121):

$$D_{\text{effective}} = \left[k \times \left(\frac{L_{\mathrm{d}}^2}{\mu_1^2}\right)\right] \tag{121}$$

Then, the mass transfer coefficient can be found out by Eq. (122):

$$h_{\mathrm{m}} = \left[Bi_{\mathrm{m}} \times \left(\frac{D_{\text{effective}}}{L_{\mathrm{d}}}\right)\right] \tag{122}$$

During growth of correlation for drying factor, authors projected the guess stating that the moisture diffusion inside the potato changes with its temperature. Hence, complete investigational mean *MR*- drying time characteristic curve for all produce shape/geometry was separated into numerous segments. Again it is assumed that for every segment, *DR* (drying rate) follows an exponential function and values of k_0 and k were found out through fitting of investigational facts by means of nonlinear regression. This process was continued for the whole drying curve. Equation (123) indicates the relationship for drying constants as

$$\begin{aligned} &\text{For Cylinder}: \quad k_0 = \left[1.0005 + 2 \times 10^{-4} \times (T_{\mathrm{S}})\right]; \\ &\qquad\qquad\qquad\quad k = \left[-1.88 \times 10^{-4} + 7.5 \times 10^{-6} \times (T_{\mathrm{s}}\ )\right] \\ &\text{For Slice}: \quad k_0 = \left[1.0005 + 4.6 \times 10^{-5} \times (T_{\mathrm{S}})\right]; \\ &\qquad\qquad\qquad\quad k = \left[-4.2 \times 10^{-5} + 2.15 \times 10^{-6} \times (T_{\mathrm{S}})\right] \end{aligned} \tag{123}$$

5.5.2 Model Validation

Statistical error analysis was used for validation of proposed diffusion model. The prediction ability was tested by determining the values for MAE (mean absolute error), RMSE (root mean square error), and SE (standard error). The statistical analysis revealed that thin-layer drying model compared to mass diffusion model gives excellent simulation outcomes.

The study indicates that proposed model in terms of drying parameters of potato can acceptably simulate the investigational *MR* facts. In other words, prediction model has closer conformity with experiments.

6 Conclusion and Future Direction

Today's increased competition due to globalization in concert with the budding customer demand for superior quality products will continue to impel innovations in the drying process. The following conclusions were drawn from this study:

- For future sustainability of solar drying, it is important to promote the efforts in improving the performance of the existing drying technologies or intensifying the new crucial concepts in solar drying. In this regard, modeling strategies must be assisted for incremental improvements.
- Drying processes for many agricultural products need to be further optimized and redesigned for improving the productivity of solar drying system.
- With tremendous developments in computing capabilities, further growth can be made in the development of sophisticated and pragmatic multiscale drying models that combine the structural changes, phase changes, complex food compositions, chemical reactions, and transport phenomenon (fluid flow, mass, and energy movement).
- A simulation model is a precious tool for forecasting the dryer concert and will be decisive in the advancement of solar drying processes.
- Computational fluid dynamics (CFD) and artificial neural network (ANN) techniques should be promoted in stimulating the drying air and temperature distributions for innovative design of drying chamber.
- A very few literature is available on development of diffusion models and requires a proper attention.
- Bulks of models formulated have not think about the equipment model, which delivers the consequence of heat and mass transport within the matter on the drying media.
- The drying unit should have a greatest utilization factor and be obliged to an endorsement of heat storage in night operation. Modeling of such system becomes complicated and needs the careful attention.

- For superior organization of drying processes during modeling, the parameters like pressure, shape of product, retention time, flow configuration, geometry of shelves, and drying media condition should be considered more precisely.

However, application of solar dryers has not pulled out owing to the high capital investment, extensive payback period, and lack of self-belief in the technology. Nonetheless nonstop research and expansion of work related to the modeling and simulation should be carried out to conquer these factors.

References

Afzal TM, Abe T (2000) Simulation of moisture changes in barley during far infrared radiation drying. Comput Electron Agric 26:137–145

Akpinar EK (2006) Determination of suitable thin layer drying curve model for some vegetables and fruits. J Food Eng 73:75–84

Akpinar EK (2008) Mathematical modelling and experimental investigation on sun and solar drying of white mulberry. J Mech Sci Technol 22:1544–1553

Akpinar EK (2010) Drying of mint leaves in a solar dryer and under open sun: modelling, performance analyses. Energy Convers Manag 51:2407–2418

Akpinar EK, Bicer Y (2005) Modeling of the drying of eggplants in thin-layers. Int J Food Sci Technol 40:273–281

Akpinar EK, Bicer Y (2008) Mathematical modeling of thin layer drying process of long green pepper in solar dryer and under open sun. Energy Convers Manag 49:1367–1375

Akpinar EK, Midilli A, Bicer Y (2003) Single layer drying behaviour of potato slices in a convective cyclone dryer and mathematical modeling. Energy Convers Manag 44:1689–1705

Bahnasawy AH, Shenana ME (2004) A mathematical model of direct sun and solar drying of some fermented dairy products (Kishk). J Food Eng 61(3):309–319

Bala BK, Chowdhury MMI, Haque MA (2011) Energy and exergy analysis of the solar drying of jackfruit leather. Biosyst Eng 110:222–229

Basunia MA, Abe T (2001) Thin-layer solar drying characteristics of rough rice under natural convection. J Food Eng 47(4):295–301

Black T (2014) A review on the Rooibos Tea Industry and thin-layer drying literature. Available on: http://efwe.ukzn.ac.za/Libraries/ResearchSeminars/Black;T.sflb.ashx. Accessed on 16 Feb 2015

Chukwunonye CD, Nnaemeka NR, Chijioke OV, Obiora NC (2016) Thin layer drying modelling for some selected Nigerian produce: a review. Am J Food Sci Nutr Res 3(1):1–15

Corzo O, Bracho N, Vasquez A, Pereira A (2010) Determination of suitable thin layer model for air drying of Coroba slices at different air temperatures and velocities. J Food Process Preserv 34:587–598

Diamante LM, Munro PA (1993) Mathematical modeling of the thin layer solar drying of sweet potato slices. Solar Energy 51:271–276

Ekechukwu OV (1999) Review of solar-energy drying systems I: an overview of drying principles and theory. Energy Convers Manag 40:593–613

El-Sabaii AA, Aboul-Enein S, Ramadan MRI, El-Gohary HG (2002) Empirical correlations for drying kinetics of some fruits and vegetables. Energy 27(9):845–859

Forson FK, Nazha MAA, Rajakaruna H (2007) Modeling and experimental studies on a mixed-mode natural convection solar crop -dryer. Sol Energy 81(3):346–357

Frejd P (2013) Modes of modeling assessment – a literature review. J Educ Stud Math 84 (3):413–438

Fudholi A, Ruslan MH, Othman MY, Zaharim A, Sopian K (2013) Mathematical modeling of solar drying of thin layer Ginger. In: Azami Z, Kamaruzzaman S (eds) Conference of proceeding: latest trends in renewable energy and environmental informatics. Kuala Lumpur, Malaysia, April 2–4, 2013, pp 273–278. ISBN:978-1-61804-175-3

Ismail MA, Ibn Idriss EM (2013) Mathematical modelling of thin layer solar drying of whole okra pods. Int Food Res J 20(4):1983–1989

Janjai S (2012) A greenhouse type solar dryer for small-scale dried food industries: development and dissemination. Int J Energy Environ 3(3):383–398

Kalogirou SA (2004) Solar thermal collectors and applications. Prog Energy Combust Sci 30:231–295

Karim MA, Hawlader MNA (2005) Mathematical modelling and experimental investigation of tropical fruits drying. Int J Heat Mass Transf 48:4914–4925

Kashaninejad MA, Mortazavi A, Safekordi A, Tabil LG (2005) Thin-layer drying characteristics and modeling of Pistachio nuts. J Food Eng

Kucuk H, Midilli A, Kilic A, Dincer I (2014) A review on thin-layer drying-curve equations. Dry Technol 32:757–773

Kumar S, Tripathy PP (2009) A methodology for determination of temperature dependent mass transfer coefficients from drying kinetics: application to solar drying. J Food Eng 90:212–218

Lahsasni S, Kouhila M, Mahrouz M, Idlimam A, Jamali A (2004) Thin layer convective solar drying and mathematical modeling of prickly pear peel. Energy 29(2):211–224

Luikov AV (1975) Systems of differential equations of heat and mass transfer in capillary porous bodies (review). Int J Heat Mass Transf 18:1–14

Madamba PS, Driscoll RH, Buckle KA (1996) Thin layer drying characteristics of garlic slices. J Food Eng 29:75–97

Maria A (1997) Introduction to modeling and simulation. In: Andradottir S, Healy KJ, Withers DH, Nelson BL (eds) Proceedings of the 1997 winter simulation conference, pp 7–13

Meisamiasl E, Rafiee S, Keyhani A, Tabatabaeefar A (2010) Determination of suitable thin layer drying curve model for apple slices. Plants Omics J 3(3):103–108

Menzies DJ, O'callaghan JR, Ballay PH (1971) Digital simulation of agric. Dryer performance. Agric Eng Res 16(3):223–244

Midilli A, Kucuk H (2003a) Energy and exergy analysis of solar drying process of pistachio. Energy 28:539–556

Midilli A, Kucuk H (2003b) Mathematical modeling of thin layer drying of pistachio by using solar energy. Energy Convers Manag 44:1111–1122

Midilli A, Kucuk H, Yapar Z (2002) A new model for single-layer drying. Dry Technol 20 (7):1503–1513

Onwude DI, Hashim N, Janius RB, Nawi NM, Abdan K (2016) Modeling the thin-layer drying of fruits and vegetables: a review. Compr Rev Food Sci Food Saf 15(3):599–618

Palipane K, Driscoll RH (1994) Thin layer drying behaviour of macadamia in shell nuts and kernels. J Food Eng 23:129–144

Panchariya PC, Popvic D, Sharma AL (2002) Thin layer modeling of black tea drying process. J Food Eng 52:349–357

Parry JL (1985) Mathematical modeling and computer simulation of heat and mass transfer in agricultural grain drying. J Agric Eng Res 32:1–29

Patil R, Gawande R (2016) A review on solar tunnel greenhouse drying system. Renew Sust Energ Rev 56:196–214

Pflug LJ, Blaisdell JL (1963) Methods of analysis of precooling data. ASHRAE J 5:33–40

Sacilik K (2007) Effect of drying methods on thin-layer drying characteristics of hull-less seed pumpkin. J Food Eng 79(1):23–30

Sacilik K, Keskin R, Elicin AK (2006) Mathematical modelling of solar tunnel drying of thin layer organic tomato. J Food Eng 73:231–238

Smitabhindu R, Janjai S, Chankong V (2008) Optimization of a solar-assisted drying system for drying bananas. Renew Energy 33:1523–1531

Togrul IT, Pehlivan D (2004) Modeling of thin layer drying kinetics of some fruits under open-air sun drying process. J Food Eng 65:413–425

Tunde-Akintunde TY (2011) Mathematical modeling of sun and solar drying of chilli pepper. Renew Energy 36:2139–2145

Usub T, Lertsatitthankorn C, Poomsa-ad N, Wiset L, Siriamornpun S, Soponronnarit S (2010) Thin layer solar drying characteristics of silkworm pupae. Food Bioprod Process 88:149–160

Van Meel DA (1958) Adiabatic convection batch drying with recirculating air. Chem Eng Sci 9:36–44

Yadollahinia AR, Omid M, Rafiee S (2008) Design and fabrication of experimental dryer for studying agricultural products. Int J Agric Biol 10(1):61–65

Yagcioglu A, Degirmencioglu A, Cagatay F (1999) Drying characteristics of Laurel leaves under different conditions. In: International congress on agricultural mechanization and energy, Adana, Turkey, pp 565–569

Yaldiz O, Ertekin C (2001) Thin layer solar drying of some vegetables. Dry Technol 19 (3&4):583–597

Yaldiz O, Ertekin C, Uzun HI (2001) Mathematical modeling of thin layer solar drying of sultana grapes. Energy 26:457–465

Zomorodian A, Moradi M (2010) Mathematical modeling of forced convection thin layer solar drying for cuminum cyminum. J Agric Sci Technol 12:401–408

Drying Kinetics in Solar Drying

Raquel de Pinho Ferreira Guiné and Maria João Barroca

Abstract From ancient times foods such as fruit, vegetables, meat or fish were dried by direct sunlight. The use of the sun as energy source is advantageous from the economic as well as environmental points of view. However, this procedure has many disadvantages concerning the efficiency and product safety and quality. The use of greenhouses can greatly minimize these problems. Inside the greenhouses the air circulates by natural convection, but they can also be equipped with chimneys for air outlet, thus increasing the airflow. In other cases, the efficiency of the drying system can be increased by incorporating a solar collector system, which uses panels for an efficient collection of the sunray's energy. Knowledge of the drying kinetics is of great importance for modelling the drying processes and to establish appropriate operating conditions. There are hundreds of mathematical models that were developed to represent the drying kinetics of foods, being mostly empirical or semiempirical or alternatively based on Fick's second law of diffusion. This chapter presents the heat and mass transfer mechanisms that regulate the drying rate, the conditions in direct and indirect solar drying, the drying curves and the mathematical modelling of the solar drying processes, with application examples in various dominions.

Keywords Modelling • Drying kinetics • Direct solar dryer • Indirect solar dryer

R. de Pinho Ferreira Guiné (✉)
CI&DETS Research Centre and Department of Food Industry, Polytechnic Institute of Viseu, ESAV, Quinta da Alagoa, Viseu, Portugal

CERNAS Research Centre, Polytechnic Institute of Coimbra, ESAC, Bencanta, Coimbra, Portugal
e-mail: raquelguine@esav.ipv.pt

M.J. Barroca
Molecular Physical-Chemistry Group, Coimbra University Research Center, Coimbra, Portugal
e-mail: mjbarroca@gmail.com

© Springer Nature Singapore Pte Ltd. 2017

O. Prakash, A. Kumar (eds.), *Solar Drying Technology*, Green Energy and Technology, DOI 10.1007/978-981-10-3833-4_10

1 Introduction

1.1 History

The drying of food products is a practice used by man since ancient times, representing still today a most important way of food preservation (Guiné 2008; Rodríguez et al. 2014). Solar drying uses the sun as energy source and includes those cases where the product is directly exposed to the solar radiation (called direct solar drying) and also the ones in which collectors are used to heat air that is then utilized for heating the food (indirect solar drying). Solar drying of fish and meat was already a documented practice in 2000 BC, and the sale of dehydrated vegetables, although not so ancient, has been done for more than a century. Also the commercialization of dehydrated soups dates from the nineteenth century. Although the terms dehydration and drying have commonly been used interchangeably, a more phenomenological approach distinguishes them, so that dehydration corresponds to any process aimed at removing the water from the food, while drying should be limited to only those processes where the moisture is removed as water vapour by means of a thermal vaporization, at a temperature usually under the boiling temperature of the water.

The drying operation has been intensively used for food preservation owing to its multiple benefits. The first reason for recurring to drying is certainly to improve the preservation and storage capacity of the food products, this being so because a significant reduction of the moisture content and, consequently, also the water activity drastically inhibits microbial growth, on one hand, and considerably slows down enzymatic modifications as well as minimizes many of the degradation reactions mediated by moisture, on the other hand (Guiné 2007a; Labed et al. 2016, Wu et al. 2007). Furthermore, the drying of foods has other advantages, such as no need to use cooling systems for preservation (avoiding equipment and energy costs) or facilitating the transport and storage due to a considerable reduction in size and weight of the product to handle due to the loss of an important amount of water. Finally, another advantage resides in the possibility of diversification of food products, with different flavours and textures, available for the consumer to choose from (Guiné 2007a, 2008; Labed et al. 2016).

Previously, the drying operation was conducted using the energy provided by the sun and consequently was limited to certain parts of the globe where the weather conditions were adequate for this practice, such as tropical and semitropical areas, where sun incidence and temperature are favourable. However, presently there are many methods using different and sophisticated equipment for the dehydration of food products that can be applied singly or in combination. These allow a substantial improvement regarding the hygiene and sanitary quality, since the drying of the foods when exposed directly to the atmospheric air turned them very susceptible to microbial contamination by the action of insects, rodents or other small animals as well as by dust, garbage or other strange materials to the product (Guiné et al. 2007b; Kituu et al. 2010). Still, the same kind of improvement in product quality

can be achieved by using greenhouses, where the product is also protected from the environmental harms and still making use of the free energy of the sun.

In solar drying of products from agricultural origin, the moisture can be removed from the product through air previously heated to a temperature between 50 and 60 °C by the energy of the sun. The solar drying under controlled conditions of temperature and moisture removing rate guarantees a correct drying process and an enhanced product quality. The moisture content in different agricultural products is variable, and, hence, for drying different products, the systems are generally classified into low- and high-temperature-operated drying systems. In the former, ventilation is used to bring the moisture content to equilibrium, whereas in the latter higher temperatures are used when a fast drying rate is necessary, particularly for products with a high moisture content (Kumar et al. 2016).

1.2 Examples of Dried Foods

1.2.1 Fruits

The diversity of fruits that have been dried in the sun since ancient times is enormous and includes grapes, figs, dates, pears, peaches and apricots, apples and pineapple slices (in quarters or in halves). However, more recently the drying of fruits has extended to less traditional fruits such as kiwi, mango, banana, orange, cherry, papaya, coconut or strawberry, among others. Although usually fruits are not blanched for drying, a procedure known as dry-scalding-drying can in some cases be used in fruits like apricots, peaches or pears. This procedure consists in an initial drying phase, where moisture is evaporated reducing the fruit weight to about half its initial value, followed by a bleaching operation made with steam for a period of about 4–5 min, after which drying continues until the desired final value of moisture. In general, as a treatment against browning, fruits are exposed to vapours resulting from the burning of solid sulphur.

1.2.2 Vegetables

Many vegetables can be found in the dried form, as it happens with the tomatoes that are dried in the sun in some countries bordering the Mediterranean or in South America or even California (USA). Besides tomatoes, perhaps the most widely known dried vegetable, other dried vegetables include green beans, peppers, cabbage, carrots, celery, spinach and broccoli. Although most vegetables are blanched and/or sulphited before drying, some other vegetables such as garlic, mushrooms, peas and onions are not sulphited, so as not to interfere with their delicate flavours.

1.2.3 Aromatic Herbs

The aromatic herbs have been dried in the sun for ages for use in the culinary preparations. However, presently they tend to be dried in vacuum to preserve their volatile compounds, responsible for the aroma and flavour, which are important characteristics. Some herbs like parsley or thyme can be dried without bleaching or sulphiting. Other aromatic herbs that can be dried include angelica, anise, balm, basil, borage, celery, chervil, chives, coriander, dill, fennel, laurel, lovage, marjoram, mint, oregano, rosemary, savoury or tarragon (Guiné and Gonçalves 2015, 2016).

1.2.4 Medicinal Plants

Many plants have been recognized for their beneficial effects for the human health, at many different levels. Because of their established utility, and in most cases limited availability due to seasonality, they used to be dried in the sun to make them available through the whole year. Some examples of medicinal plants that are preserved through drying include camomile, echinacea, Siberian ginseng, sage, melissa, lemongrass, verbena, hypericum, lemon balm, ginseng or nettle. Although for centuries the preservation of the medicinal plants was made by drying them in the sun, nowadays, the plants dried for infusions or skin formulations are dried in vacuum to preserve their bioactive compounds responsible for their bioactivities.

1.2.5 Fish

In ancient times fish used to be dried in the sun in the tropical zones or in the poles, where the effect of the wind was much important to help a fast dehydration in conditions of low temperature. The drying in the open air is only effective when the relative humidity is low and when there is solar heat and air movement. The product so obtained has an average final moisture content of approximately 50%, which determines a limited period of conservation. The drying time is influenced by factors such as the moisture content of the product, size and shape of the fish, fat content, muscle surface, spacing between samples in the environment and the thermodynamic drying conditions. Examples of species that can be dried include cod, sardine, sardinella, salmon, silver catfish and croaker, among others (Ikutegbe and Sikoki 2014; Lorentzen et al. 2016; Morales-Medina et al. 2016; Nuwanthi et al. 2016). Traditional methods of extending the shelf life of fish also comprise the salting and smoking, which indirectly are dehydration operations since they contribute for the elimination of the water and consequent preservation.

1.2.6 Meat

Similarly, to fish, also meat portions can be dried in the sun for preservation, mostly in areas around the globe where no electrical equipment is easily available at the households for other type of preservation. They can be hanged in ropes or displayed in trays for a fast dehydration. Alternatively meats can be smoked or salted, just like what happens with fish products. Industrially, the dehydrated meat products are mainly used as ingredients in dehydrated soup mixtures, sauces and ready dishes.

1.3 Quality and Properties of Dried Foods

Fruits like grapes, dates, figs, plums, apricots and peaches have been dried for centuries, and they constitute an important part of the food trade around the world. More recently, other fruits have also been dried as it is the example of apple, mango, papaya, banana, pineapple or pear (Guiné et al. 2007b). Concerning the horticultural products that have been dried, they include eggplant, zucchini, carrots, broccoli or spices such as pepper, onion, garlic and herbs. These can be consumed directly in their dried form, or alternatively they can be applied as ingredients for preparing long-term dehydrated mixtures (Brasiello et al. 2013). Foods of animal origin, such as meat or fish, are also consumed in their dried form (Darvishi et al. 2013; Traffano-Schiffo et al. 2014). The quality of dried foods is important, like in any other foods, but with particularities since drying causes intense changes in their properties, including discolouration, loss of flavour, change of texture, loss of nutritional value as well as changes in appearance and physical form (Chandan Kumar et al. 2014).

1.3.1 Structure and Texture

The main cause of change in the quality of the dehydrated foods relates to changes in their internal structure, which in turn determine the texture (Schössler et al. 2012). Other causes are the alterations in colour and the modifications in the chemical components, the nutritional value and the bioactive compounds.

The type of pretreatment and the intensity of its application have been reported to affect the structure of dehydrated fruits and vegetables. Blanching, for example, is a common preparatory operation of pronounced importance in the drying of plant materials, because it neutralizes polyphenol oxidases, among other enzymes. The polyphenol oxidases, in particular, lead to enzymatic browning during drying, with consequent alterations in colour. For those cases where the blanching operation was carried out correctly, the changes in texture are caused by phenomena such as gelatinization of starch, cellulose crystallization and internal stresses caused by localized variations in water content during dehydration. These tensions create

ruptures and compressions that originate permanent distortions in the cells, creating a wrinkled appearance. When rehydrated, these foods absorb very slowly and fail to gain back the firm texture of the original raw material. According to Guiné and Barroca (2012), increasing the drying temperature leads to changes in the textural properties, namely, a reduction in hardness and chewiness but not altering the elasticity and cohesiveness.

The texture of plant materials depends greatly on the contents of cellulose, pectin and hemicellulose present in the cell walls. These carbohydrates constitute the vegetable fibres, being cellulose and hemicellulose classified as insoluble fibres, while pectin is a water-soluble fibre. The structural changes verified along drying greatly influence the texture of the final product. The shrinkage and porosity are examples of great importance, and these determine texture because they are related to the elimination of a significant amount of water from the food. This produces different effects according to the drying method used: it results in highly porous structures in the case of lyophilized foods or, conversely, in very dense products in the case of air-dried foods, which undergo a significant degree of shrinkage (Delgado et al. 2014; Guiné et al. 2006; Koç et al. 2008; Niamnuy et al. 2014; Puig et al. 2012; Zhang et al. 2013).

The drying conditions, particularly the temperature and the drying rate, have a significant influence on the texture of the foods, and, in general, faster processes and higher temperatures cause greater changes. As the water is being eliminated, the solutes move from the inside of the food to its surface, being the mechanism that regulates this process and the water transfer rate characteristic of each solute and dependant on the food type and the operating conditions. The high temperatures have been reported as causing complex physical and chemical changes on the surface of the food, leading to the formation of a hard surface layer, which reduces the mass transfer and originates a dry crust on the surface but a moist food inside. An adequate control of the operating parameters can help minimize these effects, making the gradients between the internal and surface water content not excessively high (Vega-Gálvez et al. 2012). According to Guiné and Barroca (2012), increasing the drying temperature leads to changes in the textural properties, namely, a reduction in hardness and chewiness but not altering the elasticity and cohesiveness.

1.3.2 Colour

Drying provokes changes in the characteristics of the food surface, hence altering its colour and reflectance. Besides these physical alterations that influence colour, also some chemical changes occur in pigments like carotene and chlorophyll as a consequence of heat and oxidation that occur during drying. In general, pigments are most affected by longer drying times and higher temperatures.

During drying both the enzymatic and the non-enzymatic browning originate changes in the colour. The enzymatic browning is, hence, one of the mechanisms responsible for the loss of colour in dried foods. The polyphenol oxidases are a

group of enzymes involved in the appearance of a brownish colouration in plant foods, such as fruits and vegetables. In the case of fruits, this is particularly problematic, because they usually are not blanched before drying and also because the temperatures used in the drying process are not sufficient to inactivate them, particularly in the case of solar drying. In fact, the polyphenol oxidases are destroyed at high temperatures, so in the case of vegetables that are typically blanched prior to drying, the activity of the polyphenol oxidases is inhibited. The activity of the polyphenol oxidases is higher at the optimum pH situated in the range between 6 and 7, and therefore for a pH of 4 or lower, these enzymes become inactive. This is the reason why it is recommended the addition of citric acid or ascorbic acid to bring the pH at least two units below the optimum pH of these enzymes. Other treatments, based on sulphur compounds (e.g. the exposure to the vapours resulting from the burning of sulphur or the dipping in aqueous solutions of bisulphite or metabisulphite), have also been reported to effectively avoid the browning reactions. Nevertheless, when sulphur is involved, care must be taken in relation to the concentrations used so as to avoid unpleasant flavours in the food.

Among the non-enzymatic browning reactions stand the Maillard and the caramelization reactions. The Maillard reaction occurs between the amino acids and the reducing sugars and produces melanoidins, which diminish the nutritive value of the food. These reactions start from temperatures above 70 °C, and their rate is dependent on the type of sugars present in the food. Also the foods with water activity in the range 0.5–0.8 are more susceptible to non-enzymatic browning. Caramelization reactions happen with sugars for temperatures higher than 120 °C originating dark products named caramels. Hence, in solar drying, with relatively mild temperatures, even if inside a greenhouse, these reactions are very improbable.

The drying may affect the pigments present in the foods in variable ways. The carotenoids are pigments that in the foods give colourations going from yellow to orange and red. These, apart from their roles as colourants, also act as important functional compounds, fighting the free radicals and in some cases demonstrating provitamin A activity (like in the case of alpha-carotene, beta-carotene or beta-cryptoxanthin). The carotenoids undergo oxidation, when exposed to abundant oxygen concentrations, such as in the case of solar drying with exposure at the atmospheric air. Consequently, these compounds are extremely susceptible to oxidative reactions due to the presence of double bonds, but their stability depends also on the temperature, presence of light, water activity and acidity.

The enzymatic activity also causes losses in the pigment chlorophyll, responsible for the green colouration, turning it into pheophytin. The preservation of the green colouration could, nevertheless, be achieved altering the pH to basic by immersion in one solution of sodium bicarbonate for 1 min.

1.3.3 Chemical Composition and Nutritional Value

The changes in the nutritional value of dried foods are owing to the preparation operations prior to drying, the drying temperature and finally the storage conditions.

The losses of nutritional value during the preparation of fruits and vegetables (cut, bleaching, etc.) are normally higher than during the drying operation itself.

The water solubility of vitamins is variable according to the vitamin in question. Along the dewatering process, some vitamins (e.g. riboflavin) reach their supersaturation and so they precipitate, originating smaller losses. In other cases (e.g. vitamin C), the vitamins continue to dissolve until the food moisture is very low and react with the solutes at higher rates as the drying proceeds. Vitamin C is a water-soluble vitamins most sensitive to heat and oxidation (Kaya et al. 2010; Kowalski et al. 2013; Kurozawa et al. 2014; Solval et al. 2012; Timoumi et al. 2007). Thus, the drying times should be short, and during storage the temperatures should be kept low and both the water content and the oxygen concentration should also be low. Thiamine is a vitamin that is also relatively sensitive to heat, although not so extensively as vitamin C. Other soluble vitamins are more stable to heat and oxidation so that their losses are typically less than 5–10%; however, losses may occur due to the reaction with peroxides resulting from the oxidation of fats. The water-soluble vitamins niacin, pantothenic acid (vitamin B5), pyridoxine (vitamin B6), thiamine (vitamin B1), folic acid and riboflavin (vitamin B2) suffer important losses at drying temperatures around 70 °C, which can occur during solar drying, if done inside greenhouses with optimum solar exposure (Ekıncı 2005).

The lipid oxidation in foods is sensed by a strong characteristic smell and taste to rancid in general and, in the case of protein-rich foods, an alteration of texture. In lipid oxidation, the oxygen from the atmosphere reacts with the unsaturated fatty acids producing free radicals (chemical species highly reactive for having an unpaired electron) and peroxides (compounds with an oxygen atom with charge −1). These chemical species destroy fat-soluble vitamins and carotenoids and reduce the nutritive value of proteins. Lipid oxidation is highly dependent on the food water activity, because the water present in the food surface forms hydrogen bonds with peroxides, thus protecting them from decomposition and hence diminishing the oxidation rate. This phenomenon occurs for water activity values under 0.2 or lower than the monolayer moisture content. The fat-soluble nutrients (e.g. essential fatty acids and vitamins A, D, E and K) are generally on the dry matter of the food, and therefore their concentrations do not change so significantly along drying.

Metals like copper and iron, which are dissolved in the aqueous phase of the food, can act as catalysts for oxidation reactions of unsaturated nutrients such as lipids. However, the hydration of these metals and the formation of insoluble metal hydroxides which participate in the reaction diminish the catalytic activity, when the water activity values are under 0.5. However, for higher values of water activity, the diffusion of these catalytic metals increases, and therefore the rate of lipid degradation also augments. Consequently, when the water activity is low, the lipids are better protected, and consequently the preservation of the nutritional value of vitamins, carotenoids and proteins is higher. Dehydration does not substantially alter the biological value and digestibility of most food proteins, even though denaturation can happen in some foods and for determined drying conditions (Deng et al. 2014; Haque et al. 2013; Odjo et al. 2012).

The phenolic compounds are a family of chemical substances with the ability to act as antioxidants and therefore are considered important bioactive compounds present abundantly in fruits and vegetables. Although they are sensitive to high temperatures and can be degraded, they can be quite resistant when the temperatures are under 80 °C (Carranza-Concha et al. 2012; Gupta et al. 2002; Igual et al. 2012; Mrad et al. 2012). Therefore they resist practically unaltered for solar drying processes, where the drying temperatures are not high enough to cause their destruction.

1.3.4 Aroma

The volatile compounds present in foods are responsible for the aroma, since they vapourize and reach the nose, thus stimulating the flavour senses. The heating provoked by any drying treatment causes losses in some volatile components present in the food. However, the degree of loss is variable according to the temperature and the concentration of solids in the food as well as the vapour pressure of the volatile substances and their solubility in the water vapour. The volatile compounds with relatively high diffusivity and volatility are, naturally, those that are lost most easily. However, appropriate monitoring of conditions at the beginning and along drying can minimize the losses of aroma compounds. More expensive foods, such as herbs and spices, are preferably dehydrated at lower temperatures to minimize the loss of volatile compounds.

The protection of the flavour of dried foods can be achieved by some techniques: recover the volatile substances lost by vaporization during drying which are, after condensation, readded to the product; the mixture of recovered volatile aroma compounds with "fixing" aroma compounds and which are then added to the dried product; the activation of natural food enzymes; or the addition of external enzymes that originate aromatic substances from the natural aroma precursors. Changes in the flavour due to oxidation or enzymatic hydrolysis are avoided in the case of fruits with the use of sulphur dioxide, ascorbic acid or citric acid. Table 1 presents some works reported in the scientific literature that concern the changes in the different properties of foods submitted to solar drying.

2 Heat and Mass Transfer

The drying of products of biological nature, such as foods, involves simultaneous transfer of heat, mass and momentum in a very complex way, being therefore much difficult to accurately predict or describe these drying phenomena (Guiné 2005a; Irigoyen and Giner 2014).

Table 1 Studies about the changes in food properties caused by solar drying

Foods	Properties	References
Amaranth grains	Colour	Ronoh et al. (2009)
	Hardness	
	Crude protein	
Aromatic rice	Aroma compounds	Wongpornchai et al. (2004)
Banana	Colour	Janjai et al. (2009)
	Sensory evaluation	
Bitter gourd	Colour (greenness)	Vijayan et al. (2016)
	Volatile components	
Cambodian striped snakehead fish	Metal content	Basri et al. (2015)
	Nutritional elements	
Carrot	Vitamin C	Brătucu et al. (2013)
	Colour	
Deglet Nour dates	Browning	Mennouche et al. (2014)
Fish	Nutritional quality	Ojutiku et al. (2009)
	Organoleptic evaluation	
Fish meat (mackerels and sauries)	Vitamin D_3	Suzuki et al. (1988)
	Provitamin D_3	
Ginger	Texture	Borah et al. (2015b)
	Colour	
Green leafy vegetables (amaranth, cowpea leaves, sweet potato leaves, pumpkin leaves, wild varieties of mgagani, nsonga, ngwiba)	Carotene content	Mulokozi and Svanberg (2003)
	Vitamin A	
Green peas	Colour	Jadhav et al. 2010
	Hardness	
	Rehydration ratio	
	Shrinkage	
	Overall acceptability	
Jerky meat	Colour	Banout et al. (2012)
	Sensory analyses	
Longan	Colour	Janjai et al. (2009)
	Sensory evaluation	

(continued)

Table 1 (continued)

Foods	Properties	References
Mango	Vitamin A	Rankins et al. (2008)
	Beta-carotene	
	Sugars	
	Total coliforms	
Meat product (*Kilishi*)	Yield	Apata et al. (2013)
	Chemical properties	
	Sensory properties	
Mushrooms	Void fraction	Rahman et al. (2016)
	Average pore diameter	
Mushrooms	Shrinkage effect	Mustayen et al. (2015)
Mushrooms	Colour	Kumar et al. (2013)
	Rehydration ratio	
	Coefficient of rehydration	
Onion	Minerals	Arslan and Musa Özcan (2010)
Pea	Colour	Sahin et al. (2013)
	Shrinkage	
	Bulk and apparent densities	
	Internal and bulk porosities	
	Rehydration capacity	
	Microstructure	
Potato	Colour	Chouicha et al. (2013)
Red chilli	Colour	Banout et al. (2011)
	Vitamin contents	
	Mycotoxin contents	
Red pepper	Colour coordinates	Arslan and Musa Özcan (2010)
Sage	Microbial load	Hassanain (2011)
Strawberry	Chemical composition	El-Beltagy et al. (2007)
	Rehydration ratio	
	Texture	
	Sensory properties	

(continued)

Table 1 (continued)

Foods	Properties	References
Sweet potato	Provitamin A	Bechoff et al. (2009)
Thyme	Total phenolic compounds	Lahnine et al. (2016)
Tomato	Colour	Ringeisen and Stroeve (2014)
	Brix	
	Lycopene	
	Vitamin C	
Turmeric	Texture	Borah et al. (2015b)
	Colour	

2.1 Heat Transfer

The energy required for the evaporation of the water when drying foods is obtained by delivering an adequate quantity of thermal energy. The heat is transferred by three mechanisms: conduction, convection and radiation. The heat transfer by conduction is limited to solids, which are constituted by molecules that are in a rigid configuration and therefore have no mobility. In this case, the transfer occurs at the molecular level, so that the molecules closer to the heat source contain more vibrational energy, which is transmitted to some extent to their neighbouring molecules. The heat transfer by conduction is described by the Fourier equation:

$$\frac{dQ}{dt} = k\,A\,\frac{dT}{dx} \tag{1}$$

where dQ/dt is the amount of heat transferred per unit time [J/s], A is the sectional area which is traversed by heat [m^2], dT/dx is the temperature gradient [K/m] and k is the thermal conductivity [J/(m.s.K)].

In convection the heat transfer occurs through the movement of groups of molecules in a fluid, which may be a liquid or gas, in which the molecules have mobility. It is not possible to accurately determine the heat transfer by convection, contrarily to what happens for conduction. Although there are some theoretical models available, in most cases, empirical equations are used. The more satisfactory formulas for heat transfer by convection correspond to relations between dimensionless numbers of physical quantities. The heat transfer by convection can be either under natural or forced convection. In the former, the movement comes from differences in density produced during heating or cooling, while in the latter, an external source of energy is applied to produce movement, for example, by means of a ventilator or fan. It can happen in some cases that these two phenomena may occur simultaneously.

Heat transfer by radiation occurs by means of electromagnetic waves that reach the food and are partially absorbed being responsible for increasing its thermal energy. This form of heat transfer is independent of the means by which it operates but dependent on temperature, the geometric distribution and the surface structure of the materials which emit or absorb heat. The heat transfer by radiation is described by the Stefan-Boltzmann equation:

$$Q = \varepsilon A \sigma T^4 \tag{2}$$

where Q is the heat transferred [J], T is the absolute temperature, A is the area [m^2], σ is the Stefan-Boltzmann constant ($\sigma = 5.73 \times 10^{-8}$ J/(m^2.K^4)) and ε is the emissivity of the body, which varies from 0 to 1. Bodies which satisfy this relationship are called grey bodies. The emissivity differs according to temperature, T, and to the wave amplitude of the radiation emitted.

In drying it is also important to consider the heat transfer at the surface of the food, which is described by Newton's law:

$$Q = h_s A (T_a - T_s) \tag{3}$$

where Q is the heat transferred [J], h_s is the surface heat transfer coefficient [J/(m^2.s.K)], A is the area [m^2] and T_a and T_s are, respectively, the temperatures of the fluid and at the surface of the food [K].

The increase in the temperature of the food, due to a certain amount of thermal energy, is given by:

$$Q = m c_p \Delta T \tag{4}$$

where Q is the heat transferred [J], m is the mass of the food being heated [kg] and c_p is the specific heat at constant pressure [J/(kg.K)].

In drying a significant part of the heat received by the food is used to evaporate its water, according to the following equation:

$$Q = m \lambda_{vap} \tag{5}$$

with λ_{vap} representing the latent heat of vaporization ($\lambda_{vap} = 2257$ kJ/kg, for water boiling at atmospheric pressure).

During drying, the transfer of heat happens by the three possible mechanisms although some might be more significant than the other, depending on the case.

2.2 Mass Transfer

Drying involves the evaporation of a meaningful part of the water initially present in the food. This water moves from the inside of the food to the surface in the form

of liquid water or vapour by diffusion and then is evaporated from the surface, being removed by the surrounding air.

In a similar way to heat transfer, the mass transfer also occurs due to a gradient in concentration or pressure, being its rate proportional to that gradient as well as to the properties of the system, considered in the mass transfer coefficient. Thus, the following equation is generally used for the mass transfer:

$$\frac{dm}{dt} = k_m A \, \Delta C \tag{6}$$

where m is the mass transferred during the time period t [kg/s], k_m is the mass transfer coefficient [m/s], A is the area [m^2] and ΔC is the concentration gradient [kg/m^3]. For the mass transfer in drying, Eq. (6) becomes:

$$\frac{dm}{dt} = k'_g A \, \Delta H \tag{7}$$

where k'_g is the mass transfer coefficient to the vapour phase and ΔH is the moisture gradient.

The application of Eq. (7) for mass transfer is not so simple as the heat transfer equation because of the variations in moisture along drying. Initially the moisture is transferred from the surface of the material to the surrounding air. However, when the process moves forward, the moisture is transferred from the deeper areas of the food to the surface to be evaporated. In the study of surface/air relation, it is necessary to consider the transfer of mass and heat simultaneously. It is therefore important to consider firstly the determination of the relationship between the wet surface and the ambient air and secondly the diffusion through the food.

Most food products, including fruits and vegetables, have a porous capillary structure, wherein the food matrix contains interstitial spaces, capillary cavities and gas-filled spaces. Hence, a number of mass transfer mechanisms have to be considered, which, in turn, can act in various combinations (Guiné 2005a, b). These mechanisms include liquid diffusion due to concentration gradients; liquid transport due to capillary forces; vapour diffusion due to gradients in the partial vapour pressure; liquid or vapour transport, due to the difference in total pressure caused by external pressure and temperature; effects of vaporization and condensation; surface diffusion; and transport of liquids due to gravity (Guiné 2005a, b).

3 Solar Drying of Foods

From ancient times foods such as fruit, vegetables, meat or fish were dried by direct sunlight. While pieces of fruit or vegetables were scattered on the ground, usually on sheets or mats, products such as meat or fish were typically displayed

on shelves or alternatively hanged on ropes. However, the disadvantages of these procedures were many: the foods were exposed to countless sources of contamination (insects, birds, animals, dust), and the drying was much dependent on weather conditions (solar radiation, temperature, wind, night moist). The drying times were long and the products could get spoiled if the weather conditions were not favourable. The use of greenhouses can minimize these problems, and high temperatures are maintained as compared to the open air (due to the greenhouse effect). Furthermore, the food is protected and hence its safety and quality are improved. Inside the greenhouses the air circulates by natural convection, but they can also be equipped with chimneys for air outlet, thus increasing the airflow. In other cases, the efficiency of the drying system can be increased by incorporating a solar collector system, which uses panels for an efficient collection of the sunray's energy.

Different types of solar dryers are available varying in size and design, according to the requirements of a particular product/process. Solar dryers can be classified according to the air movement mode, solar contributions, air direction movements, type of product to be dried and insulation of the assembly (Kumar et al. 2016). The solar dryers can be with natural or forced convection with respect to the air movement. In active solar dryers or forced convection solar dryers, the air necessary for the drying of the product is forced through the solar collector to the drying chamber by means of a fan or a blower. Contrarily, in passive solar dryers or natural convection solar dryers, the flow of the air required for product drying is due to natural or buoyancy force action (Basunia and Abe 2001; Ekechukwu and Norton 1999). The solar dryers can also be classified into direct, indirect or hybrid, according to the incidence of the solar rays (Kumar et al. 2016).

3.1 Direct Solar Drying

In all solar drying processes, the energy source is the sun. However, the solar drying includes both the processes in which the product is directly exposed to solar radiation, either at open-air exposure or inside greenhouses (direct solar drying) and those in which the sun's energy is concentrated by collectors, being then used to heat air that is put in contact with the food (indirect solar drying).

For centuries, fruit, vegetables, meat and fish were dried by direct sunlight. This aimed at the preservation of such foods when no other preservation methods or equipments were available. For the drying, the pieces of fruit or vegetables were scattered on the ground, over sheets or mats. They could or could not be previously submitted to some preparation operations, such as washing, cleaning, cutting or removing the peel. Also in some cases, like for peppers, they could be gathered in ropes and hanged. Figure 1 shows the drying of pears as done traditionally in Portugal, at open-air exposure.

Fig. 1 Traditional methods for drying of pears in Portugal (Photo authored/ copyrighted by Raquel Guiné)

For the drying of meat and fish, usually they were cut into strips which were arranged on shelves or hung on ropes. These processes had in common the direct exposure to the solar radiation at open-air conditions. With these procedures, the foods were exposed to the vagaries of time and many possible sources of contamination, such as dust, insects, birds, rodents or other animals. The drying times were relatively long, and, if sometimes the weather conditions were not favourable, the foods could become rotten and spoiled because they could not reach a stable moisture content.

The use of solar covered greenhouses (Fig. 2) can minimize the problems associated with the open-air exposure of the foods by keeping the food more protected, while still using the sun as energy source. Furthermore, inside this type of structure, high temperatures are maintained as compared to the open air due to the greenhouse effect. In most of these structures, the air circulates by natural convection, and they can also be equipped with chimneys for air outlet, with the aim of increasing the airflow through the dryer. The higher the chimney, the faster is the air circulating rate. Alternatively solar tunnels provide the same advantages as greenhouses regarding the efficiency and the quality of the product (Patil and Gawande 2016).

In direct solar dryers, the moisture is removed away by the direct impingement of solar radiation directly on the product, regardless of being with or without the natural air circulation (Ekechukwu and Norton 1999). Typically, direct solar dryers consist of a drying chamber which is covered by a transparent cover made of glass or plastic and having orifices to allow the circulation of air (Fig. 3). When the solar radiation impacts on the glass cover, the air is heated and circulates either by natural

Fig. 2 Direct solar drying of pears in a greenhouse (Photo authored/copyrighted by Raquel Guiné)

Fig. 3 A direct solar dryer (Photo authored/copyrighted by Raquel Guiné)

convection owing to changes in density or by forced convection using, for example, a fan or a blower or even a combination of both (Ghazanfari et al. 2003; Seveda and Jhajharia 2012; Sharma et al. 2009).

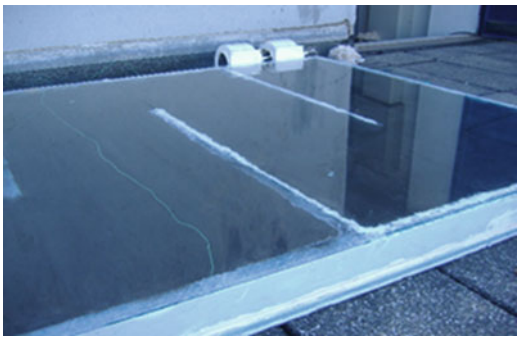

Fig. 4 A solar collector for indirect solar drying (photo authored/copyrighted by Raquel Guiné)

3.2 Indirect Solar Drying

The performance of the direct solar dryers can be increased by incorporating a solar collector system (Fig. 4), and the hot air from the collector is sent to the dryer, passing through a series of perforated shelves that support the food layers and being expelled at the top of the chamber. As alternative, the solar collector can produce electricity to heat resistances that will be used for providing the heat Pirasteh et al. 2014).

Indirect active solar dryers are constituted by a solar collector separated from the drying unit and comprise also a fan and a ducting for the circulation of the air. The solar collecting device allows reaching higher air temperatures with a controlled airflow rate, but its efficiency is reduced when higher values of temperature are achieved (Fadhel et al. 2011; Hossain et al. 2008).

The design of the systems is crucial for the performance and efficiency of the drying processes. Usually, the solar collectors are made of wood or metals covered in appropriate absorbing materials, such as black polythene, for an enhanced heat absorption, thus increasing the efficiency of the moisture removing rate (Parikh and Agrawal 2012).

4 Drying Curves

The drying rate is mainly determined by the velocity of heat transfer to the water contained in the food matrix and which will deliver its latent heat of vaporization. However, in extreme situations, the process speed may be limited by the mass transfer phenomena in the process of water removal.

Inside the food the water may be linked to the food matrix with variable intensities, being retained by forces that can be quite weak (such as those that retain the surface water) up to very strong ones (like the chemical bonds). Hence, during the drying process, the water retained with weaker forces is more easily separated from the food, and consequently the drying rate decreases as the food gets

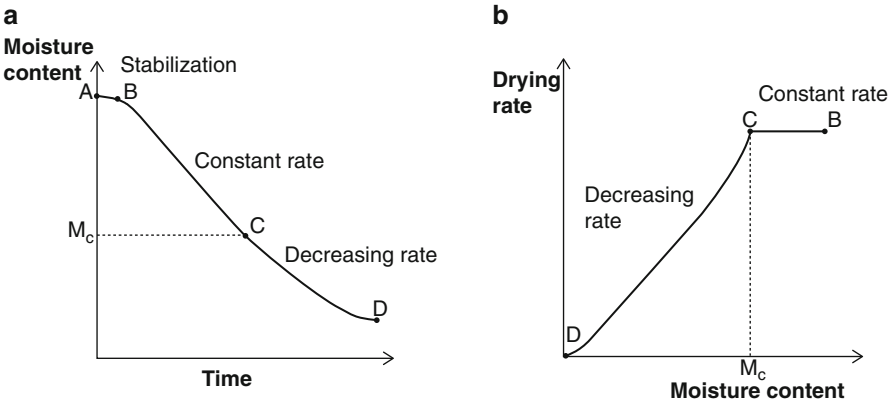

Fig. 5 Drying curves: (**a**) moisture versus time, (**b**) drying rate versus moisture content (Mc is critical moisture content) (Graphics authored/copyrighted by Raquel Guiné).

dried and the moisture content diminishes, because the remaining water gets increasingly strongly attached to the product.

Frequently, most of the water is weakly retained on the food, being considered as free water on the surface, and in such cases the drying takes place at constant rate. However, when the foods contain inner water, after the initial drying period at constant rate, the water is separated more slowly and therefore the drying rate decreases. This comportment originates a generic standard for the drying process expressed by characteristic drying curves as shown in Fig. 5a, wherein the moisture content is depicted as a function of drying time or alternatively Fig. 5b where the drying rate is expressed in terms of moisture content (Guiné 2005a, b).

In the beginning of the drying process, the heat received by the food is used to increase its temperature from its initial temperature up to the point when the water starts to evaporate. In this phase there is still no evaporation (phase AB in Fig. 5a). In the initial stages of the drying process, the material is sufficiently wet, and in that case, the water can move quickly through small distances below the surface, and diffusion rate equals the rate of evaporation at surface of the solid. Accordingly, the internal resistances to heat or mass transfer are insignificant, and the rate is limited by the external thermal resistance or the resistance to the mass transfer or even by both. Therefore, the surface remains wet and at the wet bulb temperature, maintaining a constant drying rate (phase BC in Fig. 5a). When drying reaches the point where it has been removed a quantity of water which causes the internal diffusion to no longer being able to match the evaporation rate, the vaporization front recedes inside the food increasing the resistance to diffusion of the liquid water to the surface. In this phase the surface starts to dry (phase CD in Fig. 5a). So begins the decreasing rate period, and the moisture content that separates the constant rate period from the decreasing rate one is called critical moisture content (Guiné 2005a, b).

5 Kinetic Modelling

Knowledge of the drying kinetics is of incontestable importance for the development of models that describe the drying processes and to understand the moisture removal mechanisms for the establishment of appropriate operating conditions (Guiné 2005a, b). The understanding of some of the phenomena occurring during drying can be achieved by mathematical modelling. There are hundreds of mathematical models that were developed to represent the drying kinetics of foods, being mostly empirical, owing to the complexity of the numerous phenomena involved. However, some of those empirical models include also some phenomenological parameters that, although not having a physical meaning, can allow prediction of the drying rate with relative precision. Finally, a more phenomenological approach uses Fick's second law of diffusion to describe the moisture diffusion process in foodstuffs.

Many models have been used for the description of the drying kinetics for various food products, ranging from models that are based on the laws of diffusion up to the thin-layer designs which can be grouped into theoretical, semi-theoretical or empirical (Doymaz 2007). Undoubtedly, the reliable modelling of drying processes requires a thorough knowledge of the physicochemical behaviour of food and water removal mechanisms, partially expressed through the drying kinetics. The various mathematical models developed to represent food-drying kinetics are in most cases empirical, due to the complexity of the various phenomena involved. However, some of the empirical kinetic models include phenomenological parameters that, despite not having a physical meaning, can allow prediction of the drying rate with relative precision (Guiné 2005a, b). In a more phenomenological way, many investigators use Fick's second law of diffusion to describe the moisture diffusion process in foodstuffs (Corzo et al. 2008).

5.1 Empirical Models

Thin-layer equations were developed to describe the drying phenomena in a combined way, independently of the mechanism that governs the process. This type of equation has successfully been used to obtain the drying curves for various products allowing determining the drying time. They express the variations in moisture content along the drying process as functions of certain parameters like the drying constant or the lag factor, which are responsible for combined effects of various transport phenomena during drying (Tripathy and Kumar 2009).

From the experimental data obtained from the thin-layer drying experiments, the thin-layer models can be applied either in the case of a single product exposed to the drying air or one layer of the grains as well as to a multilayer of many grain thicknesses, if the temperature and the relative humidity of the drying air can be applied for drying process calculations as being in the same thermodynamic state at

any time of the drying process (Kucuk et al. 2014). Hence, these models constitute useful tools for the prediction of drying kinetics of heat-sensitive bio-origin materials, such as foods (Chin et al. 2008).

Many different thin-layer equations can be found in the literature, ranging widely in nature, and have been used by many researchers to successfully explain the drying of various agricultural products (Nourhène et al. 2008). Most of the models include a dimensionless variable, the moisture ratio (MR), which includes the moisture content at any moment, W_t; the equilibrium moisture content, W_e; and the initial moisture content, W_0, all expressed on dry basis:

$$\mathrm{MR} = \frac{W_t - W_e}{W_0 - W_e} \tag{8}$$

Experimental studies are of the utmost importance in thin-layer drying, and the equations are important tools for the mathematical modelling of the processes. They are practical, are easy to implement and give relatively good results, thus establishing a good compromise between complexity and accuracy (Erbay and Icier 2010). Table 2 presents a sample of the most used kinetic models to describe the drying kinetics for solar drying of foods.

The drying rate constant accounts for the mechanisms of heat and mass transfer phenomena and traduces the influence that certain process variables exert on the process of moisture removal from the product during drying. It constitutes the most essential constant in the great majority of the empirical mathematical models used to describe any dehydration operation and pursues an adequate estimation of the

Table 2 Some empirical kinetic models commonly used to fit the experimental data for solar drying of foods

Model name	Equation	References
Lewis/Newton	$\mathrm{MR} = \exp.(-\mathrm{k\ t})$	Lewis (1921)
Page	$\mathrm{MR} = \exp.(-\mathrm{k\ t^n})$	Page (1949)
Modified Page	$\mathrm{MR} = \exp.[-(\mathrm{k\ t})^n]$	Overhults et al. (1973)
Henderson and Pabis	$\mathrm{MR} = a\ \exp.(-\mathrm{k\ t})$	Henderson and Pabis (1969)
Modified Henderson and Pabis	$\mathrm{MR} = a\ \exp.(-\mathrm{k\ t}) + b\ \exp.(-\mathrm{g\ t}) + c\ \exp.(-\mathrm{h\ t})$	McMinn (2006)
Two-term	$\mathrm{MR} = a\ \exp.(-\mathrm{k_0\ t}) + b\ \exp.(-\mathrm{k_1\ t})$	Henderson (1974)
Logarithmic	$\mathrm{MR} = a\ \exp.(-\mathrm{k\ t}) + c$	Yagcioglu et al. (1999)
Wang and Singh	$\mathrm{MR} = 1 + a\ \mathrm{t} + b\ \mathrm{t}^2$	Wang and Singh (1978)
Two-term exponential	$\mathrm{MR} = a\ \exp.(-\mathrm{k\ t}) + (1-a)\ \exp.(-\mathrm{k}\ a\ \mathrm{t})$	Sharaf-Elden et al. (1980)
Verma et al.	$\mathrm{MR} = a\ \exp.(-\mathrm{k\ t}) + (1-a)\ \exp.(-\mathrm{g\ t})$	Verma et al. (1985)
Diffusion approach	$\mathrm{MR} = a\ \exp.(-\mathrm{k\ t}) + (1-a)\ \exp.(-\mathrm{k\ b\ t})$	Kassem (1998)
Midilli et al.	$\mathrm{MR} = a\ \exp.(-\mathrm{k\ t^n}) + b\ \mathrm{t}$	Midilli et al. (2002)
Vega-Lemus	$\mathrm{MR} = (a + \mathrm{k\ t})^2$	Guiné (2010)

drying time as well as the behaviour of all corresponding operational factors that play an important role in the design and optimization of drying systems. The drying rate constant is determined from the experimental measurements of the moisture content along the drying process at different drying conditions (Singh et al. 2012).

Initially the drying is very rapid because the surface of the product is kept wet during the constant drying rate period. However, after that, the falling rate period begins and the drying rate is considerably lower. Hence, the drying rate decreases continuously with time and decreasing moisture content. During the falling rate period, the predominant mechanism of mass transfer is the internal transfer of moisture due to liquid diffusion inside the food, which governs the moisture transfer (Sharma et al. 1991; Toğrul and Pehlivan 2004). The drying kinetics may be fully described using the transport properties of the products together with those of the drying medium, usually air. In case of food drying, the drying rate constant, k, is used instead of the transport properties. Therefore, the drying rate constant combines all the transport properties and may be defined by thin-layer equations, in different mathematical models (Singh et al. 2012). Tables 3, 4 and 5 present some kinetic data for the drying of different food products, particularly the drying constant due to its unquestionable importance.

5.2 *Fick's Second Law of Diffusion*

Fick's second law equation for non-steady-state diffusion, assuming that the samples used can be approximated to cylinders, can be expressed by the following equation (Guiné et al. 2011):

$$\frac{\partial W}{\partial t} = \frac{1}{r}\left\{\frac{\partial}{\partial r}\left(D_e r \frac{\partial W}{\partial r}\right) + \frac{\partial}{\partial z}\left(D_e r \frac{\partial W}{\partial z}\right)\right\} \tag{9}$$

where D_e is the effective moisture diffusivity, r is the cylinder radius, z is the height and t is the time, expressed in seconds. Admitting that initially there is a uniform moisture content and that the effective diffusivity throughout the sample is constant, the analytical solution of Eq. (9) is given by:

$$\frac{W - W_e}{W_0 - W_e} = \sum_{n=1}^{\infty} \frac{4}{b_n^2} \exp\left(-D_e \frac{b_n^2 t}{r^2}\right) \tag{10}$$

where $(W-W_e)/(W_0-W_e)$ is the moisture ratio as defined by Eq. (8) (Faustino et al. 2007). Considering only the first term of the series in Eq. (10), the solution of Fick's equation becomes

Table 3 Some kinetic data relative to the solar drying of different vegetables/legumes

Food	Model name	Drying constant (unit)	References
Bitter gourd	Lewis	0.3436	Vijayan et al. (2016)
	Page	0.3906	
	Henderson and Pabis	0.3366	
	Logarithmic	0.3884	
	Two-term exponential	0.6679	
	Verma et al.	0.3436	
	Diffusion approach	0.3437	
	Midilli et al.	0.3928	
Chickpea	Henderson and Pabis	0.1391–0.1843	Lopez et al. (2014)
Jew's mallow	Newton	0.2967–0.3113	Saleh and Badran (2009)
Fenugreek leaves	Newton	0.294228	Sunil et al. (2014)
	Page	0.129662	
	Henderson and Pabis	0.397323	
	Logarithmic	0.029069	
Garlic clove	Newton	0.20804	Shringi et al. (2014)
	Page	0.59147	
	Henderson and Pabis	0.12774	
	Two-term	0.12774	
	Midilli et al.	0.88196	
Green bean	Lewis	0.10009	Doymaz (2011)
	Henderson and Pabis	0.08679	
	Modified Henderson and Pabis	0.07916	
	Logarithmic	013535	
	Two-term	0.25196	
	Two-term exponential	0.23240	
	Diffusion approach	0.18924	
	Page	0.25709	
	Midilli et al.	0.27401	
Green peas	Page	0.00092–0.01842	Jadhav et al. (2010)
	Newton	0.00171–0.00831	
	Henderson and Pabis	0.00171–0.00831	
Green peas	Newton	0.132719–0.213304	Sunil et al. (2013)
	Page	0.019292–0.059738	
	Henderson and Pabis	0.171569–0.281486	
	Logarithmic	0.007471–0.117491	
Green pepper	Newton	0.014102–0.026125	Akpinar and Bicer (2008)
	Page	0.006858–0.063688	
	Modified Page	0.118752–0.161634	
	Henderson and Pabis	0.013977–0.022276	
	Logarithmic	0.005519–0.011395	
	Two-term	0.013996–0.022237	

(continued)

Table 3 (continued)

Food	Model name	Drying constant (unit)	References
	Two-term exponential	0.261415–1.523762	
	Diffusion approach	0.022707–1.413743	
	Modified Henderson and Pabis	0.013997–0.022265	
	Verma et al.	0.023295–1.418512	
	Midilli et al.	0.047860–1.220272	
Mushroom	Newton	0.0017–0.0044	Reyes et al. (2014)
Okra	Lewis	0.03283	Doymaz (2011)
	Henderson and Pabis	0.02928	
	Modified Henderson and Pabis	0.03061	
	Logarithmic	0.02815	
	Two-term	0.25196	
	Two-term exponential	0.21453	
	Diffusion approach	0.51569	
	Page	0.06870	
	Midilli et al.	0.11109	
Potato	Newton	0.0039–0.0074	Tripathy (2015)
	Modified Page	0.0043–0.0077	
	Henderson and Pabis	0.0045–0.0083	
	Logarithmic	0.0008–0.0028	
	Two-term	0.0045–0.0083	
	Modified Henderson and Pabis	0.0040–0.0083	
	Verma et al.	0.0039–0.0074	
Red Chilli	Newton	0.0497–0.0899	Fudholi et al. (2013)
	Page	0.0091–0.0244	
	Henderson and Pabis	0.0641–0.1090	
Red seaweed	Newton	0.4019	Fudholi et al. (2014)
	Page	0.9442	
	Henderson and Pabis	0.3327	
Tomato	Newton	0.0366	Sacilik et al. (2006)
	Page	0.0591	
	Henderson and Pabis	0.0337	
	Logarithmic	0.0285	
	Two-term	0.0337	
	Two-term exponential	0.2958	
	Diffusion approach	0.4593	
	Modified Henderson and Pabis	0.0300	

(continued)

Table 3 (continued)

Food	Model name	Drying constant (unit)	References
Tomato	Newton	0.0068–0.0167	Bagheri et al. (2013)
	Henderson and Pabis	0.0074–0.0179	
	Page	0.0012–0.0048	
	Logarithmic	0.0052–0.0166	
	Two-term	0.0187–0.3571	
	Modified Page	0.0032–0.0049	
	Two-term exponential	0.0131–0.3809	
	Midilli et al.	0.0073–0.0472	
Tomato	Newton	0.04909	Gurlek et al. (2009)
	Page	0.01864	
	Henderson and Pabis	0.0562	
	Logarithmic	0.0310	
	Two-term	0.0785	
	Two-term exponential	0.0762	
	Modified Page	0.0507	
	Verma et al.	0.0929	
	Diffusion approach	0.7135	

$$\frac{W - W_e}{W_0 - W_e} = \left(\frac{4}{b_1^2}\right) \exp\left(-D_e t \frac{b_1^2}{r^2}\right), \tag{11}$$

and a plot of ln(MR) versus time will give a straight line whose slope can allow to estimate the value of the diffusion coefficient or diffusivity.

The diffusivity varies from food to food depending on its structure, which is characterized by properties such as porosity, tortuosity or pore size distribution, as well as by its composition, and particularly the quantity of water and solutes present. While sugars significantly reduce the porosity, thereby lowering the diffusivity of water through the product, on the contrary, the inert particles prevent shrinkage, causing an opposite effect on the diffusivity. The diffusivity is also dependent on the drying temperature, being suggested by many authors to correspond to an Arrhenius-type function. However, this is only valid when the temperature is controlled and kept constant, which is not the case in the direct solar drying systems, in which the temperature is variable along the hours of the day. Table 6 shows values of effective diffusion coefficient for different foods dried by various solar systems.

Table 4 Some kinetic data relative to the solar drying of different fruits

Food	Model name	Drying constant (unit)	References
Apple	Newton	0.006966	Aktaş et al. (2009)
	Page	0.006940	
	Modified Page	0.006944	
	Henderson and Pabis	0.007696	
Apricot	Newton	0.000537	Toğrul and Pehlivan (2004)
	Page	0.004006	
	Modified Page	0.000582	
	Henderson and Pabis	0.000473	
	Logarithmic	0.000528	
	Two-term	0.999984	
	Diffusion approach	0.011307	
	Verma et al.	0.009359	
	Modified Henderson and Pabis	0.000469	
	Two-term exponential	0.004544	
Fig	Newton	0.000208	Toğrul and Pehlivan (2004)
	Page	0.000991	
	Henderson and Pabis	0.000200	
	Logarithmic	0.000310	
	Two-term	0.999995	
	Diffusion approach	0.107077	
	Verma et al.	0.013803	
	Modified Henderson and Pabis	0.008389	
	Two-term exponential	0.004674	
Grape	Newton	0.0076–0.0568	Çakmak and Yıldız (2011)
	Page	0.0128–0.0847	
	Modified Page	0.0001–0.0054	
	Henderson and Pabis	0.0045–0.0564	
	Two-term	5.3086–9.9850	
	Midilli et al.	0.1277–0.3682	
Grape	Newton	0.000227	Toğrul and Pehlivan (2004)
	Page	0.000460	
	Modified Page	0.000211	
	Henderson and Pabis	0.000206	
	Logarithmic	0.000295	
	Two-term	0.999925	
	Diffusion approach	0.017607	
	Verma et al.	0.055025	
	Modified Henderson and Pabis	0.000166	
	Two-term exponential	0.010002	

(continued)

Table 4 (continued)

Food	Model name	Drying constant (unit)	References
Mango	Newton	0.0638–0.0806	Dissa et al. (2011)
	Page	0.2503–0.1888	
	Modified Page	0.0643–0.0790	
	Henderson and Pabis	0.0366–0.0604	
	Logarithmic	0.1088–0.1390	
	Two-term	0.0140–0.0284	
	Two-term exponential	0.2224–0.2473	
	Verma et al.	0.1979–0.2124	
	Diffusion approach	0.1979–0.2124	
Peach	Newton	0.000540	Toğrul and Pehlivan (2004)
	Page	0.002500	
	Modified Page	0.000564	
	Henderson and Pabis	0.000490	
	Logarithmic	0.001172	
	Two-term	0.999902	
	Diffusion approach	0.109911	
	Verma et al.	0.009573	
	Modified Henderson and Pabis	0.001710	
	Two-term exponential	0.005489	
Pear	Newton	0.0185–0.0425	Guiné et al. (2009)
	Page	0.0228–0.0534	
	Henderson and Pabis	0.0170–0.0407	
	Logarithmic	0.8610–1.0378	
	Diffusion approach	0.0185–0.0425	
Pear	Page	0.1263–0.1734	Guiné (2005b)
	Two-term exponential	0.0613–0.1266	
Plum	Newton	0.000229	Toğrul and Pehlivan (2004)
	Page	0.000324	
	Modified Page	0.000219	
	Henderson and Pabis	0.000218	
	Logarithmic	0.000236	
	Two-term	1.019951	
	Diffusion approach	0.016850	
	Verma et al.	0.000239	
	Modified Henderson and Pabis	0.000460	
	Two-term exponential	0.010806	
Pistachio	Newton	0.0417–0.0498	Midilli and Kucuk (2003)
	Page	0.0785–0.8380	
	Modified Page	0.0080–0.0243	
	Henderson and Pabis	0.0314–0.0437	

(continued)

Table 4 (continued)

Food	Model name	Drying constant (unit)	References
	Logarithmic	0.3788–0.4822	
	Two-term model	0.1199–0.4300	
	Two-term exponential	0.6170–0.7412	
Pistachio	Newton	0.0894	Kouchakzadeh (2013)
	Page	0.0587	
	Henderson and Pabis	0.0734	
	Two-term	0.1919	
Prickly pear peel	Newton	0.0057	Lahsasni et al. (2004)
	Page	0.0057	
	Modified Page	0.0063	
	Henderson and Pabis	1.0212	
	Logarithmic	1.0704	
	Two-term	0.4349	
	Two-term exponential	1.5118	
	Diffusion approach	0.0073	
	Modified Henderson and Pabis	0.0058	
	Verma et al.	0.0057	
	Midilli et al.	0.0087	
Strawberry	Newton	0.1711–0.2914	El-Beltagy et al. (2007)
Sultana grape	Newton	0.042707	Yaldiz et al. (2001)
	Page	0.088790	
	Modified Page model	0.000175	
	Henderson and Pabis	0.042707	
	Logarithmic	0.042707	
	Two-term	6.351304	
	Two-term exponential	0.226307	
White mulberries	Newton	0.021051–0.026858	Akpinar (2008)
	Page	0.042307–0.043648	
	Modified Page	0.022212–0.027777	
	Henderson and Pabis	0.018865–0.024353	
	Logarithmic	0.017859–0.017999	
	Two-term	0.018865–0.024353	
	Two-term exponential	0.202275–0.334293	
	Diffusion approach	0.508311–0.918720	
	Modified Henderson and Pabis	0.018863–0.024353	
	Midilli et al.	0.024565–0.041626	

Table 5 Some kinetic data relative to the solar drying of different herbs and spices

Food	Model name	Drying constant (unit)	References
Basil	Newton	0.0030–0.0070	Gulcimen et al. (2016)
	Page	0.0002–0.0004	
	Modified Page	1.1130–1.7030	
Basil	Newton	0.000168	Akpinar (2006)
	Page	0.000418	
	Modified Page	0.000165	
	Henderson and Pabis	0.000170	
	Logarithmic	0.100000	
	Two-term	0.000186	
	Two-term exponential	0.020361	
	Diffusion approach	0.012956	
	Verma et al.	0.000999	
	Modified Henderson and Pabis	0.000167	
Coriander	Newton	2.7472	Panwar (2014)
	Page	0.7291	
	Modified Page	0.7431	
	Henderson and Pabis	1.0000	
	Modified Henderson and Pabis	0.7113	
	Midilli et al.	0.6277	
	Logarithmic	0.6920	
	Two-term	0.7113	
Crabwood seeds (*guianensis* and *surinamensis)*	Newton	0.1168–0.1919	Mendonça et al. (2015)
	Page	0.0408–0.1181	
	Midilli et al.	0.2870–0.3867	
	Diffusion approach	0.2334–0.3329	
	Logarithmic	0.0636–0.2620	
Mint	Newton	0.2879–0.3461	Saleh and Badran (2009)
Mint	Newton	0.000148–0.000175	Akpinar (2010)
	Page	0.000261–0.000308	
	Modified Page	0.000196–0.000177	
	Henderson and Pabis	0.000178–0.000192	
	Logarithmic	0.000149–0.100000	
	Two-term	0.007400–0.000181	
	Two-term exponential	0.137759–0.147149	
	Verma et al.	0.000189–0.000219	

(continued)

Table 5 (continued)

Food	Model name	Drying constant (unit)	References
Mint	Lewis	0.2865	El-Sebaii and Shalaby (2013)
	Page	0.0794	
	Modified Page	0.3433	
	Henderson and Pabis	0.3470	
	Logarithmic	0.0760	
	Two-term	0.3470	
	Modified Henderson and Pabis	0.3470	
	Midilli et al.	0.0568	
	Diffusion approach	0.8668	
	Two-term exponential	0.2824	
Parsley	Newton	0.000128	Akpinar (2006)
	Page	0.000396	
	Modified Page	0.000116	
	Henderson and Pabis	0.000138	
	Logarithmic	0.100000	
	Two-term	0.000568	
	Two-term exponential	0.028689	
	Diffusion approach	0.010488	
	Verma et al.	0.000077	
	Modified Henderson and Pabis	0.000139	
Pepper	Newton	0.0299	Akin et al. (2014)
	Henderson and Pabis	0.0287	
	Logarithmic	0.0748	
	Two-term	0.0456	
	Page	0.0449	
	Modified Page	0.0299	
	Two-term exponential	0.1035	
	Modified Henderson and Pabis	10.520	
	Verma	0.0287	
Roselle (karkade)	Logarithmic	0.000338–0.001253	Saeed (2010)

(continued)

Table 5 (continued)

Food	Model name	Drying constant (unit)	References
Turmeric rhizomes	Lewis	0.1439–0.1727	Borah et al. (2015a)
	Page	0.0068–0.2166	
	Modified Page	0.1412–0.2239	
	Henderson and Pabis	0.1855	
Thyme	Lewis	0.0198	El-Sebaii and Shalaby (2013)
	Modified Page	0.0341	
	Henderson and Pabis	0.0279	
	Logarithmic	5.7027	
	Two-term	0.0279	
	Modified Henderson and Pabis	0.0279	
	Verma et al.	0.0198	
	Midilli et al.	0.0836	
	Diffusion approach	0.0782	
	Two-term exponential	0.0526	
Thyme	Midilli et al.	0.0450	Lahnine et al. (2016)

6 Conclusion

Despite being a very ancient method for food preservation, solar drying still assumes presently an unquestionable importance due to many reasons: it is very cheap in terms of operating costs; it is easily accessible in some regions of the globe with lower incomes and high solar incidence; it requires a low investment; and it can be efficient under some conditions. Although still much in use, it is a reality that many developments have taken place and today's solar drying processes are in fact much more effective and promote food quality in a way that the traditional open sun drying did not. These improvements can be minor, such as in the case of using a covered solar greenhouse to dry the foods, or major, such as in the cases where solar collectors are used to heat air that then is made circulating through the drying chamber.

The systematic review of the literature undertaken for the solar drying of food products showed that this method is very much employed for the drying of several foods, such as vegetables, fruits, herbs or spices. The usage of solar drying for meat and fish has not been so comprehensively studied, and therefore no studies were found to cite as in the case of the products from plant origin. However, this might

Table 6 Effective diffusivity for the solar drying of different foods

Food	Solar drying system	D_e (m^2/s)	References
Apple	Indirect drying with solar collector	1.03×10^{-8}	Aktaş et al. (2009)
Basil	Open sun drying	6.44×10^{-12}	Akpinar (2006)
Cocoa beans	Indirect drying with solar collector	8.94×10^{-11} 9.63×10^{-11}	Dina et al. (2015)
Green bean	Open sun drying	1.12×10^{-10}	Doymaz (2011)
Green peas	Solar cabinet dried	2.01×10^{-10}	Jadhav et al. (2010)
	Open sun dried	4.05×10^{-11}	
Eland meet	Double-pass solar dryer	1.43×10^{-10} 2.07×10^{-10}	Kucerova et al. (2015)
Mango	Direct solar drying	2.7906×10^{-11} 1.8489×10^{-10}	Dissa et al. (2011)
Mint	Open sun drying	7.04×10^{-12}	Akpinar (2006)
Mint	Direct dryer – natural convection	1.29×10^{-11}	Sallam et al. (2015)
	Indirect dryer – natural convection	1.20×10^{-11}	
	Direct dryer – forced convection	1.33×10^{-11}	
	Indirect dryer – forced convection	1.21×10^{-11}	
Mulberry	Solar cabinet dryer	1.09×10^{-13} 1.38×10^{-9}	Akbulut and Durmuş (2009)
Mushroom	Hybrid solar dryer	1.90×10^{-10} 1.13×10^{-9}	Reyes et al. (2014)
Okra	Open sun drying	1.52×10^{-11}	Doymaz (2011)
Parsley	Open sun drying	4.53×10^{-12}	Akpinar (2006)
Pea	Open sun drying	0.64×10^{-10}	Sahin et al. (2013)
	Solar-assisted spouted bed drying	3.27×10^{-10}	
Pear	Greenhouse	7.582×10^{-10} 8.440×10^{-10}	Guiné et al. (2007c)
Tomato	Solar tunnel dryer	1.31×10^{-9}	Sacilik et al. (2006)
	Open sun drying	1.07×10^{-9}	
Turmeric rhizomes	Solar conduction dryer	1.456×10^{-10} 1.852×10^{-10}	Borah et al. (2015a)
White mulberry	Open sun drying	2.40×10^{-9}	Akpinar (2008)
	Indirect dryer – forced convection	3.56×10^{-9}	

not mean that the solar drying does not have an economic importance for the drying of meat or fish products, and instead it might alert that those foods have not been so much studied.

In this chapter, it was possible to gather a vast set of studies devoted to the evaluation of different properties in many foods submitted to solar drying as well as to the study of the drying kinetics, both in terms of empirical thin-layer models and in terms of Fick's second law for diffusion. Finally, values for the effective diffusion coefficient for different foods dried by various solar systems were systematized for easy consultation.

The large number of studies devoted to many aspects of the solar drying of foods confirms undoubtedly the importance of this drying operation for the food processing.

References

Akbulut A, Durmuş A (2009) Thin layer solar drying and mathematical modeling of mulberry. Int J Energy Res 33(7):687–695

Akin A, Gurlek G, Ozbalta N (2014) Mathematical model of solar drying characteristics for pepper (Capsicum Annuum). ISI Bilimi ve Teknigi Dergisi-J Therm Sci Technol 34(2):99–109

Akpinar EK (2006) Mathematical modelling of thin layer drying process under open sun of some aromatic plants. J Food Eng 77(4):864–870

Akpinar EK (2008) Mathematical modelling and experimental investigation on sun and solar drying of white mulberry. J Mech Sci Technol 22(8):1544–1553

Akpinar EK (2010) Drying of mint leaves in a solar dryer and under open sun: modelling, performance analyses. Energy Convers Manag 51(12):2407–2418

Akpinar EK, Bicer Y (2008) Mathematical modelling of thin layer drying process of long green pepper in solar dryer and under open sun. Energy Convers Manag 49(6):1367–1375

Aktaş M, Ceylan İ, Yilmaz S (2009) Determination of drying characteristics of apples in a heat pump and solar dryer. Desalination 239(1–3):266–275

Apata ES, Osidibo OO, Apata OC, Okubanjo AO (2013) Effects of different solar drying methods on quality attributes of dried meat product (Kilishi). J Food Res 2(1):1–7

Arslan D, Musa Özcan M (2010) Study the effect of sun, oven and microwave drying on quality of onion slices. LWT Food Sci Technol 43(7):1121–1127

Bagheri H, Arabhosseini A, Kianmehr MH, Chegini GR (2013) Mathematical modeling of thin layer solar drying of tomato slices. Agric Eng Int CIGR J 15(1):146–153

Banout J, Ehl P, Havlik J, Lojka B, Polesny Z, Verner V (2011) Design and performance evaluation of a double-pass solar drier for drying of red chilli (Capsicum annuum L.) Sol Energy 85(3):506–515

Banout J, Kucerova I, Marek S (2012) Using a double-pass solar drier for jerky drying. Energy Procedia 30:738–744

Basri DF, Abu Bakar NF, Fudholi A, Ruslan MH, Saroeun I (2015) Comparison of selected metals content in cambodian striped snakehead fish (Channa striata) using solar drying system and open sun drying. J Environ Public Health 2015:1–6

Basunia MA, Abe T (2001) Thin-layer solar drying characteristics of rough rice under natural convection. J Food Eng 47(4):295–301

Bechoff A, Dufour D, Dhuique-Mayer C, Marouzé C, Reynes M, Westby A (2009) Effect of hot air, solar and sun drying treatments on provitamin A retention in orange-fleshed sweetpotato. J Food Eng 92(2):164–171

Borah A, Hazarika K, Khayer SM (2015a) Drying kinetics of whole and sliced turmeric rhizomes (Curcuma longa L.) in a solar conduction dryer. Inform Process Agric 2(2):85–92
Borah A, Sethi L, Sarkar S, Hazarika K (2015b) Effect of drying on texture and color characteristics of ginger and turmeric in a solar biomass integrated dryer. J Food Process Eng n/a-n/a
Brasiello A, Adiletta G, Russo P, Crescitelli S, Albanese D, Di Matteo M (2013) Mathematical modeling of eggplant drying: Shrinkage effect. J Food Eng 114(1):99–105
Brătucu G, Marin A, Florea C (2013) Research on carrot drying by means of solar energy. Bull Transilvania Univ Brasov II Forestry, Wood Industry, Agric Food Eng 6(1):91–98
Çakmak G, Yıldız C (2011) The drying kinetics of seeded grape in solar dryer with PCM-based solar integrated collector. Food Bioprod Process 89(2):103–108
Carranza-Concha J, Benlloch M, Camacho MM, Martínez-Navarrete N (2012) Effects of drying and pretreatment on the nutritional and functional quality of raisins. Food Bioprod Process 90 (2):243–248
Chin SK, Law CL, Supramaniam CV, Cheng PG, Mujumdar AS (2008) Convective drying of Ganoderma tsugae Murrill and effect of temperature on basidiospores. Dry Technol 26 (12):1524–1533
Chouicha S, Boubekri A, Mennouche D, Berrbeuh MH (2013) Solar drying of sliced potatoes. An experimental investigation. Energy Procedia 36:1276–1285
Corzo O, Bracho N, Alvarez C (2008) Water effective diffusion coefficient of mango slices at different maturity stages during air drying. J Food Eng 87(4):479–484
Darvishi H, Azadbakht M, Rezaeiasl A, Farhang A (2013) Drying characteristics of sardine fish dried with microwave heating. J Saudi Soc Agric Sci 12(2):121–127
Delgado T, Pereira JA, Baptista P, Casal S, Ramalhosa E (2014) Shell's influence on drying kinetics, color and volumetric shrinkage of Castanea sativa Mill. fruits. Food Res Int 55:426–435
Deng Y, Wang Y, Yue J, Liu Z, Zheng Y, Qian B, Zhong Y, Zhao Y (2014) Thermal behavior, microstructure and protein quality of squid fillets dried by far-infrared assisted heat pump drying. Food Control 36(1):102–110
Dina SF, Ambarita H, Napitupulu FH, Kawai H (2015) Study on effectiveness of continuous solar dryer integrated with desiccant thermal storage for drying cocoa beans. Case Stud Therm Eng 5:32–40
Dissa AO, Bathiebo DJ, Desmorieux H, Coulibaly O, Koulidiati J (2011) Experimental characterisation and modelling of thin layer direct solar drying of Amelie and Brooks mangoes. Energy 36(5):2517–2527
Doymaz İ (2007) The kinetics of forced convective air-drying of pumpkin slices. J Food Eng 79 (1):243–248
Doymaz I (2011) Drying of green bean and okra under solar energy. Chem Ind Chem Eng Q 17 (2):199–205
Ekechukwu OV, Norton B (1999) Review of solar-energy drying systems II: an overview of solar drying technology. Energy Convers Manag 46(6):615–655
Ekıncı R (2005) The effect of fermentation and drying on the water-soluble vitamin content of tarhana, a traditional Turkish cereal food. Food Chem 90(1–2):127–132
El-Beltagy A, Gamea GR, Essa AHA (2007) Solar drying characteristics of strawberry. J Food Eng 78(2):456–464
El-Sebaii AA, Shalaby SM (2013) Experimental investigation of an indirect-mode forced convection solar dryer for drying thymus and mint. Energy Convers Manag 74:109–116
Erbay Z, Icier F (2010) A review of thin layer drying of foods: theory, modeling, and experimental results. Crit Rev Food Sci Nutr 50(5):441–464
Fadhel M, Abdo R, Yousif B, Zaharim A, Sopian K (2011) Thin layer drying characteristics of banana slices in a forced convection indirect solar drying. Proceedings paper presented at the 6th IASME/WSEAS International Conference on Energy and Environment (EE 2011): Recent Researches in Energy and Environment. Cambridge, United Kingdom
Faustino JMF, Barroca MJ, Guiné RPF (2007) Study of the drying kinetics of green bell pepper and chemical characterization. Food Bioprod Process 85(3):163–170

Fudholi A, Othman MY, Ruslan MH, Sopian K (2013) Drying of Malaysian Capsicum annuum L. (Red Chili) dried by open and solar drying. Int Journal of Photoenergy 2013 Article ID: 167895:1–9
Fudholi A, Sopian K, Othman MY, Ruslan MH (2014) Energy and exergy analyses of solar drying system of red seaweed. Energ Buildings 68:121–129
Ghazanfari A, Tabil L, Sokhansanj S (2003) Evaluating a solar dryer for shell drying of split pistachio nuts. Dry Technol 21:1357–1368
Guiné RPF (2005a) Drying kinetics of some varieties of pears produced in Portugal. Food Bioprod Process 83(4):273–276
Guiné RPF (2005b) Variation of density and porosity during the drying of pears and pear halves. Braz J Food Technol 8(1):252–255
Guiné RPF (2008) Pear drying: experimental validation of a mathematical prediction model. Food Bioprod Process 86(4):248–253
Guiné R (2010) Analysis of the drying kinetics of S. Bartolomeu pears for different drying systems. Elec J Environ Agric Food Chem 9(11):1772–1783
Guiné RPF, Barroca MJ (2012) Effect of drying treatments on texture and color of vegetables (pumpkin and green pepper). Food Bioprod Process 90(1):58–63
Guiné R, Gonçalves F (2015) Chemistry and health effects of bioactive compounds in selected culinary aromatic herbs. Curr Nutr Food Sci 12(2):145–164
Guiné R, Gonçalves F (2016) Bioactive compounds in some culinary aromatic herbs and their effects on human health. Mini-Rev Med Chem 16(11):855–866
Guiné RPF, Ramos MA, Figueiredo M (2006) Shrinkage Characteristics and Porosity of Pears during Drying. Dry Technol 24(11):1525–1530
Guiné RPF, Rodrigues AE, Figueiredo MM (2007a) Modelling and simulation of pear drying. Appl Math Comput 192(1):69–77
Guiné RPF, Ferreira DMS, Barroca MJ, Gonçalves FM (2007b) Study of the solar drying of pears. Int J Fruit Sci 7(2):101–118
Guiné RPF, Ferreira DMS, Barroca MJ, Gonçalves FM (2007c) Study of the drying kinetics of solar-dried pears. Biosyst Eng 98(4):422–429
Guiné RPF, Lopes P, Barroca M, Ferreira DMS (2009) Effect of ripening stage on the solar drying kinetics and properties of s. Bartolomeu pears (Pyrus communis L.) Int J Acad Res 1(1):46–52
Guiné RPF, Pinho S, Barroca MJ (2011) Study of the convective drying of pumpkin (Cucurbita maxima). Food Bioprod Process 89(4):422–428
Gulcimen F, Karakaya H, Durmus A (2016) Drying of sweet basil with solar air collectors. Renew Energy 93:77–86
Gupta P, Ahmed J, Shivhare US, Raghavan GSV (2002) Drying characteristics of red chilli. Dry Technol 20(10):1975–1987
Gurlek G, Ozbalta N, Gungor A (2009) Solar tunnel drying characteristics and mathematical modelling of tomato. ISI Bilimi ve Teknigi Dergisi-J Therm Sci Technol 29(1):15–23
Haque MA, Aldred P, Chen J, Barrow CJ, Adhikari B (2013) Comparative study of denaturation of whey protein isolate (WPI) in convective air drying and isothermal heat treatment processes. Food Chem 141(2):702–711
Hassanain AA (2011) Drying sage (Salvia officinalis L.) in passive solar dryers. Res Agric Eng 50 (1):19–29
Henderson SM (1974) Progress in developing the thin layer drying equation. Trans Am Soc Agric Eng 17:1167–1168
Henderson SM, Pabis S (1969) Grain drying theory. I Temperature effect on drying coefficient. J Agric Eng Res 6:169–174
Hossain MA, Amer BMA, Gottschalk K (2008) Hybrid solar dryer for quality dried tomato. Dry Technol 26(12):1591–1601
Igual M, García-Martínez E, Martín-Esparza ME, Martínez-Navarrete N (2012) Effect of processing on the drying kinetics and functional value of dried apricot. Food Res Int 47 (2):284–290
Ikutegbe V, Sikoki F (2014) Microbiological and biochemical spoilage of smoke-dried fishes sold in West African open markets. Food Chem 161:332–336

Irigoyen TRM, Giner SA (2014) Drying-toasting kinetics of presoaked soybean in fluidised bed. Experimental study and mathematical modelling with analytical solutions. J Food Eng 128:31–39

Jadhav D, Annapure U, Visavale GI, Sutar N, Thorat B (2010) Studies on solar cabinet drying of green peas (Pisum sativum). Dry Technol 28(5):600–607

Janjai S, Lamlert N, Intawee P, Mahayothee B, Bala BK, Nagle M, Müller J (2009) Experimental and simulated performance of a PV-ventilated solar greenhouse dryer for drying of peeled longan and banana. Sol Energy 83(9):1550–1565

Kassem AS (1998) Comparative studies on thin layer drying models for wheat. Proceeding of 13th International congress on agricultural engineering. Morocco, 2–6

Kaya A, Aydın O, Kolaylı S (2010) Effect of different drying conditions on the vitamin C (ascorbic acid) content of Hayward kiwifruits (Actinidia deliciosa Planch). Food Bioprod Process 88(2–3):165–173

Kituu GM, Shitanda D, Kanali CL, Mailutha JT, Njoroge CK, Wainaina JK, Silayo VK (2010) Thin layer drying model for simulating the drying of Tilapia fish (Oreochromis niloticus) in a solar tunnel dryer. J Food Eng 98(3):325–331

Koç B, Eren İ, Kaymak Ertekin F (2008) Modelling bulk density, porosity and shrinkage of quince during drying: the effect of drying method. J Food Eng 85(3):340–349

Kouchakzadeh A (2013) The effect of acoustic and solar energy on drying process of pistachios. Energy Convers Manag 67:351–356

Kowalski SJ, Szadzińska J, Łechtańska J (2013) Non-stationary drying of carrot: effect on product quality. J Food Eng 118(4):393–399

Kucerova I, Hubackova A, Rohlik B-A, Banout J (2015) Mathematical modeling of thin-layer solar drying of Eland (Taurotragus oryx) Jerky. Int J Food Eng 11(2):229–242

Kucuk H, Midilli A, Kilic A, Dincer I (2014) A review on thin-layer drying-curve equations. Dry Technol 32(7):757–773

Kumar A, Singh M, Singh G (2013) Effect of different pretreatments on the quality of mushrooms during solar drying. J Food Sci Technol 50(1):165–170

Kumar C, Karim MA, Joardder MUH (2014) Intermittent drying of food products: A critical review. J Food Eng 121:48–57

Kumar M, Sansaniwal SK, Khatak P (2016) Progress in solar dryers for drying various commodities. Renew Sust Energ Rev 55:346–360

Kurozawa LE, Terng I, Hubinger MD, Park KJ (2014) Ascorbic acid degradation of papaya during drying: effect of process conditions and glass transition phenomenon. J Food Eng 123:157–164

Labed A, Moummi N, Aoues K, Benchabane A (2016) Solar drying of henna (Lawsonia inermis) using different models of solar flat plate collectors: an experimental investigation in the region of Biskra (Algeria). J Clean Prod 112(Part 4):2545–2552

Lahnine L, Idlimam A, Mahrouz M, Mghazli S, Hidar N, Hanine H, Koutit A (2016) Thermophysical characterization by solar convective drying of thyme conserved by an innovative thermal-biochemical process. Renew Energy 94:72–80

Lahsasni S, Kouhila M, Mahrouz M, Idlimam A, Jamali A (2004) Thin layer convective solar drying and mathematical modeling of prickly pear peel (Opuntia ficus indica). Energy 29 (2):211–224

Lewis (1921) The drying of solid materials. J Indian Eng 5:427–443

Lopez R, Vaca M, Terres H, Lizardi A, Morales J, Flores J, Lara A and Chávez S (2014) Kinetics modeling of the drying of chickpea (Cicer Arietinum) with solar energy. Energy Procedia: 2013 I.E. Solar World Congress 57:1447–1454

Lorentzen G, Egeness F-A, Pleym IE, Ytterstad E (2016) Shelf life of packaged loins of dried salt-cured cod (Gadus morhua L.) stored at elevated temperatures. Food Control 64:65–69

McMinn WAN (2006) Thin-layer modeling of the convective, microwave, microwave-convective and microwave-vacuum drying of lactose powder. J Food Eng 72:113–123

Mendonça AP, de Sampaio PTB, de Almeida FAC, Ferreira RF, Novais JM (2015) Determinação das curvas de secagem das sementes de andiroba em secador solar. Revista Brasileira de Engenharia Agrícola e Ambiental 19(4):382–387

Mennouche D, Bouchekima B, Boubekri A, Boughali S, Bouguettaia H, Bechki D (2014) Valorization of rehydrated Deglet-Nour dates by an experimental investigation of solar drying processing method. Energy Convers Manag 84:481–487

Midilli A, Kucuk H (2003) Mathematical modeling of thin layer drying of pistachio by using solar energy. Energy Convers Manag 44(7):1111–1122

Midilli A, Kucuk H, Yapar Z (2002) A new model for single-layer drying. Dry Technol 20 (7):1503–1513

Morales-Medina R, Tamm F, Guadix AM, Guadix EM, Drusch S (2016) Functional and antioxidant properties of hydrolysates of sardine (S. pilchardus) and horse mackerel (T. mediterraneus) for the microencapsulation of fish oil by spray-drying. Food Chem 194:1208–1216

Mrad ND, Boudhrioua N, Kechaou N, Courtois F, Bonazzi C (2012) Influence of air drying temperature on kinetics, physicochemical properties, total phenolic content and ascorbic acid of pears. Food Bioprod Process 90(3):433–441

Mulokozi G, Svanberg U (2003) Effect of traditional open sun-drying and solar cabinet drying on carotene content and vitamin A activity of green leafy vegetables. Plant Foods Hum Nutr 58 (3):1–15

Mustayen AGMB, Rahman MM, Mekhilef S, Saidur R (2015) Performance evaluation of a solar powered air dryer for white oyster mushroom drying. Int J Green Energy 12(11):1113–1121

Niamnuy C, Devahastin S, Soponronnarit S (2014) Some recent advances in microstructural modification and monitoring of foods during drying: a review. J Food Eng 123:148–156

Nourhène B, Mohammed K, Nabil K (2008) Experimental and mathematical investigations of convective solar drying of four varieties of olive leaves. Food Bioprod Process 86(3):176–184

Nuwanthi SGLI, Madage SSK, Hewajulige IGN, Wijesekera RGS (2016) Comparative study on organoleptic, microbiological and chemical qualities of dried fish, Goldstripe Sardinella (Sardinella Gibbosa) with low salt levels and spices. Procedia Food Sci 6:356–361

Odjo S, Malumba P, Dossou J, Janas S, Béra F (2012) Influence of drying and hydrothermal treatment of corn on the denaturation of salt-soluble proteins and color parameters. J Food Eng 109(3):561–570

Ojutiku RO, Kolo RJ, Mohammed ML (2009) Comparative study of sun drying and solar tent drying of Hyperopisus bebe occidentalis. Pak J Nutr 8(7):955–957

Overhults DD, White GM, Hamilton ME, Ross IJ (1973) Drying soybeans with heated air. Trans Am Soc Agric Eng 16:195–200

Page GE (1949) Factors influencing the maximum rates of air drying shelled corn in thin layers. Purdue University, Lafayette, IN, USA

Panwar NL (2014) Experimental investigation on energy and exergy analysis of coriander (Coriandrum sativum L.) leaves drying in natural convection solar dryer. Appl Solar Energy 50(3):133–137

Parikh D, Agrawal GD (2012) Solar drying in hot and dry climate of Jaipur. Int J Renew Energy Res (IJRER) 1(4):224–231

Patil R, Gawande R (2016) A review on solar tunnel greenhouse drying system. Renew Sust Energ Rev 56:196–214

Pirasteh G, Saidur R, Rahman SMA, Rahim NA (2014) A review on development of solar drying applications. Renew Sust Energ Rev 31:133–148

Puig A, Perez-Munuera I, Carcel JA, Hernando I, Garcia-Perez JV (2012) Moisture loss kinetics and microstructural changes in eggplant (Solanum melongena L.) during conventional and ultrasonically assisted convective drying. Food Bioprod Process 90(4):624–632

Rahman MM, Mekhilef S, Saidur R, Billah AGMM, Rahman SMA (2016) Mathematical modelling and experimental validation of solar drying of mushrooms. Int J Green Energy 13 (4):344–351

Rankins J, Sathe SK, Spicer MT (2008) Solar drying of mangoes: preservation of an important source of vitamin A in french-speaking West Africa. J Am Diet Assoc 108(6):986–990

Reyes A, Mahn A, Vásquez F (2014) Mushrooms dehydration in a hybrid-solar dryer, using a phase change material. Energy Convers Manag 83:241–248

Ringeisen BM, Barrett D, Stroeve P (2014) Concentrated solar drying of tomatoes. Energy Sustain Dev 19:47–55
Rodríguez J, Mulet A, Bon J (2014) Influence of high-intensity ultrasound on drying kinetics in fixed beds of high porosity. J Food Eng 127:93–102
Ronoh EK, Kanali CL, Mailutha JT, Shitanda D (2009) Modeling thin layer drying of amaranth seeds under open sun and natural convection solar tent dryer. Agric Eng Int CIGR J 11:1420
Sacilik K, Keskin R, Elicin AK (2006) Mathematical modelling of solar tunnel drying of thin layer organic tomato. J Food Eng 73(3):231–238
Saeed IE (2010) Solar drying of roselle (Hibiscus sabdariffa L.): effects of drying conditions on the drying constant and coefficients, and validation of the logarithmic model. Agric Eng Int CIGR J 12(1):167–181
Sahin S, Sumnu G, Tunaboyu F (2013) Usage of solar-assisted spouted bed drier in drying of pea. Food Bioprod Process 91:271–278
Saleh A, Badran I (2009) Modeling and experimental studies on a domestic solar dryer. Renew Energy 34(10):2239–2245
Sallam YI, Aly MH, Nassar AF, Mohamed EA (2015) Solar drying of whole mint plant under natural and forced convection. J Adv Res 6(2):171–178
Schössler K, Thomas T, Knorr D (2012) Modification of cell structure and mass transfer in potato tissue by contact ultrasound. Food Res Int 49(1):425–431
Seveda MS, Jhajharia D (2012) Design and performance evaluation of solar dryer for drying of large cardamom (Amomum subulatum). J Renew Sustain Energy 4(6):63–129
Sharaf-Elden YI, Blaisdell JL, Hamdy MY (1980) A model for ear corn drying. Trans Am Soc Agric Eng 5:1261–1265
Sharma VK, Sharma S, Garg HP (1991) Mathematical modelling and experimental evaluation of a natural convection type solar cabinet dryer. Energy Convers Manag 31(1):65–73
Sharma A, Chen CR, Vu Lan N (2009) Solar-energy drying systems: a review. Renew Sust Energ Rev 13(6–7):1185–1210
Shringi V, Kothari S, Panwar NL (2014) Experimental investigation of drying of garlic clove in solar dryer using phase change material as energy storage. J Therm Anal Calorim 118 (1):533–539
Singh SP, Jairaj KS, Srikant K (2012) Universal drying rate constant of seedless grapes: A review. Renew Sust Energ Rev 16(8):6295–6302
Solval KM, Sundararajan S, Alfaro L, Sathivel S (2012) Development of cantaloupe (Cucumis melo) juice powders using spray drying technology. LWT Food Sci Technol 46(1):287–293
Sunil, Varun, Sharma N (2014) Experimental investigation of the performance of an indirect-mode natural convection solar dryer for drying fenugreek leaves. J Therm Anal Calorim 118 (1):523–531
Sunil, Varun, Sharma N (2013) Modelling the drying kinetics of green peas in a solar dryer and under open sun. Int J Energy Environ 4(4):663–676
Suzuki H, Hayakawa S, Wada S, Okazaki E, Yamazawa M (1988) Effect of solar drying on vitamin D3 and provitamin D3 contents in fish meat. J Agric Food Chem 36(4):803–806
Timoumi S, Mihoubi D, Zagrouba F (2007) Shrinkage, vitamin C degradation and aroma losses during infra-red drying of apple slices. LWT Food Sci Technol 40(9):1648–1654
Toğrul İT, Pehlivan D (2004) Modelling of thin layer drying kinetics of some fruits under open-air sun drying process. J Food Eng 65(3):413–425
Traffano-Schiffo MV, Castro-Giráldez M, Fito PJ, Balaguer N (2014) Thermodynamic model of meat drying by infrared thermography. J Food Eng 128:103–110
Tripathy PP (2015) Investigation into solar drying of potato: effect of sample geometry on drying kinetics and CO_2 emissions mitigation. J Food Sci Technol 52(3):1383–1393
Tripathy PP, Kumar S (2009) A methodology for determination of temperature dependent mass transfer coefficients from drying kinetics: application to solar drying. J Food Eng 90 (2):212–218
Vega-Gálvez A, Ah-Hen K, Chacana M, Vergara J, Martínez-Monzó J, García-Segovia P, Lemus-Mondaca R, Di Scala K (2012) Effect of temperature and air velocity on drying kinetics,

antioxidant capacity, total phenolic content, colour, texture and microstructure of apple (var. Granny Smith) slices. Food Chem 132(1):51–59

Verma LR, Bucklin RA, Endan JB, Wratten FT (1985) Effects of drying air parameters on rice drying models. Trans Am Soc Agric Eng 28:296–301

Vijayan S, Arjunan TV, Kumar A (2016) Mathematical modeling and performance analysis of thin layer drying of bitter gourd in sensible storage based indirect solar dryer. Innovative Food Sci Emerg Technol 36:59–67

Wang CY, Singh RP (1978) A single layer drying equation for rough rice. Am Soc Agric Eng (3001)

Wongpornchai S, Dumri K, Jongkaewwattana S, Siri B (2004) Effects of drying methods and storage time on the aroma and milling quality of rice (Oryza sativa L.) cv. Khao Dawk Mali 105. Food Chem 87(3):407–414

Wu L, Orikasa T, Ogawa Y, Tagawa A (2007) Vacuum drying characteristics of eggplants. J Food Eng 83(3):422–429

Yagcioglu A, Degirmencioglu A, Cagatay F (1999) Drying characteristics of laurel leaves under different drying conditions. Proceedings of the 7th International Congress on Agricultural Mechanization and Energy in Agriculture. Adana, Turkey, 565–569

Yaldiz O, Ertekin C, Uzun HI (2001) Mathematical modeling of thin layer solar drying of sultana grapes. Energy 26(5):457–465

Zhang L, Nishizu T, Kishigami H, Kato A, Goto K (2013) Measurement of internal shrinkage distribution in spaghetti during drying by X-ray μCT. Food Res Int 51(1):180–187

Mathematical and Computational Modeling Simulation of Solar Drying Systems

Rebecca Rose Milczarek and Fatima Sierre Alleyne

Abstract Mathematical modeling of solar drying systems has the primary aim of predicting the required drying time for a given commodity, dryer type, and environment. Both fundamental (Fickian diffusion) and semiempirical drying models have been applied to the solar drying of a variety of agricultural commodities in several different dryer types (direct, indirect, and mixed mode with both forced and natural convection). Computational modeling (i.e., computational fluid dynamics or CFD), both in two-dimensional and three-dimensional modes, affords insights on geometry-specific solar drying issues, such as airflow patterns within the drying cabinet. Both mathematical and computational modeling have recently been brought to bear on solar drying innovations such as thermal storage, use of dessicants during drying, and dynamic feedback control of the drying process. Robust models are also necessary for the performance evaluation and comparison of different dryer designs and configurations. The outputs of mathematical and computational models are compared with measured drying data (whether performed outdoors or with a solar simulator) to ensure the accuracy and efficacy of the model.

Keywords Mathematical modeling • Solar drying systems • Computational modeling • Fundamental model • Semiempirical drying models

1 Mathematical Modeling

1.1 Fundamental Models

The fundamental physical model for drying (of any type, not limited to solar drying) is that of Fickian diffusion. This model states that water will move from a region of high concentration (the moist product) to a region of lower concentration (the surrounding air) until equilibrium is reached. For a given system temperature, the

R.R. Milczarek (✉) • F.S. Alleyne
United States Department of Agriculture – Agricultural Research Service, Healthy Processed Foods Research Unit, 800 Buchanan Street, Albany 94710, CA, USA
e-mail: rebecca.milczarek@ars.usda.gov

© Springer Nature Singapore Pte Ltd. 2017

O. Prakash, A. Kumar (eds.), *Solar Drying Technology*, Green Energy and Technology, DOI 10.1007/978-981-10-3833-4_11

rate of this movement is given as the effective diffusivity [D], which commonly has units of m^2/s. The temporal change in the concentration of remaining water in the product can thus be expressed as the partial differential equation known as Fick's second law:

$$\frac{\partial C}{\partial t} = D^* \partial^2 \frac{C}{\partial x^2} \tag{1}$$

where C is the concentration of water expressed on a dry basis, t is time [s], and x is distance [m]. Fick's second law can be rewritten in spherical, cylindrical, or Cartesian coordinates to describe moisture diffusion in a perfect sphere, cylinder, or infinite slab, respectively. Some common assumptions when applying Fick's second law to drying food materials are:

- The initial moisture content is uniformly distributed in the material.
- The moisture gradient in the material is symmetric about the center point (sphere) or center line (cylinder, slab).
- There is a convective boundary condition at the surface of the material due to external resistance to moisture transfer.

These assumptions lead to the initial conditions

$$C(x, 0) = C_0 \tag{2}$$

$$\frac{\partial C(0, t)}{\partial x} = 0 \tag{3}$$

and the boundary condition

$$-D^* \left(\frac{\partial C(L, t)}{\partial x} \right) = h_m [C(L, t) - C_\infty] \tag{4}$$

where L is the characteristic length of the material (radius of the sphere or cylinder, half-height of the slab), h_m is the convective mass transfer coefficient [m/s], and C_∞ is the moisture content of the ambient air.

Development of these initial and boundary conditions into mathematical models that are directly applicable to solar drying then diverges depending on the assumed geometry of the food material. Elegant developments can be found for the cylindrical geometry in Singh and Kumar (2014) and Tripathy and Kumar (2009) and for the slab geometry in Tripathy and Kumar (2009). In the end, the parameters that account for the aggregate effect of various transport phenomena during drying can be determined from a relatively simple exponential equation (Dincer and Dost 1996; Babalis and Belessiotis 2004; Ghodake et al. 2006):

$$C = k_0 \exp(-kt) \tag{5}$$

where k_0 and k represent the lag factor and drying constant of food product, respectively. It should be noted that the set of equations comprising Fick's second law and the associated initial and boundary conditions can also be solved directly by the finite difference method (Ramos et al. 2010).

A few recent works have developed solar drying models that are based on such fundamental mathematical concepts. Ramos et al. (2010) initially modeled grapes as wrinkled ellipsoids and determined an equivalent spherical radius for calculation purposes. They then approximated the individual grapes as spheres (using the equivalent radius) to apply Fick's second law for drying this commodity in a pilot convective dryer, which simulated air conditions observed in a solar dryer. The same group later coupled the Fickian diffusion equation (describing mass transfer) with a transient energy balance equation (describing heat transfer) and an equation relating instantaneous moisture content to particle size (describing geometric changes) to model the drying of grapes in a mixed-mode dryer (Ramos et al. 2015). Silva et al. (2014) approximated pear slices as continuous slabs when they applied the Fickian diffusion model to continuous drying at 30 °C, continuous drying at 40 °C, and discontinuous drying at 40 °C in an electrically heated forced convection dryer. The discontinuous drying process was assumed to be analogous to indirect solar drying, which presumably would not continue during non-daylight hours. Through this modeling approach, they showed that an evaporative condition on the surface of the drying fruit is physically more consistent than the assumption of an instantaneous equilibrium concentration on the surface, the latter of which is often adopted in many works on drying kinetics of biological products.

Tripathy and Kumar (2009) used a mixed-mode solar dryer with potato cylinders and slices to obtain the variable (temperature dependent) lag factor and drying coefficient from drying kinetics. Results indicated an increasing trend of effective diffusivity and convective mass transfer coefficients at various temperatures. Later, the same group (Tripathy and Kumar 2011) used two different approaches for the estimation of the convective mass transfer coefficient. The direct method was based on the measurement of moisture loss rate data, and the indirect method used graphically computed values of drying parameters and moisture diffusion coefficient. Drying experiments were performed with potato cylinders and slices of same thickness of 0.01 m with their respective length and diameter of 0.05 m using natural convection mixed-mode solar dryer and open-air sun drying conditions. Results of analysis revealed that for each method of estimation, the cylinders vis-à-vis slices produce higher values of convective mass transfer coefficient for both the solar drying conditions. It was also found that the mixed-mode solar drying enhances moisture transfer at food-air interface for each of the sample geometries as expected. Out of the two approaches investigated for convective mass transfer coefficient estimation, the indirect method exhibited lower values, and these values were found to be more close to the results reported in the literature.

Fundamental energy balance models can be applied to a solar dryer's various components: collector, cabinet, and – in some cases – thermal storage unit. By performing energy balances on a corrugated solar absorber and gravel-based thermal storage system, Ayadi et al. (2014) were able to predict air and gravel

temperatures in an unloaded indirect dryer, finding good agreement with experimental results. The numerical model took into account the heat transfer modes of conduction, convection, and radiation, and it used ambient environmental conditions as inputs to the model. Bennamoun (2011) has reviewed several Algerian solar drying studies in which heat balances were applied to the collectors and cabinets of indirect, direct, and mixed-mode dryers.

1.2 Empirical and Semiempirical Models

The food material in the solar dryer cabinet is often arranged on a solid, perforated, or mesh tray. When this is the case, researchers have often approximated the food as a single, thin layer. Numerous empirical and semiempirical mathematical models have been developed to describe this situation; Kucuk et al. (2014) present a recent comprehensive review of these models. Empirical models are based entirely on experimental data and dimensional analysis, while semiempirical models (sometimes termed semi-theoretical models) have some basis in Fick's second law but also incorporate terms derived from experimental data. Both empirical and semiempirical thin-layer drying models are sensitive to the experimental conditions (especially temperature), so these conditions must be known and stated when employing these models (Kucuk et al. 2014).

In the empirical and semiempirical models, moisture ratio (MR) is the response variable of interest (as opposed to dry basis moisture content (C in Sect. 1.1)). In a strict sense, MR is defined as

$$\mathrm{MR} = \frac{C - C_\mathrm{e}}{C_0 - C_\mathrm{e}} \tag{6}$$

where C is the instantaneous dry basis moisture content, C_e is the dry basis moisture content at equilibrium (i.e., at long drying times), and C_0 is the initial dry basis moisture content. Often for solar drying experiments, C_e is taken to be negligible compared to C and C_0, so for application of the empirical and semiempirical models, the equation for describing the drying curve is simply

$$\mathrm{MR} = \frac{C}{C_0} \tag{7}$$

Using this convention, Table 1 presents a collection of the thin-layer drying models applied to solar drying of agricultural commodities in the recent past. The models have been developed and revised over a number of years, so common synonyms for some of the models are listed. The most generic model name is used throughout this work, and the earliest reference for the derivation of the model is listed in Table 1.

Table 1 Empirical and semiempirical drying models applied to solar drying of food materials.

Model	Synonyms	Expression	Earliest references
Exponential	Lewis; Newton	$MR = \exp(-kt)$	Lewis (1921)
Generalized exponential	Henderson and Pabis	$MR = a\exp(-kt)$	Henderson and Pabis (1961)
Two-term		$MR = a\exp(-k_1 t) + b\exp(-k_2 t)$	Henderson (1974)
Modified Henderson and Pabis		$MR = a\exp(-k_1 t) + b\exp(-k_2 t) + c\exp(-k_3 t)$	Karathanos (1999)
Logarithmic		$MR = a\exp(-kt) + c$	Yagcioglu et al. (1999)
Page		$MR = \exp(-kt^n)$	Page (1949)
Modified Page		$MR = \exp(-(kt)^n)$	Overhults et al. (1973)
Modified Page II		$MR = a\exp(-k[t/L^2]^n)$	Diamante and Munro (1991)
Midilli-Kucuk	Midilli; Midilli et al.	$MR = a\exp(-kt^n) + bt$	Midilli et al. (2002)
Approximation of diffusion	Diffusion approach	$MR = a\exp(-kt) + (1-a)\exp(-kbt)$	Kassem (1998)
Two-term exponential		$MR = a\exp(-kt) + (1-a)\exp(-kat)$	Sharaf-Eldeen et al. (1980)
Verma et al.	Verma et al.	$MR = a\exp(-k_1 t) + (1-a)\exp(-k_2 t)$	Verma et al. (1985)
Simplified Fick's diffusion equation		$MR = a\exp(-b[t/L^2])$	Diamante and Munro (1991)
Parabolic		$MR = a + bt + ct^2$	Sharma and Prasad (2004)
Wang and Singh	Wang	$MR = 1 + at + bt^2$	Wang and Singh (1978)
Prakash and Kumar		$MR = a + bt + ct^2 + dt^3$	Prakash and Kumar (2014)
Diamante et al.		$\ln(\ln MR) = a + b\ln(t) + c(\ln(t))^2$	Diamante et al. (2010)
Thomson		$t = a\ln(MR) + b(\ln(MR))^2$	Thomson et al. (1968)

MR moisture ratio, *t* time, and *L* characteristic length of the food object. All italicized letters are model parameters, to be determined from nonlinear fitting of the model to measured drying data

The primary uses of the thin-layer models are to estimate drying times and to generalize drying curves. Researchers often measure drying curves under set or known conditions and then fit these curves to a number of empirical or semiempirical mathematical models. The best-fitting model is then chosen by evaluating one or more model performance criteria; commonly used criteria are maximization of adjusted coefficient of determination (adjusted R^2), minimization of reduced

chi-square (χ^2), and minimization of root-mean-square error (RMSE). Table 2 presents a summary of recent publications that have applied empirical and/or semiempirical thin-layer drying models to solar food drying systems.

As the wide variety of best-fitting models in Table 2 suggests, there is no single empirical model that describes all solar drying systems under all circumstances. In fact, the best-fitting model may change depending on what experimental parameters are varied to obtain the measured moisture ratios. This can be demonstrated in non-solar controlled drying experiments. For example, Zhu and Shen (2014) studied the drying of peaches. Peach slices were treated as continuous slabs with various thicknesses (0.002, 0.003, and 0.004 m) and dried in a forced-air, electrically heated drying tunnel under various conditions: temperatures (60, 65, 70, 75, and 80 °C), air velocities (0.423–1.120 m/s), and relative humidity (10 and 15%). Results of this work demonstrated that the ability of mathematical models to best predict moisture ratio, with respect to time, is dependent on the experimental conditions: thickness of samples (logarithmic model), drying temperature (Page model), and air velocity (Wang and Singh). Thus, assumptions on best-fit models cannot be automatically and universally applied when drying parameters vary.

The empirical modeling approach can also be applied to solar drying systems wherein the food particles are not assumed to be a single, thin layer but rather to be individual spheres, cubes, or cylinders. Guiné et al. (2007) approximated small (40–50 mm diameter) pears as spheres and fit their direct sun drying curves to two empirical models: a cubic polynomial and a sigmoid function. Based on four separate model performance criteria (R^2, reduced χ^2, mean bias error, and RMSE), they found that the sigmoid function better characterized the drying behavior of the pears. Kaya et al. (2015) employed two empirical models to evaluate processing parameters of potato slices in slab, cylindrical, and spherical forms under different drying conditions. Drying was conducted at various temperatures (45, 50, 55, and 60 °C) and air velocities (0.5, 1, 1.5, and 2.0 m/s). Moisture content distributions were then computed using this information and compared to experimental results. From this work, they were able to demonstrate that under both conditions, model I and model II differ in the manner in which the characteristic root is calculated with respect to the shape of the object (this is later used to determine mass transfer diffusion coefficient and moisture diffusivity). Both matched closely with the experimental data indicating that a simple calculation can be employed to quantify mass transfer diffusion coefficient.

2 Computational Modeling

Advances in computing power in the past 15 years have enabled the application of computational fluid dynamics (CFD) models to solar drying systems. CFD models can be built on finite difference time domain (FDTD) or finite element analysis (FEA) models; the latter is proving to be more popular for the analysis of solar drying systems. In the FEA approach, the software program divides a two- or three-

Table 2 Publications that have applied empirical and/or semiempirical thin-layer drying models to solar food drying systems

Reference	Dryer type	Commodity	Models employed	Best-fitting model
Akbulut and Durmuş (2009)	Active indirect	Mulberry	Exponential; Page; modified Page; generalized exponential; logarithmic; Wang and Singh; simplified Fick's diffusion equation; approximation of diffusion; modified Page II; Midilli-Kucuk	Midilli-Kucuk
Akpinar et al. (2004)	Active indirect	Apricot	Exponential; Page; modified Page; generalized exponential; logarithmic; two-term; two-term exponential; Wang and Singh; approximation of diffusion; modified Henderson and Pabis; Verma et al.; Midilli-Kucuk; Thomson	Midilli-Kucuk
Akpinar (2009)	Active indirect; passive direct	Parsley	Exponential; Page; modified Page; generalized exponential; logarithmic; two-term; two-term exponential; Verma et al.; Wang and Singh; Thomson	Parabolic
Aktaş et al. (2009)	Active indirect	Apple	Exponential; Page; modified Page; generalized exponential	Generalized exponential
Bahloul et al. (2011)	Active indirect	Olive leaves	Page; generalized exponential; exponential; logarithmic; Wang and Singh; two-term; two-term exponential	Logarithmic
Ethmane-Kane et al. (2008)	Active indirect	Mexican tea leaves	Exponential; Page; modified Page; modified Page II; generalized exponential; logarithmic; two-term; two-term exponential; Wang and Singh; approximation of diffusion; modified Henderson and Pabis; Verma et al.; Midilli-Kucuk; simplified Fick's diffusion equation	Wang and Singh
Hanif et al. (2013)	Active indirect	Onion	Exponential; Page; modified Page; two-term; Wang and Singh	Two-term exponential
Ismail and Idriss (2013)	Passive indirect	Okra	Exponential; Page	Page
Lahnine et al. (2016)	Active indirect	Thyme	Exponential; Page; two-term; generalized exponential; approximation of diffusion; logarithmic; Verma et al.; Wang and Singh; Midilli-Kucuk	Midilli-Kucuk (untreated leaves); Wang and Singh (citric acid-treated leaves)

(continued)

Table 2 (continued)

Reference	Dryer type	Commodity	Models employed	Best-fitting model
Lamnatou et al. (2012)	Active indirect	Apple, carrot, apricot	Exponential; Page; generalized exponential; logarithmic; two-term; Wang and Singh; Midilli-Kucuk; Diamante et al.	Midilli-Kucuk
Nourhene et al. (2008)	Active indirect	Olive leaves	Exponential; Page; generalized exponential	Page
Prakash and Kumar (2014)	Active mixed mode	Tomato	Exponential; generalized exponential; Page; logarithmic; two-term; Wang and Singh; modified Henderson and Pabis; Prakash and Kumar	Prakash and Kumar
Raji and Adeyemi (2012)	Passive direct, passive indirect	African baobab leaves	Exponential; Page; modified Page; generalized exponential	Modified Page
Sacilik et al. (2006)	Passive mixed mode	Tomato	Exponential; Page; generalized exponential; logarithmic; two-term; two-term exponential; Wang and Singh; approximation of diffusion; modified Henderson and Pabis; Midilli-Kucuk	Approximation of diffusion
Toğrul and Pehlivan (2002)	Active indirect	Apricot	Exponential; Page; modified Page; generalized exponential; logarithmic; two-term; parabolic; Thomson; approximation of diffusion; Verma et al.; modified Henderson and Pabis; two-term exponential; simplified Fick's diffusion equation; modified Page II	Logarithmic
Tripathy (2015)	Passive mixed mode	Potato	Exponential; modified Page; generalized exponential; logarithmic; two-term; Wang and Singh; modified Henderson and Pabis; Verma et al.	Modified Page
Tunde-Akintunde and Oke (2012)	Passive direct; passive indirect	Tiger nut	Exponential; generalized exponential; logarithmic; Page; Midilli-Kucuk; Wang and Singh	Logarithmic

dimensional virtual object into discrete elements. The partial differential equations that describe heat, mass, and/or momentum balances are set up for each element, the resulting system of equations is solved by the software, and the results are visualized for the user. FEA is especially well suited for modeling physical phenomena in food products, which are often characterized by irregular geometries that would otherwise need to be simplified in order to apply fundamental, empirical, or semiempirical drying models (Aversa et al. 2007).

CFD models can be categorized according to the scale of the fundamental geometry of interest: an individual piece of food being dried, a tray or other collection of food pieces, the cabinet of the dryer, or the entire dryer system (cabinet + collector + fan). These models can also be categorized by the mode (s) of heat, mass, and momentum transfer that are included. Standard hot-air convection dryers can be modeled considering the conduction and convection modes of heat transfer. However, solar drying presents an added modeling challenge in that the radiation mode of heat transfer must also be included. Furthermore, radiative heating from the sun [W/m^2] is inherently time varying, and the radiation that reaches the dryer collector and/or cabinet consists of both direct and scattered radiation. The radiation flux of a horizontal surface can be calculated using the following governing equations:

$$E = D_{S,\gamma} + d \tag{8}$$

$$D_{S,\gamma} = S_N \cos\theta \tag{9}$$

where E is radiation flux, D is the amount of direct radiation, S is tilt angle (the angle between vertical (zenith) and normal to the surface), γ is the azimuth angle (angle between the southward direction and direction projection of normal to surface onto the horizontal plane), θ is the zenith angle (the angle between sun and vertical direction), and d is the amount of scattered radiation. For a horizontal surface, θ is simply denoted as z. In the short-wavelength regime ($\lambda < 3 \times 10$–6 m), the total short-wavelength radiation flux on a horizontal is given by the sum of direct and scattered short-wavelength fluxes. However, the radiation flux for an inclined surface is much more complex due to radiation reflection from the ground or surroundings onto surface. Thus, the governing equation is

$$E = D_{S,\gamma} + d + R_{S,\gamma} \tag{10}$$

$$R_{S,\gamma} = \pi S_{\text{refl}} \sin^2(s/2) \tag{11}$$

where $R_{S,\gamma}$ is the amount of reflected radiation, subscript refl refers to the reflected angle, and the factor $\sin^2(s/2)$ represents the fraction of the hemisphere above the inclined surface from which the reflected radiation is received. This parameter must also be considered when modeling the behavior of a solar dryer consisting of an inclined surface.

Several research groups have applied commercial FEA software to solar food drying systems. Researchers Romero et al. (2014) used the FEA software ANSYS-Fluent (Canonsburg, PA, USA) to simulate the drying process of vanilla in an indirect solar dryer cabinet at the Cancun latitude and longitude coordinates. To model the temperature profiles within the cabinet, it was assumed that the convective heat transfer coefficient is a constant. A comparison of experimental results and simulation results revealed that the temperature profiles within the cabinet significantly differed. The model overpredicted the interior cabinet temperature in some cases by 10 °C. Results of this work revealed that variations in the convective heat transfer coefficient during the course of the day need to be accounted for in order to ensure models provide reasonable predictions.

Brasil Maia et al. (2012) also used ANSYS to model an indirect solar dryer; however, in this case, the dryer was a hybrid type – essentially, an indirect dryer with an auxiliary electric heater. The solar collector, cabinet, and chimney were modeled in three dimensions; the auxiliary heater was not included in the model. The dryer and its meshed model are shown in Fig. 1. The authors used a range of six mesh sizes (coarse to fine) to perform the simulation.

Figures 2 and 3 depict the simulated temperature fields and velocity streamlines, respectively, within the collector, cabinet, and chimney. From the model, it was predicted that the velocity and the temperature of the airflow would be homogeneous within the drying chamber, and this was confirmed with measurements by thermocouples and an anemometer within the physical dryer (with no trays and no loaded sample). The authors concluded that the use of the model to predict the airflow inside the dryer could be helpful for the design of future iterations of the geometric configurations of the device, which would improve the drying process.

Hii et al. (2013) employed a heat pump dryer to investigate the drying kinetics of cocoa beans under uniform and stepwise conditions (nonuniform process). The latter conditions, 30.7, 43.6, and 56.9 °C, were chosen to more closely represent the thermal changes experienced during conventional solar drying process (with no external/constant heat source) and to ensure temperatures detrimental to cocoa quality (> 60 °C) are avoided. The cocoa bean was modeled as an ellipsoid in the FEA software COMSOL Multiphysics using a coarse mesh size to avoid excessive computing cost. Results revealed that constant temperatures within the bean can be achieved under constant drying conditions of 56.9 °C, such that there was less than 0.3% differential in temperature from the outer to inner surface of the bean. Similarly, under typical drying conditions, bean temperatures closely resembled drying temperatures, except at the onset of drying. This could be the result of changes in texture at the surface during drying that can have profound effects on diffusion rate of water from the interior bean. Shrinkage was also deemed an irrelevant factor in cocoa bean drying, reducing the complexity of the model. Differences in moisture ratio, with respect to location in the bean, were also documented and validated in this study. Results of this study confirmed the need to incorporate factors that account for changes in texture and moisture ratio during the course of drying in modeling.

Fig. 1 Photo and three-dimensional model of a hybrid solar-electrical dryer [Reprinted from Brasil Maia C, Guimarães Ferreira A, Cabezas-Gómez L, de Morais Hanriot S, de Oliveira Martins T (2012) Simulation of the airflow inside a hybrid dryer. Int J Res Rev. Appl Sci 10 (March):382–389, with permission from ARPA Press]

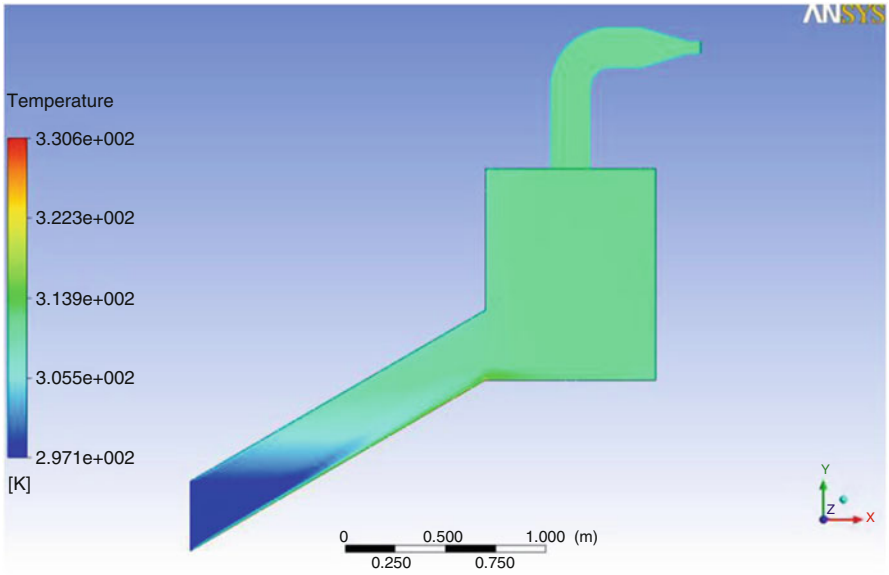

Fig. 2 Temperature field inside the middle section of a hybrid solar-electrical dryer [Reprinted from Brasil Maia C, Guimarães Ferreira A, Cabezas-Gómez L, de Morais Hanriot S, de Oliveira Martins T (2012) Simulation of the airflow inside a hybrid dryer. Int J Res Rev. Appl Sci 10 (March):382–389, with permission from ARPA Press]

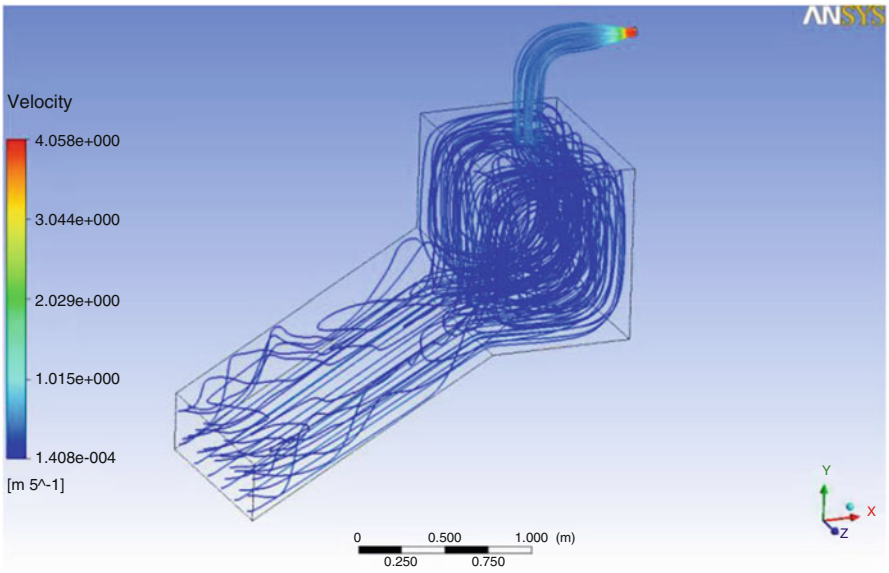

Fig. 3 Velocity streamlines inside the middle section of a hybrid solar-electrical dryer [Reprinted from Brasil Maia C, Guimarães Ferreira A, Cabezas-Gómez L, de Morais Hanriot S, de Oliveira Martins T (2012) Simulation of the airflow inside a hybrid dryer. Int J Res Rev. Appl Sci 10 (March):382–389, with permission from ARPA Press]

A similar study was conducted by Jomlapelatikul et al. (2016). In their work, COMSOL Multiphysics was employed to model the drying kinetics of carrots under both uniform and stepwise conditions (nonuniform process). Due to the drying characteristics of carrots, carrot quality is compromised at temperatures exceeding 75 °C; temperatures of 60–70 °C were chosen as design parameters. Carrots were washed, peeled, and cubed into 10 mm pieces, and then dried in an electrically heated forced-air convection dryer. Results revealed that stepwise temperature simulations are good predictors of changes in moisture content and drying time. Furthermore, the step-up process had a positive effect on thermal energy consumption savings – an indication that savings in thermal energy consumption can be achieved in dryers in which temperature differentials, in a narrow range, can be achieved during the course of drying. This is achievable in forced-air convection dryers, including active indirect solar dryers.

COMSOL Multiphysics has also been employed to understand temperature profiles within simple solar thermal cabinet dryers to inform the design of incorporating phase change materials as heat storage mechanisms to allow for overnight drying and enhance drying efficiency. The authors employed COMSOL Multiphysics to simulate the temperature profile of air in a 40.6 cm(W) x 43.1 cm(D) x 50.8 cm (H) cabinet dryer on a summer day (1 June 2014). The heat transfer fluid was air, which acted as a vehicle to transfer heat into the cabinet using the sun as the external

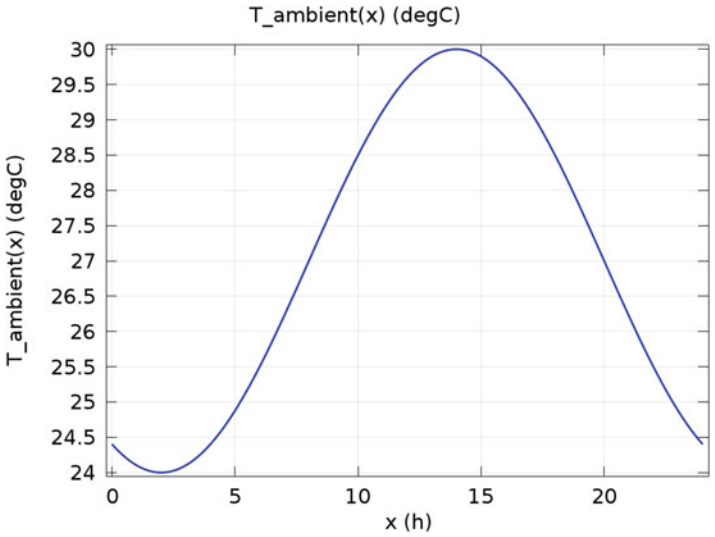

Fig. 4 Simulated ambient conditions for 1 June 2014 in Albany, CA, USA (coordinates 37.88 N 42′, -122.30 W 18′16.0″)

radiation/energy source. This led to the assumption that both convection and radiation heat transfer within the mass of air inside the cabinet are negligible. The sinusoidal expression below was used to derive the ambient temperature:

$$T_{\text{ambient}} = 27 + 3\cos\left(2\pi\left(\frac{x-14}{24}\right)\right) \tag{12}$$

The variation is shown in Fig. 4.

This simulated temperature profile matched well with the temperature conditions recorded using a Vantage Pro2 Weather Station (Davis Instruments, Vernon Hills, IL, USA).

To understand the influence of material attributes on drying conditions, optical properties of the transparent acrylic dryer cabinet lid were varied, specifically solar absorptivity and surface emissivity. Simulations were conducted based on the solar traverse at the latitudinal and longitudinal coordinates for Albany, CA, USA (location of the dryers). Results as shown in Fig. 5 revealed that at around solar noon, peak temperatures of 330 K (57 °C) can be achieved in the dryer unit designed with a material with emissivity and absorptivity values of 0.2 and 0.8, respectively.

Maximum temperatures of only 30 and 45 °C were achieved in other units with emissivity and absorptivity values of 0.8 and 0.2 and 0.5 and 0.5, respectively. In contrast, temperatures of 20 °C were consistently observed at the bottom of all dryers, which could be attributed to limited exposure to direct radiation (as indicated in Eq. 10). Thus, placement of latent heat phase change materials

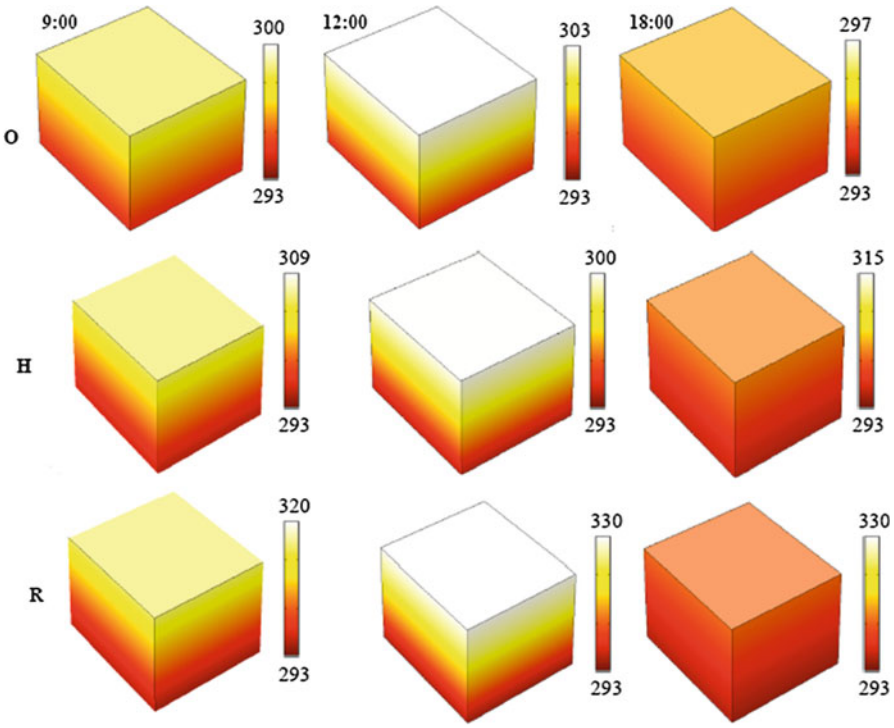

Fig. 5 Temperature profiles for the solar cabinet simulated based on the emissivity and absorptivity values for the original (O), half-half (H), and reversed (R) conditions at 9:00, 12:00, and 18:00 h

(which take up less surface area than sensible heat phase change materials) at the base of the solar thermal cabinet dryer will have limited functionality, given that appropriate temperature conditions will not be achieved to activate the heat storage capacity. Rather, temperature conditions more conducive for phase change materials appear to be near the top of the dryer, where access to direct radiation is more feasible, thereby driving increases in drying temperatures. Modifications to the solar thermal cabinet unit will be required, such as a corrugated absorber plate or other absorbing material, in order to integrate phase change materials at the base of the dryer. Based on this work, the following conclusions were drawn: materials with absorptivity and emissivity values of 0.8 and 0.2, respectively, are ideal candidates for solar thermal drying applications; foods that can be stored/dried at temperatures less than 57 °C are ideal for this drying application; and latent heat phase change materials with phase transition temperatures of 57 °C or less (e.g., Glauber's salts or paraffin wax) can be incorporated and activated in a solar thermal cabinet dryer with natural convection.

Tesfamariam et al. (2015) used the meshing program Gambit (v.2.3.16, packaged with Fluent, currently owned by ANSYS, Inc. (Canonsburg, PA, USA)) to

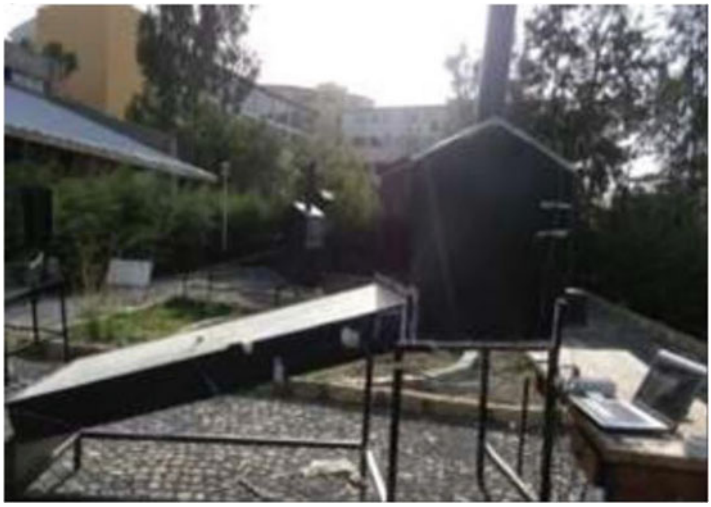

Fig. 6 Photo of an indirect, passive solar dryer; data-logging computer is shown at lower right [Reprinted from Tesfamariam DA, Bayray M, Tesfay M, Hagos FY (2015) Modeling and experiment of solar crop dryer for rural application. J Chem Pharm Sci 2015 (Special Issue 9):109–118, with permission from Journal of Chemical and Pharmaceutical Sciences]

model an indirect passive solar cabinet dryer. Using average ambient weather conditions for their location (Mekelle, Ethiopia), the authors simulated the performance of the dryer under no-load conditions. The physical dryer, two-dimensional mesh model, simulated temperature contours, and simulated velocity contours are shown in Figs. 6, 7, 8, and 9, respectively.

Actual performance of the dryer under no-load, half-load (5 kg of sliced tomatoes), and full-load (10 kg of sliced tomatoes) conditions was measured during the month of May 2012. Over all tested conditions, the average temperature of warmed air leaving the collector and entering the drying cabinet was 42 °C, and the peak temperature of this stream was 57 °C. These results agreed well with the computational modeling of the system. Both the half and full loads of tomatoes were dried within 2 days.

3 The Use of Models for Performance Evaluation and Comparison of Different Dryer Designs and Configurations

Two particular areas in which both mathematical and computational models can spur design innovations for solar dryers are performance evaluation and comparison of different dryer designs/configurations. By doing these tasks in a virtual environment, researchers can achieve rapid prototyping and exploration of the

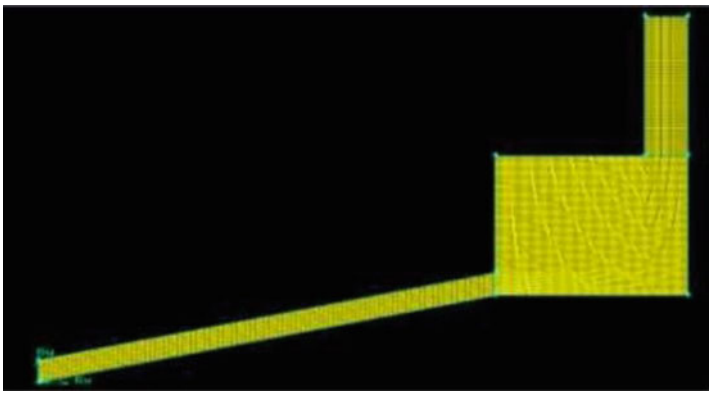

Fig. 7 Meshed two-dimensional model (center cross section) of an indirect, passive solar dryer [Reprinted from Tesfamariam DA, Bayray M, Tesfay M, Hagos FY (2015) Modeling and experiment of solar crop dryer for rural application. J Chem Pharm Sci 2015(Special Issue 9):109–118, with permission from Journal of Chemical and Pharmaceutical Sciences]

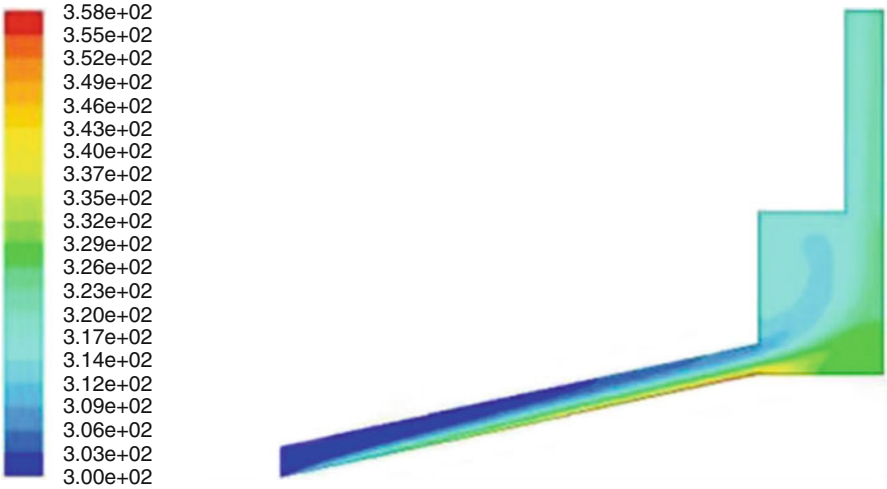

Fig. 8 Simulated temperature contours (in degrees Kelvin) of the center cross section of an indirect, passive solar dryer [Reprinted from Tesfamariam DA, Bayray M, Tesfay M, Hagos FY (2015) Modeling and experiment of solar crop dryer for rural application. J Chem Pharm Sci 2015 (Special Issue 9):109–118, with permission from Journal of Chemical and Pharmaceutical Sciences]

effects of different ambient conditions (especially insolation and wind speed/direction).

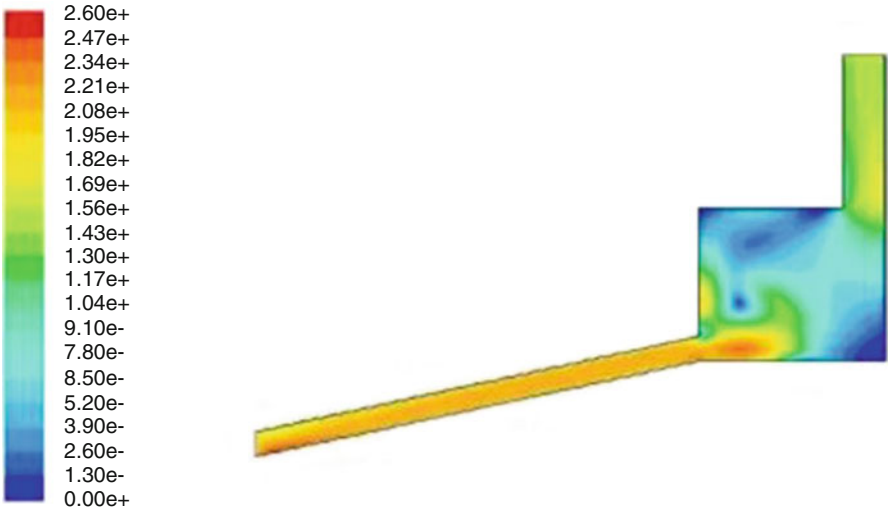

Fig. 9 Simulated contours of velocity magnitude (in m/s) of the center cross section of an indirect, passive solar dryer [Reprinted from Tesfamariam DA, Bayray M, Tesfay M, Hagos FY (2015) Modeling and experiment of solar crop dryer for rural application. J Chem Pharm Sci 2015(Special Issue 9):109–118, with permission from Journal of Chemical and Pharmaceutical Sciences]

3.1 Models for Dryer Performance Evaluation

Solar dryer performance metrics such as specific energy consumption (commonly kWh/kg) and overall efficiency (expressed as a percentage) are required under multiple circumstances:

- Operating a dryer under varying environmental conditions
- Comparing a solar dryer with an analogous conventional dryer
- Determining the payback period (or other economic metrics) for a given solar dryer design, location, and commodity being dried

In the work published by Janjai et al. (2009), mathematical modeling was used to investigate the drying performance of a photovoltaic-ventilated (PV-ventilated) solar greenhouse dryer in Thailand (PV was explored since many rural areas in Thailand have limited access to electricity grids). Modeling was employed to understand the efficiency of drying both spherical and elongated fruits, for which mass transfer and diffusion rates differ. To predict drying performance, the finite difference technique was employed for mass balance and thin-layer drying calculations with the following assumptions: no stratification of air inside the dryer, constant specific heat (air, polycarbonate, and fruit), and fraction of solar radiation loss is negligible. A time interval small enough to ensure stable air conditions was also chosen. Results of this work revealed that the temperature profiles and moisture contents predicted using the above method were a good indicator of the drying

conditions for both peeled longan and banana, when compared with experimental results. Through this modeling approach (finite difference method), drying rate and time can be estimated fairly accurately and in a more cost-effective manner for dryers, in which air stratification inside the dryer is negligible. The payback period for the solar dryer was determined to be 2.3 years – quite favorable for an agricultural technology investment.

In an effort to characterize the performance of a range of solar food dryers, Singh and Kumar (2012, 2013) have conducted experiments with the model system of a mixed-mode solar dryer loaded with cylindrical potato samples, operating under a wide range of processing conditions. In both of their studies, the variables investigated were absorbed thermal energy, airflow rate, food product loading density, and sample thickness. They developed a dimensionless dryer performance index (DPI) as well as a mathematical framework to estimate several dryer performance indicators, including drying efficiency, SEC (specific energy consumption), CO_2 emission mitigation, carbon credits earned, and amount of different fossil fuels saved due to use of solar drying. Different solar dryers with potato, banana, and wheat were tested in real climatic conditions to validate the proposed methodology for obtaining the DPI. They found that the DPI had consistent values for all test conditions, indicating a high degree of robustness for the DPI over various operating conditions and food product characteristics. For the environment-related dryer performance indicators, they found that, among different fossil fuels investigated, the replacement of coal with solar energy resulted in the maximum CO_2 mitigation potential and amount of fuel saved, compared to lower values of these metrics for replacement of natural gas with solar energy.

3.2 Models for Comparison of Different Dryer Designs and Configurations

With many solar dryer configurations (direct vs. indirect vs. mixed mode, active vs. passive, with vs. without heat storage, etc.) available, and with many design parameters associated with each configuration (size of collector, speed of forced-air convection, spatial arrangement of trays, etc.), it is critical to establish robust models for comparing these many options.

Mathematical models can help usher in new technology advances in solar drying by demonstrating the effectiveness of interventions such as heat storage units and desiccants. Vijayan et al. (2016) compared the drying of bitter gourd in open sun (passive direct) and in an active indirect solar dryer with sensible heat storage (via a pebble thermal absorber). They showed that the moisture content of bitter gourd was reduced from 92% (wet basis) to a target of 9% (wet basis) in 7 h in the active indirect drying system with thermal storage, compared to 10 h for passive direct drying. Mathematical modeling was also employed by Kabeel and Abdelgaied (2016) to investigate the effect of a rotary desiccant wheel on the thermal

performance of a solar chimney dryer. To solve the model, several assumptions were made, including but not limited to one-dimensional airflow, all honeycomb air channels are adiabatic, and air leakage in desiccant wheel is negligible. The latter can be accomplished when careful attention is made to the design such that materials are strongly adhered and material properties (such as thermal expansion coefficient) are compatible. Mathematical results for the moisture removal capacity of the rotary desiccant wheel were in reasonable agreement with the results published by Ge et al. (2008) for a rotary desiccant wheel tested under Air-Conditioning and Refrigeration Institute (ARI) summer and humid conditions at the same inlet conditions. Similarly, collector efficiency results matched well with those published by David et al. (2010). Thus, Kabeel and Abdelgaied (2016) have shown that mathematical modeling can be implemented to inform the design of a solar chimney dryer with respect to drying capacity and solar collector efficiency.

One aspect of solar drying of food that sets it apart from solar drying of other materials is the need to consider the quality of the product. A dryer may bring the moisture content of a foodstuff down quickly by providing high heat and/or airflow, but the quality of the product may be adversely impacted. Often, simple interventions will be sufficient. For example, Meas et al. (2013) used a finite difference model to determine that stirring direct sun-dried rice regularly and shading the rice during the hottest parts of the day significantly increased head rice yield, leading to better returns to the farmer.

Recently, researchers have endeavored to integrate engineering, economic, and quality parameters into a comprehensive solar dryer comparison rubric. Leon et al. (2002) presented a list of more than 20 parameters that should be considered when comparing the performance of solar dryers. Among the more common dryer performance parameters, this list also included loading density [kg product/m^2 solar aperture], duration of drying air temperature 10 °C above ambient under no-load conditions [h], quality of dried product (rehydration, color, texture, flavor, etc.), and loading/unloading convenience.

4 Modeling for the Future of Solar Drying

Both mathematical and computational models have been successfully applied to solar food drying systems in recent years. The selection of the type of model to use for a given dryer, commodity, and environment depends on the information desired from the model. Fundamental, semiempirical, and empirical models suffice for rough estimation of solar drying times. However, care must be taken to acknowledge the assumptions about geometry and heat/mass/momentum transfer that underlie these mathematical models. Computational models – made possible by dramatic advances in computer processing speed and memory – can help remove some of these assumptions by simulating the basic physical phenomena involved in solar drying for a given fundamental geometric unit (food particle, tray of food,

dryer cabinet, etc.). In order for these computational models to produce reasonable results, though, the thermophysical properties of that geometric unit must be known. So, much work remains in measuring and verifying such quantities as the desorption isotherms of food materials and the optical properties of common cabinet and collector construction materials. Both mathematical and computational models can assist researchers in establishing a dryer's performance under different environmental or product load conditions. Both types of models can also facilitate comparison of different dryer designs and configurations. The future of solar drying will heavily depend on the quality, robustness, and prudent application of both mathematical and computational models.

5 Conclusion

In this chapter, a brief review on mathematical and computational modeling simulation of solar drying system is being presented. These two modeling techniques are being applied for all three types of the solar dryer – namely, direct, indirect, and mixed mode. In the mathematical modeling, both basic and semiempirical drying models are being studied. In the computational modeling, mainly CFD modeling is being studied. Both two-dimensional and three-dimensional modes are being studied. This modeling technique is necessary for the effective evaluation of the dryer performance and proper comparative analysis of the various dryers. In order to validate the models (both mathematical and computational), the simulated results are compared with the experimental results.

References

Akbulut A, Durmuş A (2009) Thin layer solar drying and mathematical modeling of mulberry. Int J Energy Res 33(7):687–695. doi:10.1002/er.1504

Akpinar EK, Sarsılmaz C, Yildiz C (2004) Mathematical modelling of a thin layer drying of apricots in a solar energized rotary dryer. Int J Energy Res 28(8):739–752. doi:10.1002/er.997

Akpinar EK (2009) Drying of parsley leaves in a solar dryer and under open sun: modeling, energy and exergy aspects. J Food Process Eng 2009:1–22. doi:10.1111/j.1745-4530.2008.00335.x

Aktaş M, Ceylan İ, Yilmaz S (2009) Determination of drying characteristics of apples in a heat pump and solar dryer. Desalination 239(1–3):266–275. doi:10.1016/j.desal.2008.03.023

Aversa M, Curcio S, Calabro V, Iorio G (2007) An analysis of the transport phenomena occurring during food drying process. J Food Eng 78(3):922–932. doi:10.1016/j.jfoodeng.2005.12.005

Ayadi M, Mabrouk SB, Zouari I, Bellagi A (2014) Simulation and performance of a solar air collector and a storage system for a drying unit. Sol Energy 107:292–304. doi:10.1016/j.solener.2014.05.038

Babalis SJ, Belessiotis VG (2004) Influence of the drying conditions on the drying constants and moisture diffusivity during the thin-layer drying of figs. J Food Eng 65:449–458. doi:10.1016/j.jfoodeng.2004.02.005

Bahloul N, Boudhrioua N, Kouhila M, Kechaou N (2011) Convective solar drying of olive leaves. J Food Process Eng 34(4):1338–1362. doi:10.1111/j.1745-4530.2009.00432.x

Bennamoun L (2011) Reviewing the experience of solar drying in Algeria with presentation of the different design aspects of solar dryers. Renew Sust Energ Rev 15(7):3371–3379
Brasil Maia C, Guimarães Ferreira A, Cabezas-Gómez L, de Morais HS, de Oliveira MT (2012) Simulation of the airflow inside a hybrid dryer. Int J Res Rev Appl Sci 10(March):382–389
David L, Jannot Y, Nadeau J-P (2010) An oriented-design simplified model for the efficiency of a flat plate solar air collector. Appl Therm Eng 30:2808–2814. doi:10.1016/j.applthermaleng.2010.08.016
Diamante LM, Ihns R, Savage GP, Vanhanen L (2010) A new mathematical model for thin layer drying of fruits. Int J Food Sci Technol 45:1956–1962. doi:10.1111/j.1365-2621.2010.02345.x
Diamante LM, Munro PA (1991) Mathematical modelling of hot air drying of sweet potato slices. Int J Food Sci Tech 26:99
Dincer I, Dost S (1996) A modeling study for moisture diffusivities and moisture transfer coefficients in drying of solid objects. Int J Ener Res 20:531–539. doi:10.1002/(SICI)1099-114X(199606)20:6<531::AID-ER171>3.0.CO;2-6
Kane CSE, Jamali A, Kouhila M, Mimet A, Ahachad M (2008) Single-layer drying behavior of mexican tea leaves (*Chenopodium ambrosioides*) in a convective solar dryer and mathematical modeling. Chem Eng Commun 195(7):787–802. doi:10.1080/00986440701691095
Ge TS, Li Y, Wang RZ, Li Y (2008) Experimental investigation on a one-rotor two-stage rotary desiccant cooling system. Energy 33:1807–1815. doi:10.1016/j.energy.2008.08.006
Ghodake HM, Goswami TK, Chakraverty A (2006) Mathematical modeling of withering characteristics of tea leaves. Dry Technol 24(2):159–164. doi:10.1080/07373930600558979
Guiné R, Ferreira D, Barroca M, Goncalves F (2007) Study of the drying kinetics of solar-dried pears. Biosyst Eng 98(4):422–429. doi:10.1016/j.biosystemseng.2007.09.010
Hanif M, Rahman M, Amin M (2013) Convective drying and mathematical modeling of onions dried using a flat plate solar air heater. Pakistan J Nutr 12(11):1003–1007
Henderson SM, Pabis S (1961) Grain drying theory I: temperature effect on drying coefficient. J Agric Res Eng 6:169–174
Henderson SM (1974) Progress in developing the thin layer drying equation. Trans ASAE:1167–1172
Hii CL, Law CI, Law MC (2013) Simulation of heat and mass transfer of cocoa beans under stepwise drying conditions in a heat pump dryer. Appl Thermal Eng 54:264–271. doi:10.1016/j.applthermaleng.2013.02.010
Ismail M, Idriss EI (2013) Mathematical modelling of thin layer solar drying of whole okra (*Abelmoschus esculentus* (l.) Moench) pods. Int Food Res J 20(4):1983–1989
Janjai S, Lamlert N, Intawee P, Mahayothee B, Bala BK, Nagle M, Müller J (2009) Experimental and simulated performance of a PV-ventilated solar greenhouse dryer for drying of peeled longan and banana. Sol Energy 83:1550–1565. doi:10.1016/j.solener.2009.05.003
Jomlapelatikul A, Wiset L, Duangkhamchan W, Poomsa-ad N (2016) Model-based investigation of heat and mass transfer for selecting optimum intermediate moisture content in stepwise drying. Appl Thermal Eng 107:987–993. doi:10.1016/j.applthermaleng.2016.07.064
Kabeel AE, Abdelgaied M (2016) Performance of novel solar dryer. Process Safety and Env Prot 102:183–189. doi:10.1016/j.psep.2016.03.009
Karathanos VT (1999) Determination of water content of dried fruits by drying kinetics. J Food Eng 39:337–344. doi:10.1016/S0260-8774(98)00132-0
Kassem AS (1998) Comparative studies on thin layer drying models for wheat. 13th international congress on agricultural engineering, vol. 6. p 2–6 February, Morocco
Kaya A, Kamer MS, Sahin HE (2015) Determining the moisture transfer parameters for regularly shaped products. Int J Sci Technol Res 1(1):184–196
Kucuk H, Midilli A, Kilic A, Dincer I (2014) A review on thin-layer drying-curve equations. Dry Technol 32(7):757–773. doi:10.1080/07373937.2013.873047
Lahnine L, Idlimam A, Mahrouz M, Mghazli S, Hidar N, Hanine H, Koutit A (2016) Thermophysical characterization by solar convective drying of thyme conserved by an

innovative thermal-biochemical process. Renew Energy 94:72–80. doi:10.1016/j.renene.2016.03.014

Lamnatou C, Papanicolaou E, Belessiotis V, Kyriakis N (2012) Experimental investigation and thermodynamic performance analysis of a solar dryer using an evacuated-tube air collector. Appl Energy 94:232–243. doi:10.1016/j.apenergy.2012.01.025

Leon MA, Kumar S, Bhattacharya S (2002) A comprehensive procedure for performance evaluation of solar food dryers. Renew Sust Energ Rev 6(4):367–393. doi:10.1016/S1364-0321(02)00005-9

Lewis WK (1921) The rate of drying of solid materials. Indus Eng Chem 13(5):427–442

Meas P, Paterson AHJ, Cleland DJ, Bronlund JE, Mawson J, Hardacre A, Rickman JF (2013) Relating rice grain quality to conditions during sun drying. Int J Food Eng 9(4):385–391. doi:10.1515/ijfe-2013-0019

Midilli A, Kucuk H, Yapar Z (2002) A new model for single-layer drying. Dry Technol 20(7):1503–1513. doi:10.1081/DRT-120005864

Nourhene B, Mohammed K, Nabil K (2008) Experimental and mathematical investigations of convective solar drying of four varieties of olive leaves. Food Bioprod Process 86(3):176–184. doi:10.1016/j.fbp.2007.10.001

Overhults DD, White GM, Hamilton ME, Ross IJ (1973) Drying soybeans with heated air. Trans ASAE 16:195–200

Page GE (1949) Factors influencing the maximum rates of air drying shelled corn in thin layers. M. Sc. thesis, Purdue University, Lafayette

Prakash O, Kumar A (2014) Environomical analysis and mathematical modelling for tomato flakes drying in a modified greenhouse dryer under active mode. Int J Food Eng 10(4):669–681. doi:10.1515/ijfe-2013-0063

Raji AO, Adeyemi AO (2012) Thin layer drying kinetics and quality of african baobab leaf (Adansonia digitata). In: International Conference of Agricultural engineering - CIGR - AgEng 2012: Agriculture and Engineering for a Healthier Life pp 1–6

Ramos IN, Miranda JMR, Brandão TRS, Silva CLM (2010) Estimation of water diffusivity parameters on grape dynamic drying. J Food Eng 97:519–525. doi:10.1016/j.jfoodeng.2009.11.011

Ramos IN, Brandão TRS, Silva CLM (2015) Simulation of solar drying of grapes using an integrated heat and mass transfer model. Renew Energy 81:896–902. doi:10.1016/j.renene.2015.04.011

Romero VM, Cerezo E, Garcia MI, Sanchez MH (2014) Simulation and validation of vanilla drying process in an indirect solar dryer prototype using CFD Fluent program. Energy Proc 57:1651–1658. doi:10.1016/j.egypro.2014.10.156

Sacilik K, Keskin R, Elicin A (2006) Mathematical modelling of solar tunnel drying of thin layer organic tomato. J Food Eng 73(3):231–238. doi:10.1016/j.jfoodeng.2005.01.025

Sharaf-Eldeen YI, Blaisdell JL, Hamdy MY (1980) A model for ear corn drying. Trans ASAE 23:1261–1271

Sharma GP, Prasad S (2004) Effective moisture diffusivity of garlic cloves undergoing microwave-convective drying. J Food Eng 65(4):609–617. doi:10.1016/j.jfoodeng.2004.02.027

Silva V, Figueiredo AR, Costa JJ, Guiné RPF (2014) Experimental and mathematical study of the discontinuous drying kinetics of pears. J Food Eng 134:30–36. doi:10.1016/j.jfoodeng.2014.02.022

Singh S, Kumar S (2012) New approach for thermal testing of solar dryer: development of generalized drying characteristic curve. Sol Energy 86(7):1981–1991. doi:10.1016/j.solener.2012.04.001

Singh S, Kumar S (2013) Solar drying for different test conditions: proposed framework for estimation of specific energy consumption and CO_2 emissions mitigation. Energy 51:27–36. doi:10.1016/j.energy.2013.01.006

Singh S, Kumar S (2014) Performance evaluation of solar dryer system for optimal operation: mathematical modelling and experimental validation. Int J Sustain Energy 33(1):141–158. doi:10.1080/14786451.2013.772613

Tesfamariam DA, Bayray M, Tesfay M, Hagos FY (2015) Modeling and experiment of solar crop dryer for rural application. J Chem Pharm Sci 2015(Special Issue 9):109–118

Thomson TL, Peart PM, Foster GH (1968) Mathematical simulation of corn drying a new model. Trans ASAE 11:582–586

Toğrul İT, Pehlivan D (2002) Mathematical modelling of solar drying of apricots in thin layers. J Food Eng 55(3):209–216. doi:10.1016/S0260-8774(02)00065-1

Tripathy PP (2015) Investigation into solar drying of potato: effect of sample geometry on drying kinetics and CO_2 emissions mitigation. J Food Sci Technol 52(3):1383–1393. doi:10.1007/s13197-013-1170-0

Tripathy PP, Kumar S (2009) A methodology for determination of temperature dependent mass transfer coefficients from drying kinetics: application to solar drying. J Food Eng 90 (2):212–218. doi:10.1016/j.jfoodeng.2008.06.025

Tripathy PP, Kumar S (2011) Different approaches for mass transfer studies on potato cylinders and slices during solar drying. Int J Food Eng 7(1):1–18. doi:10.2202/1556-3758.1413

Tunde-Akintunde TY, Oke MO (2012) Thin-layer drying characteristics of tiger nut (*Cyperus esculentus*) seeds. J Food Process Preserv 36(5):457–464. doi:10.1111/j.1745-4549.2011.00604.x

Wang CY, Singh RP (1978) A single layer drying equation for rough rice. ASAE Paper No: 78-3001, ASAE, St. Joseph, MI

Verma LR, Bucklin RA, Endan JB, Wratten FT (1985) Effects of drying air parameters on rice drying models. Trans ASAE 28:296–301

Vijayan S, Arjunan TV, Kumar A (2016) Mathematical modeling and performance analysis of thin layer drying of bitter gourd in sensible storage based indirect solar dryer. Innov Food Sci Emerg Technol 36:59–67. doi:10.1016/j.ifset.2016.05.014

Yagcioglu A, Degirmencioglu A, Cagatay F (1999, May 26–27) Drying characteristics of laurel leaves under different drying conditions. In: Proceedings of the 7th international congress on agricultural mechanization and energy, Adana, Turkey, pp 565–569

Yaldiz O, Ertekin C, Uzun HI (2001) Mathematical modeling of thin layer solar drying of sultana grapes. Ener 26(5):457–465

Zhu A, Shen X (2014) The model and mass transfer characteristics of convection drying of peach slices. Int J Heat Mass Transf 72:345–351. doi:10.1016/j.ijheatmasstransfer.2014.01.001

Numerical Techniques for Evaluating the Performance of Solar Drying Systems

Karunesh Kant, Atul Sharma, and Amritanshu Shukla

Abstract This chapter mainly describes the various numerical methods that can be used for performance evaluation of the solar drying system. The numerical techniques help to develop solar dryers to increase drying effectiveness and analyses, and they forecast the performance of dissimilar types of solar dryers. The numerical analysis is essential for forecasting the relevant parameters, which are highly required in a solar drying system. Computational fluid dynamics (CFD) can be used to analyze and investigate the heat and mass transfer inside the solar dryer. An adaptive-network-based "fuzzy" inference system (ANFIS) is able to predict the performance of the solar drying system. The artificial neural network can be applied to estimate the quantity of the dehydrated product. Fuzzy logic is an essential tool for precisely forecasting the results with the least inaccuracy.

The numerical techniques are applied for testing the drying behavior of products in the laboratory as well as on a commercial level. These techniques are beginning to act as an effective tool for researchers and scientists, who play a vital role in saving time and money without conducting any experiments for the same purpose. Thus, the numerical analysis not only results in reduced time, but also lowers the capital cost of a solar dryer. Before the production of a solar drying system, numerical analysis is essential because it gives very supportive information regarding the design and construction of a solar drying system.

Keywords Solar dryer • Numerical methods • Drying behavior • Heat and mass transfer

1 Introduction

Solar drying is the process of reducing the moisture content in any wet product; it is one of the easiest and oldest methods applied to dry agricultural food products for storing (Augustus Leon et al. 2002). Food products, such as fruits and vegetables,

K. Kant • A. Sharma (✉) • A. Shukla
Non-Conventional Energy Laboratory, Rajiv Gandhi Institute of Petroleum Technology, Rae Bareli 229316, India
e-mail: asharma@rgipt.ac.in

© Springer Nature Singapore Pte Ltd. 2017

O. Prakash, A. Kumar (eds.), *Solar Drying Technology*, Green Energy and Technology, DOI 10.1007/978-981-10-3833-4_12

need to be heated in air within the 45-60°C temperature range (Kant et al. 2016) for safe drying, that is, reducing the wetness of the drying products to subsequently keep their edible and beneficial properties unspoiled. The required wetness content and excellence of the product can be achieved under organized humidity and temperature conditions (Sharma et al. 1995). In the case of vegetables, 50% of wet vegetables (Wahidi and Rohani 1996) are removed as undesirable items through cooking because of higher moisture content. Dehydrated vegetable peels are able to be used further for feeding animals. Furthermore, because of a decrease in the mass and size of such dehydrated products, the shipping cost of vegetables also reduces.

It has been argued that the deficiency of suitable technology and fertilization, incorrect cultivation, the nonexistence of proper advertising networks, inappropriate transport, high post-harvest losses, and so on, lead to a 10–40% food loss (Esper and Mühlbauer 1998). Consequently, food conservation is vital for decreasing food loss, and solar drying has been widely used as a key tool in this context for a long time. Consequently, well-organized drying techniques are needed to diminish moisture content from wilted food crops for conservation.

An efficient and cost-effective solar dryer can deliver an appropriate substitute for dehydrating cultivated products in developing countries (Kant et al. 2016; Mahapatra and Imre 1990; Sodha and Chandra 1994; Esakkimuthu et al. 2013; Hossain et al. 2005; Zhiqiang 2005). The use of solar energy in the farming and food industries has great potential because of the increase in the cost of fossil fuels, ecological concerns, and predictable exhaustion of conventional fuels. This places a burden on many of the fields connected to energy production and supply.

Solar energy is abundantly available on a daily basis; it can be an effective and feasible way to agree with the growing gap between energy supply and demand. Solar energy is most appropriate for drying agricultural and food products, but it alternates in nature because of the lack of solar radiation at night. The drying method helps the domestic and manufacturing sectors to produce food and agricultural products conserve food more easily, expand a certain product to be considerably more usable, upsurge the loading capacity and low cost of shipping, and harness outright or provide incidental ecological benefits.

Therefore, a well-organized solar dryer provides the highest benefits to the mankind and definitely needs the interesting task of emerging and innovative solar dryers with effective energy exhaustion for the particular product. Solar energy is thought to be quite effective for drying food and agriculture for various reasons:

1. Solar radiation available from the environment effortlessly delivers inferior thermal heat. This characteristic is good for drying products at a moderate temperature range, at a high flow rate, and with slow and low-temperature growth.

2. The intermittent nature of solar radiation does not affect drying at a low temperature, although the energy held within the product will help reduce additional moistness in the dark.
3. Solar energy is available at most of the required sites.

The drying of any product is the process of reducing its moisture content to a safe limit. The dryness fraction hangs onto moisture content during the drying process. The safe limit of different products is shown in Table 1.

The drying process takes place in a controlled environment. Consequently, the color and quality of drying products are not affected as in open sun drying. The process of drying is accomplished by various methods such as spray, electrical, mechanical, solar dryers, etc. The drying systems are contingent upon solar energy and are classified in direct mode solar dryers, indirect mode solar dryers, and mixed-mode solar dryers. In the direct mode solar dryer, the solar energy is directly used for dehydrating products. The work and design of direct solar drying is simple and operational, and maintenance costs are also lower and have the ability to dry small quantities of the food product.

The indirect solar drying system consists of a solar air heater and supplementary heater for heating air when sunshine is unavailable. The fan is used for circulating air inside the cabinet of the indirect solar dryer. The indirect method of solar dehydrating is the modern method of dehydration of wetted products without using conventional fossil fuels. The indirect solar drying system is more effective as compared to the direct solar drying system, since the air is heated by the application of a solar air heater and the heated air flow in the cabin where the product is stored (Khan et al. 2014). A mixed-mode solar dryer is the arrangement of a direct and indirect solar dryer; with this method, the product is dehydrated, either by indirect solar radiation or when atmospheric air is heated first. At that time, it is passed through the cabin where the product is stored (Bagheri 2015). Figure 1a-c shows the direct, indirect, and mixed-mode solar dryer systems, respectively (Prakash and Kumar 2013; Pardhi and Bhagoria 2013).

2 Various Numerical Techniques for Performance Evaluation of a Solar Drying System

Various numerical practices are aimed at modelling solar drying systems as follows: Artificial Neural Network (ANN); Computational Fluid Dynamics (CFD); FUZZY; ANFIS; mathematical modelling; and thermal modelling for studying the drying kinetics of solar dryers, etc. Numerical techniques are significant for explaining the drying behavior of the solar dryer in testing and designing, as well as increasing the quality of the product and saving energy consumption.

Table 1 Safe moisture limits for various products (Kumar et al. 2014; Prakash and Kumar 2013)

Product	Moisture content %		Highest temperature acceptable for drying (°C)
	Initial	Final	
Pineapple	80	10	65
Brinjal	95	6	60
Tomatoes	96	10	60
Apples	80	24	70
Apricots	85	18	65
Raw fish	75	15	30
Nutmeg	80	20	65
Fish water	75	15	50
Nutmeg	80	20	65
Potatoes	75	13	75
Chillies	80	5	65
Prunes	85	15	55
Peaches	85	18	65
Grapes	80	15-20	70
Guavas	80	7	65
Cotton	50	9	75
Bananas	80	15	70
Okra	80	20	65
Cotton seeds	50	8	75
Coffee beans	55	12	NA
Millet	21	14	NA
Cassava	62	17	NA
Spinach	80	10	NA
Cassava leaves	80	10	NA
Onion rings	80	10	55
Figs	80	24	NA
Mulberries	80	10	65
Yams	80	10	65
Sorrel	80	20	65
Coffee	50	11	NA
Cocoa beans	50	7	NA
Copra	30	5	NA
Silk cocoons	68-70	10-12	80
Ground nuts	40	9	50
Timber			
Conifers	30-40	10-15	50
Foliage trees	25-35	17-20	50
Mahogany	35	11	NA
Soaked trees	60	12	50
Leather	50	18	35
Fabrics	50	8	75

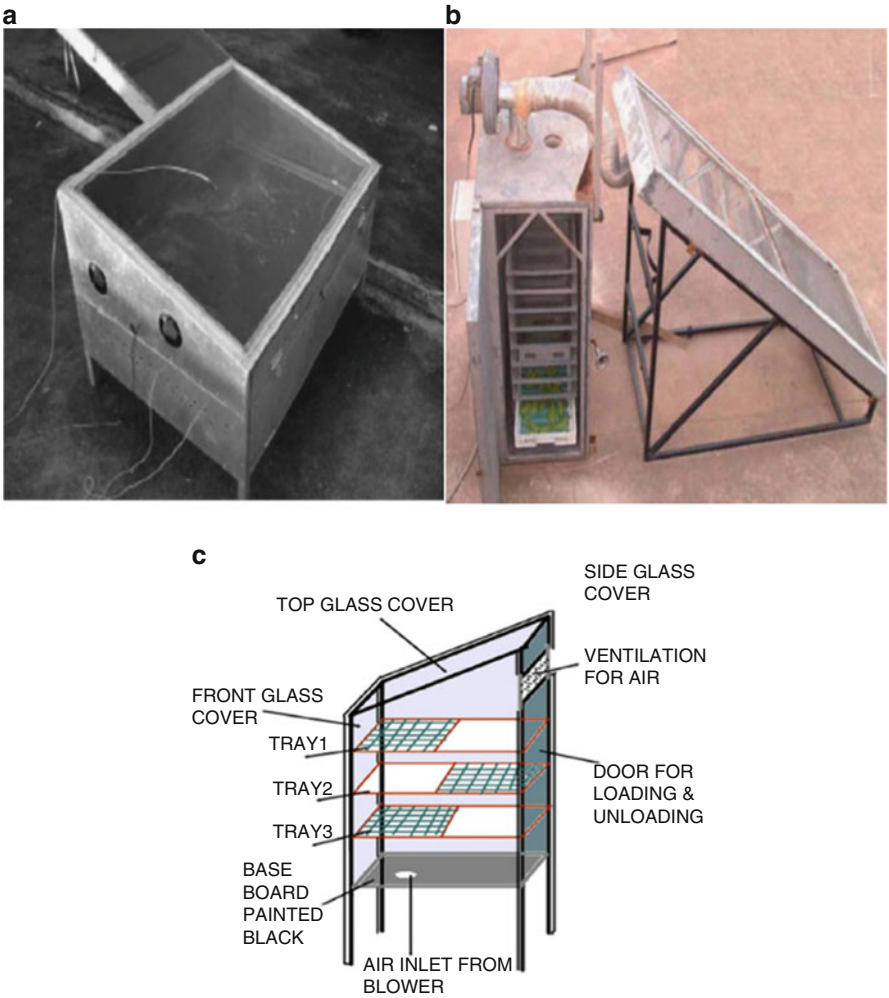

Fig. 1 Solar dryer: (**a**) Direct solar dryer (Sreekumar et al. 2008); (**b**) Indirect solar dryer (Ait Mohamed et al. 2008); (**c**) Mixed mode solar dryer (Singh Chauhan et al. 2015)

2.1 Computational Fluid Dynamic (CFD)

Computational Fluid Dynamic is connected to heat and mass transfer in the solar drying system. It can be applied to numerical analysis and solving the algorithms, and analyzing the heat and mass transfer problem. The calculations in the high-performance computer are essential to simulate the interaction between liquid and gases with the solid surface. ANSYS, COMSOL Multiphysics, and Fluent provide a widespread set of CFD tools for modelling heat and mass transfer and other connected physical phenomena. The results obtained from these solutions can

simulate a wide range of phenomena such as aerodynamics, hydrodynamics, particle dispersions, mixtures of liquids/solids/gas, reacting flows, heat transfer, and others.

2.1.1 Numerical Formulation

The steady-state and transient flow problems are easily and rapidly resolved. The governing equation for the simulation of the solar dryer is as follows (Sonthikun et al. 2016; Tekasakul et al. 2015).

Continuity equation

$$\frac{\partial \rho}{\partial t} + \nabla.(\rho \bar{u}) = 0 \tag{1}$$

Momentum equation

$$\frac{\partial (\rho \bar{u})}{\partial t} + \nabla.(\rho \bar{u}\bar{u}) = -\nabla P + \nabla.\left(\bar{\tau}_{eff}\right) + \rho g \beta (\bar{T}_0 - \bar{T}) \tag{2}$$

Energy equations

$$\frac{\partial (\rho E)}{\partial t} + \nabla.(\bar{u}(\rho E + P)) = \nabla.\left(\lambda_{eff} \nabla T - \sum_j H_j J_J + \left(\bar{\tau}_{eff}.\bar{u}\right)\right) \tag{3}$$

where E is specific energy of fluid (J/kg), u is component vector of the mean velocity (m/s), λ_{eff} is the effective thermal conductivity (W/m.K), H_j is the enthalpy of species j (J/kg), J_j is the diffusion flux of species j (kg/m^2 s), t is time (s), ρ is the density (kg/m^3), P is the pressure (N/m^2), b is the thermal expansion coefficient, g is the gravitational acceleration (m/s^2), T_0 is the surrounding temperature (K), T is the mean temperature, and τ_{eff} is an effective stress tensor and given by Eq. (4)

$$\tau_{eff} = \mu_{eff}\left[\left(\nabla \bar{u} + \nabla \bar{u}^T\right)\right] + \frac{2}{3}\nabla.\bar{u}I \tag{4}$$

where μ_{eff} is the effective viscosity (kg/m.s), I is the unit tensor and u^{-T} is the transposed mean velocity (m/s). In the E, the specific energy of fluid can be given as (5):

$$E = H - \frac{P}{\rho} + \frac{u^2}{2} \tag{5}$$

Here, H is the enthalpy (J/kg), and $u^2/2$ is the kinetic energy. The water transport during the dehydration process can be expressed through the species fraction equilibrium equation:

$$\frac{\partial(\rho Y)}{\partial t} + \nabla.(\rho \bar{u} Y) = -\nabla.J_w \tag{6}$$

and Fick's Law of Mass Transfer is

$$J_w = -\rho D_{eff} \nabla Y \tag{7}$$

where J_w is the water mass flux (kg/m^2.s), D_{eff} is the diffusion coefficient of water (m^2/s), and Y is the water mass fraction in the air (kg water = kg dry air). The dissipation rate (ε) and kinetic energy of turbulence (k) are given as follows:

k equation

$$\frac{\partial(\rho k)}{\partial t} + \nabla.(\rho k \bar{u}) = \nabla.\left[\left(\mu + \frac{\mu_t}{\sigma_k}\right)\nabla k\right] + 2\mu_t E_{ij}.E_{ij} - \rho\varepsilon \tag{8}$$

ε equation

$$\frac{\partial(\rho \varepsilon)}{\partial t} + \nabla.(\rho \varepsilon \bar{u}) = \nabla.\left[\left(\mu + \frac{\mu_t}{\sigma_\varepsilon}\right)\nabla \varepsilon\right] + C_{1\varepsilon}\frac{\varepsilon}{k}2\mu_t E_{ij}.E_{ij} - C_{2\varepsilon}\rho\frac{\varepsilon^2}{k} \tag{9}$$

The constants in the models are given as follows:

$C_{1\varepsilon} = 1.44$, $C_{\mu} = 0.09$, $C_{2\varepsilon} = 1.92$, $\sigma_{\varepsilon} = 1.3$, $\sigma_{k} = 1.0$

where $\rho\varepsilon$ is the destruction rate, E_{ij} is the turbulence rate, and μ_t is the eddy viscosity (kg/ms) as follows:

$$\mu_t = \rho C_\mu \frac{k^2}{\varepsilon} \tag{10}$$

By equating conductive and convective heat transfer at the surface, the local heat transfer coefficient (h) can be obtained

$$\lambda_g \frac{\partial \bar{T}}{\partial n}\bigg|_s = h\left(\overline{T_s} - \overline{T_a}\right) \tag{11}$$

The mass transfer coefficient due to the convective (h_m) can be obtained by a similarity between concentrating boundary layers and thermal boundary layers (known as the Chilton-Colburn Analogy):

$$\frac{h}{h_m} = \rho C_p Le^{2/3} \tag{12}$$

where L_e is the Lewis number and h_m is the convective mass transfer coefficient (m/s).

2.1.2 Heat and Mass Transfers from Drying Products

In this section, we discuss the numerical formulation used for analyzing the diffusion-based heat and mass transfer equations for the drying kinetics of food and crop products. The temperature equilibrium of heat and mass transfer means that both sides have the same temperature, as the mass equilibrium relation at the gas-solid boundary is supposed. The following assumptions are made for heat and mass transfer diffusion equations:

1. Deformation and shrinkage drying product during drying is negligible.
2. Effects of radiation are negligible.

The prevailing heat and mass transfer diffusion equations are as follows:

$$\frac{1}{\alpha_r}\frac{\partial(\bar{T})}{\partial t} = \nabla.(\nabla\bar{T}) \tag{13}$$

$$\frac{1}{D_r}\frac{\partial(\bar{M})}{\partial t} = \nabla.(\nabla\bar{M}) \tag{14}$$

where α_r is thermal diffusivity (m^2/s), $D_{r.}$ is diffusivity of the water (m^2/s). and $\bar{M}$ is the moisture content (kg/kg, db). The moisture diffusivity can be obtained by the application of the equation for the drying product:

$$D_r = 4 \times 10^{-5}\exp(-6158.47/T) \tag{15}$$

The CFD is applied to foretell the air flow field in a dryer. The numerical data from the CFD and drying experiment signify the good relationship between the velocity of air flow and drying rate. Consequently, CFD modelling can be used for appropriate designing and increasing drying effectiveness (Akpinar and Bicer 2007). Figure 2 shows the block diagrams for the process of process of CFD.

2.2 Adaptive-Network-Based Fuzzy Inference System (ANFIS)

ANFIS is established on empirical correlations having definite constraints, surrounded by a radial basis function (*RBF*) fuzzy system. The solution can be

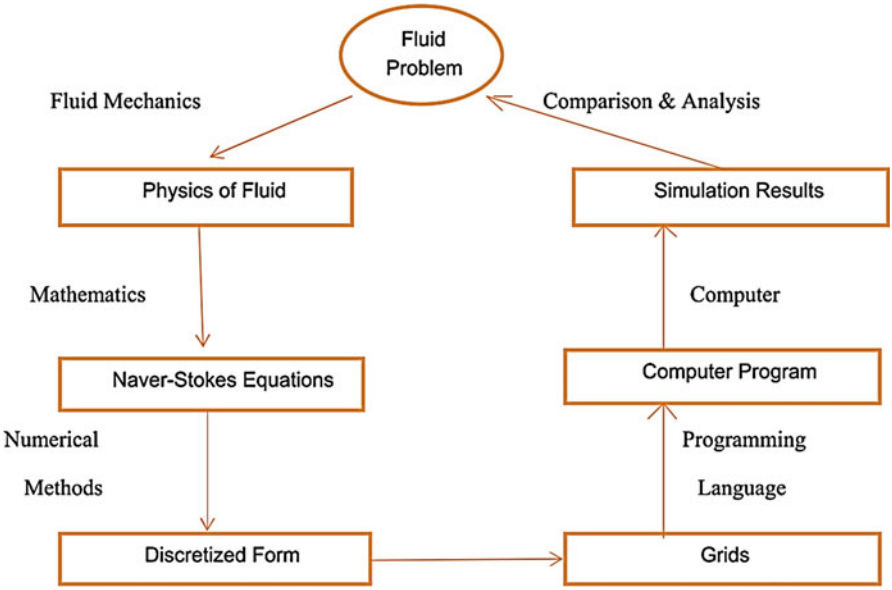

Fig. 2 Block diagrams of CFD process (Prakash et al. 2016)

directly obtained having single output by considering the input by fuzzy procedures. The instructions are completely established in the information of various input data. This technique is based on the first order of the Takagi-Sugeno model (Dymond and Kutscher 1997). The ANFIS turns out to be a better fuzzy controller due to a self-learning skill that is guided to the smallest reliable position of error (Defraeye 2014). The Sugeno fuzzy model is suitable for the complex non-linear and energetic activity systems. The standard rules that flow in a model are:

Assume that $x = s$
$y = U$; $s = f(x,y)$

where S = fuzzy set
$S = f(x,y)$ is a function of the short form of S that has two rules:

$$\text{1st rule-if } x = Z_1 \ \& \ y = U_1, \text{then} \quad f_1 = a^1x + b^1y + c^1 \tag{16}$$

$$\text{2nd rule-if } x = Z_2 \ \& \ y = U_2, \text{then} \quad f^2 = a^2x + b^2y + c^2 \tag{17}$$

Here x, y = input variable vector,
where w_1 & w_2 firing strengths, that is the product of the membership. f = output function, first layer: output function of Node i(O_i^1):

$$O_i{}^1 = \mu_1 Z_i(x); i = 1, 2 \tag{18}$$

$$O_i^1 = \mu_1 U_i(x); i = 1, 2 \tag{19}$$

2nd layer: here each swelling is a round node marked by '*w*', which is the creation of the external signs and becomes output.

$$O_i^2 = w_i; i = 1, 2 \tag{20}$$

3rd layer: Here we solve the ratio of the *i*th rule of the discharge strength of the system.

$$O_i^3 = w_1; i = 1, 2 \tag{21}$$

4th layer: Here the solution of the *i*th rule towards the complete output takes place.

$$O_i^4 = w_{1i} f_i, i = 1, 2 \tag{22}$$

5th layer: Here the complete output is computed.

$$O_i^5 = \sum w_{1i} f_i, I = 1, 2 \tag{23}$$

In the area of modelling, the ANFIS technique was researched for working out an inaccurate and uncertain method. The benefits of ANFIS are an input-output mapping of human knowledge as well as quantified input-output sets of facts.

2.3 ANN Modelling

The ANN model is used to improve the solar drying system that gives the best economic benefits. ANN techniques are successfully applied in medicine, engineering, mathematical calculations, and economics. The ANN has features that compute difficult and intricate complications of growing non-linear variables.

2.3.1 Methodology of ANN Modelling

The ANN techniques of solar drying systems investigate the mean square of the inaccuracy amid investigational and numerical time-dependent temperatures of the drying product. The arithmetical standards of the mean total error, root mean square error, standard error, and coefficient of correlation, are given by applying of following Eqs. (24), (26) and (27):

$$\mathrm{MAE} = \frac{1}{\mathrm{N}} \sum_{n=1}^{N} \left| \overline{T_{c.\exp.n}} - \overline{T_{c.evl.n}} \right| \tag{24}$$

$$RMSE = \left[\frac{1}{N} \sum\nolimits_{n=1}^{N} \left(\overline{T_{c.\exp.n}} - \overline{T_{c.evl.n}} \right)^2 \right]^{1/2} \tag{25}$$

$$SE = \frac{\sqrt{\sum_{n=1}^{N} \left(T_{c.\exp.n} - T_{c.evl.n} \right)^2}}{N - 1} \tag{26}$$

$$R^2 = \sqrt{\frac{\sum_{n=1}^{N} \left(T_{c.\exp.n} - \overline{T_{c.evl.n}} \right)^2 - \sum_{n=1}^{N} \left(T_{c.\exp.n} - T_{c.evl.n} \right)^2}{\sum_{n=1}^{N} \left(T_{c.\exp.n} - \overline{T_{c.evl.n}} \right)^2}} \tag{27}$$

2.3.2 Simulation of ANN's Modelling

The artificial neural network of the solar dryer is formulated by the constituent of the ANN model. The function of activation is the combined weight of the neuron's input. Figure 3 defines the sigmoid role, which plays a very infrequent significant role in recycled transfer. The input arriving signals represented in Fig. 3 are multiplied by the connection weights. The subjective combinations of these inputs of neurons are generally used as a transfer function, which is an active function and also known as a sigmoid function (Agatonovic-Kustrin and Beresford 2000).

2.4 Fuzzy Modelling

This technique is used for solving the intricate system. These modelling techniques are fundamentally skilled in defining the complex process. Fuzzy modelling has been considerably persistent since the beginning of fuzzy habitation by Zadeh (Momenzadeh et al. 2012). The level of theory is improved in the ill-defined program according to this method. On the other hand, the authentic applied use

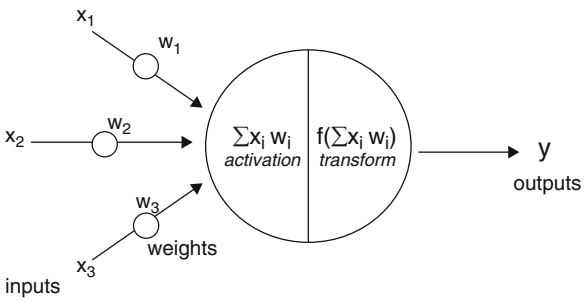

Fig. 3 Representation of an artificial neuron (Agatonovic-Kustrin and Beresford 2000)

of Fuzzy Modelling found about to continue in the direction of in such a technique to produce in the premature phase. For sampling, all the victorious commercial technical sector are executed by fuzzy logic.

2.4.1 Methodology of Fuzzy Modelling

The flow chart for fuzzy logic modelling is shown in Fig. 4. To detect the phage of nominal procedure, x = existence of certain specimens and can be completely shown by:

$$x^i = f(x, x'x'' \ldots\ldots\ldots), x^i \in R, i = [1, 2, \ldots\ldots\ldots n] \tag{28}$$

where, n = dependent variables, x^i

Here, x', x'' are the first and second-time by-products of the position vectors, respectively.

Consequently, this method fits well into fuzzy modelling and function f changed by a relation R at the moment, that is, characteristics of the fuzzy principle. This kind of sampling problem, which is non-realistic till which the extent of an only one specialist, otherwise a small classification of a dedicated. Thus, creating all codes and detectable patterns where an investigative view is lacking depends on human skill. The cooperation between insert system variables is small. That is expected to

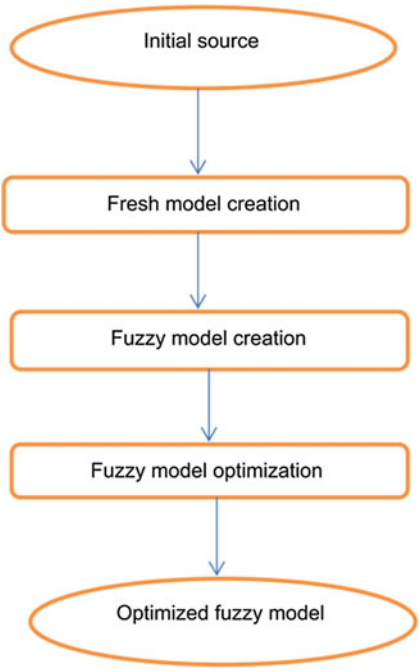

Fig. 4 Methodology of fuzzy modelling flow chart

characterize the overhead-indicated scheme, although numerous input and output systems take after a digit of distinct asymmetrical symbol Y ε X to a digit recognized on variables Z ε X via a sink of l fuzzy code as

$$Y_1^1 \cap Y_l^2 \cap \ldots\ldots\ldots\ldots\ldots \cap Y_l^n \rightarrow Z_l^{n+1} \cap \ldots\ldots\ldots\ldots\ldots \cap Z_l^m \tag{29}$$

Here $l = [1\ldots..n]$.

$$\bigcap_{k=m+1}^{n} \cap_{k=m+1}^{n} \left(Y_l^1 \cap Y_l^2 \cap \ldots\ldots\ldots\ldots\ldots \cap Y_l^m \rightarrow Z_l^k\right) \tag{30}$$

or several small preparations of the fuzzy law, beginning with

$$R = \cup_{l=1}^{l} \cap_{k=m+1}^{n} \left(\cap_{r=1}^{m} Y_l^r \rightarrow Z_l^k\right) \tag{31}$$

2.5 MATLAB Simulation

Wang et al. (2004) developed a thin layer of drying equations (TLDRY) with the help of MATLAB software, which represent the drying curves for selected grains. The reproduction of TLDRY can be numerically solved with MATLAB by including inputs, the category of grain, and temperature of the air, comparative moistness, main moistness, and speed of air. The graph for moisture ratio or a direct change in moisture content is shown in the form of output. In this program, an ending time (t_{end}) is also required to have the proper plotting span shown in the window. The reliable humidity ratio (MR) is set at 0.01 and aimed for this revision to discover the conclusion time t_{end} (Fig. 5).

I. For

$$MR = \exp(-kt) : t_{\text{end}} = \frac{-\log(MR)}{k} \tag{32}$$

II. For

$$MR = \exp\left(-kt^{\text{n}}\right) : t_{\text{end}} = \sqrt[n]{\frac{-\log(MR)}{k}} \tag{33}$$

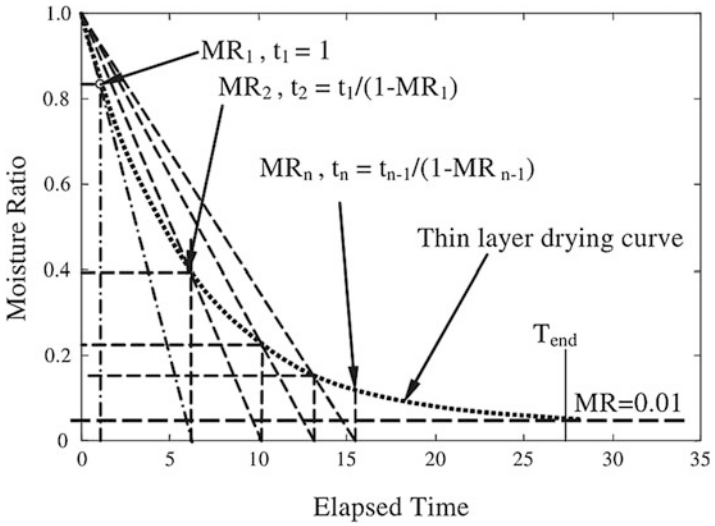

Fig. 5 Procedure for iteration to find ending time

III. For

$$MR = P_1 \exp\,(P_2 - kt) : t_{\text{end}} = \frac{-\log(MR + P_1 - l_1)}{P_2 k} \tag{34}$$

Ending time can be calculated by defining an initial time $t_1 = 1$ h, when the consistent moisture ratio $MR_1 = f(t_1)$ is calculated. For the computation of t_2, it is supposed that $t_2 = t_1/\,(1\text{-}MR_1)$ by means of matching the triangle law as shown in Fig. 6. Once the MR changes to k^{th} order, the ending time, $t_{\text{k+1}}$ will be given by:

$$t_{k+1} = \frac{t_k}{1 - MR_k} \tag{35}$$

With the application of the above-mentioned techniques, the solution converges quickly in the first half and slows down in the second half, as shown in the drying curve. The thin layer drying procedure, from initiation to conclusion time, can be accomplished by principal of a time collection knowledge as follows:

$t = 0$: increment: t_{end}

Consequently

$$t = [t1, t2, t3 \ldots t\text{end}]$$

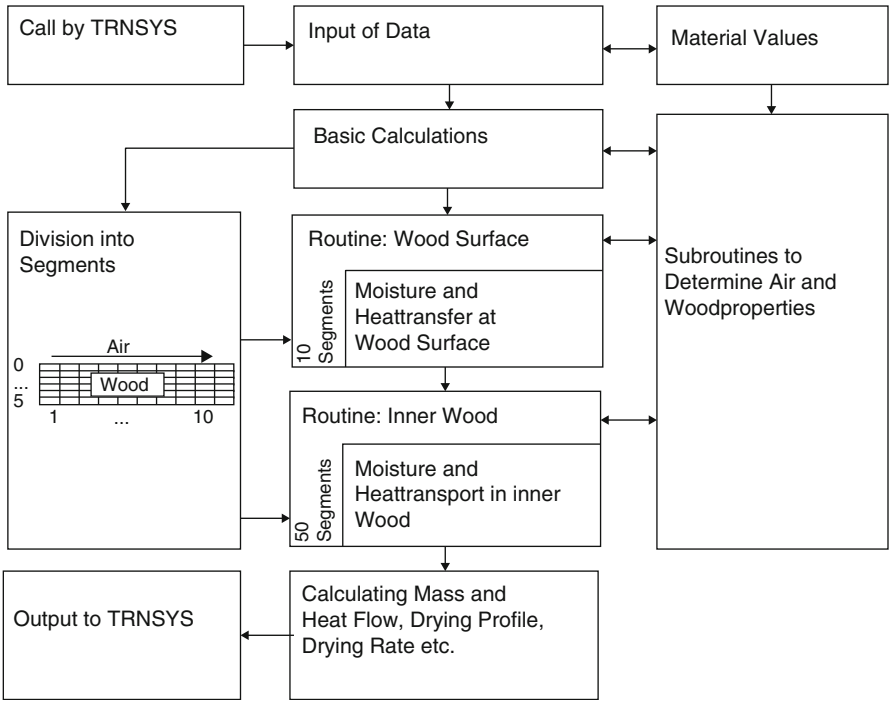

Fig. 6 *TRNSYS* module flow chart of "Wood Drying"

The moisture ratios can be expressed as follows for a given time:

$$\begin{aligned} MR &= \exp^{-kt^n} \\ &= \left[\exp^{-kt_1^n}, \exp^{-kt_2^n}, \ldots\ldots\ldots\ldots\ldots \exp^{-kt_{\text{end}}^n}\right] \\ &= [MR_1, MR_2, \ldots\ldots\ldots MR_{\text{end}}] \end{aligned} \tag{36}$$

2.6 TRNSYS Simulation

A *TRNSYS* program of timber drying was developed by Reuss et al. (1997). The *TRNSYS* "wood drying" module defines the dehydrating of timber through air, and Fig. 6 shows its flow chart. Moistness removal in drying occurs from the hard dehydrating substance to the flowing. The mass flow equation in the form of moisture transfer coefficient β gives the following relation:

$$m_A^{\bullet} = \frac{\beta}{RT}\left(p_{D,O} - p_{D,L}\right) \tag{37}$$

where $m_A^{\bullet}$ is the specific mass flow rate (kg.m^{-2} s^{-1}), β the moisture transfer coefficient (m.s^{-1}), R the gas constant (J.kg^{-1} K^{-1}), T the temperature of the drying surface (K), and $P_{D.O}$-$P_{D.L}$ is the vapor pressure difference between the air and the drying product surface (Pa). The moistness transfer in solids can be determined by Eq. (38), consequently, equivalent to Fick's Law:

$$\dot{m} = KQ_{G,t}|\nabla x| \tag{38}$$

K is the moistness transport constant (m^2 s^{-1}), $Q_{G,t}$ is the density of the dehydrated material (kgm^{-3}), and |∇x| is the moisture gradient in the material (kg kg^{-1} m^{-1}). The heat transfer relation applied aimed at all of these mechanisms, that is, convective heat transfer in liquid, heat conduction in solid body, and another for bound humidity:

$$\dot{Q} = \lambda A|\nabla T| \tag{39}$$

where $\dot{Q}$ is the heat flow, λ is heat conduction coefficient (Wm^{-1} K^{-1}), A is the area of heat flow (m^2), and |∇T| the temperature gradient in the material (K.m^{-1}).

2.7 Fortran

The concurrent partial differential equations describing heat and mass transfer during the dehydration of a product in the dryer can be modelled, and these non-linear partial differential equations can be solved using the finite difference method (FEM) in FORTRAN. FORTRAN is used to analyze solar dryers and can help reduce the capital cost of a solar drying system.

2.8 Statistical Package for the Social Sciences (SPSS)

This is an analytical tool for non-linear regression analysis. SPSS is used for fast and accurate analytical analysis such as coefficient of determination, root mean square error, and analysis of variance, reduced chi-square, etc. It is a predictive analytics software program using advanced techniques having easy-to-use user interface, and is mainly used for:

Statistical analysis and reporting: to address the entire analytical process, planning, data collection, analysis, reporting, and deployment.
Predictive modelling and data mining: to use powerful model-building, evaluation, and automation capabilities.
Decision management and deployment: analytics with advanced model management and analytic decision management.
Big data analytics: analyze big data to gain predictive insights.

3 Thermal Modeling

3.1 Concept and Working Process

Kumar and Tiwari (2006) carried out mathematical modelling of a natural convective greenhouse dryer for drying jaggery. The heat and mass balance equations of natural convective greenhouse dryers are shown in Fig. 7. The solar radiation converted into heat in the greenhouse inside the cover ($\sum I_i A_i \tau_i$) diminishes convective heat waste. The small amount of energy $(1 - F_n)F_{cr}(\sum I_i A_i \tau_i)$ will be collected partially by the crop and partially $(1 - F_n)(1 - F_{cr})(\sum I_i A_i \tau_i)$ through the surface and reveal tray zone and the rest of the solar radiation $(1 - F_n)(1 - F_{cr})(1 - \alpha_g)(\sum I_i A_i \tau_i)$ will heat the surrounding internal air surface of the greenhouse solar drying method.

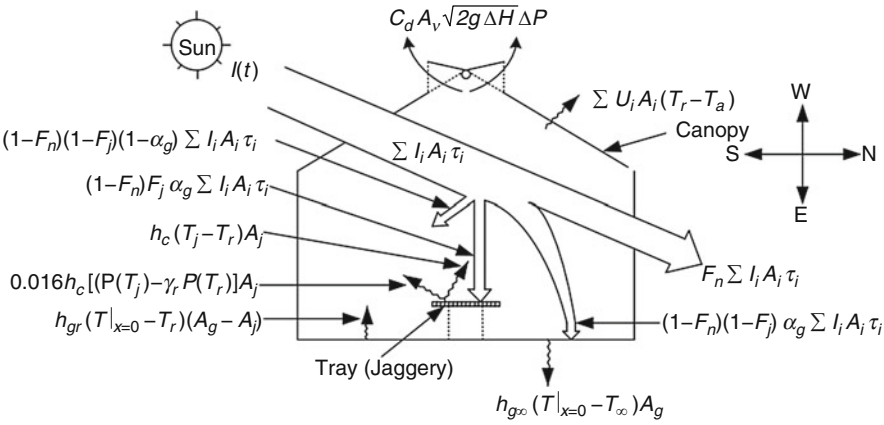

Fig. 7 Heat transfer for greenhouse dryer under natural convection

3.2 Energy Balance

Modelling heat and mass transfer were established for enhancing the effectiveness of the drying system and increasing the moisture vaporization rate by the application of energy equations. These equations are expressed with some hypotheses, as shown below:

(a) The heat absorber capacity and surface of the drying chamber were uniform.
(b) The heat transfer due to conduction convection and radiation from the tray and wall are ignored.
(c) The uniform flow is assumed inside the drying chamber.
(d) It is assumed that the collector has negligible heat waste.

1. *Energy balance equation at crop surface*:

$$\begin{aligned}&(1-F_n)F_{cr}\alpha_{cr}\sum I_iA_i\tau_i = M_cC_{cr}\frac{dT_{cr}}{dt} + h_c\left(T_{cr}-T_{ga}\right)A_{cr}\\&+0.016h_c\left[P(T_{cr})-\gamma_rP\left(T_{ga}\right)A_{cr}\right]\end{aligned} \tag{40}$$

2. *Energy balance equation at the floor of the greenhouse dryer*:

$$\begin{aligned}&(1-F_n)(1-F_{cr})\alpha_g\sum I_iA_i\tau_i = h_{g\infty}(T|y=0-T_\infty)A_g\\&+h_{gr}\left(T\middle|y=0-T_{ga}\right)\left(A_g-A_{cr}\right)\end{aligned} \tag{41}$$

3. *Equation of energy balances on a greenhouse cabin*

A coefficient of transmission and difference in vapor pressure applied to the temperature variance of greenhouse and ambient air:

$$\begin{aligned}&(1-F_n)(1-F_{cr})\left(1-\alpha_g\right)\sum I_iA_i\tau_i + h_c\left(T_{cr}-T_{ga}\right)A_{cr}\\&+0.016h_c\left[P(T_{cr})-\gamma_rP\left(T_{ga}\right)\right]A_{cr}T + h_{gr}\left(T|y=0-T_{ga}\right)\left(A_g-A_{cr}\right)\\&= C_dA_v\sqrt{2g\Delta H}\times\Delta P + \sum U_iA_i\left(T_{ga}-T_a\right)\end{aligned} \tag{42}$$

The expression of $C_dA_v\sqrt{2g\Delta H}\times\Delta P$ exposed the rapidity of heat excess by the natural cavity. The C_d is an observational loss and its implication is shown in Table 2.

$$\Delta H = \frac{\Delta P}{\rho_{ga}g} \tag{43}$$

$$\Delta P = P\left(T_{ga}\right) - \gamma_aP(T_a) \tag{44}$$

Table 2 Constants that are used in greenhouse modelling and design

Parameters	Values
A_t	0.096 m^2
C_a	1012 J/kg °C
C_j	2509.9 J/kg °C
C_d	0.0036
F_c	0.1
g	9.81 m/s^2
h_{gr}	8.0 W/m^2 °C
R_1	397.52
R_2	−7926.90
t	3600 s
γ	2.26×10^6 J/kg
σ	5.67×10^8 W/m^2 K^4
α_g	0.6
α_c	0.7
ε	0.9
τ	0.9

3.3 Thermal Model Solution

The vapor pressure is linearized as the minimum range of temperature between 26° C and 54° C for solving the above-mentioned equations, which mainly occur during solar drying, while.

$$P\,(T) = K_1 + K_2 \tag{45}$$

The linear regression analysis had been used to compute the pressure of vapor at T_r and T_a. With the help of Eq. (41), (43), (44) and (45), Eq. (42) has been simplified in the form of a third order polynomial equation to define solar dryer air temperature (T_r) for initial values of ambient and jaggery temperature as

$$AT_r{}^3 + BT_r^2 + CT_r + D = 0 \tag{46}$$

where

$$A = \left(\frac{2}{\rho_r}\right)(C_d A_v)^2 K_1^3 \tag{47}$$

$$\begin{aligned} B = {} & \left(\frac{2}{\rho_{ga}}\right)(C_d A_v)^2 K_1^2 [K_2 - \gamma_a (K_1 T_{am} + K_2)] \\ & - \left[h_c A_{cr} + 0.016 h_c A_{cr} \gamma_{ga} K_1 + (UA)_{g\infty} \sum U_i A_i\right]^2 \end{aligned} \tag{48}$$

$$
\begin{aligned}
C = &\left(\frac{2}{\rho_{ga}}\right)(C_d A_v)^2 3K_1[K_2 - \gamma_a(K_1 T_a + K_2)]^2 \\
&-2\left[h_c A_{cr} + 0.016 h_c A_{cr}\gamma_{ga} K_1\right. \\
&\left.+(UA)_{g\infty}\sum U_i A_i\right]^2 \\
&\times\left[\begin{array}{l} I_{effR} + I_{effG} H_G + T_{cr}(h_c A_{cr} + 0.016 h_c A_{cr} K_1) + T_a (UA)_{g\infty} \\ +\sum U_i A_i + 0.0167 h_c A_{cr} K_2\left(1 - \gamma_{ga}\right) \end{array}\right]
\end{aligned} \tag{49}
$$

$$
\begin{aligned}
D = &\left(\frac{2}{\rho_{ga}}\right)(C_d A_v)^2 [K_2 - \gamma_a(K_1 T_a + K_2)]^3 \\
&-\left[\begin{array}{l} I_{effR} + I_{effG} H_G + T_{cr}(h_c A_{cr} + 0.016 h_c A_{cr} K_1) + T_a (UA)_{g\infty} \\ +\sum U_i A_i + 0.0167 h_c A_{cr} K_2\left(1 - \gamma_{ga}\right) \end{array}\right]
\end{aligned} \tag{50}
$$

Applying the familiar value of in Eq. (46), the temperature (T_{cr}) of drying material may be achieved by the first-order differential equation

$$\frac{dT_j}{dt} a T_{cr} = f(t) \tag{51}$$

For the solution of Eq. (41) for the mean $\overline{f(t)}$ for 0-1, the time is

$$T_{cr} = \frac{\overline{f(t)}}{a}(1 - e^{-at}) + T_{cro} e^{-at} \tag{52}$$

Here

$$a = \frac{h_{cr} A_{cr}(1 + 0.016 K_1)}{M_{cr} C_{cr}} \tag{53}$$

and

$$f(t) = \frac{I_{effcr} + h_c A_{cr}\left[T_{ga} - 0.016\left\{K_2 + \gamma_{ga}\left(K_1 T_{ga} + K_2\right\}\right\}\right]}{M_{cr} C_{cr}} \tag{54}$$

The moistness vaporization can be given as follows:

$$m_{ev} = 0.016\frac{h_c}{k}\left[(K_1 T_{cr} + K_2) - \gamma_{ga}\left(K_1 T_{ga} + K_2\right)\right] A_{cr} t \tag{55}$$

4 Conclusions

The various authors and researchers use a number of numerical techniques for the performance evaluation of solar dryers, such as computational fluid dynamics, Adaptive-Network-based Fuzzy Inference System (ANFIS), ANN modelling, FUZZY logic, MATLAB Simulation, TRNSYS Simulation, FORTRAN, and SPSS, etc., which can be used for the numerical study of the different solar dryers for performance evaluation at load and no load conditions. The CFD study predicts the velocity field and temperature inside the solar dryer. The above-described techniques are supportive of the performance evaluation and regression analysis of the dryer. The methods described in this chapter have also been applied to finding an explanation for the intricate problem and solving the heat, mass, and moisture transfer problems in the solar drying system.

References

Agatonovic-Kustrin S, Beresford R (2000) Basic concepts of artificial neural network (ANN) modeling and its application in pharmaceutical research. J Pharm Biomed Anal 22:717–727. doi:10.1016/S0731-7085(99)00272-1

Ait Mohamed L, Ethmane Kane CS, Kouhila M, Jamali A, Mahrouz M, Kechaou N (2008) Thin layer modelling of gelidium sesquipedale solar drying process. Energy Convers Manag 49:940–946. doi:10.1016/j.enconman.2007.10.023

Akpinar EK, Bicer Y (2007) Modelling of thin layer drying kinetics of sour cherry in a solar dryer and under open sun. J Sci Ind Res 66:764–771. doi:10.1016/j.enconman.2008.01.004.

Augustus Leon M, Kumar S, Bhattacharya S (2002) A comprehensive procedure for performance evaluation of solar food dryers. Renew Sust Energ Rev 6:367–393. doi:10.1016/S1364-0321(02)00005-9

Bagheri N (2015) Development and evaluation of an adaptive neuro fuzzy interface model to predict performance of a solar dryer. Agric Eng Int CIGR J 17:112–121

Defraeye T (2014) Advanced computational modelling for drying processes – a review. Appl Energy 131:323–344. doi:10.1016/j.apenergy.2014.06.027

Dymond C, Kutscher C (1997) Development of a flow distribution and design model for transpired solar collectors. Sol Energy 60:291–300. doi:10.1016/S0038-092X(96)00157-0

Esakkimuthu S, Hassabou AH, Palaniappan C, Spinnler M, Blumenberg J, Velraj R (2013) Experimental investigation on phase change material based thermal storage system for solar air heating applications. Sol Energy 88:144–153. doi:10.1016/j.solener.2012.11.006

Esper A, Mühlbauer W (1998) Solar drying – an effective means of food preservation. Renew Energy 15:95–100. doi:10.1016/S0960-1481(98)00143-8

Hossain MA, Woods JL, Bala BK (2005) Optimisation of solar tunnel drier for drying of chilli without color loss. Renew Energy 30:729–742. doi:10.1016/j.renene.2004.01.005

Kant K, Shukla A, Sharma A, Kumar A, Jain A (2016) Thermal energy storage based solar drying systems: a review. Innovative Food Sci Emerg Technol 34:86–99. doi:10.1016/j.ifset.2016.01.007

Khan M, Ali M, Fudholi A, Sulaiman J, Ruslan MH, Yasir S (2014) Sauna technique, drying kinetic modeling and effectiveness on solar drying compared with direct drying in drying process of Kappaphycus striatum in Selakan Island, Malaysia. Energy Power Eng 6:303–315

Kumar A, Tiwari GN (2006) Thermal modeling of a natural convection greenhouse drying system for jaggery: an experimental validation. Sol Energy 80:1135–1144. doi:10.1016/j.solener.2005.09.011

Kumar A, Singh R, Prakash O (2014) Ashutosh. Review on global solar drying status. Agric Eng Int: CIGR J 16(4):161–177

Mahapatra AK, Imre L (1990) Role of solar agricultural-drying in developing countries. Int. J. Ambient Energy 11:205–210. doi:10.1080/01430750.1990.9675175

Momenzadeh L, Zomorodian A, Mowla D (2012) Applying artificial neural network for drying time prediction of green pea in a microwave assisted fluidized bed dryer. J Agric Sci Technol 14:513–522

Pardhi CB, Bhagoria JL (2013) Development and performance evaluation of mixed-mode solar dryer with forced convection. Int J Energy Environ Eng 4:23. doi:10.1186/2251-6832-4-23

Prakash O, Kumar A (2013) Historical review and recent trends in solar drying systems. Int J Green Energy 10:690–738. doi:10.1080/15435075.2012.727113

Prakash O, Laguri V, Pandey A, Kumar A, Kumar A (2016) Review on various modelling techniques for the solar dryers. Renew Sust Energ Rev 62:396–417. doi:10.1016/j.rser.2016.04.028

Reuss M, Benkert ST, Aeberhard A, Martina P, Raush G, Rentzell BV et al. (1997) Modelling and experimental investigation of a pilot plant for solar wood drying. Sol Energy 59:259 270. doi:10.1016/S0038-092X(97)00013-3

Sharma VK, Colangelo A, Spagna G (1995) Experimental investigation of different solar dryers suitable for fruit and vegetable drying. Renew Energy 6:413–424. doi:10.1016/0960-1481(94)00075-H

Singh Chauhan P, Kumar A, Tekasakul P (2015) Applications of software in solar drying systems: a review. Renew Sust Energ Rev 51:1326–1337. doi:10.1016/j.rser.2015.07.025

Sodha MS, Chandra R (1994) Solar drying systems and their testing procedures: a review. Energy Convers Manag 35:219–267. doi:10.1016/0196-8904(94)90004-3

Sonthikun S, Chairat P, Fardsin K, Kirirat P, Kumar A, Tekasakul P (2016) Computational fluid dynamic analysis of innovative design of solar-biomass hybrid dryer: an experimental validation. Renew Energy 92:185–191. doi:10.1016/j.renene.2016.01.095

Sreekumar A, Manikantan PE, Vijayakumar KP (2008) Performance of indirect solar cabinet dryer. Energy Convers Manag 49:1388–1395. doi:10.1016/j.enconman.2008.01.005

Tekasakul P, Dejchanchaiwong R, Tirawanichakul Y, Tirawanichakul S (2015) Three-dimensional numerical modeling of heat and moisture transfer in natural rubber sheet drying process. Dry Technol 33:1124–1137. doi:10.1080/07373937.2015.1014910

Wahidi R, Rohani AA (1996) The benefits of solar dryers in Iran. Renew Energy 9:700–702. doi:10.1016/0960-1481(96)88381-9

Wang D-C, Fon D-S, Fang W, Sokhansanj S (2004) Development of a visual method to test the range of applicability of thin layer drying equations using MATLAB tools. Dry Technol 22:1921–1948. doi:10.1081/DRT-200032878

Zhiqiang Y (2005) Development of solar thermal systems in China. Sol Energy Mater Sol Cells 86:427–442. doi:10.1016/j.solmat.2004.07.012

Simulation of Food Solar Drying

Inês N. Ramos, Teresa R.S. Brandão, and Cristina L.M. Silva

Abstract This chapter discusses the simulation process of food solar drying, presenting the basic issues of mass and heat transfer under time-varying conditions. Food drying embraces several phenomena, and scientists do not completely understand its underlying mechanisms. However, mathematical simulation and modelling provide comprehensions to improve the knowledge on the drying mechanisms, allow the prediction of the drying behaviour as well as being essential tools in the design of solar drying equipment. The major difficulty in simulating food solar drying arises from variable meteorological conditions that change air temperature, moisture and velocity inside the solar equipment, during the drying process. Therefore, an integrated mass and heat transfer model under dynamic conditions is presented, and appropriate assumptions are discussed. A meteorological model and desorption isotherms are taken into consideration as well. The integrated model includes food's shrinkage, changing boundary conditions and variable thermal properties and water diffusivity with time and space (non-isotropic characteristics).

Keywords Solar drying • Heat transfer • Mass transfer • Simulation • Modelling

1 Introduction

Exposing food products to the action of the sun is probably the oldest method of food preservation practised by human civilisation. Removing water from the food product decreases microbial and enzymatic activities that originate quality decline and sometimes even product spoilage. Some early archaeological findings refer to far back as the Middle Bronze Age (twenty-first to seventeenth centuries BCE) with dry and salted fish in ancient Egypt (Raban-Gerstel et al. 2008). With the Industrial Age, easier access to equipment and energy and new food drying technologies were developed, like spray drying, drum drying, fluidised bed drying, freeze-drying, etc.

I.N. Ramos (✉) • T.R.S. Brandão • C.L.M. Silva
CBQF- Centro de Biotecnologia e Química Fina, Escola Superior de Biotecnologia, Centro Regional do Porto da Universidade Católica Portuguesa, Rua Arquiteto Lobão Vital, Apartado 2511, 4202-401 Porto, Portugal
e-mail: iramos@porto.ucp.pt

© Springer Nature Singapore Pte Ltd. 2017

O. Prakash, A. Kumar (eds.), *Solar Drying Technology*, Green Energy and Technology, DOI 10.1007/978-981-10-3833-4_13

Presently, the demand for added-value dried products continues, but most of all environmental concerns in the society drive the development of eco-friendly and sustainable drying methods to produce minimal ecological and climate impact. Therefore, the improvement of solar drying techniques will play a role in a humanitarian and environmentally responsible society.

In solar drying, the temperature of the drying chamber is increased by using different methods to capture the solar energy (Fuller 1993). It is more hygienic than sun-drying (foods are exposed on the floor), since products are sheltered from rain, dust, insects and rodents. It also reduces drying time, preventing products spoilage by moulds due to the faster decrease of water activity. When compared to other drying techniques associated to sophisticated equipment, solar drying is relatively cheap, having smaller initial investment but requiring higher labour costs.

Considering the design of drying equipment, numerical simulation techniques are very useful, as they allow to minimise the investment of time, products and labour. Numerical simulation builds upon mathematical equations and appropriate boundary conditions, in order to generate a model which describes the drying process. Therefore, appropriate models are extremely important, and their approach may be mechanistic or empirical. For an appropriate decision on the approach, a careful evaluation on benefits and drawbacks should be performed, also considering the main aim and availability of 'engineering parameters'. Empirical approaches are simpler and many times properly suitable for concrete purposes like the dryer's technical plan (Mulet 1994). On the other hand, mechanistic models are more complex and require more computational effort but originate more accurate predictions. The borderline between mechanistic and empirical models is often not well defined, since mechanisms are themselves based on experimental observations (Mulet 1994). For an exhaustive and detailed review on thin-layer drying models of foods, please refer to Kucuk et al. (2014). Most solar drying processes fall into the category of 'thin-layer drying', being this term used in opposition to deep-bed drying.

The fundamental drying mechanisms of foods are not easily perceived and not yet completely understood. Inside the product, various mechanisms of mass transfer were listed in a literature review on solids' drying (Waananen et al. 1993): liquid diffusion, vapour diffusion, surface diffusion, hydrodynamic or bulk flow and capillary flow. These mechanisms may occur simultaneously and modify their process percentage along drying.

A very useful tool in identifying drying mechanisms is the well-known 'characteristic drying curve', which is an experimental plot that depicts the drying rate as a function of water content. This plot allows distinguishing the different drying periods, being the most informative regarding the drying process. The drying phases may be separated into constant-rate period and falling-rate period. Regarding food air-drying, the most common observation is a small constant-rate period and a longer falling-rate period (Mazza and Le Maguer 1980; Yusheng and Poulsen 1988; Mulet 1994; Madamba et al. 1996), until low values of equilibrium water content are reached. This observation may be attributed to the high density and low porosity of foods that originate slow drying, and molecular diffusion of the water

within the material is one of the main mechanisms (Mulet 1994). Therefore, many research works refer to Fick's second law to model the falling-rate period, and Fickian models are the most widely applied in food drying.

The extra effort in simulating solar drying when compared to other drying processes is due to the great variability on meteorological conditions along the whole process, changing with the month of the year, hour of the day and weather conditions. This variability modifies air temperature, humidity and velocity inside the solar dryer and typically produces a cyclic behaviour during the day. In a covered solar dryer, the incident radiation produces a greenhouse effect. It is the dryer's translucency that allows solar radiation to enter and be transmitted to the products inside, heating them. However, the heat emitted by the foods is not allowed to leave the dryer due to its extended wavelengths, increasing the dryer and food's temperature along the day.

An important aspect of foods' solar drying is shrinkage, although most of the mathematical models applied to solar drying until the 1980s ignored this important modification of product's characteristics (Ratti and Mujumdar 1997). Since then, methodologies have been upgraded in order to include shrinkage, meteorological aspects and time- and space-varying mass and heat transfer properties. Some works have made significant contribution to one of these aspects, although not integrating all of them simultaneously (Youcef-Ali et al. 2001; Bennamoun and Belhamri 2006; Phoungchandang and Woods 2000).

The main objectives of this chapter are:

1. To present the appropriate assumptions on heat and mass transfer mechanisms in a solar dryer
2. To describe mass and heat transfer equations for products inside a solar dryer and a meteorological model
3. To review existing literature for moisture diffusivity equations of fruits, vegetables and cereals submitted to drying
4. To incorporate in an integrated numerical model the previous equations plus product's shrinkage, variable mass diffusivity, variable thermal properties and boundary conditions
5. To validate the integrated model with a case study on grape drying in a mixed-mode solar dryer

2 Modelling Assumptions

The modelling of solar drying processes must take into account both heat and mass transfer phenomena, simultaneously. The water transfer mechanism inside the solar dryer may be diffusional and convective, in the case of an existing fan. The heat transfer mechanism involves simultaneously convection, evaporation and radiation.

Some heat and mass transfer mechanisms may be considered negligible when compared to others and therefore not accounted in the heat and mass balance equations. The criteria to make these assumptions are based on the analysis of the

values of dimensionless numbers. For instance, to assess the relation between the resistance to heat transfer inside the product and at its surface, the Biot number (Bi) is used (Ramos et al. 2015) (Eq. 1). This dimensionless number expresses the proportion between the resistance to heat conduction presented by the solid interior and the resistance to heat convection existing in the exterior fluid.

$$\mathrm{Bi} = \frac{\bar{\mathrm{h}}\,\mathrm{V}/\mathrm{A_s}}{\mathrm{Kp}} \tag{1}$$

It is assumed that when the Bi number is less than 0.1, the effect of the internal impedance to heat transfer may be ignored, and consequently the material temperature is supposed to be uniform in the entire food. An average product temperature is used in the models.

The same kind of logic may be applied to analyse the relation between internal and external resistance to mass transfer. The Biot number of mass transfer ($\mathrm{Bi_m}$ – Eq. 2) expresses the relation between internal resistance to diffusion and the external resistance to convection (Ramos et al. 2015).

$$\mathrm{Bi_m} = \frac{h_D V/A_s}{D} \tag{2}$$

When the calculated value of the $\mathrm{Bi_m}$ is smaller than 0.1, the internal resistance to mass transfer can be ignored, and the water content inside the product can be considered uniform. On the other hand, when $\mathrm{Bi_m}$ is higher than 10, the resistance to convection in the fluid is negligible, and therefore the air moisture around the food (inside the solar dryer) is supposed to be homogeneous. In this case, the average air moisture is used in the models. As referred before, in the mass transfer process inside the food product during the course of drying, diffusion is presumed to be the control mechanism.

3 Mass Transfer Model

In a situation where we have diffusion-controlled drying, the Fick's second law may be applied. When dealing with spherical foods, the inner water content (X) at a given radial position (r) and time (t) can be calculated by Eq. 3 (Ramos et al. 2015).

$$\frac{\partial X_{r,t}}{\partial t} = \frac{1}{r^2}\frac{\partial}{\partial r}\left(Dr^2\frac{\partial X}{\partial r}\right) \tag{3}$$

For simplification purposes, water diffusivity may be considered independent of temperature (T) and water content. This is the most common approach in food drying modelling. Alternatively, for a more accurate numerical simulation, a water diffusivity equation may be integrated in the mass transfer models. A survey on

Table 1 Overview on models expressing water diffusivity dependence on temperature and water content, for fruits, vegetables and cereals

Model references			Food/Drying method
$D = a(-\mathrm{b} + \mathrm{cX} - \mathrm{dX}^2)\exp(\mathrm{eT})$	(4)	Jayas et al. (1991)	Wheat
			Thin layer
$D = \exp\left(a + \frac{b}{T} + cX\right)$	(5)	Mulet et al. (1989)	Carrot
			Convective
$D = a\exp\left(-\frac{b}{T}\right)\exp\left(-\frac{c}{X}\right)$	(6)	Maroulis et al. (1995)	Potato
			Convective
$D = a\exp\left[-\frac{b}{RgT}\left(\frac{c+\frac{1}{X}}{d+\frac{T_d - T}{X_0}}\right)\right]$	(7)	Kechaou and Maâlej (2000)	Date
			Convective
$D = \exp(a + bX + cX^2)$	(8)	Vázquez et al. (2000)	Grape
			Convective
$D = a\exp\left(-\frac{b}{RgT}\right)\exp(-cT - dX)$	(9)	Azzouz et al. (2002)	Grape
			Convective
$D = a + bX + cX^2 + dX^3$	(10)	Sharma and Prasad (2004)	Garlic cloves
			Microwave+convective
$\mathrm{D} = \mathrm{D}_0\exp\left[a\frac{X}{X_0} - b\left(\frac{X}{X_0}\right)^2 - c\left(\frac{1}{T}\frac{1}{T_{av}}\right)\right]$	(11)	Ramos et al. (2010)	Grapes
			Convective

existing literature for moisture diffusivity equations regarding fruits, vegetables and cereals submitted to drying processes is presented in Table 1, listing the drying method and food product used.

When solving Fick's second law, appropriate initial and boundary conditions must be selected. In a drying process, the boundary conditions are linked with the equilibrium water content – X_e. Water content at the product's surface is usually assumed in equilibrium with the air and is dependent on air humidity and temperature. When air conditions are time varying, X_e is changing as well. Therefore, it is very important to determine X_e, which may be achieved using equations of moisture sorption isotherms, the curve representing the relationship between water activity and the water content of the product. These plots are very useful in dehydration processes, especially the desorption isotherm. There are numerous equations that mathematically represent these curves, being the most widely applied equations the following: Langmuir, Brunauer–Emmett–Teller (BET), modified Oswin, modified Halsey, modified Henderson, Chung–Pfost, Ferro–Fontan, Guggenheim–Anderson–de Boer (GAB), Peleg, Timmermann–GAB, Viollaz–GAB and Lewicki (Basu et al. 2006). The GAB model (Eq. 12) is the most popular since the 1980s, and it was more recently recommended based on statistical criteria, for fitting water sorption data in the extensive review of food isotherms by Basu et al. (2006).

$$\frac{Xe}{Xm} = \frac{CKa_w}{(1 - Ka_w)(1 - Ka_w + CKa_w)} \tag{12}$$

4 Heat Transfer and Meteorological Model

The overall energy balance to a product exposed to solar drying can be expressed in Eq. 13 (Phoungchandang and Woods 2000).

$$\frac{d(mCpT)}{dt} = \alpha A_p I(t) - \bar{h} A_s (T - T_a) - \frac{d(\lambda m_w)}{dt} - A_s \varepsilon \sigma F \left(T^4 - T_a{}^4\right) \tag{13}$$

This equation includes, on its right member, four terms that correspond to the absorbed radiant energy and the heat lost by convection, evaporation and radiation, whose sum is equal to the energy added to the drying food (left member).

I(t) is the radiation flux density at a specific day time and depends on meteorological conditions. The sampling time of radiation flux density should be as small as possible, or otherwise it may be reduced through suitable meteorological models. For instance, Charles-Edwards and Acock (1977) created a model that generates values of radiation flux density from global radiation values, considering the diurnal changes of radiation (Eq. 14). This equation is a complete sine wave, and the original purpose of its authors was to mathematically define diurnal variation in photosynthetically active radiation.

$$I(t_d) = \begin{cases} \dfrac{J_N}{g_N}\left\{1 + \cos\left[\dfrac{2\pi}{g_N}(t_d - 0.5)\right]\right\}; & 0.5 - \dfrac{1}{2}g_N \le t_d \le 0.5 + \dfrac{1}{2}g_N \\ 0; & \text{otherwise} \end{cases} \tag{14}$$

J_N represents the global radiation corresponding to day N; g_N represents the day length, varying between zero and one; and t_d represents the time normalisation of one day period, i.e. $t_d = \frac{t(h)}{24}\,(0 < t_d < 1)$. Midnight corresponds to $t_d = 0$.

In order to calculate the day length (g_N – Eq. 15), it is necessary to determine two other meteorological parameters, the solar declination (δ – Eq. 16) and the year angle (y – Eq. 17).

$$g_N = \frac{2\arccos(-\tan\phi \tan\delta)}{2\pi} \tag{15}$$

$$\begin{aligned} \delta = \; & 0.38092 - 0.76996\cos(y) + 23.26500\sin(y) \\ & +0.36958\cos(2y) + 0.10868\sin(2y) + 0.01834\cos(3y) \\ & -0.16650\sin(3y) - 0.00392\cos(4y) + 0.00072\sin(4y) \\ & -0.00051\cos(5y) + 0.00250\sin(5y) + 0.00442\cos(6y) \end{aligned} \tag{16}$$

$$y = \left(\frac{N\text{-}21}{365}\right)2\pi \tag{17}$$

In Eq. 17, N symbolises the climatological day number (the first day of May corresponds to $N = 1$), and ϕ is the latitude of the location of the solar dryer.

5 Integrated Numerical Methodology

Most partial differential equations do not have an analytical solution, and therefore discretisation methods are needed (sometimes using a numerical grid), aiming at its transformation into a system of algebraic equations. Using a computer program, these equations are solved and originate values on time and space dimensions. Numerical techniques in solar drying developed from simpler and faster approaches, such as finite differences, finite elements and finite volumes, to more complex and time-consuming methodologies, such as computational fluid dynamics (CFD) softwares, artificial neural network, fuzzy modelling, etc.

The methodology presented below applies to drying of spherical products in a mixed-mode or hybrid cabinet dryer. The forward explicit finite differences method was chosen to numerically solve Fick's second law applied to a spherical material (Eq. 3) and the energy balance equation (Eq. 13). If time and space derivatives of both equations are discretised, Eqs. 18 and 20 are, respectively, obtained.

$$X_i^{t+1} = X_i^t\left(1 - 2\frac{\Delta t D_i^t}{\Delta r^2}\right) + X_{i+1}^t\left(\frac{\Delta t D_i^t}{\Delta r^2} + \frac{\Delta t F_i^t}{2\Delta r}\right) + X_{i-1}^t\left(\frac{\Delta t D_i^t}{\Delta r^2} - \frac{\Delta t F_i^t}{2\Delta r}\right) \quad (18)$$

$$\text{being } F_i^t = \frac{1}{{r_i}^2}\,\frac{D_{i+1}^t\, r_{i+1}^2 - D_{i-1}^t\, r_{i-1}^2}{2\Delta r} \quad (19)$$

$$T_{t+1} = T_t + \left[\alpha A_p(X_t) I(t) - \bar{h} A_s(X_t)(T_t - Ta) - \frac{\lambda(X_t - X_{t+1}) m_0}{\Delta t(1 + X_0)} - A_s(X_t)\varepsilon\sigma F\left({T_t}^4 - Ta^4\right)\right] \times \frac{(1 + X_0)\Delta t}{C p m_0 (1 + X_t)} \quad (20)$$

The space domain has to be divided into a given number of nodal points. F in Eqs. 13 and 20 is a geometry factor and is usually considered equivalent to 1, when dealing with small bodies inside large areas (Ramos et al. 2015).

The following initial and boundary conditions were applied: (i) uniformity (isotropicity) of the water content in the whole product for the initial drying time, (ii) 'water content at the surface of the product always in equilibrium with the surrounding air' (Ramos et al. 2010) and is stable over time and (iii) a symmetric condition for the water content at the food's centre, indicating there is no water flow in this point.

(i) $t = 0, \quad 0 \le r \le R \quad X = X_0$
(ii) $t \ge 0, \quad r = R(t) \quad X_R = Xe(t)$
(iii) $t \ge 0, \quad r = 0 \quad \frac{\partial X}{\partial t} = 0$

This was a moving boundaries process, with changes in external dimensions of the product (R) due to shrinkage along drying, and modifications in the values of equilibrium moisture content (Xe), for being subjected to changing air conditions (Ramos et al. 2010).

The flowchart presented in Fig. 1 is a proposed integrated methodology for the numerical simulation of solar drying curves of food (Ramos et al. 2015). This methodology takes shrinkage of the product into account, including modifications on its surficial area and projected area.

It also considers some anisotropic characteristics of the food, modifications in effective moisture diffusivity with water content and temperature and changes in thermal properties of grapes.

The first input data on the flowchart are initial X_0 and R_0 values of the food, shrinkage coefficients regarding the radius, the equilibrium coefficients for the GAB model, water diffusivity coefficients (D_0, a, b, c), number of nodes, number of time steps and time interval (presented in Table 2). Air conditions (temperature and relative humidity) and radiation flux density are introduced in the flowchart as well. The next command is an external loop executed for every drying time step. The first calculation is the equilibrium water content and then an internal loop to determine the position of the nodes in the product and the corresponding particular water content at every node, with changing water diffusivity. The next step is the output of the average water content determined by integration with the trapezoidal rule and the corresponding new food radius at each drying time. The last input is the heat transfer coefficients, shrinkage parameters of A_s and A_p and their initial values and initial total mass. And finally, the convective heat loss (Qc), the evaporative heat loss (Qe), the radiation heat loss (Qr) and the specific heat are calculated. The last output is the determined food temperature.

6 Case Study

This case study was conducted in a field solar drier located in the northern region of Portugal (Mirandela), using grapes as raw material. Solar dryers may be classified into direct, indirect, mixed mode or hybrid, according to Fuller (1993). This dryer classifies as a mixed-mode or hybrid cabinet dryer and includes 'a collector for preheating the air, a drying chamber and a solar chimney' (Ramos et al. 2015). Two exhaust air fans are included on the back wall, and it has a continuous 30 cm opening for air admission. The dryer collector faces south, as is usual in the Northern Hemisphere, in order to take full advantage of solar radiation and makes an angle of 38°, being identical to the local latitude (ϕ) of 41.28 °N.

Red seedless grapes from the cultivar *Monukka* were used. Whole grape clusters were reduced to smaller portions and blanched in hot water for around 15 s. Around 5 kg of blanched grapes were placed in each wood tray of the solar dryer, totalling an initial load of approximately 250 kg. Samples were collected from different locations on the dryer, and drying was performed until reaching a constant weight.

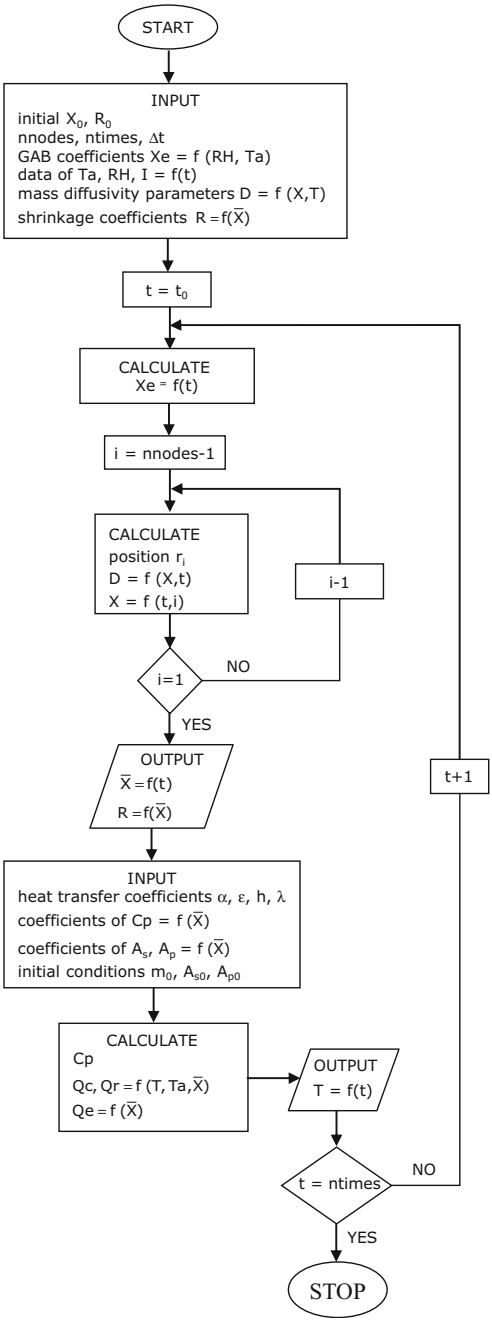

Fig. 1 Flowchart of the integrated simulation

Table 2 Coefficients and equations used in the simulation

Mass diffusivity parameters (Ramos et al. 2010) (Eq. 11)
$D_0 = 5\ \text{x}10^{-12}\ \text{m}^2\ \text{s}^{-1}$
$\text{a} = 15$
$b = 25$
$c = 2200\ \text{K}$
$T_{\text{av}} = 303.15\ \text{K}$
Heat transfer parameters
$\bar{h} = 1.263\ \text{W m}^{-2}\ ^{\circ}\text{C}$
$\lambda = 2419\ \text{kJ kg}^{-1}$
$\varepsilon = 0.73$
$\alpha = 0.823$
$Cp = 1.3767 - 3.181 \times 10^{-3}\text{T} + 2.9293\text{W(kJkg}^{-1}\text{K}^{-1})$
$Kp = -0.022 + 1.924 \times 10^{-3}\text{T} + 0.587\text{W(W m}^{-1}\ ^{\circ}\text{C}^{-1})$
Shrinkage equations (Ramos et al. 2010)
$R = R_0\left(0.3654\frac{\bar{X}}{X_0} + 0.6288\right)$
$A_p = A_{p0}\left(0.6314\frac{\bar{X}}{X_0} + 0.3521\right)$
$A_s = A_{s0}\left(0.5627\frac{\bar{X}}{X_0} + 0.4054\right)$
$R_0 = 0.75 \pm 0.07\ \text{cm}$
$A_{\text{p0}} = 1.01\ \text{m}^2$
$A_{\text{s0}} = 2.16\ \text{m}^2$
GAB coefficients for muscatel raisins (Vázquez et al. 1999)
$C = C_0\exp\left(\frac{H_1 - H_m}{RgT}\right) \quad K = K_0\exp\left(\frac{H_1 - H_q}{RgT}\right)$
$X\text{m}=0.119$
$C_0 = 0.107$
$(H_1 - H_{\text{m}})/\text{Rg} = 561.66$
$K_{\text{o}} = 0.911$
$(H_1 - H_{\text{q}})/\text{Rg} = 9.07$

Air temperature and relative humidity inside the dryer were recorded every 15 min. As expected, the air temperature increased from dawn until sunset, in the range 12–42 °C, and relative humidity in the range 8–86%. Air velocity was determined in the initial and final rows of the solar dryer twice a day, and values varied between 9 and 34 cm s^{-1}. Meteorological data from the region (daily values of global radiation, J_{N}) were collected from the Portuguese meteorological institute. They were later transformed to hourly data of radiation flux density $I(t_D)$ for each drying day, using the Charles-Edwards and Acock model (Eq. 14) and included as input data in the integrated numerical simulation. These data (Fig. 2) present a daily variation with a sinusoidal pattern, which corresponds to day rise of air temperature and night decline and respective opposite, decline and rise of air relative humidity.

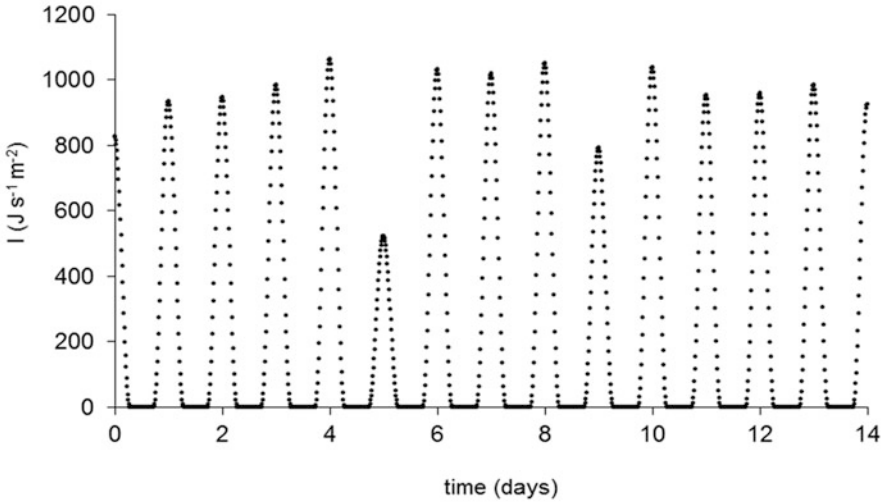

Fig. 2 Radiation flux density calculated with Charles-Edwards and Acock equations

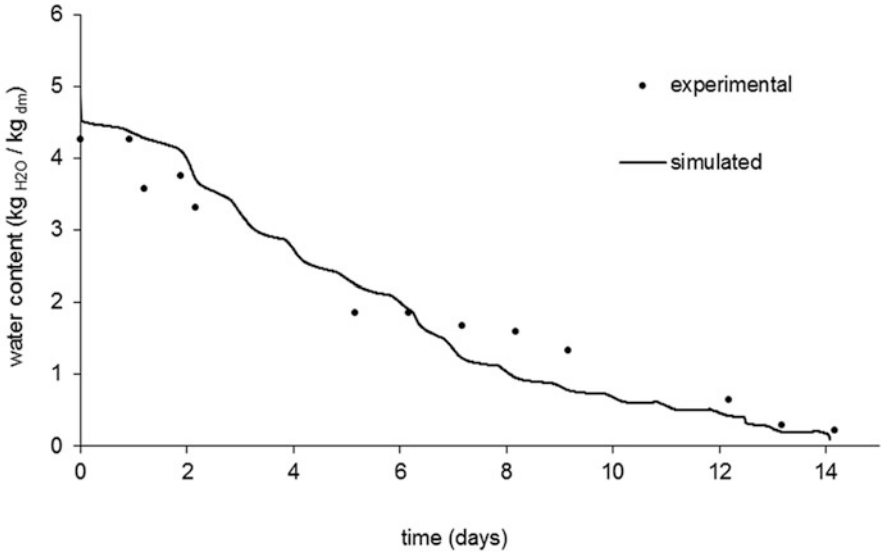

Fig. 3 Simulated drying curve (*continuous line*) and experimental data from the mixed-mode solar dryer (●)

The integrated simulation methodology allowed the estimation of drying curves. A typical example is presented in Fig. 3, as well as a set of experimental data acquired in the mixed-mode solar dryer.

Good estimations of the experimental curves were attained, considering the small number of experimental data and the high variability on their values. Steps are observed in the simulation values, which are linked to the sinusoidal cyclic pattern of day and night meteorological conditions.

Table 2 presents coefficients and equations used in the numerical simulation: water diffusivity of grapes and heat transfer parameters, shrinkage equations and equilibrium GAB coefficients. A previous study on grape convective drying at pilot scale (Ramos et al. 2010) provided the estimations range for the input of the parameters of the diffusivity model (D_0, a, b, c). The best adjust to experimental data corresponded to deviations of input values from original estimated values of 70, 4, 8 and 65%, respectively, for D_0, a, b and c parameters. These values fall within acceptable confidence intervals of the estimates.

7 Conclusions and Recommendations

Mathematical simulation and modelling are crucial to predict the drying behaviour and to design the solar drying equipment and are valuable tools to improve the knowledge on the fundamental mechanisms of drying. Numerical simulation also allows to calculate drying times and subsequently optimising drying loads and planning the production of dried foods.

The simulation methodology presented in this chapter considers a dynamic process, integrating heat and mass transfer, food's shrinkage during drying, changing thermal properties and water diffusivity along drying and within the product, variable boundary conditions and sorption isotherms. This methodology may be coupled with the heat transfer model of the whole solar dryer, obtaining a complete simulation that originates directly from meteorological data. It may be applied to simulate solar drying of other innumerable foods, besides grapes, assuming the availability of their specific characteristics.

Furthermore, the integrated model can also be enlarged to a three-dimensional model, taking into account irregular shape (like wrinkles) and anisotropic shrinkage, having all space variables varying with time. The simulation can be carried out with other diffusivity and thermal properties equations that consider water content and temperature effects.

Integrative dynamic simulations that take simultaneously into account anisotropic transient characteristics and different mass and heat transfer mechanisms should lead the way to progress on describing the drying process. The last years' improvement of knowledge on other drying scales, like microscopic, should permit taking the path into more precise and accurate simulations.

Acknowledgements Inês N. Ramos and Teresa R. S. Brandão gratefully acknowledge Fundação para a Ciência e a Tecnologia (FCT) and European Social Fund (ESF) for the financial support through the postdoctoral grants SFRH/BPD/75430/2010 and SFRH/BPD/101179/2014,

respectively. This work was also supported by national funds from FCT through project UID/Multi/50016/2013.

Nomenclature

a, b, c, d, e	Model parameters
a_w	Water activity
A_p	Projected area of the product (m^2)
A_s	Surface area of the product (m^2)
Bi	Biot number
Bi_m	Biot number for mass transfer
C	Guggenheim constant
C_0, K_0	Pre-exponential factors of C and K of GAB model on Table 2
Cp	Specific heat of the product (kJ kg^{-1} K^{-1})
D	Moisture diffusivity (m^2 s^{-1})
D_0	Pre-exponential parameter of moisture diffusivity (m^2 s^{-1})
F	Geometry factor
g_N	Day length
$\bar{h}$	Average convective heat transfer coefficient (J s^{-1} m^{-2} K^{-1})
h_D	Convective mass transfer coefficient (m s^{-1})
H_1, H_m, H_q	Parameters of C and K of GAB model on Table 2
i	Node
I	Radiation flux density (J s^{-1} m^{-2})
J_N	Global radiation in the N^{th} day (J m^{-2})
K	Factor that corrects properties of the multilayer molecules with respect to the bulk liquid
Kp	Thermal conductivity of the product (W m^{-1} $°C^{-1}$)
m	Total mass of the product (kg)
m_w	Mass of evaporated water (kg)
N	Climatological day number
Qc	Convective heat loss (J s^{-1})
Qe	Evaporative heat loss (J s^{-1})
Qr	Radiation heat loss (J s^{-1})
r	Radial position
R	Average equivalent radius (m)
Rg	Universal gas constant (8.314 J mol^{-1} K^{-1})
t	Time (s or min)
t_d	Fractional part of a day time
T	Product temperature (K)
T_a	Air temperature (K)
V	Volume (m^3)
$\bar{X}$	Average water content on dry basis (kg_{water} $kg_{dry\ matter}{}^{-1}$)
X	Water content on dry basis (kg_{water} $kg_{dry\ matter}{}^{-1}$)
Xe	Equilibrium water content on dry basis (kg_{water} $kg_{dry\ matter}{}^{-1}$)
Xm	Monolayer water content (kg_{water} $kg_{dry\ matter}{}^{-1}$)
y	Year angle

Greek Symbols

α Absorptivity of solar radiation
δ Solar declination
Δt Time interval (s)
Δr Space interval (m)
ε Emissivity
λ Latent heat of vaporisation (J kg^{-1})
ϕ Latitude (°)
σ Stefan–Boltzmann constant (5.6704×10^{-8} W m^{-2} K^{-4})

Subscripts

0 Initial Value
av Average value
r At radius r
t At time t

References

Azzouz S, Guizani A, Jomaa W, Belghith A (2002) Moisture diffusivity and drying kinetic equation of convective drying of grapes. J Food Eng 55:323–330
Basu S, Shivhare US, Mujumdar AS (2006) Models for sorption isotherms for foods: a review. Dry Technol 24:917–930
Bennamoun L, Belhamri A (2006) Numerical simulation of drying under variable external conditions: Application to solar drying of seedless grapes. J Food Eng 76(2):179–187
Charles-Edwards DA, Acock B (1977) Growth response of a chrysanthemum crop to the environment. II. A mathematical analysis relating photosynthesis and growth. Ann Bot:41–49
Fuller RJ (1993) Solar drying of horticultural produce: Present practice and future prospects. Postharvest News Inform 4(5):131N–136N
Kechaou N, Maâlej M (2000) A simplified model for determination of moisture diffusivity of date from experimental drying curves. Drying Tech 18(4,5):1109–1125
Kucuk H, Midilli A, Kilic A, Dincer I (2014) A review on thin-layer drying-curve equations. Dry Technol 32(7):757–773
Madamba PS, Driscoll RH, Buckle KA (1996) The thin layer drying characteristics of garlic slices. J Food Eng 29:75–97
Maroulis ZB, Kiranoudis CT, Marinos-Kouris D (1995) Heat and mass transfer modeling in air drying of foods. J Food Eng 26:113–130
Mazza G, Le Maguer M (1980) Dehydration of onion: some theoretical and practical considerations. J Food Technol 15:181–194
Mulet A, Berna A, Rosselló C (1989) Drying of carrots. I. Drying models. Dry Technol 7 (3):537–557
Mulet A (1994) Drying modelling and water diffusivity in carrots and potatoes. J Food Eng 22:329–348

Jayas DS, Cenkowski S, Pabis S, Muir WE (1991) Review of thin-layer drying and wetting equations. Dry Technol 9(3):551–588
Phoungchandang S, Woods JL (2000) Solar drying of bananas: mathematical model, laboratory simulation, and field data compared. J Food Sci 65(6):990–996
Raban-Gerstel N, Zohar I, Bar-Oz G, Sharon I, Gilboa A (2008) Early Iron Age Dor (Israel): A Faunal Perspective. B Am Sch Oriental Re 349:25–59
Ramos IN, Miranda JMR, Brandão TRS, Silva CLM (2010) Estimation of water diffusivity parameters on grape dynamic drying. J Food Eng 97(4):519–525
Ramos IN, Brandão TRS, Silva CLM (2015) Simulation of solar drying of grapes using an integrated heat and mass transfer model. Renew Energy 81:896–902
Ratti C, Mujumdar AS (1997) Solar drying of foods: modeling and numerical simulation. Sol Energy 60(3,4):151–157
Sharma GP, Prasad S (2004) Effective moisture diffusivity of garlic cloves undergoing microwave-convective drying. J Food Eng 65(4):609–617
Vázquez G, Chenlo F, Moreira R, Carballo L (1999) Desorption isotherms of muscatel and aledo grapes, and the influence of pretreatments on muscatel isotherms. J Food Eng 39(4):409–414
Vázquez G, Chenlo F, Moreira R, Costoyas A (2000) Effects of various treatments on the drying kinetics of Muscatel grapes. Dry Technol 18(9):2131–2144
Waananen KM, Litchfield JB, Okos MR (1993) Classification of drying models for porous solids. Dry Technol 11(1):1–40
Youcef-Ali S, Messaoudi H, Desmons JY, Abene A, Le Ray M (2001) Determination of the average coefficient of internal moisture transfer during the drying of a thin bed of potato slices. J Food Eng 48(2):95–91
Yusheng Z, Poulsen KP (1988) Diffusion in potato drying. J Food Eng 7:249–262

Applications of Soft Computing in Solar Drying Systems

Om Prakash, Saurabh Ranjan, Anil Kumar, and P.P. Tripathy

Abstract In the present scenario, the use of renewable energy is gaining more importance due to environmental degradation and limited energy resources of fossil fuel. However, solar energy is noncontinual, but it is eco-friendly, which is freely available throughout the world. In terms of energy and food security, the solar dryer is vital for reduction of postharvest food losses and electric energy consumption. The drying process of crop involves a complex analysis of heat and mass transfer parameters. In order to address this complex phenomenon, soft computing is important to analyse the drying models which in turn are useful to assess the dryer performance. It is also very helpful in predicting the crop temperature, rate of moisture evaporation, drying efficiency and dried product quality. For prediction of surrounding air temperature and quantity of evaporated moisture, the mathematical models are generated with the help of MATLAB and FORTRAN which are proved to be highly reliable in such scenario. COMSOL Multiphysics, TRNSYS, MATLAB, FORTRAN, CFD Fluent, etc. are employed for model testing and training purposes. Statistical software such as SPSS, Statistica, etc. are very useful tool for statistical data analysis. This chapter comprises different types of software and their application in designing and usage in solar dryers. This comprehensive and extensive analysis of different software will be very useful to the research community, academicians and solar dryer designers.

O. Prakash
Department of Mechanical Engineering, Birla Institute of Technology, Ranchi, India

S. Ranjan
Department of Mechanical Engineering, Birla Institute of Technology, Ranchi, India

Centre for Energy Engineering, Central University of Jharkhand, Ranchi, India

A. Kumar (✉)
Department of Energy (Energy Centre), Maulana Azad National Institute of Technology, Bhopal 462003, Madhya Pradesh, India
e-mail: anilkumar76@gmail.com

P.P. Tripathy
Department of Agricultural & Food Engineering, Indian Institute of Technology, Kharagpur, West Bengal, India

© Springer Nature Singapore Pte Ltd. 2017

O. Prakash, A. Kumar (eds.), *Solar Drying Technology*, Green Energy and Technology, DOI 10.1007/978-981-10-3833-4_14

Keywords Soft computing • Solar drying systems • Drying models • Crop temperature • MATLAB • FORTRAN • Moisture evaporation • SPSS

1 Introduction

The importance of solar energy has been growing vigorously in order to sustain development and combat energy scarcity especially in remote areas, and it is a result of global leader concerned regarding climate change and the eternal depletion of fossil fuels. Energy generation from fossil fuel is quite responsible for greenhouse gas emissions that cause environmental degradation that tends to global warming (Lotfalian et al. 2010). In an attempt to reduce harmful gas emission from the combustion of fossil fuel, the use of renewable energy is necessary, and it helps the nation to become a global leader under different environmental laws and protocols. Solar insolation provides sufficient energy in 1 min to suffice the energy requirement of the world for a year; worldwide demand is only 0.01% of the energy introduced by the sun. The total solar insolation on earth in 3 days is equivalent to stored energy of all fossil fuels. Solar energy has enough potential for fulfilment of energy demand of any country (Prakash and Kumar 2014a).

Solar drying is essential for a reduction in food losses related to postharvest conditions which include spoilage, infection by pathogens, rodent invasion and lack of modern storage house. Solar drying involves the process of moisture removal from a body by supplying heat to the body from heat sources and transferring mass as moisture which is entailed in the body to its surface. Thereafter, the transferred moisture is sailed out in the surrounding air (Prakash and Kumar 2013a). Solar dryer is used in drying applications and its demand is rising in chemical and food industries. Solar dryer is broadly classified into three categories, i.e., direct, indirect and mixed mode drying.

The direct solar dryer uses direct visible solar radiation for drying, so its construction and design are uncomplicated. Their working and upkeep are not tedious. Indirect solar dryer consists of many components such as air collector, solar radiation collector, auxiliary heater, a fan facilitating air circulation and cabinet drying chamber. Its working principle is to heat atmospheric air with the help of collector and then flow hot air through the cabin. The mixed solar dryer is an amalgamation of direct and indirect solar dryer. This system encompasses the drying of product entailed by atmospheric hot air and then passed via storage cabin (Prakash et al. 2016). Software application in solar drying system is vital for the development and analysis of mathematical models. Besides this, simulation software helps in the prediction of crop's moisture temperature, the rate of desiccation, drying kinetics and quality of crops. It is also applied for analysis and prediction of various solar drying systems' performance (Chauhan et al. 2015).

The software-based approach is essential for building and examining the mathematical models and anticipates the potential of various solar drying systems (Prakash and Kumar 2014a). Solar dryer's working is enhanced by incorporating

soft computing which also reduces the time spent in experimentation process. It can also be used for predicting the crop temperature, moisture to be evaporated, drying speed and efficiency and colour of the resulting dried sample. CFD can also be utilized in airflow study, airflow rate in the dryer, temperature distribution and variation in humidity (Chen et al. 2008). MATLAB is used for creating mathematical models to detect the variations in crop temperature, heat content in supplied air and exist moisture to be removed and also used for analysing thermal performance of solar dryer (Kumar and Tiwari 2006). SPSS, SigmaPlot V, etc. are used for statistically analysing the solar drying systems, whereas SigmaPlot V employs data filling purpose (Tripathy 2015). TRNSYS software is used for modelling of drying system which gives results in observation of drying condition (Reuss et al. 1997). This chapter presents a complete review of the application of various available software for analysis and assessment of different drying parameters for solar drying systems.

2 What Is Soft Computing

Soft computing is quite different from conventional computing; unlike complicated computing, this is forbearing of approximation and guessed values. The main principle involved in soft computing is tolerance exploitation for uncertainty, unreliability, and approximated values to achieve stability and less working cost.

The principal ingredients of soft computing (SC) are fuzzy logic (FL), machine learning (ML), probabilistic reasoning (PR), neural computing (NC) and evolutionary computation (EC). Soft computing is a partnership in which every member provides a unique method for conquering the problems faced by the user in the respective field of interest.

2.1 Importance of Soft Computing

There is a dedicated and supportive nature of EC, PR and FL and also NC which has a valuable effect; in various cases, it causes a problem which can be interpreted by appealing to FL, NC, EC and PR altogether unlike dealing with them singularly. A stunning illustration of a divine combined system is referred as “neuro-fuzzy systems”. These systems are gaining immense popularity visible as a consumer product having a good range of air conditioners and dishwashers to printing machines and cameras. Neuro-fuzzy systems have also a great deal of workload in various industrial usages. Considering both user-based ideals and industrial needs for such systems, the application of SCs has led to an environment which possesses brilliant “machine intelligence quotient (MIQ)”.

3 Solar Drying

Solar drying is an achievable substituent for sun drying. Sun drying is challenging with an approach that is enormously established in the life of many potential users. Sun drying faced various problems due to possible contamination of the sample, uncertainty in drying period and harm caused due to rain and other environmental barriers (Kumar and Tiwari 2006).

However, even the solar dryers are not fail proof; there are multiple reasons which can account for the lack of triumph of solar drying over sun dryers which are as follows:

- Solar dryers are too costly and require a large initial investment.
- In case of fluctuation in solar insolation, solar dryers are complicated for the technician.
- Solar dryers are not suitable for long-term goals.

Advantages of solar drying can be summarized as follows:

- Desirable temperature, humidty and air flow of drying air results in an increment of the drying rate.
- Food being enclosed in the drying unit is well protected from dust, birds, insects and other herbivores.
- The higher temperature disinfects a unit of any bacteria, and the faster drying rate compensates the risk of any harm caused by microbes.
- The dryers are totally waterproof, and the food does not get affected by sudden rains and doesn't need dislocation at times of rains.
- Solar dryers can be constructed from natively available substances and are relatively cheap to set up.
- More comprehensive drying allows better storage results (Amjad et al. 2015).

4 Soft Computing Methodologies for Different Solar Dryers

Solar dryer system can be classified broadly into four types, namely, direct, indirect, mixed mode and hybrid type depending on the heat transfer mode inside the drying chamber. Different simulation methods are applied in these dryers.

4.1 Direct Solar Dryer

Direct solar dryer utilizes direct visible solar radiation for drying. The design and working of such dryer are simple and easy to maintain. It can be used for the bulk

Fig. 1 Direct solar dryer (Prakash et al. 2016)

level drying and OPEM is not tedious. Cabinet dryer, greenhouse dryer and tray and tent dryers are the examples of the direct solar dryer. It can be operated either in the forced convection mode or natural convection mode. The cabinet solar dryer under natural convection mode is being shown in Fig. 1.

Various soft computing techniques applied to direct solar drying of foodstuffs are discussed below:

4.1.1 Computational Fluid Dynamic (CFD) Simulation

Mathioulakis et al. (1998) designed an industrial tray solar dryer for drying of fruits. CFD Fluent software is applied for understanding the air movement in drying chamber. In the working of this system, three boundary conditions were assumed by CFD modelling technique (Mathioulakis et al. 1998). According to the first condition, drying chamber inlet serves as inflow boundary condition comprising fixed mass. The second one has no resistance boundary condition, whereas air mass was permitted to exit the domain at the outlet window. The third condition entails the presumption of a shear stress condition in the wall which was made in the bounded domain of surfaces. The occurrence of variation in dryness state of different trays was recorded. Here the upgrading of drying process which accompanies the measurement of air velocity in the drying section of the dryer is performed by CFD Fluent. From the simulation results, it is concluded that there is a fine relation among drying rate and inside velocity of air. CFD Fluent served as an enhancing tool for solar drying optimization process. Bartzanas et al. (2004) used CFD Fluent v5.3 software to do the performance analysis of the solar greenhouse dryer. The Fluent software was utilized for exactly locating vents for air circulation inside the dryer. Air circulation rate and framework pattern of airflow were determined by tracing glass technique and three-dimensional sonic anemometer, respectively.

4.1.2 MATLAB Simulation

Various authors have used the MATLAB simulation methodology in the performance analysis of the solar dryer. Wang et al. (2004) have used TLDRY software (MATLAB based) for thin surfaced drying operation for the Newton's model for greenhouse dryer. For determining the efficiency and moisture evaporated from the crop, a specialized MATLAB-based programme is designed by Kumar and Tiwari (2006). This MATLAB-based programme was validated with experimental observations. Prakash and Kumar (2014b) have applied the adaptive neuron-fuzzy inference system (ANFIS) modelling technique for predicting various important drying parameters such as crop weight during drying, crop temperature and inside room temperature for the jaggery drying in greenhouse dryer under natural convection mode. ANFIS model is being developed in the MATLAB software. The model was able to predict with a high level of accuracy, and it was justified with various statistical parameters such as correlation of regressions, root mean square (RMS) error and coefficient of determinations. The block diagram of ANFIS working model is shown in Fig. 2.

In Fig. 3, input vector is [x, y]. The firing strengths $w1$ and $w2$ were usually taken from the product of membership grade in the prescribed parts. The ratio of each firing strength to a total of all firing strength was $E1$ and $E2$. The output "f" was average weighted of each rule.

The RMS of percentage error for jaggery and air temperature of greenhouse ranges from 0.7 to 1%. In the case of thermal modelling, the RMS of percentage error for jaggery and greenhouse air temperature ranged between 4.47% and 7.7%. Results produced by ANFIS model are more accurate than the results obtained from the thermal model.

4.1.3 FORTRAN

Mahapatra et al. (1994) have developed FORTRAN programme to analyse different drying processes. It was used to do modelling of heat flow for direct solar drying

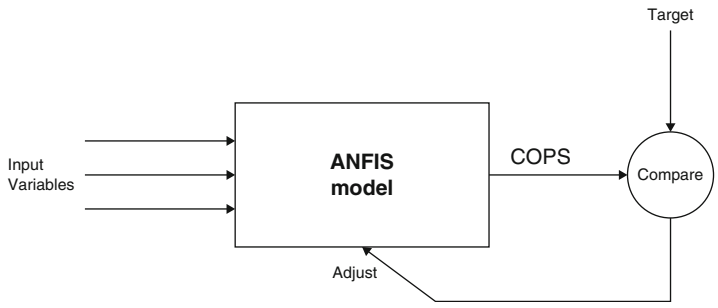

Fig. 2 ANFIS working model (Prakash and Kumar 2014a)

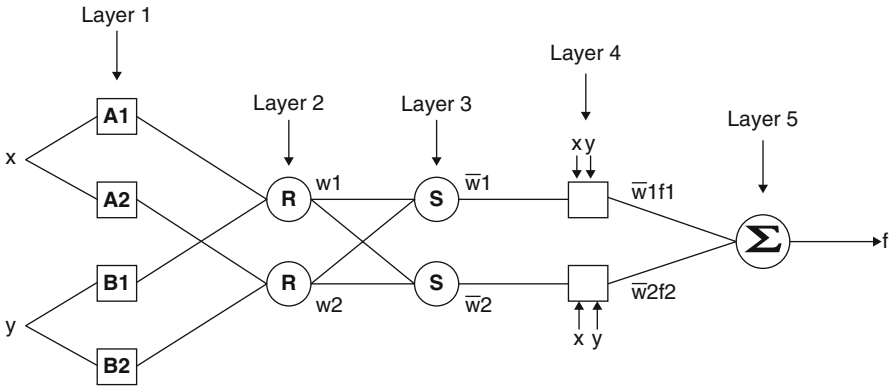

Fig. 3 First-order surgeon fuzzy inference system (Prakash and Kumar 2014a)

system. It incorporates the heat and mass transfer equations for the inside air circulation of the dryer.

4.1.4 TRNSYS Simulation

TRNSYS is widely applied in diverse solar energy-related implementations. Reuss et al. (1997) used TRNSYS software to make a model for wooden drying system. It was used to predict the natural exhaust air flow in the chimney. The parameter of surrounding conditions for the dryer was considered as system's input parameters. The modelling and coefficient of moisture transfer are being developed and evaluated for different types of wood. The output quantities consist of the temperature of the wood sample and its various heat transfer coefficient values. Awadalla et al. (2004) used TRNSYS software for solar wood drying system at WRI Munich, Germany. Figure 4 shows the flow chart of processes involved in the proper functioning of the "TRNSYS module of wood drying". There were 56 segment calculation processes employed for analysing the heating process. The time difference was taken as 15 seconds. The aim of upgrading solar dryer unit was to achieve a higher efficiency consisting better quality of dried wooden sample. This solar wooden sample heating procedure was governed theoretically under ambient conditions. This model was verified by employing the TRNSYS software in wood modelling comprising experimental values of wood drying (Awadalla et al. 2004).

4.2 Indirect Dryer

The indirect solar drying system consists of a dark painted surface capable of heat absorption, which transfers heat in the form of circulated air. This circulated air is

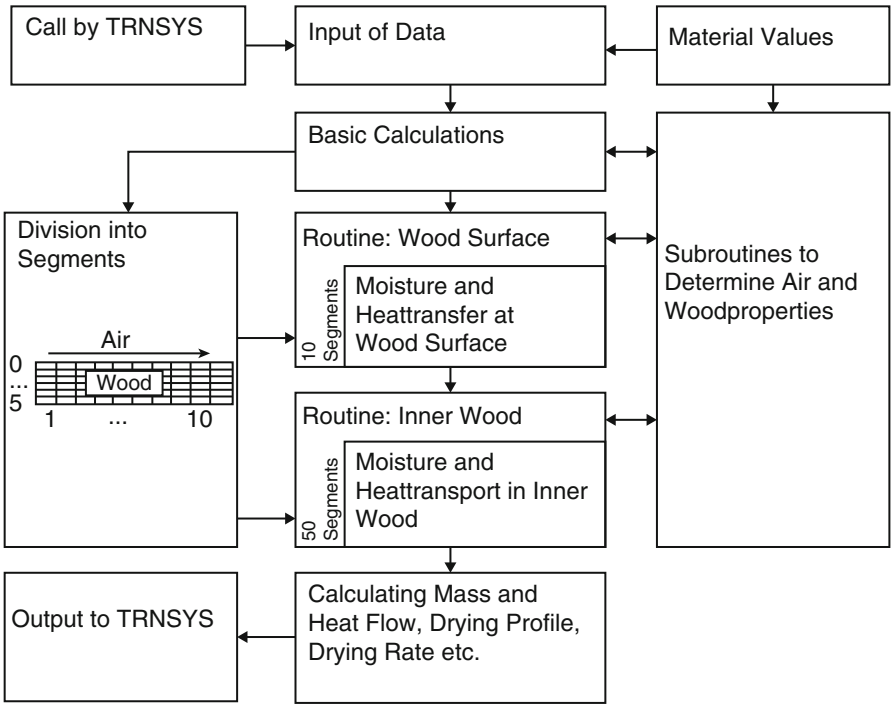

Fig. 4 Flow chart shows the working of the "TRNSYS module" applied in the drying of wooden samples (Awadalla et al. 2004)

then heated and passed through crop sample, absorbing the moisture present in it, and evacuates through the chimney (Prakash et al. 2016). Diagram of such dryer is described in Fig. 5.

4.2.1 CFD Simulation

Romero et al. (2014) developed and enhanced an indirect solar drying module having 50 kg vanilla drying capacity. They applied ANSYS-Fluent setup for working analysis and verification. The temperature variation analysis for such solar dryer was made by the help of CFD in which inputs were the temperature at inlet and outlet of the cabin. The following methods and steps were applied in solving the physical occurrence by using ANSYS-Fluent system:

Step 1: Designing the control volume structure in ANSYS modelling system.
Step 2: Parametric features of an applicable construction material and system boundary condition are mandated for individual system element.
Step 3: In the specific time period, equation's solution is used in individual mesh chamber.

Fig. 5 Indirect solar dryer (Prakash et al. 2016)

Step 4: Results are obtained in the form of graphical plots.

A huge deal of similarity was found against CFD simulation and measured value of solar collector, although in cabinet chamber, some variations were spotted in temperature difference. This variation occurs due to approximation based on the heat transfer coefficient (Romero et al. 2014).

4.2.2 COMSOL Multiphysics Simulation

Experimental analysis of indirect solar dryer is conducted by Vintila et al. (2014). This experiment was comprised of operation that was processed with COMSOL-based multiphysics. In COMSOL-based multiphysics, CFD code was employed in condensed two-dimensional model. There are two elements consisting of COMSOL physics setting, i.e. subdomain setting and boundary condition. Factors like types of material and various heat transfer schemes like convection and conduction are considered in subdomain configuration. The geometry of boundary conditions is considered as boundary condition setting (Vintila et al. 2014).

4.3 Mixed Mode Solar Dryer

In the mixed mode solar dryer, both direct and indirect ways of heating of inside air concept are being applied. This dryer takes advantage of both direct solar dryer and indirect solar dryer. The drying rate of this dryer is higher than other types of the dryer. This dryer is also operated either based on active mode or passive mode of drying. The schematic diagram of a mixed mode-type solar drying system is shown in Fig. 6.

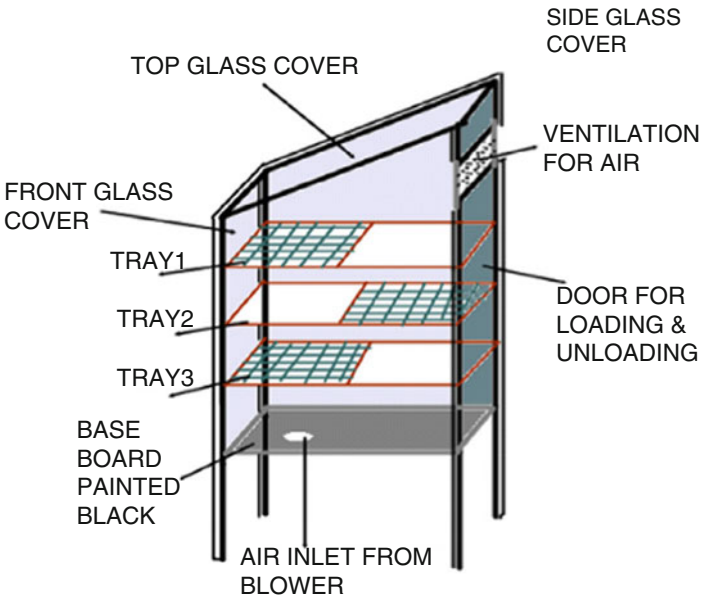

Fig. 6 Mixed mode solar dryer (Pardhi and Bhagoria 2013)

4.3.1 FORTRAN

Simate (2001) implemented FORTRAN programmes to create a mathematical tool applied in pure ventilated solar drying system for drying of grains. The experiments took place under an artificial solar simulator. This brought a good relation between practical and theoretical results. Bennamoun and Belhamri (2003) did the mathematical modelling by using FORTRAN. FORTRAN programme was developed for solving the partial differential equation of energy balance between air collector and drying section of the dryer.

4.3.2 MATLAB Simulation

Jain (2007) used MATLAB 6.1 software to figure out the equation of energy balance in onion drying. Reversed absorber system consists of condensed bed storage compromising the natural circulation of solar food drying mechanism, it was prepared to give the solution of energy balance equation for the various constituents of a solar dryer and also used to predict the quality of the supplied air in the drying chamber, absorber plate's temperature and sustained samples placed in both tray A and tray B.

4.3.3 Statistica

Midilli and Kucuk (2003) created the mathematical models of thin layer drying system in a mixed mode solar drying system. Statistica computer application was implemented for non-linear regression examination of various mathematical representations. The inference made by such application implies that the logarithmic model was best and convenient to explain the working of the mixed mode solar dryer.

4.4 Hybrid Solar Dryer

The hybrid solar dryer incorporates the usage of both conventional and solar energy which maintains internal drying condition as shown in Fig. 7 (Chauhan et al. 2015). Hence, solar energy is not singly utilized for drying operation; therefore, it can be used round the clock. Blower was used in this solar dryer for facilitating air movement inside the drying system. Solar photovoltaic cell converts photon into DC electric energy that supplies power to run the blower (Pardhi and Bhagoria 2013).

4.4.1 Computational Fluid Dynamics (CFD Simulation)

Rigit and Patrick (2010) used CFD simulation to analyse the temperature variation and moisture difference rate in the solar drying unit under unforced and forced

Fig. 7 Hybrid solar dryer (Chauhan et al. 2015)

circulation mode. STARK-CD was developed for the temperature changes and velocity patterns inside the drying unit. It approaches for drying application of "pepper fruits". CFD was helpful to examine the distribution of heat energy inside drying chamber. This helps in the modelling of unforced circulation mode of drying. Figure 8 illustrates the velocity distribution variation pattern for unforced circulation phenomenon. The ultimately high air velocity in the experiment was found to be 0.2338 m/s approximately in the vicinity of chimney outlet. This was the result of differential pressure. Accurate modelling results were obtained by this simulation software.

Figure 9 illustrates the temperature distribution pattern through contour plot inside the middle section of the solar dryer. The highest heat-absorbing region lies at the centre of the chimney, i.e. 366.6 K. The lowest heat-absorbing region lies at the nearest position of the inlet of the collector, i.e. 291.2 K. The drying chamber temperature varies between 340.9 and 352 K (Fig. 9). It gives clear temperature profile which is preferred in crop selection for drying.

Figures 10 and 11 demonstrate the movement of air and temperature variation from ingate of the silicon-based collector to the heated chamber used for drying

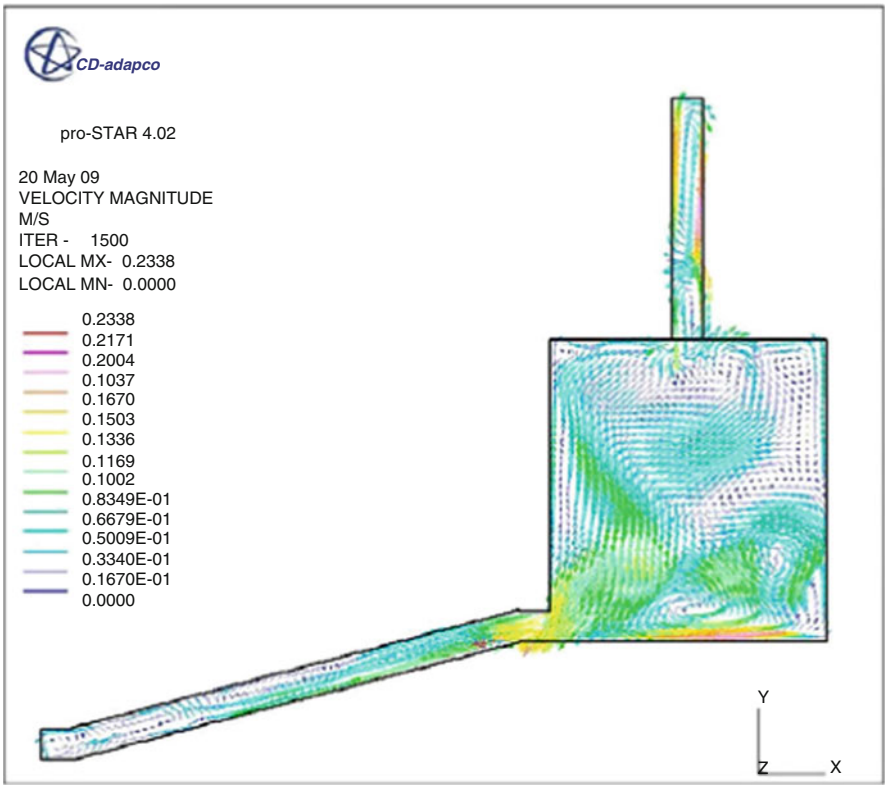

Fig. 8 Velocity distributions for natural convection (Chauhan et al. 2015)

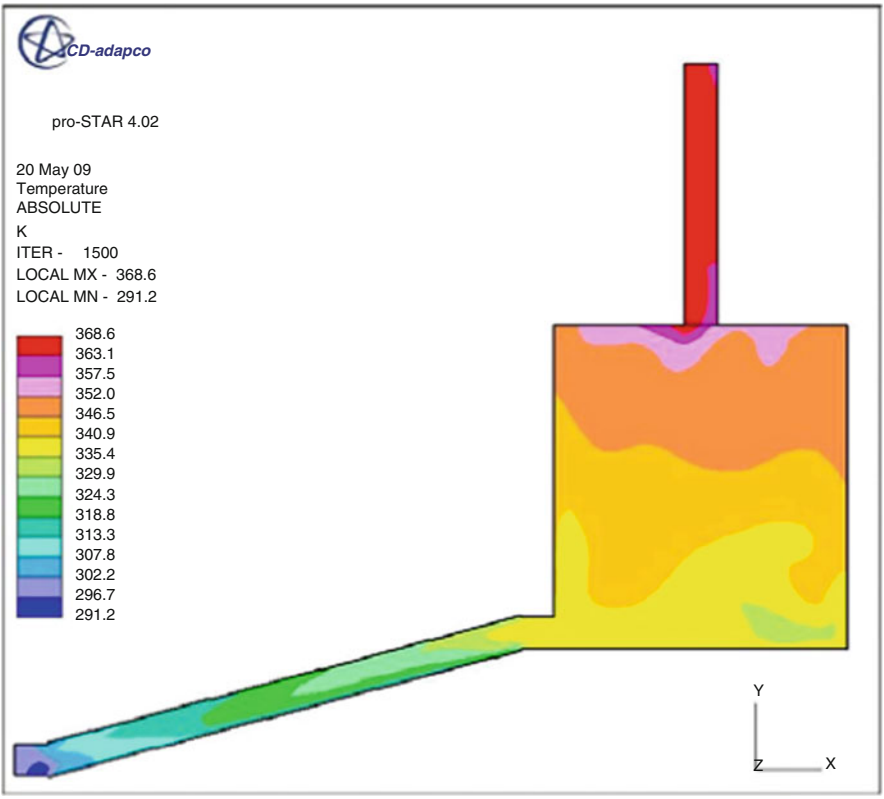

Fig. 9 Temperature distributions for natural convection (Chauhan et al. 2015)

purpose under artificial circulation stage. The highest and lowest temperatures were observed as 311.5 K and 298.3 K, respectively. Heat generated in this desiccating chamber ranges from 303 to 311.5 K. The temperature variation in the heated chamber used for drying purpose was more simplified in the case of unforced circulation model (Rigit and Patrick 2010).

4.4.2 FORTRAN

Janjai et al. (2009) used ComQ-visualized FORTRAN v6.5 for simulation and to solve the partial derivative equation. These equations were related to temperature variation and removal of moisture from peeled longan sample in PV-ventilated solar tube drying system. The predicted result of model for heating was analysed in terms of RMS change, however, small disturbance among the predicted and calculated moisture compositions was found. The change in moisture observed as RMS

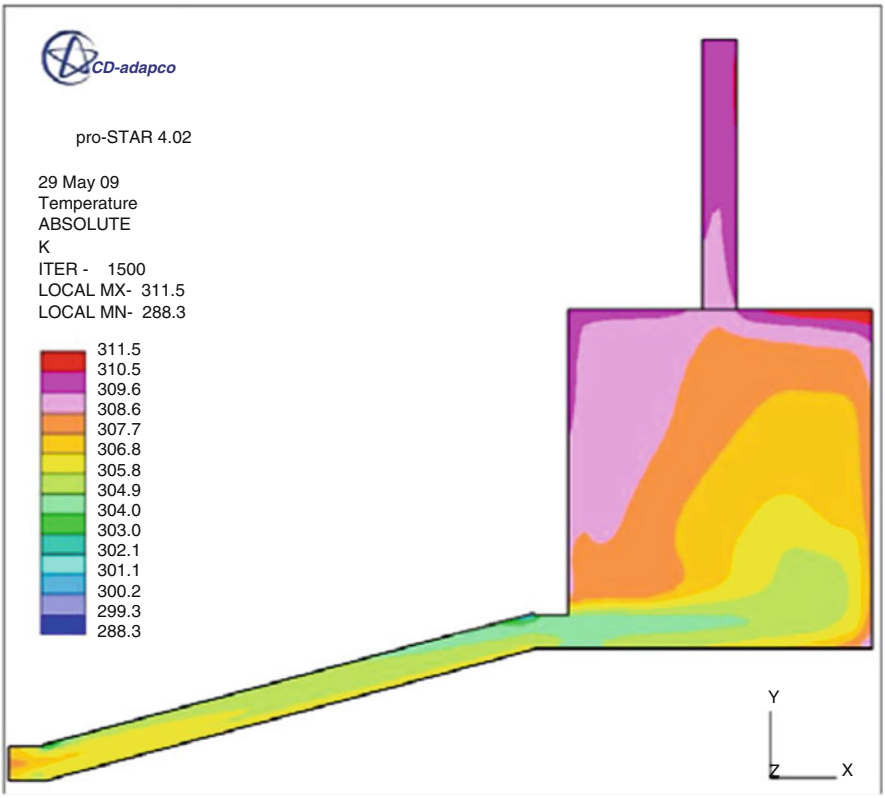

Fig. 10 Temperature distribution for forced circulation (Chauhan et al. 2015)

variation was only 6%. A similar type of variation was accounted for temperature observations which were 3% only (Janjai et al. 2009).

4.4.3 MATLAB Simulation

MATLAB 7.0 software is used to calculate the heat and mass transfer in solar dryer. This software is used to calculate the heat utilization rate of convective mass transferred and moisture evaporated. A hybrid photovoltaic and thermal greenhouse drying unit was designed for a maximum drying capacity of 100 kg agricultural produce. Thompson seedless grapes (type A and type B) were used for drying. Forced convection mode was created in the system with the help of a dc fan. The coefficient of convective heat transfers for type A grapes and type B grapes was found between 0.26–0.31 W/m^2 and 0.45–1.21 W/m^2, respectively (Barnwal and Tiwari 2008).

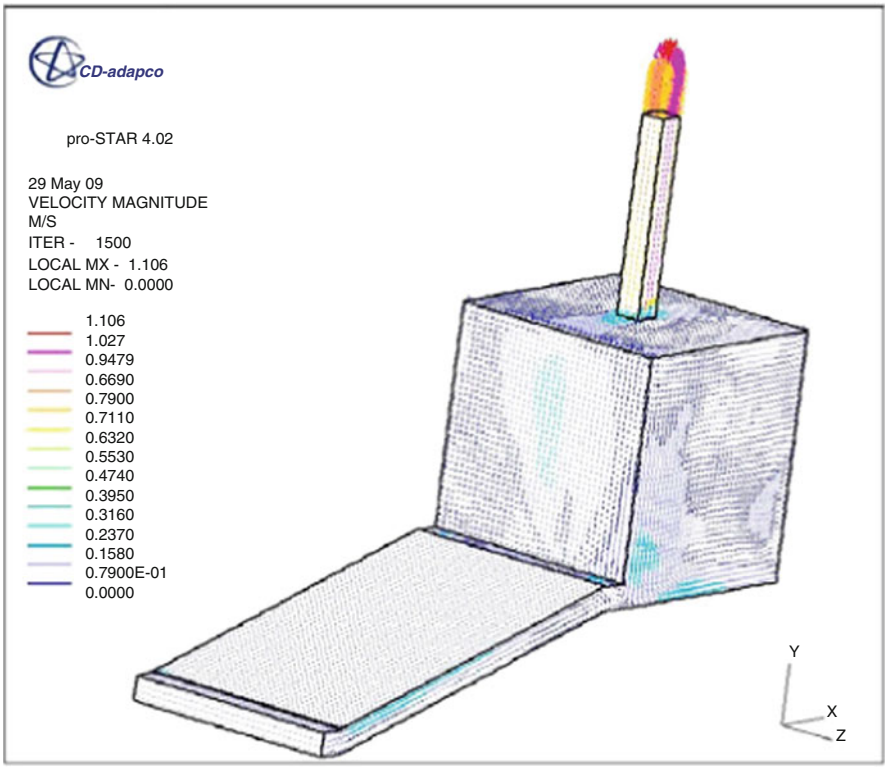

Fig. 11 Velocity distribution for forced circulation (Chauhan et al. 2015)

4.4.4 Software Package for Statistical Analysis (SPSS)

Chavan et al. (2008) used statistical analytic software "SPSS" for statistical analysis of "solar-biomass hybrid cabinet dryer". Derivation coefficient (R^2), decreased chi value (χ^2) and the amount of RMS deviation had been applied for choosing the most suited equation to understand the solar drying procedure. Statistical analysis was conducted in unordered progression using data analysis systems in all sources. In this study, various uncommon swift layer drying modules were studied according to the RMS variation, chi value (χ^2) and coefficient of derivation (R^2) (Chavan et al. 2008). Hybrid cabinet dryer of solar-biomass has recorded data of R^2 as 0.96660, 0.9720, 0.96913, 0.954 and 0.9829 describing the appearance, smell texture, taste and overall usability of the dryer, respectively. According to mackerel module of swift layer drying's observations, all modules were exhibiting symbiotic relation, whereas two-phase drying modules of Midilli were the most suitable and best predict the total moisture content in dried mackerel. The minimum RMS variation, χ^2 and maximum R^2 data were recorded. This results in the three-phase drying module (Chavan et al. 2008).

Hossain et al. (2008) analysed hybrid solar drying system statistically by using statistical software SPSS 9.0. A statistical analysis is important for colour codes, lycopenic acid, "ascorbic acid" and complete "flavonoids of sun-dried" and various altered substances. Software like SPSS 9.0 was used for such analysis. Duncan's multiple range tests were utilized for comparison of the mean resulted as per different variation compositions. The substantial air temperature was recorded at the outgate of the collection unit which was 30 °C more than the normal heating temperature. The system's efficiency was enhanced by 10% by the use of solar reflection unit. Thus, the efficiency of solar dryer increased from 17 to 29%. The colour, ascorbic acid, lycopene and total flavonoids of fruits were essentially reduced during drying process. However, the wastes obtained from nutritional and colour constituents were mounted to the large value than they were practically feasible in the market available (Hossain et al. 2008).

5 Case Study: ANFIS Prediction Model of a Modified Active Greenhouse Dryer

Under no-load scenario of modified greenhouse dryer, ANFIS prediction model is incorporated by Prakash and Kumar (2013b). There are two parameters involved in this model, i.e. input parameter and output parameter. Input parameters are weather condition. The weather condition consists of ambient temperature, ambient relative humidity, global radiation, etc., whereas output conditions are temperature inside greenhouse dryer and relative humidity. First-order Takagi-Sugeno model is derived and followed by ANFIS model. It enhanced fuzzy controllers due to self-learning ability. In the case of complex non-linear systems, Sugeno fuzzy model can be habituated. The Sugeno fuzzy model is applicable to dynamic and complex non-linear systems.

Here M and N are fuzzy set and $m = f(a, b)$ is a crisp function from M and N.

Rule 1. If a is M1 and b is N1, then $f_1 = p_1a + q_1y + r_1$.
Rule 2. If a is M2 and b is N2, then $f_2 = p_2a + q_2y + r_2$.

where $[a, b]$ is an input variable vector as shown in Fig. 12.

Here, $w1$ and $w2$ are firing strengths, which are the product of the membership grades, and output function (f) is the mean weight of each rule.

Layer 1: The output function of node t(O1).
Layer 2: In layer 2, each node is a circle node with labelled W, which predicts the incoming signals and generates output.
Layer 3: In layer 3, the ratio of the tth rules of the firing strength to the total of all firing strength of the system is calculated.
Layer 4: In layer 4, the calculation of the tth rule towards the overall output takes place; $t = 1$, 2(1.5).
Layer 5: Finally, in the fifth layer, overall output is computed; $t = 1$, 2(1.6).

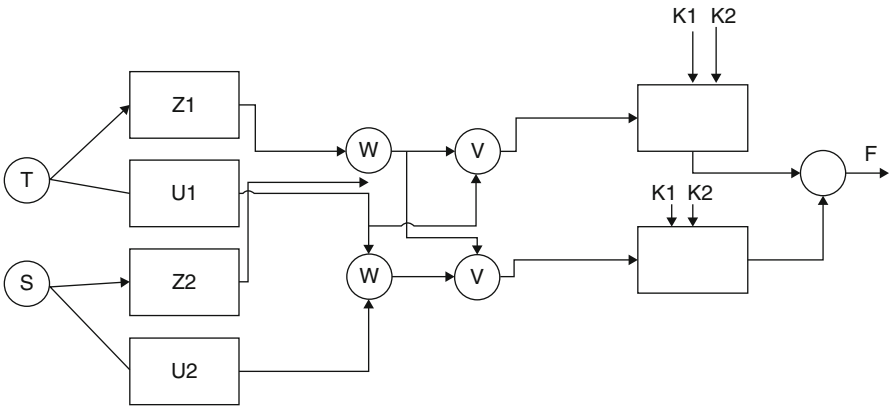

Fig. 12 ANFIS architecture (Prakash and Kumar 2013b)

Fig. 13 Active greenhouse dryer (Prakash and Kumar 2013b)

5.1 Outcome

In active greenhouse dryer, the solar cell is used to supply voltage to the exhaust fan. The mirror is used in the north wall of greenhouse dryer that made it opaque as shown in Fig. 13.

The dimension of the dryer was 1.5 × 1.0 m^2. The experimental test was conducted between 10.00 and 17.00 h on the concrete floor of MANIT Bhopal (India) in the month of January under clear sky and winter climatic condition. Solar irradiance collection, surrounding humidity pattern and surrounding temperature were taken as input parameters for ANFIS model. The average value of solar intensity was recorded as 747.17 W/m^2. The average greenhouse air temperature witnesses the rise in 11.8 °C above than surrounding environment temperature. This observation shows this dryer is very good for drying. In ANFIS prediction model,

the error was only 0.026 for greenhouse air temperature. MATLAB software was utilized for the tutelage and examination of this system as shown in Figs. 14 and 15.

The prediction of greenhouse air relative humidity encompasses error value of 0.12. This model saves the time of the experimentation (Prakash and Kumar 2013b).

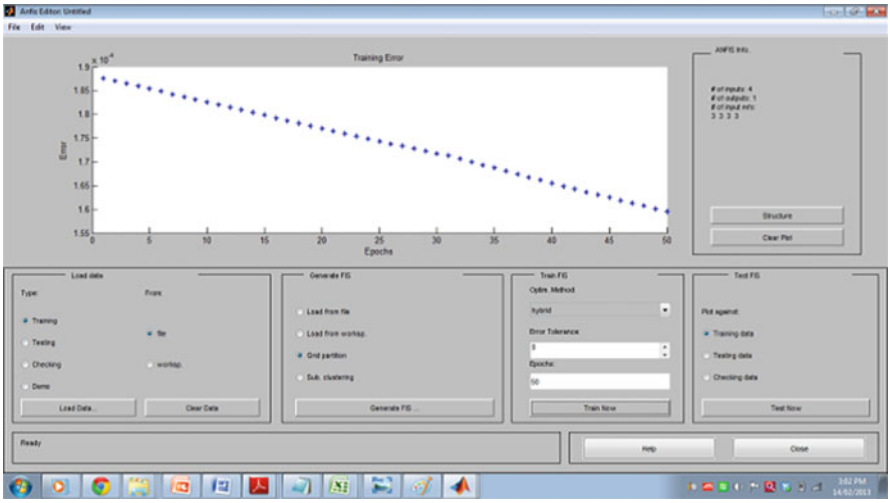

Fig. 14 ANFIS model for greenhouse air temperature (Prakash and Kumar 2013b)

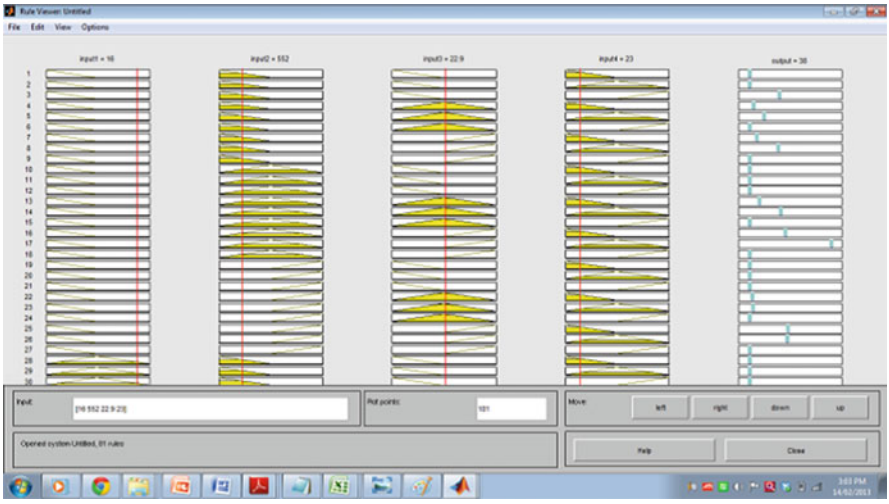

Fig. 15 Rule viewer of ANFIS model (Prakash and Kumar 2013b)

6 Conclusions

Solar drying systems are assessed and analysed by researchers with the help of a manifold number of simulation software. Soft computing is essential for optimizing design parameters of the solar dryer and helpful to design efficient dryer. Preceding fabrication process, the software facilitates the modelling of solar drying systems. In order to analyse the thermal behaviour of solar dryer, COMSOL Multiphysics, MATLAB and TRNSYS are widely used for this purpose. ANSYS and Fluent software are mainly used in computational fluid dynamics. Statistical analysis software like sigma plot V, SPSS and Statistica are usually employed for regression analysis and fitting drying kinetics data. These simulation software offer both time-saving and capital investment saving in manufacturing and working operation of the solar dryer. Software-based modelling and simulation are able to solve the complex mathematical problem and give details about the movement of air and temperature inside drying system and chamber. Academician/researcher proposed simulation model to enhance design data of solar dryer. This study will be helpful for selection of the optimal dryer and further development.

References

Amjad W, Munir A, Esper A, Hensel O (2015) Spatial homogeneity of drying in a batch type food dryer with diagonal air flow design. J Food Eng 144:148–155

Awadalla HSF, El-Dib AF, Mohamad MA, Reuss M, Hussein HMS (2004) Mathematical modelling and experimental verification of wood drying process. Energy Convers Manag 45:197–207

Barnwal P, Tiwari GN (2008) Grape drying by using hybrid photovoltaic–thermal (PV/T) greenhouse dryer: an experimental study. Sol Energy 82:1131–1144

Bartzanas T, Boulard T, Kittas C (2004) Effect of vent arrangement on windward ventilation of a tunnel greenhouse. Biosyst Eng 88:479–490

Bennamoun L, Belhamri A (2003) Design and simulation of a solar dryer for agriculture products. J Food Eng 59:259–266

Chauhan PS, Kumar A, Tekasakul P (2015) Applications of software in solar drying systems: a review. Renew Sust Energ Rev 51(2015):1326–1337

Chavan BR, Yakupitiyage A, Kumar S (2008) Mathematical modelling of drying characteristics of Indian mackerel (rastrilligerkangurta) in solar-biomass hybrid cabinet dryer. Drying Technol Int J 26:1552–1562

Chen HH, Huang TC, Tsai CH, Mujumdar AS (2008) Development and performance analysis of a new solar energy-assisted photocatalytic dryer. Dry Technol 26:503–507

Hossain MA, Amer BMA, Gottschalk K (2008) Hybrid solar dryer for quality dried tomato. Drying Technol Int J 26:1591–1601

Jain D (2007) Modeling the performance of the reversed absorber with packed bed thermal storage natural convection solar crop dryer. J Food Eng 78:637–647

Janjai S, Lamlert N, Intawee P, Mahayothee B, Bala BK, Nagle M, Muller J (2009) Experimental and simulated performance of a PV-ventilated solar greenhouse dryer for drying of the peeled longan and banana. Sol Energy 83:1550–1565

Kumar A, Tiwari GN (2006) Thermal modeling of a natural convection greenhouse drying system for jaggery: an experimental validation. Sol Energy 80:1135–1144

Lotfalian A, Ghazavi M, Hoseinzadeh B (2010) Reviewing drying of dill and spearmint by a solar dryer and comparing with traditional dryers. World Appl Sci 8:364–368
Mahapatra AK, Imre DSCL, Barcza J, Bitai A, Farkas I (1994) Simulation of a directly irradiated solar dryer with integrated collector. Int J Ambient Energy 15:195–204
Mathioulakis E, Karathanos VT, Belessiotis VG (1998) Simulation of air movement in a dryer by computational fluid dynamics: application for the drying of fruits. J Food Eng 36:183–200
Midilli A, Kucuk H (2003) Mathematical modeling of thin layer drying of pistachio by using solar energy. Energ Conver Manage 44:1111–1122
Pardhi C, Bhagoria JL (2013) Development and performance evaluation of mixed mode solar dryer with forced convection. Int J Energy Environ Eng 4:1–8
Prakash O, Kumar A (2013a) Historical review and recent trends in solar drying systems. Int J Green Energy 10:690–738
Prakash O, Kumar A (2013b) ANFIS prediction model of a modified active greenhouse dryer in no-load condition in the month of January. Int J Adv Comput Res 3:2277–7970
Prakash O, Kumar A (2014a) Solar greenhouse drying: a review. Renew Sust Energ Rev 29:905–910
Prakash O, Kumar A (2014b) ANFIS modeling of a natural convection greenhouse drying system for jaggery: an experimental validation. J Sustain Energy 33:316–335
Prakash O, Laguri V, Pandey A, Kumar A, Kumar A (2016) Review on various modeling techniques for the solar dryers. Renew Sust Energ Rev 62:396–417
Reuss M, Benkert ST, Aeberhard A, Martina P, Raush G, Rentzell BV, Sogari N (1997) Modelling and experimental investigation of a pilot plant for solar wood drying. Sol Energy 59:259–270
Rigit ARH, Patrick TK (2010) Low heat and mass transfer in a solar dryer with biomass backup burner. World Acad Sci Eng Technol 62:115–118
Romero VM, Cerezo E, Garcia MI, Sanchez MH (2014) Simulation and validation of vanilla drying process in an indirect solar dryer prototype using CFD Fluent program. Energy Procedia 57:1651–1658
Simate IN (2001) Simulation of the mixed-mode natural convection solar drying of maize. Drying Technol Int J 19:1137–1155
Tripathy PP (2015) Investigation into solar drying of potato: effect of sample geometry on drying kinetics and CO emissions mitigation. Food Sci Technol 52(3):1383–1393
Vintila M, Ghiaus AG, Fatu V (2014) Prediction of air flow and temperature profiles inside the convective solar dryer. Bull UASVM Food Sci Technol 71:188–194
Wang DC, Fon DS, Fang W, Sokhansanj S (2004) Development of a visual method to test the range of applicability of thin layer drying equations using MATLAB tools. Dry Technol 22:1921–1948

Part IV
Environomical Impact of Solar Drying Systems

Economics of Solar Drying

Deepali Atheaya

Abstract Solar drying is an ancient and inexpensive technique used for the preservation of agricultural item. Solar drying involves the removal of moisture content from crop. It is very important that the solar crop drying system should be cost-effective. Different methods of solar drying have been developed like open sun drying and greenhouse solar drying. The recent development in this area is greenhouse photovoltaic thermal mixed-mode drying in which electricity is also produced while crop drying is done. This system is quite useful for people living in remote areas. The solar drying of commercial industrial crops such as cotton, jute, sugarcane, tobacco, and ground nut has been popular and feasible. There is a need to invent cheaper solar drying methods to meet the demands of farmers of developing countries.

Keywords Cash flow • Uniform annual cost • Payback period • Net present value

1 Introduction

The controlled drying of crops is essential to ensure good quality of crops. It is evident that the cost of solar drying system should be studied to evaluate its performance and feasibility. The analysis of solar drying systems has been done on the basis of prime factors given as:

- Money spend in fabrication of solar dryer system
- Annual maintenance amount for the above system
- Life cost of solar drying system
- Salvage value of system

The economic evaluation of solar energy dryer is one of the key means which decides the overall performance of the system. The economic analysis of various solar drying systems can be done by unacost method, sinking fund factor method,

D. Atheaya (✉)
School of Engineering and Sciences, Mechanical Engineering Department, Bennett University, Plot No 8-11, Tech Zone II, Greater Noida, Uttar Pradesh, India
e-mail: deepali.atheaya@bennett.edu.in

© Springer Nature Singapore Pte Ltd. 2017

O. Prakash, A. Kumar (eds.), *Solar Drying Technology*, Green Energy and Technology, DOI 10.1007/978-981-10-3833-4_15

and cash flow diagrams, by calculating payback period. For the economic analysis of unconventional energy resources, the CO_2 credit earned by utilizing unconventional energy resources must be evaluated. Also the effect of embodied energy of renewable energy system on environment should be studied.

Bala et al. (2003) studied pineapple drying by means of solar tunnel dryer. The quality of dried pineapple was found to be best. Janjai and Tung (2005) have designed solar dryers which use air collectors placed at the rooftop. The invested rate of return and payback time period were found to be 70.3% and 3.9 years. A hybrid photovoltaic thermal greenhouse dryer has been designed and fabricated by Barnwal and Tiwari (2008). A novel mixed-mode solar greenhouse dryer to dry red pepper and grapes was proposed by Elkhadraoui et al. (2015). The economic analysis indicated payback time period as 1.6 years when the life of the system was 20 years. Kurt et al. (2015) investigated the economic performance of solar sludge drying by employing greenhouse solar dryer system. It was reported that though the capital cost of greenhouse solar dryer was more than conventional thermal dryer, but due to less energy requirements, it proved to be cost-effective. Nabnean et al. (2016) presented a novel design to dry osmotically dehydrated cherry tomatoes. The payback time of the dryer was 1.37 years. Dejchanchaiwong et al. (2016) studied mixed-mode and indirect solar drying. It was observed that the performance of mixed-mode solar dryer was excellent as compared to other methods. Recently, Misha et al. (2016) investigated the performance of solar dryer used to shrink the moisture content of crushed oil palm leaves.

The economic study of solar drying system is essential for the performance estimation. It also helps in the system optimization to benefit the user. The overall cost analysis has been done by critical understanding of system with the help of cash flow diagrams and payback diagrams. Sangamithra et al. (2014) have developed a polyhouse dryer and found it to be cost-effective. It was noted that the heat transfer coefficients between the greenhouse and open conditions were in the range 0.26–0.34 W/m^2 K. Recently Tiwari and Tiwari (2016) fabricated a PVT mixed-mode dryer. It was observed that the above system provided better product quality as compared to the conventional solar drying system.

2 Evaluation of Solar Drying Cost

If the initial present cost to fabricate solar crop system or any other system at zero time ($n = 0$) at an interest rate "i" per year is "A," the cash flow illustration is given in Fig. 1.

After year 1 the future value will be as follows:

$$F_1 = A + i \times A \tag{1}$$

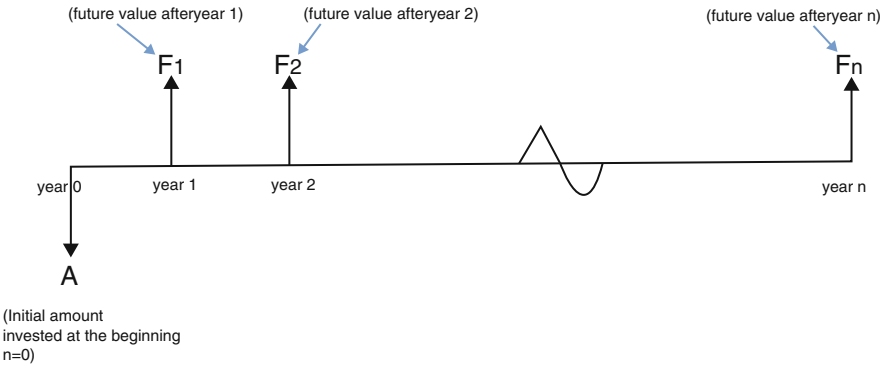

Fig. 1 Cash flow illustration for the evaluation of solar drying system cost

$$= A \times (1 + i) \tag{2}$$

Again after 2 years the new future value (F_2) will be given as:

$$\begin{aligned} F_2 &= F_1 + F_1 \times i \\ &= F_1 \times (1 + i) \\ &= A \times (1 + i)(1 + i) \end{aligned} \tag{3}$$

$$= A \times (1 + i)^2 \tag{4}$$

After a period of 3 years the future value will be as follows:

$$F_3 = A \times (1 + i)^3 \tag{5}$$

Following the above pattern, the future value after n years will be as follows:

$$F_{\mathrm{n}} = A \times (1 + i)^n \tag{6}$$

To make a general equation $F_n = F$, the expression for the determination of future value at the end of n years is given as:

$$F = A \times (1 + i)^n \tag{7}$$

Now for the case when ($F > A$; I > 0) by means of compound interest principle, Eq. (7) can be written as:

$$F = A \times F_{\mathrm{CI}} \tag{8}$$

where F_{CI} {compound interest factor} $= (1 + i)^n$.

Therefore, it can be inferred that future value is the product of present cost and compound interest factor.

Q. 1 Calculate the rate of return of an open solar dryer of cost USD 600 compounded to USD 820 over a 6-year period.

Solution

$$\text{Cost of solar dryer A} = \$\ 600$$
$$\text{n} = 6 \text{ years}$$
$$\text{Future value} = \text{F}_6 = \text{F} = \$\ 820$$
$$\text{i} = ?$$
$$820 = 600\ 1 + \text{i}$$

By solving the above equation, the rate of interest $i = 5.23\%$.

Now, let us consider the situation when 1 year has been divided into "q" equal intervals.

Therefore, new period will be equal to product of period and q equal intervals:

$$N = n \times q$$
$$i' = i/q$$

Therefore, another expression for the future value will be:

$$F = A \times (1 + i/q)^{nq} \tag{9}$$

The above expression can be rewritten as:

$$F = [A \times (1 + i/q)^{q}]^{n} \tag{10}$$

The above expression $(1+ i/q)^q$ can be further expressed as:

$$(1 + i/q)^{q} = 1 + \text{effective rate of return} \tag{11}$$

For case (a) when $q = 1$,

$$\text{Effective rate of return} = (1 + i/1)^{1} - 1 = i \tag{12}$$

For case (b) when $q > 1$,

$$\text{Effective rate of return is greater than } `i' \tag{13}$$

2.1 Simple Interest

Simple interest is calculated by multiplying the principal amount by the interest rate and the number of years in a loan:

$$\text{Future value } F = A \times (1 + n \times i) \tag{14}$$

Q. 2. Calculate the time taken for money to be tripled if compounded every year at 15% per year?

Solution The money tripled in "n" number of years or $F = 3A$.

From Eq. (7)
$$F = A \times (1 + i)^n$$
$$3A = A \times (1 + i)^n$$

The solution of above equation gives number of years as 7.95 years ~ 8 years.

Q. 3. Evaluate the effective rate of return for (i) 20% interest and $q = 2$ and (ii) 25% interest and $q = 4$.

Solution From Eq. (8) we know Effective rate of return $= (1+ i/q)^q - 1$

(i) $i = 20\%, q = 2$

$$\text{Effective rate of return} \quad (1 + 0.20/2)^2 - 1$$
$$= 0.29$$

(ii) $i = 25\%, q = 4$

$$\text{Effective rate of return} \quad (1 + 0.25/4)^2 - 1$$
$$= 0.125$$

Q.4. Mr. Smith took a loan of USD 20,000 from a bank. He returns USD 25000 at the end of the year. Calculate the rate of interest paid by Mr. Smith.

Solution From the Eq. (11)
$$F = A \times (1 + n \times i)$$
$$n = 12/12 = 1$$
$$\$25000 = \$20000(1 + 1 \times i)$$

Solving the above equation gives the value of interest rate as 0.2%.

Q. 5. Mr. Daniel borrowed USD 18,000 from bank at 15% for duration of 5 years and 6 months. Determine the money paid by him considering the compound interest.

Solution By following Eq. 11

$$F = A \times (1 + n \times i)$$
$$= 18000[1 + (6/12) \times (0.1)]$$
$$= 18000 \left[1 + 1.075\right.$$
$$= \$19350$$

Now by using Eq. (7)

$$\begin{aligned} F &= A \times (1+i)^n \\ &= 19350(1+0.15)^6 \\ &= \$44757 \end{aligned}$$

Q. 6 Mr. Niel takes a loan of USD 2500 to buy a greenhouse solar dryer, and he returns USD 3000 after 6 months. Evaluate the rate of interest paid by him.

Solution By following Eq. 11

$$\begin{aligned} F &= A \times (1+n \times i) \\ 3000 &= 2500[1+(6/12) \times i] \\ i &= 0.40 \\ i &= 40\% \end{aligned}$$

Q. 6a In the 5-year development plan of a state, it was decided to implement solar drying technologies to 30 million farmers. Calculate the required growth rate to achieve the potential of better solar drying technologies in the state in the next 5 years when the technology is distributed to 10 million.

Solution We know from Eq. 7 $F = A \times (1+ i)^n$

$$F = 30 \text{ million}, A = 10 \text{ million}, n = 5 \text{ years}$$

Taking log on both sides and solving further

$$\text{Log } (30/10) = 5 \log (1+i)$$

Solving the above equation, we get $i = 9.9\%$.

2.2 *Present Value Calculation of System*

From Eq. (7) the future value can be calculated as:

$$F = A \times (1+i)^n$$

The above equation can be rewritten as:

$$A = F \times (1+i)^{-n} \tag{15}$$

The present value can be calculated by multiplying the future value and the present value term

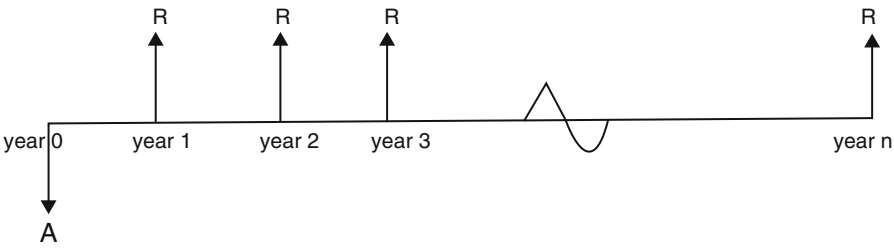

Fig. 2 Drawing showing unacost for n years

$$f_{\mathrm{PV}} = (1+i)^{-n} \tag{16}$$

From Eq. (8) we know that $F_{\mathrm{CI}} = (1+i)^{n}$

$$F_{\mathrm{CI}} \times F_{\mathrm{PV}} = 1u$$

2.3 *Uniform Annual Cost (Unacost Method)*

The comparison of various systems can be done by annualized uniform method. The term "una" means "uniform annual." Therefore, unacost implies uniform annualized cost. Figure 2 shows the unacost (R) for each year for "n" number of years.

In the above diagram, unacost is denoted as "R." Initially the present value "A" at $n = 0$. From Eq. (15) the present value A is given as:

$$A = R \times [(1+i)^{-n}]$$

$$A = A = R\left[\frac{1}{1+i} + \frac{1}{(1+i)^2} + \frac{1}{(1+i)^3} + \cdots + \frac{1}{(1+i)^n}\right] \tag{17}$$

Present worth factor $= \dfrac{1}{(1+i)^n}$

$$A = R\sum_{1}^{n} \frac{1}{(1+i)^n} \tag{18}$$

Equation (18) can be solved further as:

$$A = R\left[\frac{(1+i)^n - 1}{i(1+i)^n}\right] \tag{19}$$

Present value = Unacost × Unacost Present value factor

$$F_{RA,i,n} = \text{Unacost present value factor} \tag{19a}$$

From Eq. (19) the unacost can be calculated as:

$$R = A\left[\frac{i(1+i)^n}{(1+i)^n - 1}\right] \tag{20}$$

If the energy saving cost in a year is "R" and the carbon credit earned by utilizing the non-conventional energy resources is C_c, the money earned by utilizing renewable energy technology is as follows:

$$\text{Money earned} = [R + C_c] \times \left[\frac{(1+i)^n - 1}{i(1+i)^n}\right] \tag{21}$$

Q.7a By using a hybrid water heater, a farmer saves USD 5000 per year of fuels. Calculate the present worth of fuel which is saved by the farmer in 4th, 8th, and 12th year. Take $i = 10\%$.

Solution (i) When $n = 4$ years

$$\text{Present value factor} = \frac{1}{(1+i)^n} = \frac{1}{(1+0.1)^4} = 0.6830$$
$$\text{Present value} = 5000 \times 0.6830$$
$$= \$\ 3415$$

(ii) When $n = 8$ years

$$\text{Present value factor} = \frac{1}{(1+i)^n} = \frac{1}{(1+0.1)^8} = 0.466$$
$$\text{Present value} = 5000 \times 0.466$$
$$= \$\ 2332.52$$

(iii) When $n = 12$ years

$$\text{Present value factor} = \frac{1}{(1+i)^n} = \frac{1}{(1+0.1)^{12}} = 0.3186$$
$$\text{Present value} = 5000 \times 0.3186$$
$$= \$\ 1593.15$$

(iv) When $n = 16$ years

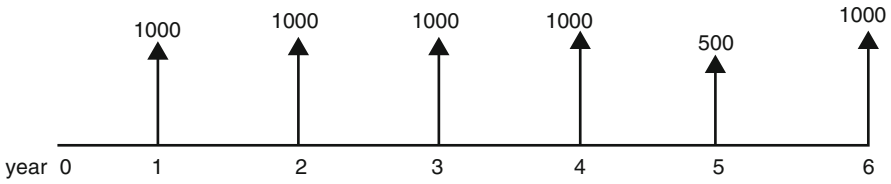

Fig. 3 Cash flow diagram in USD

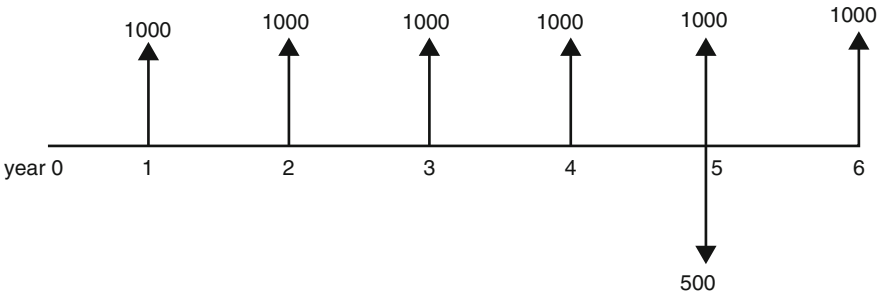

Fig. 4 Cash flow diagram in USD

$$\text{Present value factor} = \frac{1}{(1+i)^n} = \frac{1}{(1+0.1)^{16}} = 0.2176$$
$$\text{Present value} = 5000 \times 0.2176$$
$$= \$\ 1088.14$$

Q.7b Figure 3 shows the cash flow diagram (USD)S for 6 years. Determine the equivalent present value (Fig. 4).

Solution The above cash flow diagram can be redrawn as follows:

$$A = R\left[\frac{(1+i)^n - 1}{\mathrm{i}(1+i)^n}\right] + F \times (1+i)^{-n}$$
$$= 1000\left[\frac{(1+0.20)^6 - 1}{i(1+0.20)^6}\right] + 500 \times (1+0.20)^{-5}$$
$$= \$\ 3114.5$$

2.4 Sinking Fund Factor

It is a method for depreciating an asset in records and making money to buy a replacement for the asset when it reaches the end of its useful term.

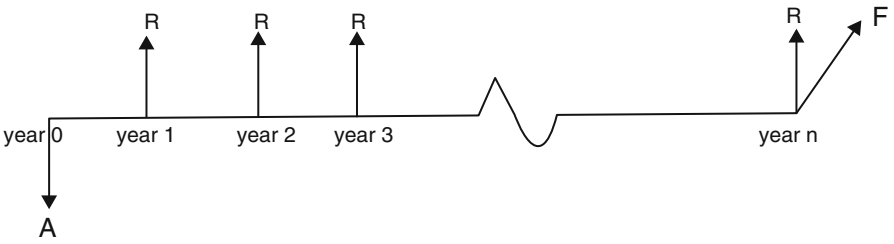

Fig. 5 Diagram showing unacost for "n" number of years

Figure 5 shows unacost (R) for each year for n number of years. From Eq. (20) the unacost is given as:

$$R = A\left[\frac{i(1+i)^n}{(1+i)^n - 1}\right]$$

From Eq. (7)

$F = A \times (1+i)^n$

The above equation can be rewritten further as:

$$A = F \times (1+i)^{-n} \tag{22}$$

So, the unacost is as follows:

$$R = F(1+i)^{-n}\left[\frac{i(1+i)^n}{(1+i)^n - 1}\right] \tag{23}$$

$$R = F\left[\frac{i}{(1+i)^n - 1}\right] \tag{24}$$

Unacost = Future value × Sinking fund factor (SFF)

$$\text{where SFF} = \left[\frac{i}{(1+i)^n - 1}\right]$$

The future value can be rewritten from Eq. (23) as:

$$\begin{aligned} F &= R\left[\frac{i}{(1+i)^n - 1}\right]^{-1} \\ F &= R\left[\frac{(1+i)^n - 1}{i}\right] \end{aligned} \tag{25}$$

Future value = Unacost × Equal payment series future value factor

3 Expression for a Uniform Beginning of the Year Annual Amount R_B

A uniform beginning of year annual amount R_B, $\underline{R}$ cash flow diagram are given below (Figs. 6 and 7).

By following Eq. $A = F \times (1 + i)^{-n}$, the R and R_B relationship is as follows:

$$\begin{aligned} R_B &= \frac{R}{(1+i)} \\ R &= R_B \times (1+i) \end{aligned} \tag{26}$$

Q. 8 Obtain an expression of RB in terms of A and F.

Solution By following Eq. 20

$$R = A\left[\frac{i(1+i)^n}{(1+i)^n - 1}\right]$$

or,

$$\begin{aligned} R_B &= \frac{A}{(1+i)} \times \left[\frac{i(1+i)^n}{(1+i)^n - 1}\right] \\ R_B &= A \times \left[\frac{i(1+i)^{n-1}}{(1+i)^n - 1}\right] \end{aligned} \tag{27}$$

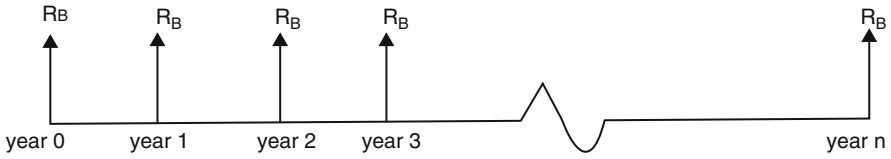

Fig. 6 Cash flow diagram showing R_B

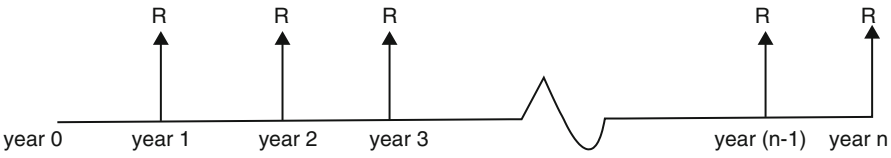

Fig. 7 Cash flow diagram showing R

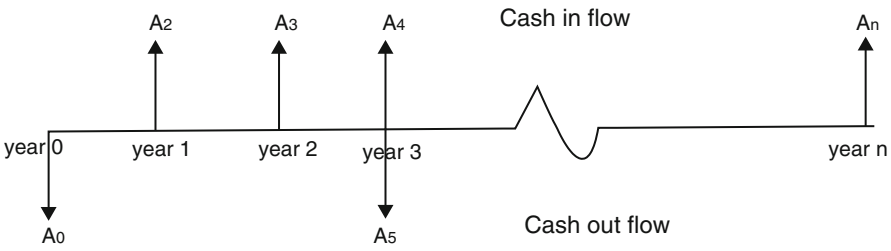

Fig. 8 Diagram depicting cash inflows and outflows

4 Diagram for Cash Flow

A cash flow diagram depicts the cash flows and outflows over a period of time. It is used to evaluate the system cost:

In Fig. 8 the upward arrows indicate the cash flows for, e.g., credit money into account, and downward arrow signifies cash outflow, e.g., withdrawing money.

Q. 6 Mr. Schmid deposits every year USD 2000 as a fourborne annuity for 10 years. He wishes to take money from bank after 16 years. Calculate the money value after 16 years. (Assume $i = 0.10$.)

Solution By following Eq. (19)

$$A = R\left[\frac{(1+i)^n - 1}{i(1+i)^n}\right]$$

$$A = 1000\left[\frac{(1+0.20)^{10} - 1}{0.20(1+0.20)^{10}}\right]$$

$$= \$4191$$

USD 4191 is deposited every year for 10 years. So, the future value at the end of 10 years will be

$$\begin{aligned} F &= A \times (1+i)^n \\ &= 4191.06(1+0.20)^{10} \\ &= \$\,25950 \end{aligned}$$

Q.7 A farmer sells a solar drying system for USD 2000 after using it for 15 years. Calculate its present value when the rate of interest is 20%.

Table 1 Cost comparison details of cabinet dryer and greenhouse dryer respectively

System	Capital cost	Maintenance cost per year	Salvage cost	Life of system	Profit as a uniform end of amount per year
Cabinet dryer	$ 2500	$ 200	$ 475	8	$ 50
Greenhouse dryer	$ 3000	$ 200	$ 325	10	$100

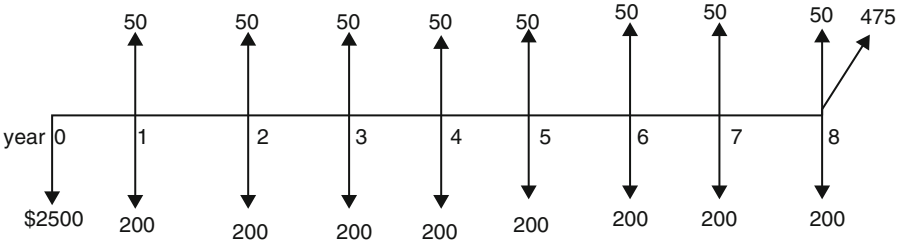

Fig. 9 Cash flow diagram of a cabinet dryer

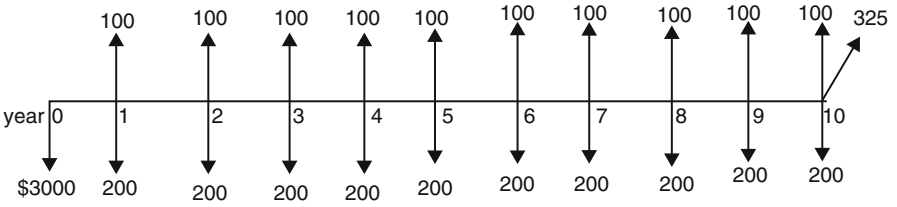

Fig. 10 Cash flow diagram of a greenhouse dryer

Solution

$$\begin{aligned} A &= F \times (1+i)^{-n} \\ &= 2000 \times (1+0.20)^{-15} \\ &= \$\ 129.81 \end{aligned}$$

Q.8 Table 1 shows the uniform cost of a cabinet dryer and a greenhouse dryer. Evaluate the economic performance of system considering the rate of interest as 20%.

Solution The cash flow diagrams of a cabinet dryer and a greenhouse dryer are as follows (Figs. 9 and 10):

For cabinet dryer

$$\text{The present value} = 2500 + (200 - 50)\left[\frac{(1+0.20)^8 - 1}{0.20(1+0.20)^8}\right]$$
$$= \$\ 3073.86$$

The greenhouse dryer is more economic.

5 Payback Period of Solar Dryer System

Payback period is the time required to recover the money invested in fabrication of solar dryer system. A system with small payback period is considered to be more economical.

Q. 9 A manufacturing firm spends USD 500000 in establishing the manufacturing plant. The firm receives USD 100000 as profit every year. Calculate the payback period.

Solution The payback period will be:

$$= \$500000/\$100000$$
$$= 5 \text{ years}$$

The payback time is 5 years.

5.1 Payback Period Calculation

The payback period is calculated by adding the annual cash flow values:
Sum of annual cash flows – money invested in business = 0.

Case (a) When annual savings are equal

$$Payback\ \ period = \frac{Initial\,\text{Pr}esent\,\text{Cos}t}{Annual\,cash\,flow} \tag{28}$$

Case (b) When annual savings are unequal

$$0 = -A + \sum_{T=1}^{n} CF\left(f_{\text{PV,i\%,T}}\right) \tag{29}$$

Here CF_{T} is cash flow at the end of the year T. If cash flow is the same every year, $\boldsymbol{F_{RA,i,n}}$ factor may be used in the relation:

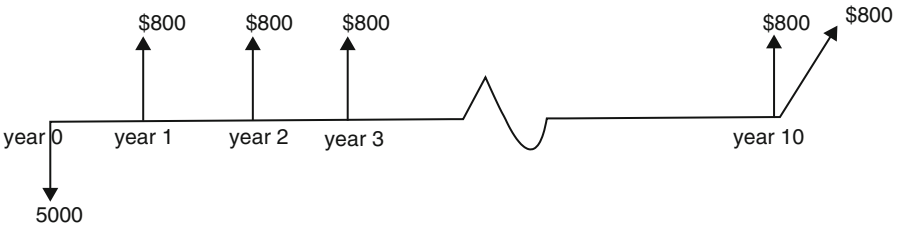

Fig. 11 Cash flow diagram of a greenhouse dryer

$$0 = -A + CF_{\mathrm{T}}(F_{RA,i,n,}) \tag{29a}$$

After n years, the cash flow will be recovered from the money spent.
If $i = 0$ then above equation becomes:

$$0 = -A \sum_{T=1}^{n} CF_T \tag{29b}$$

And if cash flow is equal at the end of year T are equal, then:

$$\mathrm{n} = \mathrm{A}/\mathrm{CF} \tag{29c}$$

Q.9 The cost of mixed-mode solar greenhouse dryer is $ 5000. It gives profits of $800 annually. The salvage value of dryer is $800 at any time till 10 years. Calculate the payback time period (take $i = 15\%$) (Fig. 11).

Solution From Eq. 29a

$$0 = -A + CF_{\mathrm{T}}\left(F_{RA,15\%,n}\right) + \text{Salvage value}\left(f_{\mathrm{PV},15\%,n}\right)$$
$$0 = -5000 + 800\,\frac{(1+0.15)^n - 1}{0.15 \times (1+0.15)^n} + 800 \times \frac{1}{(1+0.15)^n}$$

Solving the above equation, we get $n = 18.06$ years.

Therefore, it can be observed that $n = 18.06$ years is not cost-effective with high interest rate.

For $i = 0$,

$$0 = -5000 + 800\,n + 800$$

Or $n = 5.25$ years.

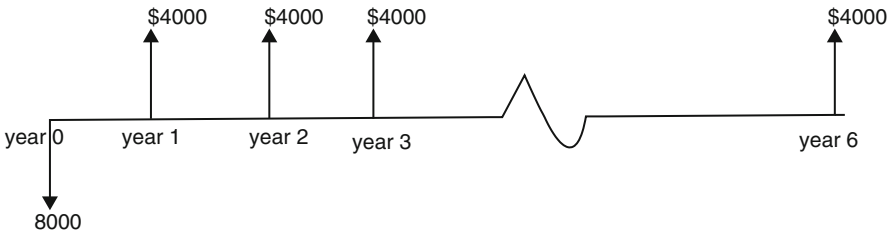

Fig. 12 Cash flow diagram of solar dryer

The payback period time is 5.25 years which turns out to be a cost-effective option.

Q.10 The table gives the information about indirect solar dryer system and hybrid solar dryer system. Calculate the payback period of the systems.

	Indirect solar dryer system	Hybrid solar dryer
Capital cost	$ 8000	$12,000
returns per year	$4000	5000
Maximum life	6 years	7 years
Rate of interest	15%	15%

Solution For Indirect solar dryer system (Fig. 12).

Using Eq. 29a

$$0 = -8000 + 4000 \times F_{RA,15\%,n}$$
$$0 = -8000 + 4000 \times \frac{(1+0.15)^n - 1}{0.15 \times (1+0.15)^n}$$

Solving the above equation, $n = 2.5$ years (Fig. 13).

5.1.1 For Hybrid Solar Dryer

Following Eq. 29a

$$0 = -12000 + 5000 \times F_{RA,15\%,n}$$
$$0 = -12000 + 5000 \times \frac{(1+0.15)^n - 1}{0.15 \times (1+0.15)^n}$$

Solving the above equation, $n = 3.17$ years which is less than the maximum life.

Depreciation It can be defined as the decrease in the value of a product with respect to time. It may give rise to profit when there is tax advantage because of depreciation (Fig. 14).

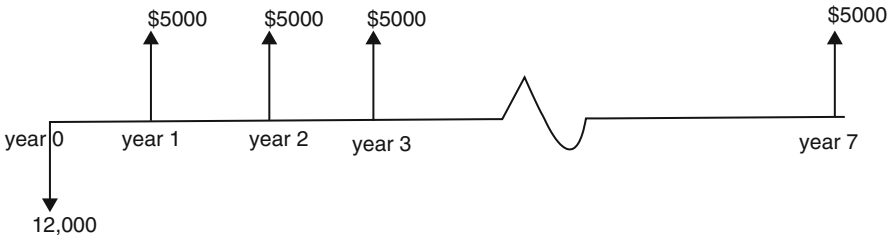

Fig. 13 Cash flow diagram of hybrid solar dryer

Fig. 14 Graph showing the cumulative cash with respect to years

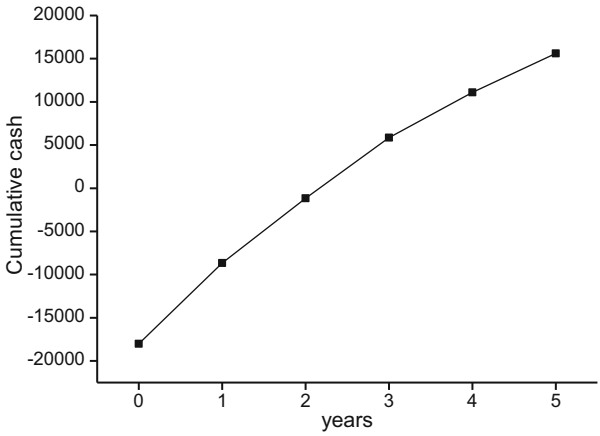

Table 2 Record showing profit and cash flow in USD

Time (year)	Profit after tax USD (I)	Tax benefit because of depreciation USD (II)	Cash flow (I + II)
0	−18,000	0	−18,000
1	4850	4500	9350
2	3000	4500	7500
3	2500	4500	7000
4	750	4500	5250
5	0	4500	4500

$$\text{Taxes} = (\text{Income} - \text{deduction})\text{tax rate}$$

Q. 11 Determine the payback time for the following record as shown in Tables 2 and 3.

From the above records, it can be seen that the payback time is between 2 and 3 years.

Table 3 Record showing cumulative cash flow

Time (years)	Cumulative cash flow
0	−18,000
1	−8650
2	−1150
3	5850
4	11,100
5	15,600

6 Various Terms Used for Economic Analysis

6.1 Initial Cost (c_i)

It is defined as the total cost involved in the installation of system. It comprises of the actual cost, delivery cost, installation charges, and service charges spent for the working of the system.

6.2 Salvage Cost (c_{sa})

It is basically the cost of an asset at the end of valuable life of the asset.

6.3 Depreciation (c_d)

It is the reduction in value of a system with time. The decrease in the worth of a system is termed as depreciation:

$$c_{\mathrm{d}} = c_{\mathrm{i}} - c_{\mathrm{sa}}$$

6.4 Book Value (B_V)

It is defined as the asset value mentioned in the firm's book. It is evaluated by subtracting asset value from the accumulated depreciation. It is calculated at the end of every year.

6.5 Depreciation Rate

It is ratio of depreciation cost of the asset to the number of years:

$$\text{Depreciation rate} = c_{\mathrm{d}} = (c_{\mathrm{i}} - c_{\mathrm{sa}})/(N)$$

6.6 Recovery Period (Expected Life, N)

It is defined as the number of years the value of an asset can be recovered.

6.7 Market Value

It is the price of a commodity after selling it in open market. The market price of a house will increase with time. Its book value will decrease if depreciation charges are considered. A mobile phone will have less market value than book value because of technology change.

Q. 12 Evaluate the rate of depreciation and book value of a commodity having first cost of USD 30,000 and salvage value of USD 5000 after 4 years.

Solution Depreciation rate $= c_{\mathrm{d}} = (\mathrm{c_i} - c_{\mathrm{sa}})/(N)$

$$= \frac{30000 - 5000}{4} = \$\ 6250 \text{ for 4 years}$$

(i) The book value at the first year end $= B_{\mathrm{V1}} = 30{,}000\text{–}1 \times 5000 = \$\ 25{,}000$
(ii) The book value at the second year end $= B_{\mathrm{V2}} = 30{,}000\text{–}2 \times 5000 = \$\ 20{,}000$
(iii) The book value at the third year end $= B_{\mathrm{V3}} = 30{,}000\text{–}3 \times 5000 = \$\ 15{,}000$
(iv) The book value at the fourth year end $= B_{\mathrm{V4}} = 30{,}000\text{–}4 \times 5000 = \$\ 15{,}000$.

7 Analytical Expression for Book Value

Let first cost of an asset be "$\mathrm{c_i}$."
Also salvage value after N years = "$\mathrm{c_{sa}}$."

$$\text{Therefore, depreciation,} \quad c_{\mathrm{d}} = c_{\mathrm{i}} - c_{\mathrm{sa}} \tag{30}$$

Let F_{d1}, F_{d2}, F_{d3}, and F_{d4} be the fractional depreciation for each year.
So, depreciation for xth year will be as follows:

$$F_x = F_{dx} \times c_d \tag{31}$$

Book value = First cost × accumulated cost

$$\begin{aligned} B_V &= c_i - c_d \Sigma F_{di} \\ &= c_i - c_d + c_d + c_d \Sigma F_{di} \\ &= c_{sa} + c_d[1 - c_d \Sigma F_{di}] \end{aligned} \tag{32}$$

7.1 Straight Line Depreciation

If fractional depreciation is same for all years,

$$\begin{aligned} &\text{Let } F_{d1} = F_{d2} = F_{d3} = F_{d4} = \cdots = F_{dn-1} = F_{dn}, \text{or Let } F_d = 1/N \\ &\text{Depreciation for x}^{\text{th}}\text{year} = c_d/N \end{aligned} \tag{33}$$

Accumulated depreciation up to *x*th year:

$$\begin{aligned} B_{VX} &= c_i - c_d \Sigma F_{di} \\ &= c_i - c_d(X/N) - c_d + c_d \\ &= c_{sa} + c_d[1 - (X/N)] \end{aligned} \tag{34}$$

Book value = Salvage value × Future depreciation.

8 Net Present Value (NPV)

The purpose of calculating net present value is to determine whether the project will turn out to be profitable or not. If NPV is positive, the investor will gain profits after taking the project. If NPV is negative, the investor will lose money by taking the project:

$$\text{NPV} = \sum_{k=0}^{n} \frac{(B_k - C_k)}{(1+i)^k} \tag{35}$$

where B_k is profit gained after time period "k".

C_k is cost after time period "k".

N is life of project and "i" is the interest rate.

Case(i) when $k = 0$, (Bk - Ck) is constant:

$$\text{NPV} = (B_0 - C_0) + \sum_{k=0}^{n} \frac{(B_k - C_k)}{(1+i)^k} \tag{36}$$

B_0 is the profit in the "0" year, $B_0 = 0$, $C_0 =$ initial money invested in the project, and $(B_k - C_k)$= constant $(B - C)$for $k = 1$ to n:

$$\begin{aligned} \text{NPV} &= (-C_0) + (B - C) \sum_{k=0}^{n} \frac{1}{(1+i)^n} \\ \text{NPV} &= (-C_0) + (B - C)\left[\frac{(1+i)^n - 1}{i(1+i)^n}\right] \end{aligned} \tag{37}$$

Q.13 A hybrid PVT solar water heater system cost price is USD 12000. The usage of this system leads to savings of USD 2000. The maintenance cost every year is USD 200. Evaluate the net present value of the money invested in system. Consider useful life of the system as 20 years and interest rate as 20 years:

Solution

$$\text{NPV} = (-C_0) + (B - C)\left[\frac{(1+i)^n - 1}{i(1+i)^n}\right]$$

$$\text{NPV} = (-1000) + (2000 - 200)\left[\frac{(1+0.1)^{20} - 1}{0.20 \times (1+0.20)^{20}}\right]$$

$$= \$\ 5304.34$$

As NPV is positive, the hybrid PVT solar water heater is profitable.

The calculation of NPV is a decisive factor of taking an assignment and is as follows:

(a) If NPV is **positive**, then take the assignment.
(b) NPV is **negative** then decline the assignment.

When the interest rate "I" varies with time:

$$\text{NPV} = (B_0 - C_0) + \frac{(B_1 - C_1)}{(1+i_1)} + \frac{(B_2 - C_2)}{(1+i_1)(1+i_2)} + \cdots + \frac{(B_n - C_n)}{(1+i_1)(1+i_2)\cdots(1+i_n).}$$

where i_1, i_2, i_3 and i_n are the interest rate for 1st year, 2nd year, 3rd year and nth year.

9 Conclusions

Developments of solar drying system technologies are economically feasible way to tackle problems of food spoilage in developing countries. It is considered as the cheapest way to reduce the moisture contents of dried products. Also, it drastically reduces environmental pollution problems and gives rise to huge energy savings in terms of cost. In this chapter various methods such as annual cost methods, sinking fund method, cash flow diagrams, payback periods, and net present value have been discussed.

References

Bala BK, Mondol MRA, Biswas BK, BLD C, Janjai S (2003) Solar drying of pineapple using solar tunnel Drier. Renew Energy 28:183–190

Barnwal P, Tiwari GN (2008) Grape drying by using hybrid photovoltaic-thermal (PV/T) greenhouse dryer: an experimental study. Sol Energy 82:1131–1144

Dejchanchaiwong R, Arkasuwan A, Kumar A, Tekasakul P (2016) Mathematical modeling and performance investigation of mixed-mode and indirect solar dryers for natural rubber sheet drying. Energy Sustain Dev 34:44–53

ELkhadraoui A, Kooli S, Hamdi I, Farhat A (2015) Experimental investigation and economic evaluation of a new mixed mode solar greenhouse dryer for drying of red pepper and grape. Renew Energy 77:1–8

Janjai S, Tung P (2005) Performance of a solar dryer using hot air from roof-integrated solar collectors for drying herbs and spices. Renew Energy 30:2085–2095

Kurt M, Aksoy A, Sanin FD (2015) Evaluation of solar sludge drying alternatives by costs and area requirements. Water Rese Arch 82:47–57

Misha S, Mat S, Ruslan MH, Salleh E, Sopian K (2016) Performance of a solar-assisted solid desiccant dryer for oil palm fronds drying. Sol Energy 132:415–429

Nabnean S, Janjai S, Thepa S, Sudaprasert K, Songprakorp R, Bala BK (2016) Experimental performance of a new design of solar dryer for drying osmotically dehydrated cherry tomatoes. Renew Energy 94:147–156

Sangamithra GJS, Prema RS, Priyavarshini R, Chandrasekar V, Sasikala S (2014) An overview of a poly house dryer. Renew Sust Energ Rev 40:902–910

Tiwari S, Tiwari GN (2016) Exergoeconomic analysis of photovoltaic-thermal (PVT) mixed mode greenhouse solar dryer. Energy 114:155–164

Techno-economic Analysis of Solar Dryers

S. Selvanayaki and K. Sampathkumar

Abstract Worldwide demand for energy is increasing at an increasing rate owing to the population bang and technological advancement. So, it is imperative to go for consistent, cost effectual and eternal nonconventional energy sources for meeting the raising demands. The possible utilization of solar energy in the industrialized/farming segment has improved due to the environmental concerns and expected fatigue of conventional fossil fuel. Drying using solar energy is one of the best methods with respect to environmental concern and hopeful application of solar energy utilization all over the world. In this context, many types of solar dryers were invented, namely, hybrid solar dryer, direct solar dryer and indirect solar dryer, for various drying applications. However, the availability of suitable drying system which is technically and economically feasible is limited. As of now only few solar dryers which meet the valued parameters like economical, technical and socio-economical requirements commercially exist. This chapter presents their importance of economic consideration of solar dryers and review of techno-economic study of an assortment of solar dryers developed over the years.

Keywords Solar dryer • Economics • Payback period • Cost benefit analysis

1 Introduction

All over the world, particularly in developing countries, open sun drying is a well-liked, efficient and cost-effective method used for drying of agricultural and other products. Direct sun drying requires large open space area and is highly dependent on the availability of sunshine, prone to contamination by foreign materials such as

S. Selvanayaki
Department of Agricultural and Rural Management, TamilNadu Agricultural University, Coimbatore 641003, India
e-mail: sselvanayaki@tnau.ac.in

K. Sampathkumar (✉)
Department of Mechanical Engineering, Tamilnadu College of Engineering, Coimbatore 641659, India
e-mail: ksktce@gmail.com

© Springer Nature Singapore Pte Ltd. 2017

O. Prakash, A. Kumar (eds.), *Solar Drying Technology*, Green Energy and Technology, DOI 10.1007/978-981-10-3833-4_16

dusts and litters, and is exposed to birds, insect and rodents (Fudholi et al. 2010). Based on the size and design requirements, various types of solar dryers are available in the market. Generally, solar dryers are classified on the basis of air movement mode, solar contributions, air direction movements, type of product to be dried and insulation of the assembly (Toshniwal and Karale 2013). Solar dryers are generally alienated into three grouping, namely, hybrid solar dryers, direct solar dryers and indirect solar dryers. Solar dryer gives enviable product quality with minimal ecological bang. This is a very low-cost, effective and safe method for food and agricultural drying applications. VijayaVenkataRaman et al. (2012) listed the three key barriers in increasing the use of solar crop drying, viz. lack of consciousness regarding cost-effectiveness of solar drying systems, lack of good scientific information and lack of good realistic practices.

No solar energy device is useful unless it is cost-effectively viable. Economic feasibility will directly link to the cost variables like material, maintenance, manufacturing, operational, etc., and it should be low during optimization of solar drying system under specified design condition. The major problems associated with solar drying technologies are high manufacturing cost, operating cost, maintenance cost and interest rate. The success of the solar drying system is purely dependent on the drastic reduction of capital cost in drying system of the construction. Research efforts that will help lower the cost of such units should be sustained. The progress and use of cheaper, more robust, locally accessible materials for construction of drying units, without endangering their performance, should be an ongoing endeavour (Sharma et al. 1994a).

Techno-economic investigation of solar drying system is a significant facet to analyse overall viability of a designed solar system. The capital cost of the system, operational and maintenance cost, dryer efficiency, efficient design, climatic condition during drying and physical characteristics directly influence this analysis. From the review of literature and general observation, the traditional drying methods followed over the years or open sun drying methods are obliviously cheap as compared to solar drying systems. However, the product quality obtained from such systems are very poor and may not compete with present market standards. On other hand, solar dryers have been found as successful drying devices with trouble-free operation and competent in producing eminent products with very less investment cost (Kumar 2016).

In the present chapter, a brief overview of economic analysis of various types of solar dryers and key factors associated with techno-economic and exergoeconomic evaluation has been presented in detail.

2 Review on Economic Analysis of Various Solar Dryers

Solar energy utilization particularly solar drying systems usually requires a vast initial investment as compared to conventional energy conversion equipments. Therefore, economic analysis is the most significant move to determine the

practical utility of the system. Solar drying systems should be used continuously on a year-round basis to be cost-effective compared to the conventional drying systems like electric, oil and gas. With multiple cropping becoming the craze in developing countries, the economics of solar dryers can be significantly improved through drying of summer as well as winter crops. In that case, the cost of solar drying would be less than that of conventional system. Dang and Bansal (1985) reviewed various methods of economic evaluation of solar energy system. The initial cost plus interest over its lifetime of any solar system would be more economical only if it functions for several years. Most of the solar energy systems include a secondary energy source due to nonavailability of sunshine for its year-round performance. Thus, the annual loads are met by a combination of energy sources like solar and conventional. The ultimate amount of interest is, in any case, the cost of the delivered useful energy. The factors in determining this cost are the price of the solar system, labour and operating expenses. The above variables should be suitably weighed with the interest rate, resale value of the equipment, income tax, maintenance cost, insurance, etc.

Govind and Tiwari (1984) presented the cost analysis of three types of solar energy systems namely solar dryers, solar water heating systems and solar distillation units. They followed uniform cost analysis procedure for economic analysis of different solar systems. In their study, three types of economic analysis have been suggested for solar dryers, namely, annual cost method, annual cost per unit of useful energy and annual cost per unit mass of the product. Various types of solar dryers developed in different countries with their economic considerations are listed in Table 1.

Techno-economic analysis of emblematic was dryers with diverse kinds of energy sources has been carried out by Sodha et al. (1991). From the study, it was found that the plastic collectors with a lifespan of 5–10 years are the cheapest among all solar energy systems. The conventional collectors with a lifespan of 10 years are more economical than wood, oil and electricity, whereas those with a lifespan equal to or more than 20 years are more economical than other fuel systems for drying applications.

The payback period and internal rate of return are the most significant economic parameters in the life cycle cost analysis as suggested by Sharma et al. (1994b). In totting up, initial investment, fuel price, interest on fuel price, etc. are the other important and most dominant parameters in analysing the solar system economics. Always economic analysis includes estimation of both investment and production costs systematically. Production costs may be contentious, as these are site specific, depending on local manufacturing costs, labour cost and availability of raw materials. Many authors have reported and applied some sophisticated economic concepts for evaluation of solar drying systems. The real applications of solar drying systems are with farmers, and hence well-defined sophisticated economic analysis is hard to understand for decision-making. From the above discussion, it is observed that simple economic methodology/analysis is to be developed on imperative basis to improve the acceptance rate of end users. A functional analysis based on the

Table 1 Economic variables of different solar dryers (Govind and Tiwari 1984)

Sl. No.	Country	Product	Type of dryer	Capacity (kg)	Life (year)	Total cost ($)	Cost/ m^2 ($)	Annual cost/m^2 ($)	Cost/ product ($/kg)
1.	Colombia	Coffee	Paseras	106	8	4	2.10	0.684	0.0013
2.	India	Prunes	Cabinet	75	10	20	0.15	5.16	0.028
3.	Brazil	Banana	Chamber	200	5	64.10	32.5	11.88	0.0011
4.	USA	Apricots	Chamber	27.5	20	34	27.2	5.998	0.015

market price can be carried out based on the manufacturing, operational costs and output available from the system.

The economic analysis is very usable in finding the internal rate of return and finding out the different possible technical options available to satisfy the end customers. The capital cost of the project, maintenance cost, interest rate, conventional fuel cost and salvage value are the main parameters for the calculation of net cost of the useful energy delivered by the solar drying system. Dividing the annual cost by the annually delivered useful energy gives the cost of per unit energy. The total cost of the system can be articulated in terms of initial capital investment, yearly fuel costs, interest rate, maintenance and operational costs, etc. From their realistic understanding, it was concluded that the use of solar drying technology in Southern Italy was more economical for drying forage, vegetables and a variety of other agricultural products.

Palaniappan and Subramanian (1998) presented the economic analysis of roof-integrated solar air heating system installed in few tea factories in South India with an area of 212 m^2 which were in operation for nearly three years. Major findings of the study were:

1. Twenty five percent of the fossil fuel used in tea factories will be saved annually if the conventional system is replaced with solar drying system. Because most (>40%) of the tea factories in South India are using wood/fossil fuels as fuel for running the drying system. This will directly create a significant impact in reducing the pressure on forests.
2. Payback period for the solar drying system was less than two years for a profit-making company. This was achieved through the subsidy provided by Government of India for solar energy promotion. The corresponding payback period for non-profit-making company was three years and four months, and it was obviously higher as compared to profit-making companies. This was because of the interst on capital cost to a tune of 16%, a 10% escalation rate on parasitic energy and maintenance cost and an 8% escalation rate on fuel cost. From the analysis, it is understood that, the solar air preheating "ped" system for tea processing was found to be economically viable.
3. Tea processing industries in India are using coal or wood as fuel for drying applications, and the annual fuel consumption is approximately 454 million kg. We can reduce this by 25%, if the solar drying system is used with an area 0.6 million m^2.

Multi-shelf domestic solar dryer developed at Punjab Agricultural University (PAU), India, has been tested, and results were presented by Singh et al. (2006a). In their study, the economic analysis was performed by three different methods. The following assumptions were made for the analysis:

Rate of inflation (A) = 5%
Real interest rate (B) = 3%
Discount rate = $A + B$ = 8%

The current capital cost of a PAU domestic solar dryer (CCC) is Rs.1600/–, and its life has been taken as 20 years.

(a) *Method 1 – Annualized cost method*
The important variables and values are listed with calculated values:

(a) Annual maintenance cost = 3%
(b) Salvage value = 10%
(c) Number of usable days of dryer = 150 days
(d) Capital cost of electric dryer = Rs.800/–
(e) Cost of electric energy = Rs.4/kWh
(f) Efficiency of electric dryer = 80%
(g) Annualized cost of the solar dryer = Rs.164.35
(h) Amount of dried fenugreek = 4.25kg/year
(i) Cost of drying fenugreek leaves using solar dryer = Rs.38.67/kg

(b) *Method 2 – Life cycle cost saving*
This method is mainly intended for comparing the cost of drying the fenugreek in PAU was domestic solar dryer with commercially branded products available in the market. From the calculations, it is observed that the current saving per day was Rs.8.5/day. The annual saving, present worth of annual saving and cumulative present worth of annual saving for each year of life of the domestic solar dryer were also calculated for solar dryer. For drying fenugreek leaves, the cumulative present worth of the annual savings over the life of the domestic solar dryer is calculated as Rs.18,315.69.

(c) *Method 3 – Payback period*

Payback period	Equivalent drying days	Product
1.36 years	204 drying days	Fenugreek
0.57 years	86 drying days	Chillies

The calculated payback period is shown in the above table. The payback period is very short when compared to the life of the dryer (20 years), so it would dry the product free of cost for almost its entire life period.

Sreekumar (2010) conducted an economic analysis and compared the costs of solar dried and branded dried using other drying methods, such as dryers that used fossil fuels. Two different types of products are available in the market, namely, branded product and unbranded product. From the general viewpoint, the

unbranded product has lower cost, and it is often in substandard worth and produced under unhealthy conditions. The product developed under such condition is often unfit for human consumption. On the other side, branded products are available in the market with comparatively high cost due to production under hygienic conditions. Three methods were normally adopted for the economic analysis and comparison of the product costs.

The first method is annualized cost method and it is used for comparison of cost of drying a product of unit weight with the solar dryer with drying the same in electric dryer. The total annualized cost of the dryer is defined as the ration between the amounts of product dried in a year to obtain the cost of drying per unit weight of the dried product. The main disadvantage of this method is that the cost of drying does not fully confine the economics of the solar dryer due to cost of drying varies petite over the entire life of the dryer, say 20 years. The rapid increase in cost of conventional energy is in turn increasing the cost of drying in the case of dryers using conventional energy (Table 2).

To overcome the disadvantage of the above method, it is essential to determine the savings over the life of the dryer to understand the economic benefits. The second method proposed is life cycle cost analysis, which satisfies the above factor for economic benefits. In this method, the present worth of annual savings over the life of the system is calculated. From that, we calculate the payback period of the system, which will be purchased by low, normal people. On the other hand, they will not be fascinated to buy if long, substantial long-term savings are possible. Therefore, the authors also highlighted the third method, namely, payback period. From the study, it is observed that the cumulative present worth of annual savings for drying bitter gourd over the life of the solar dryer is approximately Rs.17 million. The other results are listed below from the economic analysis:

Capital investment of the dryer = Rs.5,50,000/–
Payback period of the dryer = 0.54 year,
Cost of drying pineapple in the solar dryer = 20% of drying in electric dryer
The life of the system = 20 years, (Material used in the construction is corrosion proof.)

Hollick (1999) made an economic analysis of crop solar drying and estimated the total price of the solar dryer as 3,200,000 Indian rupees. The fuel savings were 0.5l/m^2 panel per day, and the annual fuel consumption was 168,000 l oil. The price per litre of fuel was Rs.9; thus, the savings was Rs.1,512,000 per year, and the payback period is approximately two years. It exhibits better returns in using the solar energy for drying. The calculated payback period was based on the solar plate costs, and the expenses for the complete dryer system were not considered. If the total cost of a new solar dryer project is evaluated, the other advantages such as improved quality, higher yields and less land use should be included in the analysis to obtain more accurate cost-benefit analysis.

Four different economic indicators of solar drying system were recommended by Panwar et al. (2014), namely, cost benefit ratio (CBR), internal rate of return (IRR), net present worth (NPW) and payback period. The internal rate of return is

Table 2 Economic analysis of solar dryer (pineapple as product), with 250 days of use of solar dryer (Sreekumar 2010)

Year	Annualized cost of dryer (Rs.)	Annual saving (million rupees)	Present worth of annual saving (million rupees)	Present worth of cumulative saving (million rupees)
1	0.073	1.19	1.19	1.10
2	0.073	1.25	1.07	2.18
3	0.073	1.32	1.04	3.22
4	0.073	1.38	1.01	4.24
5	0.073	1.45	0.99	5.23
6	0.073	1.52	0.96	6.19
7	0.073	1.60	0.93	7.12
8	0.073	1.68	0.91	8.03
9	0.073	1.76	0.88	8.91
10	0.073	1.85	0.86	9.77
11	0.073	1.94	0.83	10.60
12	0.073	2.04	0.81	11.41
13	0.073	2.14	0.79	12.20
14	0.073	2.25	0.76	12.96
15	0.073	2.36	0.74	13.70
16	0.073	2.48	0.72	14.43
17	0.073	2.60	0.70	15.13
18	0.073	2.73	0.68	15.81
19	0.073	2.87	0.67	16.48
20	0.073	3.02	0.65	17.13

calculated by a trial-and-error method to find that discount rate, which will make the net present worth of the incremental net benefit stream equal to zero. The two vegetable crops (i.e. cucumber and tomato) were cultivated in a naturally ventilated solar greenhouse, and their economic feasibility was studied. The economic indicators used to assess the feasibility of the solar greenhouse are presented in Table 3. The cost benefit ratio of cucumber was 2.17 which was higher compared to that of tomato (1.77). General rule of the cost benefit ratio is that the product is economically viable if the calculated value is greater than one.

A framework for techno-economic evaluation of solar crop dryers was presented by Purohit and Kandpal (2005). Unit cost of drying and the unit cost of useful energy was estimated for different crops. The monetary benefits accrued to the end user was quantified on the basis of commercial fuel saved. The effect of internalizing the benefits of CO_2 emission mitigation on the financial performance indicators has also been presented. Haque and Somerville (2013) presented the techno-economic and environmental evaluation of biomass dryer. From this study, they concluded that increasing temperature will decrease drying time and increase throughput but not necessarily decrease the drying cost. This is due to higher energy use and higher cost of capital inputs such as loading/unloading and heat plant. Thus, low drying temperature can be used if throughout is not an issue for an operation.

Table 3 Economic indicators of selected crops (Panwar et al. 2014)

Crop	Net present value (US$)	Cost benefit ratio	Payback period	IRR (%)
Cucumber	28,341.60	2.17	5 years and 3 months	35
Tomato	15,993.94	1.77	6 years and 11 months	20

The total global warming potential of biomass drying process as expressed in CO_2 equivalent units is 9.3 kg/t of oven dry biomass using dry wood waste as fuel for a rotary drum dryer.

Lhendup (2005) analysed the scientific and economic feasibility of a solar dryer in Bhutan and found that the technical performance of the dryer was found satisfactory. However, from the economic point of view, the dryer is financially un viable in Bhutan. Nevertheless, compared to a fully electrical heating system, a solar dryer is more attractive. The total investment cost for a non-optimized solar dryer is US$ 2343. The corresponding cost of an optimized system is US$ 3437 due to the increased cost of collector and its accessories. The cost of electric heating system dryer is US$ 1174. The net present value of the optimized solar system dryer is US$ 4373, while the NPV of an electric heating system dryer is US$ 7066. The negative NPV is unlikely to attract private investors. The drying cost of the solar dryer in Bhutan is US$ 5.77 and 6.20/kg of dry matter for chilli and respectively using the solar dryer system. The study revealed that the solar drying system is cheaper to dry beef and electric heating/drying system is cheap to dry chilli.

Experimental study and economic assessment of a new mixed-mode solar greenhouse dryer for drying of grape and red pepper were presented by Elkhadraoui et al. (2015), and economic parameters are listed in Table 4. The solar dryer was manufactured using flat plate solar collector and a chapel-shaped greenhouse for fast drying application. The drying time obtained from solar greenhouse dryer is much higher than open sun drying (OSD). The newly developed solar greenhouse dryer substantially reduced the drying time of red pepper and grape by seven and 17 h, respectively. The experimental drying curves show only the falling rate period. The payback period of the dryer was calculated to be 1.6 years, and it is much less than the estimated life of the solar system (20 years).

Fudholi et al. (2015a) described the techno-economic examination of solar drying system for seaweed in Malaysia, and economic parameters are listed in Table 5. From the techno-economic analysis, the drying time is found to be 15 h at average solar radiation of about 507W/m^2 and air flow rate of 0.0536kg/s. The results also revealed that the collector, drying system and pickup efficiencies are found to be 35, 27 and 95 percent, respectively, for solar drying system. Double-pass solar collector is best suited for developed or marketed marine products based on the results obtained from economic analysis and potential market price. The payback period is calculated as 2.33 years and it is comparatively low for frying of seaweed.

Economic investigation of hybrid photovoltaic-thermal (PVT) integrated solar dryer was presented by Nayak et al. (2012). From the study, it is observed that the total energy payback period of hybrid PVT solar dryer is 5.6 years, which is much less than the expected life of the dryer (Table 5).

Table 4 Economic parameters of solar dryer with capital cost (Elkhadraoui et al. 2015)

Economic parameter	Value
Capital cost of dryer	2000 DT
Annual electricity cost for fans	15 DT/year
Capacity of dryer	80 kg (pepper), 130 kg (grape)
Price of fresh grape	1 DT/kg
Price of fresh pepper	0.5 DT/kg
Price of dried grape	10 DT/kg
Price of dried pepper	10 DT/kg
Life of dryer	20 years
Interest rate	8%
Inflation rate	5%
Payback period	1.6 years

Note: 1US Dollar = 1.6 DT

Table 5 Parameters used in calculation of the LCS and PP (Fudholi et al. 2015a)

Parameter	Unit	Value
Inflation rate (i)	%	3
Discount rate (d)	%	10
$C_{\text{unit. elect}}$	USD	0.07
Daily electricity consumption	kWh	60
Cost of electricity per annum	USD	1533
Ratio of resale value at end of period of analysis to initial investment (Rv)	%	30
Solar system performance degrade	%	1
Cost of solar assisted chemical heat pump dryer	USD	5068
Annually solar fraction (SF)		0.335
Solar saving (LCS)	USD	1224.5
Pay back period (PP)	Year	3.9

The solar drying system is not technically viable sometimes due to energy availability in the particular period. To overcome this issue, other conventional equipments may also include getting the desired load to dry the products in desired timescale. In such conditions, the cost invested for other energy sources plays an important role for finding the economic competitiveness of the solar drying system. Optimum variables by using simulation programme and payback period of the system are presented by Rahman et al. (2013). Economic analysis shows that the solar system has adequate amount of savings during life cycle with a least payback period of about 4.37 years. Also they observed that the variations in the fuel inflation rate and discount rate have a significant effect on payback period. It is also revealed that the optimal system is insensitive to the variations in the fuel inflation rate and discount rate. Figure 1 shows the variation of payback period with respect to air collector area. From the figure, it is understood that the payback period falls sharply with increase in collector area. This observable fact may be

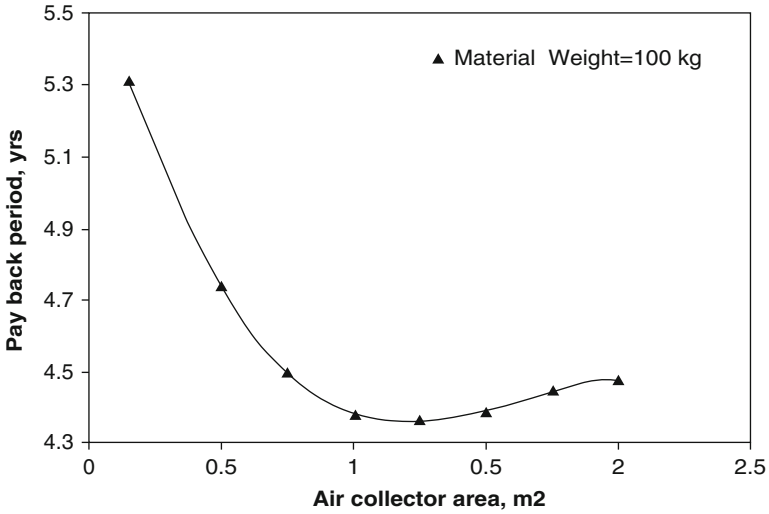

Fig. 1 Variation of payback period with air collector area (Rahman et al. 2013)

explained that, with the increase in collector area, auxiliary fuel saving increases very rapidly compared to the cost of the system. Again payback period reaches a least value and then rises with increase in collector area which agrees with the real expected phenomena.

An economic analysis of a PV powered, forced convection solar grain dryer with passive temperature control was presented by Mumba (1995). The analysis concluded that the dryer is very cost-effective with a payback period of less than a year.

Pirasteh et al. (2014) concluded from their review that solar energy is feasible for drying system, including industrial processes, given the amount of energy consumed by dryers and considering that solar radiation is unlimited and available with an average value of 200–500 W/m^2 in most parts of the world. Solar drying has positive economic, environmental and social effects on human life. Solar drying can mitigate monetary burdens via a payback period of 1 year or less than 10 years at most. Solar drying can also reduce the greenhouse effect and CO_2 production and make possible the establishment of appropriate policies in different countries.

Mustapha et al. (2014) analysed the qualitative performance and economics of low-cost solar fish dryers in sub-Saharan Africa. The dryers were found to be better than the other dryers because they are cheap, reliable, safe to use, easy to repair, well insulated and cost-effective. These solar dryers are compact and efficient with drying of fish with lowest moisture content achieved within few days, and the dried products of good quality, with long shelf life, are highly acceptable by the consumers. The adaptation of dryers will contribute to the wealth of rural people in developing countries where there is no electricity and the challenges of deforestation are becoming prominent. The low-cost solar dryers described in their analysis are better than the traditional open sun drying, smoking kiln and electric oven on the account of being cheap and cost-effective and possess many of the good attributes of an effective solar dryer as listed in Table 6.

Table 6 Qualitative performance evaluation and cost benefits of the solar dryers, open sun drying, smoking kiln and electric oven (Mustapha et al. 2014)

Performance evaluation	Open	Mosquito	Plastic	Aluminum	Gloss	Glass + stone	Smoking kiln	Electric oven
Moisture reduction in fish sample (%)	69.46	69.48	69.51	70.69	69.98	71.25	69.54	75.20
Drying rate/efficiency	Law	High	High	high	High	Very high	High	Very high
Maximum capacity (kg)	50	20	20	20	20	20	40	30
Drying time fur 10 kg of fish	12 days	9 days	10 days	7 days	7 days	6 days	1 day	3 h
Quality of dried products	Low	High	High	High	High	High	High	High
Radiation losses	Very high	High	Low	Low	Low	Very low	High	Very low
Heat losses	Very high	High	Low	Low	Low	Very low	High	Very low
Environmental pollution	None	None	None	None	None	None	High	None
Shelve life of dried fish	Short	Long	Long	Very long	Lung	Very long	Long	Very long
Life span (years)	5	8	8	10	10	10	5	15
Safety	Very safe	Very safe	Very safe	Very safe	Very safe	Very safe	Nat very safe	Not very safe
Installation cost	0	0	0	0	0	0	0	3000
Maintenance cost	Low	Low	Low	Low	Low	Law	High	Very high
Installation	Easy	Easy	Easy	Easy	Easy	Easy	Nat so easy	Not so easy
Insulation	Bad	Good	Good	Good	Good	Good	Bad	Good
Repair	Easy	Easy	Easy	Easy	Easy	Easy	Nat so easy	Not so easy

(continued)

Table 6 (continued)

Performance evaluation	Open	Mosquito	Plastic	Aluminum	Gloss	Glass + stone	Smoking kiln	Electric oven
Technicality/operability	None	None	None	None	None	None	Yes	Yes
Durability/handling	Not durable but easy	Very durable and easy	Very durable and easy	Very durable and easy	Very durable and easy	Very durable and easy	Nat durable and easy	Very durable and easy
Hygiene of products	Not hygienic	Very hygienic	Very hygienic	Very hygienic	Very hygienic	Very hygienic	Very hygienic	Very hygienic
Energy source	Solar	Solar	Solar	Solar	Solar	Solar	Wood	Electricity
Avaliability/local adaptability	Yes	Yes	Yes	Yes	Yes	Yes	Yes	No
Affordability	Very high	High	High	High	High	High	High	Law
Reliability	Law	Not high	High	High	High	High	Not high	Law
Spate	Less	Less	Less	Less	Less	Less	More	Less
Fixed cast of drier! (*N*)	1300	300	2300	2700	3300	3400	6000	20000
Operational cost of drying 10 kg of fish (*N*)	0	0	0	0	0	0	1000	3000
Market value of dried fish (*N*)	10,500	12,000	13,500	15,000	15,000	15,000	16,500	17,500
Net income (*N*)	3000	4500	6000	7500	7500	7500	7000	7000
Pay back (month/s)	L	3	3	3	3	3	12	36
Cast benefit ratio	3:1	2.5:1	3.3:1	4.1:1	4.4:1	4.5:1	2.1:1	1.5:1

Tiwari and Tiwari (2016) evaluated different parameters of hybrid photovoltaic-thermal greenhouse solar dryer and found that greenhouse dryer performs well in all weather conditions as it utilizes direct as well as diffused radiation. Energy payback time was 1.23 years and 10 years on the basis of energy and exergy, respectively, which is less compared to other existing systems. CO_2 mitigation and carbon credit earned for 25 years were found to be 81.75 tons and $817.50, respectively, which would contribute to its sustainability.

Boroze et al. (2014) reviewed the inventory and comparative characteristics of dryers used in the sub-Saharan zone. Different types of dryers were taken into account for techno-economic analysis and to find a suitable dryer for adaptation with respect to all possible factors. The selected dryers will be re-employed by the users in line with the investment and maintenance costs and enable them to earn profit for drying operations. From the techno-economic analysis, it is observed that two types of dryers have met those conditions. First one is the traditional simple sun dryer used by families and groups and second one is Atesta gas dryer. The economic analysis showed costs of €0, 01/kg of evaporated water equal to seven percent of daily capital gain for the first system and cost of €0.07/kg of evaporated water equal to nine percent of daily capital gain for the second dryer. The thermo-economic investigation of six different types of dryers are presented in Table 7.

A Life Cycle Net Energy Analysis (LNEA) of solar thermal applications for wood drying with fastidious position of two typical greenhouse type solar kilns (Oxford and Boral) was presented by Hasan and Langrish (2016). The results indicated that net present profit ratio (NPPR), net present energy value (NPEV) and the internal rate of return (IRR) were higher for the Oxford kiln compared to Boral kiln and values are estimated approximately as 37 percent, 55 percent and 47 percent, respectively. However, the present value of energy losses (PVEL) and the discounted energy payback period (DEPP) were smaller for the Oxford kiln by 24 and 85 percent, respectively, as compared to the Boral kiln. The other decision-making parameter such as the NPER, IRR and the DEPP has also influenced much. In this analysis, the consequence of discount rate on the decision-making parameters for the two kilns was also analysed. The results of the three different discount rates obtained from the sensitivity analysis are given in Table 8.

The techno-economic analysis of various solar dryers was reviewed by Kumar et al. (2016). The review mainly concentrated on the solar dryer analysis with overall feasibility of the designed system. The techno-economic analysis normally considered the associated variables like physical characteristics of drying product, design effectiveness, drying climatic conditions, system efficiency, interest rate and operating and maintenance cost as well. They also concluded that the open sun drying and other traditional drying methods are very cost-effective or had no cost as compared to solar drying system. However, the quality of the product developed in those methods is poor and not in position to compete with products available in the market. So, the solar dryers have been identified as effective in the drying process. Also the operation of this solar drying system is

Table 7 Thermo-economic analysis of six dryers (Boroze et al. 2014)

Dryer	Alesla	Geho	Chamber	Shell	Direct cupboard	Cover dryer
Products to be dried	Pineapple	Cassava pasta	Rice	Tomato	Tomato	Maize
Dryer data						
Dryer cost C_{inv} (€)	3050	1220	7630	115	76	6
Life Cycle Δt_{life} (year)	10	5	20	10	10	2
Annual maintenance cost C_{maint} (€/year)	15.3	15.3	7.6	4.5	0.8	0.3
Number of days of dryer use per year $N_{d/y}$ (day/year)	360	180	284	100	100	90
Operating						
Humid product initial mass per cycle m_i (kg/cycle)	120	150	2000	5	2	50
Initial moisture content X_i (dry basis)	400%	223%	32%	1718%	1718%	54%
Final moisture content X_f (dry basis)	14%	10%	12%	12%	12%	15%
Raw material cost per day m_{RM} (€/d)	0.15	0.31	0.14	0.15	0.15	0.15
Dried product price per kg P_{DP} (€/kg)	4.03	3.31	0.92	1.83	1.33	0.27
Drying time Δt_{yc} (day/cycle)	1	2	1	3	1.5	5
Theoretical calculation						
Energy received per day by the dryer E (kJ/day)	575,000	439,900	1,452,300	18,200	18,600	67.700
Water mass evaporable by the dryer E/L_v (kg/day)	256	196	646	8.1	8.3	30.1
Practical calculation						
Final mass of dried product per day m_f (kg/day)	27	26	848	0.1	0.1	7.5
Daily evaporated water mass from the product M_w (kg/day)	92.6	49.5	152	1.6	1.3	2.5
ε = Evaporated water mass/evaporable water mass	36%	25%	23%	19%	15%	8%
Daily turn-over TO_d (€/day)	110	85	777	0.19	0.15	2.05
Drying cost per kg of evaporated water C_{dry} (€/kg)	0.07	0.09	0.01	0.10	0.07	0.01
Daily capital gain CC_d (€/d)	73.7	54	640	-0.14	-036	0.53

(continued)

Table 7 (continued)

Dryer	Alesla	Geho	Chamber	Shell	Direct cupboard	Cover dryer
Part of drying cost in capital gain $C\%_{dry}$ (%)	8%	9%	0.2%	–	–	7%
Dryer cost/daily evaporated water mass (€d/kg)	33	25	50	73	61	2.4
Profit per evaporated water mass (€/kg)	0.7	1.0	4.2	−0.2	−0.4	0.2

Table 8 Persuade of discount rates (Hasan and Langrish 2016)

	Discount rate (4%)		Discount rate (7%) (base case)		Discount rate (10%)	
Parameters	Oxford	Boral	Oxford	Boral	Oxford	Boral
NPEV (GJ)	1515	870	1414	633	885	468
NEPR	4.9	2.27	4.12	1.84	3.44	1.48
IRR (%)	71	37	71	37	71	37
EPBP (years)	2	3.43	2	3.6	2.19	3.78

very simple and competent of producing quality product with the aid of low initial investment.

In developing countries, the most prevalent practice for drying is open sun drying, and steps taken for dissemination of large-scale solar dryers for agriculture-based application will meet severe competition. However, it increases the awareness among end users for their acceptance with respect to exceptionally striking financial achievement. A modest attempt to develop a simple framework to make possible a comparison of the financial viability of solar drying as besides open sun drying has been made and presented by Purohit et al. (2006). The sensitivity analysis shows the effect of uncertainties associated with input variables to find the breakeven price of the solar collector. The analysis also revealed that the breakeven price of collector for tea drying was found to be quite sensitive. The annual repair and maintenance cost has a reasonable effect on the breakeven price of collector. The effect of an uncertainty produced the same effect in the value of daily solar radiation availability on the breakeven price of the solar collector and similar percentage change in the value of overall efficiency of drying. Unit cost with various products used in a solar dryer is presented in Table 9 (Purohit et al. 2006).

Kumar and Kandpal (2005) estimated the potential utilization of solar crop drying for certain cash crops in India. The study revealed that the solar drying has direct effect on saving biofuels and fossil fuels, which is a major energy source for drying in present-day condition for tobacco, tea and coffee. The study also noted that some of these crops are presently being sun-dried in developing countries like India and there is a very huge potential for solar dryer to avoid losses during open

Table 9 Unit cost of drying of various products in solar dryer of 100kg capacity (Purohit et al. 2006)

Product	Moisture content (initial)	Moisture content (final)	Drying time (days)	Annual cost	Unit cost of drying (Rs./kg)	Unit cost of energy used (Rs./MJ)	Wholesale selling price (Rs./kg)
Onion	0.80	0.10	1	121,275	10.11	1.18	44.55
Grapes	0.80	0.15	4	32,150	14.29	1.58	150.00
Chilli	0.80	0.05	1	67,317	8.98	0.95	40.25
Ginger	0.80	0.10	1	21,342	19.92	1.90	55.00
Cabbage	0.80	0.04	2	67,603	5.01	0.53	2.00
Cardamom	0.72	0.06	14	7610	7.10	0.95	403.77
Potato	0.75	0.13	3	30,341	6.07	0.95	2.50
Tomato	0.85	0.10	1	89,765	6.65	0.53	3.00
Pepper	0.71	0.13	1	34,714	5.14	1.05	73.66

sun drying. The major finding also highlighted the importance of solar dryer at the community level to avoid the problem associated with poor utilization by individual farmers. These findings also provide a pathway to improve purchasing power of potential end users.

Janjai et al. (Janjai et al. 2008) studied the performance of a roof-integrated solar drying system (SDS) for drying herbs and spices, and the findings are presented below:

For rosella flowers (200 kg):

Initial moisture content = 90% (wb)
Final moisture content = 18% (wb)
Payback period = 5 years

For chilli (200 kg):

Initial moisture content = 80% (wb)
Final moisture content = 18% (wb)
Payback period = 5 years

Janjai (2012) reported that the payback period was very low (0.6 year) while using greenhouse solar dryer with a capacity of 1000 kg for tomatoes and time taken was observed as 40 h. Janjai et al. (2009) examined the performance of a PV-ventilated solar greenhouse dryer for drying bananas and peeled longans. The result obtained from the study is that the payback period was 2.3 years for both banana and longans with normal drying time of 36 h.

Banout and Ehl (2010) used double-pass solar dryer (DPSD) to dry bamboo and concluded that it is economically and technically suitable for drying of bamboo

under specific conditions. They concluded that the payback period for the said driyer was 1.6 years. The efficiencies of the collector, drying system and pickup were also calculated, and it is approximately 56 percent, 23 percent and 61 percent, respectively. Kamble at al. (2013) dried chilli using a solar cabinet dryer coupled with a gravel bed heat storage system. The analysis revealed that the payback period was 0.6 year with the collector efficiency of 34 percent. They also dried the same with open sun drying, and the drying time was estimated as 104 h which is 48 h more than the solar drying system.

Bala et al. (2009) experimentally studied the solar tunnel dryer for drying mushroom. They examined the capacity of 160 kg mushroom, and the moisture content was reduced from 89 percent to 6 percent (wb) with a span of 8 h. The study estimated the collector, and the drying efficiencies were 34 percent and 52 percent, respectively, and payback period of solar tunnel dryer was 0.7 year. Schirmer et al. (1996) analysed the performance of solar tunnel dryer for bananas and concluded that the payback period was 3 years. They also reported that drying time of bananas using solar tunnel dryer was 36 h and open sun drying was 54 h. Manjarekar and Mohod (2010) presented the economic assessment of solar tunnel dryer for drying peeled prawns. The study revealed that the net present value of investment made in solar dryer for drying of peeled tiny prawns under solar tunnel dryer and in open sun drying system were Rs.2,086,165/– and Rs.85,822/–, respectively. The cost benefit ratio, profitability index and internal rate of return calculated for solar tunnel dryer and open sun drying were 1.21, 11.08 and 23.90 and 1.02, 1.80 and 11.15, respectively. The payback period for solar tunnel dryer and open sun drying was found to be 2.84 and 7.01 years, respectively. The comparative study between solar tunnel dryer and open sun drying is given in Table 10.

The performances of solar drying system with air- and water-based solar collectors as reported by various authors were summarized by Fudholi et al. (2015b) and Fudholi et al. (2015c) and presented in Table 11.

Numerous studies reported on methods used to dry red chilli using solar drying system as listed in Table 12.

Table 10 Economic indicators

S. No.	Indicator	By solar tunnel dryer	By open sun drying
1.	Capital investment	188,353.00	47,603.00
2.	NPW at 10% D.R.	2,274,518.32	133,425.05
3.	NPV at 10% D.R.	2,086,165.32	85,822.05
4.	BCR	1.21	1.02
5.	Profitability index	11.08	1.80
6.	Payback period	2.84	7.01
7.	IRR	23.90	11.15

Table 11 Performances of solar drying system as reported by various authors

Product/load	M (%wb)		Time(h)		Efficieny (%)			PP	References
	M_i	M_t	OS	SDS	η_t	η_d	η_p		
Rosella/200	90	18	–	27	–	–	–	5	Manjarekar and Mohod (2010)
Bamboo/40	96	17	–	33	56	23	61	1.6	
Banana/300	69	30	54	36	–	–	–	3	
Longan/100	81	12	–	27	–	–	–	2.3	
Mushroom/160	89	6	–	8	34	52	–	0.7	
Tomato/1000	54	17	–	40	–	–	–	0.6	
Chilli/–	89	7	104	56	46	34	–	0.6	
Chilli/300	75	10	45	27	–	–	–	2.5	Fudholi et al. (2015b)
Chilli/500	74	9	70	30	–	–	–	2	
Chilli/200	80	18	–	24	–	–	–	5	
Chilli/38	90	10	–	32	64	24	22	3.3	
Mackerel/25	72	16	48	27	–	20	–	1.5	
Banana/100	70	24	–	36	–	–	–	2.3	
Seaweed/40	90	10	–	15	35	27	95	–	
Grapes/320	85	16	–	70	–	30	–	–	

Table 12 Performances of SDSs for chilli as reviewed by (Fudholi et al. 2015b)

Load (kg)	M (% wb)		t (h)		SEC	E	S_t	Efficiency (%)				IP	PP
	M_i	M_t	OS	SDS	(kWh/kg)	(kg/h)	(%)	η_t	η_d	η_p	η_{Ex}	(W)	(year)
24	80	10	65	31	–	–	52	38	6	30	–	–	–
350	76	9	105	50	–	–	52	–	–	–	–	–	–
300	75	10	45	27	–	–	40	–	–	–	–	–	2.5
500	74	9	70	30	–	–	57	–	–	–	–	–	2.0
80	–	–	–	–	–	–		–	28	–	–	–	4.0
118	–	–	–	–	–	–	–	–	28				3.2
115	–	–	–	–	–	–	–	–	28	–	–	–	3.2
38	90	10	–	32	–	–	–	62	24	22	–	–	3.3
40	73	9	–	24	–	–	–	–	21	–	–	–	–
40	80	10	65	33	5.26	0.97	49	28	13	45	57	47	–
200	80	18	–	24	–	–	–	–	–	–	–	–	5

3 Economic Analysis of Solar Dryers

From the literature, it is understood that huge amount of work has been invested for the development of new designs of solar dryers; also further work is in progress with respect to new materials and from economic point of view. The economic viability is a major variable for effective utilization of solar dryers. From the literature, it is observed that three methods were used for the economic

analysis (Sreekumar 2010). The first method is annualized cost method, where the annual cost was the sum of annual cost and maintenance cost, annual salvage value. The total annualized cost of the dryer is dived by the amount of product dried in a year to obtain the cost of drying per unit weight of the dried product. The main disadvantage of this method is that the cost of drying does not fully consider the economics of the solar dryer because it varies little over the entire life of the dryer, say 20 years (only cost incurred is that required to operate the blower and axial fans), while in the case of conventional energy dryers, cost of drying is directly proportional to the increasing cost of conventional energy. Therefore, for evaluating the economic benefits of the solar dryer, it is essential to determine the savings over the life of the dryer.

The savings over the life of the dryer is calculated using the life cycle savings method. The first step is to determine the savings per drying day for the solar drying system in the present year. Based on that, the present worth of annual savings over the life of the system is calculated. If the payback period of the system is small, people will come forward to acquire the solar drying system, and if it is long, people may not prefer to purchase even if substantial long-term savings are possible. In this context, the third method, namely, payback period, is invented to find the optimum return time from the investment. A similar approach was also employed by Sreekumar et al. (2010) with pertinent equations for economic analysis of a solar dryer for domestic use.

3.1 Annualized Cost Method

The annualized cost method is to compare the cost of drying for solar drying system and other drying systems using the conventional energy sources. In this method, the annualized cost of the dryer is divided by the amount of product dried per year.

3.2 Annualized Cost

Annualized cost is the cost per year of retaining, functioning and sustaining an asset over its lifetime. The annualized cost of a dryer is intended by

$$AC = C_{\text{acc}} + C_{\text{mc}} - S_a + C_{\text{rfc}} + C_{\text{rec}} \tag{1}$$

$$C_{\text{acc}} = C_{\text{ccd}} \times \text{CRF} \tag{2}$$

$$S_a = S \times \text{SFF} \tag{3}$$

where CRF is the capital recovery factor and it is defined as

$$\mathrm{CRF} = \frac{i(1+i)^n}{(1+i)^n - 1} \tag{4}$$

and SFF is the salvage fund factor and it is defined as

$$\mathrm{SFF} = \frac{i}{(1+i)^n - 1} \tag{5}$$

The cost of drying per kg of dried product is defined by

$$CD_{\mathrm{kg}} = \frac{AC}{M_{year}} \tag{6}$$

(i) Solar dryer: the quantity of product dried in the solar dryer per year, M_{year} is calculated using

$$M_{year} = \frac{M_{\mathrm{dry}} D_{year}}{D_b} \tag{7}$$

For general assumption, the annual running fuel cost of the solar dryer is zero. C_{rc} is the running cost for fans in the dryer:

$$C_{\mathrm{rc}} = R_a \times W_p \times C_{\mathrm{ee}} \tag{8}$$

R_a is the number of hours the blower and fans are running each year, W_p is the rated power consumption of fans and C_{ee} is the unit charge for electricity.

(ii) Electric dryer: the product dried by solar dryer is taken into account, and the same quantity is dried using electric dryer, and the corresponding annual running fuel cost is calculated.

The annual running cost, $C_{\mathrm{rfc}}$of the electric dryer, is given by

$$C_{\mathrm{rfc}} = M_{year}\left[\left(\frac{m_{\mathrm{oi}}}{100}\right)\frac{LC_{\mathrm{ee}}}{\eta_e \times 3600}\right] \tag{9}$$

where m_{oi} is the moisture content in dry basis and is given by

$$m_{\mathrm{oi}} = \left(\frac{M_{\mathrm{fre}} - M_{\mathrm{dry}}}{M_{\mathrm{dry}}}\right) \times 100 \tag{10}$$

3.3 Life Cycle Cost Savings

In the life cycle savings method, the first step is to calculate the savings per drying day for the solar dryer in the base year.

3.4 Savings per Day

The cost of fresh product per kg of dried product is found out using the following equations:

$$C_{\text{dry}} = C_{\text{fre}} \times \frac{M_{\text{fre}}}{M_{\text{dry}}} \tag{11}$$

$$C_{drys} = C_{\text{dry}} + CD_{\text{kg}} \tag{12}$$

$$B_{\text{kg}} = C_{\text{bdp}} - C_{drys} \tag{13}$$

$$B_b = B_{\text{kg}} \times M_{\text{dry}} \tag{14}$$

$$B_d = \frac{B_b}{D_b} \tag{15}$$

3.5 Present Worth of Annual Savings

For the life of the system, the annual savings (B_j)for drying a product in the jth year are obtained using Eq. (16), and the present worth of annual savings in the jth year is obtained from Eq. (17):

$$B_j = B_d \times D_{year} \times (1 + r)^{j-1} \tag{16}$$

$$P_{was} = F_{\text{pwf}} \times B_j \tag{17}$$

$$F_{\text{pwf}} = \frac{1}{(1 + i)^j} \tag{18}$$

The life cycle saving = present worth of the annual savings over the life of the system.

3.6 Payback Period

This is the simplest method of evaluating the investment proposals in a systematic way. Payback period is the period (i.e. number of years) necessary to recover the original cash outlay invested in a project. It is one of the simplest savings

assessment techniques used over the decades. The payback period is useful from a risk analysis viewpoint, since it gives a quick picture of the amount of time that the initial investment will be at risk. Unlike net present value method and internal rate of return method, payback method does not consider the present value of cash flows. It is the period during which the initial outlay is recovered in the form of cash benefits. The payback period is calculated by dividing the initial investment by the annual cash flows.

The payback period (N) is calculated from

$$N = \frac{\ln\left(1 - \frac{C_{\text{ccd}}}{B_1}(i - r)\right)}{\ln\left(\frac{1+r}{1+i}\right)} \tag{19}$$

where

AC – annualized cost of dryers (Rs)
B_{b} – savings per batch for solar dryer (Rs./kg)
B_j – annual savings for domestic solar dryer in the jth year (Rs.)
B_{kg} – savings per kg in comparison to branded product for solar dryer (Rs./kg)
B_d – savings per day for domestic solar dryer in the jth year (Rs.)
C_{acc} – annualized capital cost (Rs.)
C_{bdp} – selling price of branded dried product (Rs./kg)
C_{ee} – cost per kWh of electric energy (Rs./kWh)
C_{dry} – cost of fresh product per kg of dried product (Rs./kg)
C_{drys} – cost per kg of dried product for domestic solar dryer (Rs./kg)
C_{fre} – cost per kg of fresh product (Rs./kg)
CD_{kg} – cost of drying per kg of dried product in dryer (Rs./kg)
C_{mc} – annualized maintenance cost (Rs.)
C_{rfc} – annual running fuel cost (Rs.)
C_{rec} – running electricity cost of fans in the dryer (Rs.)
C_{ccd} – capital cost of dryer (Rs.)
D_b – number of drying days per batch
D_{year} – number of days of use of domestic dryer per year
F_{pwf} – present worth factor for jth year
CRF – capital recovery factor
SFF – salvage fund factor
i – rate of interest on long-term investment
M_{dry} – mass of dried product removed from solar dryer per batch (kg)
m_{oi} – moisture content (dry basis) (%)
M_{fre} – mass of fresh product loaded in solar dryer per batch (kg)
M_{year} – mass of product dried in the dryer per year (kg)
n – life of solar dryer (year)
R_a – annual running hours of blower and axial fans
S – salvage value (Rs.)
S_a – annualized salvage value (Rs.)

W_p – rated power of electric blower and axial fans (kW)
η^e – efficiency of electric dryer (%)

3.7 Net Present Value

Net present value is used to compare the present value of the future benefits with the present value of the investment. This is done by discounting the cash flows by an appropriate rate of interest. When the present value of investment, is more than the present value of benefits the proposal for investment should be discarded. Even if the life span of the project differs, comparison is possible by just artificially extending the life of those projects which have short span to the extent of other project lives.

The formula for finding out the total present value of all cash inflows generating out of an investment may be stated as follows:

$$\text{NPV} = \sum_{t=1}^{t=n} \frac{B_t - C_t}{(1+i)^t} \tag{20}$$

where B_t = benefit in each year (US$), C_t = salvage value or cost in each year (US $), $t = 1, 2. \ldots n$ and i = discount rate (%)

3.8 Salvage Value

For any product, life is designed or assumed numerically say, for example, 20 years or 25 years. After that period, the value of product is calculated using a salvage value. It is defined as the approximate resale value of an asset after its economic life. Salvage value is based on the initial investment of the asset/project. The value is based on the estimation of the asset's value, or the value can be determined by a regulatory body. For numerical calculation, the salvage value of the system is taken as S and the sinking fund factor is given as follows:

$$\text{SFF} = \left[\frac{i}{(1+i)^n - 1}\right] \tag{21}$$

3.9 Capital Recovery Factor (CRF)

Capital recovery factor is earning back the initial capital amount invested for the product development. Normally this factor converts a present value into a stream of

identical annual payments in excess of a particular time, at a precise interest rate. The CRF can be interpreted as the amount of equal (or uniform) payments to be received for n years such that the total present value of all these equal payments is equivalent to a payment at present. If interest rate is "i" and it is denoted as

$$\mathrm{CRF} = \left[\frac{i(1+i)}{(1+i)^n - 1}\right] \tag{22}$$

3.10 Cost Benefit Ratio

A cost benefit ratio is a discounted method of capital budgeting applied to identify the relationship between the cost and benefits of a proposed project. It explains about the relationship between all possible benefits and costs that are discounted to the current time factor. It is arrived by dividing the sum of discounted value of benefits by the sum of discounted value of the costs. In other words, it is the ratio between the present worth of the benefit stream and the present worth of the cost stream. The cost benefit ratio as a selection criterion for acceptability of a project specifies a value of one or more. The ratio is computed by taking the present worth of the gross benefit less associated cost and then dividing it by the present worth of the project cost. The cost of the project is the sum of installation costs, operation and maintenance cost and replacement costs. Cost benefit ratio can be computed mathematically employing the following formula:

$$\text{Benefit} - \text{Cost ratio (BCR)} = \frac{\sum_{t=1}^{t=n} \frac{B_t}{(1+i)^t}}{\sum_{t=1}^{t=n} \frac{C_t}{(1+i)^t}} \tag{23}$$

3.11 Internal Rate of Return (IRR)

Internal rate of return is again a discounted method of capital budgeting technique that considers the time value of money. This method is employed to identify the discount rate that equates the present value of benefits to that of the present value of costs. It is the rate at which the present value of cash inflows is equal to the present value of cash outflows of a project. At internal rate of return, the net present value of an investment is zero. A trial-and-error method is normally employed to find the IRR such that the net present value becomes zero:

$$\sum_{t=1}^{t=n} \frac{B_t - C_t}{(1+i)^t} = 0 \tag{24}$$

4 Energy Analyses

The annual energy can be calculated by summing up all the monthly available energy. Further, embodied energy is calculated which is used in construction of experimental setup. Payback period and carbon credit earned for the system have been calculated with the help of embodied energy and thermal energy gain throughout the year (Tiwari and Tiwari 2016).

4.1 Energy Payback Time (EPBT)

The energy payback time is mainly dependent on the energy utilized or spent to make the materials used for manufacturing of solar drying system and its components, i.e. embodied energy and the annual energy yield (output) obtained from the solar system. Energy payback time is the total time duration which is required to recuperate the total energy given to make the resources (embodied energy) used for construction of solar dryer. It is defined as the ratio of embodied energy and the annual energy output from the system, which can be written as

$$\text{EPBT} = \frac{\text{Embodied Energy}\,(E_{\text{in}}, \text{kwh})}{\text{Annual Energy output}\left(E_{\text{out}}, \frac{\text{kwh}}{\text{year}}\right)} \tag{25}$$

4.2 Carbon Dioxide (CO_2) Emission

The average CO_2 equivalent intensity for electricity generation from coal is approximately 0.98kg of CO_2 per kWh at the source.

$$\text{Annual } CO_2 \text{ emission/year} = \frac{E_{\text{in}}}{L} \times \frac{1}{1 - L_a} \times \frac{1}{1 - L_t} \times 0.98\,\text{kg} \tag{26}$$

where E_{in} is embodied energy, L is the life of the system, L_t is transmission losses and L_a is domestic appliances losses.

4.3 Net CO_2 Mitigation

The net CO_2 mitigation over the lifetime of the system = total CO_2 mitigation – total CO_2

$$Emission = (E_{aout} \times L - E_{in}) \times \frac{1}{1 - L_a} \times \frac{1}{1 - L_t} \times 0.98\,\text{kg} \tag{27}$$

where

L = No. of year (5, 10, 15, 20, 25 years)
E_{aout} = total energy out per year (kWh/year)

4.4 Carbon Credit

If CO_2 emission is being traded at 10 US$ per ton of CO_2 mitigation, then the carbon credit earned by the system is obtained as follows:

$$The\ \ carbon\ \ credit\ \ earned = \text{Net}\ \ CO_2\ \ mitigation \times 10\text{US\$} \tag{28}$$

The techno-economic studies of various solar dryers developed over the years by different scientists are listed in Table 13.

5 Conclusion

Solar drying of various products is one of the most important potential applications of solar energy. High moisture content in the agricultural products would lead to microbial spoilage and, hence, it is essential to remove the free water available in order to avoid the activities of harmful organisms. Open solar drying has been used by the farmers from time immemorial. However, the hygiene of such open drying system is still a question. Many artificial drying systems are available but still are not economically feasible. Introduction of PV technology and hybrid technology in drying agricultural produce provides solution to the problems of both artificial dryers and open solar drying systems. Moreover, solar dryer would definitely be a best option for future energy demand since it is superior in terms of availability, capacity and efficiency compared to other renewable energy sources.

Zarezade and Mostafaeipour (2016) suggested that creating awareness among individuals, consumers, managers and officials about the solar drying systems and their cost-effectiveness would encourage more investments. On the other hand, the more private investors are attracted in these projects, the more would be the implementation of such projects, including acquisition of updated knowledge, design and manufacturing technology. This will ultimately increase the efficiency of solar drying systems. Therefore, it is necessary to improve the awareness of the general public and especially farmers about the benefits of using solar dryers which would increase the readiness to accept the solar dryers. As a result, these systems

Table 13 Techno-economic study of various solar dryers

S. No.	Authors	Year	Remarks
1.	Zarezade and Mostafaeipour (2016)	2016	They developed the model which clearly pointed the important factors and risks for effective utilization of solar dryers. The analysis revealed the issues related to designing, development and implementation of such system in real-time implementation process
2.	Hasan and Langrish (2016)	2016	Invented the new methodology to identify the performance of solar dryers in terms of life cycle energy effectiveness in present value term.
3.	Fudholi et al. (2015c)	2015	Presented the techno-economic analysis of solar drying system with water-based solar collectors in Malaysia and concluded that payback period was 1 year. The developed solar drying system with water-based solar collectors has produced higher performance and temperature for drying application
4.	Elkhadraoui et al. (2015)	2015	Experimentally investigated the novel mixed-mode solar greenhouse dryer with forced convection. The developed solar dryer was more effective to dry red pepper and sultana grapes
5.	Aravindh and Sreekumar (2014)	2014	Presented the techno-economic analysis of a solar matrix collector designed for various drying applications. The major economic factors of annual cost, net present value, present worth of annual savings and present worth of cumulative savings are systematically valued for analysis
6.	Boroze et al. (2014)	2014	Reviewed the various types of solar dryers with respect to techno-economic analysis to scientifically identify the most effective solar dryer. The results clearly stated the dissatisfaction of the end users and suggested the possible methods for adaptation of solar dryers. The social, economic and physical criteria were found to be the major factors for the implementation of solar dryers
7.	Pirasteh et al.(2014)	2014	A complete review was carried out to find the role of drying system in industry and agriculture, the energy consumption capacity and the availability of the required energy for the products to be dried. The major positive effect of solar drying is positive economic development, reduction in environmental degradation and social effects on end users
8.	Panwar et al. (2014)	2014	In their article, studied the economic feasibility of two vegetable crops cultivated in a naturally ventilated greenhouse. The major economic indicators like NPV, CBR, PP and IRR for these crops on the basis of year-round cultivation were presented. The study revealed that the low-cost technologies would be more suitable for farmers
9.	Eswara and Ramakrishnarao (2013)	2013	Reported that Solar drying system is the effective drying method with low drying cost. They concluded that the government policies and international agencies play an important role for the development of solar drying system in large-scale industrial system

(continued)

Table 13 (continued)

S. No.	Authors	Year	Remarks
10.	Rahman et al. (2013)	2013	Developed the solar-assisted heat pump drying system and optimized the evaporator and air collector area from economic point of view. The model focused on the life cycle cost analysis and the payback period of four years
11.	Nayak et al. (2012)	2012	Conducted an economic investigation of hybrid photovoltaic thermal integrated solar dryer. The study concluded that the total energy payback period for hybrid PVT solar dryer was 5.6 years, which was much less than the expected life of the dryer
12.	Fudholi et al. (2010)	2010	Reviewed the solar dryers for agricultural and marine products and listed the sample prices of various solar dryers developed over the years around the world
13.	Purohit et al. (2006)	2006	Comparative study was conducted for solar drying system with open sun drying in terms of financial feasibility. The operational and financial parameters identified the effectiveness
14.	Singh et al. (2006b)	2006	Designed and tested the multi-shelf design, consisting of three perforated trays arranged one above the other. They concluded that the payback period was low (<2 years) as compared to the life of the dryer (20 years). This general observation states that the dryer will dry the product free of cost virtually during its complete life period
15.	Purohit and Kandpal (2005)	2005	Presented a new techno-economic assessment of solar dryers for different crops. The analysis is based on the different commercial fuel savings and their breakeven points
			Effect on mitigation of CO_2 emissions is also an important factor these days due to Kyoto protocol. Its effect on the system financial performance has also been analysed in the study
16.	Kumar and Kandpal (2005)	2005	Estimated the potential utilisation of solar dryers in cash crops such as tobacco, tea and coffee in India. The solar drying system effectively saved the CO_2 emission mitigation with respect to different conventional fuels used for drying applications
17.	Lhendup (2005)	2005	The solar dryer developed in Khao-Kho, Thailand, was examined technically and economically for possible implementation of the same in Bhutan. The developed solar dryer system was found inexpensive to dry chilli, and the comparative study identified that the electric drying system was found cheaper to dry beef
18.	Palaniappan and Subramanian (1998)	1998	The study presented the economic analysis of 212 m^2 solar dryer in tea factory in operation period for a period 2.75 years. The developed economic model systematically considered the subsidy provided by the government and external agencies. The results revealed that the payback period was 2–4 years in two different cases

(continued)

Table 13 (continued)

S. No.	Authors	Year	Remarks
19.	Mumba (1995)	1995	Economic analysis of a photovoltaic, forced convection and solar grain dryer was presented. The dryer had a payback period of less than one year and was cost-effective
20.	Sodha et al.(1991)	1991	Presented the techno-economic analysis of various types of dryers with different solar energy collectors. Based on the analysis, it was observed that the plastic collectors used for drying with a lifespan of 5–10 years were cheaper than other collectors
21.	Dang and Bansal (1985)	1985	Reviewed various economic approaches to assess solar energy drying systems. Results revealed that the developed solar drying system cost was be less than that of conventional energy system
22.	Govind and Tiwari (1984)	1984	Economic investigation of some solar energy systems was discussed with the adaptation of uniform cost analysis. Paseras dryers used for drying coffee were identified as very cheap as compared to other dryers

could be promoted between the specific and general consumers, more easily. The more the experience in the design, construction, operation and management of solar dryer's system, the more the chances of success would be of solar dryer-related projects. In this chapter, a detailed description of the economic analysis of solar dryers has been presented. It is concluded that it is mandatory to optimize each and every step involved in solar drying for better techno-economic feasibility. The developments in economics of various solar dryers were also summarized with remarks.

References

Aravindh MA, Sreekumar A (2014) Design and techno economic analysis of a solar matrix collector for drying application. Res Civil Environ Eng 2(3):160–171

Bala BK, Morshed MA, Rahman MF (2009) Solar drying of mushroom using solar tunnel dryer. In: International solar food processing conference, pp. 1–11

Banout J, Ehl P (2010) Using a double pass solar dryer for drying of bamboo. J Agric Rural Dev 111(2):119–127

Boroze T, Desmorieux H, Meot JM, Marouze C, Azouma Y, Napo K (2014) Inventory and comparative characteristics of dryers used in the sub-Saharan zone: criteria influencing dryer choice. Renew Sust Energ Rev 40:1240–1259

Dang A, Bansal NK (1985) Economic analysis of solar systems. Energy Convers Manag 25 (2):159–169

Elkhadraoui A, Kooli S, Hamdi I, Farhat A (2015) Experimental investigation and economic evaluation of a new mixed-mode solar greenhouse dryer for drying of red pepper and grape. Renew Energy 77:1–8

Eswara AR, Ramakrishnarao M (2013) Solar energy in food processing – a critical appraisal. J Food Sci Technol 50(2):209–227

Fudholi A, Sopian K, Ruslan MH, Alghoul MA, Sulaiman MY (2010) Review of solar dryers for agricultural and marine products. Renew Sust Energ Rev 14:1–30

Fudholi A, Otman MY, Ruslan MH, Yahya M, Zaharim A, Sopian K (2015a) Techno-economic analysis of solar drying system for seaweed in Malaysia. Recent Res Energy Environ Landsc Archit 1:89–95

Fudholi A, Sopian K, Bakhtyar B, Gabbasa M, Othman MY, Ruslan MH (2015b) Review of solar drying systems with air based solar collectors in Malaysia. Renew Sust Energ Rev 51:1191–1204

Fudholi A, Sopian K, Bakhtyar B, Gabbasa M, Bakhtyar B, Yahya M, Ruslan MH, Mat S (2015c) Techno-economic of solar drying systems with water based solar collectors in Malaysia: a review. Renew Sust Energ Rev 51:809–820

Govind FR, Tiwari GN (1984) Economic analysis of some solar energy systems. Energy Convers Manag 24(2):131–135

Haque N, Somerville M (2013) Techno-economic and environmental evaluation of biomass dryer. Procedia Eng 56:650–655

Hasan M, Langrish TAG (2016) Time-valued net energy analysis of solar kilns for wood drying: a solar thermal application. Energy 96:415–426

Hollick JC (1999) Commercial scale solar drying. Renew Energy 16:714–719

Janjai S (2012) A greenhouse type solar dryer for drying for small scale dried food industries: development and dissemination. Int J Energy Environ 3(3):383–398

Janjai S, Srisittipokakun N, Bala BK (2008) Experimental and modelling performances of roof-integrated solar drying system for drying herbs and spices. Energy 33:91–103

Janjai S, Lamlert N, Intawee P, Mahayothee B, Bala BK, Nagle M (2009) Experimental and simulated performance of a PV-ventilated solar greenhouse dryer for drying of peeled longan and banana. Sol Energy 83:1550–1565

Kamble AK, Pardeshi II, Singh PL, Ade GS (2013) Drying of chilli using solar cabinet dryer coupled with gravel bed heat storage system. J Food Res Technol 1(2):87–94

Kumar M (2016) Sunil Kumar Sansaniwal and Pankaj Khatak. Progress in solar dryers for drying various commodities. Renew Sust Energ Rev 55:346–360

Kumar A, Kandpal TC (2005) Solar drying and CO_2 emissions mitigation: potential for selected cash crops in India. Sol Energy 78:321–329

Lhendup T (2005) Technical and financial feasibility of a solar dryer in Bhutan. Energy Sustain Dev 9(4):17–24

Manjarekar RG, Mohod AG (2010) Economic evaluation of solar tunnel dryer for drying peeled prawns. Int J Agric Eng 3(1):68–72

Mumba J (1995) Economic analysis of a photovoltaic, forced convection, solar grain drier. Energy 20(9):928–928

Mustapha MK, Salako AF, Ademola SK, Adefila IA (2014) Qualitative performance and economic analysis of low cost solar fish driers in Sub-Saharan Africa. J Fish 2(1):64–69

Nayak S, Naaz Z, Yadav P, Chaudhary R (2012) Economic analysis of hybrid photovoltaic-thermal (PVT) integrated solar dryer. Int J Eng Invent 1(11):21–27

Palaniappan C, Subramanian SV (1998) Economics of solar air pre-heating in south Indian tea factories: a case study. Sol Energy 63(1):31–37

Panwar NL, Koushik SC, Kothari S (2014) Cost-benefit and systems analysis of passively ventilated solar greenhouse for food production in arid and semi-arid regions. Environ Syst Decis 34:160–167

Pirasteh A, Saidur R, Rahman SMA, Rahim NA (2014) A review on development of solar drying applications. Renew Sust Energ Rev 31:133–148

Purohit P, Kandpal TC (2005) Solar crop dryer for saving commercial fuels: a techno economic evaluation. Int J Ambient Energy 26(1):3–12

Purohit P, Kumar A, Kandpal TC (2006) Solar drying vs open sun drying: a framework for financial evaluation. Sol Energy 80:1568–1579

Rahman SMA, Saidur R, Hawlader MNA (2013) An economic optimization of evaporator and air collector area in a solar assisted heat pump drying system. Energy Convers Manag 76:377–384
Schirmer P, Janjai S, Esper A, Smitabhindu R, Muhlbauer W (1996) Experimental investigation of the performance of the solar tunnel dryer for drying bananas. Renew Energy 7(2):119–129
Sharma VK, Colangelo A, Spagna G, Pistocchi F (1994a) Preliminary economic appraisal of solar air heating system used for drying of agricultural products. Energy Convers Manag 35 (2):105–110
Singh PP, Singh S, Dhaliwal SS (2006a) Multi-shelf domestic solar dryer. Energy Convers Manag 47:1799–1815
Sodha MS, Chandra R, Pathak K, Singh NP, Bansal NK (1991) Techno-economic of typical dryers. Energy Convers Manag 31(6):509–513
Sreekumar A (2010) Techno-economic analysis of a roof-integrated solar air heating system for drying fruit and vegetables. Energy Convers Manag 51:2230–2238
Tiwari S, Tiwari GN (2016) Exergoeconomic analysis of photovoltaic-thermal (PVT) mixed mode greenhouse solar dryer. Energy 114:155–164
Toshniwal U, Karale S (2013) A review paper on solar dryer. Int J Energy Res 3:869–902
VijayaVenkataRaman S, Iniyan S, Goic R (2012) A review of solar drying technologies. Renew Sust Energ Rev 16:2652–2670
Zarezade M, Mostafaeipour A (2016) Identifying the effective factors on implementing the solar dryers for Yazd province, Iran. Renew Sust Energ Rev 57:765–775

Economic Analysis of Various Developed Solar Dryers

Om Prakash, Saurabh Ranjan, Anil Kumar, and Ravi Gupta

Abstract In the era energy in security, the solar emerges as alternative source of renewable energy. Although it is unavailable at night, it provides sufficient energy in the daytime. In the region of tropical and subtropical countries, solar drying system is the most mesmerizing and utile application of solar energy. In order to make solar dryer popular and easy to use, it is very important to do its economic analysis. In this chapter, the main aim is to discuss various methodologies to do the economic analysis of the solar dryers such as annualized cost, capital cost, savings earn in its entire working life, and payback period with and without interest. It is being overserved that the most of the solar dryer have payback period less than 4 years and their life span is about 20 years.

Keywords Solar energy • Solar dryer • Economic analysis • Payback period

1 Introduction

Solar energy application attracts many nations worldwide for mitigation of global warming as well as energy scarcity. Solar energy conversion process and solar industry deals with high investment cost that tends economic problem for under-developed and developing countries (Prakash and Kumar 2013) Proper site survey,

O. Prakash
Department of Mechanical Engineering, Birla Institute of Technology, Ranchi, India

S. Ranjan
Department of Mechanical Engineering, Birla Institute of Technology, Ranchi, India

Centre for Energy Engineering, Central University of Jharkhand, Ranchi, India

A. Kumar (✉)
Department of Energy (Energy Centre), Maulana Azad National Institute of Technology, Bhopal 462003, Madhya Pradesh, India
e-mail: anilkumar76@gmail.com

R. Gupta
Department of Agricultural Engineering, Rajmata Vijayaraje Scindia Krishi Vishwavidyalaya, Gwalior, India

© Springer Nature Singapore Pte Ltd. 2017

O. Prakash, A. Kumar (eds.), *Solar Drying Technology*, Green Energy and Technology, DOI 10.1007/978-981-10-3833-4_17

market survey, load management, demand side management, policies, economic factors, etc. should be analyzed before manufacturing and installing solar thermal applications such as solar dryer, solar pond, solar collectors, and various solar power generation systems. The main purpose of economic analysis refers to maximizing net benefit or minimizing cost for a given level of benefits. In many cases, it is being seen that the techniques for energy conversion may be quite efficient in engineering terms but it can be financially inferior to another option with less efficient technology. Thus, economic or financial efficiency is different from engineering efficiency. The financial/economic analysis is vital for introducing any product (gadget, device) in the market. This analysis also helps to make the product available for maximum people, in accordance with mankind and environmental implication (Adeaga et al. 2015).

Techno-economic assessment of solar dryer is based on some factors. These are as follows:

- Primary investment regarding solar drying construction
- Primary cost for supplement heating, if applicable
- Functioning cost
- The cost of yearly maintenance of the system
- Finally, annual cost of crops to be dried
- Life of solar dryer and its salvage value

A software program is also used to predict performance and economic analysis of solar dryer (Prakash and Kumar 2014). In order to do dryer performance analysis, the following parameters, description, and modeling are required, namely:

- Climatic data: Meteorological condition of the site is required for economic assessment of solar drying system. Average value of global radiation, ambient temperature, and wind speed data is used in the economic evaluation.
- Load description: Magnitude and distribution of the load are important to analyze for the economic performance of the system. It maximizes the use of the energy available in the dryer.
- Mathematical modeling: Mathematical equations are used to describe the performance of different components of the solar dryer (Adeaga et al. 2015).

2 Methodologies for Economic Analysis of Solar Dryer

In this section, some of the most important methodologies of economic analysis for solar dryer are being discussed, which are as follows (ELkhadraoui et al. 2015):

- Annualized cost method
- Life cycle saving
- Payback period

Annualized cost method consists of details of study regarding the comparison between drying cost per unit weight of product in the solar dryer and the drying cost per unit weight of product in an electric dryer. The cost of drying the product by using solar energy remains the same in the entire life of the solar dryer. Annual fluctuation of drying cost is observed in the electric dryer which is a result of an abrupt rise in conventional fuel cost. It is essential to determine the life cycle saving for analysis of the economic benefit of solar dryer. Therefore, one more method is needed to calculate life cycle savings, i.e., "life cycle analysis." In the life cycle analysis, how much savings earned in each drying day in the base year is calculated. Then**,** the annual saving's present worth of system life should be determined, namely, "payback period." Systems pertaining to long payback period are generally discarded by people. Hence, the payback period is the benchmark in the economic analysis of solar dryer (Sreekumar 2010).

2.1 Annualized Cost Method

Annualized cost method is used to determine drying cost and comparative analysis of drying cost employing different energy resources. The drying cost per unit weight of dried product is obtained by dividing annualized cost of the dryer to the amount of dried product in a year (Sreekumar 2010). Equation 1 shows how to calculate the annualized cost of dryer (C_a):

$$C_a = C_{ac} + C_{am} + V_{as} + C_{af} + C_{ae} \tag{1}$$

Salvage value (V_{as}) and yearly capital cost (C_{ac}) are expressed in Eqs. 2 and 3, respectively:

$$C_{ac} = C_{cc} \times F_{cr} \tag{2}$$

$$V_{as} = V_s \times F_{sr} \tag{3}$$

Expressions for salvage fund factor (F_{sr}) and capital recovery factor (F_{cr}) are given in Eqs. 4 and 5, respectively (ELkhadraoui et al. 2015):

$$F_{cr} = \frac{i(1+i)^n}{(1+i)^n - 1} \tag{4}$$

$$F_{sr} = \frac{i}{(1+i)^n - 1} \tag{5}$$

In Eq. 1, the yearly maintenance cost is taken as a static percentage of year-wise capital cost. The drying cost per kg of dried product can be determined as in Eq. 6:

$$C_{\mathrm{dp}} = \frac{C_{\mathrm{a}}}{M_{\mathrm{dp}}} \tag{6}$$

Equation 7 is used to determine the mass of product dried annually in the solar dryer (M_{dp}):

$$M_{\mathrm{dp}} = \frac{M_{\mathrm{pr}} N_{\mathrm{d}}}{N_{\mathrm{dd}}} \tag{7}$$

The cost of fuel which is spent in the operation of the solar dryer is zero except the cost required for running blower in the dryer. C_{re} is the cost of operation for the blower in the dryer:

$$C_{\mathrm{re}} = N_{\mathrm{h}} \times W \times C_{\mathrm{e}} \tag{8}$$

The fuel cost associated with the operation of the electric dryer to dry the product. Electric dryer's year-wise running fuel cost (C_{rf}) may thus be enumerated by following Eq. 9:

$$C_{\mathrm{rf}} = M_{\mathrm{dp}} \left[\left(\frac{m_{\mathrm{db}}}{100} \right)_{\eta_{\mathrm{e}}} \frac{h_{\mathrm{l}} C_{\mathrm{ee}}}{\eta_{\mathrm{ed}} \times 3600} \right] \tag{9}$$

where m_{dp} is the moisture content in dry basis that can be determined in Eq. 10:

$$m_{\mathrm{db}} = \left(\frac{M_{\mathrm{fp}} - M_{\mathrm{dp}}}{M_{\mathrm{dp}}} \right) \times 100 \tag{10}$$

Operational economic expenditure of fan should be considered.

2.2 *Life Cycle Savings*

Life cycle savings method explains how much savings occur in each drying day for the solar dryer; after this, it determines the present worth of annual saving throughout the life of solar dryer.

2.2.1 Savings per Day

Deduction of fresh product's cost per kg of dried product by using Eq. 11 (ELkhadraoui et al. 2015):

$$C_{\mathrm{fd}} = C_{\mathrm{fp}} \times \frac{M_{\mathrm{fp}}}{M_{\mathrm{dp}}} \tag{11}$$

Fresh product's cost (C_{dp}) and drying cost per kg of dried product (C_{s}) are constitute to the cost of 1 kg of dried product (C_{ds}):

$$C_{\mathrm{dp}} = C_{\mathrm{fp}} + C_{\mathrm{s}} \tag{12}$$

If the solar dryer product quality is the same as the commercially available product quality, thence, the saving per kilogram of dried product (S_{kg}) occurring in the reference year due to usage of solar dryer is expressed in Eq. 13:

$$S_{\mathrm{kg}} = C_{\mathrm{b}} - C_{\mathrm{ds}} \tag{13}$$

Now batchwise saving (S_{b}) and the saving on drying days' basis (S_{d}) in the base year can be obtained by using Eqs. 14 and 15, respectively:

$$S_{\mathrm{b}} = S_{\mathrm{kg}} \times M_{\mathrm{d}} \tag{14}$$

$$S_{\mathrm{d}} = \frac{S_b{}^{b}}{D_{\mathrm{b}}} \tag{15}$$

2.2.2 Annual Saving's Present Worth

In lieu of system's life assessment, year-wise savings are obtained for desiccating the typical product using Eq. 16:

$$S_j = S_{\mathrm{d}} \times D \times (1+i)^{j-1} \tag{16}$$

Equation 17 is used for calculation of present worth of savings in *j*th year:

$$P_j = F_{pj} \times S_j \tag{17}$$

The present worth factor in the *j*th year may be computed as in Eq. 18:

$$F_{pj} = \frac{1}{(1+i)^j} \tag{18}$$

The total present worth of system's life savings, i.e., savings of life cycle, is obtained by summation of year-wise saving's present worth over the time period of the system.

2.3 Payback Period

In general, payback period is the time required to recover its initial investment. Payback period is also called as payment time, payback time, or payout time, but the motto is to find the time required to recover the gross initial investment. Payback period is one of the criteria for profitability. It is categorized into payback period without interest and payback period with interest (Lin et al. 2015).

2.3.1 Payback Period Without Interest

Here, working capital is not included in evaluating payment time without interest. It is important to know depreciation; thence, tax depreciation is the loss in value of a physical asset such as equipment and machinery with the passage of time and uses:

$$\text{Taxes} = (\text{Income} - \text{Deduction}) \times \text{Tax rate} \tag{19}$$

2.3.2 Payout Time with Interest

This method allows for a return on investment and is subjected to variations. The variation includes an interest in working capital. Here, the following relation computes an investment for the year:

$$\begin{aligned}\text{Investment for year} = {} & (\text{Investment for previous year}) \\ & - (\text{Cash Flow} - \text{Interest rate for previous year})\end{aligned} \tag{20}$$

Equation 21 is used to determine the payback period (P_n) (Prakash and Kumar 2014):

$$P_n = \frac{\ln\left(1 - \frac{C_{cc}}{S_1}(i_{\text{interest}} - i_{\text{inflation}})\right)}{\ln\left(\frac{1 + i_{\text{interest}}}{1 + i_{\text{inflation}}}\right)} \tag{21}$$

2.3.3 Dynamic Method for Payback Period

In dynamic method, the influence of inflation is also considered for calculating payback time. Payback is obtained if accumulated savings (S) satisfy the sum of capital investment which includes yearly interest (I) and accumulated cost (E) as shown in Eq. 22:

$$\boldsymbol{S = I + E} \tag{22}$$

The year-wise accumulated savings are obtained by using Eq. 23:

$$S = \frac{(1+r)^n - (1+e)^n}{r-e} D \tag{23}$$

where

r is annual interest.
e is yearly inflation rate.
n is number of years.

For solar dryers, D is the price of substituted conventional energy, and for natural solar dryer, D is the net income.

The first investment cost (C) associated with interest rate in n years is obtained as given in Eq. 24:

$$I = C(1+r)^n \tag{24}$$

The accumulated yearly costs for equipment are calculated by using Eq. 25:

$$E = \frac{M_c(1+r)^n - M_c(1+i)^n}{r-i} \tag{25}$$

where M_c is the yearly chargeable fixed charge rate and i is inflation rate.

3 Cash Flow Diagram

Cash flows are the most important economic analysis. In any financial analysis, there are usually cash receipts (credits) and cash disbursement (expense) which occur over an interval of time. These receipts and disbursements (expenses) in each time are referred to as cash flows. Receipts are represented by positive cash flows, whereas disbursements are represented by negative cash flow. In general, cash flow is the movement of money in and out in each time of any business:

$$\text{Net cash flow} = \text{Receipts} - \text{Expenses} \tag{26}$$

Cash flow diagram gives net cash flow. Figure 1 (Nayak et al. 2012) shows the graphical representation of cash flow in cash flow line diagram on time scale, where P_i is principal investment (Rs.), CF is cash flow/annual income (Rs.), R_m is operational and maintenance expenses (Rs.), n is life of the dryer (years), and S is salvage value of the dryer (Rs.).

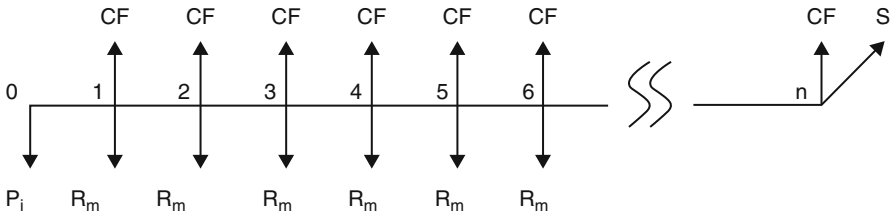

Fig. 1 A sample cash flow diagram (Nayak et al. 2012)

4 Case Studies

4.1 Economic Evaluation of a Mixed and Indirect Mode Solar Dryer

Simate (2003) has studied the economic analysis of mixed and indirect mode solar dryer. The system was used to dry the maize. The system was design and developed in Newcastle University in Tyne, UK. The system was developed to dry the crop up to 90 kg at a time. Figures 2 and 3 shows the schematic diagram of the mixed mode and indirect mode solar dryer.

The detailed dimension of both types of solar dryer is being presented in Table 1.

The proposed dryer was fabricated with the locally available material. The 18 mm of the plywood is being used in the sides of the collector and drying compartment. The leg width of the dryer is only 75 mm. The 3-mm clear glass thickness is being used as the collector. The major fabrication materials are wood, US $ 8.9/m^2; transparent glass, US $ 7.2/m^2; and wire mesh with fine hole, US $3.13/$m^2$. The fixed costs of US $ 11.50 happen and for insulation sawdust is being used. The charge of this is being negligible because it is being collected from the institute workshop. The interest and inflation rate is taken 15% and 12%, respectively. The total life of the dryer is being taken as 5 years, and the no. of working days per year is taken as 90. Table 2 presents the cost of both dryers in US $.

From the study, it is observed that the drying produce output of the indirect mode solar dryer is 15% more than mixed mode solar dryer. However, the total cost of the indirect dryer is also more due to large collector area. Figure 4 presents the comparative analysis of both dryers with the variation of mean moisture content per drying time.

4.2 Techno-economic Analysis of a Solar Air Heating System-Based Solar Dryer

Sreekumar (2010) investigated the system ability and viability of a roof-integrated solar air heating system for drying fruit and vegetables. The solar air heater-based solar dryer was loaded with 200 kg of fresh pineapple slices (5 mm thickness). The

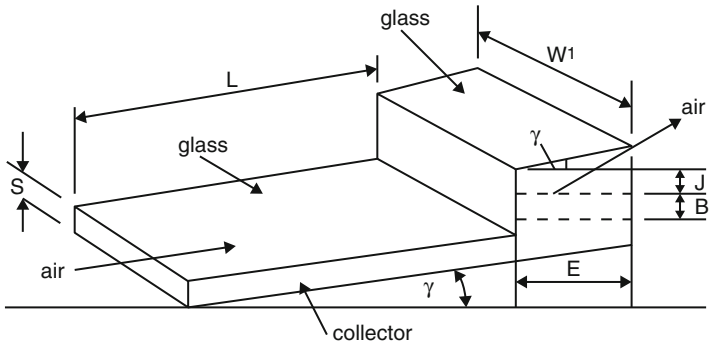

Fig. 2 Schematic diagram of the mixed mode solar dryer

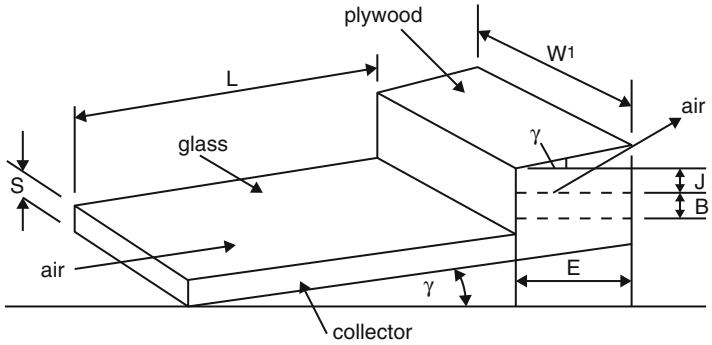

Fig. 3 Schematic diagram of the indirect mode solar dryer

Table 1 Dimension of the indirect and mixed mode solar dryer

	Solar dryer	
Parameters (m)	Indirect mode	Mixed mode
Collector length	3.34	1.8
Collector and dryer width	2.03	2.1
Grain depth	0.083	0.084

Table 2 Comparison of the cost

	Solar dryer	
Parameters	Indirect mode	Mixed mode
Dryer cost (US $)	16.05	12.76
Annual cost (US $)	52.07	35.88
Total cost (US $)	220.29	151.79
Quantity of dry grain per year (ton)	3.24	2.81

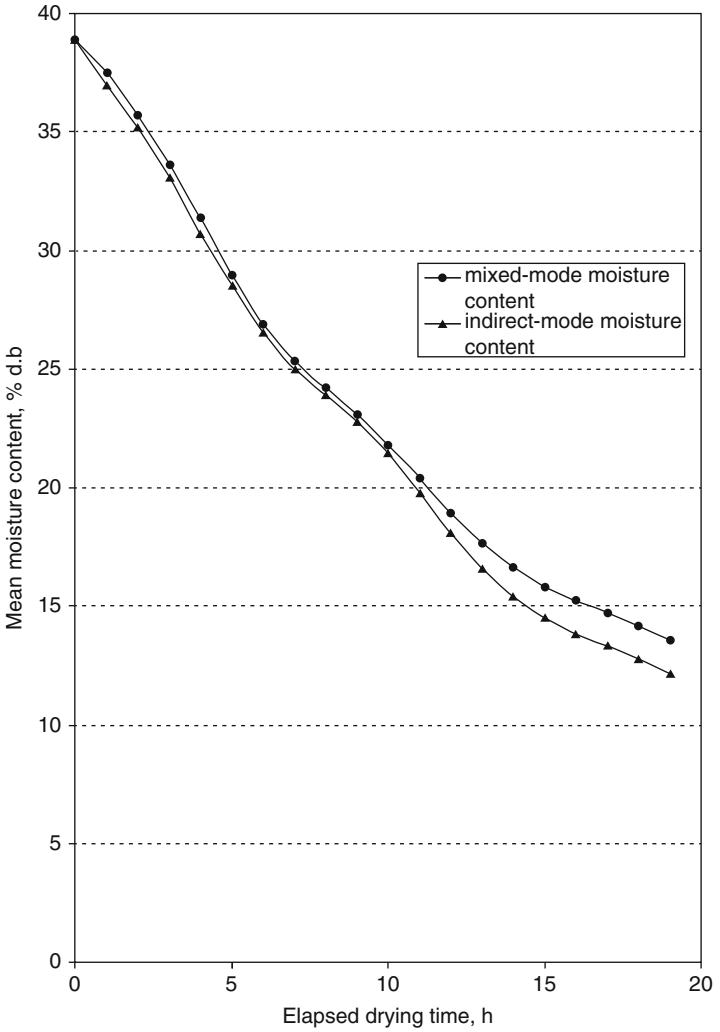

Fig. 4 Variation of mean moisture content with drying time

economic performance of the proposed solar dryer is done by using the following methods, viz., annualized cost, life cycle saving, and payback period of the dryer. The solar dryer consists a baffles board that direct the flow of drying air as shown in Fig. 5. Three baffles were attached in the air flowing region of the dryer. These baffles create turbulence inside the system. Turbulence inside the system makes airflow nearer to the absorber plate and reduces thermal sublayer.

Convective losses can be reduced at front side by creating space between the glass and absorber as shown in Fig. 6.

Figure 7 shows the integration of solar air heater with the building's roof.

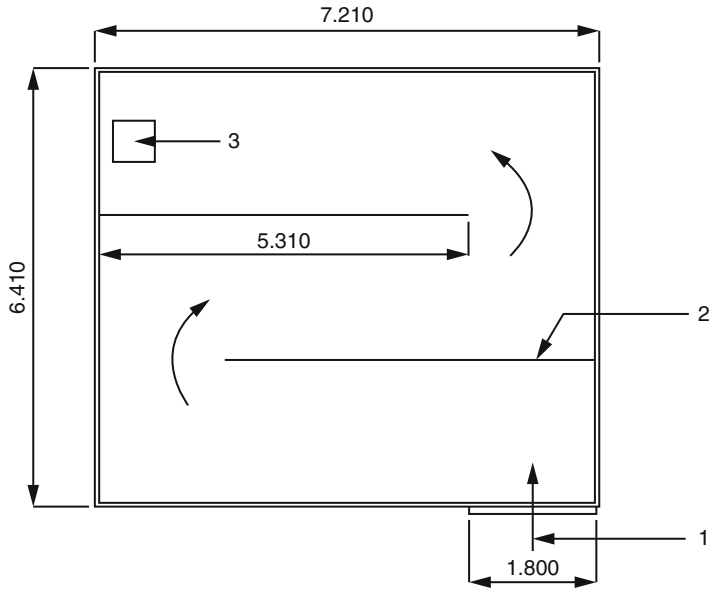

Fig. 5 Diagram showing air flowing the solar air heater where *1* represents the air inlet, *2* represents the metal partition, and *3* represents the outlet of the inside drying air (Sreekumar 2010)

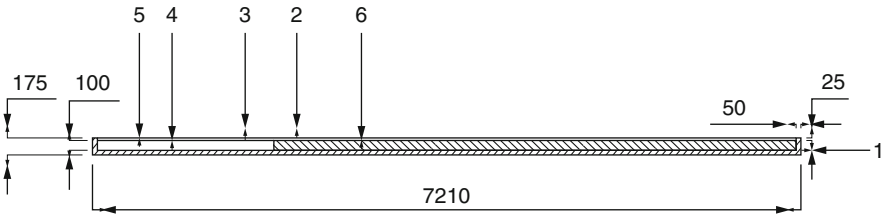

Fig. 6 Cross-sectional views of solar air heater (Sreekumar 2010)

4.2.1 Annualized Cost

The annual maintenance cost was 10% of the annual capital cost (C_{ac}). Ten percent of the annual cost was assumed as salvage value. Solar dryer's annual cost is turned out to be Rs. 55,990. The number of drying days of the dryer was 250 days per year (assumed value). By employing domestic solar dryer, drying cost per kg of pine-apple slices was Rs. 11, and drying cost in the electric dryer was Rs.19.73/kg. The cost of dried product in the domestic solar dryer was only 44.42% of cost of drying same product in an electric dryer. The cost of an electric dryer, the cost of electric

Fig. 7 Photograph of solar air heater (Sreekumar 2010)

energy, and electric dryer efficiency were Rs. 275,000, Rs. 4/Kwh, and 75%, respectively.

4.2.2 Life Cycle Savings

Calculation of drying cost for 1 kg pineapple in the case of the electric dryer and solar dryer is done previously. Calculation of dryer's annualized cost, the current value of yearly savings, and the current value of present worth of solar dryer's annual total saving is given in Table 3. Daily current saving is deduced as Rs. 4773. The cumulative present worth turned out to be Rs. 17 million, whereas the capital cost of the solar dryer was only Rs. 550,000.

4.2.3 Payback Period

The resulting payback period was only 191 days which is meager as compared to system's life span (20 years). In the first year of operation, Rs. 550,000 is recovered as a total investment. This finding hints that solar dryer will dry the pineapple slices free of cost through its entire life period.

4.3 Economic Analysis of Multi-shelf Domestic Solar Dryer

Singh et al. (2006) analyzed economic analysis of multi-shelf solar dryer for drying fenugreek leaves. Here solar dryer is structured with multi-shelf composition. It consists of three porous trays, one stacked over the other. It captured more solar

Table 3 Cost and economic parameters of solar dryer (Sreekumar 2010)

S. no.	Parameters	Values
1.	Assumed dryer life	20 years
2.	Construction cost of the solar dryer	Rs. 550,000
3.	Cost of fresh pineapple	Rs. 10/kg
4.	Electricity consumption cost	Rs. 4.00 Kwh
5.	Inflation rate	5%
6.	Price of dried pineapple	Rs. 200/kg
7.	Rate of interest	8%
8.	Real interest rate	3%

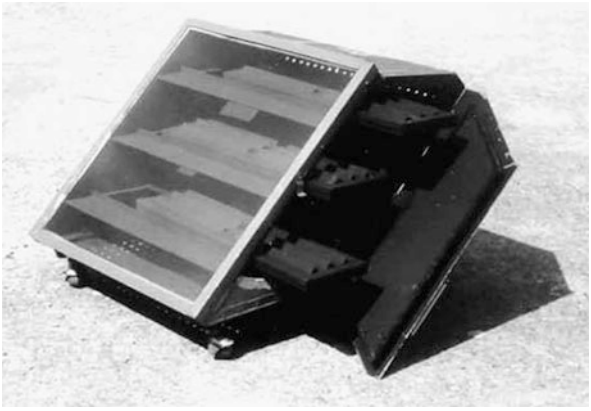

Fig. 8 Photograph of PAU domestic solar dryer with open doors (Singh et al. 2006)

energy in the different season due to its variable inclination. As per requirement, options are available for drying the product either under the shade or without shade. The design of a noncommercialized, small-sized domestic solar dryer, namely, "PAU solar dryer," was presented by them which perceives a natural convection as shown in Fig. 8.

The key working components of the dryer were a dry box, base frame, trays, and shading plates. Three different levels are equipped with three perforated trays stacked over subsequently in a hot box as shown in Fig. 7. The perforated tray was put inside a dry box arranged one above the other at a different level. The area of each tray was 0.105 m^2 which was placed on a tray support as shown in Fig. 9.

Dryer's side view represents the respective locations of tray supports. The product was loaded in the tray and the tray was loaded in the dryer. The shading plate provided over each tray is to dry product under shade in a specific condition. The shading plate is removable and attached optionally above each tray as shown in Fig. 10.

They analyzed economic evaluation of solar drying system by using three methods, viz., years cost method, life cycle method, and payback time. In the case of economic analysis, inflation rate and interest rate had taken as 5% and 3% simultaneously. Dryer's capital cost was Rs. 1600 and its working life was estimated as 20 years.

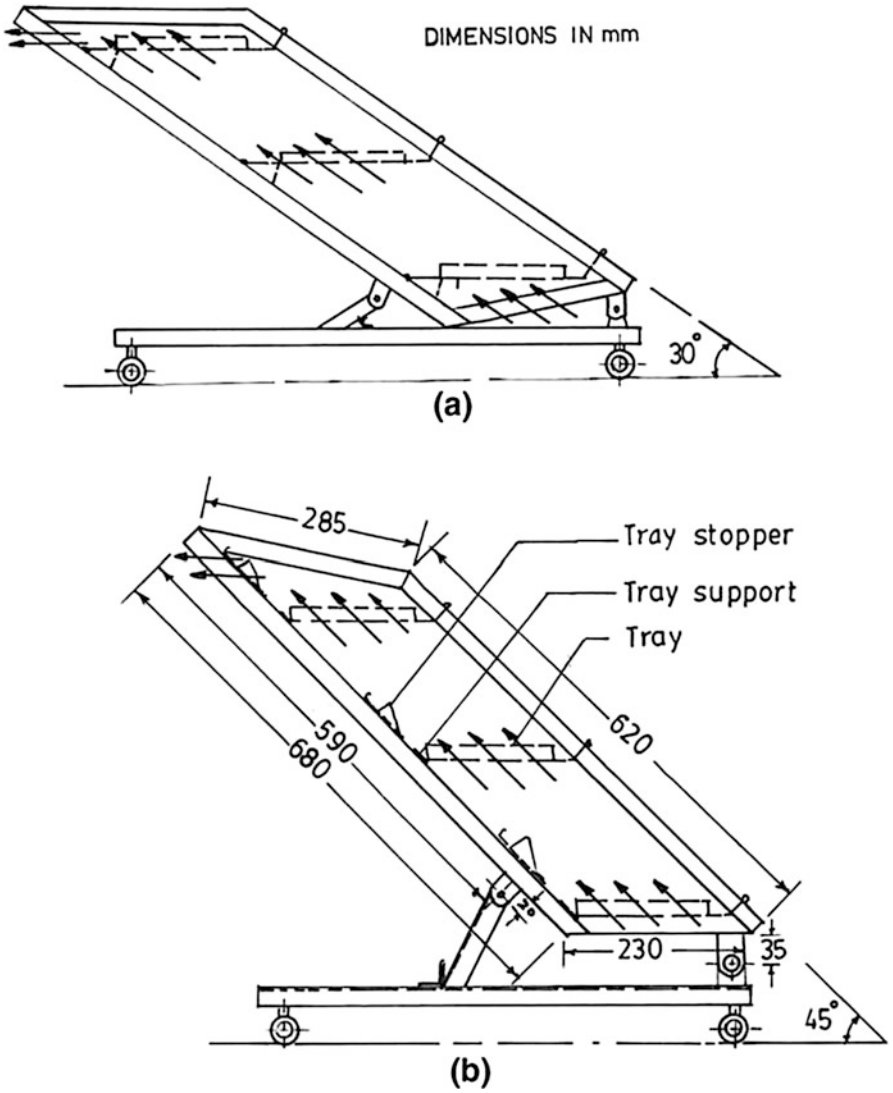

Fig. 9 Side view of the dryer showing the position of tray supports at different inclination: (**a**) 30°, (**b**) 45° (Singh et al. 2006)

4.3.1 Annualized cost

The year-wise cost for maintenance was 3% of the annual capital cost (C_{ac}). Ten percent of the annual cost was assumed as salvage value. Solar dryer's annual cost is turned out to be Rs. 164.35. Since, the experiment was conducted at northern Indian plain, the number of drying days of the solar dryer were 150 days per year (assumed value). Therefore, the dried fenugreek leaves obtained in a year were only

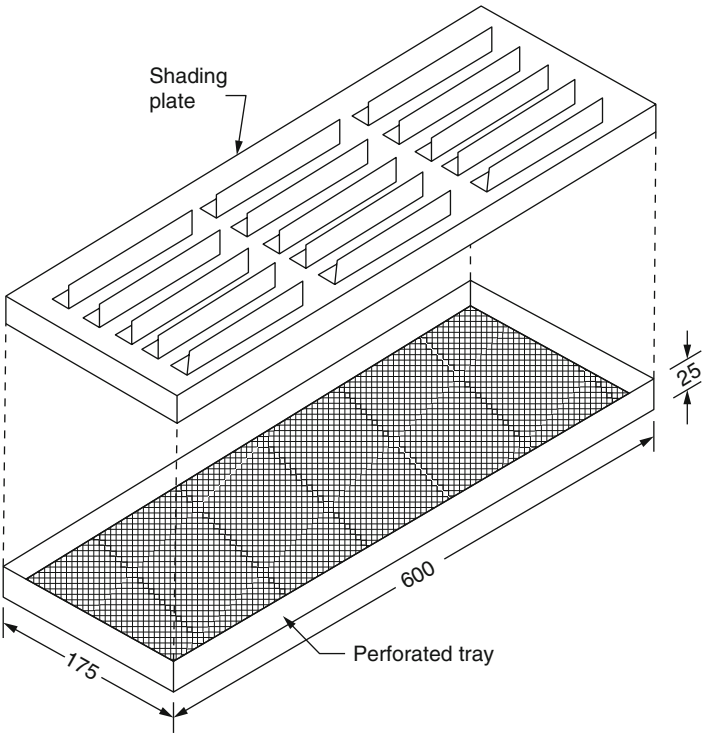

Fig. 10 Perforated tray with shading (Singh et al. 2006)

4.25 kg. By employing domestic solar dryer, drying cost per kg of fenugreek leaves was deciphered as Rs. 38.67. The drying product's cost was only 60% of the cost involved in drying the same product using an electric dryer. Singh et al. (2006) assumed the electric dryer's capital cost, electric energy cost, and electric dryer efficiency as Rs. 800, Rs. 4/kwh, and 80%, respectively.

4.3.2 Life Cycle Savings

The current saving per day was Rs. 8.5/day. The cumulative present worth of yearly savings for drying fenugreek leaves was taken out as Rs. 18,315.69. It means by investing Rs. 1600 to buy a multi-shelf domestic solar dryer, the consumer will save Rs. 18,315.69 through the estimated life of the dryer. The result of annualized cost of the dryer, annual savings, present worth of annual saving, and the present worth of cumulative saving is given in Table 4.

A similar calculation was also done for drying chilies. For chilies, the total present value of yearly savings in the total life span of the domestic solar dryer was Rs. 43,073.98, and saving per drying day was Rs. 20/day. The increment in total

Table 4 Savings for each year or 150 days/year throughout the life of the dryer (Singh et al. 2006)

Year	Annualized cost (Rs.)	Annual savings (Rs.)	Present worth of annual savings (Rs.)	Present worth of cumulative savings (Rs.)
1	164.35	1275.64	1181.15	1181.15
2	164.35	1339.42	1148.34	2329.49
3	164.35	1406.39	1116.44	3445.93
4	164.35	1476.71	1085.43	4531.36
5	164.35	1550.55	1055.28	5586.64
6	164.35	1628.08	1025.96	6612.61
7	164.35	1709.48	997.46	7610.08
8	164.35	1794.95	969.76	8579.84
9	164.35	1884.70	942.82	9522.66
10	164.35	1978.94	916.63	10,439.30
11	164.35	2077.89	891.17	11,330.47
12	164.35	2181.78	866.41	12,196.89
13	164.35	2290.87	842.34	13,039.24
14	164.35	2405.41	818.95	13,858.19
15	164.35	2525.68	796.20	14,654.39
16	164.35	2651.97	774.08	15,428.48
17	164.35	2794.57	752.58	16,181.06
18	164.35	2923.80	731.67	16,912.74
19	164.35	3069.99	711.35	17,624.09
20	164.35	3223.48	691.59	18,315.69

current value of yearly savings for life span of the domestic solar dryer was based on increasing number of drying days. The result of Fig. 11 can be represented by Eq. 27:

$$C_{\mathrm{pn}} = m \times D \tag{27}$$

where $m = 14.36 \times S_{\mathrm{d}}$.

S_{d} is saving each day in solar dryer (Rs, Indian National Rupees).
D is no. of days involving usage of domestic solar dryer annually.

4.3.3 Payback Period

The calculated payback time was 204 drying days for fenugreek leaves and 86 drying days for drying chilies. These findings proved that dryer work is free of cost in the entire life period. The payout time is very less as compared to the life of the dryer.

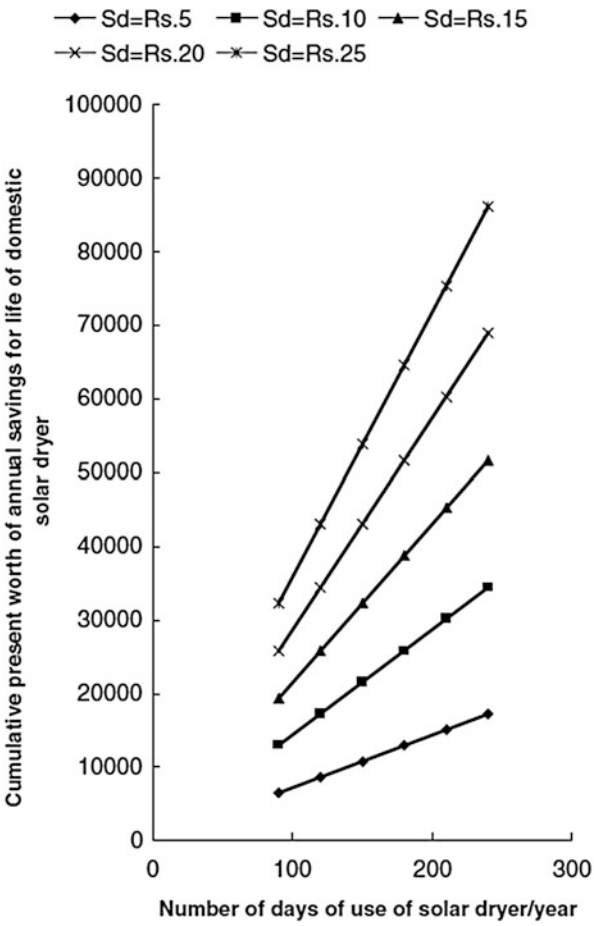

Fig. 11 Graphical representation between cumulative current value of yearly savings and no. of days dedicated to drying days (Singh et al. 2006)

5 Conclusion

In this chapter, solar dryer's economic analysis is demonstrated including methodologies and case study. Economic analysis is vital for promoting devices or products in the related market. Solar dryer is economically benefited for small- and medium-scale enterprises, entrepreneur, farmers, etc. People refer the system having shorter payback period. Solar dryer is having shorter payback time as compared to its capital investment.

Nomenclature

B	Grain depth of the dryer
C	First investment cost
C_a	Annualized cost of dryer (Rs.)
C_{ac}	Yearly capital cost (Rs.)
C_b	Selling price of branded dried product (Rs./kg)
C_{cc}	Capital cost of dryer (Rs.)
C_{fd}	Cost of fresh product per kg of dried product (Rs./kg)
C_{ds}	Cost per kg of dried product for domestic solar dryer (Rs./kg)
C_{ee}	Cost per kW h of electric energy (Rs./kWh)
C_{fp}	Cost per kg of fresh product (Rs./kg)
C_{am}	Annualized maintenance cost (Rs.)
C_{af}	Yearly running fuel cost (Rs.)
C_{ae}	Yearly electricity cost for fans (Rs.)
C_s	Cost of drying per kg of dried product in dryer (Rs./kg)
C_{dp}	Fresh product's cost
C_{ds}	Cost of 1 kg of dried product
C_e	Electricity unit charge
C_{fp}	Cost of fresh product
C_{re}	Cost of operation for the blower in dryer
C_{rf}	Electric dryer's year-wise running fuel cost
D	Net income/ price of substituted conventional energy
D_b	Number of drying days per batch
E_{ch}	Input energy in the chamber
E_m	Embodied energy (kWh)
e	Yearly inflation rate
F_{cr}	Capital recovery factor
F_{sr}	Salvage fund factor
η_{ed}	Efficiency of the electric dryer
F_{pj}	Present worth factor for jth year
h_l	Latent heat of water (kJ/kg)
i	Rate of interest on long-term investment
j	No. of year
L	Length of collector
m_{db}	Moisture content (dry basis) (%)
M_d	Mass of dried product removed from solar dryer per batch (kg)
M_{dp}	Mass of dried product removed from solar dryer per batch (kg)
M_{fp}	Mass of fresh product loaded in solar dryer per batch (kg)
M_{pr}	Mass of product dried in the dryer per year (kg)
M_c	Yearly chargeable fixed charge rate
m_w	Mass of removed water
N_d	Number of days of use of domestic dryer per year
N_{dd}	Number of drying days per batch
N_h	Number of operating hours of fan and blower
n	Life of solar dryer (year)
P_n	Payback period (year)
P_j	Present worth of annual saving in jth year (Rs.)
r	Annual interest
S_l	Salvage value of the solar dryer (Rs.)
S_b	Saving per batch for solar dryer (Rs./kg)
S_d	Saving per day for domestic solar dryer in the jth year (Rs.)

S_j	Annual savings for domestic solar dryer in the jth year (Rs.)
S_{kg}	Savings per kg in comparison to branded product for solar dryer (Rs./kg)
V_s	Salvage value (Rs)
V_{as}	Annualized salvage value (Rs)
W	Rated power of electric blower and axial fans (kW)
W_1	Width of the drying chamber
Y	Exchange rate of carbon credit
Rs	Indian national rupee
MGD	Modified greenhouse dryer
BCC	Black-coated concrete
BPVC	Black polyvinyl chloride
EPBT	Energy payback time
BPCF	Black-painted concrete floor

References

Adeaga OA, Dare AA, Odunfa KM, Ohunakin OS (2015) Modeling of solar drying economics using Life Cycle Savings (L.C.S) method. J Power Energy Eng 3:55–70

ELkhadraoui A, Kooli S, Hamdi I, Farhat A (2015) Experimental investigation and economic evaluation of a new mixed mode solar greenhouse dryer for drying of red pepper and grape. Renew Energy 77:1–8

Lin WM, Chang KC, Chung KM (2015) Payback period for residential solar water heaters in Taiwan. Renew Sustain Energy Rev 41:901–906

Nayak S, Naaz Z, Yadav P, Chaudhary R (2012) Economic analysis of hybrid photovoltaic–thermal (PVT) integrated solar dryer. Int J Eng Invent 1(11):21–27

Prakash O, Kumar A (2013) ANFIS prediction model of a modified active greenhouse dryer in no-load conditions in the month of January. Int J Adv Comput Res 3(1):220–223

Prakash O, Kumar A (2014) Environomical analysis and mathematical modelling for tomato flakes drying in a modified greenhouse dryer under active mode. Int J Food Eng 10(4):669–681

Simate IN (2003) Optimization of mixed-mode and indirect-mode natural convection solar dryers. Renew Energy 28(3):435–453

Singh PP, Singh S, Dhaliwal SS (2006) Multi-shelf domestic solar dryer. Energy Convers Manage 47:1799–1815

Sreekumar A (2010) Techno-economic analysis of a roof-integrated solar air heating system for drying fruit and vegetables. Energy Convers Manage 51:2230–2238

Economic Analysis of Hybrid Photovoltaic-Thermal (PV-T) Integrated Indirect-Type Solar Dryer

Sujata Nayak and Kapil Narwal

Abstract Drying of agricultural crops is a very energy consuming activity and most methodologies adopted for it draw this energy form non-renewable sources. It also exists on records that the unavailability and therefore the shortage of fossil fuel result in the higher cost of energy generated from such sources. In recent years, renewable energy sources have emerged out as possible alternatives to the nonrenewable energy sources, and among others, solar energy has got significant recognition between energy researchers. The present chapter deals with the economic analysis of drying process using a hybrid photovoltaic-thermal (PV-T) integrated indirect-type solar dryer. In the dryer, a DC fan has been directly coupled with the photovoltaic (PV). The dryer works under forced air circulation without any external power supply and has been coupled to a solar heater. The solar heater is equipped with a sun-tracking facility and is having blackened surface to absorb to increase its energy collection efficiency. The dryer also consists of a dryer chamber with a chimney which is used for the drying of agriculture products. The experiments carried for the force air circulation under no load and load conditions have been discussed. Further, a techno-economic analysis has been explained in detail.

Keywords Solar photovoltaic • Techno-economic analysis • Solar dryer • Solar thermal • Exergy

1 Introduction

Drying of agricultural produce under the open sun is quite a time-consuming process, which also needs a lot of labor and land for per unit throughput. Moisture removal process for the produce involves both heat transfer and mass transfer phenomena, and the produce undergoes various physical and chemical changes, which at times may not be needed depending upon the kind of conditions and quality sought by the consumer. Over the year, researchers have studied and utilized various methods of achieving the efficient drying using various renewable and

S. Nayak (✉) • K. Narwal
Department of Mechanical Engineering, Manav Rachna University, Faridabad, India
e-mail: dashsuj@gmail.com; mr.k.narwal@gmail.com

© Springer Nature Singapore Pte Ltd. 2017

O. Prakash, A. Kumar (eds.), *Solar Drying Technology*, Green Energy and Technology, DOI 10.1007/978-981-10-3833-4_18

nonrenewable sources of energy, but the study of drying process under forced circulation of heated air has not been studied that widely. The fan used for the forced circulation of heated air inside the drying area can be powered by the electricity from the grid or the one generated from solar power photovoltaic modules. The electricity generated by solar powered photovoltaic to ensure the forced circulation of air in the hybrid photovoltaic solar dryer has been studied by Mumba (1995). It has been observed after studying a solar dryer with photovoltaic cells, for driving a direct current fan, incorporated within the section of solar air heater, that a moisture content of 33-20% can be dried from a maize grain in a single day, which in comparison to sun drying conditions, reduces the drying time by over 70%. Farkas et al. (1999) developed a modular structure of solar dryer which had a dedicated module with a photovoltaic panel attached in the front side of dryer with an arrangement to adjust angle elevation as per the position of sunshine throughout the year, to power an electric fan artificial circulate the air. Hossain et al. (2005) did the optimization of a solar tunnel dryer which they had designed for the agricultural produces. Experiments were carried out at Bangladesh using chili as agricultural product. It was observed that there was a very negligible effect of various fixed and variable costs but indeed was very sensitive to the cost of construction material, intensity of solar radiation, and the air velocity with which air flow through the dryer. A thermal model for indirect sun drying of banana was developed, and it showed to be in good agreement with experimental results by a similar setup and field data obtained by Phougchandag and Woods (2000), in Thailand. Togrul and Pehlivan (2002) generated the drying curve from recorded data, which was also validated with a number of mathematical/thermal models and studied the effect of drying air temperature, velocities, and relative humidity on the model constants and coefficients. These values were further evaluated by multiple regression analysis and compared with previously given models. The logarithmic drying model was found to be satisfactory with a correlation coefficient (r) of 0.994 for solar drying curve of apricots. A plastic-covered solar tunnel dryer was designed for drying of fruits, vegetables, cereals, grain, legumes, oil seeds, spices, fish, and even meat by Bala et al. (2003). Hossain and Bala (2007) developed solar tunnel dryer for drying of chili. Numerous tests have been carried out for different vegetables, fruits, and cereals in different tropical and subtropical regions. Saleh and Sarkar (2002) designed, fabricated, and tested a domestic solar dryer with transparent external surfaces. Thin-layer drying models described the drying phenomena in a unified way, regardless of the controlling mechanism which has been used to estimate the drying period for several products. The performance was tested under different operational conditions, and the drying characteristics were experimentally investigated by conducting the experiments on two local herbs, Jew's mallow and mint leaves. The dryer was able to reduce moisture of the tested products to the recommended level (6% wb) in about a 12 h period. The reliability of the exponential model was evaluated by comparing the experimental with the predicted data. Ghazanfari et al. (2003) studied the feasibility of drying pistachio nuts in thin-layer forced air solar dryer. The result showed that the quality of solar dried nuts was better than the conventional heated air due to slower drying rates. Performance

analysis of a conventional PV-T mixed-mode dryer under no load condition has been carried out by Dubey and Tiwari (2008). The experiment was conducted for forced mode under no load conditions during April 2008 and validated with theoretical results for New Delhi climatic condition. Among the important parameters that influence the performance of the collector are temperature of the photovoltaic cell, air mass flow rate, radiation intensity, depth of the first and second channel, inlet temperature, packing factor of the photovoltaic cell, and collector length. Barnwal and Tiwari (2008) had conducted grape drying by using hybrid photovoltaic-thermal (PV-T) greenhouse dryer: An experimental study. Various hourly experimental data, namely, moisture evaporated, grape surface temperature, ambient air temperature and humidity, greenhouse air temperature and humidity, etc., are recorded to evaluate heat and mass transfer for the proposed system.

Celma and Cuadros (2009) presented the energy and exergy analysis of the drying method of olive mill wastewater (OMW) using an indirect-type natural convection solar dryer. An energy analysis has been carried out for estimating the amount of energy obtained from solar air heater and the ratio of energy utilization of the drying chamber using the first law of thermodynamic, and exergy analysis was carried out by using the second law, to determine the type and magnitude of exergy losses during the solar drying process. The exergetic efficiencies of the drying chamber decreased as inlet temperature was increased, provided that exergy losses became more significant. Maia et al. (2013) studied the energy and exergy analysis of the airflow inside a solar chimney. The results showed that the exergy losses were lower and the efficiency was higher for the lowest ambient temperature, which used as the dead state temperature, when compared to the instantaneous ambient temperature. Motevali et al. (2014) calculated the energy output, thermal output, drying efficiency, and specific energy in various drying methods for drying of chamomile. These methods included convective, infrared, convective-infrared, microwave, microwave-convective, microwave-vacuum, vacuum, and hybrid photovoltaic-thermal solar (with/without heat pump). Results of data analysis showed that the highest energy output of 49.99% belonged to the microwave dryer, while the lowest 1.41% belonged to the vacuum dryer. Results of analysis indicated that adding a heat pump to the photovoltaic solar dryer increases drying efficiency, energy output, and thermal output, while it reduces the required specific energy. An energy and exergy analysis was carried out for thin-layer drying of coroba slices at three different air temperatures and velocities, and also the effects of inlet air temperature and velocity and drying time have been studied by Corzo et al. (2008). Mumba (1996) achieved a 70% efficiency in grain drying using a solar powered DC fan against open sun drying. Chowdhury et al. (2011) discussed the energy and exergy analysis of a solar tunnel dryer, which was used for solar drying of jackfruit leather. It was found that with the increase in solar radiation, exergy input and exergy loss increase for the dryer. The dryer was found to be 42% efficient for energy, and the exergy efficiency for the collector was found to be varying between 32% and 69% and the mean exergetic efficiency of dryer 42%. Dincer and Sahin (2004) developed a new model for thermodynamic analysis, in terms of exergy, of a drying process. Exergy efficiencies are derived as functions of

heat and mass transfer parameters. The proposed model should be useful to people seeking (i) to optimize the design of drying systems and their components and (ii) to identify appropriate applications and optimal configurations for drying systems.

Fudholi et al. (2015) described the techno-economic analysis of solar drying system (SDS) with water-based solar collector in Malaysia. The design, performance, and economic analysis of four types of SDSs with water-based solar collectors in Malaysia were described: (1) SDS with hybrid PV-T mechanical heat pump, (2) SDS with chemical heat pump, (3) SDS with dehumidification system, and (4) greenhouse SDS with heat exchanger. The energy and exergy analysis of SDS with water-based collector was presented. Moreover, the energy and exergy analysis of PV-T water collector was presented in this paper. Panwar et al. (2012) analyzed solar dryers for its energy and exergy with case studies. Sopian et al. (2000) proposed a double pass photovoltaic thermal solar collector for solar drying applications. Sami et al. (2011) analyzed an indirect cabinet solar dryer using a previously developed dynamic mathematical model for performance, and microscopic energy and exergy analysis for the same dryer was carried out. The results showed that in spite of high energy efficiency, the indirect solar cabinet dryer had relatively low exergy efficiency. The maximum exergy losses were observed in midday. The effect of some operating parameters, including length of the collector, its surface, and airflow rate, was investigated on the exergy destruction and efficiency. ELkhadraoui et al. (2015) presented an experimental analysis to investigate the performance of a novel mixed-mode solar greenhouse dryer with forced convection which was used to dry red pepper and sultana grape. The payback period of the dryer was found to be 1.6 years, much less than the estimated life of the system (20 years). Boughali et al. (2009) constructed and investigated a new specific prototype of an indirect active hybrid solar-electrical dryer for agricultural products and evaluated an economic/cost analysis using the criterion of payback period, which was found to be very small (i.e., 1.27 years) as compared to the life of the dryer (15 years). Rahman et al. (2013) studied an economic optimization of evaporator and air collector area of a solar-assisted heat pump drying system. Identification of optimum variables by using a simulation program and an effect of load and different economic variables based on payback period of the system were also presented. Economic analysis revealed that system had sufficient monetary savings during the life cycle with a minimum payback period of about 4 years.

A photovoltaic solar dryer was a self-sustained and efficient dryer, as it had not needed any external energy sources during operation. Therefore it would be a better proposition for rural and other remote areas, where electricity is very scarce and irregular. A photovoltaic-based hybrid mixed solar dryer has been designed, fabricated, and installed at rooftop of Manav Rachna University, Faridabad, Haryana, which consists of an air heater and drying chamber with chimney and a supporting stand. A techno-economic analysis of the dryer has also been calculated and discussed in this chapter.

2 Methodology

2.1 Detail Description of PV-T Integrated Solar Dryer and Working Principle

Solar air heater and solar chamber are two principal components of a solar drying system. Solar air heater which has been used for heating the ambient air available at the inlet point of air duct consists of a photovoltaic panel for converting solar radiation into electricity, which is integrated with flat-plate collector at 30^{o} angle so as to receive maximum solar radiation.

Working Principle

The system works on the principle of solar energy collection. Schematic diagram for the hybrid photovoltaic solar dryer has been presented in Fig. 1, in which the dying unit has been connected to air heater. The solar radiations coming from the sun fall on the photovoltaic module, which converts these radiations into electricity. Collector absorbs the radiation and converts the same into the thermal energy. The energy so absorbed by the collector is utilized to increase the temperature of working fluid, in this case air. The high temperature working fluid is utilized to reduce the moisture content from agricultural products. The fan of capacity 12 V ensures the forced circulation of heated air in drying chamber which is operated by the electricity generated from PV module.

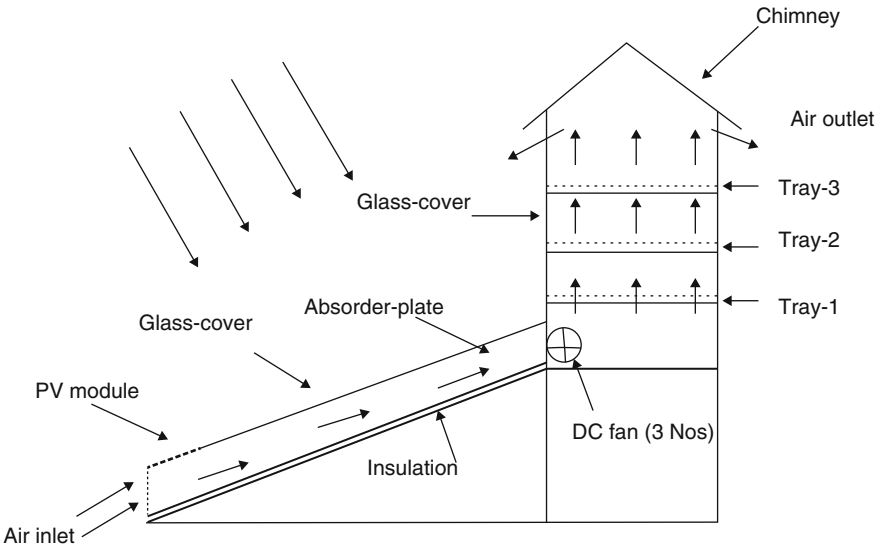

Fig. 1 Schematic diagram of hybrid photovoltaic-thermal integrated solar dryer

2.2 Experimental Observations

The hybrid mixed photovoltaic/thermal solar dryer under discussion has been utilized to dry the agricultural produces, which have been placed in three trays in the dying chamber. The experiments were carried out under no load and load conditions in order to measure the efficiency of dryer and payback time. Energy and exergy analysis was further performed for the economic evaluation of solar dryer. Particular specifications of the solar dryer can be found in the Table 1. The dryer was placed on the rooftop of Manav Rachna University, Faridabad, where all the experiments were carried out. The hot air was made to flow through the air heater under forced circulations using the exhaust fan, which on the other hand was powered by the electricity generated from photovoltaic modules, and was forced into the drying chamber, wherein all the fresh agriculture produces were placed for drying in the three trays. After giving out the heat for the drying of produces and absorbing the moisture content in it, moist air was made to pass through the chimney, which was placed on the east and west side of the drying chamber.

S. No.	Parameter measured	Unit
1	Dryer inlet temperature	°C
2	Dryer outlet temperature	°C
3	Ambient temperature	°C
4	PV module temperature	°C
5	Total and diffuse solar intensity on collector	W/m^2
6	Load current (I_L) and load voltage (V_L)	Amp. and Volt.
7	Short circuit current (I_{sc}) and open circuit voltage (V_{oc})	Amp. and Volt.

Table 1 Hybrid mixed photovoltaic/thermal solar dryer particulars

S. No.	Detail of particulars	Specifications
1	Air duct	Length, 2.2 m; breadth, 0.65 m; height, 0.05 m
2	Photovoltaic module	Length, 0.65 m; breadth, 0.55 m; power, 35 W
3	Absorber and glass gap	0.10 m
4	Fan (DC)	12 V, 1.3 A
5	Chimney	Length, 0.65 m; breadth, 0.26 m; height, 0.60 m
6	Trays (3 Nos.)	3
7	Gap between trays	0.15 m
8	Angle of air duct with ground	30^o

A copper constantan thermocouple, well calibrated, was used for temperature measurements. Temperature was measured at the inlet and outlet of solar dryer; also ambient temperature was measured. Very accurate digital thermometers with indicator accuracy of 1° were used to make hourly temperature measurements. A solarimeter (accuracy 20 W/m^2) was used to measure hourly solar radiations received at the air collectors. An AC/DC digital clamp meter (accuracy 0.1 A and 0.1 V) was used to measure the current and voltage. The experiments were performed during the summers of 2016 (Fig. 2, Tables 2a and 2b).

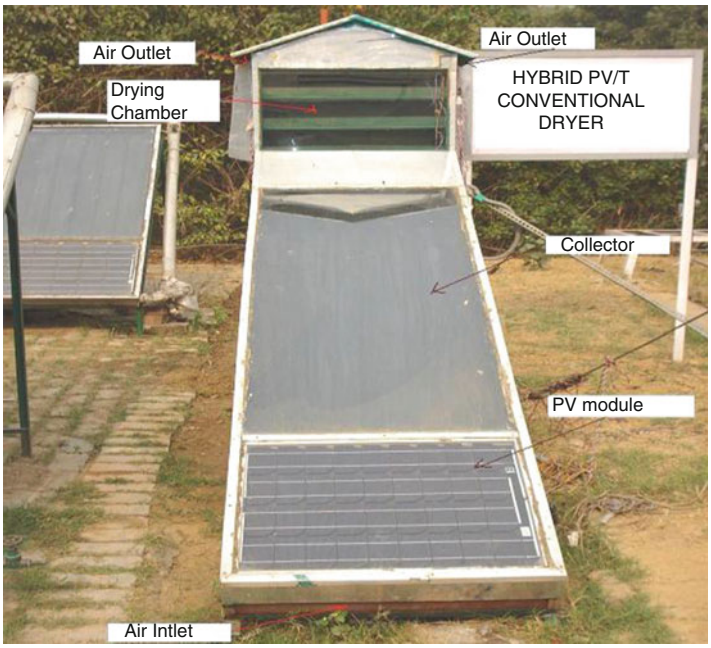

Fig. 2 Hybrid photovoltaic-thermal integrated solar dryer (actual picture)

No Load Experiment Observation

Table 2a Temperatures measured (hourly)

Time (h)	Inclined solar radiation W/m^2	Ambient temp. $T_{fi} = T_a$	Collector output temp. T_{chfo}	Temp. at first tray T_1	Temp. at second tray T_2	Temp. at third tray T_3	Temp. at outlet
t	(I_t)	°C	°C	°C	°C	°C	°C
9.00	520	35.5	46.5	46	45.5	45	44.5
10.00	550	36	47	46.5	46	45.5	45

(continued)

Table 2a (continued)

Time (h)	Inclined solar radiation W/m^2	Ambient temp. $T_{fi} = T_a$	Collector output temp. T_{chfo}	Temp. at first tray T_1	Temp. at second tray T_2	Temp. at third tray T_3	Temp. at outlet
t	(I_t)	°C	°C	°C	°C	°C	°C
11.00	670	37	47.5	47	46.5	46	45.5
12.00	790	38	49.5	49	48.5	48	47.5
13.00	670	38.5	48.5	48	47.5	47	46.5
14.00	660	39	48.5	48	47.5	47	46.5
15.00	560	39.5	47.5	47	46.5	46	45.5
16.00	300	40.5	46.5	46	45.5	45	44.5

Table 2b Current, voltage, ambient temperature, and solar radiation intensity (hourly)

Time (h)	Ambient temp.	Inclined solar radiation (W/m^2)	Open circuit voltage (Volts)	Short circuit current (Amp.)	Load voltage (Volts)	Load current (Amp.)
t	$T_{fi} = T_a$	(I_t)	(V_{oc})	(I_{sc})	(V_L)	(I_L)
9.00	35.5	520	15.5	1.6	15.3	0.5
10.00	36	550	15.5	1.7	15.3	0.5
11.00	37	670	15.2	1.7	16.8	0.5
12.00	38	790	17	1.9	17.5	0.6
13.00	38.5	670	16.4	1.8	17.2	0.6
14.00	39	660	16	1.7	16.4	0.5
15.00	39.5	560	15.8	1.5	16.3	0.5
16.00	40.5	300	15.1	0.9	16	0.4

2.3 Testing Under Load Condition

(a) *Product selection*

Freshly produced white and compact cauliflowers (*Brassica oleracea* var. *botrytis*) were purchased from the city market, with all the leaves and stems removed.

(b) *Cutting and washing*

The cauliflower heads were cut into small pieces of sizes 3 × 1.5 cm (3 cm length and 1.5 cm width)
and were duly washed under fresh tap water in order to remove all the unwanted dust and dirt.

(c) *Blanching*

A muslin cloth was then used to wrap the cut parts of cauliflower and was immerged into the hot water bath for 2–4 min at around 80 °C to prevent any inactivation of peroxide and catalase. Further moisture content was measured from the cut parts by taking samples.

(d) *Testing procedure*

The cut parts were then placed on the trays inside the drying chamber, and hourly temperature was measured using the thermocouples. A standard oven dry method was used to measure the moisture content. Samples were prepared and spread uniformly in trays and trays were put inside the dryer. Three sample trays of size (60 cm × 26 cm × 13 cm) cm each were used for each drying tray to study the drying behavior of material. The weight of sample tray was recorded at each hour to determine the quantity of moisture removed.

3 Techno-economic Analysis

Techno-economic analysis of hybrid mixed photovoltaic/thermal solar dryer solar dryer was done for drying of cauliflower. The embodied energy for hybrid mixed photovoltaic/thermal solar dryer integrated solar dryer has been calculated.

4 Annual Thermal Outputs

Energy output per year from hybrid mixed photovoltaic/thermal integrated solar dryer

= Net electrical output + Thermal output

$$\begin{aligned}&\text{Net daily average output from a PV module}\\&\quad = \text{No load output} - \text{on load output}\\&\quad = (0.8 \times I_{sc} \times V_{oc} - I_L \times V_L)\\&\quad = 27 - 8\\&\quad = 19\text{W}\end{aligned} \tag{1}$$

Net annual average electrical output

= Net daily average electrical output (W) X peak sunshine hours per day (N)
X No.of clear sunny days in a year X10^{-3}kWh/year (2)

$$= 19 \times 8 \times 300 \times 10^{-3}$$
$$= 45.6\,\text{kWh/year}$$

Net annual average equivalent thermal output

$$= \frac{\text{Net annual average electrical output}}{0.38}$$
$$= \frac{45.6}{0.38} \tag{3}$$
$$= 120\,\text{kWh per year}$$

The daily thermal output of the dryer $\left(\dot{Q}_u\right)_{\text{daily}}$

$$= \text{moisture evaporated (kg)} \times \text{latent heat of evaporation (J/kg)}$$
$$= \frac{\left(0.35 \times 2.26 \times 10^6\right)}{\left(3.6 \times 10^6\right)}\ \text{kWh} = 0.227\ \text{kWh} \tag{4}$$

Therefore, annual thermal output of the dryer, E_{aout}

=Daily thermal output of the dryer (kWh) $\times \frac{300}{2}$
=0.227 × 150 = 34.05 kWh

For three trays, average annual thermal output of the dryer

=34.05 × 3 = 120.15 kWh

Therefore, total annual energy output of the dryer

=120 + 102.15 = 222.15 kWh

5 Energy Payback Time (E_{PBT})

$$= \frac{1311.05}{222.15} = 5.9\,\text{years} \tag{5}$$

It has been concluded that the energy payback time of hybrid PV-T (50 W) dryer, under New Delhi climatic condition, has been calculated as 5.9 years.

Annual Income, Cash Flow (CF)
Wt. of dried product in each tray = 100 g
Wt. of dried product in three trays per year = 100 × 3 × 150 = 45,000 = 45 kg
Average cost of dried cauliflower per year = Rs. 30/kg
Annual income, CF(Rs.) = 45 × 30 = Rs. 1350

Annualized Salvage Value (R')

$$R' = S\frac{i}{(1+i)^n - 1}$$
$$R' = SF_{SR,i,n}$$
$$R' = 1762.8 \times 0.0178 = \text{Rs.}31.42$$
$$\text{Annualized cost of dried cauliflower (Rs.)} = (R - R') = 1092.42 - 31.42 = \text{Rs.}988 \quad (6)$$

Cost of Drying (C_d)
If M_P is dried product output per year (in kg), then cost of drying (C_d) can be evaluated as:

Cost of drying C_d(Rs./kg) = annualized cost (Rs.) /dried product output per year (kg)

$$= \frac{R}{M_P} = 24.5\,(\text{Rs./kg}) \quad (7)$$

Total Benefits (Rs.) =Rs. 1350 – 988 = Rs. 362

6 Results and Discussion

Economic analysis of hybrid PV-T solar dryer has been carried out for the drying of cauliflower. Embodied energy for the experimental setup has been calculated for evaluating the energy payback time of the dryer. Table 3 shows the embodied energy calculation for the hybrid PV-T solar dryer. It is observed that the embedded

Table 3 Embodied energy

S. No.	Items used	Weight (kg)	Embodied energy (kWh/kg)	Embodied energy (kWh)
1	Glass	15.00	7.28	101.92
2	Steel sheet	12.00	8.89	88.9
3	Black paint	1.00	25.11	25.11
4	Plastic sheet and rubber parts	1.00	25.64	25.64
5	Various bolts, washers, screws (steel), and rivets	1.00	8.89	8.89
6	Al. sheet	11.00	55.28	552.8
7	Wood	21.00	2.89	57.8
8	Photovoltaic module (length, 0.6 m; breadth, 0.55 m; and height, 0.01 m)	1 No.	369.5	369.5
9	Fan (operated on DC)	1 No.	26.83	26.83
	Grand Total			**1257.39**

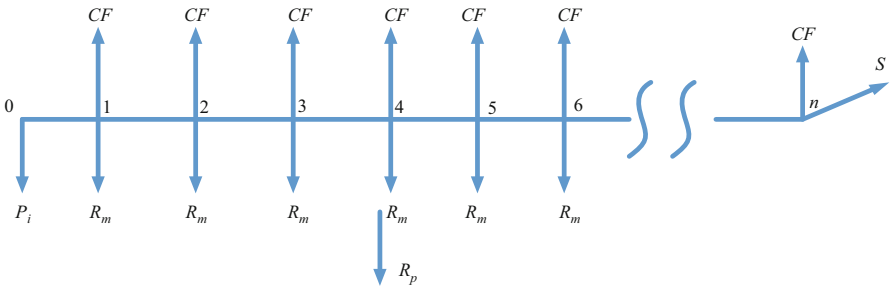

Fig. 3 Cash flow diagram for hybrid PV integrated solar dryer

energy for different items for fabrication of hybrid PV-T solar dryer is calculated as 1257.39 kWh. Thereafter the annual energy output for the above dryer has been calculated as the sum of the net annual electrical output and annual thermal output. Net annual electrical output has been calculated by multiplying daily electrical output with the number of clear sunny days in a year, and it has been calculated as 45.6 kWh per year. Similarly, the net annual equivalent thermal output is calculated as 120 kWh per year. Therefore, the total energy output of the dryer has been calculated as 222.15 kWh.

The dryer was used for drying of 450 g cauliflower in each tray. The experiments were conducted in October 2015 to dry cauliflower. The cauliflowers were purchased from a local market, manually sorted, and washed with fresh water to remove undesirable materials, e.g., dust and foreign materials. The drying time was 2 clear sunny days of 8 h (10.00 to 5.00) by using hybrid PV-T integrated solar dryer. About 350 g moisture was removed in 2 days from drying 450 g cauliflower.

Figure 3 shows the cash flow diagram for the hybrid PV-T integrated solar dryer. Annual income of the dried cauliflower has been calculated as Rs. 1350. The annualized salvage value is calculated as Rs. 31.42 as shown in Eq. (6). From the results, the cost of drying of the dryer is calculated as Rs. 24.5 as given in Eq. (7).

7 Conclusion

The following conclusions are drawn from economic analysis of hybrid photovoltaic-thermal (PV-T) integrated indirect-type solar dryer:

1. PV-based solar dryer is a self-sustained solar dryer harnessing abundantly available solar energy.
2. The total energy payback period for hybrid PV-T solar dryer is 5.6 years, which is much less than the expected life of the dryer.
3. Total benefit of dried cauliflower is calculated as Rs. 362, and benefits of dried product will be higher if large quantities of products are taken for drying.

Nomenclature

A	Area, m^2
b	Width of PV module, m
L	Length of PV module, m
C_d	Cost of drying, Rs./kg
C_s	Specific heat, J/kg °C
CF	Net cash flow
CRF	Capital recovery factor
E_{aout}	Annual thermal output, kWh
E_{PBT}	Energy payback time, years
i	Annual rate of interest (in fraction) is taken as 4% = 0.04
$I(t)$	Incident solar intensity, Wm^2
I_L	Load current, Amp
I_{SC}	Short circuit current, Amp
M_p	Mass of product, kWh
n	Life of the dryer = 30 years
N	Number of sunshine hours, h
Pi	Initial investment (Rs.) = 17,628.8
$(Q_u)_{daily}$	Daily thermal output, kWh
R_m	Operational and maintenance expenses (Rs.) = 0
R	Annualized present cost (Rs.)
R'	Annualized salvage value of the dryer
S	Salvage value of the dryer at the end of the life (Rs.) = 10% of initial investment = Rs. 1762.8
T	Temperature, °C
V_L	Load voltage, V
V_{OC}	Open circuit voltage, V

Subscripts

a	Ambient
c	Solar cell
d	Drying

References

Bala BK, Mondol MRA, Biswas BK, Chowdhury BLD, Janjai S (2003) Solar drying of pineapple using solar tunnel drier. Renew Energy 28(2):183–190

Barnwal P, Tiwari GN (2008) Design, construction and testing of hybrid photovoltaic integrated greenhouse dryer. Int J Agric Res 3(2):110–120

Boughali S et al (2009) Crop drying by indirect active hybrid solar – electrical dryer in the eastern Algerian Septentrional Sahara. Solar Energy 83(12):S. 2223–S. 2232. doi:10.1016/j.solener.2009.09.006

Celma AR, Cuadros F (2009) Energy and exergy analyses of OMW solar drying process. Renew Energy 34(3):S. 660–S. 666. doi:10.1016/j.renene.2008.05.019

Chowdhury MMI et al (2011) Energy and exergy analysis of the solar drying of jackfruit leather; Biosyst Eng 110 (2), S. 222–229. doi:10.1016/j.biosystemseng.2011.08.011
Corzo O et al (2008) Energy and exergy analyses of thin layer drying of coroba slices; J Food Eng 86 (2), S. 151–161. DOI: 10.1016/j.jfoodeng.2007.05.008
Dincer I, Sahin AZ (2004) A new model for thermodynamic analysis of a drying process. Int J Heat Mass Transf 47(4):S. 645–652. doi:10.1016/j.ijheatmasstransfer.2003.08.013
Dubey S, Tiwari GN (2008) Thermal modeling of a combined system of photovoltaic thermal (PV/T) solar water heater. Solar Energy 82:602–612
ELkhadraoui A et al (2015) Experimental investigation and economic evaluation of a new mixed-mode solar greenhouse dryer for drying of red pepper and grape; Renew Energy 77, S. 1–8. doi:10.1016/j.renene.2014.11.090
Farkas I, Seres I, Meszaros CS (1999) Analytical and experimental study of a modular solar dryer. Renew Energy 16:773–778
Fudholi A et al (2015) Techno-economic of solar drying systems with water based solar collectors in Malaysia: a review. Renew Sustain Energy Rev 51, S. 809–820. doi:10.1016/j.rser.2015.06.059
Ghazanfari A et al (2003) Evaluating a solar dryer for in-shell drying of split pistachio nuts. Dry Technol 21(7):1357–1368
Hossain MA, Bala BK (2007) Drying of hot chilly using solar tunnel drier. Solar Energy 81 (1):85–92
Hossain MA, Woods JL, Bala BK (2005) Optimization of solar tunnel drier for drying of chilly without color loss. Renew Energy 30:729–742
Maia CB et al (2013) Energy and exergy analysis of the airflow inside a solar chimney. Renew Sustain Energy Rev 27:S. 350–361. doi:10.1016/j.rser.2013.06.020
Motevali A et al (2014) Comparison of energy parameters in various dryers. Energy Convers Manage 87:S. 711–725. doi:10.1016/j.enconman.2014.07.012
Mumba J (1995) Development of a photovoltaic powered forced circulation grain dryer for use in the tropics. Renew Energy 6(7):855–862
Mumba J (1996) Design and development of a solar grain dryer incorporating photovoltaic powered air circulation. Energy Convers Manage 37(5):615–621
Panwar NL et al (2012) A review on energy and exergy analysis of solar dying systems. Renew Sustain Energy Rev 16(5):S. 2812–2819. doi:10.1016/j.rser.2012.02.053
Phougchandag S, Woods JL (2000) Solar drying of banana: mathematical model, laboratory simulation and field data compared. J Food Sci 65(6):990–996
Rahman SMA et al (2013) An economic optimization of evaporator and air collector area in a solar assisted heat pump drying system. Energy Convers Manage 76:S. 377–384. doi:10.1016/j.enconman.2013.06.058
Saleh T, Sarkar MAR (2002) Performance study of a PV operated forced convection solar energy dryer. In: The 8th international symposium for renewable energy education (ISREE-8), Orlando, University of Florida
Sami S et al (2011) Energy and exergy analysis of an indirect solar cabinet dryer based on mathematical modeling results; Energy 36 (5), S. 2847–2855. DOI: 10.1016/j.energy.2011.02.027
Sopian K, Liu HT, Kakac S, Veziroglu TN (2000) Performance of a double pass photovoltaic thermal solar collector suitable for solar drying systems. Energy Convers Manage 41:353–365
Togrul IT, Pehlivan D (2002) Mathematical modelling of solar drying of apricots in thin layers. J Food Eng 55(3):209–216

Energy Analysis of the Direct and Indirect Solar Drying System

Om Prakash, Anil Kumar, Prashant Singh Chauhan, and Daniel I. Onwude

Abstract The energy study is very important for any energy system due to rise in fuel cost, raw materials cost, and higher environmental impact of the energy system. Hence, a study on energy analysis of solar drying system becomes indispensable. In order to highlight the energy requirements of solar drying system, this chapter attempts to show extensive energy analysis of direct/indirect solar dryers. The CO_2 discharge per year, embodied energy, energy payback time, carbon mitigation, and carbon credit have all been considered. The embodied energy of greenhouse dryers in passive mode and the life cycle cost have also been evaluated. The finding shows about 17.6% reduction in per unit cost of the fossil fuel-generated electricity. The net mitigation of CO_2 for the dryer is 38.06 tons, and the earned carbon credit varies from INR 12,561.70–50,245.49. This finding suggests that energy analysis of direct/indirect solar dryers is important in protecting the environment from pollution and is also a viable tool in the design of efficient drying system.

Keywords Energy • Embodied energy • Energy payback time • Carbon mitigation • Carbon credit

O. Prakash
Department of Mechanical Engineering, Birla Institute of Technology, Mesra, Ranchi 835215, India

A. Kumar (✉)
Department of Energy (Energy Centre), Maulana Azad National Institute of Technology, Bhopal 462003, Madhya Pradesh, India
e-mail: anilkumar76@gmail.com

P.S. Chauhan
Department of Energy (Energy Centre), Maulana Azad National Institute of Technology, Bhopal 462003, India

D.I. Onwude
Department of Agricultural and Food Engineering, Faculty of Engineering, University of Uyo, 52021 Uyo, Nigeria

© Springer Nature Singapore Pte Ltd. 2017

O. Prakash, A. Kumar (eds.), *Solar Drying Technology*, Green Energy and Technology, DOI 10.1007/978-981-10-3833-4_19

1 Introduction

Energy has become the basic need for human existence. This need cuts across all aspects of life: domestic, transportation, industrial, medical, agricultural, and so on, where energy is required for proper functioning. Therefore, energy security has become an important requirement in the present social set-up. It can be ensured by the conservation of non-renewable energy sources and utilization of renewable energy sources. Bentley (2002) has suggested that non-renewable energy sources are being depleted due to unrestricted harnessing and fixed resources.

Till now, the generation of electricity is mainly dependent on non-renewable energy sources, mostly fossil fuel. However, this energy source is diminishing with alarming rate day by day (Prakash and Kumar 2014). Another disadvantage is air pollution and environment pollution. These are mostly due to CO_2 emission, which is due to burning of fossil fuels. Therefore, it necessitates exploring renewable energy sources with great seriousness and urgency.

Among all renewable energy sources, the solar energy is freely available everywhere and can easily be harnessed. This energy is also environmentally friendly and pollution-free. In recent years, awareness about the application of solar energy to fulfil various needs in domestic as well as the industrial level has increased rapidly. This includes the development of more environmentally friendly solar collectors (photovoltaic), which are often deployed in solar dryers (Kumar and Mandapati 2012).

The photovoltaic (PV) system is used to generate direct current (DC) directly from solar radiation. The generated DC current can be used as alternating current (AC) with the help of an inverter. The main limiting factor of this system is low electrical efficiency. It serves as the promising substitute to generate electricity from fossil fuel. By the suitable provision in this system, the PV system provides daylighting and thermal energy. Due to intensive research, the application of PV is increasing day by day. It also mitigates the CO_2 emissions, which decrease the environmental pollution substantially.

Based on the study of previous chapters, the performance of solar dryers under active mode is found to be better in the drying of crop containing high moisture content than passive mode dryers (Prakash et al. 2016). The active mode solar dryer requires the exhaust fan to continuously ventilate the moist and humid air. Therefore, PV system can be applied to supply power to run the exhaust fan of the dryer.

Alsema and Niluwlaar (2000) have computed total required energy, CO_2 emission, and EPBT for the making of PV scheme. It is observed that they did not pay attention to parameters such as support structure, the frequency of battery spare, and effectiveness of balance of system (BOS). Krauter and Ruther (2004) simply calculated energy constraint and CO_2 emission in the manufacturing of PV and did not consider above factors. Frankl et al. (1998) have measured maintenance structure to evaluate energy constraint for making PV scheme. However, a review of their study shows that the life cycle of battery was assumed to be the same as PV system. Kumar and Mandapati (2012) designed a stand-alone photovoltaic system

for conference hall of the Department of Energy, Maulana Azad National Institute of Technology, Bhopal, India. The life cycle cost (LCC), EPBT, carbon credit, and CO_2 emission were considered for the proposed system. They also reported a 17.6% reduction in per unit cost of the fossil fuel-generated electricity. Nawaz and Tiwari (2006) presented embodied energy (EE) analysis for PV system applied in micro and macro level for the inclined surface in India. They also analyzed the EPBT and CO_2 emission. The EPBT is calculated with and without BOS for two different conditions, namely, open field and rooftop. The study reveals that the EE of the macro level is lower than micro level EE. The local authorities of Spain have supported an SPV project of 65 sites having a capacity of 50 kWp.

Bhuiyan and Asgar (2003) had developed a stand-alone photovoltaic system which can be used in residential houses. The design concept is based on the standard procedure for Dhaka, Bangladesh. For any SPV system, the main expenditure is on PV arrays' size and battery. By optimal sizing of the SPV system, the substantial amount of the investment cost can be reduced.

Kumar and Mandapati (2012) defined the insolation value (kWh/m^2) for flat sheet. In this study, all essential techno-economic and environmental parameters for the installation of the SPV system such as sizing of PV array, life cycle cost analysis, earned carbon credit, and mitigation of CO_2 emissions were taken into considerations. In addition, energy analysis and thermal performance of mud house located in IIT Delhi, India, show that 5.2 metric tons/year of CO_2 emission was mitigated by such system. This is also valid in different parts of India. Chel and Tiwari (2011) demonstrated 2.32 kWp SPV for New Delhi in the composite climate in their study. The outdoor experiment was conducted each month of the year in different weather conditions, namely, clear, partially cloudy, hazy, and fully cloudy. The hourly efficiency of the system was evaluated and reported. The LCC, EPBT, and energy production factor (EPF) have been calculated and presented.

Chel and Tiwari (2009) have done the energy analysis of the earth to air heat exchanger integrated with adobe building for New Delhi composite climate. Experimental result reveals that the rise in room temperature is 5–15 °C as compared to ambient temperature in the winter season, and temperature decreased in summertime. This concept saves the energy. About 16 tons/year of CO_2 emission is mitigated. The payback period of the system is not greater than two years.

2 Embodied Energy

The total energy needed to produce any substances or service in entire life cycle is called embodied energy (EE). This concept is quite useful for evaluating the energy saving substances or service. In Tables 1 and 2, the embodied energy of some commonly used materials is given.

Table 1 Embodied energy of some selected materials (Hammond and Jones 2008)

Material	Energy (MJ Per Kg)	C (Kg Per Kg)	Density (Kg/m^3)
Aggregate	0.083	0.0048	2240
Concrete (1:1.5:3)	1.11	0.159	2400
Bricks (common)	3	0.24	1700
Concrete block (Medium density)	0.67	0.073	1450
Aerated block	3.5	0.3	750
Limestone block	0.85	–	2180
Marble	2	0.116	2500
Cement mortar (1:3)	1.33	0.208	
Steel (general, av. recycled content)	20.1	1.37	7800
Stainless steel	56.7	6.15	7850
Timber (general, excludes sequestration)	8.5	0.46	480–720
Glue laminated timber	12	0.87	–
Cellulose insulation (loose fill)	0.94–3.3	–	43
Cork insulation	26	–	160
Glass fibre insulation (glass wool)	28	1.35	12
Flax insulation	39.5	1.7	30
Rockwool (slab)	16.8	1.05	24
Expanded Polystyrene insulation	88.6	2.55	15–30
Polyurethane insulation (rigid foam)	101.5	3.48	30
Wool (recycled) insulation	20.9	–	25
Straw bale	0.91	–	100–110
Mineral fibre roofing tile	37	2.7	1850
Slate	0.1–1.0	0.006–0.058	1600
Clay tile	6.5	0.45	1900
Aluminium (general & incl 33% recycled)	155	8.24	2700
Bitumen (general)	51	0.38–0.43	–
Medium density fibreboard	11	0.72	680–760
Plywood	15	1.07	540–700
Plasterboard	6.75	0.38	800
Gypsum plaster	1.8	0.12	1120
Glass	15	0.85	2500
PVC (general)	77.2	2.41	1380
Vinyl flooring	65.64	2.92	1200
Terrazzo tiles	1.4	0.12	1750
Ceramic tiles	12	0.74	2000
Wool carpet	106	5.53	–
Wallpaper	36.4	1.93	–
Vitrified clay pipe (DN 500)	7.9	0.52	–
Iron (general)	25	1.91	7870
Copper (average incl 37% recycled)	42	2.6	8600

Table 2 Embodied energy of different photovoltaic cells (Hammond and Jones 2008)

Photovoltaic (PV) cell types	Energy (MJ per m^2)	C (Kg per m^2)
Monocrystalline (average)	4750	242
Polycrystalline (average)	4070	208
Thin film (average)	1305	67

3 Energy Payback Time (EPBT)

Energy payback period is the essential time to recover embodied energy of the product. The unit is the year. It is calculated as

$$\text{Energy Payback Time(EPBT)} = \frac{\text{Embodied Energy}}{\text{Annual Energy Output}} \text{(year)} \quad (1)$$

Therefore, energy payback time depends on a live energy and annual energy output.

4 CO_2 Emission

Watt et al. (1998) have suggested that by coal-generated electricity, the emission of average CO_2 is approximately equivalent to 0.98 kg of CO_2/kWh. The lifetime of greenhouse dryer is found to be 35 years (Prakash and Kumar 2014). Therefore, the carbon dioxide emission per year can be calculated as

$$CO_2 \text{ emissions per year} = \frac{\text{Embodied energy} \times 0.98}{\text{Lifetime}} \quad (2)$$

5 Carbon Mitigation and Earned Carbon Credit

The mitigation of carbon dioxide (CO_2) is applied for the measure of climate change potential. The net CO_2 mitigations are measured per kilowatt-hour; hence it can be compared with other power production systems. The carbon credit can be defined as "a key component of national and international emissions trading schemes that have implemented to mitigate global warming". It provides a means to minimize the greenhouse effect emission on a commercial scale by capping total annual emissions and providing an opportunity to compensate any shortfall of assign mitigation of greenhouse gas emission. The exchange of carbon credit can be purchased and sold in international market or business at the current price. This can be employed in financial carbon reduction schemes.

The daily efficiency is calculated as

$$\eta_{\mathrm{d}} = \frac{\text{Daily Output Energy}}{\text{Daily Input Energy}} = \frac{M \times \lambda}{I_{\mathrm{m}}(t) \times A} \times 100, \tag{3}$$

where M is the mass of evaporated water (kg); λ is latent heat of vaporization (J/kg), that is, 2.26×10^6 J/kg; $I_{\mathrm{m}}(t)$ is mean instance solar emission on the dryer (W/m^2); and A is the area of the dryer (m^2).

$$\begin{aligned}&\text{Daily thermal output of dryer(kwh)}\\ &= \frac{\text{Moisture evaporated(kg)} \times \text{latent heat of evaporation(J/kg)}}{3.6 \times 10^6}\end{aligned} \tag{4}$$

$$\begin{aligned}&\text{Yearly thermal output energy of the dryer } (E_a)\\ &= \text{Daily thermal output energy of dryer} \times N_d\end{aligned} \tag{5}$$

where N_d is the total number of sunshine days in a year, which is 300 (Assume), and N_h is the number of sunshine hour per day, which is 7 h.

$$\text{Daily input energy} = I_{\mathrm{m}}(t) \times N_h \times A_r \times 10^{-3}\text{kWh} \tag{6}$$

The various losses of energy by the consumer in domestic appliances in unit power consumption are taken as L_{a} (10%) then transmitted power $\frac{1}{1-L_{\mathrm{a}}}$ units; the loss of energy per unit in transmission and distribution is L_{td} (taken 45%). Hence the generation of power in the plant would be $\frac{1}{1-L_{\mathrm{a}}} \times \frac{1}{1-L_{\mathrm{td}}}$ unit.

Since the mean CO_2 equivalent intensity from coal-based power is 0.98 kg of CO_2/kWh, then the amount of CO_2 mitigation of the system would be

$$X = \frac{1}{1-L_{\mathrm{a}}} \times \frac{1}{1-L_{\mathrm{td}}} \times 0.98 = 2.01 \text{ kg per unit.} \tag{7}$$

$$\textit{The } \mathrm{CO_2} \textit{ mitigation in the lifetime of the dryer} = E_m \times X, \tag{8}$$

where E_{m} has embodied energy in kWh.

$$\begin{aligned}&\textit{The net mitigation of } \mathrm{CO_2} \textit{ over lifetime (kg)}\\ &= \textit{Total } \mathrm{CO_2} \textit{ Mitigation} - \textit{Total } \mathrm{CO_2} \textit{ emission} = [E_a \times n \times X - E_m]\, k,\end{aligned} \tag{9}$$

where n is the life span of the dryer which is taken as 35 years.

$$\textit{Earned Carbon credit would be} = \text{net } \textit{mitigation of } \mathrm{CO_2} \textit{ in life span (tones)} \times D \tag{10}$$

Here, D is the cost of carbon credit which varies from INR 300 to 1200/tons of CO_2 mitigation.

6 Case Study

6.1 Case Study 1

6.1.1 Energy Analysis of Modified Greenhouse Dryer Under Active Mode for Tomato Flakes Drying

Prakash and Kumar (2014) carried out energy analysis of tomato flakes drying in the modified greenhouse dryer under active mode as shown in Fig. 1. The dimension of the dryer is $1.5 \times 1.0 \times 0.712$ m^3 with one exhaust DC fan (12 V, 0.32 A) of 127 mm diameter which was positioned in the upper portion of the west wall of the dryer. The dryer was powered by the six-polycrystalline solar cell of 1 kWp with battery backup connected through a solar charge controller. The structure of the dryer was made of an aluminium edge enclosed by a polycarbonate piece nevertheless on the north wall. The north wall was made opaque by a 3 mm thick mirror to minimize the solar radiation losses. In order to minimize the heat conduction losses through the ground surface inside the dryer, a dark PVC piece was spread on the ground.

The EE of individual items used in fabrication of the improved greenhouse dryer under active mode is presented in Table 3.

From Table 3, it can be seen that the aluminium section consumed the highest amount of energy when compared with other materials used in fabricating the dryer. Figure 2 further illustrates the breakup of items used in the fabrication of modified

Fig. 1 Photograph of active mode modified greenhouse dryer (Prakash and Kumar 2014)

Table 3 Embodied energy of different component used in the fabrication of modified greenhouse dryer under active mode

S. No.	Material	Quantity	Embodied energy coefficient	Total (kWh)
1	Polycarbonate sheet	15.600 kg	10.1974 (kWh/kg)	159.0794
2	Glass	5.400 kg	7.2800 (kWh/kg)	39.3120
3	Silver coating	0.750 m^2	0.2780 (kWh/m^2)	0.2085
4	Black PVC sheet	0.325 kg	19.4400 (kWh/kg)	6.3180
5	Wire mesh steel tray	0.700 kg	9.6700 (kWh/kg)	6.7690
6	Aluminium section			
	(i) 1"×1 mm section	3.590 kg	55.2800 (kWh/kg)	198.4552
	(ii) 4"×1 mm section	0.820 kg	55.2800 (kWh/kg)	45.3296
	(iii) 1"×3 mm angle	0.080 kg	55.2800 (kWh/kg)	4.4224
7	Fitting			
	(i) Hinges/*kabja*	0.200 kg	55.2800 (kWh/kg)	11.0560
	(ii) *Kundi*(door lock)	0.025 kg	55.2800 (kWh/kg)	1.3820
	(iii) Handle	0.100 kg	55.2800 (kWh/kg)	5.5280
	(iv) Steel screw	0.250 kg	9.6700 (kWh/kg)	2.4175
8	DC fan	–	–	–
	(i) Plastic	0.120	19.4400 (kWh/kg)	2.3328
	(ii) Cooper wire	0.050	19.6100 (kWh/kg)	0.9805
9	Polycrystalline solar cell	0.059 m^2	1130.6000 (kWh/m^2)	66.1378
10	Battery	–	–	46.0000
11	Solar charge controller	–	–	33.0000
	Grand total (kWh)			**628.7287**

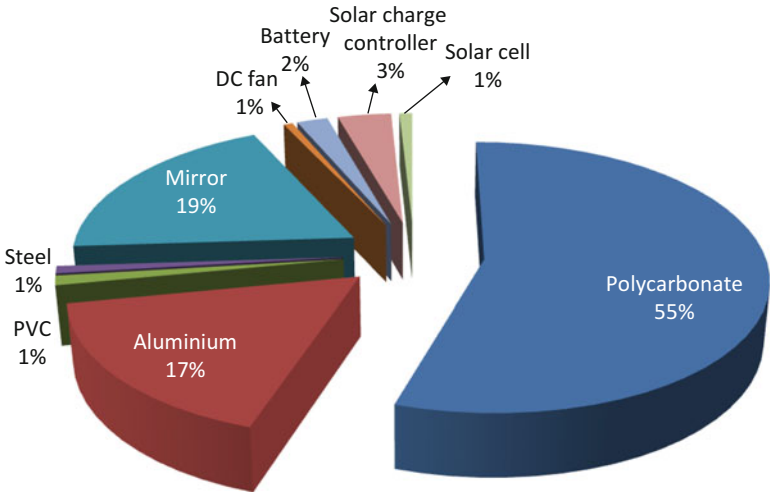

Fig. 2 Breakup of items used in the fabrication of modified greenhouse dryer under active mode (Prakash and Kumar 2014)

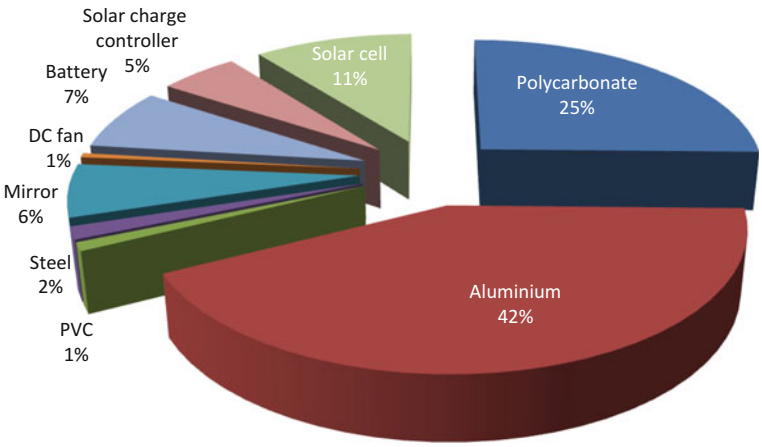

Fig. 3 Breakup of embodied energy of the various items used in modified greenhouse dryer under active mode (Prakash and Kumar 2014)

greenhouse dryer under active mode. Here contribution of polycarbonate is highest. The breakup of embodied energy of used materials in the dryer is presented in Fig. 3 (Prakash and Kumar, 2014). Aluminium contributes the highest percentage of embodied energy in the system. The total EE of this system is 628.73 kWh. The increase in the embodied energy in the modified greenhouse dryer under active mode is due to the application of drain DC fan and its renewable arrangement for the supply of power.

Furthermore, Table 4 shows the energy payback time for different dryers. The comparative analysis of the annual energy output from the dryers and their energy payback time for crops containing high to moderate moisture content, such as tomato and potatoes, are also highlighted in Table 4. The dryer developed by Prakash and Kumar (2014) has low energy payback period as compared to other modified/hybrid greenhouse dryer. The study reveals that under both conditions, the EPBT of the altered greenhouse dryer in passive mode has the lowest value. This is due to its simplicity in construction and operation. The high EPBT for the modified greenhouse dryer under active mode is due to the application of exhaust fan and their provision to power it through solar energy. The comparative analysis of the various solar dryer is further presented in Table 4 (Prakash and Kumar 2014).

The CO_2 emission in kg per year has been calculated for greenhouse dryer in active and passive mode. The CO_2 emission of passive mode dryer is only 13.45 kg per year. However, under active mode it is 17.6 kg per year. The relative study of CO_2 secretion of the various solar dryer is presented in Fig. 4 (Prakash and Kumar 2014).

The net mitigation of CO_2 for the dryer is 38.06 tons, and the earned carbon credit varies from INR 12,561.70 per ton of C to 50,245.49 per ton of C.

Table 4 Energy payback time for various solar dryers (Prakash and Kumar 2014)

S. No.	Solar dryer	EPBT (years)
1	Cabinet dryer	13.27
2	Greenhouse crop dryer	1.43
3	Reverse absorber cabinet dryer	54.01
4	Active (conventional) solar dryer	102.5
5	Hybrid PV/T greenhouse dryer	155.54
6	Hybrid conventional PV/T dryer	41.07

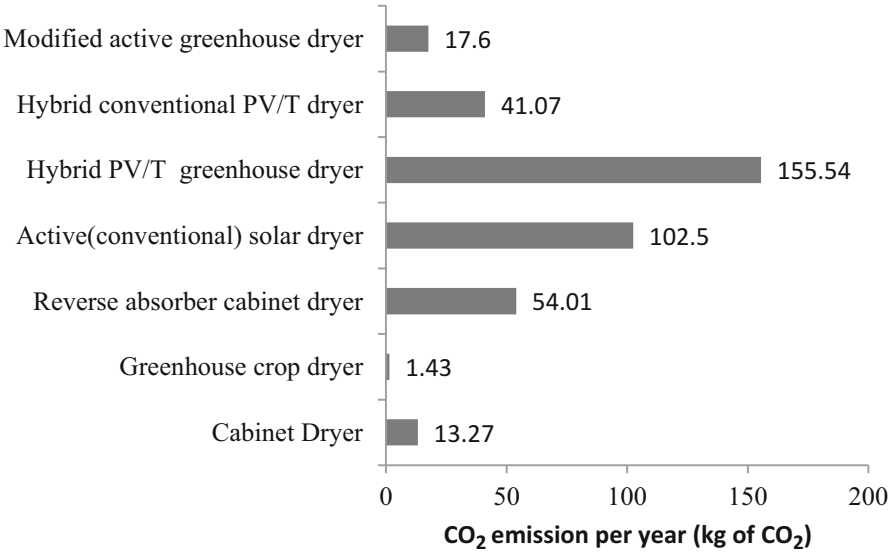

Fig. 4 CO_2 emission of different solar dryers (Prakash and Kumar 2014)

6.2 Case Study 2

6.2.1 Energy Analysis of the Hybrid PVT-Based Greenhouse Dryer for Mint Drying

Nayak et al. (2011) demonstrated the drying of mint in a hybrid photovoltaic-thermal-centred greenhouse dryer. The source of the fossil fuel is depleting day by day, and the price of the fossil fuel is increasing day by day. In order to decrease the cost of the drying and saving energy from fossil fuel, a hybrid PVT ultraviolet (UV)-stabilized polyethylene greenhouse dryer (PGD) emerges as one of the alternatives. It is cost-effective. This dryer comprised aluminium units, two PV units, three DC fans, an ultraviolet-stabilized polyethylene slip, and so on. Aluminium units were recycled in manufacture to escape rusting erosion from environments, increasing the life span of the dryer equivalent to the life of PV module, which is 30 years. The PV units were placed on the south roof of the

greenhouse dryer. Easy opening–closing of the PV module and symmetrical air vents (placed on the north roof) was facilitated by using hooks, hinges, etc. The UV-stabilized polyethylene sheet was fixed to the physical frame of the dryer with the help of steel screws with washer, rivets, nuts, and bolts. Each tier of the drying system consisted of two wire mesh trays, with a base area of 0.9 m ×1.30 m. The dryer had (a) a floor area of 2.50 m×2.60 m, (b) a central height of 1.80 m, and (c) sidewalls of 1.05 m. Its north and south roofs had leanings of 30 degree each positioned horizontally, which is the latitude of New Delhi.

The integrated dryer consisted of two PV units (glass to glass; dimensions, 1.20 m×0.55 m×0.01 m; 75kWp) integrated on its south roof and two openings (dimension, 1.10 m × 0.55 m) in the north roof. The drying unit was evaluated to dry the mint leaf. The location of the greenhouse was as east–west in the experiments due to the motion of the sun from east to west due south. The greenhouse was erected above the ground to allow air to pass through the base of the tray for thermal heating and extracting moist air from the product. Inside the greenhouse, three DC fans were fitted at the upper end of the east and west sides in order to increase the mass flow rate for faster removal of moisture and thus further the drying course to the necessary level. More, the effects show that the efficiency of the dryer and net carbon dioxide mitigation throughout the lifetime was 34.2% and 140.97 tons, correspondingly. The variation of earned carbon credit is INR 47,929.8 per ton of carbon–191,719.2 per ton of carbon.

6.3 Case study 3

6.3.1 Energy Analysis of the Indirect Solar Dryer

Shrivastava and Kumar (2015) developed an indirect solar dryer as shown in Fig. 5. The system was designed, developed, and tested in the Department of Energy (Energy Centre), Maulana Azad National Institute of Technology, Bhopal, India. The system consists of solar air heater, air supply unit which consists of four AC fans, four 12 V DC fans, and a drying chamber. The drying chamber also comprises two drying trays of dimension 0.7 m × 0.7 m with a combined capacity of 4 kg (2 kg in each tray). The top transparent glass of solar air heater of 1m ×1m dimension was used. The top transparent surface is made of toughened glass of thickness 0.005 m. The whole system is well insulated with glass wool and putty. The enclosed surface of the air heater is made of fibre reinforced polymer (FRP). The thickness of FRP is 3 mm and its dimension is 1 m × 1 m × 0.15 m. Below the transparent toughen glass, the galvanized iron sheet was used as absorber plate of the air heater. The dimension of this plate is 0.9 m×0.85 m×0.002 m.

The working process of the system involved (1) the introduction of ambient air by the air supply unit to the solar air heater unit. Here, the inlet air gets heated up due to greenhouse effect in the solar air heater. The hot air is being supplied to the

Fig. 5 Photograph of the system (Shrivastava and Kumar 2015)

drying chamber through the duct. The dimension of the duct is 0.063 m diameter and 3 m length.

In order to examine the performance of the drying unit, fenugreek was dried. 2 kg of the fenugreek was put in each tray with a total of 4 kg and was used during the experiment. Drying of the product was achieved after 2 consecutive days. The final weight of the dried product was 0.454 kg. The embodied energy of the system is presented in Table 5. The total embodied energy of the system is 1081.8 kWh.

The drying efficiency of the system is 31.42%. The value of EPBT is 4.36 per annum, CO_2 emission per annum is 85.46, CO_2 mitigation is 391.52 kg per annum, and earned carbon credit lies between INR 46,982 per ton C and INR 187,931 per ton of C in the product life time.

7 Conclusion

Due to rapid depletion and increase in the price of fossil fuel, there is an increase in the importance of energy analysis for solar dryers. At present, the energy efficient solar dryers have gained increased interest as seen in the literature. Five different energy analysis techniques were applied in highlight the energy efficiencies of

Table 5 Embodied energy of the system

S. No.	Material	Embodied energy (kWh/kg)	Quantity (kg)	Total (kWh)	References
1	Plywood	2.88	17.57	50.60	Baird and Haslam (1997)
2	Glass wool	4.044	5.97	24.13	Baird and Haslam (1997)
3	Aluminium sheet	55.28	13.07	722.5	Baird and Haslam (1997)
4	Steel wire mesh tray	8.89	3.79	33.63	Baird and Haslam (1997)
5	FRP sheet	19.39	5.31	102.96	Baird and Haslam (1997)
6	Absorber plate	9.636	2.98	28.74	Baird and Haslam (1997)
7	PVC pipe	19.39	2.29	44.40	Baird and Haslam (1997)
8	Glass cover	7.2800	5.16	37.56	Baird and Haslam (1997)
9	Plastic	19.440	0.12	2.33	Baird and Haslam (1997)
10	Copper wire	19.6100	0.050	0.98	Baird and Haslam (1997)
11	Fittings (nuts, bolts, screw and rivets)	8.89	1	8.89	Baird and Haslam (1997)
12	Paint	25.11	1	25.11	Baird and Haslam (1997)
Total				**1081.83 kWh**	

different direct/indirect solar dryers. They include embodied energy, CO_2 emission in kg per year, energy repayment time, C mitigation, and earned C acclaim. The analysis from literature showed that the earned carbon credit can be exchanged as the international market values. For the indirect solar dryer, the variation of the earned carbon credit per ton of carbon is INR 46,982–INR 187,931. However, for the modified greenhouse dryer, it varies from INR 12,561.70–50,245.49. This analysis is important in protecting the environment from pollution and is also a viable tool in the design of efficient drying system.

References

Alsema EA, Niluwlaar E (2000) Energy viability of photovoltaic system. Energy Policy 28:999–1010

Baird AG, Haslam P (1997) The energy embodied in building materials-updated New Zealand coefficients and their significance, IPENZ Transactions 24

Bentley RW (2002) Global oil and gas depletion: an overview. Energy Policy 30(3):189–205

Bhuiyan MH, Asgar MA (2003) Sizing of a stand-alone photovoltaic power system at Dhaka. Renew Energy 28:929–938

Chel A, Tiwari GN (2009) performance evaluation and life cycle cost analysis of earth to air heat exchanger integrated with adobe building for New Delhi composite climate. Energy Buildings 41:56–66

Chel A, Tiwari GN (2011) A case study of a typical 2.32 kWp Stand-Alone Photovoltaic (SAPV) in composite climate of New Delhi (India). Appl Energy 88:1415–1426

Frankl PP, Masini A, Gamberale M, Toccaceli D (1998) Simplified life cycle analysis of PV system in building present situation and future trends. Prog Photovoltaic Res Appl 6 (2):137–146

Hammond GP, Jones CI (2008) Embodied energy and carbon in construction materials. Pro ICE Energy 161(2):87–98

Krauter S, Ruther R (2004) Consideration for the calculation of greenhouse gas reduction by photovoltaic solar energy. Renew Energy 29:345–355

Kumar A, Mandapati R (2012) Designing and lifecycle assessment of SPV system for conference hall at Dept. of Energy, MANIT, Bhopal. Int J Wind Renew Energy 1(2):79–83

Nawaza I, Tiwari GN (2006) Embodied energy analysis of photovoltaic (PV) system based on macro- and micro-level. Energy Policy 34:3144–3152

Nayak S, Kumar A, Mishra J, Tiwari GN (2011) Drying and testing of mint (Mentha piperita) by a hybrid photovoltaic-thermal (PVT)-based greenhouse dryer. Dry Technol 29(9):1002–1009

Prakash O, Kumar A (2014) Environomical analysis and mathematical modelling for tomato flakes drying in modified greenhouse dryer under active mode. Int J Food Eng 10(4):669–681

Prakash O, Kumar A, Laguri V (2016) Performance of modified greenhouse dryer with thermal energy storage. Energy Rep 2:155–162

Shrivastava, V, Kumar A (2015) Embodied energy analysis of the indirect solar drying unit. Int J Ambient Energy http://dx.doi.org/10.1080/01430750.2015.1092471

Watt M, Johnson A, Ellis M, Quthred N (1998) Life cycle air emission from PV power system. Prog Photovolt Res Appl 6(2):127–136

Part V
Innovations in Solar Drying

Energy Conservation Through Recirculation of Hot Air in Solar Dryer

Kamaruddin Abdullah

Abstract The use of pneumatic conveying system is quite new in solar drying system. The study of the application of pneumatic conveyor in solar drying system experiments using single unheated and heated pipe was conducted. It was found that the power requirement to convey rough rice was about 1.02 W/kg/h less than that used in the industry. The experiments also have found an expression of two-phase pressure of air and grains similar to Ergun's correlation. Testing with both inclined and vertical drying chamber of a recirculation-type solar dryer indicated that with the initial load of between 104 and 380.5 kg and initial moisture content on wet basis of 27.3–31%, less than a day of drying time is required. The drying efficiency and the specific energy of the solar dryer with inclined drying chamber were on an average less than the vertical type. The drying capacity (initial load) of the inclined drying chamber was larger than the vertical chamber type.

Keywords Drying efficiency • Energy requirement • Pneumatic conveyor • Specific energy • Power requirement

1 Introduction

Most of the available solar dryers use a stationary system in which the products to be dried are kept standstill in a box or cabinet. In this case, the final products will vary in their moisture content between the upper layer and the bottom layer. The use of pneumatic conveyor in a solar drying system is quite new. The reason for using the system was because it only requires small power to drive the centrifugal blower. In addition, the final moisture content is almost homogeny due to turbulent drying process that takes place within the pneumatic conveyor. Test results indicate that the required power to convey rough rice was between 500 and 600 W or 1.02 W/kg/h. Here, two types of tests were conducted to verify the practicality of the pneumatic drying system. The first type was a series of drying tests using an unheated

K. Abdullah (✉)
Universitas Darma Persada (UNSADA), Jl Radin Inten II, Pondok Kelapa, Jakarta Timur 13450, Indonesia
e-mail: kamaruddinabd@gmail.com

© Springer Nature Singapore Pte Ltd. 2017

O. Prakash, A. Kumar (eds.), *Solar Drying Technology*, Green Energy and Technology, DOI 10.1007/978-981-10-3833-4_20

and heated single pipe. The second type of test was using the completed system of pneumatic conveyor and the solar drying system. In the field test using inclined drying integrated collector drying chamber (ICDC) where a pneumatic conveyor was also used, loading with 380.5 kg of rough rice (initial mc of 27.1% wb), the required time to reach 14% wb was 8.48 h. Under this drying condition, the drying temperature was between 42 and 66 °C. Using a vertical cylinder ICDC solar dryer with 200 kg load of rough rice (initial mc of 27.3% wb) and also using a pneumatic conveyor, the required drying time to reach the final mc of 16.6% wb was 8 h, with average drying temperature of 42 °C. Here, the drying efficiency achieved was 31.7% and a specific energy of 10.7 MJ/kg of water evaporated.

2 Test Using Single Pipe

2.1 Instrumentation

A 4 inch single steel pipe was used in the test, as shown in Fig. 1. It comprises of a centrifugal blower, a feed hopper and pneumatic conveying pipe, and a receiving hopper. Besides that, an electric panel to measure power required during handling of grains and a U-tube manometer were also installed. At critical locations on the pipe, pressure taps were imbedded to measure the two-phase pressure drop, while a digital balance was used to measure the mass flow rate of the grains. To measure the airflow rate, a LT Lutron anemometer was used. The consumed electric power was measured using a volt- and amperemeter located in the electric panel. The dimension of the experimental setup is arbitrary.

2.2 Testing Procedure

Before starting the experiment, the average equivalent diameter of rough rice was measured from the sample. The test was started by opening the valve located beneath the feed hopper while making the blower to start operating. When steady state has been reached, the change in weight of rough rice on the digital balance under a specific time was recorded using a stopwatch. At the same time, the airflow rate was measured using LT Lutron anemometer from the pipe end. Pressure drop was recorded by reading the U-tube manometer level.

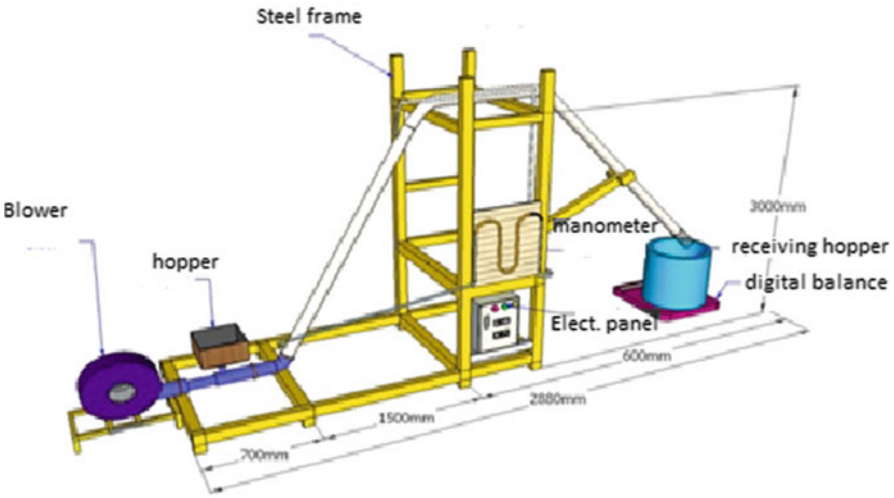

Fig. 1 Experimental setup for unheated pneumatic conveyor test (Kamaruddin et al. 2010a)

2.3 Test Results and Discussions

Figure 2 shows the results indicating that the of grains' flow rate Gp (kg/hr) increased as power (Watt) was increased. From this data, it was possible to formulate an empirical relation between the airflow rate and the required conveying power.

$$W_p = 1.15Pw + 7.52 \tag{1}$$

From the slope of the curve, it was found that the conveying capacity of the pneumatic system was 1.02 W/kg/hr. This value was smaller than the capacity of industrial pneumatic conveyor which was between 1.25 and 1.5 W/kg/hrs (Hanafi 2006).

Figure 3 shows the relation between the conveying power and the ratio between mass flow rate of the air W_a and that of the grains, W_p. The empirical relation was found to follow the following formula. It shows that with the increasing ratio, the power required was also increased proportionally.

$$Pw = 55.42\left(W_a/W_p\right) + 465.63 \tag{2}$$

Next is the relation between the mass flow rate of the grains and the two-phase (air and grains) pressure drop. The empirical relation follows to that of Ergun's such that:

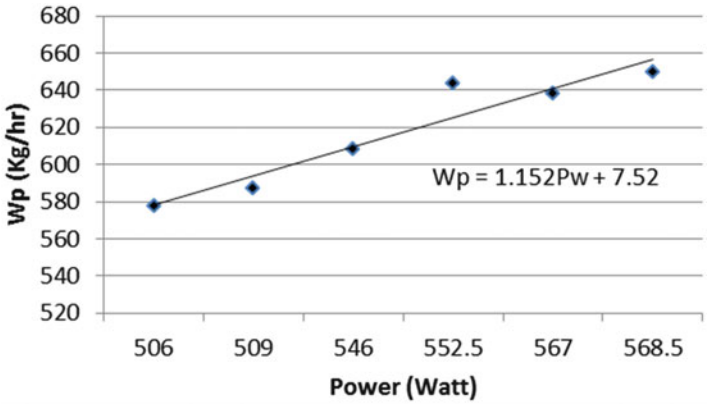

Fig. 2 Relation between the conveying power to the mass flow rate of the grains

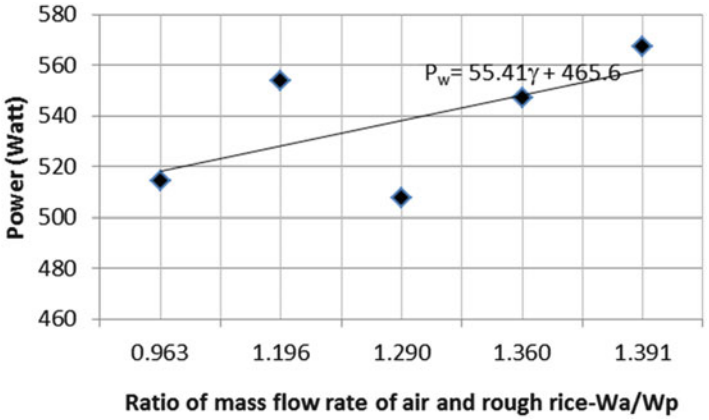

Fig. 3 Relation between power and ratio of mass flow rate of the air and that of the grains

$$\left(\frac{(P_0 - P)\rho_a.}{Go}\right)\left(\frac{\gamma}{(1-\gamma)}\right)\left(\frac{D_p}{L}\right) = 150\left(.\frac{(1-\gamma)\mu}{G_o D_p}\right)^{1.52} \tag{3}$$

Figure 4 shows the relation between the mass flow rate of the grains and the two-phase (solid and gas) pressure drop per unit length of pipe.

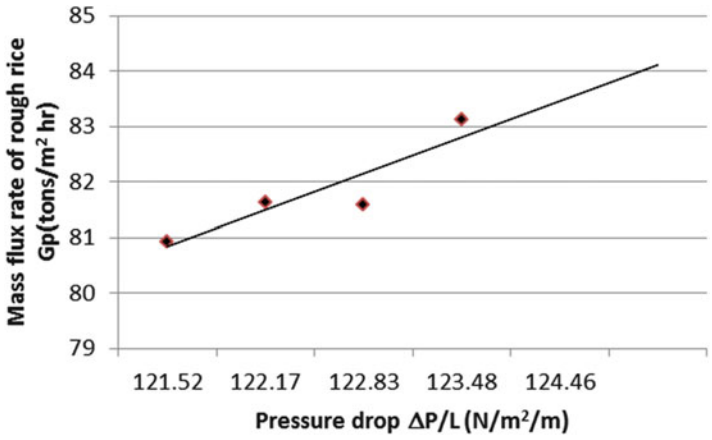

Fig. 4 Relation between the mass flow rate of the grains and the two-phase pressure per unit length of the pipe

3 Drying in a Heated Single Pneumatic Conveyor Pipe

Using the control volume shown in Fig. 5, an energy and mass balance equation can be developed.

$$\frac{\partial T_a}{dy} = \frac{-\left[h_{cv}(T_a - T_g) + G_a\left(\frac{\partial H}{\partial y}\right)Cp_w(T_a - T_g)\right] - U_v(T_a - T_r)}{G_a(Cp_a + Cp_w H)} \tag{4}$$

Since the absolute humidity is assumed to be constant within the heating shell, then the temperature change within the shell, T_r, becomes

$$\frac{\partial T_r}{dy} = \frac{-U_v(T_r - T_a)}{G_r Cp_a} \tag{5}$$

where Uv is the volumetric heat transfer coefficient; whereas for cylindrical shell, it can be expressed as follows:

$$U_v = U_a(4/D) \tag{6}$$

With the assumption of heat loss at 0.8 kW/m^2 °C, change in particle temperature along the pipe can be expressed as

$$\frac{\partial T_g}{dy} = -\frac{\left\{h_{cv}(T_a - T_g) + \left\{G_p(\Delta H_{fg} + (Cp_w - Cp_l)T_g\right\}\left(\frac{\partial H}{\partial y}\right)\right\}}{G_p(Cp_g + Cp_l M)} \tag{7}$$

In which the change in absolute humidity along the pipe is given by

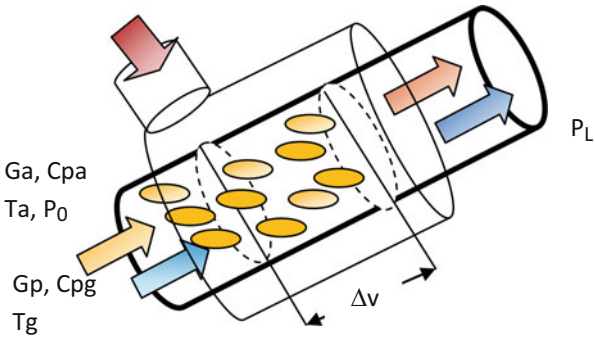

Fig. 5 Control volume in single heated pipe

$$\frac{\partial H}{\partial y} = -\frac{G_{\mathrm{p}}}{G_{\mathrm{a}}}\frac{\partial M}{\partial y} \tag{8}$$

and the change in moisture content along the pipe is given by

$$\frac{\partial M}{\partial y} = \frac{\partial M}{\partial t}\frac{\partial t}{\partial y} = -\mathrm{k}(M - M_{\mathrm{e}})\frac{1}{V} \tag{9}$$

The volumetric heat transfer coefficient, h_{cv}, can be expressed as

$$h_{\mathrm{cv}} = 86,9{G_{\mathrm{a}}}^{1,3} \tag{10}$$

The value of specific heat capacity, C_{pg}, was taken as a constant value at C_{pg} 2 kJ/kg °C. The equilibrium moisture content, (M_{e}), was calculated from the following relation:

$$Me = \left\{\frac{\ln(1 - Rh)}{-1.9187 \times 10^{-5} \times (T + 51.161)}\right\}^{1/2.4451} \tag{11}$$

while the drying constant, k, of the rough rice was taken from:

$$k = \exp(-1.9283 - 2803.4/T_{\mathrm{abs}}) \tag{12}$$

the latent heat of evaporation of rough rice, ΔH_{fg}, is given by:

$$\Delta H_{\mathrm{fg}} = 1.298\Delta H_{\mathrm{fgw}} \quad \text{at} \quad 30{-}50^{o}C \tag{13}$$

while the latent heat of evaporation of pure water, ΔH_{fgw}, is given by

$$\Delta H_{\mathrm{fgw}} = 2501.64 + 1.88T_{\mathrm{a}} \tag{14}$$

Psychrometric equation was used to calculate vapor pressure:

$$P = \frac{R\,\mathrm{Exp}\left(A + BT + CT^2 + DT^3 + ET^4\right)}{FT - GT^2} \tag{15}$$

where:

$R = 22105649.25$
$A = -27405.526$
$B = 97.5413$
$C = -0.146244$
$D = 0.000126$
$E = -0.0000000485$
$F = 4.34903$
$G = 0.00394$

Heat capacity of the air is given by

$$C_\mathrm{p} = R_1\left(A_1 + B_1T + C_1T^2 + D_1T^3 + E_1T^4\right) \tag{16}$$

And the constants are as follows:

$A_1 = 4.07$
$B_1 = -1.108 \times 10^{-3}$
$C_1 = 4.152 \times 10^{-6}$
$D_1 = -2.964 \times 10^{-9}$
$E_1 = 0.807 \times 10^{-12}$
$R_1 = 8314/18$

3.1 The Instrument

Testing of heated 4 inch pipe (3) was done using experimental setup shown in Fig. 6. The pipe was enclosed with an 8 inch steel pipe to function as shell where hot air from an electric heater was blown in. The whole pipe was wrapped with glass wool and aluminum foil. At each entrance and outlet of both the pipe and the shell, cc thermocouples were imbedded and recorded with digital thermometer Lutron type TM-903A with the smallest reading of 0.1 °C. The airflow rate for both pipes was measured using a LT Lutron anemometer, while the mass flow rate of rough rice using a digital balance (5) was located under the receiving hopper (4). To measure the change in moisture content of rough rice, a Crown-type TA-5 moisture tester was used.

Fig. 6 Experimental setup for testing using heated pipe (Kamaruddin et al. 2014)

3.2 Testing Procedure

Before testing, the shell was heated first by blowing hot air into the shell until steady state was reached and then a valve beneath the rough rice feed hopper (2) was opened and the blower (1) was started. The mass flow rate of rough rice was measured by knowing the change in weight in the receiving hopper (4) on the balance (5) within a specific time. At the same time, the airflow rate was measured from the pipe end. The temperature readings both from the pipe and from the shell were recorded using digital recorder Lutron type TM-903A.

3.3 Test Results and Discussions

Table 1 shows the experimental results showing the change in moisture content of rough rice under different inlet temperatures of both the drying air within the pneumatic conveyor pipe and the heating air within the shell. As shown in Table 1, the power requirement varied between 485 and 553 W. The conveying power was found to be 1.02 W/kg/h. The moisture change from inlet to outlet or with 3 m conveying distance varies between 0.67 and 2.2% wb. Table 2 shows the results of the experiments under different heating temperatures as compared to the calculated values. It shows that on average, the moisture content of the calculated values was somewhat higher than the experimental data. This may be due to the use of smaller drying constant, while in fact the drying took place under turbulent condition so that mass and heat transfer should have been intense which made the greater value of the drying constant. Figure 7 shows the change in air temperature at shell inlet and outlet and the comparison between the calculated results and

Table 1 Experimental data (Kamaruddin et al. 2011)

Air temperature in cell/ velocity			Pneumatic conveyor temperature/velocity			Moisture content (% wb)		Power	Mass flow rate of grains
T_{in} (°C)	T_{out} (°C)	V_{in} (m/s)	T_{in} (°C)	T_{out} (°C)	V_{in} (m/s)	Inlet	Outlet		(Watt) Ton/h
127	61.9	6.4	30.2	34.4	28.6	27.48	26.04	484.6	645.9
101	65.7	7.5	30.6	34.6	28.4	26.04	24.86	504.4	650.5
118	60	14.3	34.4	36.0	25.6	24.64	23.97	509	551
106.1	66.8	14.3	33.7	36.7	28.4	26	23.8	553	488
120.3	89.6	10.2	34.6	39.2	25.4	27.4	26.2	514.08	763.68

Table 2 Experimental results as compared with calculated values

Air temperature within shell °C			Air temperature within pneumatic conveyor °C			Moisture content (5 wb)		
	Outlet			Outlet			Outlet	
Inlet	Calculated	Data	Inlet	Calculated	Data	Inlet	Calculated	Data
101	55.7	65.7	30.6	32.41	34.6	26.04	25.87	24.86
106.1	75.88	66.8	33.7	36.63	36.7	26	25.76	23.8
118	83.2	60	34.4	38.2	36	24.64	24.36	23.97
120.3	74.55	89.6	34.6	36.81	39.2	27.4	27	27.22
127	59.3	61.9	30.2	32.7	34.4	27.48	27.33	26.04

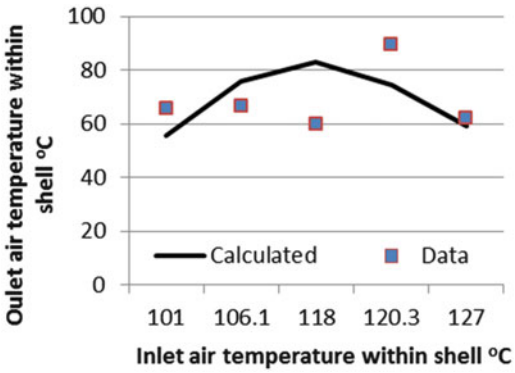

Fig. 7 Change in inlet and outlet air temperature within the shell

experimental data. Figure 8 shows how the value is calculated as compared to experimental data of the air temperature within the conveyor pipe. Figure 9 shows the comparison between the calculated values and experimental data of moisture content at pipe outlet. The drying constant used in the calculation was the same as for thin-layer drying, and therefore the effect of turbulence could not be observed. This is probably that the drying process is already in the stage of falling-rate period

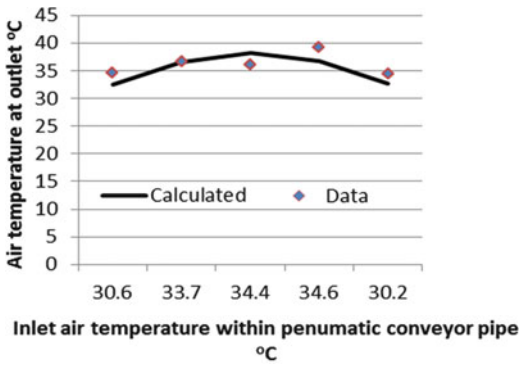

Fig 8 Change in air temperature at inlet and outlet of conveyor pipe

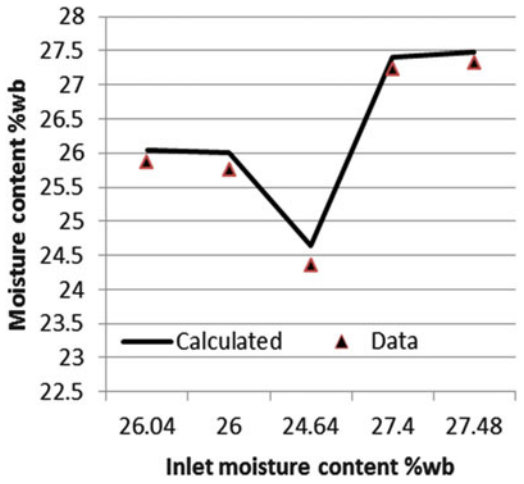

Fig. 9 Comparison between the calculated values data of moisture content at pipe outlet

where the effect of turbulence was insignificant. From these figures, we can judge that the mathematical model used could estimate each change in heating and drying air temperatures and moisture content of rough rice.

Figure 9 shows the calculated changes of each air temperature with the shell and within the pneumatic conveyor pipe and the changes in moisture content of rough rice along the conveyor pipe.

Figure 10 shows the simulation results indicating the change in drying air and grain temperatures within the pneumatic conveyor pipe, change in air temperature within the shell, and change in moisture content along the conveyor pipe. Although the drying air and grain temperature were at the same level, the drying air temperature was a little higher than the grain temperature.

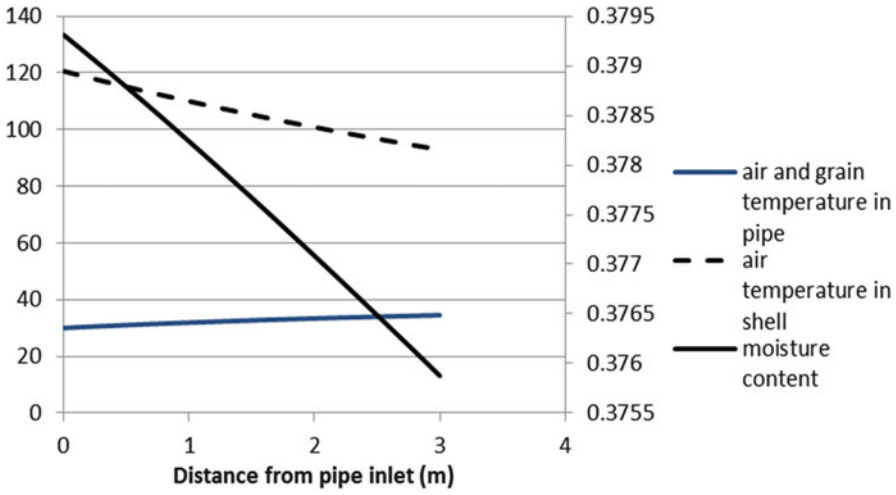

Fig. 10 Simulation results for inlet shell temperature of 120 °C

4 Recirculation-Type ICDC Solar Dryer with Inclined Drying Chamber

4.1 Introduction

In Indonesia and in most rural areas in the developing countries, direct sun drying has been a common practice to extend shelf life of agricultural products such as food crops, high-value cash crops, and forest, animal, and marine products. Although this method seems very cheap, the results of drying are susceptible to contamination with dirt and other foreign materials and therefore are not hygienic. As the climate is changing and global warming continues to prevail, direct sun drying may become difficult to perform due to the uncertainty of rainy and cloudy days which can hamper the drying process. Consequently, the unavoidable delay of drying process due to prolonged and unexpected rain fall can result in rapid decomposition of the products and, therefore, may not suitable for consumption. In Indonesia, experiences have shown that using direct sun drying of rough rice with initial moisture content of 26–27% wb, just after harvest, may take a week or more to reach the final moisture content of 14% wb in cloudy and rainy days.

On the other hand, mechanical drying using fossil fuel encountered problems at village level due to scarcity and high prices of fossil fuel. In addition, most of these dryers are imported overseas, making their price unaffordable by local farmers. As a possible alternative, many researchers have proposed to use solar energy instead of fossil fuels as the heat source (Belessiotis and Delyannis 2011). In such a dryer, solar radiation is utilized in a way so that the airflow, air temperature, and RH are controlled at a desired level to achieve faster and even drying process. Modern solar

dryer is usually provided with auxiliary heating unit such as biomass stove connected to heat exchanger unit to provide clean hot air. The use of auxiliary heater can make it possible to perform drying process continuously day and night and all year round regardless of the availability of solar radiation.

Up to now, many solar dryers have been developed overseas, but nowadays, some domestic designs are also available. Their practical applications, however, differ from country to country, but the majority of them have been ended as laboratory prototypes or as demonstration models. Many solar dryers introduced to the farmers have stopped operating due to lack of continuous financial support from the project owners, as the projects are mostly implemented on a short-term basis, from 10 months to 1 year only. Another important reason has been due to lack of access to working capitals and market of processed product.

4.2 Literature Study

Solar dryer for granular materials may be divided into two categories. The first type is solar dryer using stationary drying bin (such as flatbed dryer) or tray where the products are kept within a bin or on tray. These types of solar dryer are the most popular and have been widely studied by several workers in the past such as Sharma et al. (2009) and many others. Belessiotis and Delyannis (2011) had made a review on the current design of solar dryer, but none have discussed on a continuous solar dryer using pneumatic conveying system.

In Indonesia, solar dryer with rectangular bin with perforated floor has also been studied. The problems encountered using this type of dryer are due to the different drying rate at each grain layer, where the fastest drying rates occur at the bottom of the bin where hot drying air is coming in. This condition results in different moisture content between the upper layer and bottom layer of the grains within the bin. The difference can be as large as 4% (Hien et al. 2003). As the airflow moved upward across each grain layer, its temperature would be decreasing and consequently the drying rate would also decrease. This has resulted in difference in moisture content of the grains at the top and those at the bottom layer. The thicker the bed depth, the greater the variation in final moisture content of the grains. Other types of solar dryer are those where the products are allowed to move, being mixed continuously using mechanical mixer such as the work of Manalu (1999) or being mixed and flowing in a rotating drum (Kamaruddin and Nelwan 2006). A new type of solar dryer has been proposed by Kamaruddin et al. (2010a, b) where the products are allowed to flow under turbulent manner within a pneumatic conveyor during transportation within the dryer system. This latter system of solar drying was found to consume less electric power per unit mass flow rate of the commodity. Due to the turbulent and mixing action of the commodity while flowing within the conveyor, the drying process could be accomplished faster than the traditional method with more even distribution of final moisture content of the dried product.

4.3 Working Principle of the Proposed Dryer

Figure 11 shows the basic design of the proposed recirculation-type ICDC (integrated solar collector drying chamber) hybrid solar dryer (Yefri et al. 2015). Granular materials such as rough rice, soybeans, corn kernels, peppers, or even coffee berries are first loaded into a hopper (6). In this newer design, hot air generated from a gas stove (4) is introduced into the blower inlet (7) and then blown directly into the pneumatic conveyor unit (3). From the pneumatic conveyor, the grains are then transported, while drying is conducted, into an inclined ICDC unit, with UV stabilized transparent cover (5) after passing a grain distributor (2). The drying process occurring within the inclined ICDC unit (5) is conducted by passing ambient air flowing counter currently upward against the falling grains and out through the vortex (1). As the air is flowing across the ICDC unit (5), its temperature increases due to the heating of the solar collector plate which is made of blackened metal sheet. The moisture generated from the drying process occurring both within the pneumatic conveyor and within the ICDC unit is then discharged to the surrounding air through the wind vortex (1), while the falling grains from the ICDC unit (5) are distributed evenly within the hopper (6).

The grains on the top layers of the hopper (6) will receive heat from the incoming solar radiation through the two sides of the transparent louvers (7) to perform drying process, and the resulting water vapor will be blown by the passing wind through louver openings (7).

As the collected grains within the hopper (6) flow freely down toward the hopper's outlet pipe, located at the bottom section, tempering process will take place releasing the grains from thermal stresses and simultaneously allowing even

Fig. 11 Schematic diagram of the second generation of a recirculation-type hybrid ICDC solar dryer (Kamaruddin et al. 2014)

distribution of moisture to occur within the individual grain. The similar recirculation process will go on and on until the moisture within the grains will finally reach 14% wb, a safety level for long storage time and for milling. One drying cycle may start from the hopper exit (6) and then continue after grains enter the pneumatic conveyor (3), completing the cycle after the grains fall freely across the ICDC unit (5) and back into the top section of the hopper (6).

4.4 Estimation of Drying Time

A rough rice grain undergoing drying process can be regarded as a spherical body with radius r (m) and mass diffusivity, Dv (m^2/s); the change in its moisture content M (% db) under constant drying air temperature and RH can be expressed using the following formula (Thuwapanichayanan et al. 2011):

$$\partial M/\partial t = Dv\left\{\frac{\partial^2 M}{\partial r^2} + \frac{2}{r}.\frac{\partial M}{\partial r}\right\} \tag{17}$$

Under the initial condition, at $t = 0$, $0 <$ r0, $r =$ R, $M =$ Me, $D_v =$ constant, Eq. (17) can be solved to obtain the average moisture content, expressed in a simpler form such as

$$\frac{\bar{M} - M_e}{M_0 - M_e} = A\exp(-kt). \tag{18}$$

Here, M_e is the equilibrium moisture content of the grain, in % db; A, the geometric coefficient; (−), t, the unit time, while the mass diffusivity, D_v (m^2/h), can be expressed in terms of a drying constant k, (1/h) such that

$$k = Dv\pi^2/r^2 \tag{19}$$

Therefore, using Eq. (18), the change in average moisture content of the grains can be calculated by calculating the travel time of the grains during each recycling stage within the dryer component.

4.5 Estimation of the Travel Time of Grains Across the Conveyor and the ICDC Unit

The traveling time of grains passing through the pneumatic conveyor can be calculated from the known value of mass flow rate, W_P (kg/h); the void ratio, ε (-);

and the cross section of the conveying pipe A_P (m^2) and bulk density of the grains ρ_p (kg/m^3). The traveling velocity V_P (kg/h) t then can be written as in Eq. (20):

$$V_p = \frac{W_p}{(1-\varepsilon)\rho_p A_p} \tag{20}$$

For a pipe of length, L_{pc}, (m) of pneumatic conveyor, the time of travel t_{pc} (h) is given by

$$t_{pc} = \frac{L_{pc}}{V_p} \tag{21}$$

For the case of free fall occurring in the ICDC unit with length, L_d, (m), inclined at θ degree from horizontal, the time of fall t_d (h) can be calculated using the following relation:

$$t_d = L_d / \sqrt{2gL_d \sin\theta} \tag{22}$$

4.6 The Tempering and Travel Time Within the Hopper

The tempering time, t_T (h), is the time required by the grains to fall due to gravity force within the hopper. It can be estimated by establishing a mass balance within the hopper using Fig. 12, such that:

$$A_p dH_h/dt = -A_1 C_1 \sqrt{2gH_h} \tag{23}$$

Here, C_1 is the discharge coefficient (−); A_o is the cross-sectional area of the top grain layer (m^2) at any height, H_h, (m), of the grain column within the hopper; A_1 is the cross-sectional area of the connecting pipe to the pneumatic conveyor (m^2); and g is the gravitational forces (m^2/s). The integration of Eq. (23) will give the following results after some rearrangements:

$$t_T = -\frac{2}{C_1\sqrt{2g}}\left(\frac{A_o}{A_1}\right) H_h^{0.5} \tag{24}$$

Here

$$H_h = 2W_p/\rho_p A_o \tag{25}$$

and the value of the discharge coefficient, C_1, can be determined from the experiment by measuring the time to discharge the grains at appropriate column height.

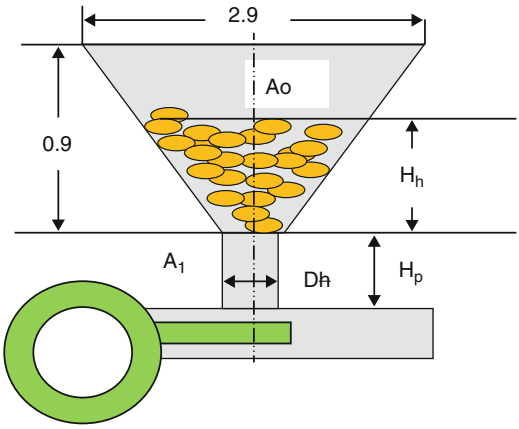

Fig. 12 Schematic diagram of the hopper for determining the discharge coefficient C_1 and the tempering time t_T (Kamaruddin et al. 2014)

4.7 The Experiment

Experiment was conducted using the complete system of the second-generation recirculation-type hybrid ICDC solar dryer under outdoor climatic condition heated by both solar radiation and by the auxiliary heating unit. This second test was used to confirm the results of the first test regarding the power requirement for the pneumatic conveyor and the effect of tempering and to determine the overall drying performance of the system which occurs simultaneously across the pneumatic conveyor and within the ICDC unit. During the calculation, the effect of additional drying occurring on the top of the hopper was neglected. The complete system of the recirculation-type hybrid ICDC solar dryer shown in Fig. 11 was tested under the outdoor condition. Newly harvested rough rice grains were obtained from the nearby farm. Before each of the experimental runs, all cc thermocouple temperature sensors were placed each at both the inlet and outlet of the pneumatic conveyor and at the inlet and outlet of the ICDC unit having dimension of 3 m × 3 m. The digital Lutron type BG-UT-02P RH and temperature meter were used to measure the RH and temperature of the environment and the drying air within the ICDC unit. Pressure taps were placed in the specified locations in the conveyor pipes, and all are connected to a U-tube manometer to measure the occurring two-phase pressure drop. A digital solar pyranometer (Tenmarr Type TM 206) was used to measure global solar radiation, while voltmeter and amperemeter were used to measure the power required and the energy consumed during each test runs. A Lutron type DW-6060 anemometer was used to measure airflow rate at the blower inlet.

4.7.1 Experimental Procedure

After installing all sensors and recorders, the experiment then was conducted only during daytime. During the drying test, hot air from an auxiliary heating unit using gas stove was supplied directly into the blower inlet which later was blown into the

pneumatic conveyor pipe. The latter was used to heat and transport the falling grains from the feed hopper into the ICDC compartment. Experiment using 212 kg (26% wb initial moisture) of rough rice grains was conducted by first loading the grains into the hopper through the side wall opening of the dryer. This first experiment was terminated in the afternoon when the final moisture of the grains has reached 19.8% wb after 4 h and 22 min of drying time. Using the same grains that now become 192 kg (initial moisture of 19.6% wb), the drying test was continued in the following day. The drying test was started at 11:30 WIST and was terminated at 17:45 after the moisture content of the grains has been reduced to 16.3% wb, with effective drying time of 4 h. Since the moisture content of the grains was still high and unsafe for long storage, the drying test was then continued again in the following day for another 3 h, to reach the final moisture content of 14.2% wb. Therefore, the total drying time was 11 h and 22 min. A similar drying test was also conducted using 380.5 kg load with the initial moisture content of the grains at 27.1% wb.

4.7.2 Measurement of the Tempering Time

The tempering time was determined from the known height of the grain column within the hopper and the time required to discharge the grains from the hopper using a stopwatch. Using 192 kg load, with column height of 0.2 m, the time required to empty the hopper was 36.4 s, and therefore, by using Eq. (24), the value of C_1 was found to be $C_1 = 0.00021$.

4.8 Experimental Results

4.8.1 Drying Performance of the Complete Solar Drying Setup

Figure 13 shows experimental results with 212 kg load and 26% wb initial moisture content. The drying time to reduce the moisture content of rough rice to 19.8% wb was attained in 4 h and 22 min or equivalent to nine recycles of the grains within the dryer. Experimental results of the first stage experiments with 212 kg load and 26% wb initial moisture content as compared with theory (solid line) are $k = 1, 25$ (1/hr), $M_e = 6\%$ db (Kamaruddin et al. 2014). It shows that the drying time calculated using Eq. (2) was longer than the observed value. This deviation might be due to the neglected influence of solar radiation during the drying process within the ICDC unit. Using Eqs. (21), (22), and (24), the travel time of the grains across the pneumatic conveyor (t_{Pc}), the solar collector drying chamber (t_D), and the tempering time within the hopper (t_T) were $t_{PC} = 0.0018$ h, $t_D = 0.0003$ h, and $t_T = 0.028$ hrs., respectively. During these experiments, the change in solar radiations and conveyor inlet and outlet air temperatures are shown, respectively, by Figs. 14 and 15. These figures show that during the test the weather condition

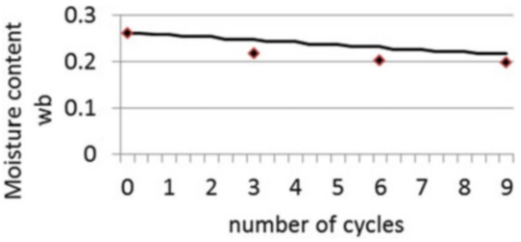

Fig. 13 Drying with 212 kg load with initial mc of 26% wb as compared with calculated values

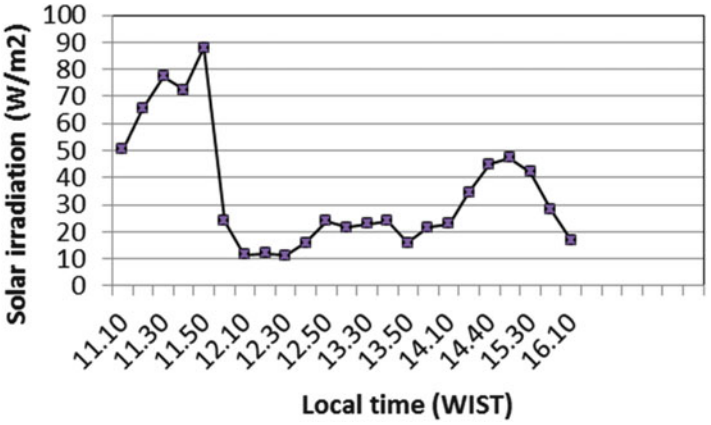

Fig. 14 Change in solar irradiation during the first 3 h of the drying experiment from 26 to 19.8% wb (Kamaruddin et al. 2014)

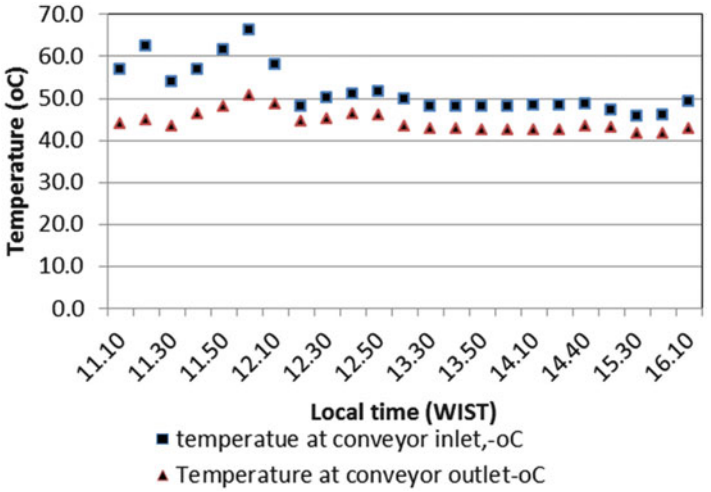

Fig. 15 Variation in conveyor inlet and outlet temperatures during the experiment (Kamaruddin et al. 2014)

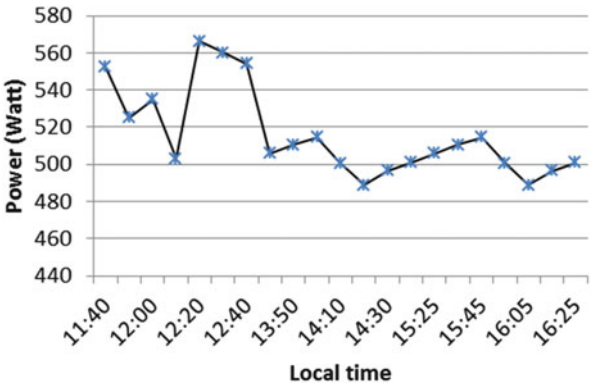

Fig. 16 Variation power consumed during the experiments (Kamaruddin et al. 2014)

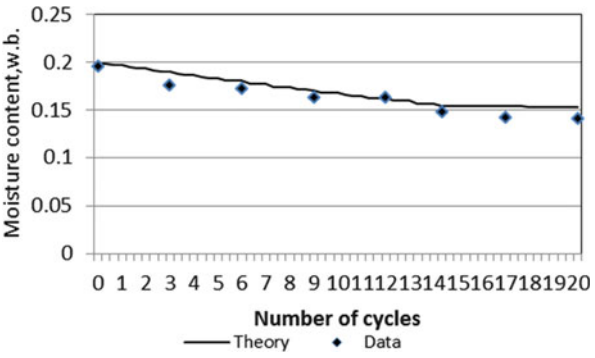

Fig. 17 Comparison between calculated results and data for drying test with 192 kg,19.8% wb initial moisture of rough rice, ($k = 1.25$ in (1/h), $M_e = 6\%$ db (Kamaruddin et al. 2011)

was mostly cloudy, and fluctuating, where 78.3% of incoming solar radiation was below 500 W/m^2.

By operating the auxiliary heating unit using a gas stove, however, it was possible to maintain a relatively constant inlet and outlet temperature of the pneumatic conveyor between 40 and 50 °C and the drying chamber temperatures between 37.2 and 42.5 °C. During the experiments, the electric consumption of the recirculation blower was high at the first hours but tends to be a relatively constant value of 516 W as shown in Fig. 16, where the mass flow rate of the recirculating grains was 602 kg/h as estimated using Eq. (2).

Figure 17 shows the results of continuing test during the next day after the first test was terminated at 19.8% wb grain mc. The drying time required to reduce the moisture content from the initial moisture of 19.8% (now with 192 kg load of rough rice) to the final moisture of 14.2% wb was attained within 7 h. This is comparable to the calculated drying time of 20 cycles or 20 cycles × 0.347 h/cycles = 6.94 h. Therefore, the total drying time from the first experiment with initial load of 212 kg was 11 h 22 min. This is shorter than using direct sun drying which requires days of drying time to reach 12–18% wb from 20 to 30% wb under continuous sunshine (Figs. 18 and 19).

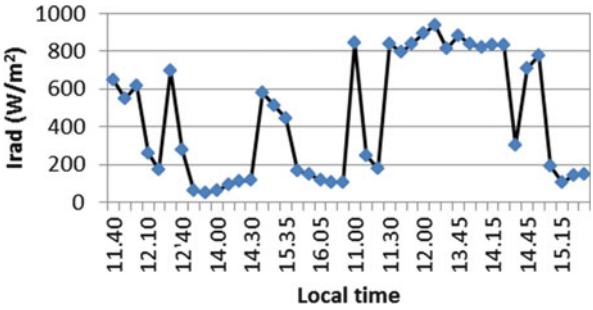

Fig. 18 Change in solar radiations during drying test with 192 kg rough rice (Kamaruddin et al. 2014)

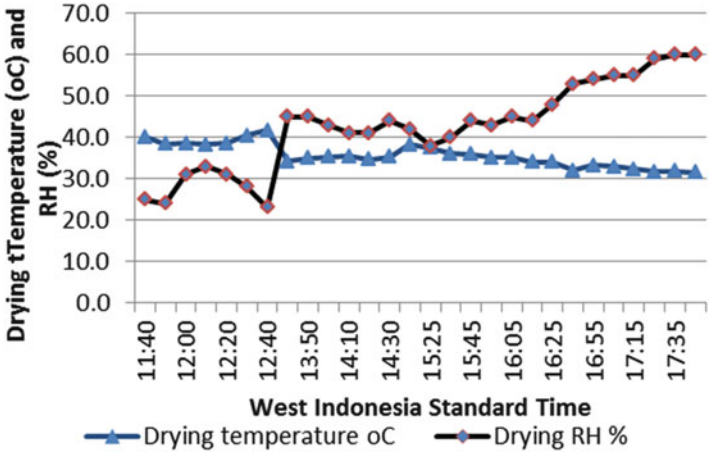

Fig. 19 Variation in drying temperature and RH (Kamaruddin et al. 2014)

Figure 20 shows that the consumed electric power was almost constant all the time at 500 W. The total gas consumption was 12 kg or equivalent to 563.64 MJ, the electric power consumed was 506.8 W, and the total energy consumed was 6081.3 Wh or 21.89 MJ. Total solar radiation received was 8470 Wh/m^2 which is equivalent to 274.4 MJ. Therefore, the total energy input during the drying process was 894.6 MJ.

Figure 21 shows the drying process using 380.5 kg (at initial mc of 27.1% wb). Under this condition, the flow rate of rough rice was at 584.5 kg/h. Based on the calculated trend, to reach 14% wb, the drying process would require 13 recirculations or equivalent to 13 × 380.5 kg/584.5 kg/h = 8.48 h, which means that the drying process can be accomplished within 1 day. Figure 22 shows the operating conditions during the test where the ICDC unit temperatures were fluctuating between 42 and 66 °C. The pneumatic conveyor temperature, however, was maintained relatively constant between 65 and 70 °C at inlet and between 51 and 59 °C at the outlet location. Figures 23 and 24 show, respectively, the variation in ICDC unit temperature with average value of 40 °C with solar

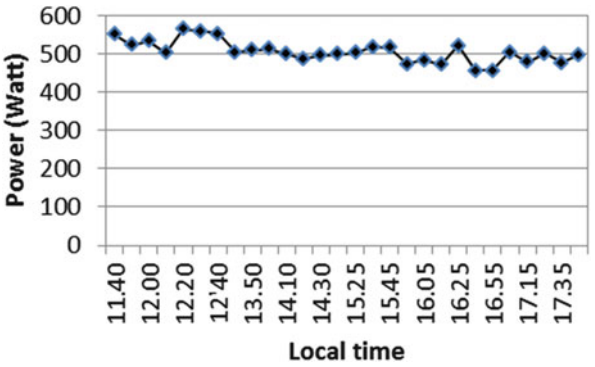

Fig. 20 Change in electric consumption during drying test (Kamaruddin et al. 2014)

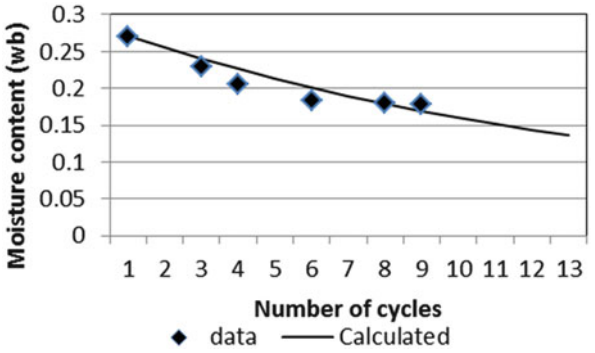

Fig. 21 Comparison between measured and calculated change in moisture content during drying test of 380.5 kg (initial mc, 27.1% wb) (Kamaruddin et al. 2014)

radiation level always above 600 W/m^2 . Total radiation received during the drying was 124.92 kW or 449.7 MJ, total gas consumed was 8.48 kg or 398.3 MJ, while the electricity consumed was 497.2 W or 4.216 kWh or 128.7 MJ, and the total energy input was 976.7 MJ.

4.8.2 The Specific Energy and Drying Efficiency

Specific energy, S_E, is defined as the ratio of total input of commercial energy to the amount of water evaporated during the entire drying process. It can be expressed as

$$S_{\mathrm{E}} = \frac{Pwt_{\mathrm{D}} + W_{\mathrm{g}}CV_{\mathrm{g}} + I_{\mathrm{rad}}A_{\mathrm{c}}t_{\mathrm{D}}}{\left\{\frac{(X_{\mathrm{i}}-X_{\mathrm{f}})W}{(1-X_{\mathrm{f}})}\right\}} \tag{26}$$

Here, W_{g} is the amount of consumed LPG and CV_g is its calorific value, of 46.97 MJ/kg.I_{rad} is solar irradiation (W/m^2) and A_{c} is the collector area (m^2). Here X_{i} is the initial moisture content of the grains (% wb), X_{f} is the final moisture content, and W is the initial mass of rough rice before drying. The denominator of

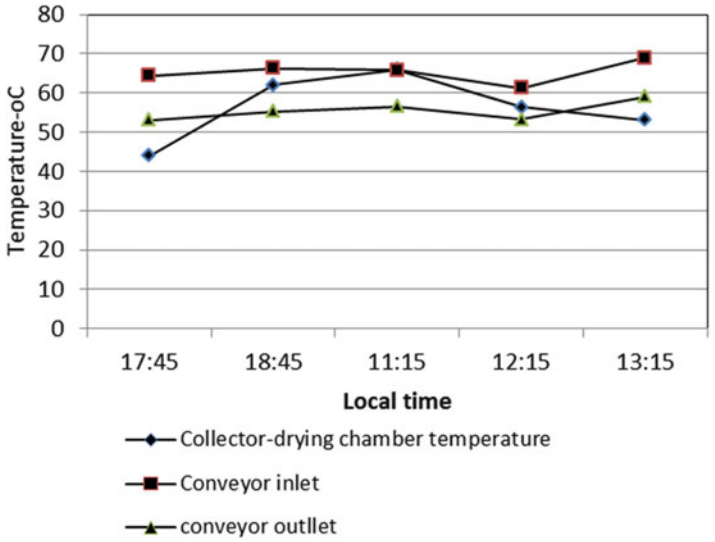

Fig. 22 Variation in air temperature within the ICDC unit during the experiment with 380.5 kg load of rough rice (Kamaruddin et al. 2014)

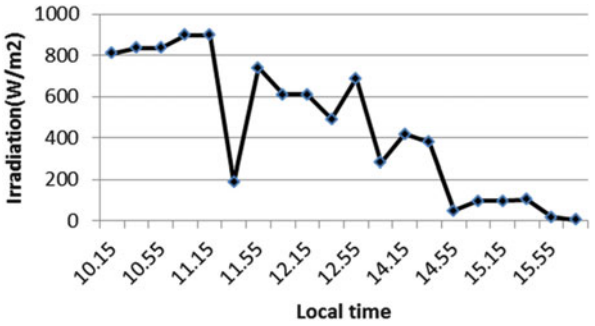

Fig. 23 Variation in solar radiation during the drying test with 380.5 kg of rough rice (Kamaruddin et al. 2014)

Eq. (26) is in fact the total amount of water evaporated during the drying process. Using data of drying test with 212 kg load (26% wb initial mc), the specific energy, as defined above, was found to be 23.82 MJ/kg of water evaporated when input from solar radiation was included and becomes 14.4 MJ/kg of water evaporated when excluded.

The drying efficiency is defined as the ratio between total energy used for drying divided by total input energy. Hence,

$$\eta_D = \frac{\left\{\frac{(X_i - X_f)W}{(1-X_f)}\right\}\Delta H_{fg}}{Pwt_D + W_g C V_g + I_{rad} A_c t_D} \tag{27}$$

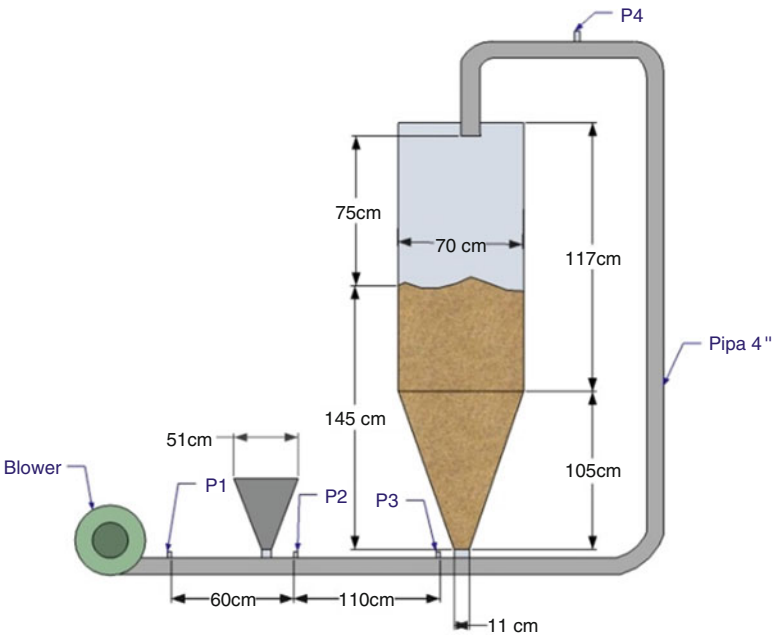

Fig. 24 Diagram showing the dimension of the recirculation dryer (Nining 2015)

The drying efficiency was calculated using Eq. (27), neglecting the sensible heat of the rough rice. Using drying data of the 212 kg load, the drying efficiency was 14% when solar radiation input was included and becomes 16.9% when solar radiation was excluded. Using Eq. (26) and data from the 380.5 kg load, the calculated specific energy was 23.4 MJ/kg of water evaporated when solar radiation was included and becomes 20.4 MJ/kg of water evaporated when excluded. The calculated drying efficiency was found to be 14.3% when solar radiation was included and becomes 26.5% when excluded.

4.8.3 The Drying Quality

Regarding the quality of the drying process using pneumatic conveyor, it was found that from 100 samples of dried grains, only one cracking was detected from two groups of ten grain samples. There was no occurrence of cracking detected in the remaining 80 grain samples. Therefore, it is recommended that pneumatic conveying system should be used as a proper means of conveyance method in a continuous solar drying system since besides causing less damage to the grains, it also consumes less energy during the transportation of the grains.

5 Recirculation-Type ICDC Solar Dryer with Vertical Drying Chamber

The system was cleaned thoroughly prior to experimentation. The system was used to dry the rough rice.

5.1 Estimation of the Drying Curve

5.1.1 The Drying Process

For the spherical shape crop, the following equation is being used:

$$\frac{\partial M}{\mathrm{d}t} = D_v\Big\{\frac{\partial^2 M}{\partial r^2} + \frac{2}{r}.\frac{\partial M}{\partial r}\Big). \tag{28}$$

If $M = M_e$, then solution of Eq. (28) can be written as follows:

$$\frac{\bar{M} - M_e}{M_0 - M_e} = A\exp\left(-Dv\pi^2 t/r^2\right) \tag{29}$$

The recycling time (θ_R) can be calculated as follows:

$$\theta_R = \frac{W_h}{W_R} \tag{30}$$

5.1.2 The Drying Efficiency and Specific Energy

The drying efficiency (η_D) is the ratio of useful energy per total input energy of the system. It can be calculated as

$$\eta_D = \frac{\left(m_{pf}Cp_f T_{pf} - m_{pi}Cp_i T_{pi}\right) + \left\{\frac{(X_i - X_f)W}{(1-X_f)}\right\}\Delta H_{fg}}{Pwt_D + W_g CV_g + I_{rad}A_c} \tag{31}$$

The total specific energy (S_E) is the ratio of the total input energy and total quantity of water evaporated:

$$S_E = \frac{Pwt_D + W_g CV_g + I_{rad}A_c}{\left\{\frac{(X_i - X_f)W}{(1-X_f)}\right\}} \tag{32}$$

5.2 The Experiment

Figure 24 shows the dimension of the recirculation dryer comprising mainly of a blower, feed hopper, receiving hopper, pneumatic conveyor pipe, and LPG gas stove. The experiment setup is shown in Fig. 25 (Nining 2015).

The temperature sensor is being used to observe the temperature of the system. The humidity is being measured by the hygrometer manufactured by Lutron, and the model no. of this is BG-UT-02 P. The intensity of the solar radiation is being measured by the solar power meter which is manufactured by Tenmars, and the model no. of this instrument is TM 206. The airflow is being measured by the anemometer which is developed by Lutron, and the model no. is DW-6060.

5.3 Results

Table 3 shows the results of field test performance of the recirculation-type ICDC solar dryer. The drying time varies between 4.4 and 8 h for initial load of between 104 and 200 kg under drying temperature varying between 47 and 83 °C. The RH of the drying chamber varied between 19.6 and 21.7%. The drying efficiency excluding solar energy input varied between 22 and 32%, while the specific energy excluding solar energy input varied between 9.25 MJ/Kg of water evaporated and 10.6 MJ/kg of water evaporated.

Fig. 25 Blower (1), feed hopper (2), LPG stove (3), transparent structure (4), pneumatic conveyor (5), and receiving hopper (6) (Nining 2015)

Table 3 Summary of experimental results (Nining 2015)

Test Item	Test run	Test run	Test run
Initial mass of rough rice (kg)	124	104	200
Final mass (kg)	102.3	90	170.3
Drying time (h)	12.7	5	8
Initial mc (% wb)	31	28.6	27.3
Final mc (% wb)	16.4	14.56	14.6
Drying temperature °C	58.53	50	47
RH of drying chamber (%)	19.6	21.7	N.a.
Final variation in moisture content (%)	0.7	0.4	0.3
Energy consumed for drying (MJ)	72.643	472.94	100.651
Total drying efficiency (%)	0.27	0.20	28.4
Drying efficiency excluding solar energy input (%)	0.29	0.22	0.32
Total specific energy (MJ/kg of water evaporated)	12.368	16.635	11.939
Specific energy excluding solar energy input (MJ)	10.617	9.255	10.504
Energy input (MJ)	267.837	232.902	354.593
Gas (MJ)	230.500	198.230	276.600
Electricity (MJ)	211.326	211.326	353.83
Solar (MJ)	162.048	135.4	426.09

5.3.1 Drying Time and Energy Consumption

The drying curve of the rough rice is being presented in the Fig. 26. The drying time of this experiment is 5 h till the moisture content reaches 14.3% wb from 28.4% wb. The temperature of drying air was 50 °C and 21.73% is the relative humidity (Figs. 27 and 28).

Figure 29 shows the results of drying with 124 kg initial load with an initial moisture of 31% wb. The drying room temperature recorded was between 44.7 and 65.4 °C, while the power consumed was between 518.1 W and 585.3 W. It took 12 h and 40 min to dry from the initial moisture content of 31 to 16.46% wb. The energy consumption during the drying process was 230.5 MJ for gas, electricity of 21.13 MJ, and solar radiation of 16.2 MJ.

Figure 30 shows the drying curve for the 200 kg load test. It took 8 h to dry from 27.3% wb of rough rice to the final moisture content of 14.6% wb. The electricity consumption was 578.2 W (353.38 MJ) on the average, and the LPG consumption was 6 kg (276.6 MJ) with solar radiation of 42.608 MJ. The average drying temperature was 47 °C.

5.3.2 The Drying Efficiency and Specific Energy

The drying efficiency of the 104 kg initial load was calculated using Eq. (31) and was found to be 20% when solar energy input was included and becomes 22% when

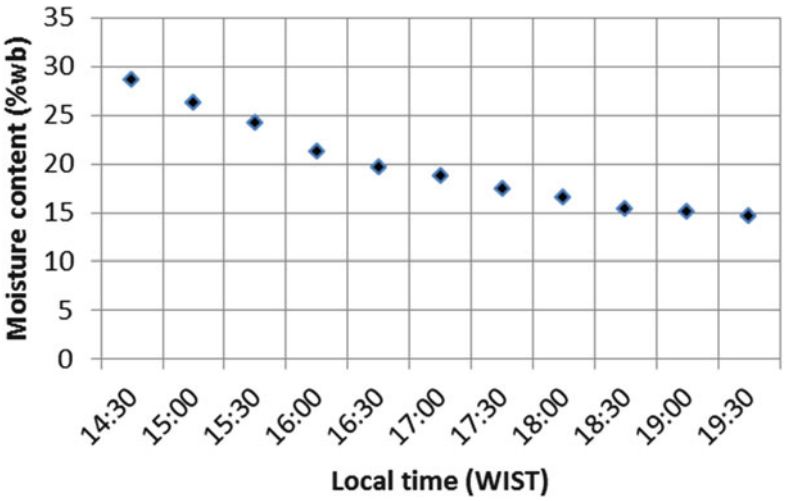

Fig. 26 Drying curve of 104 kg load of rough rice (Yefri et al. 2015)

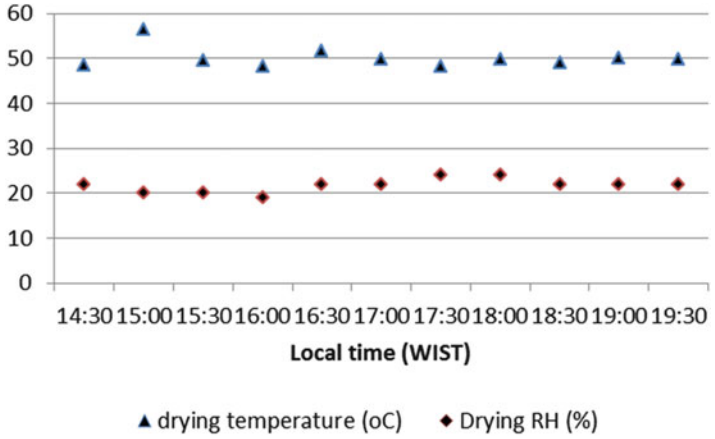

Fig. 27 Variation in drying chamber temperature and RH (Nining 2015)

solar energy input was excluded, while the total specific energy calculated using Eq. (32) was found to be 16.6 MJ/kg of water evaporated when solar radiation was included and becomes 9.25 MJ/kg of water evaporated when solar energy input was excluded. The drying efficiency of the 124 kg initial load was 27% when solar radiation was included and becomes 29% when solar radiation input was excluded. When solar energy was included, the specific energy was 12.4 MJ/kg of water evaporated and becomes 10.6 MJ/kg of water evaporated when solar energy input was excluded. For the test result using initial load of 200 kg, the calculated drying efficiency was 28.4% when solar energy input was included and becomes 32.3% when solar energy input was excluded, while the total specific energy was 11.94

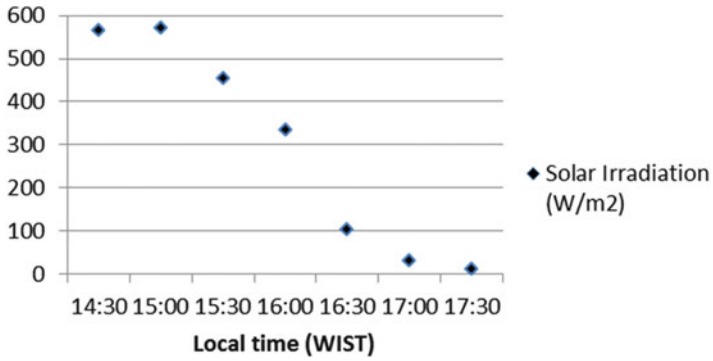

Fig. 28 Variation of solar radiation during the experiment (Yefri et al. 2015)

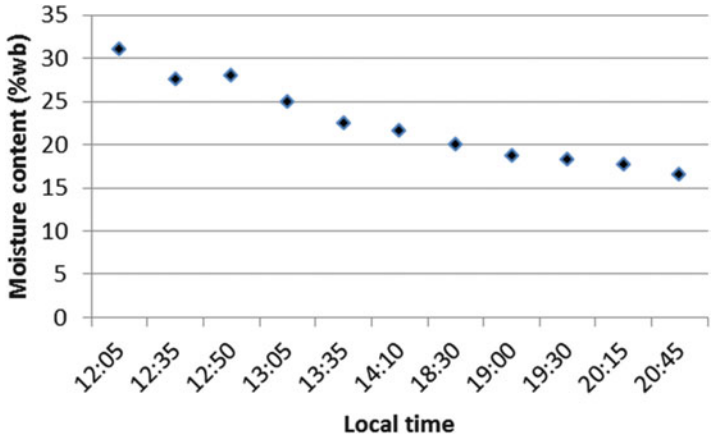

Fig. 29 Drying with 124 kg load and initial mc of 31% wb (Yefri et al. 2015)

MJ/Kg of water evaporated when including solar energy input and becomes 10.5 MJ/kg of water evaporated when solar energy input was excluded.

5.3.3 Comparison Between Calculated Values and Data

Figure 31 shows the comparison between the calculated drying curve using Eq. (29) (Yefri et al. 2015). It shows that the model used predicted quite well of the data obtained. The value of the drying constant used was 0.78 (1/h) with $M_e = 6\%$ db. Here, the value of the shape factor, A, was given as unit larger than for the case of spherical body which is $6/\pi^2$. This k value was relatively smaller than the previous test using inclined drying chamber which was 1.25 (1/h) and comparable to the thin-layer value obtained.

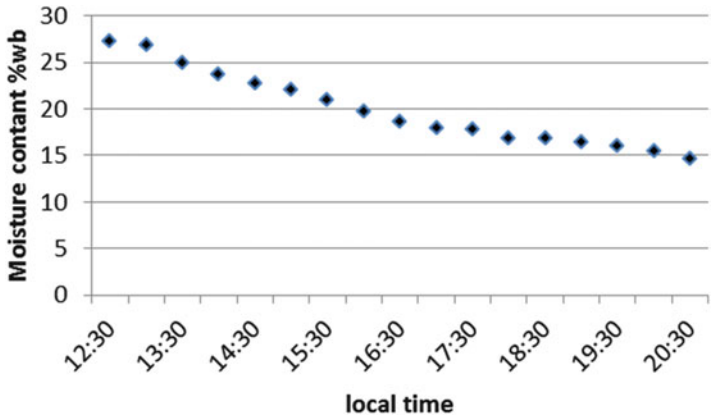

Fig. 30 The drying curve for the 200 kg load test (Yefri et al. 2015)

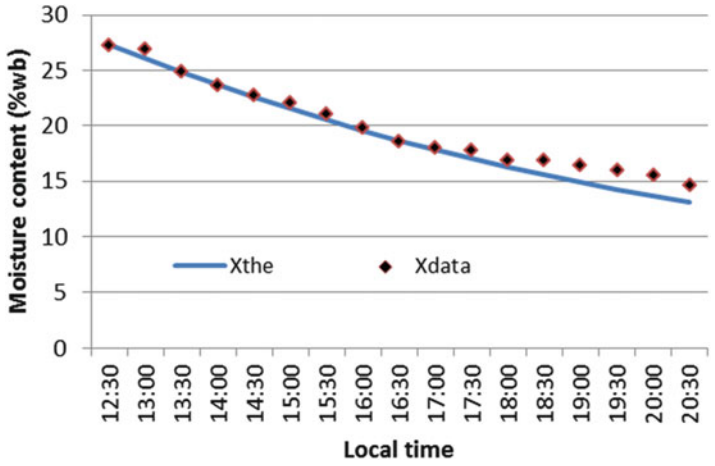

Fig. 31 Comparison between calculated and observed data for the initial load of 200 kg (Yefri et al. 2015)

5.3.4 Homogeneity in Moisture Content

The final moisture content for the 104 kg initial load is depicted in Fig. 32. Here, the variation of the final moisture content obtained was about 3% at the beginning of the drying process, but at the end of the drying process, it reduced to less than 0.5%. Final variation for initial load of 124 kg was 0.7% and for the 200 kg load was 0.3%, all showing the homogeneity in the final moisture content of dried rough rice.

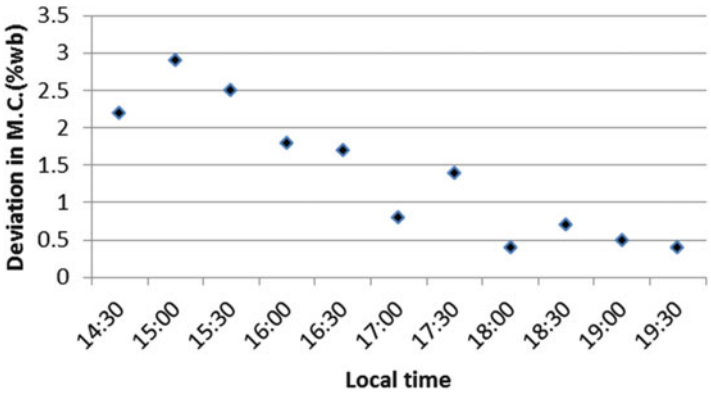

Fig. 32 Variation in final moisture content (Yefri et al. 2015)

6 Conclusions

The following conclusions are drawn from the present study:

1. The first experiments with single unheated and heated pneumatic conveyor pipe were conducted, and later the results were applied to the complete solar drying system.
2. Important results obtained from the first experiments with unheated were, namely, the two-phase gas-solid pressure drop and the relation between the pressure drop and mass flow rate of rough rice, the relation of electric power consumed and the mass flow rate of rough rice, and the relation between power consumption and the ratio between mass flow rate of the carrying air and the rough rice.
3. Results from experiment of drying test with heated single pipe have shown that the mathematical model used to predict the drying process was in good agreement with the experimental data except that the predicted value was somewhat higher than the data.
4. From the field experiment with the inclined and vertical drying chamber, all results indicated that the drying time required was less than 1 day, the final moisture content of the grains was relatively homogenous, and less cracking occurred.

Nomenclature

A	area (m^2)
A	coefficient of Eq. (15)
A	geometric coefficient in Eq. (2)
A_1	coefficient of Eq. (16)
A_1	cross section of pipe below the hopper (m)
A_o	cross section area of hopper on top of grain column (m^2)
A_p	cross section area of pipe (m^2)
B	coefficient of Eq. (15)

B_1	coefficient of Eq. (16)
C	coefficient of Eq. (15)
C_1	coefficient of Eq. (16)
$C1$	discharge coefficient (−)
C_{pi}	initial heat capacity of the grains (kJ/kg °C)
C_{pf}	final heat capacity of the grains (kJ/kg °C)
C_{pw}	specific heat of water vapor (kJ/kg °C)
C_{pl}	specific heat of liquid (kJ/kg/°C)
C_f	friction coefficient (-)
CV_g	calorific value of LPG (MJ/kg)
D	coefficient of Eq. (15)
D	pipe diameter (m)
D_1	coefficient of Eq .(16)
D_h	pipe diameter below the hopper (m)
D_v	mass diffusivity (m^2/h)
E	coefficient of Eq. (15)
E_1	coefficient of Eq. (16)
F	coefficient of Eq. (15)
G	coefficient of Eq. (15)
g	acceleration due to gravity (m/s^2)
Go	mass flux of air under superficial air velocity (kg/m^2 h)
W_a	mass flow rate of the air (kg/s)
G_a	mass flux of air (kg/m_2 s)
W_p	mass flow rate of the grains (kg/s)
G_p	mass flux of grains (kg/m^2 s)
G_r	mass flux of air within the shell (kg/m^2)
h	heat transfer coefficient (W/m^2 °C)
h_{cv}	volumetric heat transfer coefficient (W/m^2 °C)
H	pressure head (Pa)
H	absolute humidity (kg of moisture/kg of dry air)
H_1	height of pipe below the hopper (m)
H_0	height of grain column in hopper (m)
H_h	height of grain column in hopper (m)
$\Delta Hfgw$	latent heat of pure water (kJ/kg)
ΔHfg	latent heat of evaporation of grains (kJ/kg)
I_{rad}	solar irradiation (W/m^2)
k	the drying constant (1/hr)
L_p	pipe length (m)
L_{pc}	pneumatic conveyor pipe length (m)
L_d	length of drying chamber solar collector (m)
M	moisture content (% db)
$\bar{M}$	average moisture content (% wb)
m_{pf}	final mass of grains (kg)
m_{pi}	initial mass of grains (kg)
Me	the equilibrium moisture content (% db)
P	pressure (N/m^2)
Po	pressure at conveyor inlet (N/m^2)
P_L	pressure at conveyor outlet (N/m^2)
Pw	power of blower (W)
Qa	volumetric flow rate of air (m^3/s)
r	radius of grains modeled as spherical body (m)
R	coefficient of Eq. (15)
R_1	coefficient of Eq. (16)
R_h	relative humidity (%)
S_E	specific energy (MJ/kg of water evaporated)

t	time (h)
t_D	drying time (h)
t_T	tempering time (h.)
t_D	travel time of grains within solar collector drying chamber (h.)
tpc	travel time of grains within pneumatic conveyor (h.)
Ta	temperature of the air (°C)
T_g	temperature of the grains (°C)
Ua	overall heat transmission from the shell (w/m^2 °C)
Uv	volumetric heat transmission from the shell (W/m^3 °C)
Vo	superficial velocity of the air (m/s)
Vp	velocity of rough rice (m/h)
W	initial mass of the grains (kg)
Wg	consumption of LPG (kg)
Wa	mass flow rate of air (kg/s)
Wp	mass flow rate of rough rice (kg/s)
Xi	initial moisture content of the grains (% wb)
Xf	final moisture content of the grains (% wb)
y	distance traveled by grain from pneumatic conveyor inlet (m)

Greek Letters

ε	void ratio (−)
γ	ratio between mass flow rate of air and that of rough rice (−)
μ	absolute viscosity of the air (kg/m s)
ρ_p	bulk density of the grains (kg/m^3)
ρ_a	density of the air (kg/m^3)
η_D	drying efficiency (−)

Subscript

a	air
D	collector drying chamber
i	inlet, initial
o	outlet
p	rough rice, pipe
p_c	pneumatic conveyor
T	tempering

References

Belessiotis V, Delyannis E (2011) Solar drying, Solar energy, 8(8)

Hanafi RA (2006) Graduation thesis, Department of Agricultural Engineering, Fateta, IPB, Indonesia

Hien PH, Tam NH, Van Xuan N (2003) Study on the reversal timing for the sra reversible dryer. Paper for presentation at the seminar on "Agricultural Engineering and Agro-products

Processing towards Mechanization and Modernization in Rural Areas“ at Nong-Lam University, HoChiMinh City, 11–12 December 2003

Kamaruddin A, Nelwan LO (2006) Installation of solar dryer with rotating drum in Kamare village, Sulawesi, Report to the Directorate General of Electricity and Energy Utilization, CREATA, IPB

Kamaruddin A, Uyun AS, Chan Y, Esye Y (2010a) Final report of the 1st year competence Grant of the Directorate General of Higher Education, Contract No.413/SP2H/PP/DP2M/VI/2010, June 11, 2010

Kamaruddin A, Uyun AS, Chan Y, Esye Y (2010b) Pengembangan Prototype Pengering Surya Hybrida ICDC Tipe Resirkulasi untuk Kapasitas 2.5 ton (Development of Recirculation Type ICDC Hybrid Solar Dryer for Capacity of 2.5 tons). Proposal for the 2nd year research grant to the Directorate General of Higher Education

Kamaruddin A, Uyun AS, Chan Y, Esye Y (2011) Pengembangan Prototype Pengering Surya Hybrida ICDC Tipe Resirkulasi untuk Kapasitas 2.5 ton (Development of Recirculation Type ICDC Hybrid Solar Dryer for Capacity of 2.5 tons). Second year final report

Kamaruddin A, Uyun AS, Chan Y (2014) Performance of a continuous flow solar drying system. Int Energy J 14(1):1–14

Manalu L (1999) Pengering surya dengan pengaduk mekanis untuk pengeringan kakao, thesis S2, (Solar drying with mechanical mixer for cocoa drying), Agricultural Engineering Science Division, the Graduate School, IPB, Indonesia

Nining DMT (2015) Analisis Keekonomian Pengering Surya Resirkulasi Tipe Pancuran Untuk Pengeringan Gabah. (Economic analysis of spray type recircuation solar dryer for rough rice). MS thesis proposal, the Graduate School Renewable Energy, Darma Persada University

Sharma A, Chen CR, Lan NV (2009) Solar drying system: a review. Renew Sust Energ Rev 13 (6–7):1185–1210

Thuwapanichayanan R, Prachayawarakorn S, Kunwisawa J, Soponronnarit S (2011) Determination of effective moisture diffusivity and assessment of quality attributes of banana slices during drying. LWT-Food Sci Technol 44(6):1502–1510

Yefri C, Nining Dyah TM, Kamaruddin A (2015) Solar dryer with pneumatic conveyor. Energy Procedia 65:378–385

Development and Performance Study of Solar Air Heater for Solar Drying Applications

Partha Pratim Dutta and Anil Kumar

Abstract Open sun drying for drying of rural agro-based produces is an age-old practice for preservation as well as for the use of dried products in the future. However, open sun drying takes longer duration, and thus, it gives inconsistent quality for drying of agro-based produces. Hence, solar dryer emerges as a device to overcome the demerits of the open sun dryer and incorporates its advantage to the maximum extent. Different improved designs of solar air heater cum dryers are available to get efficient solar drying. The present investigation explores general theoretical thermodynamic performance studies of some improved solar air heater for drying applications. It follows with a detailed thermal performance studies of an improved hemispherical protruded solar air heater. The protrusion height (e) varied as 2.4, 3.0, and 3.7 mm, and the long way length (p) varied as 24, 36, and 52 mm, respectively. The effect of $\frac{e}{D}$ (0.055, 0.045, 0.035) of hemispherical protruded absorber on constant $\frac{p}{e} = 12$ had been observed. It was seen that maximum thermal efficiency of 82% is achievable for $\frac{p}{e} = 12$ and $\frac{e}{D} = 0.055$. Moreover, with $\frac{e}{D}$, value of 0.035 and 0.055 gives maximum and minimum effective efficiency (74 and 64%), respectively, at 12,000 Reynolds number. From economic analysis, it has been estimated that if 400 m^2 of black tea processing factory galvanized roof were converted by using black painting, plywood insulation, and tempered glass enclosure to convert it into a solar air heater, then average 20% of conventional thermal energy for black tea drying may be saved. The annual carbon dioxide reduction of 2189 t is achievable by using improved solar air heater. The payback period of the hybrid renewable thermal energy-based system is less than 15 months, and the benefit-cost ratio is 1:1.

Keywords Solar drying • Improved solar air heater • Hemispherical protrusion • Payback period

P.P. Dutta (✉)
Department of Mechanical Engineering, Tezpur University, Tezpur 784028, India
e-mail: ppdutta06@gmail.com

A. Kumar
Department of Energy (Energy Centre), Maulana Azad National Institute of Technology, Bhopal 462003, Madhya Pradesh, India

© Springer Nature Singapore Pte Ltd. 2017

O. Prakash, A. Kumar (eds.), *Solar Drying Technology*, Green Energy and Technology, DOI 10.1007/978-981-10-3833-4_21

1 Introduction

Solar thermal energy-based drying is nonpolluting, freely available in abundant quantity, and renewable. However, the inherent problem of solar thermal energy for drying is temporal variation of solar radiation over the year or within a day for a location. This difficulty may be eliminated if appropriate solar thermal energy storage device is incorporated with the system. Since solar radiation has low energy density, therefore for a given drying load, the amount of collector surface area requirement is quite high. Therefore, the techno-economic studies of solar drying system give insight to principal factors and their role for viability of the system in the long run (Prakash and Kumar 2014). The number of sunny days in a year and incident radiation intensity give variable energy gain on different geographical locations of the Earth's surface. A seasonal change of solar radiation suggests the use of solar drying in the maximum radiation intensity spell (Twidell et al. 1993). Cost and maximum temperature achievable of concentrating-type solar collector are comparatively higher compared to flat-plate collectors. Therefore, for low-temperature drying of agro-products, flat-plate solar thermal collector-based dryer is economically more appropriate and effective. Low-cost solar collector is available by simple construction techniques with cheap locally available materials. However, one may have to compromise with quality of such solar air heater with inadequate reliability. Roof-integrated solar air heater/thermal collector may be useful for multipurpose applications. Likewise, the same solar collector may be used for hot air and water generation as the need arises over the year with certain modification. Such multipurpose utility of solar thermal energy system reduces the total cost involved.

To dry plants, seeds, fruits/vegetables, fish, meat, and other agricultural products, open sun drying process has been used since ancient time. However, open sun drying has certain limitations like solar radiation is not consistent over the daytime that results in uncontrolled drying temperature and longer drying time coupled with deterioration of finally dried products' quality. With large-scale production of agricultural produces, open sun drying has other limitations like high manual labor involvement, large space requirement, unwanted biochemical and microbiological reactions, and insect invasion. To harness solar thermal energy effectively for drying process, efficient solar dryers evolved over time. Therefore, it is imperative to understand appropriately different designs of solar dryer, heat and mass transfer phenomenon during solar drying, its economic evaluation and environment benefits, etc. (Prakash and Kumar 2013).

It has been reported that due to volatile nature and uncertainty of international crude oil prices, many developing countries have been considering exploration of renewable energy option over the last one decade (Mahapatra and Imre 1989). Moreover, most of the developing countries receive considerably higher than world average insolation of 3.82 kWh/m^2 day (Zandler et al. 2016). Therefore, trapping of

this naturally abundant solar thermal energy with intervention of appropriate drying technology has certain justification as follows. Solar dryer provides uniform drying of agro-products, and as a result the quality of final product remains consistent. The drying time is considerably reduced than open sun drying, and farmer may get additional income from quality dry products thus produced (Prakash and Kumar 2013). It is expected that the additional investment incurred for procurement of improved solar dryer may recovered from such additional income generated. However, due to a bit higher initial cost involved for solar drying system, performance evaluation and techno-economic study will be useful before fabrication and installation.

2 Thermodynamic Performance Parameter of Solar Dryer

The thermal efficiency of solar collector is the ratio of solar collector output (gained) heat to its plane irradiation energy, and it is expressed in Eq. (1) (Vlachos et al. 2002; Fudholi et al. 2014a, 2014b):

$$\eta_{\text{col}} = \frac{\frac{Q_{\text{o,col}}}{Q_{\text{i,col}}} = \int_{t_{\text{i}}}^{t_{\text{f}}} \dot{m}_{\text{da}} c_{\text{p,da}} (T_{\text{col,o}} - T_{\text{col,i}}) \text{d}t}{SA\text{col}t} \times 100 \tag{1}$$

where η_{col} is the collector efficiency (%); $Q_{\text{ i,col.}}$ and $Q_{\text{ o,col.}}$, respectively, are the input and output energy of solar collector (kJ); $\dot{m}_{da}$ is the mass flow rate of air (kg/s); $c_{\text{p,da}}$ is the specific heat of drying air (J/kg); $T_{\text{col,i}}$ and $T_{\text{col,o}}$, respectively, are the input and output air temperature of solar collector (°C); t_{i} and t_{f} are the initial and final time of drying experiment (s); S is the solar radiation on horizontal plane (W/m^2); and A_{col} is the effective surface of solar collector (m^2). Drying efficiency is defined as the ratio of the energy required for moisture evaporation of product to the heat supplied by solar collector. The drying efficiency measures the overall effectiveness of a dehydrating arrangement and may be obtained using Eq. (2) (Fudholi et al. 2014a, b, 2015):

$$\eta_{\text{d}} = \frac{Q_{\text{dc,o}}}{Q_{\text{dc,i}}} = \frac{\int_{t_{\text{i}}}^{t_{\text{f}}} (m_{\text{w}} \times \lambda) \text{d}t}{\left(mc_{\text{p,a}}(T_{\text{o,col}} - T_{\text{i,col}}) + E_{\text{fan}}\right)t} \times 100 \tag{2}$$

where η_d is the dryer efficiency (%); $Q_{\text{dc,i}}$ and $Q_{\text{dc,o}}$, respectively, are the input and output energy of drying chamber (kJ); m_{w} is the mass of water evaporated from the product (kg/s); λ is the latent heat of water vaporization at exit air temperature (kJ/kg); $T_{\text{dc,i}}$ and $T_{\text{dc,o}}$, respectively, are the input and output air temperatures of drying compartment (°C); and E_{fan} is the fan energy consumption (kW). Equations

(3) and (4) calculate, respectively, the energy of single-phase fan and the mass of water removed (m_w) from the wet material (Fudholi et al. 2015):

$$E_{fan} = U.I.\ \text{Cos}\ \theta \tag{3}$$

$$m_w = \frac{m_i(X_i - X_f)}{100 - X_f} \tag{4}$$

where U is the voltage (V), I is the electric current (A), Cos θ is the phase angle difference between voltage and electric current ($\sim$0.85), m_i is the initial weight of product (kg), and X_i and X_f are the initial and final moisture content of drying product (wet basis, wb%). Pickup efficiency (expressed by Eq. (5)) measures the ability of drying air, and it is the ratio of the moisture of wet material picked up by the air in the drying chamber to the theoretical capacity of drying air to absorb moisture (Mumba 1996):

$$\eta_P = \frac{m_w}{m_{da}t(w_{as} - w_i)} \times 100 \tag{5}$$

where η_p is the pickup efficiency (%), w_{as} is the absolute humidity of air arriving the dryer at the point of adiabatic saturation (%), and w_i is the absolute humidity of air entering the drying chamber (%). Equation (6) shows the specific moisture extraction rate (SMER) or the energy required to remove 1 kg of water from drying product (kg of H_2O/kW h) (Fudholi et al. 2014b):

$$\text{SMER} = \frac{m_w}{(A_{col}S + E_{fan})t} \tag{6}$$

Specific energy consumption (SEC) is the ratio of total energy supplied in drying process to the amount of water removed during drying (kWh/kg of H_2O). Equation (7) explains how to calculate SEC in the solar drying system (Fudholi et al. 2014b):

$$\text{SEC} = \frac{1}{\text{SMER}} \tag{7}$$

The general energy conservation (first law of thermodynamics) is expressed in Eq. (8) (Midilli and Kucuk, 2003):

$$\sum \dot{E}_i - \sum \dot{E}_o = \Delta \dot{E}_{sys} = \frac{d\dot{E}_{sys}}{dt} \tag{8}$$

It is assumed that the arrangement is in a steady-state and time-independent process ($\Delta \dot{E}_{sys} = 0$). Equation (9) shows its energy balance:

$$\sum \dot{E}_i = \sum \dot{E}_o \tag{9}$$

In Eqs. (8) and (9), $\Sigma \dot{E}_{\mathrm{i}}$ is the whole input energy of the system (kJ/s or kW), $\Sigma \dot{E}_{\mathrm{o}}$ is the whole output energy of the system (kJ/s or kW), and $\Delta \dot{E}_{\mathrm{sys}}$ is the difference or remaining energy within the system (kJ/s or kW). The energy balance for an open system under steady state for air (as an inviscid and nonconducting fluid flow) is expressed in Eq. (10) (Bernoulli's principle):

$$\sum_{i=1}^{n} m_{\mathrm{da,i}} \left(h_{\mathrm{i}} + \frac{u_{\mathrm{i}}^2}{2} + g z_{\mathrm{i}} \right) + Q = \sum_{o=1}^{n} m_{\mathrm{da,o}} \left(h_{\mathrm{o}} + \frac{u_{\mathrm{o}}^2}{2} + g z_{\mathrm{o}} \right) + \dot{W} \tag{10}$$

Since there was no major mechanical work involved in the solar drying of whole drying material, $\dot{W} = 0$, and no subsequent motion is involved in the solar drying process, the momentum components $\frac{u_{\mathrm{i}}^2}{2}$ and $\frac{u_{\mathrm{o}}^2}{2}$ can be eliminated. Furthermore, there was no physical displacement for the drying product in solar dryer ($z_{\mathrm{i}} = z_{\mathrm{o}}$), and the input and output mass of airflow rates in the solar dryer were equal ($\dot{m}_{\mathrm{da,i}} = \dot{m}_{\mathrm{da,o}} = \dot{m}_{\mathrm{da}}$); it is possible to convert Eq. (10) (Bernoulli's principle) to Eq. (14) and calculate energy variation of solar drying system:

$$Q = m_{\mathrm{da}} (h_{\mathrm{o}} - h_{\mathrm{i}}) \tag{11}$$

In Eqs. (10) and (11), h_{i} and h_{o}, respectively, are air enthalpies at the dryer inlet and outlet temperatures (kJ/kg); u_{i} and u_{o}, respectively, are air velocities at dryer inlet and outlet (m/s); g is the gravitational acceleration (9.8 m/s^2); z_{i} and z_{o} are the height of the product in the inlet and outlet of dryer (m); Q is the heat energy inflow (kJ/s); and $\dot{\mathrm{W}}$ is the rate of mechanical work output (kJ/s).

Equation (12) is a good tool to calculate the energy utilization ratio (EUR) in drying unit using Eq. (11) (Aghbashlo et al. 2008):

$$\mathrm{EUR} = \frac{m_{\mathrm{da}} (h_{\mathrm{dc,i}} - h_{\mathrm{dc,o}})}{m_{\mathrm{da}} (h_{\mathrm{dc,i}} - h_{\mathrm{col,i}})} \tag{12}$$

where $h_{\mathrm{dc,i}}$ is the enthalpy of air at the input of drying chamber (kJ/kg), $h_{\mathrm{dc,o}}$ is the enthalpy of air at the output of drying chamber (kJ/kg), and $h_{\mathrm{col,i}}$ is the enthalpy of air at the input of collector (kJ/kg). Equation (13) was used to calculate the enthalpy values noted in Eq. (12):

$$h = 1.005(T - T_{\infty}) + w(2501.4 + 1088(T - T_{\infty})) \tag{13}$$

where T is the temperature of drying air (°C) and T_{∞} is the ambient temperature (°C). This equation was used by Therdthai and Zhou (2009) to calculate the enthalpy of drying air based on the temperature rise as compared to ambient air temperature (T-T_{∞}), absolute humidity of air (w), and latent heat of water equal to 2501.4 kJ/kg. Equation (14) (Akbulut and Durmus 2010) may be used to compute the specific humidity (w) value noted in Eq. (13):

$$w = 0.622 \frac{\phi P_{vs}}{P_{sur} - \phi P_{vs}} \tag{14}$$

Equation (15) (Bagheri et al. 2011) may be used to estimate the saturated vapor pressure of air noted in Eq. (14):

$$P_{vs} = 0.1 \exp\left(27.0214 - \frac{6887}{T_{abs}} - 5.31 \ \ln\left(\frac{T_{abs}}{273.16}\right)\right) \tag{15}$$

Equation (16) (Bagheri et al. 2011) may be used to estimate the surrounding pressure noted in Eq. (14):

$$P_{sur} = 1.01325 \times 10^5 \left(1 - 2.25577 \times 10^{-5} \times Z\right)^{5.2559} \tag{16}$$

In Eqs. (14, 15 and 16), w is the absolute humidity (kg H_2O/kg Da), φ is the RH (%), P_{sur} is the atmospheric pressure (for Sabzevar City is 90.118 kPa), P_{vs} is the saturated vapor pressure of air (kPa), T_{abs} is the absolute temperature (K), and Z is the height of drying place from sea level (977.6 m). Equation (17) was used to calculate the mass flow rate of air used in Eq. (12):

$$m_{da} = \frac{Va}{v} \tag{17}$$

Finally, Eqs. (18) and (19) (Therdthai and Zhou 2009) may be used to calculate the specific volume and volumetric flow rate of air noted in Eq. (20):

$$v = (0.082T_a + 22.4)\left(\frac{1}{29} + \frac{w}{18}\right) \tag{18}$$

$$V_a = A\bar{u} \tag{19}$$

In Eqs. (17, 18 and 19), V_a is the volumetric flow rate of air (m^3/s), V_a is the specific volume (m^3/kg), and $\bar{u}$ is the average air velocity (m/s). For analysis of applied energy, we assumed that the primary and secondary collectors both had a single inlet and outlet, and the ambient air is ideal fluid, and the drying systems were at steady-state conditions.

Exergy of pistachio drying system is described as the maximum amount of work that can be produced theoretically in a reversible process by a stream of matter, heat, or work as it comes to equilibrium with a reference environment (Kurtbas and Durmus 2004; Hepbasli et al. 2010; Erbay and Hepbasli 2013). According to the second law of thermodynamics, part of entering exergy to a drying system is dissipated due to its irreversibility process in real systems. In this study, exergy is a criterion to explain how the quantity of solar energy is reduced during the actual drying process. Equation (20) calculates the general exergy in terms of specific heat

and temperature difference between ambient air and the drying system (Vlachos et al. 2002; Fudholi et al. 2014a):

$$\mathrm{Ex} = m_{\mathrm{da}} c_{\mathrm{p,da}} \left[(T - T_{\infty}) - T_{\infty} \ \ln \frac{T}{T\infty} \right] \tag{20}$$

The entering (inflow) and leaving (outflow) exergy of drying chamber are expressed, respectively, in Eq. (21) and Eq. (22) (Vlachos et al. 2002; Fudholi et al. 2014a):

$$\mathrm{Ex}_{\mathrm{dc,i}} = m_{\mathrm{da}} c_{\mathrm{p,da,i}} \left[(T_{\mathrm{dc,i}} - T_{\infty}) - T_{\infty} \ \ln \frac{T_{\mathrm{dc,i}}}{T_{\infty}} \right] \tag{21}$$

$$\mathrm{Ex}_{\mathrm{dc,o}} = m_{\mathrm{da}} c_{\mathrm{p,da,o}} \left[(T_{\mathrm{dc,o}} - T_{\infty}) - T_{\infty} \ \ln \frac{T_{\mathrm{dc,o}}}{T_{\infty}} \right] \tag{22}$$

The specific heat in Eqs. (21) and (22) was obtained from Eq. (26) (Hans et al. 2009):

$$c_{\mathrm{pda}} = 1.0029 + 5.4 \times 10^{-5} T_{\mathrm{dc}} \tag{23}$$

Since the difference between the maximum and real works is called lost work or exergy loss (Hepbasli et al. 2010), Eqs. (21) and (22) may be used to obtain this loss in drying chamber [Eq. (24)]:

$$\mathrm{EX}_{\mathrm{L,dc}} = \mathrm{EX}_{\mathrm{dc,i}} - \mathrm{EX}_{\mathrm{dc,o}} \tag{24}$$

$$\mathrm{IP} = \left(1 - \eta_{\mathrm{Ex,dc}}\right) \mathrm{EX}_{\mathrm{L,dc}} \tag{25}$$

In Eqs. (21, 22, 23 and 24), $\mathrm{Ex}_{\mathrm{dc,i}}$, $\mathrm{Ex}_{\mathrm{dc,o}}$, and $\mathrm{Ex}_{\mathrm{L,dc}}$ are, respectively, the inlet exergy, outlet exergy, and exergy loss in kJ/s. The exergy efficiency can be defined as the ratio of useful exergy (difference between entering and loss) to the entering exergy of drying air supplied for drying material dehydration. Thus, the general form of exergy efficiency is written in Eq. (25) (Mahapatra and Imre 1990; Odunukwe 1987; Fudholi et al. 2013), and its simplified form is in Eq. (26):

$$\eta_{\mathrm{Ex,dc}} = \frac{\mathrm{EX}_{\mathrm{dc,i}} - \mathrm{EX}_{\mathrm{L,dc}}}{\mathrm{EX}_{\mathrm{dc,i}}} \tag{26}$$

$$\eta_{\mathrm{Ex,dc}} = 1 - \frac{\mathrm{EX}_{\mathrm{L,dc}}}{\mathrm{EX}_{\mathrm{dc,i}}} \tag{27}$$

To improve and maximize the exergy efficiency of a drying system, the exergy loss ($\mathrm{Ex}_{\mathrm{loss}}$) should be minimized. Researchers used improvement potential (IP) parameter to clarify and analyze the concept of an exergy for different

processes (Vlachos et al. 2012; Fudholi et al. 2014a). Equation (27) can be used to calculate the IP:

$$\mathrm{IP} = \left(1 - \eta_{\mathrm{Ex,dc}}\right)\mathrm{EX}_{\mathrm{L,dc}} \tag{28}$$

In Eqs. (25, 26 and 27), $\eta_{\mathrm{Ex,dc}}$ is exergy efficiency (%) and IP is exergetic IP (kJ/s).

3 Development and Performance Study of Solar Air Heater

3.1 Solar Air Heater

Solar air heater is becoming increasingly popular in India. However, there is scope of improvement in the performance. Moreover, Mishra and Sharma (1981) had done critical review on the development, performance, and testing of improved solar air heaters which are available. However, the application of solar air heater cum dryer is not available in the market particularly for tea drying application. It has been observed that in most of the solar air heater, the absorber plate in mentioned literature had used galvanized iron or steel sheet. Therefore, a different solar thermal absorber material (aluminum plate of 2 mm thickness) had been selected for the design. An improved solar air heater has been considered for its performance evaluation in actual outdoor condition at Tezpur University campus, Tezpur-784,028, India (latitude 26° 42′ 03″ N and longitude 92° 49′ 49″ E), in the month of May–June 2012. Both the thermal performance and thermo-hydraulic performance would be evaluated for the hemispherical protruded solar air heater at variable dimensionless protrusion height and pitch (roughness parameter) and Reynolds number. This series of exercise has been performed with an aim to examine the prospect of solar thermal energy in black tea drying.

3.2 Major Components and Development of Solar Air Heater

The different components of a solar air heater had been discussed (Choudhuri and Garg 1993). Therefore, two rectangular ducts measuring 2400 (L) × 375 (W) × 37.5 (H) mm^3 were fabricated at Tezpur University, Tezpur, India. The top of the air heater was covered with two number of 5 mm thick commercial transparent glass. The other five sides of the air heater were covered with 10 mm thick plywood boards. Moreover, the lengths of entry and exit sections were provided with 900 mm and 500 mm as per established standards (ANSI/ASHRAE 2003). The hydraulic diameter (D_h) of the solar air heater duct was calculated from Eq. (29):

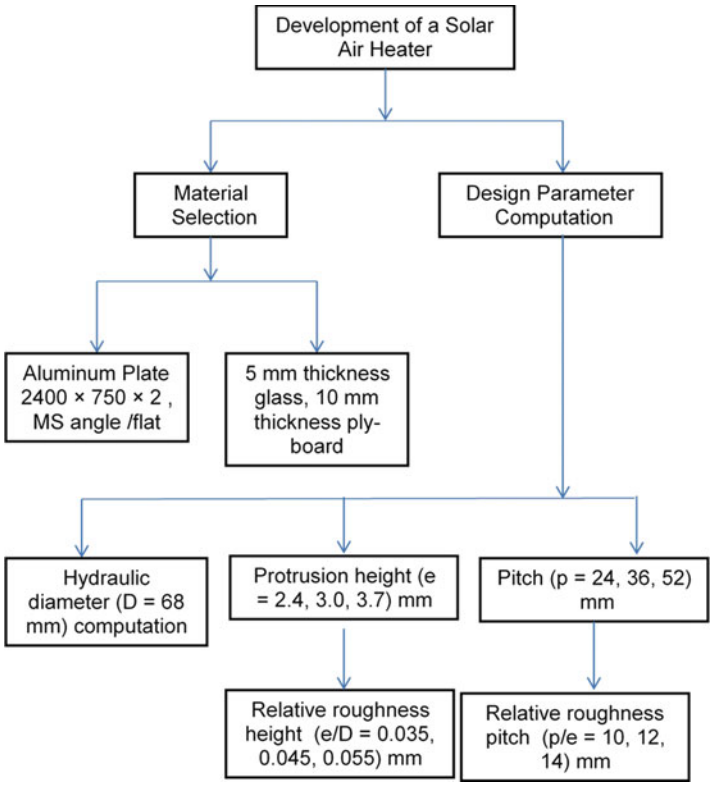

Fig. 1 Design methodology of solar air heater thermal energy absorber

$$D_h = \frac{2WH}{W+H} \tag{29}$$

where W is the duct width (mm) and H is the duct height (mm). The design methodology of the solar air heater has been presented in Fig. 1.

3.2.1 The Designed and Developed Solar Air Heater Absorber

The absorber plate is considered as a critical component of solar air heater design. Hemispherical protrusion on aluminum sheet and dimension of hemispherical protrusion shown in Figs. 2 and 3 are being used in the proposed system.

The protrusion height (e) varied as 2.4, 3.0, and 3.7 mm (Figs. 2 and 3). The long way length (p) varied as 24, 36, and 52 mm, respectively (Fig. 4).

Nusselt number for the hemispherical protruded absorber may be calculated from experiment data of average heat transfer coefficient ($\bar{h}$), thermal conductivity (k), and hydraulic diameter (D_h) of the duct. Nusselt number for smooth rectangular

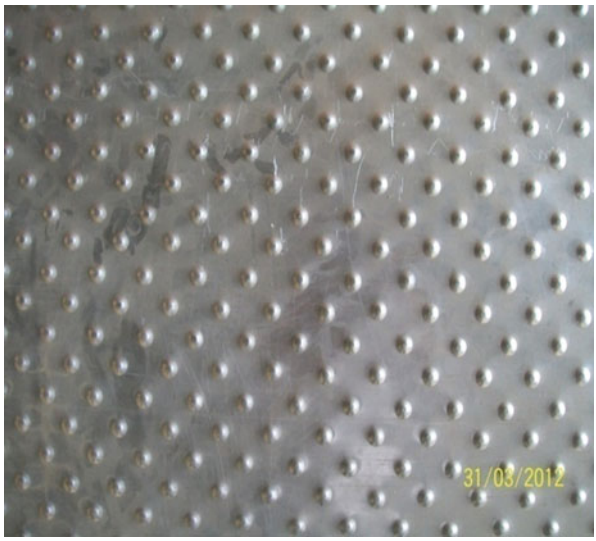

Fig. 2 Hemispherical protrusion on aluminum sheet

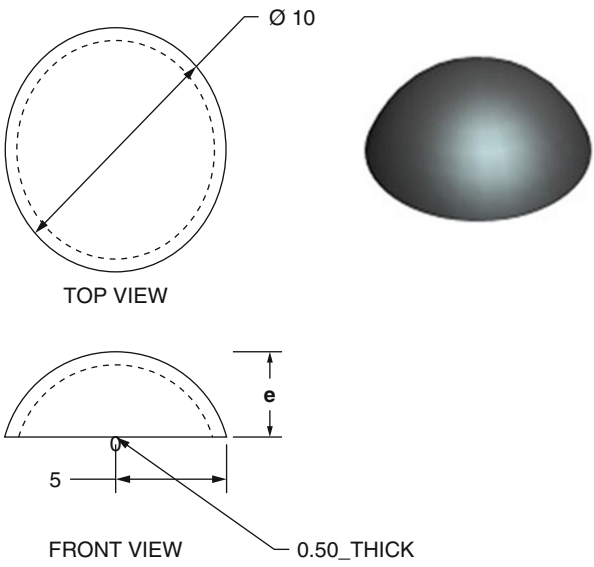

Fig. 3 Dimension of hemispherical protrusion

duct is given by Dittus-Boelter (Eq. 30) (Han et al. 1985). Roughness parameters, namely, $\frac{e}{D}$ and $\frac{p}{e}$, are strong function of Nusselt number for artificially roughen solar air heater. The cross section of air heater is shown in Fig. 5:

$$\mathrm{Nu}_s = 0.034\mathrm{Re}^{(0.8)}\mathrm{Pr}^{(0.4)}2\left(\frac{R_{\mathrm{av}}}{D}\right) \tag{30}$$

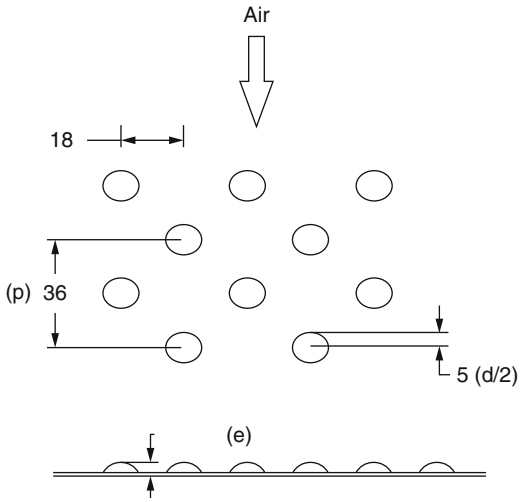

Fig. 4 Different dimensions of solar air heater absorber

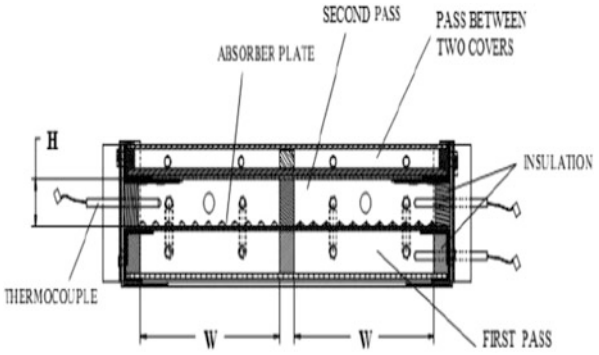

Fig. 5 Cross-sectional view of solar air heater

3.3 Experimental Methodology

ASHRAE 93–2003 (2003) standard was followed for testing of high-performance solar air heater for tea drying air. One improved solar air heater of gross absorber area of 1.8 m^2 was considered for present study. The collector temperature and pressure measurement points were made close to the collector rigid duct section. The measured variables included inlet and outlet air temperatures, ambient temperature, airflow rates, wind velocity, pressure drop, and solar radiation.

The ten numbers of PT-100-type thermocouples (24 SWG) with digital display units (Electra, made in India) and temperature accuracy of 0.1 °C had measured the duct air temperatures. Similarly, 15 thermocouples were pasted on the plate to measure average plate temperatures.

The mass flow rate of air was measured with the help of a calibrated hot-wire anemometer (Testo 425, made in Germany) [(0–20) m/s, resolution = 0.01 m/s,

accuracy = 0.03 m/s]. Average pressure drop across the air heater duct was measured with micromanometer (Testo 525, made in Germany) [(0–200) hPa, resolution = 0.1 hPa]. Air velocity varied by using a variable speed blower (Black and Decker, India, maximum discharge = 3.5 m^3 min^{-1}, maximum rpm = 16,000). The hot-wire anemometer was calibrated with a gas turbine flowmeter (discharge, 6–2500 m^3 h^{-1}; linearity = ± 0.5%; Make:Rockwin, India).

The computed hydraulic diameter (D) was 68 mm for this roughen duct air heater. The relative roughness height $\frac{e}{D}$ (Figs. 2 and 3) varied as 0.035, 0.045, and 0.055, and relative roughness pitch $\frac{p}{e}$ varied as 10, 12, and 14 during the experiments (Fig. 4) for a total of nine absorbers. The Reynolds number varied from 3500 to 17,000 for the experiments by using a variable speed blower. Flow of air was measured with a gas turbine flowmeter.

To analyze the performance of solar air heater, the following assumptions had been made: (1) The temperature difference between the plate and protrusion was neglected due to the large thermal conductivity of the absorber plate and hemispherical protrusion. (2) The thermal process in roughened air collector was approximately in steady state. (3) Centrifugal blower caused negligible rise in air temperature. (4) The glazing material had negligible heat capacity. The improved air heater performance testing experiments were normally conducted on sunny days from 9.00 a.m. to 15.00 p.m. at Tezpur University campus (latitude 26° 42′ 03″ N and longitude 92° 49′ 49″ E), Tezpur, India. The air heater experimental setup is given in Figs. 6 and 7.

4 Economic Analysis

An effort had been made to investigate economic feasibility of solar air heater cum dryer for tea drying. There are different procedures available in literatures for economic feasibility analysis of a new energy system. However, in the present investigation, a specific procedure was followed where (1) net present value, (2) - benefit-cost ratio, and (3) payback period pertaining to a new renewable energy technology were assessed. The difference between the present value of all future returns (F_{n1}) and present money required to make an investment (F_{n2}) with rate of interest (i) for n years is related with net present worth by Eq. (31):

$$\mathrm{NPV} = \sum_{n=1}^{n=n} \frac{F_{n1} - F_{n1}}{(1+i)^n} \tag{31}$$

Benefit-cost ratio is defined as the present worth of benefit stream to present worth of cost stream. An acceptable project must have benefit-cost ratio greater than 1. Mathematically, benefit-cost ratio is expressed as in Eq. (32):

Fig. 6 Improved solar air heater: experimental setup

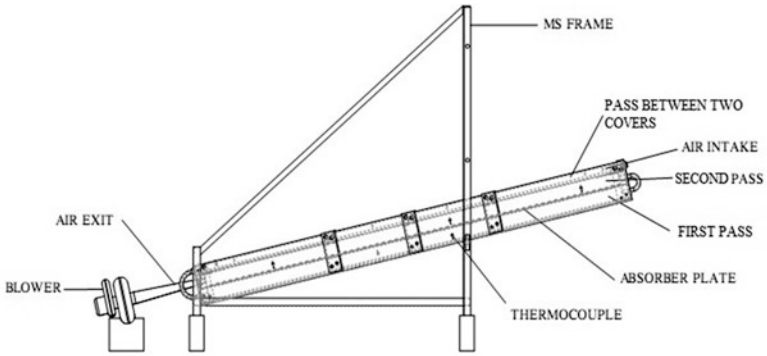

Fig. 7 Experimental setup of solar air heater in CAD

$$Benefit\ \ cost\ \ ratio = \frac{\sum_{n=1}^{n=n} \frac{F_{n1}}{(1+i)^n}}{\sum_{n=1}^{n=n} \frac{F_{n2}}{(1+i)^n}} \tag{32}$$

The principal amount of capital (P) with rate of interest (i) (minimum attractive rate of return, $MARR$) for n years yield future amount of money (F_n) given by the following Eq. (33) (Audsley and Wheeler 1978):

$$P = \frac{F_n}{(1+i)^n} \tag{33}$$

The necessary condition for attractive payback period for an investment C_0, the amount accumulated A_t in m years, is given by inequality (Eq. 34), and a project investment has to be attractive, and internal rate of return must be greater than minimum attractive rate of return (IRR > MARR):

$$\text{PBP} = the\ \ smallest\ \ m\ \ such\ \ that \sum_{(t=1)}^{(t=m)} A_t > C_0 \tag{34}$$

The payback period is the total length of time from the beginning of the project until the net value of the incremental production stream recovers the total amount of capital investment.

5 Results and Discussions

The computation for collector efficiency was performed for incident of solar radiations (average 790 W m^{-2}). Data were measured from 9.00 a.m. to 3.00 p. m. at automatic weather station of Tezpur University, Tezpur, India. Therefore, Fig. 8 shows variation of solar radiation and improved air heater air temperature with time from 9.00 a.m. to 3.00 p.m. The maximum outlet air temperature was 65 °C around 12.00 p.m. at solar irradiance of (950) W m^{-2}. The testing was performed as per established standards (Kalogirou 2003).

Figure 9 shows variation of solar air preheater output air temperature and efficiency with hot air mass flow rate (kg/s m^{-2}) against collector area. It is clear that thermal efficiency increases with increase in air mass flow rate. The output temperature of hot air decreases with increase hot air mass flow. Beyond hot air mass flows rate of 0.028 kg/s m^{-2}, the falling rate of outlet temperature of air heater becomes steady, although collector efficiency still increases. From these data, the best operating point of solar air heater may be found out around air mass flow rate of 0.028 kg/s m^{-2}.

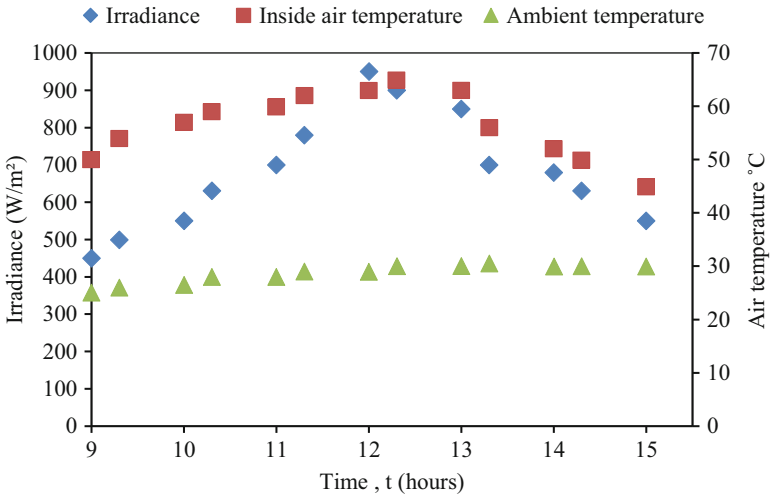

Fig. 8 Variation of solar radiation and improved air heater air temperature with time

Beyond this mass flow rate, even if there is an increase of collector efficiency, due to fall in outlet air temperature, it is not economical to operate the solar air heater. Therefore, performance studies have been made at mass flow rate of 0.028 kg/s m^{-2}. Figure 10 shows the effect of variable $\frac{p}{e}$ (10–14) for fixed value of roughness parameter, $\frac{e}{D}$ (0.055). It is clear that Nusselt number is maximum for $\left(\frac{p}{e}\right)$ value of 12, and it decreases in either side of 12. This might be due to separation of airflow over hemispherical protruded surface, and reattachment of free shear layer occurs for $\frac{p}{e}$ (12). This gives rise to maximum heat transfer near reattachment region. Reattachment may not occur near $\frac{p}{e}$ (10 or 14), and therefore, Nusselt number is smaller in these regions. For higher value of $\frac{e}{D}$ (0.055) ratio, more reattachment of free shear layer might occur that enhances Nusselt number.

The effect of $\frac{p}{e}$ on performance of hemispherical protruded absorber has been shown at Fig. 11. It is seen that maximum thermal efficiency of 82% is achievable for $\frac{p}{e} = 12$ and $\frac{e}{D} = 0.055$. The corresponding F_0U_1 and $F_0(\alpha\tau)$ are 10, 09, and 07 W m^{-2} K^{-1} and 0.837, 0.721, and 0.572 for $\frac{p}{e}$ (12, 10, and 14). Similarly, Fig. 12 shows the effect of $\frac{e}{D}$ (0.055, 0.045, 0.035) of hemispherical protruded absorber on constant $\frac{p}{e} = 12$. The values of F_0U_1 and $F_0(\alpha\tau)$ are 10, 09, and 08 W m^{-2} K^{-1} and 0.884, 0.746, and 0.664, respectively. Average solar radiation was above 790 W m^{-2} for all experiments.

Figure 13 presents the variation in effective efficiency of hemispherical protruded solar air heater with Reynolds number. It is clear that effective efficiency increases with Reynolds number for all three values of $\frac{e}{D}$ (0.035, 0.045, and 0.055) and attains maximum value for Reynolds number around 12,000. Effective

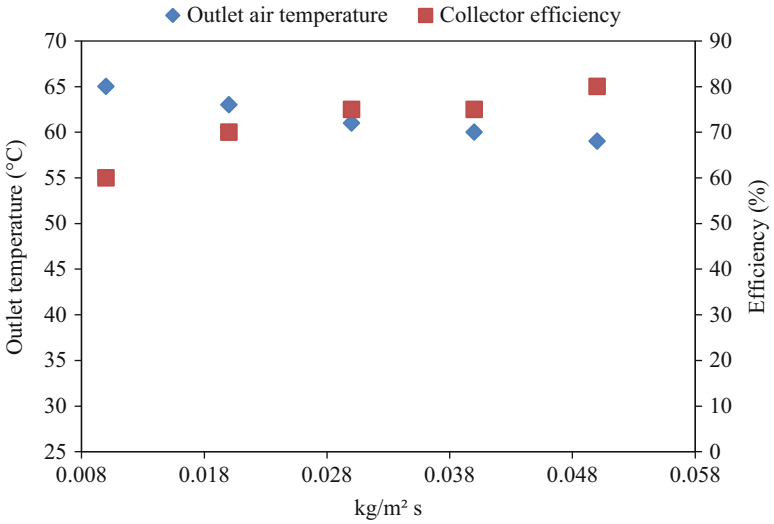

Fig. 9 Variation of collector outlet temperature and efficiency with air mass flow rate

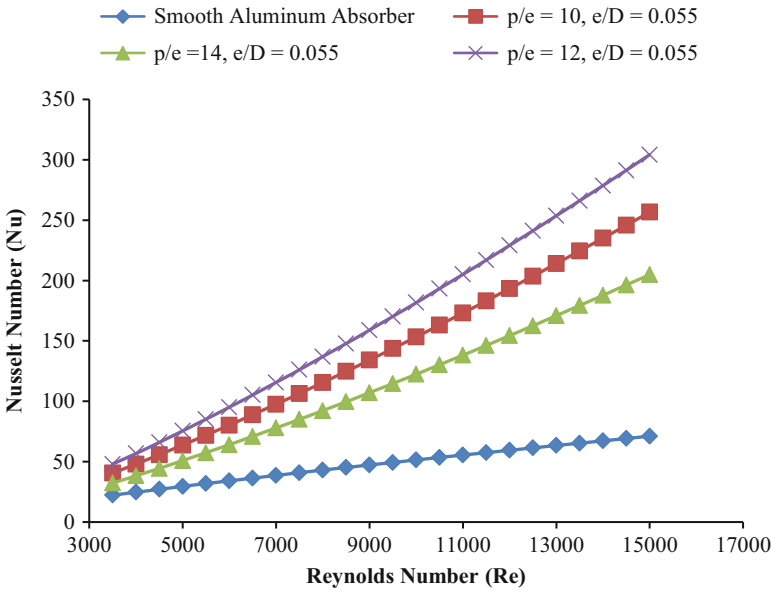

Fig. 10 Variation of Nu number with Re number for constant *e/D* and variable *p/e*

efficiency for smooth solar air heater absorber was minimum up to Reynolds number 14,000, and beyond this Reynolds number, effective efficiency of smooth solar air heater becomes maximum. Therefore, beyond this region, there is no gain in effective efficiency of artificially roughen air heater. It is also clear that with $\frac{e}{D}$,

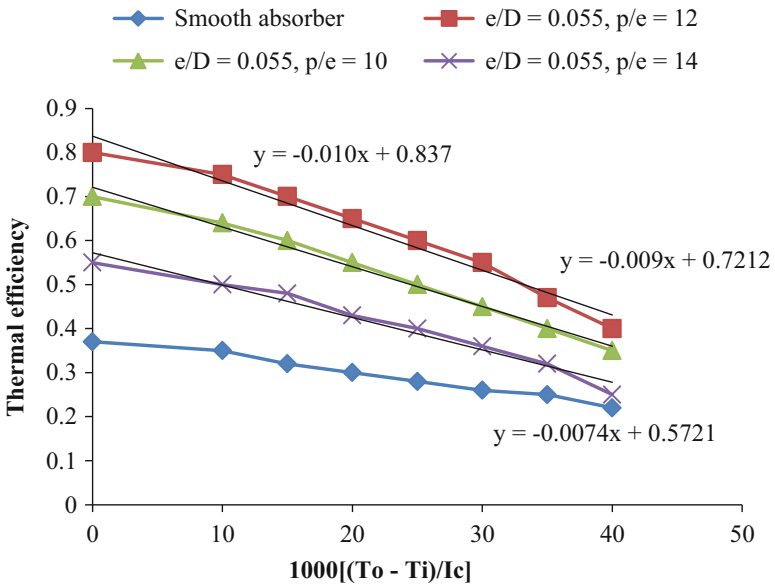

Fig. 11 Effect of *p*/*e* on the performance of hemispherical protruded air heater

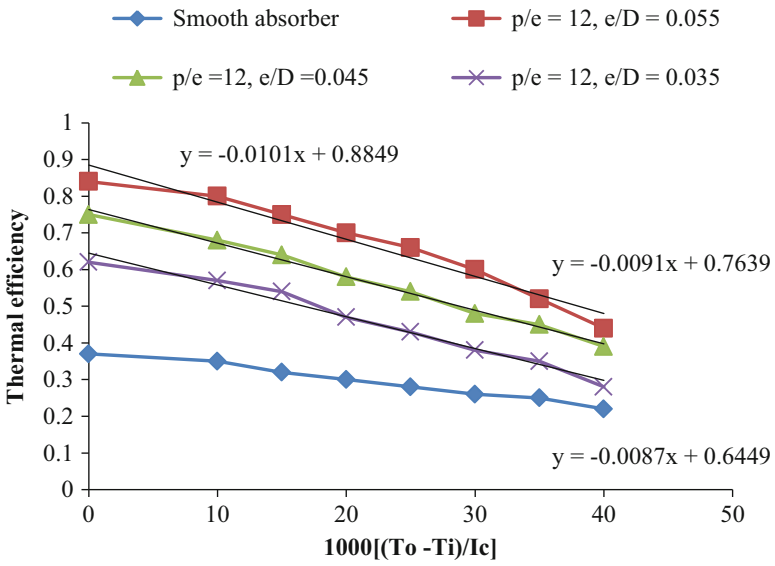

Fig. 12 Effect of *e*/*D* on the performance of hemispherical protruded solar air heater

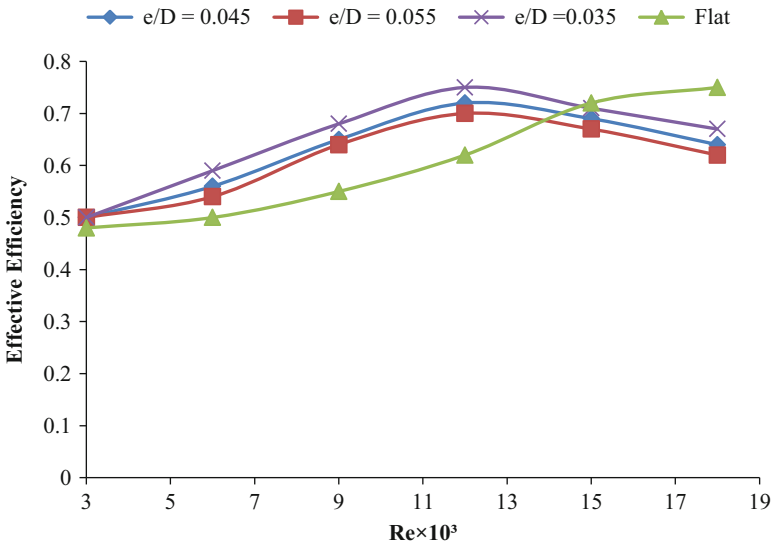

Fig. 13 Variation of effective efficiency of hemispherical protruded solar air heater with Reynolds number

value of 0.035 and 0.055 gives maximum and minimum effective efficiency (74 and 64%), respectively, around Reynolds number 12,000.

Figure 14 shows variation of useful energy of hemispherical protruded solar air heater with Reynolds number. It is clear that with decrease in dimensionless protrusion height ($\frac{e}{D}$, 0.055, 0.045, 0.035), useful heat gain by the hemispherical protruded solar thermal absorber increases. All three solar thermal energy absorbers gain maximum energy around Reynolds number 12,000, and beyond this useful energy gain decreases because more high-grade energy is required to propel air than it acquires from roughen air heater.

Figure 15 presents comparison of effective efficiency of hemispherical protruded solar air heater with smooth air heater. The maximum efficiency enhancement takes place for dimensionless protrusion height ($\frac{e}{D} = 0.035$) that is about 8.9% around Reynolds number 6000–10,000. The minimum efficiency enhancement about 5.5% takes place for protrusion height ($\frac{e}{D} = 0.055$).

For performance testing of solar air heater, it has been observed that hemispherical protrusion with ($\frac{e}{D} = 0.035$) and ($\frac{p}{e} = 12$) geometry gave the best thermo-hydraulic efficiency of 74% around Reynolds number 12,000. Therefore, this configuration of improved solar air heater has been selected for producer gas solar hybrid studies of black tea drying analysis:

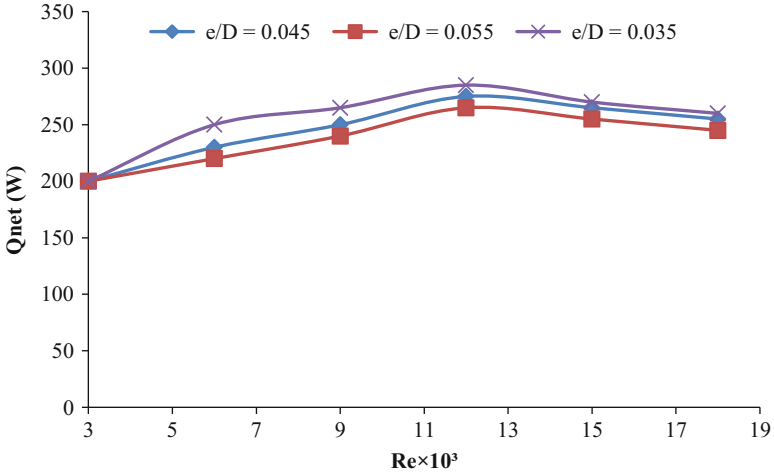

Fig. 14 Variation of useful energy of solar air heater with Reynolds number

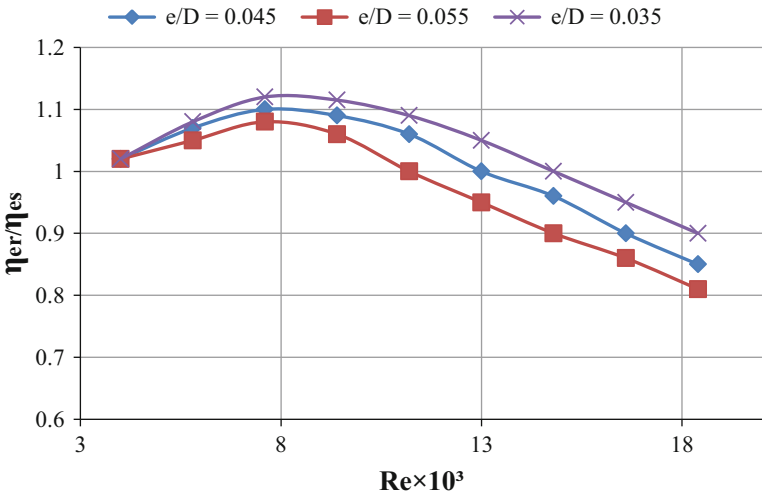

Fig. 15 Comparison of efficiency of hemispherical protruded solar air heater with smooth air heater

$$\mathrm{Nu_{rh}} = 5.2 \times 10^{(-4)} \mathrm{Re}^{1.27} \left(\frac{p}{e}\right)^{(3.15)} \exp(-2.12) \left[\log\frac{p}{e}\right]^{p/6e} \left(\frac{e}{D}\right)^{0.33} \exp(-1.30) \left(\log\frac{e}{D}\right)^{2} \tag{35}$$

A modified correlation of Nusselt number had been developed from analysis of our experimental data of hemispherical protruded solar air heater as given by correlation in Eq. (35) similar to that developed by Saini and Verma (2008).

6 Economic Analysis of Biomass Gasification and Improved Solar Air Heater Hybrid System for Tea Drying

Annual black tea manufactured by an average-sized tea estate in Sonitpur district (Assam, India) was 990 t in the year 2011–2012 as computed by geographical information system mapping. The average yield of black tea manufactured was assumed as 02 t ha^{-1} to compute annual black tea production for a representative average-sized tea estate. The total back tea production was calculated by multiplying yield of black tea by total mapped area of the tea estate (Project Report, National Remote Sensing Centre, Hyderabad 2006).

Since annual black tea manufactured by an average-sized tea estate in Sonitpur district (Assam) was 990 t (GIS mapping), the corresponding coal requirement is 825 t (coal 1.35 kg kg^{-1} of black tea manufactured). It was also observed from this study that thermal efficiency was 20% for a conventional coal-fired furnace and 80–90% for proposed producer gas-fired furnace used for tea drying. Therefore, producer gas-fired furnace is a better option over coal-fired system. Coal international price was 95 \$ t^{-1} (Birol 2010), and that of woody biomass was 11 \$ t^{-1} in the year 2011–2012. A 454 kW thermal woody biomass gasifier was considered that could substitute 28% of this thermal load (Varshney et al. 2010). It is estimated that by plantation of 22.5 ha *Bambusa tulda*, this thermal load of the said biomass gasifier may be met. It has been estimated that if 400 m^2 of tea factory galvanized roof were converted by using black painting, plywood insulation, and tempered glass enclosure to convert into solar air heater, then average 20% of biomass energy may be saved. The annual carbon dioxide reduction of 2189 t is achievable (Dutta 2014). The payback period of the hybrid renewable thermal energy-based system is less than 15 months, and the benefit-cost ratio is 1:1.

7 Conclusion

Open sun drying takes longer duration, and as a result, it gives inconsistent quality for drying of agro-based produces. Different improved designs of solar air heater cum dryers are available to get efficient solar drying. The present investigation explores general theoretical thermodynamic performance studies of some improved solar air heater for drying of rural agro-based produces. An improved hemispherical protruded solar air heater has been designed and developed. It follows with a detailed thermal performance studies of an improved hemispherical protruded solar air heater. The protrusion height (e) varied as 2.4, 3.0, and 3.7 mm, and the long way length (p) varied as 24, 36, and 52 mm, respectively. The effect of $\frac{e}{D}$ (0.055, 0.045, 0.035) of hemispherical protruded absorber on constant $\frac{p}{e} = 12$ had been observed. It was seen that maximum thermal efficiency of 82% is achievable for $\frac{p}{e} = 12$ and $\frac{e}{D} = 0.055$. Moreover, with $\frac{e}{D}$, value of 0.035 and 0.055 gives

maximum and minimum effective efficiency (74% and 64%), respectively, around Reynolds number 12,000. From economic analysis, it has been estimated that if 400 m^2 of black tea processing factory galvanized roof were converted by using black painting, plywood insulation, and tempered glass enclosure to convert it into a solar air heater, then average 20% of conventional thermal energy for black tea drying may be saved. The annual carbon dioxide reduction of 2189 t is achievable by using improved solar air heater. The payback period of the hybrid renewable thermal energy-based system is less than 15 months, and the benefit-cost ratio is 1:1.

Nomenclature

Cos θ	The phase angle difference between voltage and electric current, ~0.85
c_p	Specific heat of drying air, kJ/kg
$\dot{E}$	Energy, kJ/s
E_{fan}	Fan energy consumption, kW
Ex	Exergy, kJ/s or kW
EUR	Energy utilization ratio, dimensionless
g	Gravitational acceleration, 9.8 m/s^2
h	Enthalpy, kJ/kg
I	Electric current, ~4 A
IP	Exergetic improvement potential, kJ/s or kW
$\dot{m}$	Mass flow rate of air, kg/s
m_i	Initial weight of product, kg
m_w	Mass of water evaporated from the product, kg/s
N	The number of days, in January N ¼1 and in December N ¼365
n_i	Number of holes in length or width of heat-absorbing plate
n_j	Total number of holes in heat-absorbing plate
P	Pitch of holes in heat-absorbing plate, m
P_{sur}	Pressure, kPa (for Sabzevar City is 90.118 kPa)
P_{vs}	Saturated vapor pressure of air, kPa
Q	Heat energy, kJ/s
S	Solar radiation, W/m^2
SEC	Specific energy consumption, kW h/kg
SMER	Specific moisture extraction rate, kg/kW h
T	Air temperature, °C or K
t	Time (s)
u	Air velocity, m/s
ū	Average velocity, m/s
U	Voltage, 220 V
V	Volumetric flow rate of air, m^3/s
$\dot{W}$	Mechanical work, kJ/s
w	Absolute humidity, kg H_2O/kg Da
w_{as}	Absolute humidity of the air entering the dryer at the point of adiabatic saturation, %
w_i	Absolute humidity of air entering the drying chamber, %
X	Moisture content, wb%
Z	Height from sea level, m (for Sabzevar City is 977.6 m)
z	Height from base level, m

Greek Letters

Δ	Difference between two values
η	Efficiency, %
λ	Latent heat of water vaporization at exit air temperature, kJ/kg
φ	Relative humidity, %
υ	Specific volume, m^3/kg
σ	Void in the heat-absorbing plate
Σ	Sum between several values
∞	Surrounding or ambient (reference)

Subscripts

a	Air
abs	Absolute
col	Collector
d	Dryer
da	Drying air
dc	Drying chamber
ex	Exergy
f	Final
I	Initial, input, inflow
L	Loss
o	Output, outflow
p	Pickup
sur	Surrounding
sys	System

References

ANSI/ASHRAE (2003) Standard 93–2003. Methods of testing to determine the thermal performance of solar collectors. ISSN: 1041–2336, ASHRAE, Inc., 1791 Tullie Circle, Ne, Atlanta, GA, 30329

Audsley E, Wheeler J (1978) The annual cost of machinery calculated actual cash flows. J Agric Eng Res 23:89–201

Aghbashlo M, Kianmehr MH, Arabhosseini A (2008) Energy and exergy analyses of thin-layer drying of potato slices in a semi-industrial continuous band dryer. Dry Technol 26(12):1501–1508

Akbulut A, Durmus A (2010) Energy and exergy analyses of thin layer drying of mulberry in a forced solar dryer. Energy 35(4):1754–1763

Bagheri N, Keyhani A, Mohtasebi SS, Alimardani R, Rafiee SH, Mansoori GH (2011) Design, construction and evaluation of a fan speed controller in a forced convection solar dryer to optimize the overall energy efficiency. Agric Sci Technol 13:503–515

Birol F (2010) World energy outlook 2010. International Energy Agency, France

Choudhuri C, Garg HP (1993) Performance of air heating collectors with packed air flow passage. Sol Energy 50(3):205–221

Dutta PP (2014) Prospect of renew able thermal energy in black tea processing in Assam: an investigation for energy resources and technology. Ph.D. thesis, School of Engineering, Department of Energy, Tezpur University

Erbay Z, Hepbasli A (2013) Advanced exergy analysis of a heat pump drying system used in food drying. Dry Technol 31(7):802–810
Fudholi A, Othman MY, Ruslan MH, Sopian K (2013) Drying of Malaysian Capsicum annuum L. (red chili) dried by open and solar drying. Int J Photoenergy 2013:1–9. doi:10.1155/2013/167895. (Article ID 167895)
Fudholi A, Sopian K, Othman MY, Ruslan MH (2014a) Energy and exergy analyses of solar drying system for red seaweed. Energ Buildings 68:121–129
Fudholi A, Sopian K, Yazdi MH, Ruslan MH, Gabbasa M, Kazem HA (2014b) Performance analysis of solar drying system for red chili. Sol Energy 99:47–54
Fudholi A, Sopian K, Alghoul MA, Ruslan MH, Othman MY (2015) Performances and improvement potential of solar drying system for palm oil fronds. Renew Energy 78:561–565
Han JC, Park JS, Lei CK (1985) Heat transfer enhancement in channels with turbulence promoters. Trans ASME J Eng Gas Turbine Power 107(30):628–635
Hans VS, Saini RP, Saini JS (2009) Performance of artificially roughened solar air heaters – a review. Renew Sust Energ Rev 13:1854–1869
Hepbasli A, Colak N, Hancioglu E, Icier F, Erbay Z (2010) Exergy economic analysis of plum drying in a heat pump conveyor dryer. Dry Technol 28(12):1385–1395
Kalogirou S (2003) The potential of solar industrial process heat applications. Appl Energy 76:337–381
Kurtbas I, Durmus A (2004) Efficiency and exergy analysis of a new solar air heater. Renew Energy 29(9):1489–1501
Mahapatra AK, Imre L (1989) Energy alternatives: the Indian perspective. Int J Ambient Energy 10(3):163–166
Mahapatra AK, Imre L (1990) Role of solar agricultural-drying in developing countries. Int J Ambient Energy 11(4):205–210
Midilli A, Kucuk H (2003) Energy and exergy analyses of solar drying process of pistachio. Energy 28:539–556
Mishra CB, Sharma SP (1981) Performance study of air heated packed bed solar energy collectors. Int J Energy 6:153–157
Mumba J (1996) Design and development of a solar grain dryer incorporating photovoltaic powered air circulation. Energy Convers Manag 37(5):615–621
Odunukwe CG (1987) Proceeding of biennial congress of ISES, vol 3. Pergamon Press, Hamburg, FRG, p 2515
Prakash O, Kumar A (2013) Historical and recent trend of solar drying system: a review. Int J Green Energy 10(7):690–738
Prakash O, Kumar A (2014) Environomical analysis and mathematical modeling for tomato flakes drying in modified greenhouse dryer under active mode. Int J Food Eng 10(4):669–681
Project Team natural resource census: national land use and land cover analysis using multi-temporal LISS-III (LULC-LII: 50K) e Project manual. Document No.: NRSA/RSGIS-A/NRC/NLULCL3/TECHMAN/R02/JANUARY. National Remote Sensing Centre, Hyderabad (2006)
Saini RP, Verma J (2008) Heat transfer and friction factor correlations for a duct having dimple-shape artificial roughness for solar air heaters. Energy 33:1277–1287
Therdthai N, Zhou W (2009) Characterization of microwave vacuum drying and hot air drying of mint leaves (Mentha cordifolia Opiz ex Fresen). J Food Eng 91(3):482–489
Twidell JW, Muniba J, Thornwa T (1993) The Strathclyde solar crop dryer: air heater, photovoltaic fan and desiccants. In: Proceeding of ISES solar world congress, vol 8. Budapest, pp 55–60
Varshney R, Bhagoria JL, Mehta CR (2010) SMALL Scale Biomass Gasification Technology in India – an overview. J Eng Sci Manag Educ 3:33–40
Vlachos NA, Karapantsios TD, Balouktsis AI, Chassapis D (2002) Design and testing of a new solar tray dryer. Dry Technol 20(5):1239–1267
Zandler H, Mislimshoeva B, Samimi C (2016) Scenarios of solar energy use on the "roof of the world": potentials and environmental benefits. Mt Res Dev Int J 36(3):256–266

Thermal Energy Storage in Solar Dryer

Ajay Kumar Kaviti and Harsh Deep

Abstract Energy storage not only plays an important role in conserving the energy but also improves the reliability and performance of a wide range of energy systems. In general, there is gap between the energy supply and energy demand in any system. The energy storage can neutralize this imbalance and thereby helps in savings of capital. Energy storage is more important where the energy source is irregular such as solar. Developing countries are taking so many initiatives to take advantage of solar energy. Among many applications of solar energy, drying of farming food products is extensively used in developing countries. Development of dexterous energy storage devices with less cost is as significant as budding new energy sources and, thus, decreases the time gap between demand and supply of energy, by this means playing a very indispensable mission in energy conservation. In the past few decades, various small-scale designs of solar dryers with storage of thermal energy have been developed for different purposes. Therefore, in this chapter an attempt has been made to study the recent and past research on different thermal storage systems for solar dryers like latent heat storage, sensible heat storage, and thermochemical storage which are commonly used for domestic and industrial applications.

Keywords Latent heat • Sensible heat • Thermal storage • Solar dryer

1 Introduction

One of the important topics of discussion in the current research and scientific literature is energy. It is obvious that it is going to face energy problem at local level, national level, and at the international level, if the rate of population and use

A.K. Kaviti (✉)
Department of Mechanical Engineering, Vallurupalli Nageswara Rao Vignana Jyothi Institute of Engineering and Technology, Hyderabad 500090, India
e-mail: ajaykaviti@gmail.com

H. Deep
Department of Mechanical Engineering, Birla Institute of Technology, Mesra, Ranchi 835215, India

© Springer Nature Singapore Pte Ltd. 2017

O. Prakash, A. Kumar (eds.), *Solar Drying Technology*, Green Energy and Technology, DOI 10.1007/978-981-10-3833-4_22

of exiting available energy of fossil fuels continues in the same rate. Hence, efforts of scientific research and technology have been moved in the direction of development of alternative and renewable energy sources. However, developing effective and low-cost energy storage devices is as essential as developing new sources of energy.

Energy storage can triumph over the time lag between the demand and supply of energy and, thus, plays a significant role in conservation of energy. It helps in improving the performance of energy system by smooth functioning and increases consistency. Especially, some of the renewable energies like solar, wind can endow with only irregular energy supply. So, an additional backup energy source is necessary. Provision of a solar thermal energy storage can reduce the additional backup energy consumption to considerable rate, thus saving the reserves of energy in fossil fuels.

Mother Earth is source of storing plenty of solar energy. But, they are huge in quantity, unpredictable, and frequently locally unavailable, so it is very difficult to be portable. So, an efficient means for storing energy would significantly reduce the problem and would make available low-cost energy for everybody. It seems that not much attention has been given toward the problem of storage as much attention given to generation of energy. So, the storage of energy in suitable form for suitable use is topic of research in the field of science and technology.

It is obvious that solar energy is one of the important renewable energy sources used widely in many aspects of our life like space heating of houses, hot water supply, desalination, drying, and cooking. So, the need of energy storage devices is increasing day by day to mitigate the drawback of intermittence of solar energy. Applications of solar energy in the agricultural area have enlarged due to fluctuation in the price of fossil fuels, environmental concerns, and expected running down of conventional fossil fuels. Figure 1 shows the sudden increment in the energy consumption being noticed in the food and related sector. This is creating a pressure on many fields related to energy production as well as energy transmission.

It has been noticed that a food loss in the range of 10–40% is caused due to lack of appropriate technology, inappropriate farming, fertilization, the nonexistence of marketing channels, inappropriate transportation, high postharvest losses, etc. (Esper and Mühlbauer 1998). Hence, food preservation is needed to reduce the food loss. Hence, drying is widely accepted as an important tool in this direction, since a long time. The drying is the one of the oldest and the most basic process to reduce moisture from a product usually agricultural or food products storage (Leon et al. 2002). In order to keep the edible and nutritious properties of the food product intact, drying is done. To dry reasonably and rapidly to a safe moisture content and to ensure a good quality of the food product, drying should be done under controlled condition of temperature and humidity (Sharma et al. 1995).

Solar drying is advantageous in domestic as well as industrial sector for a number of food and agricultural products, like it makes the preservation process much easier, turns some products into much more usable form, increases the storage capacity and reduces the transportation cost, and also utilizes the direct or indirect ecological benefits. Hence, an efficient solar dryer system could be of great use for

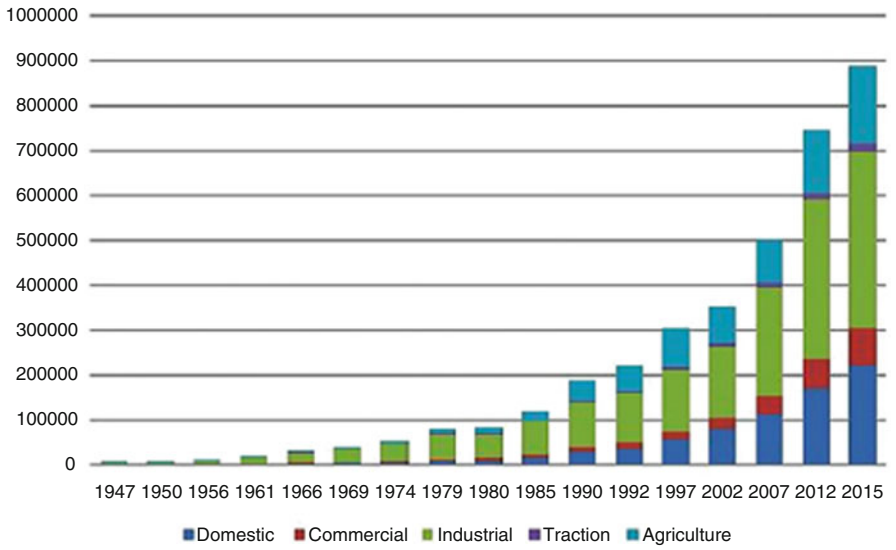

Fig. 1 Showing sector-wise electricity growth in India (GWh) (Source: Central Electricity Authority 2015)

the betterment of the mankind. This is truly a challenging task to develop a solar drying technique with efficient energy consumption for the desired product because of its significant limitation of intermittence.

In order to avoid the intermittent effects in solar dryers, some of the researchers integrated it with a thermal energy storage to store excess heat energy in the sunshine time and utilize it in the off-sunshine time. The surplus solar energy can be stored in solids or well-insulated fluids in the form of sensible heat or latent heat or thermochemical. Among these methods latent heat storage provides higher storage with small temperature difference between storing and releasing energy. Khanna (1967) constructed a solar dryer with thermal storage using heat exchanger. It was observed that shell and tube heat exchanger helped in drying a specific food product. Ayensu and Asiedu-Bondzie (1986) designed and fabricated a solar dryer with thermal storage which was capable to transfer 118 W/m^2 of radiation to the drying chamber. Ayensu (1997) fabricated a solar dyer with rock storage system and observed that thermal storage material reduced the drying period. Therefore, in this chapter attempt has been made to study the recent and past research on different thermal storage systems for solar dryers like latent heat storage, sensible heat storage, and thermochemical storage commonly used for domestic and industrial applications.

2 Thermal Energy Storage

Solar energy can be stored using mechanical, electrical, and thermal method (Khartchenko 1997). In well-insulated materials, thermal energy can be stored as sensible heat, as latent heat, as change in internal energy of the material and thermochemical, or any combination of above mentioned. Figure 2 shows some of the major techniques involved in thermal energy storage.

2.1 Sensible Heat Storage

In the sensible heat storage (SHS), change in temperature of a liquid or solid results in change in heat stored as sensible heat. The amount of sensible heat storage depends on rise in temperature of the storage medium, the specific heat capacity of storage medium, and mass of the storage material.

$$Q = m \int_{T_1}^{T_2} C_{\mathrm{p}} \, \mathrm{d}T \tag{1}$$

where m is the mass and Cp is the specific heat at constant pressure. T_2 and T_1 signify the range of upper and lower temperature levels within which the storage functions. The difference of upper and lower temperature denotes the temperature swing (Gogus 2009).

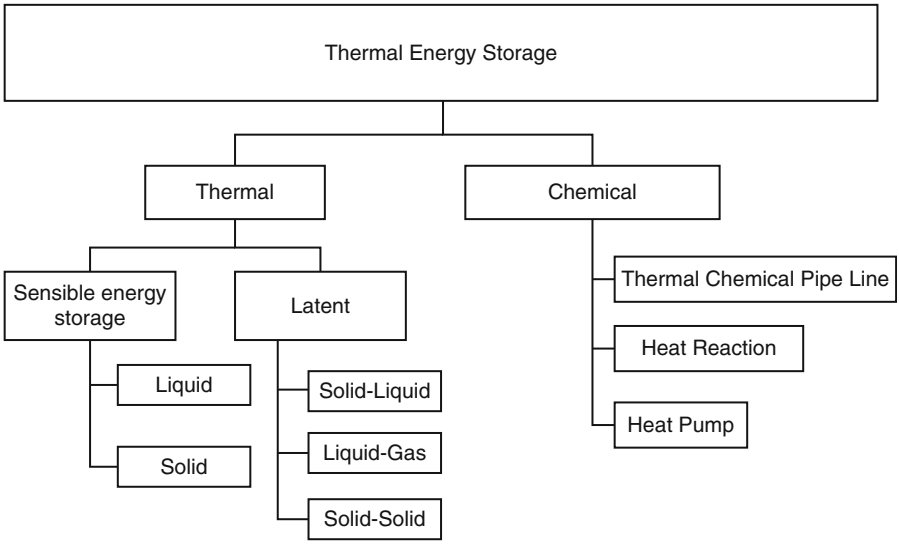

Fig. 2 Various types of thermal energy storage (Bal et al. 2010)

2.1.1 Indirect Solar Dryers

Aboul-Enein et al. (2000) performed a study on solar crop drying with natural airflow using reversed absorber plate type collector. It was observed that the thermal storage materials affected the usual mass current rate in the drying system. On the basis of energy equation, thermal model was developed. The inclined absorber, packed bed, reversed absorber, and dryer are shown in Fig. 3. The thermal storage is provided in absorber plate inclined at 30° with length and breadth each of 1 m having 0.15 m packed bed, when operated for 24-h drying period, and could dry 95 kg of onion from a moisture content of 6.14–0.27 kg water/kg of dry substance.

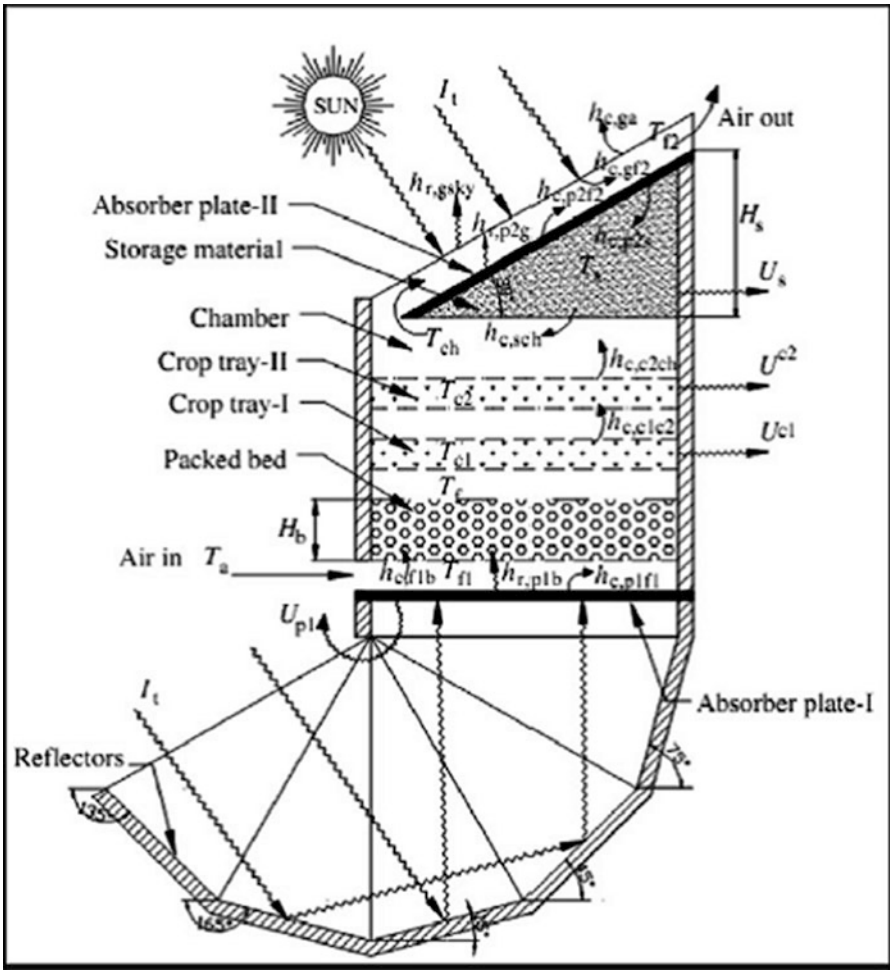

Fig. 3 Sectional view of reversed absorber plate solar crop dryer with energy storage (Aboul-Enein et al. 2000)

Due to the thermosiphon effect, natural airflow takes place. These types of solar dryers are operated completely independent from any external power.

Mohanraj and Chandrasekar (2009) designed and fabricated indirect forced convection solar dryer. They performed experimental study of chili drying by integrating different sensible heat storage materials to the indirect forced convection solar dryer as shown in Fig. 4. The absorber plate is coated with black color paint and glass cover was present in the solar air heater. The aluminum scraps mixed in sand is used to fill the gap between insulation and absorber plate to obtain hot air during no sunny hours and store the heat during sunny hours. The capacity of the dryer is to hold about 50 kg of chili per batch. With the help of glass wool of 10 mm width, the drying chamber was isolated. At an angle about 25°, the solar air heater was tilted w.r.t. horizontal surface (Shariah et al. 2002). By integrating sensible heat storage materials, the drying time was increased by about 4 h in a day, and consistent air temperature was also maintained. Moisture content in the chili was observed as 72.8% at the beginning, and after drying the moisture content was about 9.7% and 9.2% in top and bottom trays, respectively.

Jain and Jain (2004) demonstrated an analytical model of solar dyer with thermal storage as shown in Fig. 5. And it was evaluated in the month of October for drying paddy crop for climatic condition of capital of India. In extension to above, Jain (2005) used the multi-tray instead of single tray and analyzed the proficiency of the solar dyer. The increase in the tilt angle and the collector area of solar air heater up to its definite critical value resulted in the increase of grain temperature. During the off-sunshine hours, the thermal energy storage gets affected, and mathematical model is developed to predict the performance of the solar air heater. A study on solar-assisted heat pump dryer and water heater was done by Hawlader et al. (2003). The performance of the system was evaluated on the basis of the solar indices such

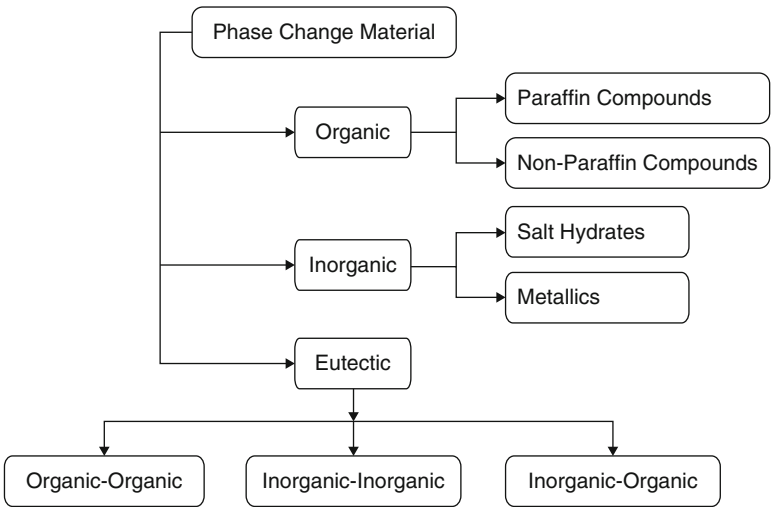

Fig. 4 Classification of phase change materials (Kant et al. 2016)

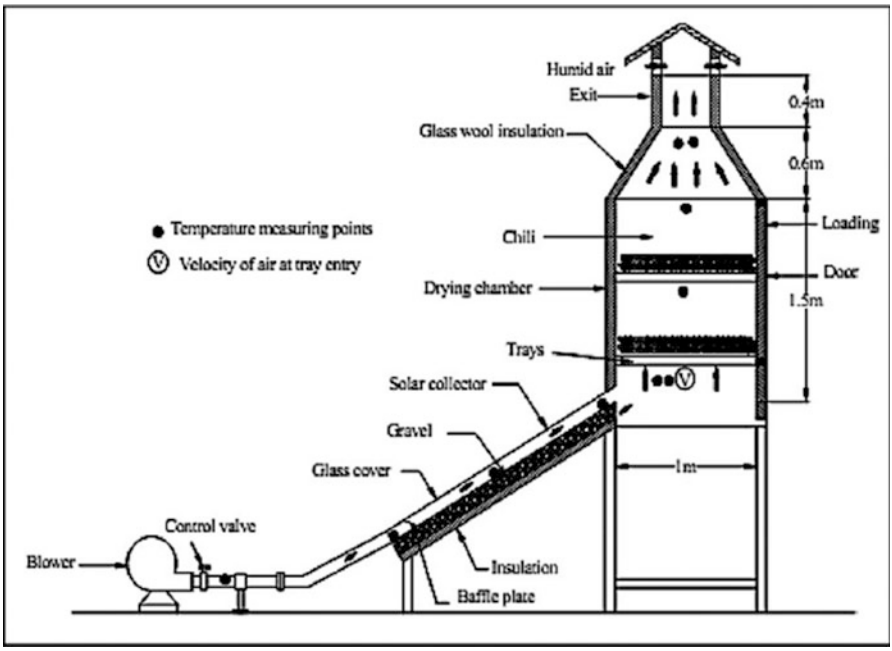

Fig. 5 Schematic view of experimental setup (Jain and Jain 2004)

as solar fraction (SF) and coefficient of performance (COP) with and without a water heater. From the experiment and simulation, the values of COP are found to be 5 and 7, respectively. Similarly, the solar fraction (SF) values from experiment and simulation are noted as 0.61 and 0.65, respectively.

2.1.2 Greenhouse Dryers

A solar tunnel dryer integrated with sensible heat storage material has been designed and fabricated by Ayyappan and Mayilsamy (2012) to test its performance for copra drying. During the clear day and off-sunshine hours, the temperature gradient inside the tunnel dryer is 10–25 °C and 7–12 °C, respectively. The % moisture in copra is reduced in the dryer from 52 to 7.1%. The overall thermal efficiency of the solar tunnel dryer is 15%. The dryer efficiency is increased by 2–3% by the use of heat storage material. Ayyappan et al. (2016) designed and developed a greenhouse dryer to predict the thermal performance of concrete, sand, and rockbed. A 4″ thickness was found to be optimum size for sand and rockbed, as it improved drying condition during both day- and nighttime. The dryer with concrete material reduced the moisture content from 52 to 7% in 78 h, whereas open sun drying took 174 h for the same % reduction of moisture content.

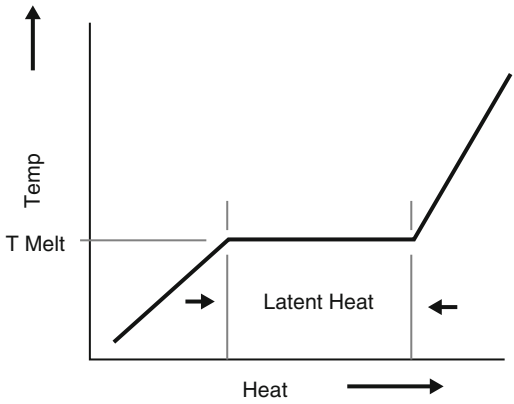

Fig. 6 Changes in heat and temperature during the phase change (Nuckols 1999)

2.2 *Latent Heat Storage*

When a thermal storage material undergoes a phase change from solid state to liquid state or from liquid state to gaseous state or vice versa at constant temperature, then the heat absorption or release is considered as latent heat storage (LHS) which is presented graphically in Fig. 6 (Nuckols 1999). The heat storage capacity of the latent heat storage system with a phase change material medium (Sharma et al. 2009) is given by Eq. 2.

$$Q = \int_{T_i}^{T_m} mC_p dT + ma_m \Delta h_m + \int_{T_m}^{T_r} mC_p dT \tag{2}$$

2.2.1 Indirect Solar Dryer

The latent heat storage with paraffin wax as a phase change material to store sufficient thermal energy and release when the energy availability is not sufficient was investigated by Devahastin and Pitaksuriyarat (2006a, b). The schematic diagram of experimental setup is shown in Fig. 7a. The complete diagram of LHS tank in which PCMs are stored is shown in Fig. 7b. Due to heat loss from surrounding, the solidification in PCM takes place from outer to inner surface. When the inlet air velocity is 2 and 1 m/s, then the extractable energy per unit mass flow rate was 1386 and1920 kJ min/kg, respectively.

The performance of an indirect forced convection and desiccant integrated solar dryer was investigated by Shanmugam and Natarajan (2007) as shown in Fig. 8 without and with the reflective mirror operated in both sunshine hours and off-sunshine hours.

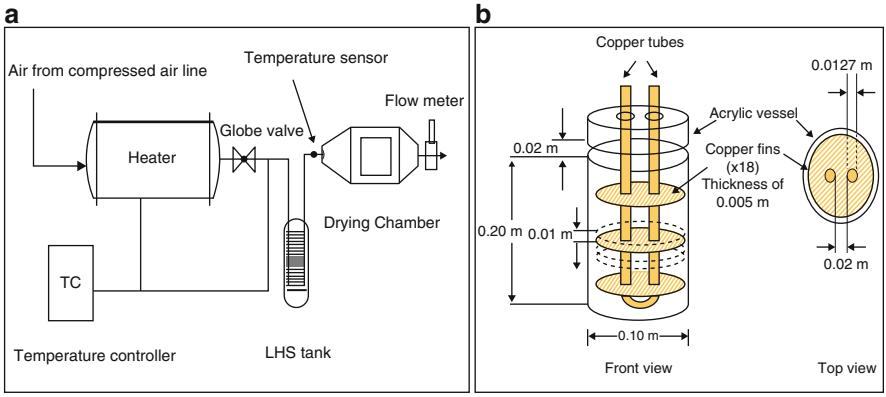

Fig. 7 (**a**) A simple sketch of the setup with drying chamber. (**b**) Detailed diagram of the LHS vessel (Devahastin and Pitaksuriyarat 2006a)

The efficiency of drying is increased by 20% with the inclusion of reflective mirror on the desiccant bed. The drying time was reduced by 4 and 2 h for pineapple and green peas, respectively, along with the increase of 10 °C temperature with the presence of mirror.

Drying performance of a novel indirect solar dryer with PCMs was studied by Shalaby et al. (2014). Important components of the dryer are two air heaters, drying chamber, PCMs, and blower. Performance of the dryer is tested with PCM and without PCM. The results indicated that air temperature is 3.5–6.5 °C higher with PCM in comparison to without PCM.

Shringi et al. (2014) designed and developed a dryer to dry garlic cloves with PCMs using indirect solar air heater. The initial % of moisture in garlic cloves is 55.5% (w.b.), and final moisture content is 6.5% (w.b.) for the duration of 8 h. The efficiency of dryer with recirculation of air and without is varied from 3.98 to 14.95% and 43.06 to 83.73%, respectively.

Jain and Tiwari (2015) developed an experimental setup of a solar dryer with PCMs. Important components of the dryer are drying chamber, packed bed for thermal storage, flat plate collector, and natural draft system as shown in Fig. 9. Thermal storage assisted in maintaining the temperature in the range of 40–45 °C, which in turn helped in increase the duration of drying. Dryer thermal efficiency was observed as 28.2% with a payback period of 1 year 6 months, and it was also observed good performance in the night.

Sain et al. (2013) fabricated solar dryer with natural convection and further integrated with thermal heat storage in the form of latent heat. Experiments were conducted under no load and full load condition. In full load condition, the ginger dehydrated from initial moisture content of 74% (w.b.) to a final moisture content of 3% (w.b.) in a day. The average daily drying efficiency was observed as 12.4%. The collector efficiency varied in the range of 53–96% and 40–65% in no load and full load conditions, respectively. The overall thermal efficiency of the natural convection type solar dryer with latent heat storage was found to be 22.7%.

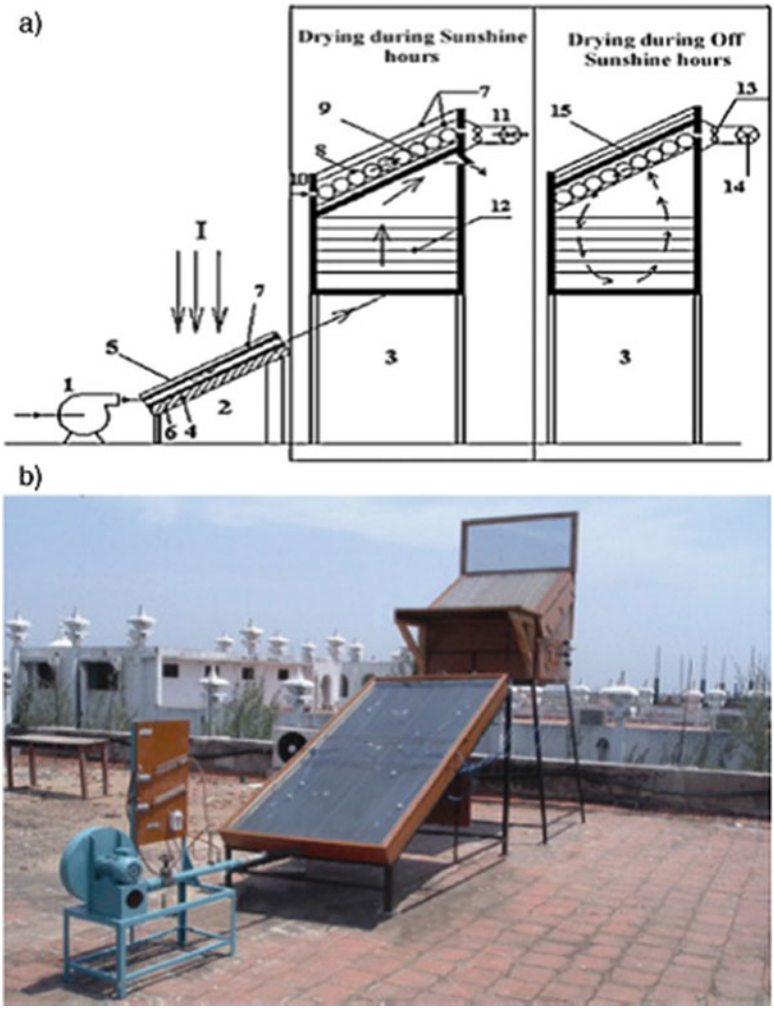

Fig. 8 (**a**) Sketch of the desiccant integrated solar dryer. (**b**) A pictorial view of the experimental setup (Shanmugam and Natarajan 2007)

Dina et al. (2015) performed experimental study on incessant solar dryer with energy storage for drying cocoa beans as shown in Fig. 10. They have used desiccant molecular sieve as adsorbent and $CaCl_2$ as absorbent in thermal storage, and it showed 9–12 °C higher temperature of drying chamber during sunshine hours.

Cakmak and Yildiz (2011) designed and fabricated a setup for drying seeded grapes. The designed solar drying system contains expanded-surface solar air collector which assisted in increase turbulence effect, and heat transfer is shown in Fig. 11.

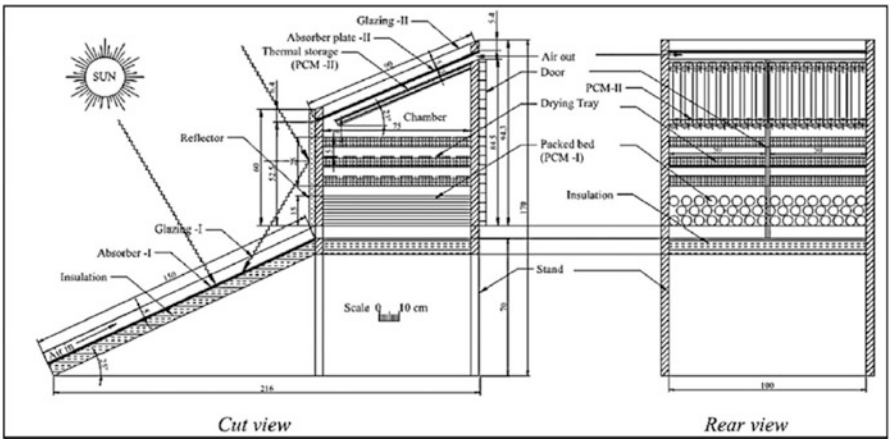

Fig. 9 Sketch of natural convective solar crop dryer with the thermal storage (Jain and Tiwari 2015)

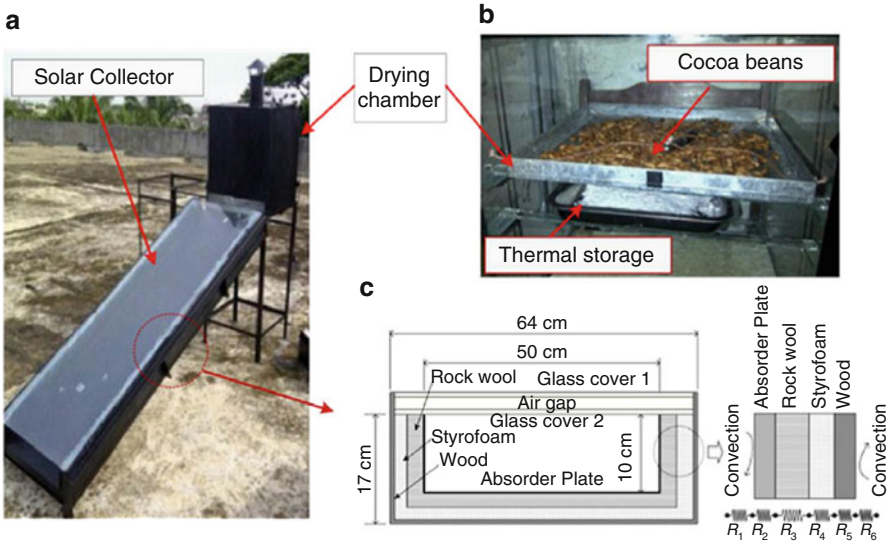

Fig. 10 Pictorial view of the experimental setup of solar dryer: (**a**) solar collector, (**b**) drying chamber and thermal storage, and (**c**) solar collector envelope (Dina et al. 2015)

Esakkimuthu et al. (2013) fabricated solar dryer with PCM thermal energy storage. The area of collector is made of three panels with 6 m^2 area. A V-corrugated aluminum sheet of 38 mm height and 1.1 mm thick is used as absorber plate. The distance linking the bottom surface and the absorber plate is 15 cm, and a case-hardened glass with thickness 5 mm was positioned above absorber plate. The bottom and sides of the collector are insulated with rock

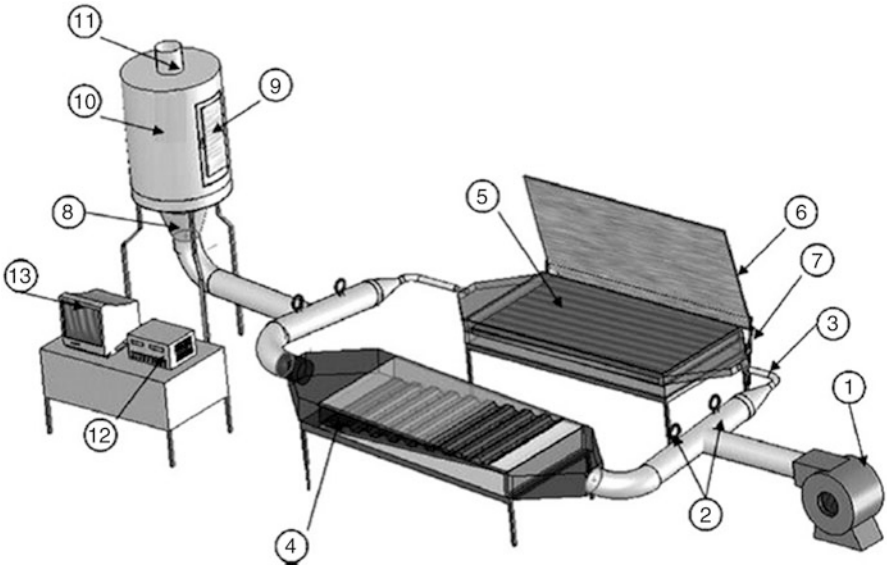

Fig. 11 Schematic view of solar dyer (Cakmak and Yıldız 2011)

wool. It was observed that the collector efficiency and heat transfer coefficient were increased with increase in the mass flow rate. Another important factor is selection of PCM with appropriate temperature to have proper drying of food products. They suggested that at 200 kg/h mass flow rate, almost consistent heat exchange takes place with nominal extra energy expenditure, which also helped in surmounting the drop-in pressure all through the solidification and melting of PCM. Furthermore, it was observed that at lower mass flow rate, uniform supply of the storage system achieved with maximum capacity of the PCM.

2.2.2 Greenhouse Dryer

Berroug et al. (2011) investigated the effect of greenhouse dryer with $CaCl_2 \cdot 6H_2O$ as PCM integrated its north side wall. The solar greenhouse dryer is oriented in east–west direction and 40-mm-thick PCM north wall as a storage medium. It was observed 4–5 °C rise in cover temperature and 6–12 °C rise in inside air temperature. Fluctuation of temperature and % relative humidity are relatively lower with PCM in comparison to without PCM in greenhouse dryer.

2.2.3 Hybrid Solar Dryer

Reyes et al. (2014) designed and fabricated a hybrid solar dryer with PCMs for drying of mushrooms. Many runs were performed in a day by maintaining temperature up to 60 °C with recycling of air (70–80%), and each run comes up with different shrinkage and darkening of mushroom. The accumulator panel efficiency varied between 10 and 21%, while thermal efficiency fluctuates between 22 and 62%.

2.3 Thermochemical Energy Storage

Thermochemical energy storage system depends on energy absorbed at the time of breaking molecular bonds and release of energy during reformation of the molecular bonds in a chemical reaction which is completely reversible. So, in thermochemical storage, the amount of stored heat depends on the quantity of storage material and the endothermic reactions.

$$Q = a_{\mathrm{r}} m \Delta h_{\mathrm{r}} \tag{3}$$

Among the all above stated thermal heat storage methods, latent heat thermal storage is more attractive because of its higher-energy storage density per mass and per unit volume.

3 Conclusion

The above discussion gives an overview of various designs of solar dryers with heat storage systems. Effective method of utilizing solar energy plays a key role to future's unlimited energy source; thus, it will fulfill the time gap between supply and demand of energy. A vast amount of experimental and theoretical research has been presented in the last three to four decades, which has by now confirmed for drying of various food products using solar dryer combined with storage in the form of sensible and latent heat storages. Heat storage by means of phase change materials is a prudent alternative. One of the predictable development solar drying with PCMs is drying of medical plants. It is bringing into being that use of metallic fins, encapsulation, and the addition of nanoparticles can enhance the thermal conductivity of PCMs considerably.

References

Aboul-Enein S, El-Sebaii AA, Ramadan MRI, El-Gohary HG (2000) Parametric study of a solar air heater with and without thermal storage for solar drying applications. Renew Energy 21 (3):505–522

Ayensu A (1997) Dehydration of food crops using a solar dryer with convective heat flow. Sol Energy 59:121–126

Ayensu A, Asiedu-Bondzie V (1986) Solar drying with convective self-flow and energy storage. Solar Wind Technol 3:273–279

Ayyappan S, Mayilsamy K (2012) Solar tunnel drier with thermal storage for drying of copra. Int J Energy Technol Policy 8(1):3–13

Ayyappan S, Mayilsamy K, Sreenarayanan VV (2016) Performance improvement studies in a solar greenhouse drier using sensible heat storage materials. Heat Mass Transf 52(3):459–467

Bal LM, Satya S, Naik SN (2010) Solar dryer with thermal energy storage systems for drying agricultural food products: a review. Renew Sust Energ Rev 14(8):2298–2314

Berroug F, Lakhal EK, El Omari M, Faraji M, El Qarnia H (2011) Thermal performance of a greenhouse with a phase change material north wall. Energy Build 43(11):3027–3035

Cakmak G, Yıldız C (2011) The drying kinetics of seeded grape in solar dryer with PCM-based solar integrated collector. Food Bioprod Process 89(2):103–108

Devahastin S, Pitaksuriyarat S (2006a) Use of latent heat storage to conserve energy during drying and its effect on drying kinetics of a food product. Appl Therm Eng 26(14):1705–1713

Devahastin S, Pitaksuriyarat S (2006b) Use of latent heat storage to conserve energy during drying and its effect on drying kinetics of a food product. Appl Therm Eng 26(14):1705–1713

Dina SF, Ambarita H, Napitupulu FH, Kawai H (2015) Study on effectiveness of continuous solar dryer integrated with desiccant thermal storage for drying cocoa beans. Case Stud Ther Eng 5:32–40

Esakkimuthu S, Hassabou AH, Palaniappan C, Spinnler M, Blumenberg J, Velraj R (2013) Experimental investigation on phase change material based thermal storage system for solar air heating applications. Solar Energy 88:144–153

Esper A, Mühlbauer W (1998) Solar drying-an effective means of food preservation. Renew Energy 15(1):95–100

Gogus Y (2009) Energy storage systems: storage of thermal energy. Eolss Publishers Company Limited, Oxford

Hawlader MNA, Chou SK, Jahangeer KA, Rahman SMA, KW EL (2003) Solar-assisted heat-pump dryer and water heater. Appl Energy 74(1):185–193

Jain D (2005) Modeling the system performance of multi-tray crop drying using an inclined multi-pass solar air heater with in-built thermal storage. J Food Eng 71(1):44–54

Jain D, Jain RK (2004) Performance evaluation of an inclined multi-pass solar air heater with in-built thermal storage on deep-bed drying application. J Food Eng 65(4):497–509

Jain D, Tiwari P (2015) Performance of indirect through pass natural convective solar crop dryer with phase change thermal energy storage. Renew Energy 80:244–250

Kant K, Shukla A, Sharma A, Kumar A, Jain A (2016) Thermal energy storage based solar drying systems: a review. Innovative Food Sci Emerg Technol 34:86–99

Khanna ML (1967) Design data for solar heating of air using a heat exchange and storage system. Sol Energy 11:142–144

Khartchenko NV (1997) Advanced energy systems. Institute of Energy Engineering & Technology University, Berlin

Leon MA, Kumar S, Bhattacharya SC (2002) A comprehensive procedure for performance evaluation of solar food dryers. Renew Sust Energ Rev 6(4):367–393

Mohanraj M, Chandrasekar P (2009) Performance of a forced convection solar drier integrated with gravel as heat storage material for chili drying. J Eng Sci Technol 4(3):305–314

Nuckols ML (1999) Analytical modeling of a diver dry suit enhanced with micro-encapsulated phase change materials. Ocean Eng 26(6):547–564

Reyes A, Mahn A, Vásquez F (2014) Mushrooms dehydration in a hybrid-solar dryer, using a phase change material. Energy Convers Manag 83:241–248

Sain P, Songara V, Karir R, Balan N (2013) Natural convection type solar dryer with latent heat storage. In: Renewable energy and sustainable energy (ICRESE), 2013 international conference on IEEE, pp 9–14

Shalaby SM, Bek MA, El-Sebaii AA (2014) Solar dryers with PCM as energy storage medium: a review. Renew Sust Energ Rev 33:110–116

Shanmugam V, Natarajan E (2007) Experimental study of regenerative desiccant integrated solar dryer with and without reflective mirror. Appl Therm Eng 27(8):1543–1551

Shariah A, Al-Akhras MA, Al-Omari IA (2002) Optimizing the tilt angle of solar collectors. Renew Energy 26(4):587–598

Sharma VK, Colangelo A, Spagna G (1995) Experimental investigation of different solar dryers suitable for fruit and vegetable drying. Renew Energy 6(4):413–424

Sharma A, Tyagi VV, Chen CR, Buddhi D (2009) Review on thermal energy storage with phase change materials and applications. Renew Sust Energ Rev 13(2):318–345

Shringi V, Kothari S, Panwar NL (2014) Experimental investigation of drying of garlic clove in solar dryer using phase change material as energy storage. J Therm Anal Calorim 118 (1):533–539

Development of Phase Change Materials (PCMs) for Solar Drying Systems

Anand Jain, Anil Kumar, A. Shukla, and Atul Sharma

Abstract Solar drying is an effective way for drying food products. Therefore, the development of efficient and cost-effective solar dryer has become a feasible alternative to fossil fuels. Solar energy is freely available during daytime; henceforth, it can't be utilized during off-sunshine hours. Therefore, solar dryer with thermal energy storage (TES) is becoming important for drying of food and agriculture crop. The interest in TES along with PCMs has increased in the past, as the suitable PCMs, i.e., paraffins, fatty acids, salt hydrate, eutectics, and binary mixtures, generally have all relevant thermophysical properties for the thermal applications. In comparison with the other categories, few selected fatty acids, i.e., commercial-grade lauric acid (LA), myristic acid (MA), palmitic acid (PA), stearic acid (SA), and acetamide (AC), are generally used in solar drying applications. The abovementioned fatty acids have been tested through differential scanning calorimeter (DSC) thermal analysis technique and concluded as potential PCMs for TES applications. Based on the DSC analysis, it may be concluded that the developed binary mixtures were in the melting range of 40–60 °C with an adequate amount of energy. The main aim of this chapter is to provide an idea about the methodology to develop the promising PCMs for TES applications.

Keywords Phase change materials • Differential scanning calorimeter • Thermal energy storage • Solar drying

A. Jain
Department of Energy (Energy Centre), Maulana Azad National Institute of Technology, Bhopal 462003, India

A. Kumar
Department of Energy (Energy Centre), Maulana Azad National Institute of Technology, Bhopal 462003, Madhya Pradesh, India

A. Shukla • A. Sharma (✉)
Non-Conventional Energy Laboratory, Rajiv Gandhi Institute of Petroleum Technology, Jais, Amethi 229304, India
e-mail: asharma@rgipt.ac.in

© Springer Nature Singapore Pte Ltd. 2017

O. Prakash, A. Kumar (eds.), *Solar Drying Technology*, Green Energy and Technology, DOI 10.1007/978-981-10-3833-4_23

1 Introduction

With the decline of the fossil fuels and an increase in the CO_2 content in the air, which leads to the greenhouse effect and causes a major role in climate change in the whole world, therefore, there is an increased demand for renewable sources in the worldwide market. With the prompt development of urbanization and therefore the aggravation of energy shortage within the developing countries, energy conservation is turning into an additional essential in recent years.

The establishment of energy systems and acceleration in its development resemble nurturing babies in the history of mankind. Energy systems are continually evolving, with the aims of improving technological efficiencies, reducing losses, and lowering the cost of production and supply. The higher levels of renewable energy infiltration will require a continuation of increasing market shares in all end use sectors. Therefore, in addition, the complete world annually needed an incredible growth within the renewable energy sector to fulfill the demand.

To enhance the present-day scenario of renewable energy systems (RES), it increases its share in the energy sector under enabling conditions and social acceptance; however, it will take adequate time. Immediately, some additional integration efforts should be put into the practice to accelerate the process in which include the understanding of the renewable energy resource characterization, its accessibility, monetary investments required for building up the infrastructure, and research, development, and demonstrations (RD&D). Worldwide short-term goal should also include the addition of RES into the already existing technologies effectively while finding ways to combat the challenges and the potential obstacles, whereas, the globally long-term goal should include integration of RES into future technologies and aim for an energy sector dominated by renewable energy.

Worldwide, today is the biggest crises being the energy crises as the usage of the conventional and non-renewable resources such as crude and oil; however, it is a well-known fact that such type of energy sources will be depleted eventually depending on the usage in the systems. The other major concern of their usage is that these energy sources release greenhouse gasses in bulk to the atmosphere, which is the main reason for the global warming, climate change, and ozone layer depletion, and due to that, ultraviolet rays affect the human life by causing different skin-related disease. Therefore, it is necessary for the worldwide society to find the other sources of energy, which should be cleaner and can be used for longer terms. Presently, the most popular renewable energy sources are solar energy, which is generally used in two ways, i.e., thermal or electrical.

Right now, in the entire world, solar energy usage for different purposes is in common practice. One of the most prominent processes involving its usage is in the drying process. The main countries of the earth and the application of solar energy-based thermal systems in the agricultural, to preserve vegetables and fruits and occasional and alternative crops, have revealed to be a convenient, inexpensive, and conscientious approach environmentally. Solar drying systems can enhance the value of the produce and at the same time reduce waste produce and consumption

of ancient fuels – consequently enhancing the class of life; on the other hand, the accessibility of worthy information is deficient in many of the nations where solar food processing systems are highly required as well as desired. Solar drying process reduces energy and time consumption, conquers less space, enhances the product quality, develops efficient methods, and preserves from the atmospheric degradation. The drying technology using solar radiation can be applied in moderate food processing industries to yield hygienic and good quality food products (Sharma et al. 2009a). Conventionally, the crop has been dried beneath the open sun that is called open sun drying and accomplished by burning fossil fuels and timber in chambers. These approaches suffer from several issues. In open sun drying, the products are lost owing to meagerly drying, because it's unprotected to a variety of impurities with external materials. Another difficulty is demanding large open space area with the availability of sunlight (Fudholi et al. 2015; Kant et al. 2016b; Prakash and Kumar 2014).

2 Disadvantages of Solar Dryers

As the solar radiation energy is alternating by its nature, though, there is no sunshine availability throughout the nighttime. The value of total available solar radiation is periodic and is hooked on the atmospheric conditions at the locations. However, irregularity is the major issue for widespread solar energy consumption for any type of the applications. Solar energy cannot be stored as such; therefore, a storage device along with the latent heat storage materials, i.e., PCMs, is needed to store the thermal energy throughout the process and can be reused later when it's required (Sharma et al. 2009b). The demerits of solar dryer are as follows:

- More expensive as compared to open sun drying.
- It may necessitate some parts of the material to be imported.
- Work only sunshine hours.
- High capital cost.

3 Classification of PCMs

PCMs are materials that may absorb or release the thermal energy throughout the method of melting and solidification. As a PCM melt or solidify, it absorbs or discharges the bulk amount of thermal energy in the form of latent heat. PCMs usually store 5–14 times additional heat per unit volume than sensible heat storage materials. Along with a variety of heat storage materials, PCMs are predominantly pretty as they offer high-energy storage density per unit volume and store thermal energy within a narrow temperature range. A huge number of PCMs (organic,

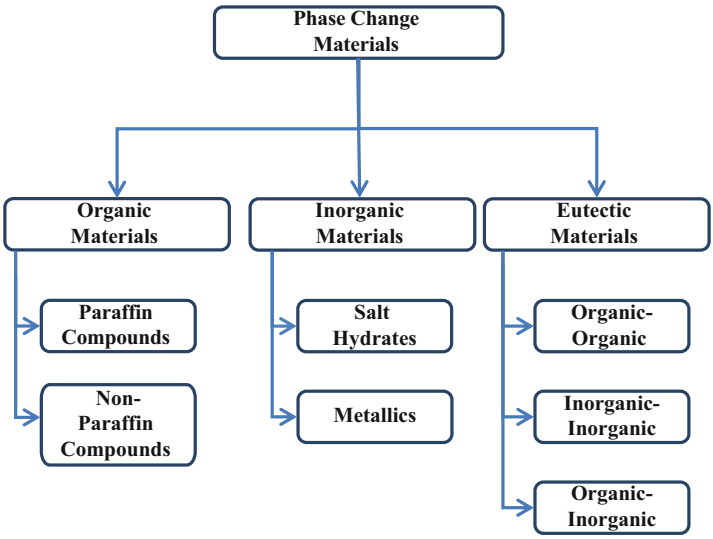

Fig. 1 Classification of PCM

inorganic, and eutectic) are on hand in the local market with an essential temperature range. Classifications of PCMs are given in Fig. 1.

Organic PCMs These PCMs can be classified into paraffins and non-paraffins. It includes congruent melting and self-nucleation.

- Paraffins: They consist of mainly straight-chain alkanes. Crystallization of (CH_3) chain releases a huge amount of hidden heat.
- Non-paraffins: Various non-paraffinic materials such as fatty acids, alcohols, glycols, and esters are often used as PCMs (Sharma et al. 2009b). Their chemical and physical properties are suitable to be used, but their costs limited their use as PCMs. The main properties of fatty acids are that having a high latent heat of fusion values comparable such as that of paraffins. The fatty acids are also spectacle that they have reproducible melting and freezing behavior and freeze with no supercooling. Their major drawback is the cost, which is 2–2.5 times greater than that of technical-grade paraffins. Some fatty acids have importance to low-temperature latent heat thermal energy storage applications and are tabulated in Table 1.

Inorganic PCMs It can further classify as salt hydrates and metallics.

- Salt hydrates: Inorganic salts and water together form a typical crystalline solid of general formula AB.nH2O, known as salt hydrates, which generally melts to a salt hydrate with fewer molecules of water.
- Metallics: Metal eutectics and low-melting metals are regarded as metallics. They have not yet been completely well thought out for PCMs due to their excessive weight.

Table 1 Melting temperature and latent heat of some fatty acids

Material	Capric acid	Elaidic acid	Lauric acid	Pentadecanoic acid	Tristearin	Myristic acid	Palmitic acid	Stearic acid	Acetamide
Melting point (OC)	36	47	49	52.5	56	58	55	69.4	81
Latent heat (kJ/ kg)	152	218	178	178	191	199	163	199	241

Eutectics A eutectic is a mixture of chemical compounds or elements that have a single chemical composition that solidifies at a lower temperature than any other composition. They approximately always meet and freeze without segregation since they freeze to a close mixture of crystals, leaving little chance for the components to separate.

There are huge quantities of organic and inorganic PCMs, which may be known by transition temperature and heat energy of fusion. Though, except for the transition temperature in the operating temperature range, the bulk of PCMs doesn't fulfill the standards essential for a suitable storage medium. As no single material will have all the specified properties for a perfect thermal storage media, one has got to use the available market materials and take a look to create up for the poor property by suitable system approach. The PCMs to be applied in any design TES should pass desirable thermophysical, kinetic, and chemical properties, which are given in Table 2.

4 Role of PCMs in Solar Drying

Nowadays, TES devices are majorly used to store the solar thermal energy for later use. As the solar energy is intermittent in nature, i.e., available only in sunshine hours and unavailable in the off-sunshine hours, therefore, the excess heat in the daytime may be stored and used later in the off-sunshine hours. The thermal energy storage assists in the development of energy-efficient thermal systems and decreases the consumption of energy and capital cost which leads to development of cost-efficient solar drying system. TES can be used for either short- or long-term energy storage in various solar thermal systems. If vitality is stored for insufficient hours, it is labeled as instant storage and is vital in many industrial and domestic solicitations; while if energy is stored for a month or more, it is generally deliberated as a durable storage device, which may also be essential in some applications.

Latent heat storage (LHS) through the PCMs is a promising technology for thermal energy storage, because of its high-thermal energy storage density and its isothermal nature during the phase transition from solid to liquid or liquid to gas (Fig. 2). LHS can be proficient through solid–liquid, liquid–gas, solid–gas, and solid–solid phase transformations from onto another. Though, solid–liquid and solid–solid phase transition are important for practical application. Solid–gas

Table 2 Desirable properties of PCMs for thermal energy storage

Thermal properties	Physical properties	Kinetic properties	Chemical properties	Economic properties
Suitable melting temperature in desirable range	Favorable phase equilibrium	No supercooling	Durable chemical stability	Abundantly available
High latent heat of transition so that it can store large amount of thermal energy	High density to store large amount of heat in small volume	Adequate crystallization rate	Compatibility with materials of construction	Have lower cost
High thermal conductivity in both liquid and solid phases	Slight volume change on phase transition		Nontoxic	
Good quality heat transfer	Low vapor pressure		Inflammable	
High-specific heat therefore can absorb heat during sensible heating				

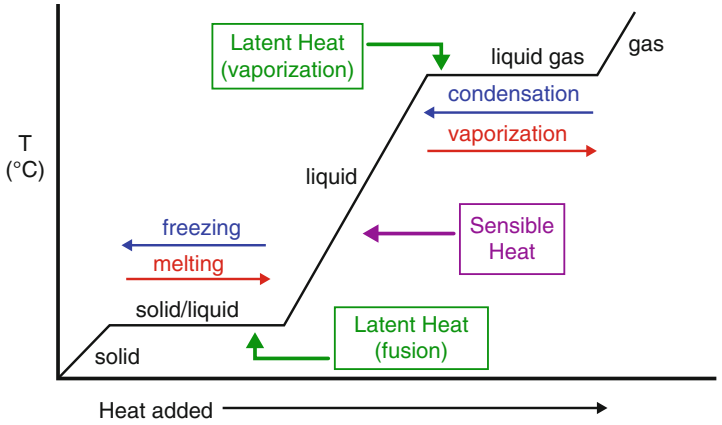

Fig. 2 TES heat flow diagram

and liquid–gas PCMs are related to the higher latent heat of fusion. Nevertheless, the difficulties with them are their higher volume changes on phase transition. This directed out their potential utility in thermal storage systems. The changes in volume make the system intricate and unrealistic. In addition, PCM is an option to rationalize the high cost and power utilization in thermal energy storage (TES). Electrical energy cost is rising gradually and the desire for better load management. In recent past, many researchers have been made a vast progress in TES systems along with PCMs (Abhat 1983; Khudhair and Farid 2004; Sharma et al. 2009b; Zalba et al. 2003). On the other hand, the high cost of the PCMs is a major disadvantage, which restricts their use in TES system. In recent times, many

inorganic and organic materials used as a PCM and their mixtures have been studied for impregnating into TES systems (Alkan and Sari 2008; Karaipekli and Sari 2008; Tunçbilek et al. 2005).

As of now, there will be short of commercial contemptible PCMs for the solar drying applications. However, in general, the higher price of these materials is a major shortcoming, which restrains the effectiveness of them in TES systems. Due to this, the use of fatty acids (commercial grade) as form-stable PCM will upsurge their viabilities with respect to the cheap price for TES applications (Sharma et al. 2013, 2014). Among the studied fatty acids, the lauric acid (LA), myristic acid (MA), palmitic acid (PA), stearic acid (SA), and acetamide (AC) are potential, abundant, and commercial materials for heat storage in TES systems from points of view of melting temperature and latent heat of fusion (Abhat 1983; Hasan 1994; Sarı and Kaygusuz 2001, 2002; Sharma et al. 2000). An experimental model of a solar dryer integrated with PCM is given in Fig. 3.

5 Applications of PCMs

PCMs are capable to absorb and discharge thermal energy in controlled environments. They have several applications such as solar drying (Kant et al. 2016b), solar energy storage (Murat Kenisarin et al. 2007), thermal regulation of photovoltaic

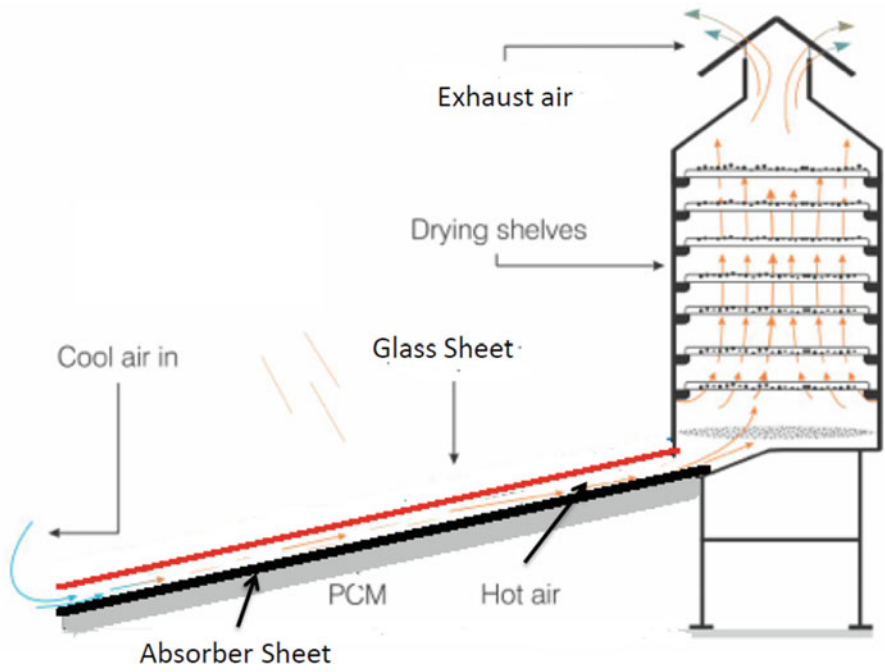

Fig. 3 Solar dryer with installed PCMs

(Kant et al. 2016a; Shukla et al. 2017a, b), waste heat recovery, smart air-conditioning in buildings (Sharma et al. 2013), thermal energy in solar stills (Shukla et al. 2017a, b), temperature adaptation in greenhouses (Shukla et al. 2016), and thermal comfort in textiles (Mondal 2008) due to their benefits of the high latent heat of fusion per unit mass, phase transition at nearly uniform temperatures, and low thermal expansion during phase change. There are numerous organic and inorganic, binary mixtures polymeric blends, and composites are testified as PCMs by several researchers. The application of energy storage with phase change is not limited to solar energy heating and cooling but has also been considered in other applications, i.e., buildings, shifting the peak heating load (Abhat 1983; Khudhair and Farid 2004; Sharma et al. 2009b; Zalba et al. 2003), solar drying (Kant et al. 2016b), desalination of water (Shukla et al. 2017a), and thermal regulation of photovoltaic (Kant et al. 2016a).

Some of the different uses found in the literature are given below:

- Solar thermal energy storage
- Passive thermal energy storage in architecture (HDPE)/bioclimatic building
- Safety: temperature regulation of electronic devices
- Food preservation: transport, hotel trade, ice cream, etc.
- Food agro-industry, wine, milk products (absorbing peaks in demand), and drying
- Thermal protection of electronic devices (integrated into the appliance)
- Water desalination (Shukla et al. 2017a, b) and greenhouse (Shukla et al. 2016)
- Medical applications: transport of blood, operating tables, and hot–cold therapies
- Solar power plants
- Spacecraft thermal systems
- Softening of exothermic temperature peaks in chemical reactions

6 Development of Materials

Commercial-grade fatty acids (capric, lauric, myristic, palmitic, and stearic, purity >98%) supplied from the Burgoyne Pvt. Ltd. firm utilized as favorable PCMs for this study without sanitization. Authors choose the fatty acids for this study because the basic materials of fatty acids are derivative from the ordinary vegetable and animal sources, which assured a frequent supply even though the lack of fuel sources (Cedeño et al. 2001; Chuah et al. 2006; Feldman et al. 1989). In general, only small volume changes are found during melting or solidification in fatty acids. Additionally, little or no supercooling has seen within these materials during the phase transition, which is also a significant advantage over many other PCMs. Generally, fatty acids are commercially available in the local market, which mostly are manufactured in large extents of plastics, cosmetics, textile, and other industries.

The phase change temperatures of a PCM can be easily adjusted to a proper temperature by mixing with other PCM/additives at a suitable ratio. Appropriate phase change temperature and a high melting enthalpy are two essential necessities for a PCM to be valid in any type of TES systems. Hence, in recent times, several research works were mostly centered toward the synthesis of solid–liquid PCMs. The main purpose of this study is to manufacture low-cost PCMs for solar drying applications. Therefore, the binary mixtures based on commercial-grade fatty acids, i.e., LA, MA, PA, SA, and AC, were chosen as possible materials for heat storage in TES applications, which are majorly based on the melting temperature, latent heat of fusion, and other thermophysical properties. To develop the PCMs, a series of binary mixtures are prepared with different weight percentages (05/95, 10/90, 15/85, 20/80, 25/75, 30/70, 35/65, 40/60, 45/55, 50/50, 55/45, 60/40, 65/35, 70/30,75/25, 80/20, 85/15, 90/10, and 95/05 wt.%) as also specified in the previous research work of the author's group, and their thermal properties are measured through the DSC technique (Sharma et al. 2013, 2014). Many samples of binary eutectic (100 g each) were formed by mixing it in a melted state and retained at room temperature for 1 h. A semi-analytical digital balance (accuracy ± 0.0001 g) additionally used to quantify the weight of the developed samples (g).

7 Measurement Techniques of Melting Temperature and Latent Heat of Fusion

The most important thermal properties are the latent heat of fusion, and melting and solidification temperatures, which can be measured by the differential scanning calorimetry (DSC) thermal analysis technique. The DSC analytical technique was developed by Watson in 1962. The equipment that is used for this purpose is named as DSC. The equipment has the ability to directly measure the energy storage capacity during melting and allow accurate measurement of heat capacity. The temperatures and heat flow associated with material changes as a function of time are measured in a controlled environment (Michael E. Brown 1998). The qualitative and quantitative data about physical and chemical changes measured that involve endothermic or exothermic processes (DSC 2010). According to Kuznik et al. (David et al. 2011), the name DSC is very clear:

- Calorimetry: The measurement of the quantity of heat absorbed or released of a sample with the change in temperature.
- Differential: The measurements have been carried out on sample with respect to reference sample with known properties.
- Scanning: The thermal excitation with a linear temperature ramp.

8 Working Principle of Differential Scanning Calorimetry (DSC)

DSC is a technique for determining the energy required to establish a nearly zero temperature variance between a sample material and an inert reference material, as the two samples are subjected to same temperature regimes in an environment heated/cooled at a controlled rate. There are two categories of DSC systems in common use: (1) heat flux DSC and (2) power compensation DSC (Fig. 4).

In the present study, the authors used the heat flux-based DSC (PerkinElmer model - DSC 4000) to measure the thermophysical properties of the binary mixtures. The reference material used as sample must have a distinct heat capacity over the range of temperatures. The suggested reference material sample is alumina (Al_2O_3) for PCMs. The elementary fundamental of this method is that when the sample experiences a physical transformation such as phase changes, so as to keep both reference and sample at the equal temperature, more or less heat will be required as compared to the reference sample. The condition of heat flow to the sample depends on whether the process is endothermic or exothermic.

By detecting the dissimilarity in heat flow between the material sample and reference sample, DSC is able to evaluate the amount of heat absorbed or discharged during such phase transitions. The sample's latent heat of fusion can be calculated using the area below the DSC curve. The phase transition temperature of the sample is taken as the onset obtained by curve fitting of the growing part of the DSC peak and is calculated between onset temperatures, and temperature corresponds to the peak of the curve. The transition temperature of sample is evaluated by the tangent at the point of maximum slope on the face part of the peak in DSC curve. In the present study, the authors used DSC 4000. The scan rate of sample is 2 °C min^{-1} under a continuous flow of nitrogen at a flow rate of 20 ml min^{-1}. The maximum deviation in enthalpy estimation was ± 2%, and the maximum deviation in temperature estimation was ± 0.1 °C. The thermophysical

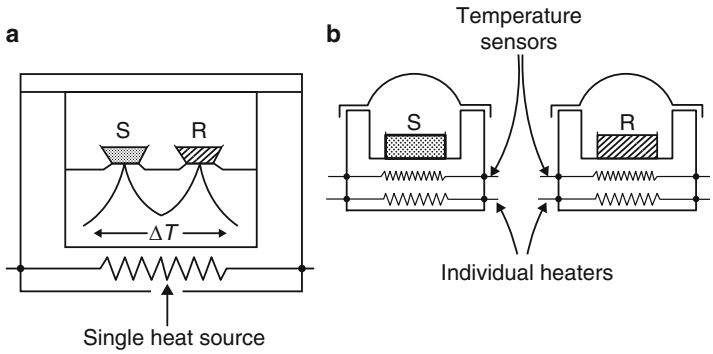

Fig. 4 (a) Heat flux DSC and (b) power compensation DSC

properties of pure fatty acids provided by the manufacturer are taken from Sharma et al. (2014).

9 Results and Discussion

A few major hurdles typically faced within the TES systems, such as unreliability regarding the durable thermal performance and the lesser number of proper PCMs for the TES utilization. Several authors already conducted such type of the research study; however, still there is a necessity of innovative PCM developments, which might carry out the requirements of the users and would be effortlessly obtainable in the local commercial market. A couple real obstacles regularly confronted inside the TES frameworks, for example, instabilities with respect to the long haul warm execution and furthermore the fewest number of suitable PCMs for the TES applications. A ton of examination has been done in this specific course, nonetheless; still, there is a prerequisite for new PCMs advancements, which may satisfy the necessities of the client and would be effectively accessible in the nearby business market.

For the present study, the authors has selected five technical-grade fatty acids, i.e., LA ($T_m = 45.93$ °C, $\lambda_m = 175.77$ kJ/kg), MA ($T_m = 56.83$ °C, $\lambda_m = 168.27$ kJ/kg), PA ($T_m = 64.25$ °C, $\lambda_m = 206.11$ kJ/kg), SA ($T_m = 57.73$ °C, $\lambda_m = 180.79$ kJ/kg), and AC ($T_m = 83.58$ °C, $\lambda_m = 214.59$ kJ/kg) as these materials have high latent heat of fusion and also easily available at low cost in the Indian market. The heating/cooling curves for binary mixture of PA and SA at the zeroth cycle are given in author's newly published research articles (Sharma et al. 2013, 2014). The several binary mixtures were prepared in the laboratory, which was based on the identified materials as classified in above text. All developed materials were characterized through DSC analysis technique to find out their phase transition temperature and latent heat of fusion with the scan rate of 2 °C min^{-1}, and data achieved from the DSC curves is given in Table 3.

It had been hard to discover techniques to guess phase change temperature and latent heat of fusion in binary mixtures based on the pure fatty acids (Cedeño et al. 2001). It had been also perceived that the phase change temperature in a binary mixture of two fatty acids was forever lower as compared to pure fatty acid. The phase change temperature vs. composition in binary eutectic mixtures of fatty acids, where the existence of lowest melting points is seen, is being revealed that the approach of fatty acid mixtures was entirely non-ideal (Sharma et al. 2013). The similar trend was found during this research work.

Several samples developed with a unique mass fraction of PA and SA fatty acids with proper mixing. Taking into account these outcomes, it can be clarified that the transition temperature of the samples follows a turndown behavior with an increase in the concentration of PA within the binary mixture. The binary mixture of PA-SA (05/95 wt. %) showed that 61.45 °C as transition temperature as well as 160.36 kJ/kg as a value of the latent heat of fusion. On the other hand, the melting

Table 3 Thermophysical properties of eutectic mixture developed using fatty acids

S. No.	Code[a]	A (%)	B (%)	Melting point (°C)	Latent heat of fusion (kJ/kg)
1	LA-AC	90	10	41.25	193.10
2	MA-AC	80	20	46.04	188.39
3	Lauric acid	–	–	46.13	190.21
4	MA-PA	60	40	46.82	176.63
5	MA-AC	60	40	48.08	160.13
6	MA-SA	50	50	48.27	150.41
7	LA-PA	50	50	48.29	183.69
8	MA-AC	70	30	48.99	170.13
9	MA-AC	90	10	50.69	195.93
10	SA-AC	30	70	53.50	153.37
11	PA-AC	60	40	55.72	143.98
12	PA-AC	50	50	55.82	144.01
13	PA-SA	55	45	57.25	183.32
14	PA-AC	90	10	58.00	184.79
15	PA-SA	45	55	58.14	184.14
16	PA-SA	65	35	58.23	181.49
17	PA-SA	35	65	58.44	194.05
18	PA-SA	25	75	59.20	178.58
19	PA-AC	70	30	59.42	187.03
20	PA-AC	80	10	59.61	190.34
21	PA-SA	15	85	59.84	179.57
22	PA-SA	75	25	60.97	170.09
23	PA-SA	85	15	60.97	170.09
24	PA-SA	5	95	61.45	160.36
25	PA-SA	95	5	63.67	196.98

[a]Thermal cycle testing is also required for these samples before employment to any TES system

temperature of PA-SA samples (shown in Table 3) were in the range of 57–65 °C melting temperature range along with the range of 160–200 kJ/kg, which is quite appropriate for the solar drying applications. Figure 5 shows the DSC (heating/cooling) curve of the PA-SA (65/35 wt.%) material with 2 °C min^{-1} scanning heating/cooling rate, which clearly shows the thermal behavior of the developed material as expected by the authors.

On the other hand, authors identified several other possibilities based on the other identified possible material. In this series, several other binary materials were identified and listed in Table 3. It's clear from the table that these materials also lie in the temperature range of 40–60 °C; however, the value of the latent heat of fusion was nearly same as quoted in the above text. Overall, it can be concluded that these developed materials may be used in the solar drying application as well as for the relevant thermal application.

A cost assessment could not be mentioned because of the non-accessibility of the standard information for the same; however, the PCMs developed within the

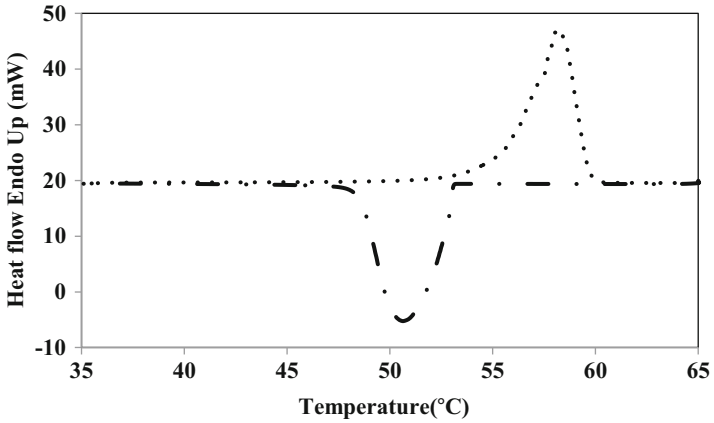

Fig. 5 DSC graph of PA-SA (65/35 wt. %) with the scan rate of 2 °C/min

author's lab is reasonably at the cheaper price as associated to available materials for the alike TES uses. The evaluated cost for the developed PCMs can be reduced up to 3–4 $/kg, once produced in large scale. It may be outlined that these materials are having an expanded life, reasonable and simple to handle, and exceptionally easy to revive thermally.

10 Conclusion

The eutectic binary mixtures of fatty acids were developed to form-stable PCMs for drying applications. The prepared binary samples were based on LA, MA, PA, SA, and AC with different weight fractions and were also characterized through DSC analysis methods. The DSC analysis showed that many binary mixture of fatty acid samples were found satisfactory in the desired operating temperature range (40–60 °C), along with high latent heat of fusion (140–200 kJ/kg), which is also a very important parameter to recommend any material for the applications. The thermal stability testing of the developed samples up to 1000 cycles are on track and will communicate for publication in the due course of time. Overall, this chapter provides an idea about the methodology of the suitable energy storage material development for drying applications. Finally, the authors could conclude that fatty acid-based binary mixtures may be incorporated as prompt PCMs because these materials have shown suitable melting point with adequate of the latent heat of fusion for the solar drying application.

Acknowledgment Authors are highly thankful to Director, RGIPT, Jais, Amethi for supporting to carry out the work at RGIPT.

References

Abhat A (1983) Low temperature latent heat thermal energy storage: heat storage materials. Solar Energy 30:313–332. doi:10.1016/0038-092X(83)90186-X

Alkan C, Sari A (2008) Fatty acid/poly(methyl methacrylate) (PMMA) blends as form-stable phase change materials for latent heat thermal energy storage. Solar Energy 82:118–124. doi:10.1016/j.solener.2007.07.001

Brown ME (1998) Handbook of thermal analysis and calorimetry, 1st edn. Elsevier B.V, Amsterdam

Cedeño FO, Prieto MM, Espina A, García JR (2001) Measurements of temperature and melting heat of some pure fatty acids and their binary and ternary mixtures by differential scanning calorimetry. Thermochim Acta 369:39–50. doi:10.1016/S0040-6031(00)00752-8

Chuah TG, Rozanna D, Salmiah A, Thomas Choong S, Sa'ari M (2006) Fatty acids used as phase change materials (PCMs) for thermal energy storage in building material applications

David D, Johannes K, Roux J-J, Kuznik F, David D, Johannes K, Roux J-J (2011) A review on phase change materials integrated in building walls. Renew Sustain Energy Rev 15:379–391. doi:10.1016/j.rser.2010.08.019

DSC (2010) Differential Scanning calorimeter operator's manual

Feldman D, Shapiro MM, Banu D, Fuks CJ (1989) Fatty acids and their mixtures as phase-change materials for thermal energy storage. Solar Energy Mater 18:201–216. doi:10.1016/0165-1633(89)90054-3

Fudholi A, Sopian K, Gabbasa M, Bakhtyar B, Yahya M, Ruslan MH, Mat S (2015) Techno-economic of solar drying systems with water based solar collectors in Malaysia: A review. Renew Sustain Energy Rev 51:809–820. doi:10.1016/j.rser.2015.06.059

Hasan A (1994) Phase change material energy storage system employing palmitic acid. Solar Energy 52:143–154. doi:10.1016/0038-092X(94)90064-7

Kant K, Shukla A, Sharma A, Biwole PH (2016a) Heat transfer studies of photovoltaic panel coupled with phase change material. Solar Energy 140:151–161. doi:10.1016/j.solener.2016.11.006

Kant K, Shukla A, Sharma A, Kumar A, Jain A (2016b) Thermal Energy storage based solar drying systems: A review. Innovative Food Sci Emerg Technol 34:86–99. doi:10.1016/j.ifset.2016.01.007

Karaipekli A, Sari A (2008) Capric-myristic acid/expanded perlite composite as form-stable phase change material for latent heat thermal energy storage. Renew Energy 33:2599–2605. doi:10.1016/j.renene.2008.02.024

Khudhair AM, Farid MM (2004) A review on energy conservation in building applications with thermal storage by latent heat using phase change materials. Energy Convers Manag 45:263–275. doi:10.1016/S0196-8904(03)00131-6

Mondal S (2008) Phase change materials for smart textiles – an overview. Appl Therm Eng 28:1536–1550. doi:10.1016/j.applthermaleng.2007.08.009

Murat Kenisarin A, Mahkamov K, Kenisarin M, Mahkamov K (2007) Solar energy storage using phase change materials. Renew Sustain Energy Rev 11:1913–1965. doi:10.1016/j.rser.2006.05.005

Prakash O, Kumar A (2014) Solar greenhouse drying: a review. Renew Sustain Energy Rev 29:905–910. doi:10.1016/j.rser.2013.08.084

Sarı A, Kaygusuz K (2001) Thermal performance of myristic acid as a phase change material for energy storage application. Renew Energy 24:303–317. doi:10.1016/S0960-1481(00)00167-1

Sari A, Kaygusuz K (2002) Thermal performance of palmitic acid as a phase change energy storage material. Energy Conver Manage 43:863–876. doi:10.1016/S0196-8904(01)00071-1

Sharma SD, Buddhi D, Sawhney RL, Sharma A (2000) Design, development and performance evaluation of a latent heat storage unit for evening cooking in a solar cooker. Energy Convers Manag 41:1497–1508

Sharma A, Chen CR, Vu Lan N (2009a) Solar-energy drying systems: A review. Renew Sustain Energy Rev 13:1185–1210. doi:10.1016/j.rser.2008.08.015

Sharma A, Tyagi VV, Chen CR, Buddhi D (2009b) Review on thermal energy storage with phase change materials and applications. Renew Sustain Energy Rev 13:318–345. doi:10.1016/j.rser.2007.10.005

Sharma A, Shukla A, Chen CR, Dwivedi S (2013) Development of phase change materials for building applications. Energy Buildings 64:403–407. doi:10.1016/j.enbuild.2013.05.029

Sharma A, Shukla A, Chen CR, Wu TN (2014) Development of phase change materials (PCMs) for low temperature energy storage applications. Sustain Energy Technol Assess 7:17–21. doi:10.1016/j.seta.2014.02.009

Shukla A, Sharma A, Kant K (2016) Solar Greenhouse With Thermal Energy Storage: a Review. Curr Sustain/Renew Energy Rep 3:58–66. doi:10.1007/s40518-016-0056-y

Shukla A, Kant K, Sharma A (2017a) Solar still with latent heat energy storage: A review. Innov Food Sci Emerg Technol 41:34–46. doi:10.1016/j.csl.2006.06.005

Shukla A, Kant K, Sharma A, Biwole PH (2017b) Cooling methodologies of photovoltaic module for enhancing electrical efficiency: A review. Solar Energy Mater Solar Cells 160:275–286. doi:10.1016/j.solmat.2016.10.047

Tunçbilek K, Sari A, Tarhan S, Ergüneş G, Kaygusuz K (2005) Lauric and palmitic acids eutectic mixture as latent heat storage material for low temperature heating applications. Energy 30:677–692. doi:10.1016/j.energy.2004.05.017

Zalba B, Marin JS, Cabeza LF, Mehling H (2003) Review on thermal energy storage with phase change: materials, heat transfer analysis and applications. Appl Therm Eng 23:251–283. doi:10.1016/S1359-4311(02)00192-8